SREE CHITRA TIRUNAL INSTITUTE OF MEDICAL SCIENCES & TECHNOLOGY TRIVANDRUM -695011

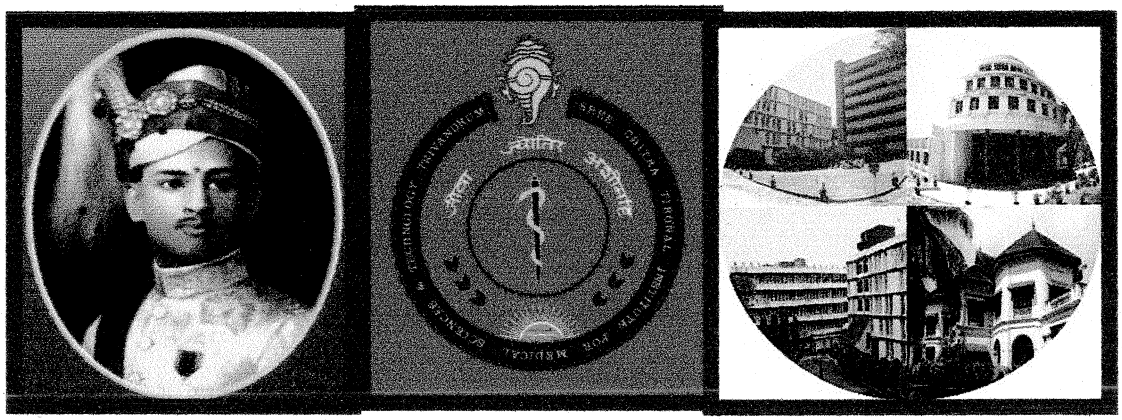

DIPLOMA IN ADVANCED MEDICAL IMAGING TECHNOLOGY

Work book submitted by: ***LALITHA. R.S***

DAMIT Student
Dept of Imaging Sciences and
Interventional Radiology
SCTIMST,
Thiruvananthapuram.

Place: Thiruvananthapuram
Date: 30-11-2006.

2005-2006

SREE CHITRA TIRUNAL INSTITUTE FOR MEDICAL SCIENCES AND TECHNOLOGY

CERTIFICATE

I Miss. LALITHA.R.S here by declare that I have actually performed all the procedures listed under the course of diploma in advanced imaging technology (DAMIT)

Place : Thiruvananthapuram

Date : 30-11-2006

signature

name Lalitha R.S.

Signature,

Head of the Dept
Dept .of
Imaging science
&
interventional radiology

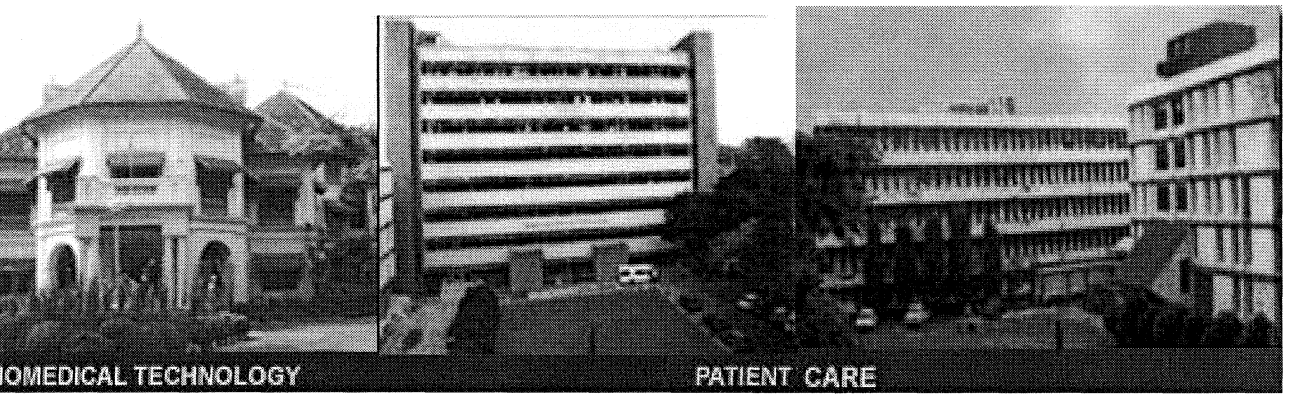

The Sree Chitra Tirunal Institute for Medical Sciences &Technology (SCTIMST), Thiruvananthapuram is an Institute of National Importance established by an Act of the Indian Parliament. It is an autonomous Institute under the administrative control of the Department of Science and Technology, Government of India.

The Institute signifies the convergence of medical sciences and technology and its mission is to enable the indigenous growth of biomedical technology, besides demonstrating high standards of patient care in medical specialties and evolving postgraduate training programs in advanced medical specialties, biomedical engineering and technology, as well as in public health

It has a 239-bedded hospital for tertiary care of cardiovascular and neurological diseases, a biomedical technology wing with facilities for developing medical devices from a conceptual stage to commercialization, and a center of excellence for training and research in public health.

The Institute has the status of a University and offers postdoctoral, doctoral and postgraduate courses in medical specialties, public health, nursing, basic sciences and health care technology. It is a member of the Association of Indian Universities and the Association of Commonwealth Universities

ACKNOWLEDGEMENT

First and fore most, I would like to thank my Head of the Department Prof.. Dr. Arun Kumar Gupta and Addl. Prof Dr Kapilamoorthy T.R, Dr Kesavadas C and all other faculty members who had guided me through the different phases of my studies encouraged and helped me on all aspects of my training.

I thank the Director of the institute Dr K Mohandas, Dean Prof Dr Radhakrishnan.K and the Registrar Dr A.V George, for their advices and kind attention towards me.

I extent my heartful thanks to all the Radiographers, other staffs of radiology, staff members of different depts, for their help during my stay in the institute. I am thankful to the patients who were the core medium of study.

At last, I would like to acknowledge my sincere thanks to PG residents, senior and junior DAMITS for their co-operation at work place and in studies.

PREFACE

This work book, I have done as part of my training in the dept of radiology for diploma in Advanced Medical Imaging Technology (DAMIT) course includes brief details of the equipment used in the Dept, basic physics and working involved with the equipments, the routine protocols and the procedures followed in our different labs, number of cases which I have individually done in X-RAY,CR,CT, MRI,PACS&3D WORKSTATION, and the cases which I have assisted in Neuro and Cardiac Cath Lab, I also have included the seminars and projects I have done .

DAMIT is a two years full time residential programme in advanced medical imaging technology for qualified radiographers to excel and learn the newer techniques in medical imaging. Selection is done by a national level entrance examination. At present institute offers 3 seats.

The students are posted in the department of radiology equipped with all modern medical imaging facilities-State of art and top of the line-MRI system, Spiral CT system, DSA suit, Colour Doppler ultra sound scanner and a radiology network with a central workstation with added 3D software and the division of Interventional Radiology make it a distinguished Radiology Dept .The course schedule contains theory classes, practical training, seminar presentations & projects. Diploma is awarded after successful completion of 2 Year term based on a written examination with viva-voce and internal assessment.

INDEX

MAGNETISM

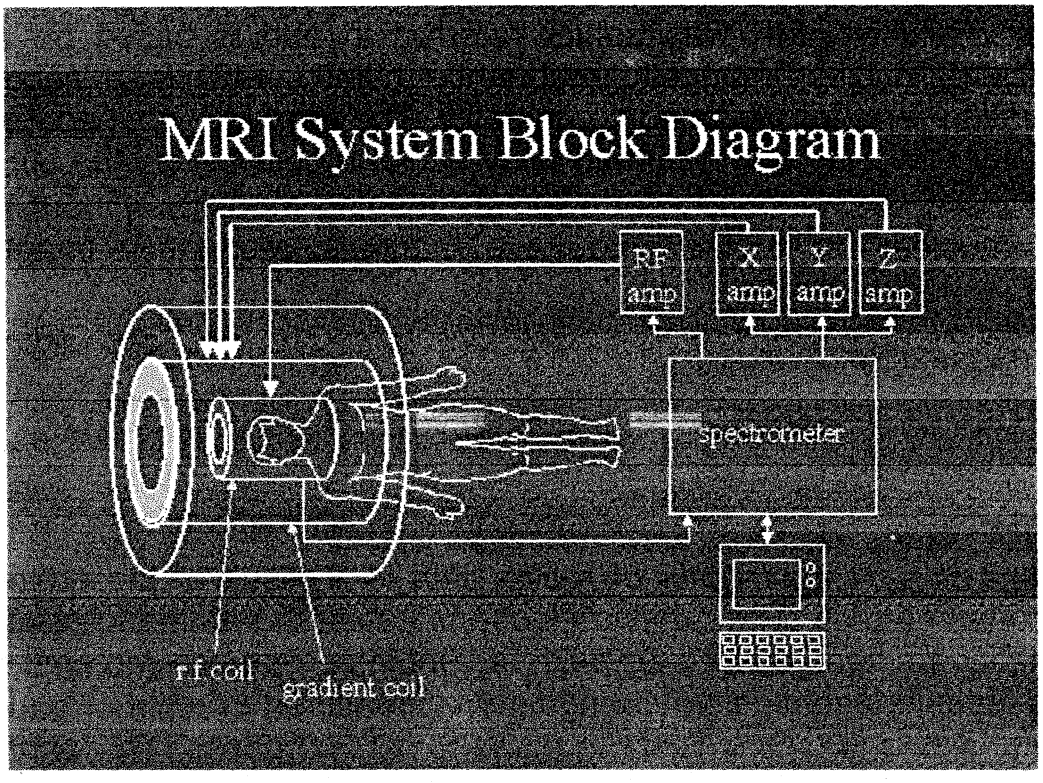

History of Magnetic Resonance

In 1946, Felix Bloch and Edward Purcell independently discovered that a magnetically energized substance bombarded with RF emitted a "tune" similar to a tuning fork. They found that the nuclei of different atoms absorbed radio waves at different frequencies. In 1952, Bloch and Purcell received the Nobel Prize for their discovery of what was referred to as Nuclear Magnetic Resonance (NMR), eventually to be known as Magnetic Resonance (MRI). In 1970, the medical imaging world significantly changed with the contributions of Dr. Raymond Damidian. Dr. Damidian discovered that the structure and abundance of water in the human body was the key to MR imaging, and that the water (hydrogen) emitted a signal that was both detectable and recordable. Dr. Damidian and his team spent the next seven years

ently designing and creating the first MRI scanner for medical ging of the human body. It was Paul Lauterbur, however, who lemented the concept of tri-plane gradients used for tingselective areas of the body (G_x, G_y, and G_z). **Felix Bloch**

BlochFelix BlochMR was earlier referred to and is based on the sics of nuclear magnetic resonance (NMR). MRI is a second eration term for this imaging modality. The term MRI was adopted n after imaging of the human body became possible as the public ld more easily adopt a term for an imaging modality without the d "nuclear" in it. Thus we have magnetic resonance imaging RI).

Magnetism
Resonance and RF
Relaxation

gnetism

Magnetism is a property of matter that is a result of the orbiting ctrons in atoms. The orbiting electrons cause the atoms to have a gnetic moment associated with an intrinsic angular momentum ed 'spin'. Magnetic field strengths are measured in units of gauss and Tesla (T). One Tesla is equal to 10,000 gauss. The earth's gnetic field is about 0.5 gauss. The strength of electromagnets d to pick up cars in junk yards is about the field strength of MRI chines (1.5-2.0T). Four terms describing the magnetic properties materials, used in MRI. These terms are ferromagnetism, amagnetism, superparamagnetism, and diamagnetism

Ferromagnetism
Paramagnetism
Superparamagnetism
Diamagnetism

Ferromagnetism

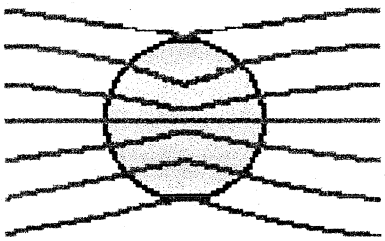

Ferromagnetic materials generally contain iron, nickel, or cobalt. These materials include magnets, and various objects one might find in a patient, such as aneurysm clips, parts of pacemakers, shrapnel, etc. These materials have a large positive magnetic susceptibility, i.e., when placed in a magnet field, the field strength is much stronger inside the material than outside. Ferromagnetic materials are also characterized by being made up of clusters of 10^17 to 10^21 atoms called magnetic domains, that all have their magnetic moments pointing in the same direction. The moments of the domains is random in unmagnetized materials, and point in the same direction in magnetized materials. The figure to the above illustrates the effect of a ferromagnetic material (grey circle) on the magnetic field flux lines (blue). The ability to remain magnetized when an external magnetic field is removed is a distinguishing factor compared to paramagnetic, superparamagnetic, and diamagnetic materials. On MR images, these materials cause susceptibility artifacts characterized by loss of signal and spatial distortion. This can occur with even fragments to small to be seen on plain x-ray. This is a common finding in a cervical spine MRI post anterior fusion.

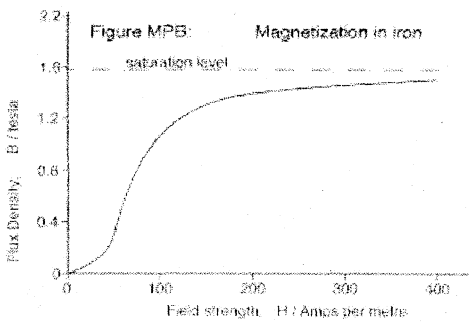

amagnetism

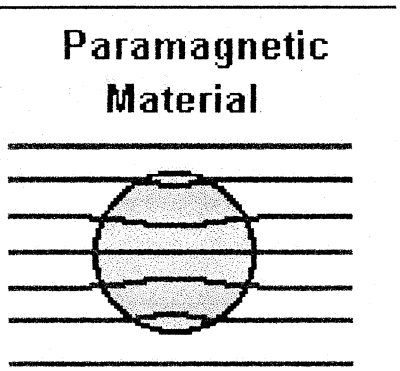

Paramagnetic materials include oxygen and ions of various als like Fe, Mg, and Gd. These ions have unpaired electrons, lting in a positive magnetic susceptibility. The magnitude of this ceptibility is less than one one-thousands of that of ferromagnetic erials. The effect on MRI is increase in the T1 and T2 relaxation s (decrease in the T1 and T2 times).

erparamagnetism

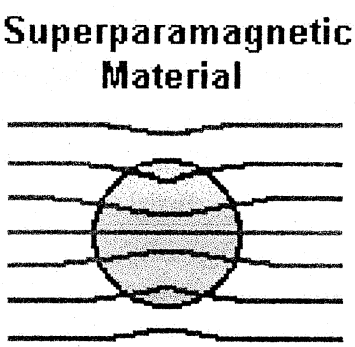

erparamagnetic materials consist of individual domains of nents that have ferromagnetic properties in bulk. Their magnetic ceptibility is between that of ferromagnetic and paramagnetic erials. The figure to the left illustrates the effect of a erparamagnetic material (grey circle) on the magnetic field flux s (blue). Examples of a superparamagnetic materials include iron taining contrast agents for bowel, liver, and lymph node imaging.

Diamagnetism

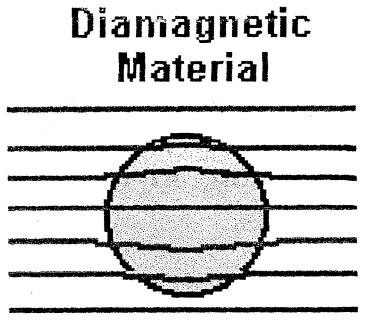

Diamagnetism is a very weakform of magnetism that is only exhibited in the presence of an external magnetic field. It is the result of changes in the orbital motion of electrons due to the external magnetic field. The induced magnetic moment is very small and in a direction opposite to that of the applied field. When placed between the poles of a strong electromagnet, diamagnetic materials are attracted towards regions where the magnetic field is weak. Diamagnetism is found in all materials; however, because it is so weak it can only be observed in materials that do not exhibit other forms of magnetism. Also, diamagnetism is found in elements with paired electrons. Oxygen was once thought to be diamagnetic, but a new revised molecular orbital (MO) model confirmed oxygen's paramagnetic nature.

An exception to the "weak" nature of diamagnetism occurs with the rather large number of materials that become superconducting, something that usually happens at lowered temperatures. Superconductors are perfect diamagnets and when placed in an external magnetic field expel the field lines from their interiors (depending on field intensity and temperature).

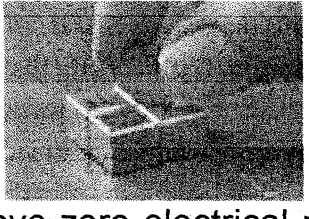

Superconductors also have zero electrical resistance, a consequence of their diamagnetism. Superconducting structures have been known to tear themselves apart with astonishing force in their attempt to escape an external field. Superconducting magnets are the major

ponent of most magnetic resonance imaging systems, perhaps only important application of diamagnetism

haps the substance that displays the strongest diamagnetism is nuth, used as an alternative to lead shot in shotgun shells. Melting n bismuth and then molding it is a very efficient way of capturing diamagnetic properties. Pyrolitic Graphite is stronger than muth in only one direction; in the other two directions it is still magnetic, but it is weaker

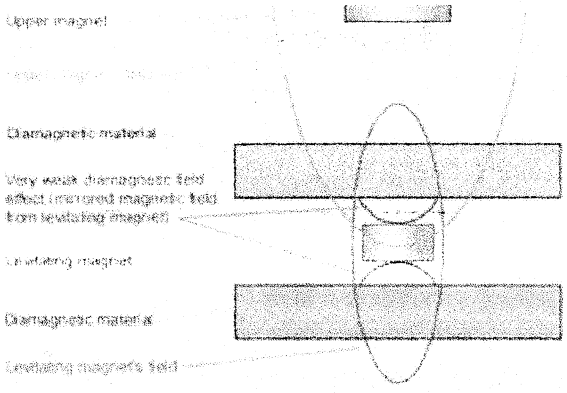

per Conductors

erparamagnetic materials consist of individual domains of elements that e ferromagnetic properties in bulk. Their magnetic susceptibility is veen that of ferromagnetic and paramagnetic materials. The figure to the illustrates the effect of a super paramagnetic material (grey circle) on the netic field flux lines (blue). Examples of a super paramagnetic materials ude iron containing contrast agents for bowel, liver, and lymph node ging. Diamagnetic materials have no intrinsic atomic magnetic moment, when placed in a magnetic field weakly repel the field, resulting in a ll negative magnetic susceptibility. Materials like water, copper, ogen, barium sulfate, and most tissues are diamagnetic. The figure above trates the effect of a diamagnetic material (grey circle) on the magnetic l flux lines (blue). The weak negative magnetic susceptibility contributes he loss of signal seen in bowel on MRI after administration of barium ate suspensions.

The Atom

In order to understand MRI, it is necessary to understand the properties of atoms. Atoms consist of a dense nucleus surrounded by orbiting electrons. The nucleus of most atoms is made up of positively charged particles called protons, and neutrally charged particles called neutrons. The nucleus of an atom is always positively charged due the positive protons. The electrons orbiting around the nucleus are extremely small negatively charged particles which balance the positive charge of the nucleus. Chemical properties of elements vary based on the electrical charge of the atoms. An atom with the same number of protons and electrons is chemically neutral and stable. Often, electrons are added or knocked out of the orbits around nuclei, which alters the charge of atom thus creating a positively or negatively charged particle. An atom which is positively or negatively charged is referred to as ionized

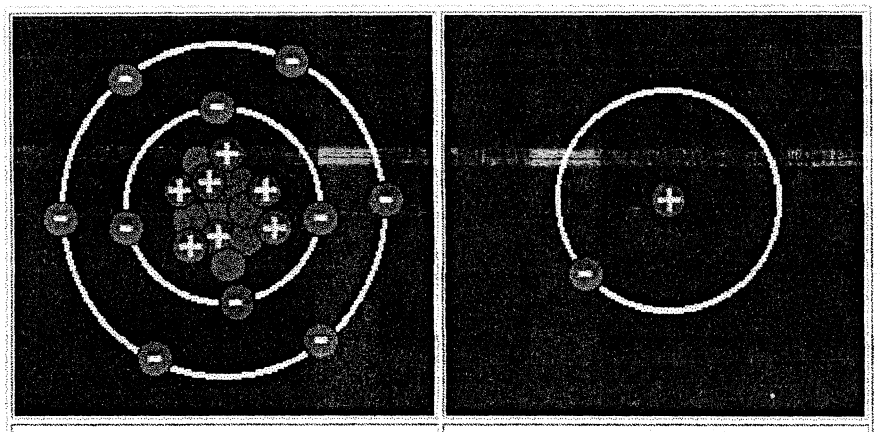

Ionized Atom | Hydrogen Atom

The simple nucleus of the **hydrogen atom** consists of one **proton,** and no **neutrons**. The hydrogen atom has a positive charge and an atomic number of 1 due to the presence of only one proton in its nucleus. For the purposes of MR, the hydrogen atom is referred to as a **proton**. The abundance of the hydrogen atoms in the human body, and the large **magnetic moment** (discussed below) created by the single proton in the nucleus of the atom, make hydrogen atoms extremely sensitive to magnetic resonance. Based on these facts, we will concentrate on the **hydrogen atom** for the duration of this section. Hydrogen has the simplest atomic structure compared to all other elements. There is an abundance of hydrogen in the human

y. Approximately 70% of the body is made up of water which tains two hydrogen atoms and one oxygen atom. It is the rogen atoms that are focused on to produce an MR image.

e proton

h spin and parity $1/2^+$, charge +1, and mass of 938 MeV, the on is the nucleus of a hydrogen atom ($^1H_1$). It has a magnetic ment of 2.79 nuclear magnetons. The electric dipole moment is sistent with zero; the bound on it is that it is less than $0.54\times10^{-}$ -cm.

ome speculative grand unified theories it may decay. The half-life this decay has been limited to be greater than 2.1×10^{29} years. The rge radius is measured mainly through elastic electron-proton ttering and is 0.870 fm. For specific decay modes, into antilepton epton and a meson, the bound is often better than 10^{32} years. The on is therefore taken to be a stable particle, and baryon number is umed to be conserved.

e neutron

e neutron has no charge, has spin and parity of $1/2^+$, and mass of MeV. The most precise measurements of its decay lifetime are inly from traps of various kinds and in beams. The lifetime of a tron is 886 s. It has the weak decay

$$n \rightarrow p + e + \overline{\nu}_e$$

magnetic moment is -1.91 nuclear magnetons. Both time reversal l parity invariance of the strong interactions implies that the tron's electric dipole moment must be zero; the current servational bound is that it is less than 0.63×10^{-23} e-cm. The mean-uare charge radius related to the scattering length measured in low rgy electron-neutron scattering for the neutron is -0.116 fm^2.

lation of baryon number conservation may give rise to oscillations ween the neutron and antineutron, through processes which nge **B** by two units. Using free neutrons from nuclear reactors, as l as neutrons bound inside nuclei, the mean time for these nsitions is found to be greater than 1.3×10^{8} seconds. The much rer bound, as compared to protons, is related to the difficulty of observations.

mit on electric charge non-conservation comes from the observed k of the decay

$$n \rightarrow p + \nu_e + \overline{\nu}_e$$

The observations which limit the branching fraction of the neutron in this decay channel to less than 8×10^{-27} are all done looking for appropriate decays of nuclei ($A\rightarrow A$ and $Z\rightarrow Z+1$).

Spin

The moving (**spinning**) hydrogen protons create a **magnetic field**, and thus perform as a tiny magnet with a north and a south pole. Since there are two magnetic poles, the protons are referred to **magnet dipoles**. Based on the laws of electromagnetism, any electrically charged particle which moves creates a magnetic field called a **magnetic moment**. This is the property that allows hydrogen protons to behave predictably within an external magnetic field. The motion or the "spin" of the hydrogen atoms can be described as a random combination of the spinning of a top, the spin of a bowling ball and the rotation of the earth around its axis. Understanding the magnetic moment of the hydrogen protons, will lead to an understanding of the **alignment** of the protons within a magnet.

Nuclear spin and magnets

Electrons, neutrons and protons, the three particles which constitute an atom, have an intrinsic property called spin. This spin is defined by the fourth quantum number for any given wave function obtained by solving relativistic form of the Schrödinger equation (SE). It represents a general property of particles which we can describe using the properties of electrons. Electrons flowing around a coil generate a magnetic field in a given direction; this property is what makes electric motors work. In much the same way electrons in atoms circulate around the nucleus, generating a magnetic field. This generated field has an angular momentum associated with it. It so turns out that there is also an angular momentum with the electron particle itself, denoted the spin, and this gives rise to the spin quantum number, m_s.
Spin angular momentum is quantized and can take different integer or half-integer values depending on what system is under study. If we solve the relativistic SE for the electron we get the values +½ and -½. Since the Pauli principle states that no two fermions can have the same quantum number, it is why only two electrons, paired

parallel (one with positive spin and one negative with negative
), can appear in a single atomic orbital.
e the electron, protons and neutrons also have a spin angular
mentum which can take values of + ½ and –½. In the atomic
leus, protons can pair with other antiparallel protons much in the
ne way that electrons pair in a chemical bond. Neutrons do the
ne. Paired particles, with one positive and one negative spin, thus
e a net spin of zero "0". We can see that a nucleus with unpaired
tons and neutrons will have an overall spin, with the number
aired contributing ½ to the overall nuclear spin quantum number,
/hen this is larger than zero, a nucleus will have a spin angular
mentum and an associated magnetic moment, μ, dependent on
direction of the spin. *It is this magnetic moment that we*
nipulate in modern NMR experiments.
worth noting here that nuclei can have more than one unpaired
ton and one unpaired neutron, much in the same way that
ctronic structures in transition metals can have many unpaired
ns. For example ^{27}Al has an overall spin I=5/2.
echnique related to nuclear magnetic resonance is electron spin
onance that exploits the spin of electrons instead of nuclei. The
ciples are otherwise similar.

ues of spin angular momentum

e spin angular momentum of a nucleus can take ranges from +*I* to
n integral steps. This value is known as the magnetic quantum
nber, *m*. For any given nucleus, there is a total (2*I*+1) angular
mentum states. Spin angular momentum is a vector quantity. The
omponent of which, denoted I_z, is quantised:

$$I_z = mh/2\pi$$

ere *h* is Planck's constant.
e resultant magnetic moment of this nucleus is intrinsically
nected with its spin angular momentum. In the absence of any
ernal effects the magnetic moment of a spin ½ nucleus lies
roximately 52.3° from the angular momentum axis or 127.7° for
opposing spin. This magnetic moment is intrinsically related to *I*
a proportionality constant γ, called the gyromagnetic ratio:

$$\mu=\gamma I$$

Spin behaviour in a magnetic field

Consider the case of nuclei which have a spin of a half, like ^{1}H, ^{13}C or ^{19}F. The nucleus thus has two possible magnetic moments it could take, often referred to as up or down, +1/2 or -1/2, which are also called the spin states α and β. The energies of each state are degenerate - that is to say that they are the same. The effect is that the number of atoms, their *population*, in the up or α state is the same as the number of atoms in the β state.

If a nucleus is placed in a magnetic field, the angular momentum axis coincides with the field direction. The resultant magnetic momenta, space quantised from the angular momentum axis, *no longer have the same energy* since one state has a z-component aligned with an external field and are lower in energy (positive I values) and the other opposes the external field and is higher in energy. This causes a population bias toward the lower energy states.

The energy of a magnetic moment μ when in a magnetic field B_0, the zero subscript is used to distinguish this magnetic field from any other applied field, is the negative scalar product of the vectors:

$$E = -\mu_z \boldsymbol{B}_0$$

We've already defined $\mu_z=\gamma I_z$. So placing this in the above equation we get:

$$E = -mh\gamma B_0 / 2\pi$$

Where γ is the gyromagnetic ratio of the nucleus being scanned

Alignment of protons in magnet

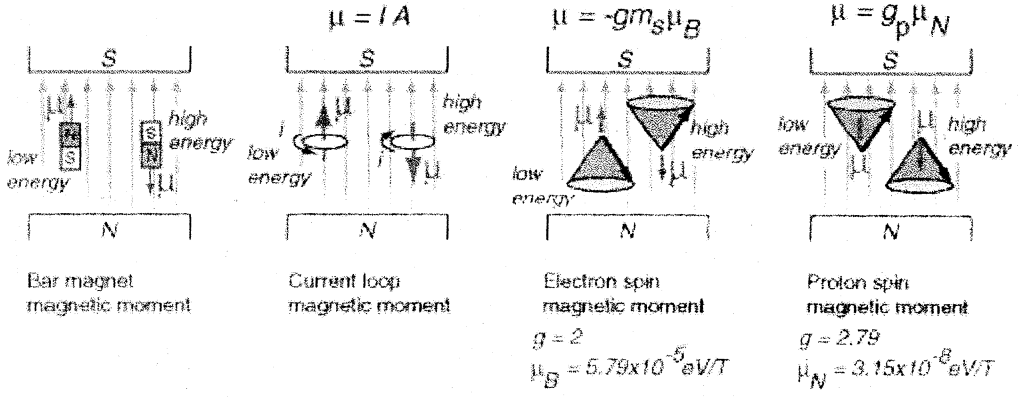

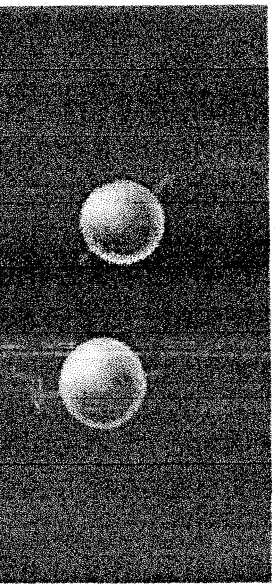

Random Distribution

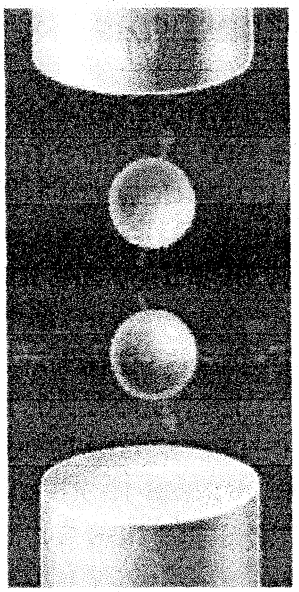

Aligned In Field

drogen nuclei magnetic moments are randomly oriented in the sence of an external magnetic field and are considered to have a **t magnetization** of zero. Once hydrogen protons are placed in the esence of an external magnetic field, they align themselves in one two directions, **parallel** or **anti-parallel** to the net magnetic field ich is commonly referred to as the vector $\mathbf{B_0}$. The strength of the ternal magnetic field and the thermal energy of the atoms are the ctors which affect the direction of alignment of the hydrogen otons. The high energy protons are strong enough to align emselves against or anti-parallel to the magnetic field, whereas the wer energy protons will align themselves with or parallel to the agnetic field. As the magnetic field increases, there are fewer otons which are strong enough to align anti-parallel to the magnetic ld. There are always a larger number of protons aligned parallel h the magnetic field (B_0), so once the parallel and anti-parallel otons cancel each other out, only the small number of low energy otons left aligned with the magnetic field create the overall net agnetization of the patient's body. Even though there are relatively ly a few protons creating the net magnetization of the patient's dy, this **difference** is all that counts. The magnetic moments of ese protons are added together and are referred to as **net agnetization vector (NMV)** or the symbol '**M**'.

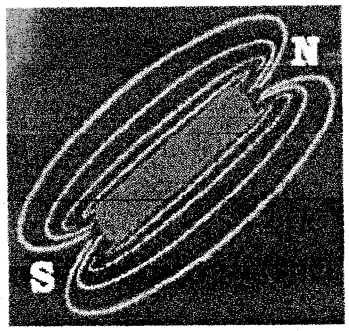

Bar magnet

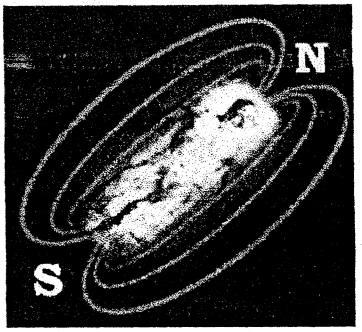

Human magnet

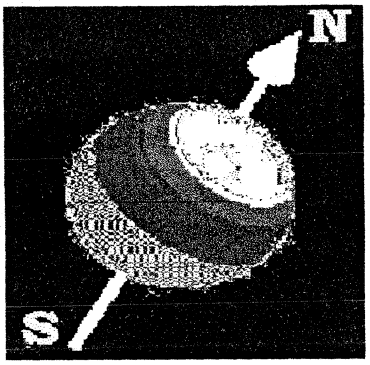

Spinning proton

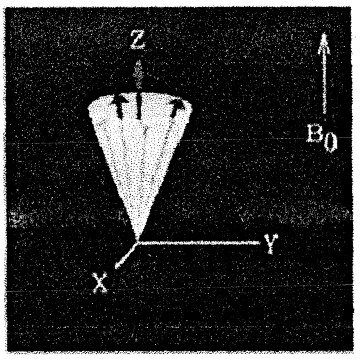

Precession

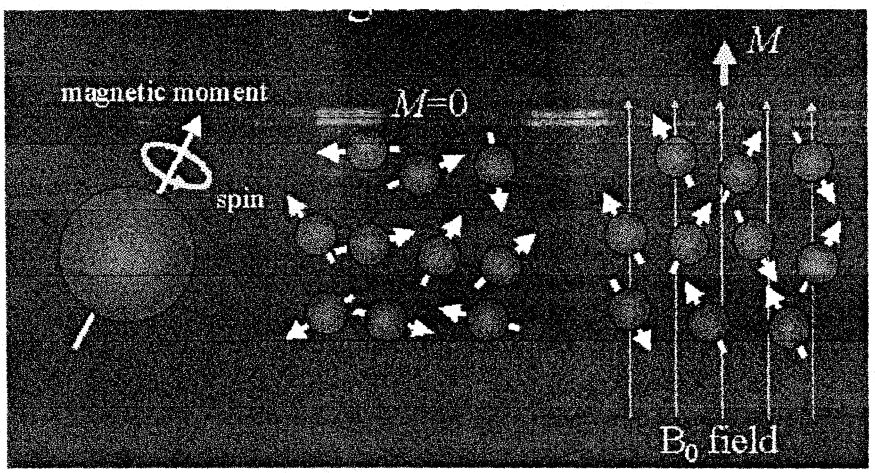

Aliengment of spins in a magnetic field

e Larmor Frequency

sla (T) or **gauss** is the measure of strength of the magnetic field. e Tesla is equivalent to 10,000 gauss, and is about 20,000 times onger than the earth's magnetic field. All protons precess at the me frequency within a magnetic field. The **gyro-magnetic ratio** of drogen is 42.57 MHz/Tesla. The gyro-magnetic ratio is different for ch nucleus of different atoms. The frequency is determined by the o-magnetic ratio of atoms and the strength of the magnetic field. e **Larmor** equation is important because it is the frequency at ich the nucleus will absorb energy. The absorption of that energy cause the proton to alter its alignment. In MR imaging, the energy t is transferred is radio frequency waves (RF) and ranges from 1- 0 MHz. The Larmor equation governs the value of the precessional quency, and is follows:

ecessional frequency (w_o) = B_0 x I

= the magnetic field strength of the magnet

the gyro-magnetic ratio.

1 T the precessional frequency of hydrogen is 42.57 MHz (1 T x 57 MHz)

1.5 T the precessional frequency of hydrogen is 42.57 MHz (1.5 T 3.86 MHz)

e stronger the magnetic field, the higher the **precessional quency**. If an RF pulse at the Larmor frequency is applied to the cleus of an atom, the protons will alter their alignment from the ection of the main magnetic field to the direction opposite the main gnetic field. As the proton tries to realign with the main magnetic d, it will emit energy at the frequency of the Larmor frequency.

sonance is referred to as the property of an atom to absorb ergy only at the Larmor frequency. This is the basis of MR. An m will only absorb external energy if that energy is delivered at cisely it's resonant frequency. The energy must also be delivered 90° to the net magnetic vector (NMV) and main magnetic field (B_0).

Otherwise, no energy will be absorbed, resonance will not have occurred and an image cannot be created. **Excitation** occurs when the proton absorbs the applied energy or resonates. As resonance occurs and the NMV moves out of alignment with the B_0 to a pre-specified angle. The deflection of the magnetization or total angle created after the end of the RF pulse is referred to as the **flip angle.**

Longitudinal and Transverse Magnetization

The stronger the RF energy applied to the protons, the greater the angle of deflection for the magnetization. The two most common flip angles in MR are **90°** and **180°** . A 90° pulse will flip the magnetization into the **x-y plane (Mxy)**. A 180° pulse will flip the magnetization through the x-y plane and into the opposite direction of B_0.

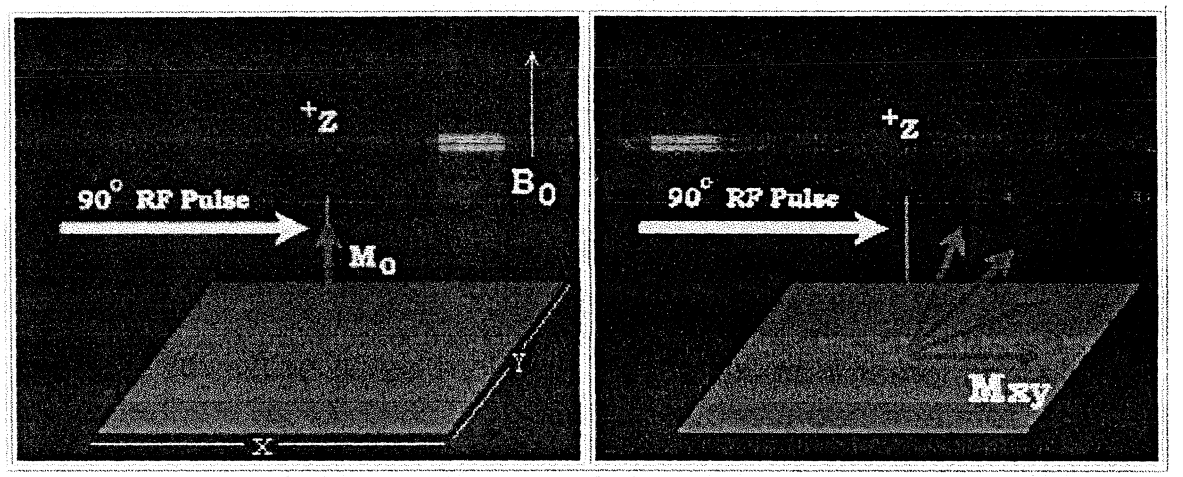

When a 90° pulse is applied and the protons are given enough energy to be flipped into the x-y plane, the net magnetization vector is now in the transverse plane. B_0 or **z-axis** is now referred to as the longitudinal plane. The protons are now rotating in the transverse plane at the Larmor frequency. As well as flipping into the transverse plane, the protons also begin rotating in phase with each other. When resonance occurs, all the magnetic moments move into the same path or all flip the same number of degrees, and they all precess in phase with other.

th the net magnetization in the transverse plane (created with a ° flip angle), and a receiver coil or antenna in the transverse plane, voltage is induced within the receiver coil. This oscillating signal tage over time is the MR signal. The magnitude of the signal is pendent on the magnetization present in the transverse plane. At termination of the RF, the freely precessing protons in the nsverse plane **(Mxy)** give up energy (RF) in order to try to realign h B_0. As the transverse magnetization starts to **decay** due to the s of phase coherence, the protons eventually realign with B_0. This **nal** produced by the decay of transverse magnetization is called **e induction decay (FID).** The amplitude of the FID signal comes smaller over time as net magnetization returns to uilibrium. Simultaneously, the longitudinal magnetization begins to cover and return to B_0 to a state of equilibrium just as if nothing had curred.

er the external RF signal is turned off, two phenomenons nultaneously occur.

- Longitudinal magnetization gradually increases and is called **T1 recovery**
- Transverse magnetization gradually decreases and is called **T2 decay**

ese phenomena are discussed in more detail below. In summary, oms rotate randomly outside the presence of a magnetic field. nen in the presence of an external magnetic field, the atoms align her with or opposed to the main magnetic field. The parallel and ti-parallel protons cancel each other out, leaving a relatively small mber of protons aligned with the main magnetic field. As an RF nal is applied at the Larmor frequency, the individual protons sonate, or absorb the applied energy, and precess in phase. pending on the strength of the applied energy, the protons will flip

o the x-y plane (transverse magnetization), or exactly the opposite ection of the main magnetic field. The transverse magnetization luces a voltage in an antenna or receiver coil which will be entually become the MR signal. As the RF is turned off, the protons phase and lose their coherence as they try to realign with B_0. Two enomenons occur simultaneously. Transverse magnetization

resonate, or absorb the applied energy, and precess in phase. Depending on the strength of the applied energy, the protons will flip

into the x-y plane (transverse magnetization), or exactly the opposite direction of the main magnetic field. The transverse magnetization induces a voltage in an antenna or receiver coil which will be eventually become the MR signal. As the RF is turned off, the protons dephase and lose their coherence as they try to realign with B_0. Two phenomenons occur simultaneously. Transverse magnetization decreases (T2 decay), while longitudinal magnetization increases (T1 recovery).

Longitudinal and Transverse Relaxation

Relaxation is a very important process in MR imaging as it determines the type of signal obtained greatly impacting the type of image generated. When the RF pulse is terminated, the net magnetic vector (NMV) is once again influenced by the main magnetic field (B_0) and tries to re-align with it along the longitudinal axis. Protons attempt to return from a state of non-equilibrium to a state of equilibrium. As the NMV gives up its absorbed RF energy while trying to return to B_0, the process of relaxation occurs. As relaxation is occurring, magnetization is recovering in the longitudinal plane while decaying in the transverse plane. Longitudinal and transverse magnetization occur at simultaneously but are two completely different processes. To examine the relaxation phenomena further, the net magnetization vector needs to be divided into its two processes; longitudinal and transverse magnetization.

Longitudinal relaxation is the return of longitudinal magnetization to equilibrium (B_0) and is termed **T1 recovery.**

- **Transverse relaxation** is the return of transverse magnetization to equilibrium and is termed **T2 decay.**

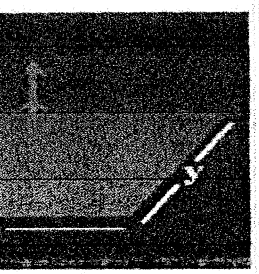

l
on

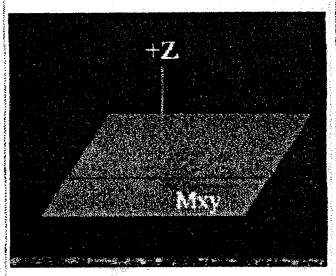

90 Degree RF Pulse

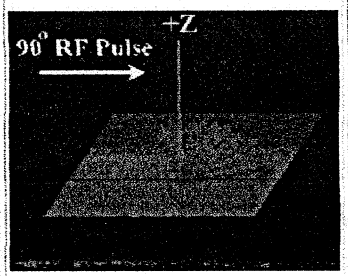

T2 Dephasing

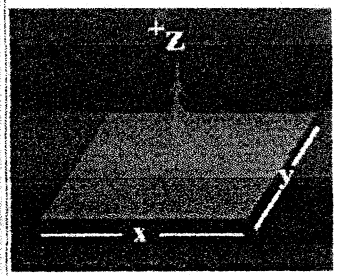

Longitudinal Relaxation - T1

ngitudinal Relaxation

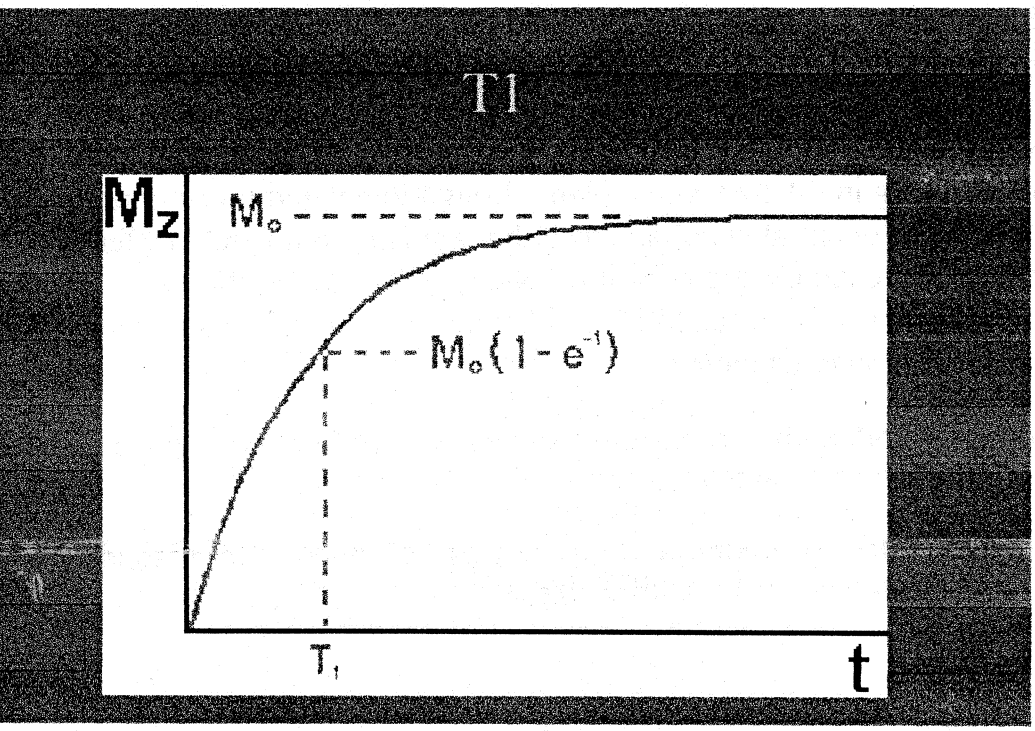

ngitudinal relaxation is the return of longitudinal magnetization to uilibrium (B_0) and is termed T1 recovery. As the hydrogen atoms ease their energy they previously absorbed to the surrounding sue (lattice), in their attempt to realign with the main magnetic field, relaxation or T1 recovery occurs. This phenomenon is sometimes

Transverse Relaxation

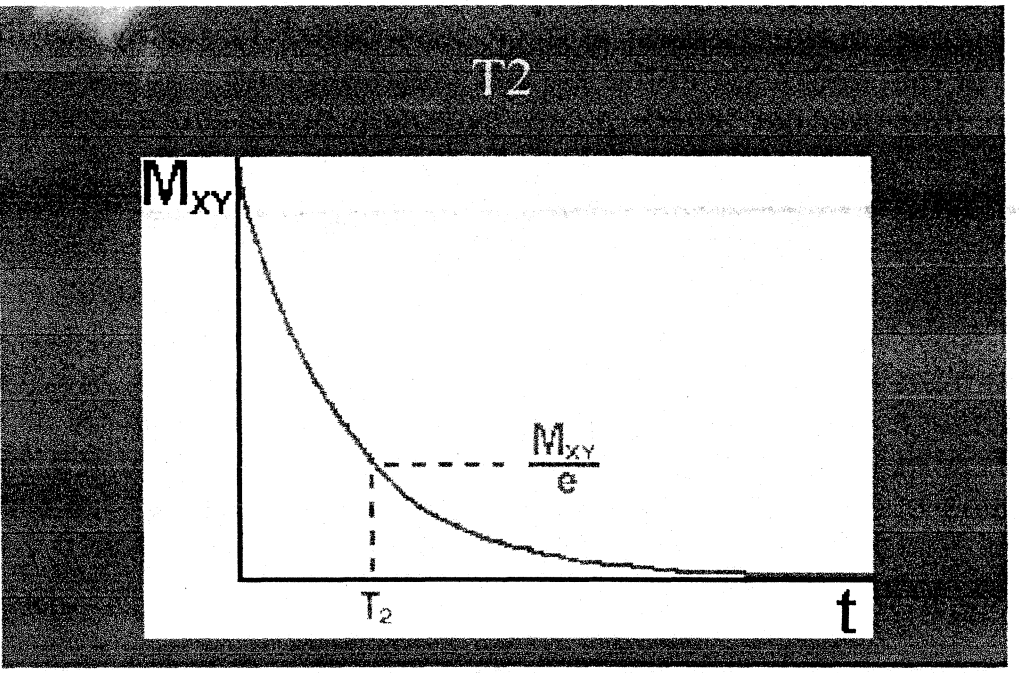

As longitudinal magnetization is occurring, it is accompanied by transverse relaxation. **Transverse relaxation** is the return of transverse magnetization to equilibrium. Although these two processes occur at the same time, they are quite different and thus contribute significantly different information to the resulting MR image. Unlike longitudinal relaxation, transverse relaxation is not a process of dissipation or absorption of energy into tissue. The **decay of transverse magnetization** is a process called T2 decay. As the amount of magnetization in the x-y (transverse) plane decreases, T2 decay increases. After an RF pulse, hydrogen nuclei are spinning in unison or in-phase with each other. As the magnetic fields of all the nuclei interact with each other, energy is exchanged between those nuclei. The nuclei which began spinning "in-phase",
lose their phase coherence or dephase over time and spin in a random fashion. This process results in an exponential decrease or decay in transverse magnetization. Because T2 decay is the result of the exchange of energy between spinning hydrogen nuclei, it is referred to as "**spin-spin**" relaxation. As T2 decay occurs, the MR signal dies out. The rate of T2 decay is also expressed as a time constant. T2 decay occurs when the transverse magnetization has decreased to **37%** of its initial value

ge. Unlike longitudinal relaxation, transverse relaxation is not a cess of dissipation or absorption of energy into tissue. The **decay transverse magnetization** is a process called T2 decay. As the ount of magnetization in the x-y (transverse) plane decreases, T2 ay increases. After an RF pulse, hydrogen nuclei are spinning in son or in-phase with each other. As the magnetic fields of all the lei interact with each other, energy is exchanged between those lei. The nuclei which began spinning "in-phase",
e their phase coherence or dephase over time and spin in a dom fashion. This process results in an exponential decrease or ay in transverse magnetization. Because T2 decay is the result of exchange of energy between spinning hydrogen nuclei, it is erred to as "**spin-spin**" relaxation. As T2 decay occurs, the MR nal dies out. The rate of T2 decay is also expressed as a time nstant. T2 decay occurs when the transverse magnetization has creased to **37%** of its initial value

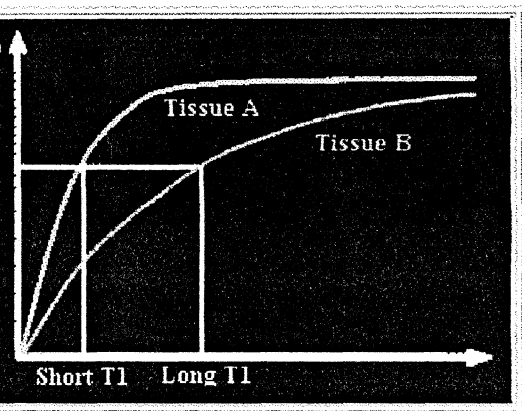

ecovery Curve

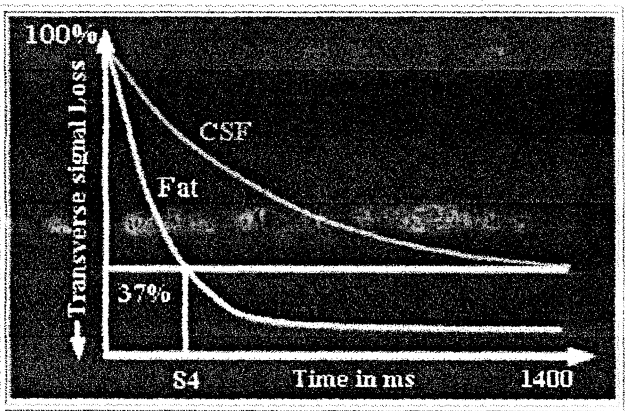

T2 Decay Curve

ngitudinal relaxation is a regrowth or an increase in value, whereas nsverse relaxation is a decrease or decay. Although these two cesses occur together, T2 decay almost always occurs more idly than the regrowth of longitudinal magnetization.

sue Contrast

e to the T1 and T2 relaxation properties, we can differentiate ween various tissues in the body. As well as T1 and T2 contrast tissues, proton density can also be measured. **Proton density** is asured by the **number of protons per unit of tissue**. Various

tissues have different T1 and T2 values. These T1 and T2 values significantly influence the type of signal generated during MRI and thus contribute greatly to the MR image. **Tissue contrast** is affected by not only the T1 and T2 values of specific tissues, but the differences in the magnetic field strength, temperature changes and many other factors. It is not imperative that one memorize the absolute T1 and T2 values in different tissues, but being aware of the values may make a difference when the technologist is programming values for pulse sequences.

Fat Versus Water

Due to the slow molecular motion of fat nuclei, longitudinal relaxation occurs rather rapidly and longitudinal magnetization is regained quickly. The net magnetic vector realigns with B_0 leading to a short T1 time for fat. Water is not as efficient as fat in T1 recovery due to the high mobility of the water molecules. Water nuclei do not give up their energy to the lattice (surrounding tissue) as quickly as fat, and therefore take longer to regain longitudinal magnetization resulting in a long T1 time.

As we know, T2 decay is dependent on the interaction of nuclei and the exchanging of energy with near by nuclei. Fat has a very efficient energy exchange and therefore has a relatively short T2. Water is less efficient than fat in the exchange of energy, and therefore has a long T2.

1 and T2 CONSTANTS

	T1 Constants at 1.5 T Controlled by TR	*T2 Constants at 1.5 T Controlled by TE*
at		85
uscle	860	45
hite matter	780	90

y matter	920	100
	3000	1400

R and TE are parameters controlled by the operator and are usually easured in milliseconds.

- **TR** stands for repetition time, or the elapsed time between successive RF excitation pulses.
- **TE** stands for echo delay time, or the time interval between the RF pulse and the measurement of the first echo.

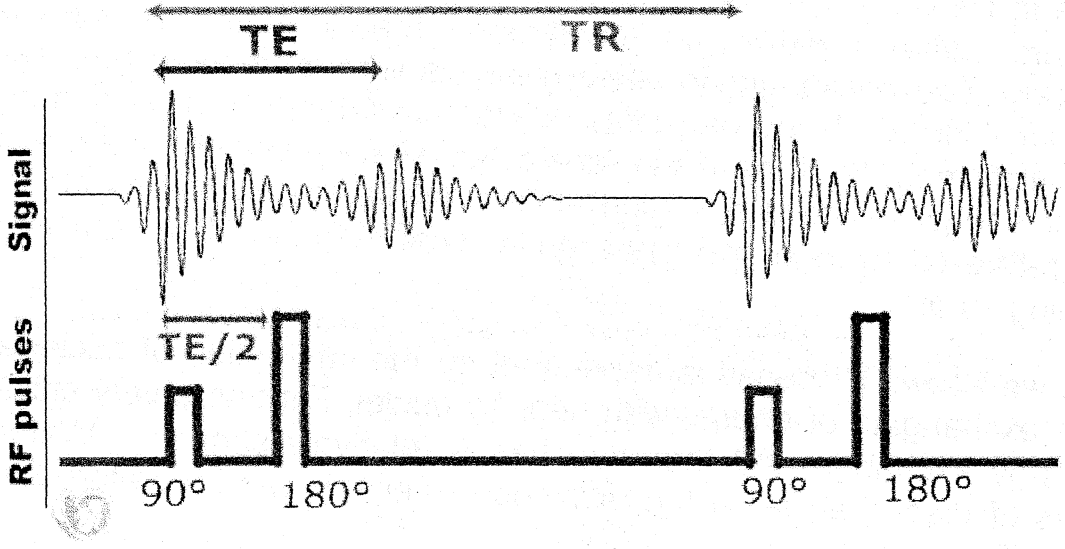

-

ne T1 constants above will indicate how quickly the spinning nuclei ll emit their absorbed RF into the surrounding tissue. The T2 onstants above will indicate how quickly the spinning nuclei will ecay to 37% of the initial transverse magnetization.

1, T2 and Proton Density Contrast

at has a shorter T1 time than water, therefore the fat vector will align more quickly with the main magnetic field. It is obvious then at fat has a larger longitudinal component than water. After a 90° ulse, the longitudinal magnetization of both fat and water are flipped to the transverse plane. As previously mentioned, fat has a larger ngitudinal component prior to an RF pulse, and it has a larger

ransverse component after an RF pulse. Due to the larger ongitudinal and transverse magnetization, fat has a higher signal and will appear bright on a T1 contrast MR image. Conversely, water has ess longitudinal magnetization prior to an RF pulse, therefore less ransverse magnetization after an RF pulse yielding low signal appearing dark on a T1 contrast image. Images created with TR's and TE's to enhance T1 contrast are referred to as T1-weighted mages.

The previously learned concepts of transverse magnetization apply for T2 contrast. Fat has a shorter T2 time than water and relaxes or decays more readily than water. Since the amount of transverse magnetization in fat is small, fat generates very little signal on a T2 contrast image and appears dark. Water has a very high T2 constant, therefore has very high T2 signal and thus appears bright on a T2 contrast image. Images created with TR's and TE's to enhance T2 contrast are referred to as T2-weighted images.

Proton density contrast is a quantitative summary of the number of protons per unit tissue. The higher the number of protons in a given unit of tissue, the greater the transverse component of magnetization, and the brighter the signal on the proton density contrast image. Conversely the lower the number of protons in a given unit of tissue, the less the transverse magnetization and the darker the signal on the proton density image.

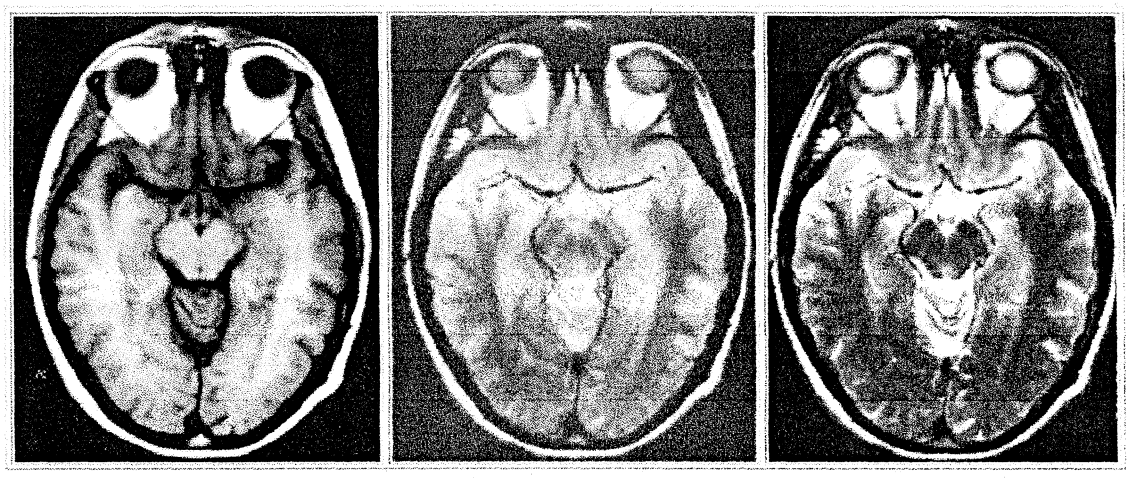

l Weighting	Proton Density Weighting	T2 Weighting

AND T2 WEIGHTING (Proton weighting imaging)

st all MR imaging will entail T1 and T2-weighted images among ny other types of imaging. T1 and T2 images are the most mmon contrasts obtained in MRI. T1-weighted images are obtained compare the T1 differences in tissues or to compare the relaxation es of the tissue being examined. T2-weighted images are ained to compare the T2 contrast in tissues and compare the nsverse relaxation rates. Parameters are manipulated by the user btain the type of image contrast desired

RF SIGNAL INTENSITIES IN TISSUE	
High-Intensity Signal	Low-Intensity Signal
Short T1	Long T1
Long T2	Short T2

previously stated, **TR** will control the T1-weighting of an MR imag rt TR maximizing T1-weighting and a long TR maximizing proton ghting

controls the T2-weighting of an MR image with a short TE imizing T2-weighting and a long TE maximizing T2-weighting.

TYPICAL TE and TR Values	
Short TE	10-25 ms

IMAGE PARAMETERS	*WEIGHTING*	
	TR	TE

Long TE	60-100+ ms	T1 Weighting	Short	Short
Short TR	100-900 ms	Proton Density Weighting	Long	Short

T1-Weighted Imaging:

Emphasis is made on the differences on longitudinal relaxation rates by utilizing a short TR and short TE. The short TR allows full recovery of tissues with a short T1 (fat) to recover quickly while allowing only partial recovery of tissues with a long TR (CSF). The short TE used to obtain a T1-weighted image will allow minimal loss of transverse magnetization due to T2relaxation. Basically, short TR increases T1 effects with the short TE minimizes T2 effects of tissue.

T2-Weighted Imaging:

Emphasis is made on the differences on transverse relaxation rates by utilizing a long TR and long TE. The long TR allows tissues to reach complete longitudinal magnetization which will reduce T1 effects. The long TE will allow for the loss of transverse signal enhancing T2 effects. Fluid has a very long T2 and is frequently associated with pathology, so it is important to take advantage of the imaging parameters to accentuate signal differences.

There are many parameters which significantly contribute to the contrast of an image. Most of these parameters are controlled or at least influenced by the technologist creating the images. Care must be taken to create the best possible MR images which will ensure a more accurate diagnosis by the radiologist. Parameters contributing to an MR image should be manipulated only by an experienced MR technologist who is aware of all the factors which are changing during the manipulation

On a macroscopic level, exposure of an object or person to RF radiation at the Larmor frequency, causes the net magnetization to spiral away from the Bo field. In the rotating frame of reference, the

magnetization vector rotate from a longitudinal position a distance portional to the time length of the RF pulse. After a certain length me, the net magnetization vector rotates 90 degrees and lies in transverse or x-y plane. It is in this position that the net netization can be detected on MRI. The angle that the net netization vector rotates is commonly called the 'flip' or 'tip' angle. ngles greater than or less than 90 degrees there will still be a ll component of the magnetization that will be in the x-y plane, therefore be detected.

INSTRUMENTATION

section will cover the following topics:

- Magnets
- RF and Gradient Coils
- Electronics and Data Processing

GNET

Fig. MPM: The concept of magnetic moment.

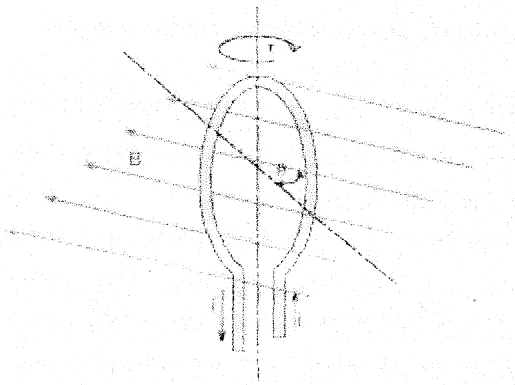

gnetic resonance imaging (MRI) is based on the magnetic onance phenomenon, and is used for medical diagnostic ging since ca. 1977 (see also MRI History). first developed MRI devices were constructed as long narrow

tunnels. In the meantime the magnets became shorter and wider. In addition to this short bore magnet design, open MRI machines were created. MRI machines with open design have commonly either horizontal or vertical opposite installed magnets and obtain more space and air around the patient during the MRI test. The basic hardware components of all MRI systems are the magnet, producing a stable and very intense magnetic field, the gradient coils, creating a variable field and radio frequency (RF) coils which are used to transmit energy and to encode spatial positioning. A computer controls the MRI scanning operation and processes the information.
The range of used field strengths for medical imaging is from 0.15 to 3 T. The open MRI magnets have usually field strength in the range 0.2 Tesla to 0.35 Tesla. The higher field MRI devices are commonly solenoid with short bore superconducting magnets, which provide homogeneous fields of high stability.

There are THREE different types of magnets:

- Resistive Magnet
- Permanent Magnet
- Super conducting magnet

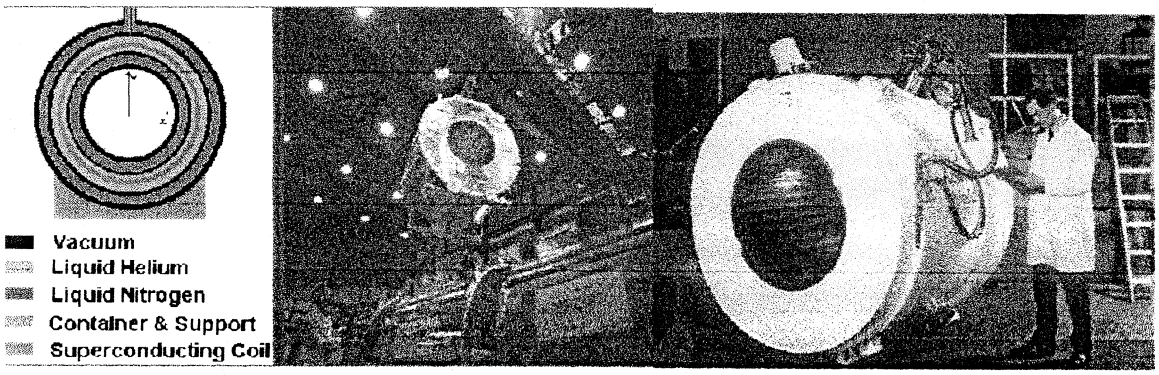

the point at which the magnet becomes demagnetized by an xternal field. (1Oersted is like 2.02 ampere-turns/inch) **Hmax** is a term of overall energy density. The higher the number, emorepowerfulthmagnet.

coef of Br is the temperature coefficient of Br in terms of % per egree Centigrade. This tells you how the magnetic flux changes th respect to temperature. -0.20 means that if the temperature creases by 100 degrees Centigrade, its magnetic flux will decrease 20%!

max is the maximum temperature the magnet should be operated . After the temperature drops below this value, it will still behave s it did before it reached that temperature (it is recoverable). egreesCentigrade)

curie is the Curie temperature at which the magnet will become emagnetized. After the temperature drops below this value, it will ot behave as it did before it reached that temperature. If the magnet heated between Tmax and Tcurie, it will recover somewhat, but not lly (it is not recoverable). (degrees Centigrade)

uperconducting Magnet

type of magnet whose field is generated by current in wires ade of a superconducting material such as niobium-titanium, that as no resistance when operated at temperatures near absolute ero (-273,15°C, -459°F, 0K).

he coil of wire is kept at a temperature of 4.2K by immersing it in quid helium. The coil and liquid helium is kept in a large dewar. In arly magnet designs, this dewar was typically surrounded by a quid nitrogen (77.4K) dewar, which acts as a thermal buffer etween the room temperature (293K) and the liquid helium. In ter magnet designs, the liquid nitrogen region was replaced by a ewar cooled by a refrigerator. This design eliminates the need to dd liquid nitrogen to the magnet.

uperconducting magnets typically exhibit field strengths of eater than 0.5 T, operate clinically up to 3 T and have a orizontal field orientation, which makes them prone to missile fects without significant magnetic shielding.

tunnels. In the meantime the magnets became shorter and wider. In addition to this short bore magnet design, open MRI machines were created. MRI machines with open design have commonly either horizontal or vertical opposite installed magnets and obtain more space and air around the patient during the MRI test. The basic hardware components of all MRI systems are the magnet, producing a stable and very intense magnetic field, the gradient coils, creating a variable field and radio frequency (RF) coils which are used to transmit energy and to encode spatial positioning. A computer controls the MRI scanning operation and processes the information.
The range of used field strengths for medical imaging is from 0.15 to 3 T. The open MRI magnets have usually field strength in the range 0.2 Tesla to 0.35 Tesla. The higher field MRI devices are commonly solenoid with short bore superconducting magnets, which provide homogeneous fields of high stability.

There are THREE different types of magnets:

- Resistive Magnet
- Permanent Magnet
- Super conducting magnet

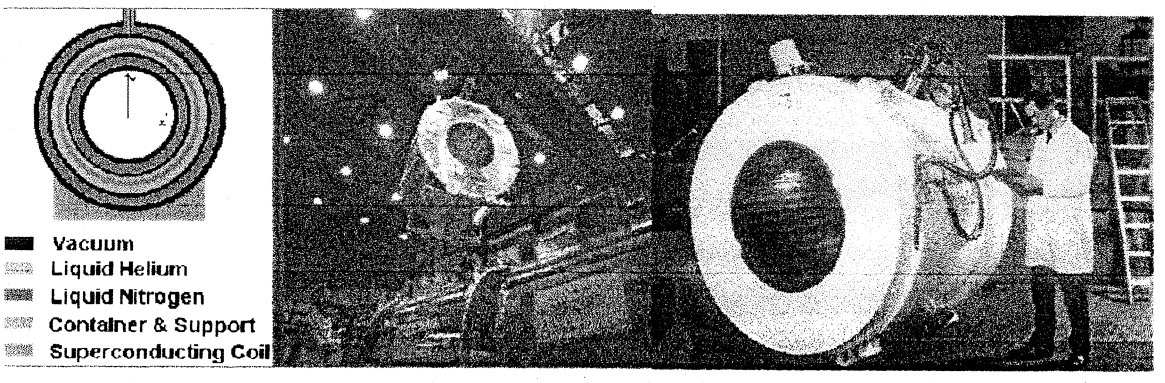

esistive Magnet

type of magnet that utilizes the principles of electromagnetism generate the magnetic field. Typically large current values and gnificant cooling of the magnet coils is required. The **resistive agnet** does not require cryogen's, but needs a constant power pply to maintain a homogenous magnetic field, and can be quite pensive to maintain.

esistive magnets fall into two general categories - iron-core and r-core. Iron-core electromagnets provide the advantages of a rtically oriented magnetic field, and a limited fringe field with le, if any, missile effects due to the closed iron-flux return path. r-core electromagnets exhibit horizontally oriented fields, which ve large fringe fields (unless magnetically shielded) and are one to missile effects. Resistive magnets are typically limited to aximum field strengths of approximately 0.6T.

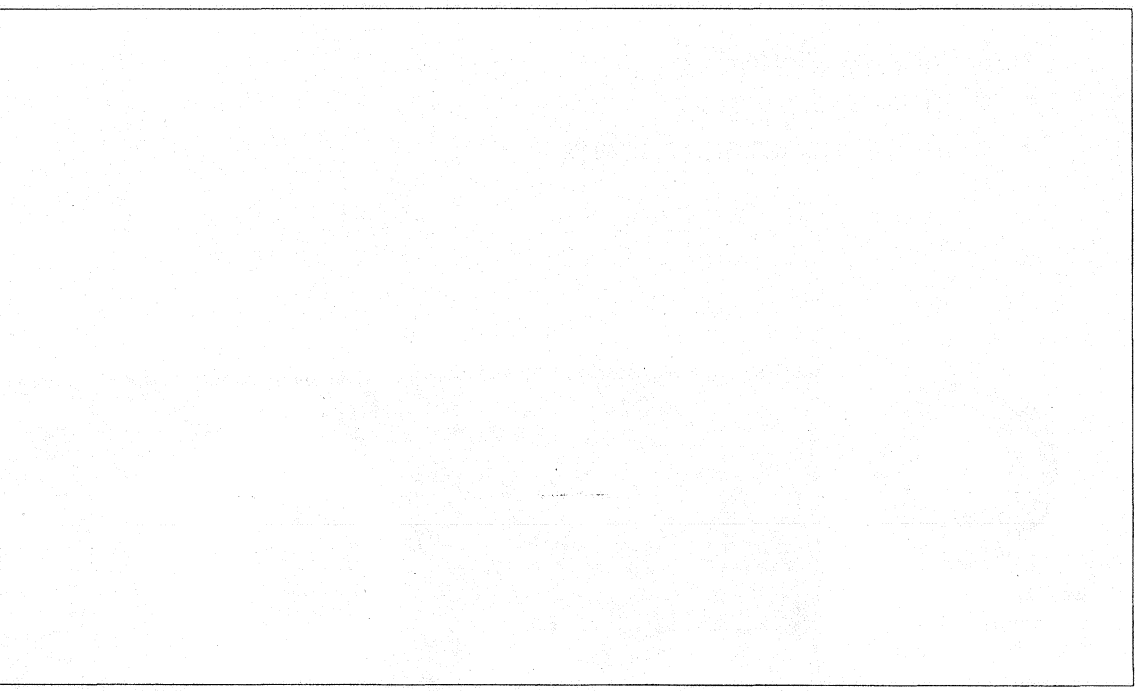

ne main advantages of these types of magnets are:
1) No liquid cryogen, 2) The ability to "turn off" the magnetic field,
3) Relatively small fringe field.

ermanent Magnet

field and no missile effect. Due to weight considerations, **permanent magnets** are usually limited to maximum field strengths of 0.4 T. The main disadvantages of a **permanent magnet** are the cost of the magnet itself and supporting structures and the varying changes in the magnetic field. Field homogeneity can be an on-going problem in **permanent magnets**.

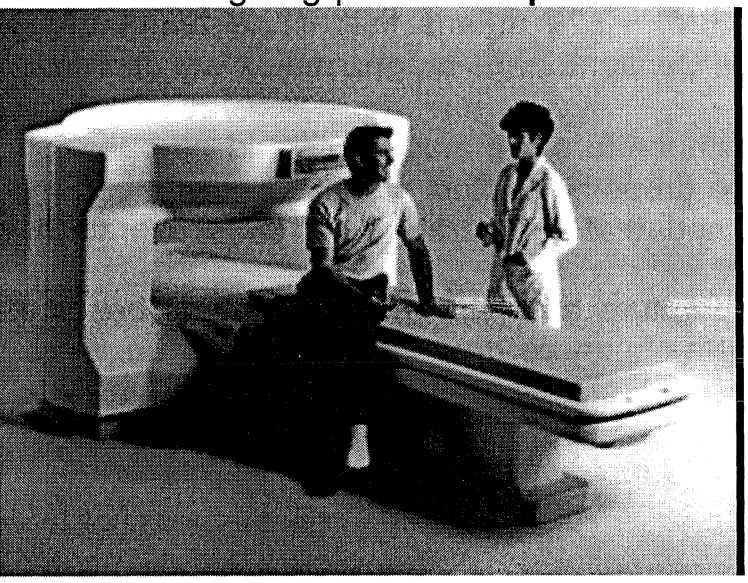

The patient lies on a scanning table between these two plates. Advantages of these systems are: 1) Relatively low cost, 2) No electricity or cryogenic liquids are needed to maintain the magnetic field, 3) Their more open design may help alleviate some patient anxiety, 4) Nearly nonexistent fringe field. It should be noted that not all vertical field magnets are permanent magnets.

Materials used for permanent magnets

- There are four classes of permanent magnets:
  1, Neodymium Iron Boron (NdFeB or NIB)
  2,Samarium Cobalt (SmCo)
  3, Alnico
  4,Ceramic or Ferrite

Br is the measure of its residual magnetic flux density in Gauss, which is the maximum flux the magnet is able to produce. (1Gauss islike6.45lines/sqin)
Hc is the measure of the coercive magnetic field strength in Oersted,

the point at which the magnet becomes demagnetized by an ernal field. (1Oersted is like 2.02 ampere-turns/inch) **max** is a term of overall energy density. The higher the number, morepowerfulthmagnet.

oef of Br is the temperature coefficient of Br in terms of % per gree Centigrade. This tells you how the magnetic flux changes n respect to temperature. -0.20 means that if the temperature reases by 100 degrees Centigrade, its magnetic flux will decrease 20%!

ax is the maximum temperature the magnet should be operated After the temperature drops below this value, it will still behave it did before it reached that temperature (it is recoverable). egreesCentigrade)

urie is the Curie temperature at which the magnet will become magnetized. After the temperature drops below this value, it will behave as it did before it reached that temperature. If the magnet heated between Tmax and Tcurie, it will recover somewhat, but not y (it is not recoverable). (degrees Centigrade)

perconducting Magnet

type of magnet whose field is generated by current in wires de of a superconducting material such as niobium-titanium, that s no resistance when operated at temperatures near absolute ro (-273,15°C, -459°F, 0K).

e coil of wire is kept at a temperature of 4.2K by immersing it in uid helium. The coil and liquid helium is kept in a large dewar. In rly magnet designs, this dewar was typically surrounded by a uid nitrogen (77.4K) dewar, which acts as a thermal buffer tween the room temperature (293K) and the liquid helium. In er magnet designs, the liquid nitrogen region was replaced by a war cooled by a refrigerator. This design eliminates the need to d liquid nitrogen to the magnet.

perconducting magnets typically exhibit field strengths of eater than 0.5 T, operate clinically up to 3 T and have a rizontal field orientation, which makes them prone to missile ects without significant magnetic shielding.

Boil off Rate

Rate of cryogen (liquid helium) evaporation in **superconducting magnets**, usually measured in liters of liquid per hour. It increases during ramping of the magnet and with eddy currents induced in the cryoshields by pulsed field gradients. In calculating cryogen consumption additional transfer and filling losses have to be considered

Cryogen

A cooling agent, typically liquid helium or liquid nitrogen used to reduce the temperature of the magnet windings in a **superconducting magnet**. All cryogenic liquids are gases at normal temperatures and pressures. Different cryogens become liquids under different conditions of temperature and pressure, but all have two properties in common: they are extremely cold, and small amounts of liquid can expand into very large volumes of gas. The boiling points of cryogens are commonly below -150°C(- 238°)

Ramping Up.

Ramping up of oxford magnet.

The supercon contains minimum 80% He and 20% Nitrogen. The normal ramp up procedure consumes 7 – 10 % of He. Normal ramp down consume 5% of He. Normal ramp up takes 5 hrs. and normal ramp down takes 4 hrs. to complete. Before start to ramp up ensure that all magnet power supplies are okay and install the magneto meter at the centre probe. Do not start ramp up procedure with below 80% He. For proceeding the ramp up first give a warm up heating to the heater (resistance) for a period of 3 – 5 minutes and set voltage as 2V (for high current). After the warm-up procedure set the current to 250A. The current will first jump to 4 A and comes down to 1A per minute. Synchronize the magnetometer until the field is approximately 7000 gauss. Once the magneto meter shows the reading of 14750 gauss, set the current level which is less than 250A and allow the field to stabilize for 45 minutes. The magnetometer reading is stable at the stabilization time. By making the fine control we can get a magnetic field strength of 15008 +/- 0.2 gauss. When

field reaches 15008 turns, off the heater switch and allow 5 utes to cool. After this turn the current and voltage limit to zero. en reaches zero wait 5 minutes for stabilization. Selective manual p down can also do with proper current and voltage to the heater vercoming this problem is to use a secondary compensating netic field generated by a **set** of so-called shim coils to bring the all field to the level of desired homogeneity.

mming

rection of inhomogeneity of the magnetic field produced by the n magnet of a MRI system due to imperfections in the magnet o the presence of external ferromagnetic objects. May involve nging the configuration of the magnet or the using of shim coils ive **shimming**) or adding or removing steel from the magnets es (passive **shimming**) to fine-tune the magnetic field.

COILS USED IN MRI SYSTEM

COILS And Gradient coils

coils are the "antenna" of the MRI system that broadcasts the RF al to the patient and/or receives the return signal. RF coils can be eive-only, in which case the body coil is used as a transmitter; or smit and receive (transceiver).

oil consist of one or more loops of a conductor used to create a gnetic field or to detect a changing magnetic field by voltage uced in the wire. A coil is usually a physically small antenna. perfect coil produces a uniform magnetic field without significant ation.

dio Frequency Coil

coils create the B_1 field which rotates the net magnetization in a se sequence. They also detect the transverse magnetization as it cesses in the XY plane. RF coils can be divided into three general egories; RF coils can be divided into three general categories

- transmit and receive coils
- receive-only coils
- transmit-only coils

Transmit Receive Coil

(T/R) Also called transceiver coil. An RF coil that acts as a transmitter (T) producing the B1 excitation field and as a receiver (R) of the MRI signal. Such a coil requires a T/R switching circuit to switch between the two modes. A body coil is typically a T/R coil, but smaller volume T/R coils (head/extremities) are often used at high field as a possibility of reducing RF power absorption (SAR).

Transmitter Coil

The coil of the RF transmitter, inside the MR imager is used in excitation of the spins. Also called transmit-only coil it is used to create the B1 field. As a radio frequency generator send this coil bursts of RF pulses. These pulses serve to disturb the spins in the patient.

Receiver Coil

A coil, or antenna, positioned within the imaging volume and connected to the receiver circuitry that is used to detect or receive the MR signal from the patient as the disturbed spins relax back into their equilibrium distribution. Also called receive-only coil. Special-purpose coils are designed to optimize the SNR from a given region of the body. State-of-the-art coil systems include the use of four or more coils with four separate receivers. This method is often referred to as a phased array system. Receiver coil types include also solenoid, planar, volume and quadrature coils. The quality of the MR images depends on the SNR of the acquired signal from the patient. SNR is of the utmost importance in obtaining clear images of the interior of the human body

Multiply Tuned Coil

RF coil designed to operate at more than one resonance frequency, so that NMR of more than one kind of nucleus can be observed with the same coil.

OLUME COIL

adio frequency coil that surrounds a portion of the body. Volume ils have a better RF homogeneity than surface coils

rd Cage Coil

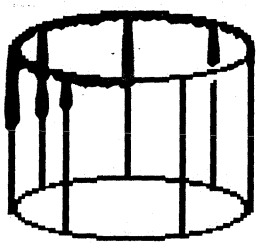

Bird Cage Coil

transmit and receive RF imaging coil, which looks like a bird cage. e bird cage coil works on a different principle to conventionally ned local and surround coils in that it behaves like a tuned nsmission line with one complete cycle of standing wave around e circumference.The bird cage coil provides the best RF mogeneity of all the RF coils. One advantage is that it is simple to oduce an exceedingly uniform B1 radio frequency field over most of e coil's volume, with the result of images with a high degree of iformity. A second advantage is that nodes with zero voltage occur ° away from the driven part of the coil, thus facilitating the roduction of a second signal in quadrature, which produces a cularly polarized radio frequency field. The bird cage coil is the coil choice for imaging the head and brain. This type of coil is also d occasionally for imaging of the extremities, such as the knees.

rcularly Polarized Coil

coil designed to excite or detect spins using two orthogonal nsmit and/or receive channels. As a transmitter coil, there is a tor of 2 reductions in power required. The receiver coil has a better IR than a linearly polarized coil.

Crossed Coil

RF coil pair arranged with their magnetic fields at right angles to each other in such a way as to minimize their mutual magnetic interaction.

Helmholtz Pair Coil

The Helmholtz pair coil consists of two circular coils parallel to each other. They are used as z gradient coils in MRI scanners. They are also used occasionally as RF coils for pelvis imaging and cervical spine imaging

Paired Saddle Coil

Paired saddle coils are commonly used for imaging of the knee. These coils provide better homogeneity of the RF in the area of interest and are used as volume coils, unlike surface coils. Paired saddle coils are also used for the x and y gradient coils. By running current in opposite directions in the two halves of the gradient coil, the magnetic field is made stronger near one and weaker near the other

Quadrature Coil

A coil that produces an RF field with circular polarization. The RF power received from the RF power amplifier comes in two signals (quadrature detection), which have a phase difference of 90°. The RF transmit coil converts the power into a circularly polarised RF magneticfield. Quadrature coils can be used as both, transmit and/or receive coil. When used as a transmitter coil a factor of two power reduction over a linear coil results; as a receiver an increase in SNR of up to a factor of 1.41 can be achieved.

gle Turn Solenoid

ransmit and receive RF imaging coil that, in general, has a ndrical shape. This small volume coil differs somewhat from a flat face coil. The single turn consists of a significantly wider copper e whose width is wider than the diameter of the coil. The single n solenoid is useful for imaging extremities, such as wrist or knee.

RFACE COIL

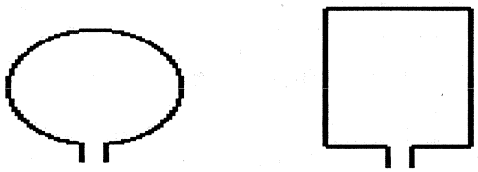

Surface Coils

ype of receiver coil, which is placed directly on or over the region nterest for increased magnetic sensitivity. Surface coils have a od SNR for tissues adjacent to the coil and the signal decrease n the distance, an eligibility homogeneity correction will balance over the FOV. As only the region close to the surface coil will tribute to the noise, there is an improvement in the SNR for ions close to the coil, compared to the use of receiver coils that round the corresponding part of the body. These coils are ecifically designed for localized body regions, and provide proved signal to noise ratios by limiting the spatial extent of the itation or reception. When a surface coil is used, a larger coil on imager is used as the transmitter of RF energy to producing the and 180° pulses.

ay Coil

array coil combines the advantages of smaller coils (high SNR) n those of larger coils (large measurement field). This type of RF is composed of separate multiple smaller coils, which can be ed individually (switchable coil) or combined. en used simultaneously, the elements can either be:
upled array coils - electrically coupled to each other through mmon transmission lines or mutual inductance

isolated array coils - electrically isolated from each other with separate transmission lines and receivers and minimum effective mutual inductance, and with the signals from each transmission line processed independently or at different frequencies
phased array coils - multiple small coils arranged to efficiently cover a specific anatomic region and obtain high-resolution, high-SNR images of a larger volume. The data from the individual coils is integrated by special software to produce the high-resolution images.

Body Wrap Around Coil(BWA)

A flexible surface coil for body imaging.

Linearly Polarized Coil(LP Coil)

A coil designed to excite or detect spins using one RF transmit and/or receive channel. The magnetic field has predominantly a single direction

Phased Array Coil

The phased array coils are typically operated as a receive only coil. A larger coil on the imager is used as the transmitter of RF energy to producing the 90° and 180° pulses. State-of-the-art coil systems include the use of four or more coils with four separate receivers. This method is often referred to as a phased array system, although the signals are not added such that the signal phase information is included. The use of phased array coils allows the number of signal averages to be decreased with their superior SNR and resolution, thereby decreasing scan time Fast parallel imaging techniques using surface phased array multichannel coils, such as sensitivity encoding (SENSE) or simultaneous acquisition of spatial harmonics (SMASH) to further improve spatial and temporal resolution. High-sensitivity RF coils and digital processing algorithms have been developed that speed image acquisition and reconstruction during MRI. Also called linear array coil or synergy coil.

Saddle Coil

A coil geometry, which has two loops of a conductor wrapped around opposite sides of a cylinder. RF coil configuration design commonly used when the static magnetic field is coaxial with the axis of the coil along the long axis of the body (e.g., superconducting magnets and most resistive magnets) as opposed to solenoid or surface coil.

Surface Coil NMR

A surface coil placed over a region of interest will have an effective selectivity for a volume approximately subtended by the coil circumference and one radius deep from the coil center. Such a coil can be used for simple localization of sites for measurement of chemical shift spectra, especially of phosphorus, and blood flow studies. Some additional spatial selectivity can be achieved with magnetic field gradients.

GRADIENT COIL

Gradient coils are used to produce controlled variations in the main magnetic field (B0) to provide spatial localization of the signals and to apply reversal pulses in some imaging techniques. The standard magnetic resonance coordinate system, a gradient in B_o in the Z direction is achieved with an antihelmholtz type of coil. Current in the two coils flow in opposite directions creating a magnetic field gradient between the two coils. The B field at one coil adds to the B_o field while the B field at the center of the other coil subtracts from the B_o field

The X and Y gradients in the B_o field are created by a pair coils. The X axis coils create a gradient in B_o in the X direction due to the direction of the current through the coils. The Y axis coils provides a similar gradient in B_o along the Y axis.

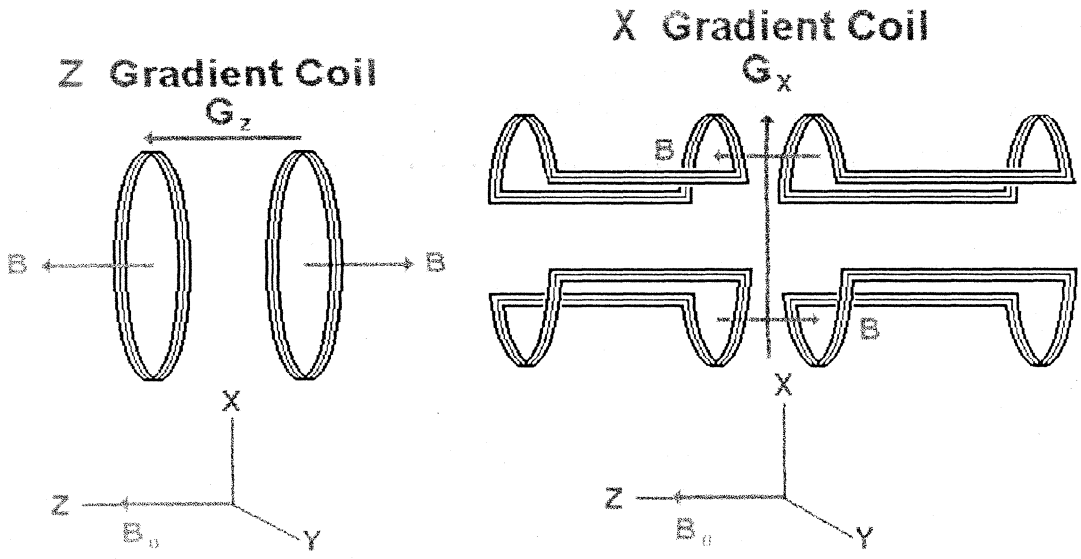

Current carrying coils designed to produce a desired magnetic field gradient (so that the magnetic field will be stronger in some locations than others). Proper design of the size and configuration of the coils is necessary to produce a controlled and uniform gradient. Three paired orthogonal current-carrying coils located within the magnet that are designed to produce desired gradient magnetic fields, which collectively and sequentially are superimposed on the main magnetic field (Bo) so that selective spatial excitation of the imaging volume can occur. Gradients are also used to apply reversal pulses in some fast imaging techniques. Gradient coils are used to produce deliberate variations in the main magnetic field (Bo). The set of gradient coils for the z-axis are, e.g. Helmholtz pairs, and for the x- and y-axis, paired saddle coils.

Figure 8 Coil

A magnetic field gradient coil shaped like the number eight.

lay Coil

m commonly used for a particular kind of gradient coil, commonly ed to create magnetic field gradients perpendicular to the main gnetic field

lmholtz Coil

Helmholtz
Pair Coil

r of current carrying coils used to create uniform magnetic field in center of the space between them. For circular coils, their paration equals their radius

xwell Coil

particular kind of gradient coil, commonly used to create magnetic d gradients along the direction of the main magnetic field

ired Saddle Coil

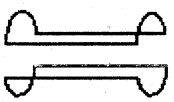

Paired Saddle
Coil

ired saddle coils are commonly used for imaging of the knee. ese coils provide better homogeneity of the RF in the area of erest and are used as volume coils, unlike surface coils. ired saddle coils are also used for the x and y gradient coils. By nning current in opposite directions in the two halves of the gradient l, the magnetic field is made stronger near one and weaker near other.

Shielded Gradient Coils

Current-carrying gradient coils with reduced gradient fringe field inside of the magnet cryostat structures like cryoshields and He-vessel. The shielding can be accomplished by secondary actively driven coils or by passive screens, which are inductively coupled to the gradient coils. In both cases eddy currents outside of the gradient system will be reduced.

Gradient coil designs

Gradient coils are carefully designed to produce linearly varying magnetic fields, as well as to have other features. The two simplest coil designs for use with a cylindrical whole body imaging system are shown in figures 3 and 4.:

Gradient coil designs

Gradient coils are carefully designed to produce linearly varying magnetic fields, as well as to have other features. The two simplest coil designs for use with a cylindrical whole body imaging system are shown in figures 3 and 4.:

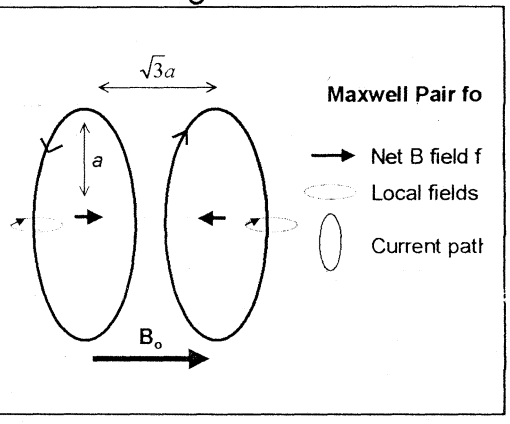

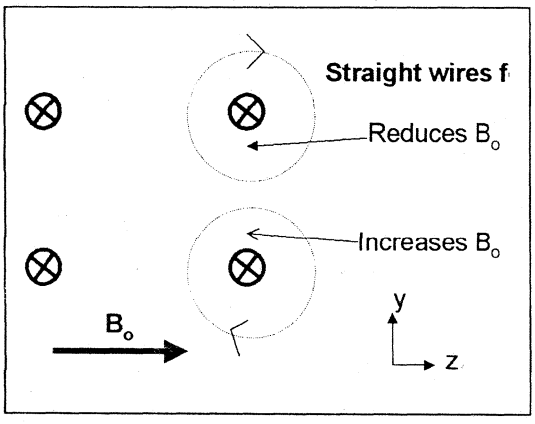

The movement of the gradient coil wires in the magnetic field as electric currents are pulsed through them is the reason that MRI is so accoustically noisy.

ce selection

select a slice, a magnetic field gradient is applied in a certain ection, let us say z. This means that the Larmor frequency now ies along x (eqn.2, fig.5).

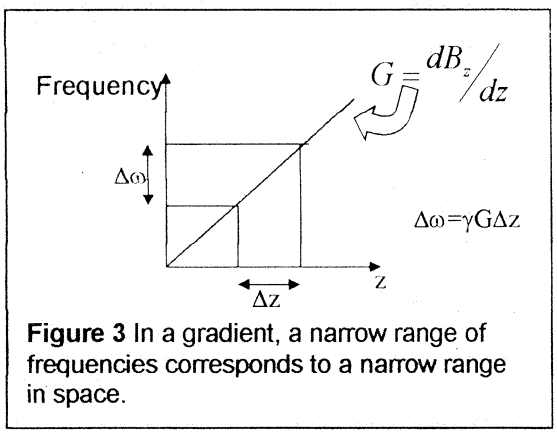

Figure 3 In a gradient, a narrow range of frequencies corresponds to a narrow range in space.

order to select a slice it is cessary to apply an RF radiation er a narrow bandwidth of quency, so that only spins in that ge of frequencies are excited. In s way it is possible to select a slice rpendicular to the z-axis.

t how can a narrow range of quencies be excited?

radiation oscillates at a single carrier frequency (corresponding to ingle spike in the Fourier transform of the radiation time course). pulses are created by modulating the carrier frequency at audio quencies (ie carrier signal is multiplied by an audio frequency ndow. The audio frequency window defines the pulse shape).\

member that if you multiply two functions in time, it is equivalent to nvolving them in frequency space. Therefore if the carrier signal is ltiplied by a shaped envelope (eg a sinc function), this responds to convolving the spike with the Fourier transform of the ape of the envelope (for a sinc function in time, this is a rectangle frequency).

nce an RF pulse can be designed to excite a range of frequencies out ω_o. By varying the shape of the pulse you can control ckness (and in fact the position) of the imaging slice.

You may be interested to know that Sir Peter Mansfield (from Nottingham) invented the slice selection technique. The patent income from this discovery paid for a large part of the building of the SPMMRC Centre.

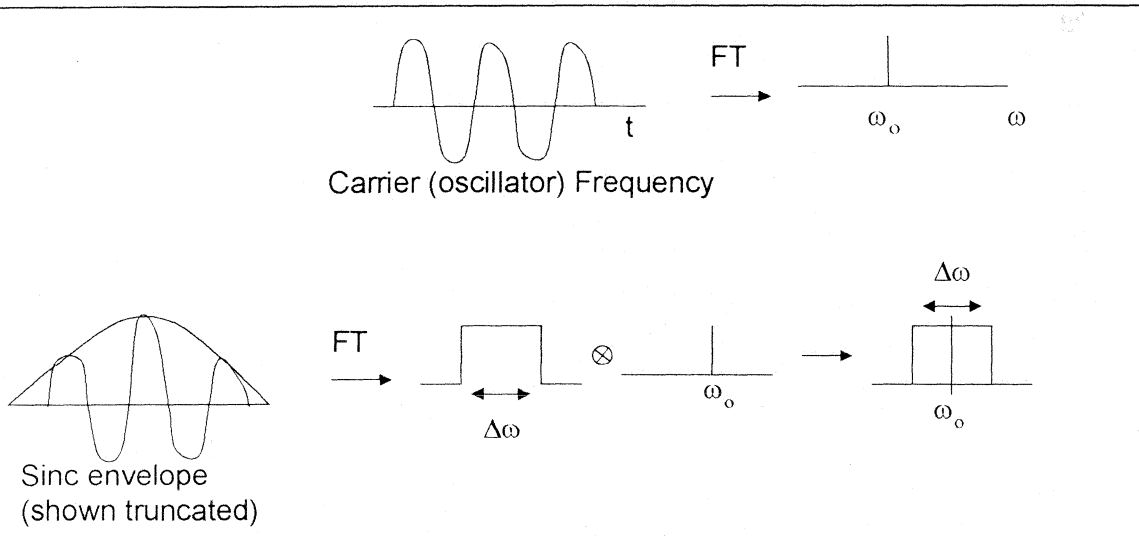

Figure 6 Amplitude modulation of an RF pulse can be used to select a narrow range of frequencies to be excited. Multiplying the MHz carrier RF signal by a sinc pulse envelope (only the centre of the

K- SPACE

The inverse relationship between time and frequency: if the period of a function is T s, then its frequency is 1/T Hz..

Spatial encoding using magnetic field gradients

Virtually all modern MRI scanners use spatially variations in the applied magnetic field (Bo), to make the Larmor frequency spatially dependant. Magnetic field gradients can be formed in any direction

$(G_x = \frac{dB_z}{dx}, G_y = \frac{dB_z}{dy}, G_z = \frac{dB_z}{dz})$.

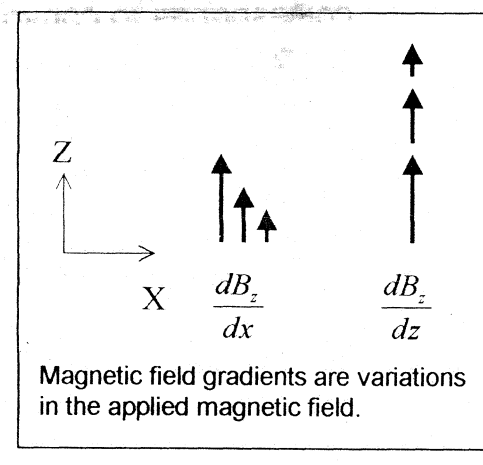

Magnetic field gradients are variations in the applied magnetic field.

Therefore in the present of a magnetic field gradient, the local applied magnetic field is given by:

$B(r) = B_o + G_r r$

where

B_o = applied field from magnet (T)

G_r = applied gradient along r (mT/m) from the gradient coils

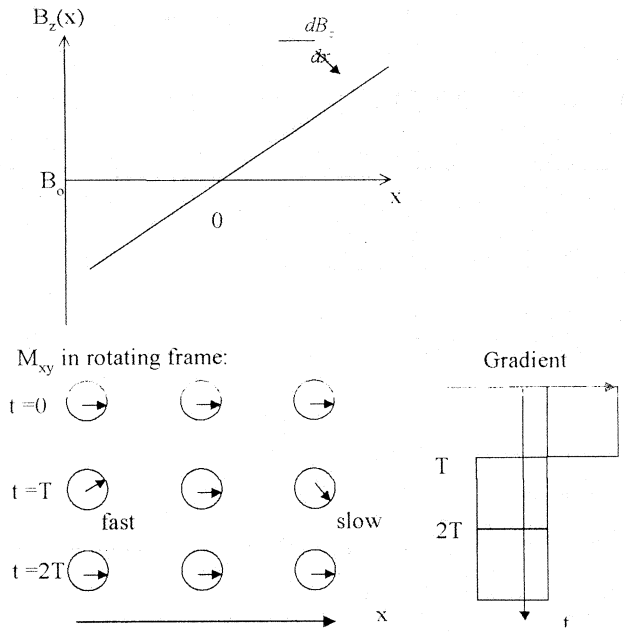

refore the Larmor frequency now depends on the position of the as within the sample:

$$\omega = \gamma(B_o + G_r r)$$

different parts of sample will produce transverse magnetisation cessing at different frequencies.

FOR Imaging sequences

ce a slice has been selected we want to be able to create a picture distribution of the spins within it. There are many ways of ducing an image in MRI, and we are going to consider just a few nem.

jection reconstruction

s is closely related to the method of CT imaging.
er a slice has been excited using a gradient along z, another dient is applied along x. Now the precessional frequency of the ns that have been excited depends on their position in x. Therefore

the time varying signal will be the sum of signals at a range of frequencies.
If the signal is Fourier transformed, so that the frequency spectrum is obtained, then the spectrum is the same as the projection through the object along the gradient.

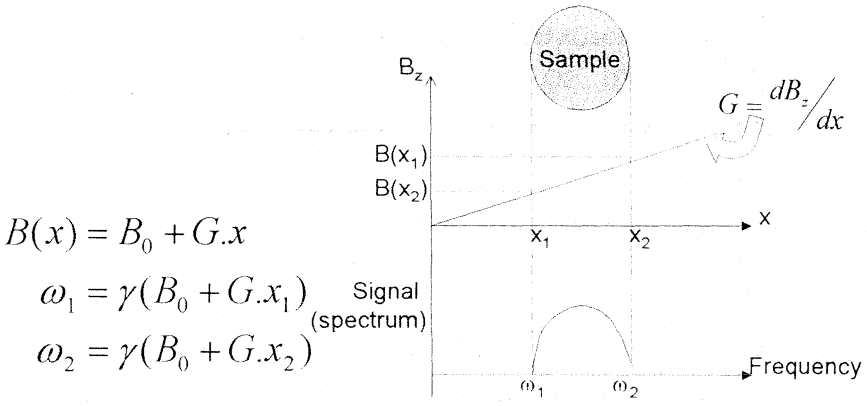

Figure 7 The use of gradients to produce a projection through a sample.

If this process is repeated for different directions of the gradient (ie at various angles between x and y), then projections through the object can be acquired at a variety of angles. The image can then be reprocessed back projections

Gradients can be produced at various angles between x and y, by using combinations of the x and y gradients. The relative amplitudes of the currents through the Gx and Gy coils, determines the angle of the gradient with respect to the x axis. (figure 8).

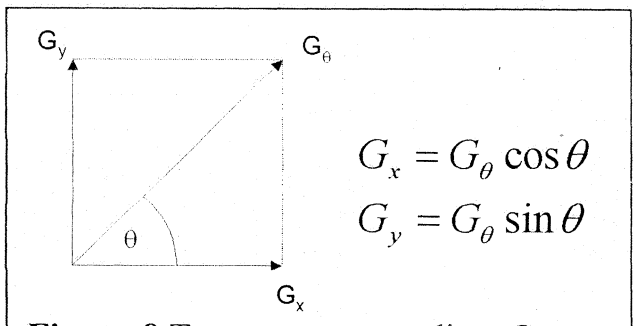

Figure 8 To generate a gradient G at

Look at this analytically. The signal from a sample at position x is given by:

$S_x(t) = \rho(x)e^{i\omega t}$

re

$\gamma(G_x x + B_o)$ i.e. the frequency of rotation in the x y plane

= total spin density at position x (ie projection along x)

vever the signal we measure is summed over the whole sample, ver all values of x:

$(t) = \int \rho(x) e^{i\gamma(B_o + G_x x)t} dx$

we know, phase sensitive detection mixes out the central Larmor uency, ie the B_o term, so that the total signal after detection is en by

$= \int \rho(x) e^{i\gamma G_x x t} dt$

ne projection through the object along the direction of the gradient be obtained by taking the Fourier transform of the signal (NB this

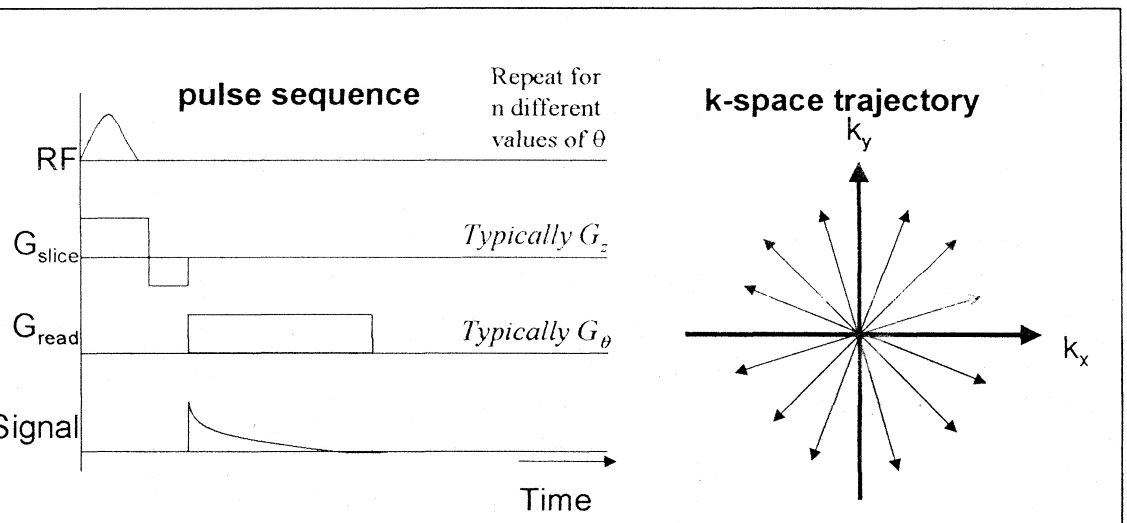

Figure 9 Projection reconstruction sequence

lysis neglects T2* decay). (If filtered backprojection reconstruction be used, then the signal can be multiplied by the appropriate rier domain filter before Fourier transforming).

projection reconstruction imaging 'pulse sequence' is shown in re 9. This shows the time course of the gradient and RF veforms. The first line shows the slice selective RF pulse, and the ond line shows the slice selection gradient. The third line shows image encoding (frequency encoding/ readout) gradient. The th line shows the magnitude of the signal that will be acquired (ie magnitude of the transverse magnetization, so net frequency ets cannot be seen).

Applications of back projection reconstruction:

because imaging can start sampling very quickly after excitation, projection reconstruction is useful for imaging things with a short T_2^* eg
Lungs (which have a very short T2* because of susceptibility differences between lung tissue and lung gas)
Sodium imaging (which has a very short T2)
Microscopy (where susceptibility artefacts can also be a problem)
The images can be badly affected by inhomogeneities in the main magnetic field (Bo)
The total scan time is long.

k-space imaging

MR pulse sequences are best compared in k-space (reciprocal space), (which contains the spectrum of spatial frequencies contained in the image. If we define

$$k = \gamma \int G(t)dt$$

(for the general case where G is varying) so that the Fourier transform in eqn. 5 can be rewritten

$$S(k) = \int \rho(x) e^{-ik.x} dx$$

i.e. signal obtained can be directly mapped into 'reciprocal' space (spatial frequency space). To sample higher spatial Frequencies (responsible for sharp edges and high resolution) you need higher (or longer) gradients.

Conventional Fourier Imaging

Fourier imaging resolves spatial information by three distinct procedures, called ***selective excitation, phase encoding***, and ***frequency encoding***).The slice-selection gradient spreads out the Larmor frequency over a broad range so that the frequencies contained in the RF pulse affect only a slice. The phase-encoding gradient is pulsed briefly after the RF excitation pulse has been

ed off, making the Larmor frequency depend on spatial position
ng the phase-encoding direction. Afterwards, magnetization
nponents everywhere in the slice regain the same Larmor
uency, but the phase depends on their position along the phase-
oding direction. Spatial information in the phase-encoding
ction can be resolved if many separate MR signals are collected.
amplitude of the phase-encoding gradient for each signal is
reased systematically. Each of these signals is measured as an
o while the frequency-encoding gradient is active, which creates a
ribution of Larmor frequencies along the frequency-encoding
ction. The first pulse of the frequency-encoding gradient is
essary for an echo to form during the middle of the second pulse.

Spin-warp imaging

ou remember, the problems of crude back projection
onstruction stem from the fact that k-space is not sampled
formly. In spin warp imaging k space is sampled on a regular grid.

member that moving across k space you are increasing the
nber of radians per meter acquired by the spins. Therefore in
er to move across the k space in the k_y direction, you must apply a
rection gradient (so that the spins gains relative phase shifts
ng y).

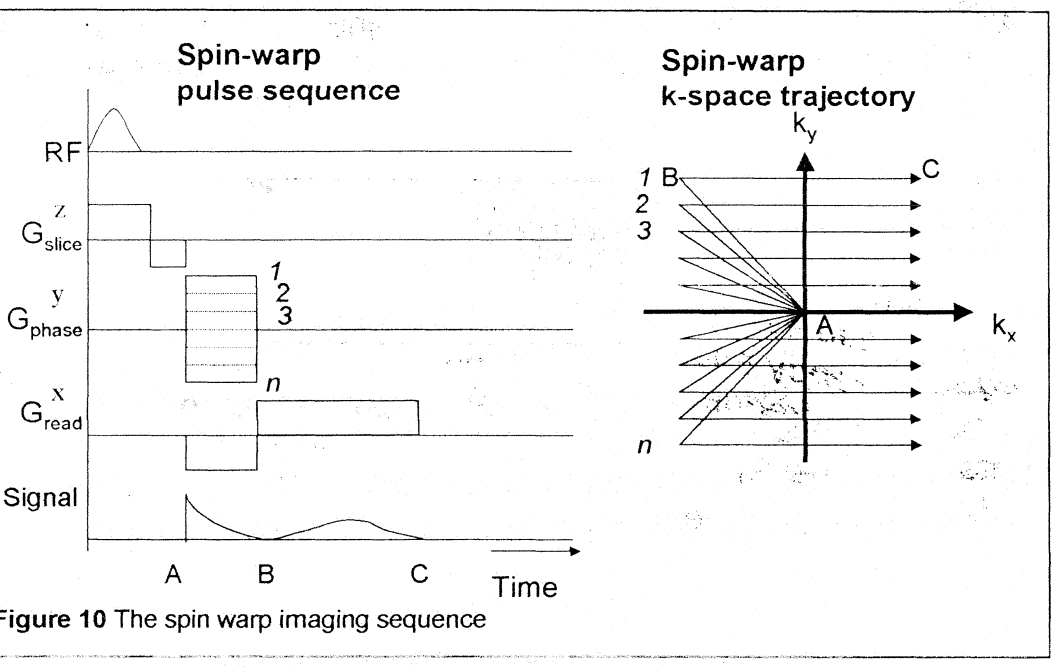

Figure 10 The spin warp imaging sequence

Figure 10 matches up the k space trajectory and the imaging sequence. Frequency encoding: The line BC in k space is acquired between the points B and C in the pulse sequence diagram, whilst the spins evolve under the read gradient. This part of the sequence looks very much like a standard projection reconstruction sequence: whilst the gradient is applied (and the signal is readout), we move across k space in the reciprocal direction of the gradient. You may have noticed that a negative read gradient is actually applied during the period AB, so that a gradient echo is acquired in the period BC .This corresponds to the fact that the line AB in the k-space trajectory is moving in a negative k_x direction. Phase encoding During the period AB an additional phase encoding gradient is applied. This makes the initial phase of the signal depend on both G_y and the position of sample in y (Morris 1985) and moves us in the y direction in k space.

Advantages:

Most widely used imaging sequence Field errors cause distortion, not blurring

Disadvantages

Long imaging times... motion causes ghost artifacts

Cine imaging.

Uses a single thick slice (10 – 40 mm) is acquired in the plane that best include the vessel. Acquisition is carried indexed to the patient's heart rate. The heart beat interval is divided in to several segments called cardiac phases. This is achieved using a gradient echo with small flip angle leaving enough magnetization on the longitudinal axis of the magnet for a multiple data collection from same slice throughout the cardiac cycle, as heart rate varies the time for T1 relaxation recovery also vary from one encoding cycle to the next. This motion can be corrected by giving ECG triggering and respiratory compensation. When displayed in a movie mode this images give excellent functional aspect of flow during the cardiac cycle through the vessel.

PROPELLER IMAGING

Periodically rotated overlapping parallel lines with enhanced reconstruction.
Multiple sets of parallel lines in k-space are filled

An angle is then shifted ,and another sets of parallel lines are filled

It overlapping first sets of parallel lines in the center It is continued until full range of k-space is filled

Central region of the k-space is sampled repeatedly
It suppress motion artifact.
FFT is required to collect the row data
Chemical shift artifact are more

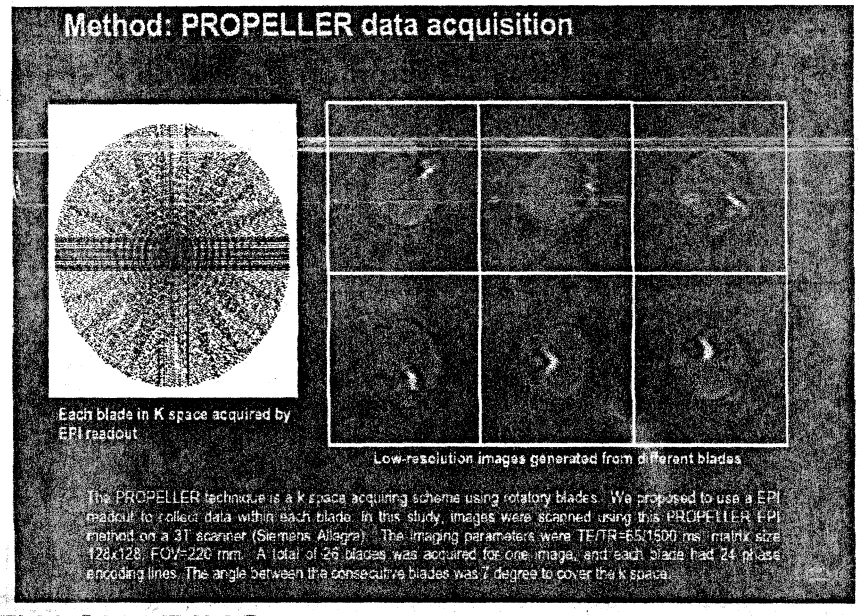

VIEW SHARING

The acquired views to reconstruct a given image slice or volume ,the data can be shared between one or more images.This will decrease the amount of data that must be newly sampled per images .It increase the temporal resolution of fast mri techniques Approach is similar to the radiographic fluoroscopy

Real time images are generated by continuously replacing the alternate lines in the CRT .It effectively doubling the apparent temporal resolution .
MR Fluoroscopy –intermittently refreshing some of the image data .
An image with 128 lines in the Kx, replacing 8 lines we can generate 16 images .
view sharing-increase the efficiency of dual TE FSE

Center of the k-space obtain separately with in each of the echo train portion Cardiac imaging,
Dynamic contrast –enhanced MR images

Dynamic events during fMRI ,
View sharing –impressive reduction imaging time

KEYHOLE IMAGING

A variant of the shared echo techniques K-space is covered completely on the first image only the central part (20%),which provide the most of the contrast,is updating on subsequent image
It speed up the imaging by a factor of 5 Is very useful in fast recitative imaging of the same slice Its disadvantages is high frequency outer 80% of k space is shared information

Two major limitation of keyhole imaging techniques

If any motion between the baseline higher resolution images& dynamic contrast enhanced images
It will produce misregistration between the contrast &fine detail of the image
It produce some distortion in the contrast enhanced small vessel or finely heterogeneous pattern of tissue

Keyhole hybrid technique

It intermittently updating the peripheral views
Periphery of the k-space is filled in an interleaved manner.This has been applied to 3D MRA
Contrast enhanced application,3D-TRICKS .
Hybrid keyhole-spin echo,fse,gre

ZIP IMAGING

Zero fill interpolation processing.
Zip are used with any MR acquisition

The portion of the K-space are not directly filled during the read out

These are filled with zeros ,FFT can be performed This techniques allows for interpolation of large matrix
Zip create 512X512 matrix image from 256X256 image

Using this we can increase the apparent resolution
It reducing the scanning time with out much loss in resolution & SNR
It increase the truncation artifact

ELECTRONICS AND DATA PROCESSING

This will be an abbreviated description of the MRI scanner. To get a general idea of the major components of a MRI scanner I have included the following schematic diagram:

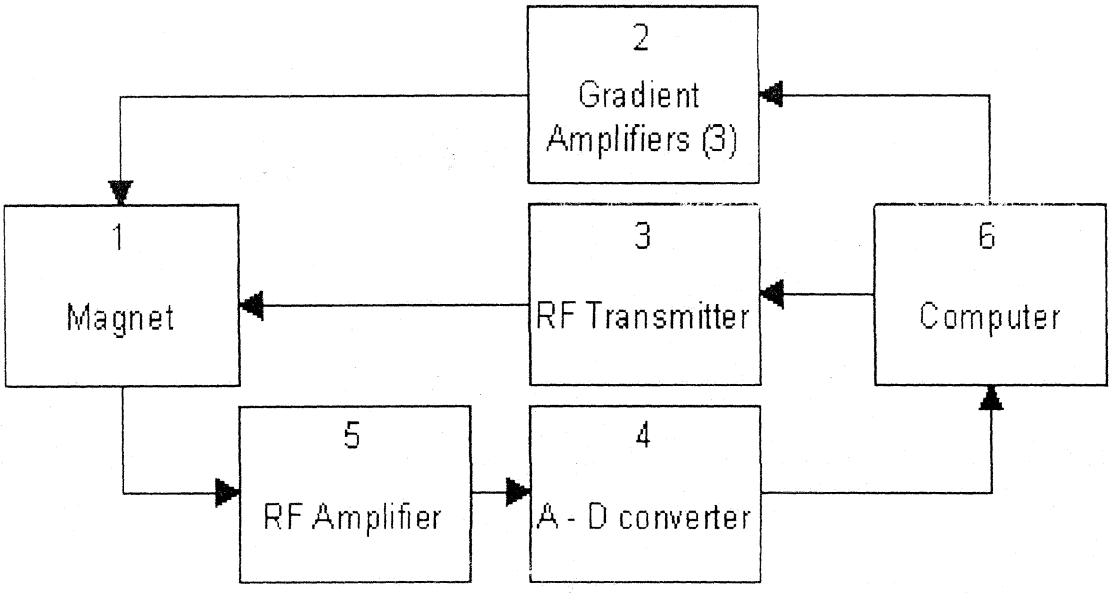

Starting from the right hand side, we have the computer that directs all of the action in the MRI acquisition and acquires and processes the data. The computer tells the gradient amplifiers and RF transmitter when to turn on and off to obtain the proper pulse sequence. The RF receiver amplifier is also controlled by the computer and relays the signal received by the RF coil from the patient to the A-D converter that digitizes the signal, and from there to the computer to be reconstructed into

Equipment: The MR Console

The MR Console is the "brains' of the system. It consists of one or more computers, complete with software, and the control electronics. It controls all the hardware, collects the data and presents it to the user.

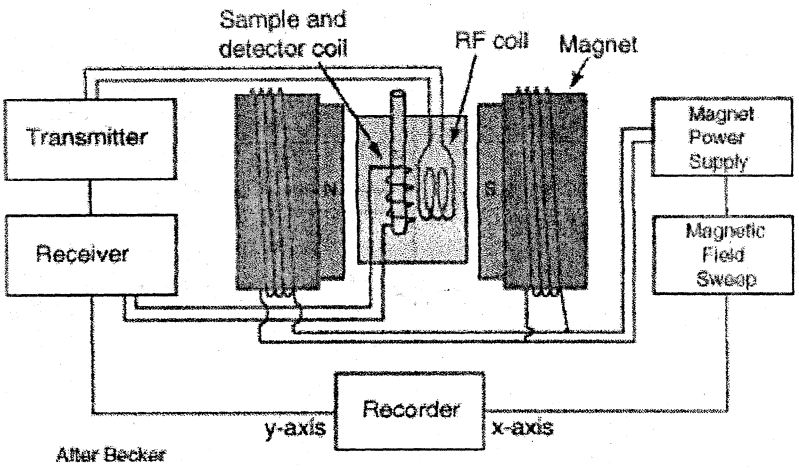

MRI PULSE SEQUENCE

A preselected set of defined RF and gradient pulses, usually repeated many times during a scan, wherein the time interval between pulses and the amplitude and shape of the gradient waveforms will control NMR signal reception and affect the characteristics of the MR images. Pulse sequences are computer programs that control all hardware aspects of the measurement process.

A recommended shorthand designation of interpulse times and excitation pulse used to generate a particular image is to list the repetition time (TR), the echo time (TE) and, if using inversion recovery, the inversion time (TI) with all times given in milliseconds and if using a gradient echo sequence the flip angle. For example, 3000/30/1000 would indicate an inversion recovery pulse sequence with TR of 3000 msec, TE of 30 msec, and TI of 1000 msec. Specific pulse sequence weightings are dependent on the field strength, the manufacturer and the pathology. See also Interpulse Times.

SPIN ECHO SEQUENCE

The most common pulse sequence used in MR imaging is based of the detection of a spin or Hahn echo. It uses 90° radio frequency

pulses to excite the magnetization and one or more 180° pulses to refocus the spins to generate signal echoes. In the pulse sequence timing diagram, the simplest form of a spin echo sequence is illustrated. The 90° pulse is first applied to the spin system and rotates the magnetization down into the X'Y' plane. The transverse magnetization begins to dephase. At some point in time after the 90° pulse, a 180° pulse is applied. This pulse rotates the magnetization by 180° about the X' axis. The train of refocusing 180° pulses serves to generate repetitive signal echoes (hence the name spin echo). The 180° pulses occur at time, ½TE + iTE i = 0,1,...,n, and the signal echoes at iTE. The echoes serve to rephase all the coherence in the x y-magnetization which are lost during the time between 90° and 180° pulse due to dephasing.

The recovery of the z-magnetization occurs with the T1 relaxation time and typically at a much slower rate than the T2-decay, because in general T1 is greater than T2 for living tissues and is in the range of 100–2000 ms. The SE pulse sequence was devised in the early days of NMR days by Carr and Purcell and exists now in many forms: the multi echo pulse sequence using single or multislice acquisition, the fast spin echo (FSE/TSE) pulse sequence, echo planar imaging (EPI) pulse sequences and the GRASE pulse sequence are all basically spin echo (SE) sequences. In the simplest form of SE imaging, the pulse sequence has to be repeated as many times as the image has lines.

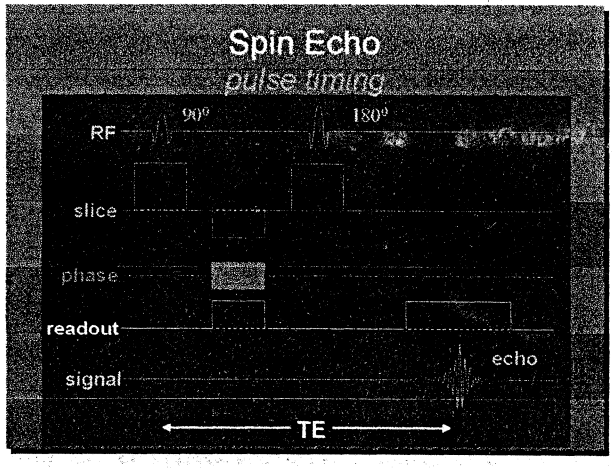

slice selective 90° RF pulse is applied in conjunction with a slice election gradient. A period of time equal to TE/2 elapses and a 180° lice selective 180° pulse is applied in conjunction with the slice election gradient. A phase encoding gradient is applied between the 0° and 180° pulses The phase encoding gradient could be applied fter the 180° pulse, however if we want to minimize the TE period he pulse is applied between the 90° and 180° RF pulses. The requency encoding gradient is applied after the 180° pulse during the me that echo is collected. The recorded signal is the echo. The FID, hich is found after every 90° pulse, is not used. One additional radient is applied between the 90° and 180° pulses. This gradient is long the same direction as the frequency encoding gradient. It ephases the spins so that they will rephase by the center of the cho. This gradient in effect prepares the signal to be at the edge of -space by the start of the acquisition of the echo. The entire equence is repeated every TR seconds until all the phase encoding teps have been recorded.

DWeighted:ShortTE(20Ms)AndLongTR.

T1Weighted:ShortTE(10-20Ms)AndShortTR(300-600Ms)

T2Weighted:LongTE(GreaterThan60Ms)AndLongTR(GreaterThan1600Ms)

With Spin Echo Imaging No T2* Occurs.

Dual Echo Sequen (DE - dual / double echo)

Dual echo sequences include images with different weightings and or echo times and are used to obtain both, proton density and T2 veighted images or in phase and out of phase gradient echo images, simultaneously without increasing the measurement time.

Modified Spin Echo(MSE)

A spin echo technique with a flip angle over 90°.

Multi Echo Multiplanar (MEM)

Sequence with a multislice and multi echo acquisition in one TR.

Partial Saturation Spin Echo (PSSE)

Partial saturation sequence in which the signal is detected as a spin echo. Even though a spin echo is used, there will not necessarily be a significant contribution of the T2 relaxation time to image contrast, unless the echo time, TE, is on the order of or longer than T2.

Variable Echo Multiplanar (VEMP)

MR imaging spin echo pulse sequence in which signals for multiple variable echoes are collected

FAST SPIN ECHO (FSE)

In conventional spin echo, depending up up on the phase encoding steps we repeat the TR and fill the k-space for each echo (e.g. for an 8 echo train we will get a eight different images), but in FSE we wil get only one K-space and also we get 8 lines at a time depending up on the ETL. In this one TR we will get 8 lines next TR we will get 8 more lines. If your phase encoding steps is 256 & ETL-8 ,we only have to repeat the k-space to 32 times

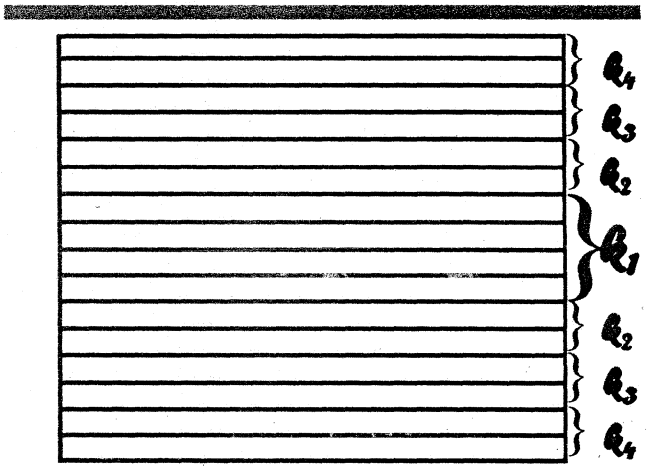

ETL

It refers to the number of echoes used in-FSE and it ranges typically from 3-32.The time interval between successive echoes is called the echo spacing (ESP) ,the typical ESP is in the order of 16-20ms at a

ical high field band width of 32 khz .in FSE the only TEs we can oose are integral multiples of the echo spacing this is called ective TEeff

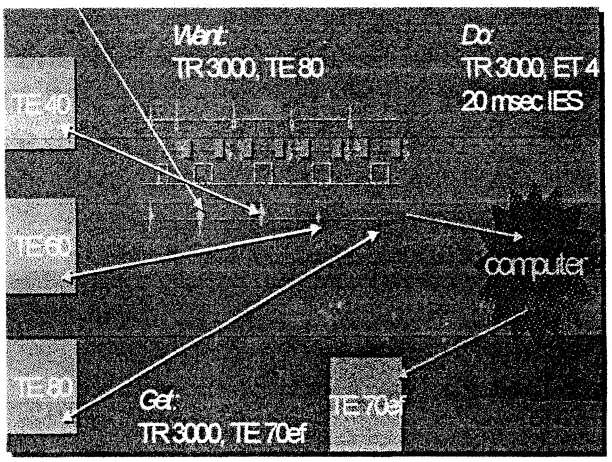

enter of k-space has maximum signal .Edges of k-space ,we get ss signal .we use phase encoding with lowest strength for effective E. Each subsequent phase encoding steps will have a gradient with ore and more amplitude

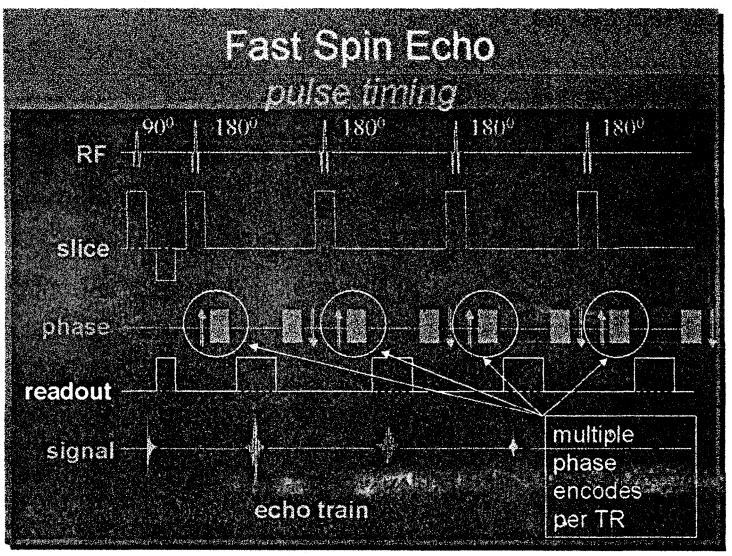

case of the acquisition of 2 echoes this type of a sequence is amed double fast spin echo / dual echo sequence, the first echo is ually density and the second echo is T2 weighted. ther terms for this technique are

with 90° phase shift in the rotating frame of reference between the 90° pulse and the subsequent 180° pulses in order to reduce accumulating effects of imperfections in the 180° pulses. Suppression of effects of pulse error accumulation can alternatively be achieved by switching phases of the 180° pulses by 180

Double Fast Spin Echo(DFSE)

Simultaneously acquired T2 and proton density weighted TE in FSE echo images

Double Turbo Spin Echo(DTSE / DE TSE)

Simultaneously acquired T2 and proton density weighted echoes in a TSE sequence.

Half Fourier Acquisition Single Shot Turbo Spin Echo(HASTE)

A pulse sequence with data acquisition after an initial preparation pulse for contrast enhancement with the use of a very long echo train (Single shot TSE), whereat each echo is individually phase encoded. This technique is a heavily T2 weighted, high speed sequence with partial Fourier technique, a great sensitivity for fluid detection and a fast acquisition time of about 1 sec per slice. This advantage makes it possible for using breath-hold with excellent motionless MRI, e.g. used for liver and lung imaging.

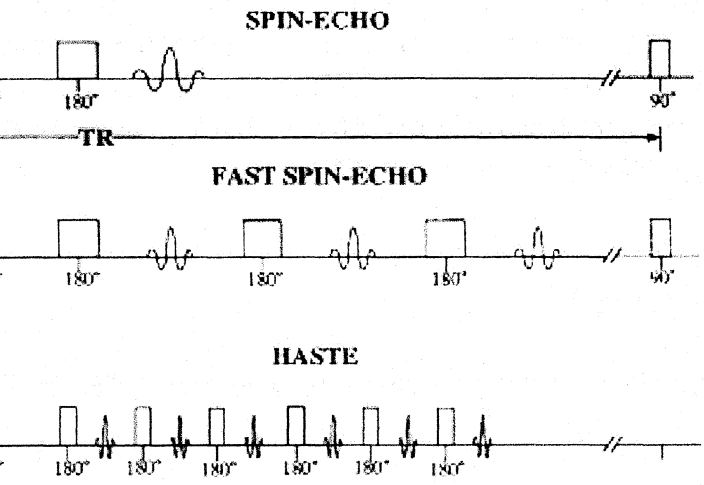

oid Acquisition with Refocused Echoes(RARE) (GE)

e image lines from multiple echoes are used for the same image, results in the RARE pulse sequence. The sequence is similar to spin echo.

bo Spin Echo (TSE)

ulse sequence characterized by a series of rapidly applied 180° asing pulses and multiple echoes.(SIEMENS)

rashort Turbo Spin Echo

rbo spin echo (TSE / FSE) technique with extremely short echo cing, resulting in shorter scan times. This is an advantage in s where motion is a problem, for example dynamic or abdominal ging. The shorter scan time and echo spacing are achieved by g a higher TSE factor and an increased data sampling. dvantages are the decrease in SNR (caused through the ease of the bandwidth) and artifacts if minimum echo spacing is l (incomplete dephasing of the 180° pulse FID).

INVERSION RECOVERY(IR)

Inversion recovery is a MR technique, which can be incorporated into MR imaging, wherein the nuclear magnetization is inverted at a time on the order of T1 before the regular imaging pulse-gradient sequences. The resulting partial relaxation of the spins in the different structures being imaged can be used to produce an image that depends strongly on T1. This may bring out differences in the appearance of structures with different T1 relaxation times. Note that this does not directly produce an image of T1. T1 in a given region can be calculated from the change in the MR signal from the region due to the inversion pulse compared to the signal with no inversion pulse or an inversion pulse with a different inversion time. This sequence involves successive 180° and 90° pulses. The **inversion recovery** sequence is specified in terms of three parameters, inversion time (TI), repetition time (TR) and echo time (TE).

Inversion Recovery Sequence

This pulse sequence produces signals, which represent the longitudinal magnetization existent after the application of a 180° inversion RF pulse and rotates the net magnetization down to the negative z-axis. The magnetization undergoes spin Lattice relaxation and returns toward its equilibrium position along the positive z-axis. Before it reaches equilibrium, a 90° pulse is applied that rotates the longitudinal magnetization into the xy plane. Once magnetization is present in the xy plane it rotates about the z-axis and dephases giving a FID.

In the pulse sequence timing diagram, the basic **inversion recovery** sequence is illustrated. The 180° inversion pulse is attached prior to the 90° excitation pulse of a spin echo acquisition. The **inversion recovery** sequence has the advantage, that it can provide very strong contrast between tissues having different T1 relaxation times or to suppress tissues like fluid or fat. But the disadvantage is, that the additional inversion radio frequency RF pulse makes this sequence less time efficient than the other pulse sequences.

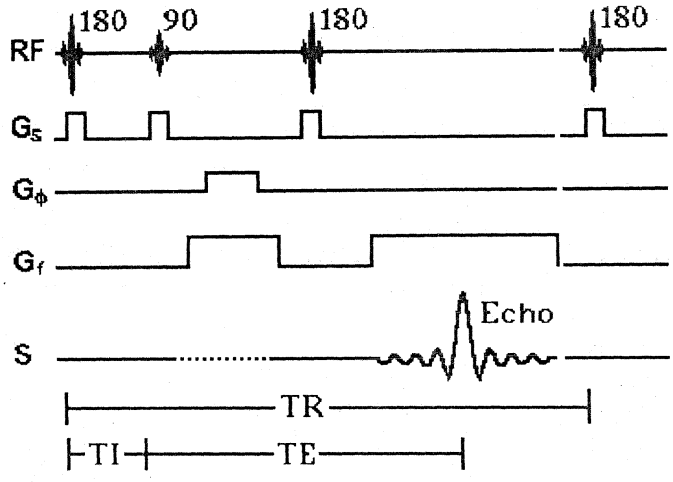

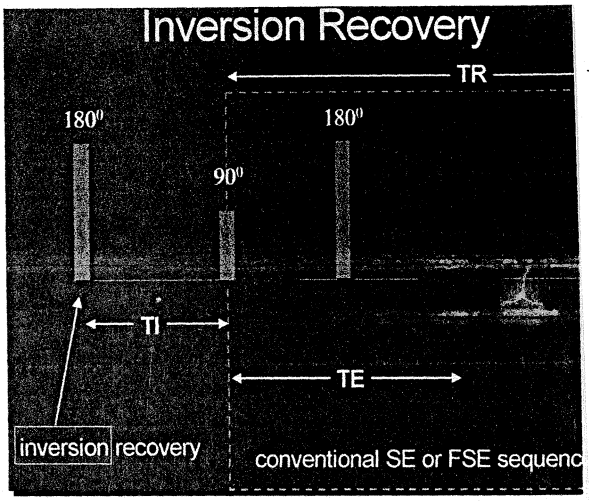

Inversion Recovery Spin Echo (IRSE)

Form of **inversion recovery** imaging in which the signal is detected as a spin echo. For TE short compared to the T2 relaxation time, there will be only a small effect of T2 differences on image intensities; for longer TE's, the effect of T2 may be significant

Short T1 Inversion Recovery(STIR)

Also called Short Tau (TI-inversion time) **Inversion Recovery**. It is an **inversion recovery** sequence where the TI time is set to T1ln2, where T1 is the spin Lattice relaxation time of the component that should be suppressed. For fat suppression that component is fat, for water suppression it is water. This technique only works when the T1 values for the two components are different. Inversion recovery doubles the distance spins will recover, allowing more time for T1 differences. A 180° preparation pulse inverts the net magnetization to the negative longitudinal magnetization prior to the 90-degree excitation pulse. This specialized application of the **Inversion Recovery** pulse sequence set the inversion time (TI) of the sequence at 0.69 times

the T1 of fat. The T1 of fat at 1.5T is approximately 250 with a null point of 170 ms while at 0.5T its 215 with a 148 ms null point. At the moment of excitation, about 120 to 170 ms after the 180° inversion pulse (depending of the magnetic field) the magnetization of the fat signal has just risen to zero from its original, negative, value and no fat signal is available to be flipped into the transverse plane. When deciding on the optimal T1 time, factors to be considered include not only the main field strength, but also the tissue to be suppressed and the anatomy. In comparison to a conventional spin echo where tissues with a short T1 are bright due to faster recovery, fat signal is reversed or darkened. Because body fluids have both a long T1 and a long T2, it is evident that STIR offers the possibility of extremely sensitive detection of body fluid. This is of course, only true for stationary fluid such as edema, as the MR signal of flowing fluids is governed by other factors.

Flow Sensitive Alternating Inversion Recovery(FAIR)

In this sequence 2 inversion recovery images are acquired, one with a nonselective and the other with a slice selective inversion pulse. The z-magnetization in the first sequence is independent of flow. Inflowing spins give z-magnetization from second pulse. A major signal loss in FAIR is the T1 relaxation of tagged blood in transit to the imaging slice. Sharper edges of the inversion pulse give narrow spacing between the inversion edge and the 1st slice because reduced transit time gives lower T1 relaxation induced signal loss. The difference of the images in a consequence contains information proportional to flow (blood partition coefficient). Standard adiabatic inversion RF pulse does not have good slice-profile, because of power/SAR limitation. A c-shaped frequency offset corrected inversion (FOCI) RF pulse can help to increase the signal. Perfusion imaging, e.g. myocardial, using tissue water as endogenous contrast is suggested

Attenuation Inversion Recovery(FLAIR)

ecial inversion recovery sequence with long TI to remove the s of fluid from the resulting images. The TI time is set to the tion time of the component that should be suppressed. For fluid ession the inversion time (long TI) is set to the zero crossing of fluid, resulting in the signal being 'erased'.

ns that are normally covered by bright fluid signals using ntional T2 contrast are made visible by the dark fluid technique fore it is an important technique for the differentiation of brain pine lesions. This sequences is used in the brain to suppress bring out the periventricular hyper intense lesion ,such as le sclerosis plaques

Inversion Recovery(TIR / TIRM / IR-TSE)

Spin Echo / FIR - Fast **Inversion Recovery**) o / fast **spin echo sequence** with long TI for fluid suppression R) or with short TI for fat suppression (STIR). This sequence for a true **inversion recovery** display that shows the netic sign of the signal.
means a turboIR with a **magnitude** display.

DIENT ECHO SEQUENCE(GRE - sequence)

adient echo is generated by using a pair of bipolar gradient s. In the **pulse sequence timing diagram**, the basic gradient sequence is illustrated. There is no refocusing 180° pulse and ata are sampled during a gradient echo, which is achieved by **asing** the spins with a negatively pulsed gradient before they ephased by an opposite gradient with opposite polarity to ate the echo.

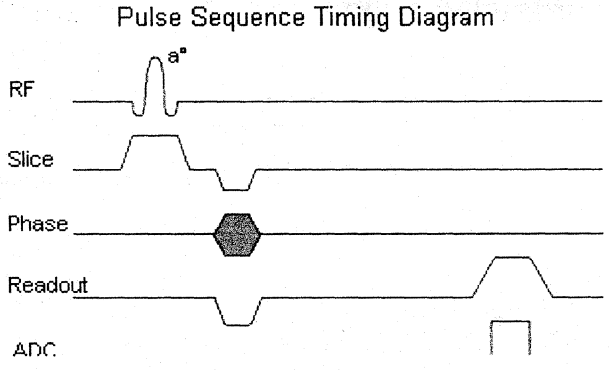

There you will find a description of the components. The excitation pulse is termed the alpha pulse . It tilts the magnetization by a flip angle □, which is typically between 0° and 90°. With a small flip angle there is a reduction in the value of transverse magnetization that will affect subsequent RF pulses. The flip angle can also be slowly increased during data acquisition (variable flip angle: tilt optimized non-saturation excitation). The data are not acquired in a steady state, where z-magnetization recovery and destruction by ad-pulses are balanced. However, the z-magnetization is used up by tilting a little more of the remaining z-magnetization into the xy-plane for each acquired imaging line. Gradient echo imaging is typically accomplished by examining the FID, whereas the read gradient is turned on for localization of the signal in the readout direction. T2* is the characteristic decay time constant associated with the FID. The contrast and signal generated by a gradient echo depend on the size of the longitudinal magnetization and the flip angle. When flip angle is 90° the sequence is identical to the so-called partial saturation or saturation recovery pulse sequence. In standard GRE imaging, this basic pulse sequence is repeated as many times as image lines have to be acquired. Additional gradients or radio frequency pulses are introduced with the aim to spoil to refocus the xy-magnetization at the moment when the spin system is subject to the next pulse.

As a result of the short repetition time, the z-magnetization cannot fully recover and after a few initial α pulses there is an equilibrium established between z-magnetization recovery and z-magnetization reduction due to the □ pulses.

Gradient echoes have a lower SAR, are more sensitive to field in homogeneities and have a reduced crosstalk, so that a small or no slice gap can be used. In or out of phase imaging depending on the selected TE (and field strength of the magnet) is possible. As the flip angle is decreased, T1 weighting can be maintained by reducing the TR. T2* weighting can be minimized by keeping the TE as short as

ssible, but pure T2 weighting is not possible. By using a reduced angle, some of the magnetization value remains longitudinal (less e needed to achieve full recovery) and for a certain T1 and TR, re exist one flip angle that will give the most signal, known as the nst angle"

ntrast values:

weighted: Small flip angle (no T1), long TR (no T1) and short TE (no T2*)

weighted: Large flip angle (70°), short TR (less than 50ms) and short TE

weighted: Small flip angle, some longer TR (100 ms)and long TE (20 ms

assification of GRE sequences

1. T1 weighted or incoherent/(RF or gradient) spoiled GRE sequences
2. T1/T2* weighted or coherent/refocused GRE sequences.
3. T2 weighted contrast enhanced GRE sequencesultrafast GRE sequences.

RADIENT RECALLED ECHO SEQUENCE

MRI sequence producing signals called gradient echoes as a sult of the application of a refocusing echo. In the gradient called echo sequence, a slice selective RF pulse is applied to e imaged object. This RF pulse typically produces a rotation gle of between 10° and 90°.

slice selection gradient is applied with the RF pulse. A phase coding gradient is applied and a dephasing frequency encoding adient is applied at the same time so as to cause the spins to be phase at the center of the acquisition period. This gradient is gative in sign from that of the frequency-encoding gradient ned on during the acquisition of the signal. An echo is produced en the frequency encoding gradient is turned on because this adient refocuses the dephasing, which occurred from the adients.

GRADIENT ECHO FAST SCANNING TECHNIQUES

DRIVEN EQUILIBRIUM FAST GRADIENT RECALLED ACQUISITION IN THE STEADY STATE DEPHASING GRADIENT(DE FGR)

A gradient echo sequence using a pulse, which sensitizes the sequence to variations in T2, rather than waiting for T1 relaxation

Fast Gradient Recalled Echo(FGRE)

In the gradient recalled echo sequence, a slice selective RF pulse is applied to the imaged object.

SPGR(Spolied Gradient)

With SPGR T2 dependence is almost completely eliminated. If we use this sequence with short TE and moderate flip angle, one could achieve T1 weighted gradient echo images. This pulse sequences uses very short TR values neither a transverse or longitudinal state has enough time to become fully established during the course of imaging. Because the image acquisition has not taken place under steady state condition, non uniform weighting of the data along phase encoded axis will occur and can cause loss of image resolution. Because the TR value are so short, small flip angle may be used to minimize saturation to preserve the SNR. In SPGR uses a simple preparative non-selective 180^0 pulse along the phase encoding axis(Spoiling gradient) which invert the tissue magnetization across the sample and produces T1 weighted images. The SPGR spoiling is achieved by adding phase shift to each successive RF excitation pulse. This result in tilting of residual magnetization in out of phase with each other to prevent the build up of steady state component and thus eliminate T2 contribution. This approaches only works if the transmitter and receiver keep a constant phase relationship for each transmit and receive function.

There are various way to get SPGR images

1,By applying RF spoiling
2,BY applying variable gradient spoilers
3,BY lengthening TR

RF spoiling

n this scheme ,a phase offset is added to each successive RF pulse. This causes a corresponding phase shift in successive Mss vectors.By maintaining a constant phase relationship between the ransmitter and the receiver

Variable Gradient Spoilers

Spoiling can also be achieved by using gradient spoilers . This is accomplished by introducing an additional gradient with variable strength from cycle to cycle

Lengthening TR

When TR is sufficiently large ,there is enough time to allow complete dephasing of the spin in the transverse plane

CE-FFE-T1: Contrast Enhanced Fast Field Echo with T1 Weighting,
GFE:Gradient Feildf Echo,
FLASH: Fast Low Angle Shot,
PS: Partial Saturation,
RF spoiled FAST: RF Spoiled Fourier Acquired Steady State Technique,
RSSARGE: Radio Frequency Spoiled Steady State Acquisition Rewound Gradient Echo
S-GRE: Spoiled Gradient Echo,
SHORT: Short Repetition Techniques,
SPGR: Spoiled Gradient Recalled (spoiled GRASS),
STAGE: T1W T1 weighted Small Tip Angle Gradient Echo,
T1-FAST: T1 weighted Fourier Acquired Steady State Technique,
T1-FFE :T1 weighted Fast Field Echo.

Abdominal Imaging

General MRI of the abdomen can consist of T1 or T2 weighted spin echo, fast spin echo (FSE, TSE) or gradient echo sequences with fat suppression and contrast enhanced MRI techniques. The examined organs include liver, pancreas, spleen, kidneys, adrenals as well as parts of the stomach and intestine. Respiratory compensation and breath hold imaging is mandatory for good image quality.

T1 weighted sequences are more sensitive for lesion detection than T2 weighted sequences at 0.5 T, while higher field strengths (greater than 1.0 T), T2 weighted and spoiled gradient echo sequences are used for focal lesion detection. Gradient echo in phase T1 breath hold can be performed as a dynamic series with the ability to visualize the blood distribution. Phases of contrast enhancement include the capillary or arterial dominant phase for demonstrating hypervascular lesions, in liver imaging the portal venous phase demonstrates the maximum difference between the liver and hypovascular lesions, while the equilibrium phase demonstrates interstitial disbursement for edematous and malignant tissues.

Out of phase gradient echo imaging for the abdomen is a lipid-type tissue sensitive sequence and is useful for the visualization of focal hepatic lesions, fatty liver, haemochromatosis, adrenal lesions and renal masses. The standards for abdominal MRI vary according to clinical sites based on sequence availability and MRI equipment. Specific abdominal imaging coils and liver-specific contrast agents targeted to the reticuloendothelial system (RES) of the liver and spleen, achieve the goals of improved detection and localization in the liver.

Contrast Enhanced Fast Field Echo with T1 Weighting(CE-FFE-T1)
A T1 weighted gradient echo sequence
Fast Spoiled Gradient Echo(FSPGR)
A sequence similar to Turbo FLASH or Turbo Field Echo

Refocused Gradient Echo Sequence

Refocused GRE sequences use a refocusing gradient in the phase encoding direction during the end module to maximize (refocus) remaining xy- (transverse) magnetization at the time when the next excitation is due, while the other two gradients are, in any case, balanced.
When the next excitation pulse is sent into the system with an opposed phase, it tilts the magnetization in the □ direction. As a result the z-magnetization is again partly tilted into the xy-plane, while the remaining xy-magnetization is tilted partly into the z-

ection.
mpanies use different acronyms to describe certain techniques.
fferent terms for these gradient echo pulse sequences:
GRE:RefocusedGradientEcho,
ST: Fourier Acquired Steady State,
E: Fast Field echo,
SP: Fast Imaging with Steady State Precession,
SHORT SHORT Repetition Technique Based on Free duction Decay,
FEC: Gradient Field Echo with Contrast,
RASS: Gradient Recalled Acquisition in Steady State,
DAST: Resonant Offset Averaging in the Steady State,
SFP: Steady State Free Precession.
TERF: Steady State Technique with Refocused FID

st Field Echo(FFE)
n echo signal generated from a FID by means of a bipolar itched magnetic gradient. The preparation module of the pulse quence consists of an excitation pulse. The magnetization tilts a flip angle between 0° and 90°.

st Gradient Recalled Echo(FGRE)

the gradient recalled echo sequence, a slice selective RF pulse applied to the imaged object.

st Low Angle Recalled Echoes (FLARE)

sequence producing signals called gradient echoes as a result the application of a refocusing echo with low flip angles.

SFP (Steady State Free Precession) / PSIF
eady state gradient sequence is designed to operate either single multi- section mode by using extremely short TR values R<50mSec.) and to produce a coherent steady state free ecession. The steady state can be controlled in two ways .Through e use of resonant offset averaging on the read and slice select adients. Through the application of rewinder gradients on the phase coded axis.Steady state is the sum of two components-

FID occurring early in the cycle (just after each RF pulse) and A stimulated echo(St.E) occurring late in the cycle (just before next RF pulse.) It is possible to recover both signals simultaneously and coherently, provided gradient profiles are perfectly balanced.
If the sequence were run for only one cycle no echo is formed. An echo is formed in this sequence by magnetization brought in to trasverse plane by RF pulse in the preceding cycle. The effective echo time is TR + TE [SSFP => TE =2(TR-9)
Relatively long evaluating period before echo collection allows for natural transverse decay of magnetization to occur. So the images from SSFP sequence is highly T2 weighted. In this each □ pulse contains some 90° and 180° pulses embedded in it

ADVANTAGES

1,Decreased dephasing due to in homogeneities in B0 compared with GRASS and SPGR
2, Decreased magnetic susptibility artifacts compared with GRASS and SPGR
3,Dcreased chemical shift artifact s

DIS ADVANTAGES

1, Decreased SNR secondary to the use of longer TE
2, Increased sensitivity to non stationary tissue

ULTRAFAST GRADIENT ECHO SEQUENCE

In simple ultrafast GRE imaging, TR and TE are so short, that tissues have a poor imaging signal and — more importantly — poor contrast except when contrast media enhanced (contrast enhanced angiography). Therefore, the magnetization is 'prepared' during the preparation module, most frequently by an initial 180° inversion pulse.
In the pulse sequence timing diagram, the basic ultrafast gradient echo sequence is illustrated. The 180° inversion pulse is executed one time (to the left of the vertical line), the right side represents the data collection period and is often repeated depending on the acquisition parameters.
Ultrafast GRE sequences have a short TR,TE, a low flip angle and TR is so short that image acquisition lasts less than 1 second and typically less than 500 ms. Common TR: 3-5 msec, TE: 2 msec, and the flip angle is about 5°. Such sequences are often labeled with the

refix "Turbo" like TurboFLASH, TurboFFE and TurboGRASS. his allows one to center the subsequent ultrafast GRE data cquisition around the inversion time TI, where one of the tissues of terest has very little signal as its z-magnetization is passing through ero.

nlike a standard IR sequence, all lines or a substantial segment of -space image lines are acquired after a single inversion pulse, which an then together be considered as readout module. The readout odule may use a variable flip angle approach, or the data cquisition may be divided into multiple segments ("shots"). The latter useful particularly in cardiac imaging where acquiring all lines in a ngle segment may take too long relative to the cardiac cycle to rovide adequate temporal resolution. multiple lines are acquired after a single pulse, the pulse sequence a type of gradient echo echo planar imaging (EPI) pulse sequence

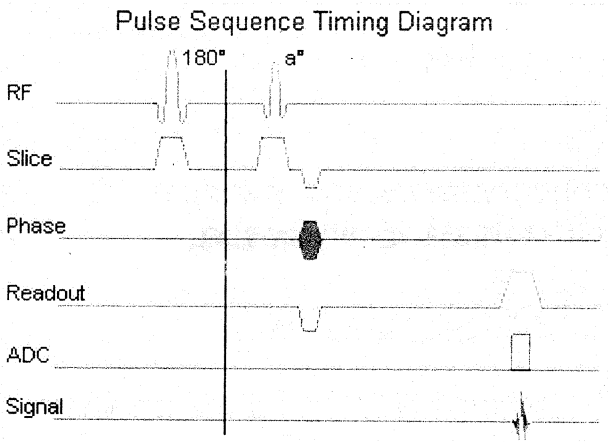

alanced Sequence

his family of sequences uses a balanced gradient waveform. This aveform will act on any stationary spin on resonance between 2 onsecutive RF pulses and return it to the same phase it had before e gradients were applied. A balanced sequence starts out with a RF ulse of 90° or less and the spins in the steady state. Before the next R in the slice, phase and frequency encoding direction, gradients e balanced so their net value is zero. Now the spins are prepared to ccept the next RF pulse, and their corresponding signal can become art of the new transverse magnetization. If the balanced gradients aintain the longitudinal and transverse magnetization, the result is at both T1 and T2 contrast are represented in the image.

This pulse sequence produces images with increased signal from fluid (like T2 weighted sequences), along with retaining T1 weighted tissue contrast. Because this form of sequence is extremely dependent on field homogeneity, it is essential to run a shimming prior the acquisition.
This sequences include e.g. Balanced Fast Field Echo (bFFE), Balanced Turbo Field Echo (bTFE), Fast Imaging with Steady Precession (TrueFISP), Completely Balanced Steady State (CBASS) and Balanced SARGE (BASG).

Balanced Fast Field Echo(bFFE)

A FFE sequence using a balanced gradient waveform. A balanced sequence starts out with a RF pulse of 90° or less and the spins in the steady state. Before the next TR in the slice phase and frequency encoding, gradients are balanced so their net value is zero. Now the spins are prepared to accept the next RF pulse, and their corresponding signal can become part of the new transverse magnetization. Since the balanced gradients maintain the transverse and longitudinal magnetization, the result is, that both T1 and T2 contrast are represented in the image. This pulse sequence produces images with increased signal from fluid, along with retaining T1 weighted tissue contrast. Because this form of sequence is extremely dependent on field homogeneity, it is essential to run a shimming prior the acquisition. A fully balanced (refocused) sequence would yield higher signal, especially for tissues with long T2 relaxation times.

Balanced SARGE(BASG)

The spoiled steady state acquistion rewinded gradient echo sequence with balanced waveform.

Balanced Turbo Field Echo(BTFE)

A gradient echo pulse sequence with a balanced gradient waveform and data acquisition after an initial preparation pulse for contrast enhancement.

ast Imaging with Steady Precession(TrueFISP)

ue fast imaging with steady state precession is a coherent chnique that uses a fully balanced gradient waveform. The image ntrast with TrueFISP is determined by T2*/T1 properties and ostly depending on TR. The speed and relative motion insensitivity acquisition help to make the technique reliable, even in patients no have difficulty with holding their breath. ecent advances in gradient hardware have led to a decreased nimum TR. This combined with improved field shimming pabilities and signal to noise ratio, has allowed TrueFISP imaging become practical for whole-body applications. There's mostly T2* eighting. With the used ultra short TR-times T1 weighting is almost possible. One such application is cardiac cine MR with high yocardium-blood contrast. Spatial and temporal resolution can be bstantially improved with this technique, but contrast on the basis the ratio of T2* to T1 is not sufficiently high in soft tissues. By oviding T1 contrast, TrueFISP could then document the hancement effects of T1 shortening contrast agents. These operties are useful for the anatomical delineation of brain tumors d normal structures. With an increase in SNR ratio with minimum R, TrueFISP could also depict the enhancement effect in myoma eri. True FSIP is a technique that is well suited for cardiac MR aging. The imaging time is shorter and the contrast between the ood and myocardium is higher than that of FLASH.

educed k-Space Sampling

Reduced k-space sampling methods include MR Fluoroscopy, urier-encoded keyhole imaging, random k-space sampling ethods. Spiral scan imaging and other fast or ultra-fast techniques n be included among these methods if acquisition yields complete k-space filling. Also, the Half Excitation method] uses half space filling exploiting k-space symmetry. images acquired using duced k-space sampling may suffer from reduced spatial resolution, ifacts, low tissue contrast, or be restricted to a small FOV. educed k-space sampling methods exploit different imaging gorithms - Fourier spatial encoding ordering strategies - for

temporal efficiency, and, in theory, can utilize a number of fundamental pulse sequence approaches. Also, some of these methods use the strategy of updating, rather than waiting to refill, the k-space image reconstruction buffer so that fast computing hardware can reconstruct and display images (from the mixture of image data in the buffer) in real-time without the delay of the standard acquire-delay-reconstruct-display paradigm.

MR FLUOROSCOPY

MR fluoroscopy techniques have been available for the last decade but predominantly based on gradient echo or EPI acquisitions providing T1 or proton weighted imaging . They have primarily been applied to cardiac and angiographic imaging. As a result of their limited contrast and spatial resolution, combined with their sensitivity to off resonance artefacts,

MR Fluoroscopy combines a fast MR pulse sequence (GRASS) and an efficient imaging algorithm (partial zero-filling of k-space) with specialized hardware for image reconstruction, and was developed for real-time visualization of dynamic processes. The approach of the MR Fluoroscopy method is to acquire less data for image reconstruction in order to improve temporal resolution in dynamic studies and to create the appearance of real-time image display. Improved temporal resolution is obtained, however, at the expense of reduced spatial resolution since the acquisition of higher spatial frequency information is bypassed in order to more rapidly update low spatial frequency image data

SPIRAL SCANNING,

A way of sampling image data for MR imaging in k space. As opposed to a standard procedure, where k-space is examined by sampling data points linearly, in spiral scanning k-space is scanned in one or several intertwined . Spiral scanning is more demanding on image reconstruction than standard scanning. When moving through k-space in a spiral fashion, the gradient fields are continously changing in a sinus-like form with decreasing frequency. Data acquisition requires nonlinear sampling. Potential advantages of

piral scanning are: k-space can be sampled more efficiently, omitting ata points at its edge where image information is less important; and nage data in the centre of k-space are acquired first, where the radient strength needed is small and thus flow effects are smaller, i. images acquired using spiral scanning are less prone to flow tefacts.

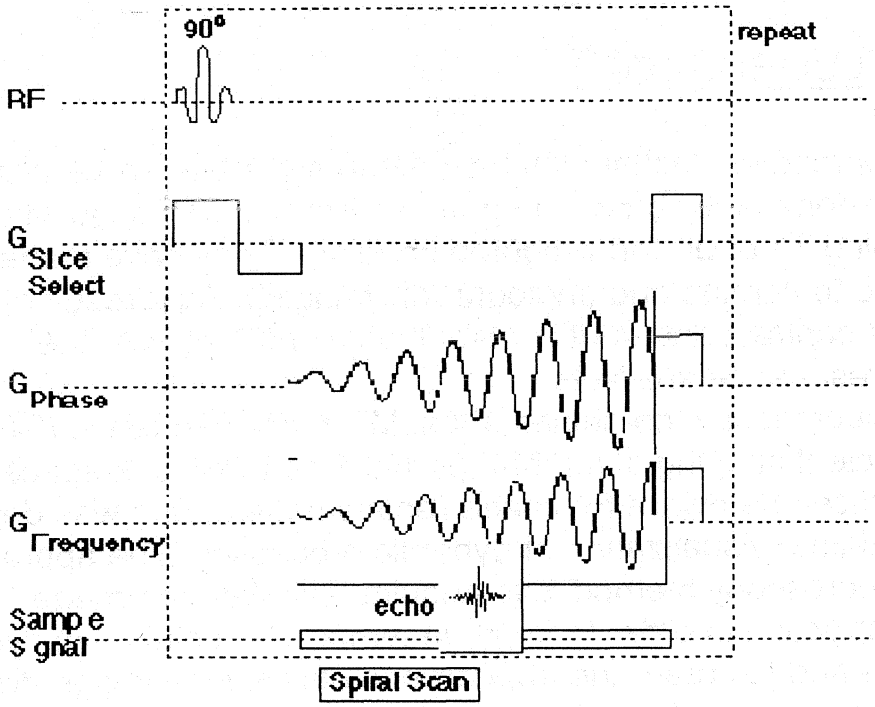

piral scanning is an echo planar imaging EPI sequence, as after a ngle excitation pulse the entire k-space is sampled, entailing the roblem that the signal amplitude decays with T2* during the neasurement. Hence, the signal from image data measured further ut on the spiral is underestimated to an unknown and variable egree. This problem can be remedied by using an interleaving or multishot" data acquisition technique .Where multiple intertwined pirals originating at the centre of k-space are traced consecutively, ut with fever turns per radial distance increment

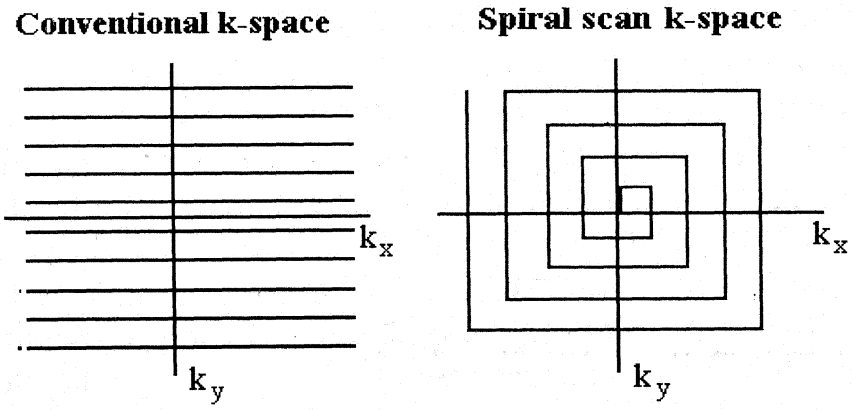

ECHO PLANAR IMAGING

This was also invented by Professor Sir Peter Mansfield..
In 2003,he got Nobel prize in medicine
1981-82-the first snap shot EPI image
1983-Firsy EPI images of the brain
EPI is a very fast MR imaging technique. It acquiring the entire mr image in fraction of seconds. In this multiple lines of imaging data are acquired after a single RF pulse. Its advantages over conventional

IR imaging is reduced imaging time, reduced motion artifact,
ossible to imaging the rapid physiological process of human body
In this technique the whole of k space is sampled in a single FID, so
iat the total scan time is typically less than 100 ms. This is a major
dvantage of EPI is, there are no motion artefacts, dynamic
rocesses (such as brain activation) can be scanned, quantitative
naging (measurement of T1 and T2 and other parameters) can be
erformed in a reasonable time However the images have a low
trinsic signal to noise ratio (although the signal to noise per unit time
very high, and this is what really matters), The magnetic field
radients have to be switched very rapidly. This means that low
nductance gradient coils are required, (and the sequence can be
ery loud at high field) The images are very sensitive to distortions
nd signal loss arising from gross variations in the magnetic field
cross the sample (T_2^* effects).High performance of gradient are
eeded to to allow rapid on and of switching of the gradient

YPES OF EPI
wo main types exist
1,single-shot EPI
2,multi-shot EPI
lewer techniques use as blipped phase-encoded gradient
lipped-EPI

ingle-shot EPI

In single-shot EPI all the lines in K-space are filled by multiple
radient reversal ,producing multiple echoes in a single RF-pulse
o achieve this ,read out gradient must be reversed rapidly from
naximum positive to maximum negative value. Each lobe of the read
ut gradient above or below the base line correspond to a separate
$_y$ line in the k-space. so the number of phase encoding steps Ny is
qual to the +ve & -ve lobes of read out gradient In earlier EPI
nethods,the phase-encoding gradient was kept on continuously
uring the acquisition resulting in the zigzag coverage of k-space
This lead to some artifacts during FT compared with conventional
-space trajectories.To rectify this problem ,the phase encoding
radient was subsequently applied briefly during the time when the

read out gradient was zero .This method was reffered to as blipped phase encoding and this k-space trajectory is much easier on FT.

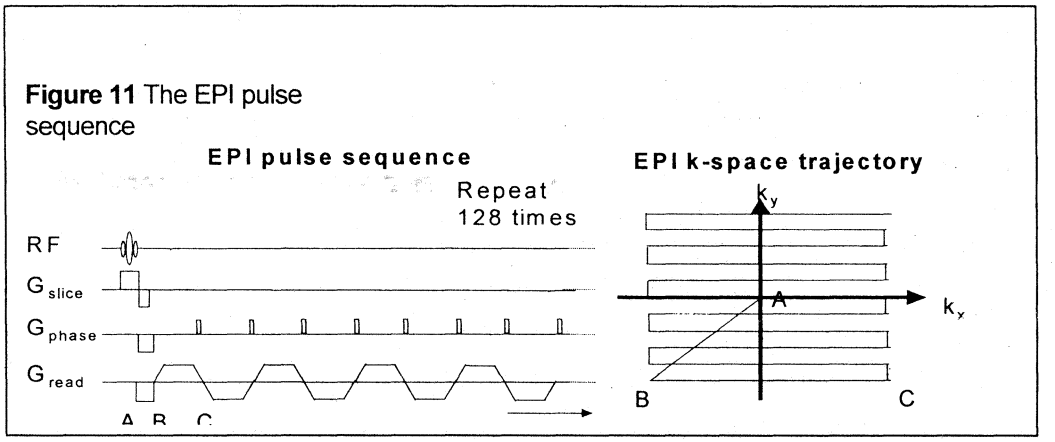

Figure 11 The EPI pulse sequence

The susceptibility artifact is more in single shot EPI, and the phase errors tends to propagates along the phase-encode axis,

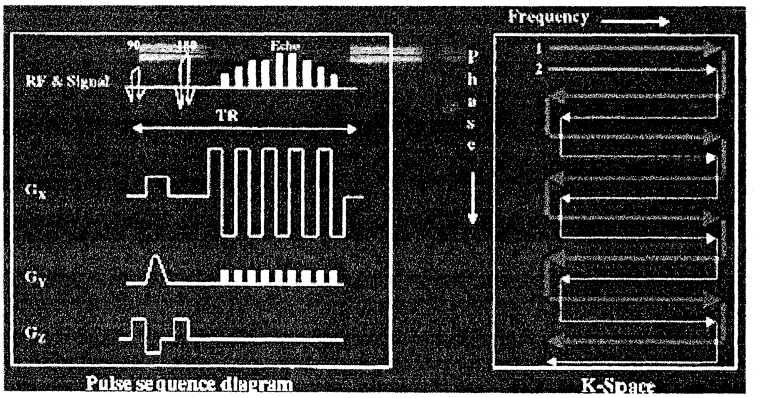

Multishot- EPI

ulti-shot EPI ,the readout is divided in to multi-shot EPI or nents (Ns),so that

Ny=Ns X ETL

is echo train length ,is the number of lines in each segment .this so called **segmental EPI**

antages of multi-shot EPI (compared with single-shot EPI)

s technique places less stress on the gradients compared with e-shot EPI

ase errors susceptibility artifact are less

dvantages of multi-shot EPI (compared with single-shot EPI)

ulti-shot EPI takes longer to perform than does single-shot EPI

lti shot EPI is more susceptible to motion artifact

ITRAST IN EPI

rast in EPI depends on the root pulsing sequence .For SE-EPI are using 90°-180°-SE root sequences is applied before the module ,like that we can produce the gradient echo,IR-uences, diffusion etc

Spin Echo EPI

,Gradient EPI

pin Echo EPI

efocusing pulses can be applied after th initial excitation pulse application of the refocusing pulse helps to clean up some of the acts by magnetic field inhomogenities and chemical shift.

dient Echo EPI

EPI is acquired with a RF pulse followed by a number of ent blips creating a train of gradient echoes.in this sequence es are acquired in one TR pass in milliseconds.

dient EPI is less time than SP EPI

Special Hardware Requirements

gradient strength, rise time, and duty cycle are markedly increased
gradient coils capable of a maximum amplitude of 20 mT/m
minimum rise time of 0.1 msec
slew rate of 200 T/m per second
duty cycle of 50%–60%
First generation Epi hardware-resonant systems
Second generation Epi hardware-nonresonant systems

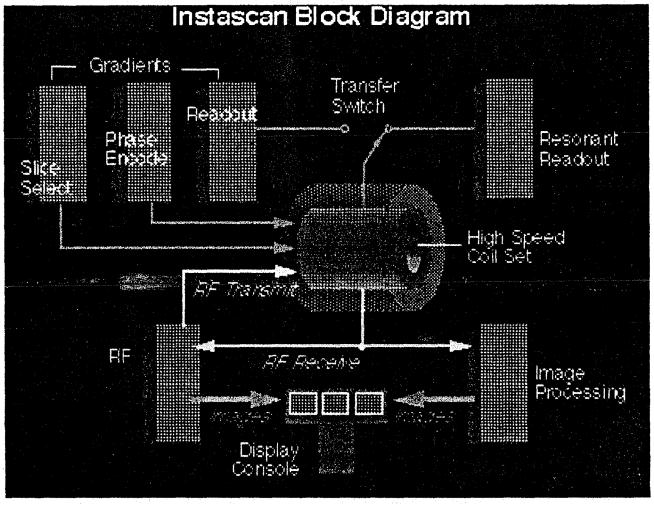

Saturation Recovery Sequence

The saturation recovery (SR) sequences are rarely used for imaging now. Their primary use at this time is as a technique to measure T1 times more quickly than an inversion recovery pulse sequence. Saturation recovery sequences consist of multiple 90 degree RF pulses at relatively short repetition times (TR). An example of a SR sequence is shown below. Residual longitudinal magnetization after the first 90-degree RF pulse is dephased by a spoiling gradient (in this case with the slice select gradient). Longitudinal magnetization that develops during the TR period after the dephasing gradient is rotated into the transverse plane by another 90 degree pulse. A gradient echo is acquired immediately after this. The signal will reflect T1 differences in tissues because of different amounts of longitudinal recovery during the TR period.

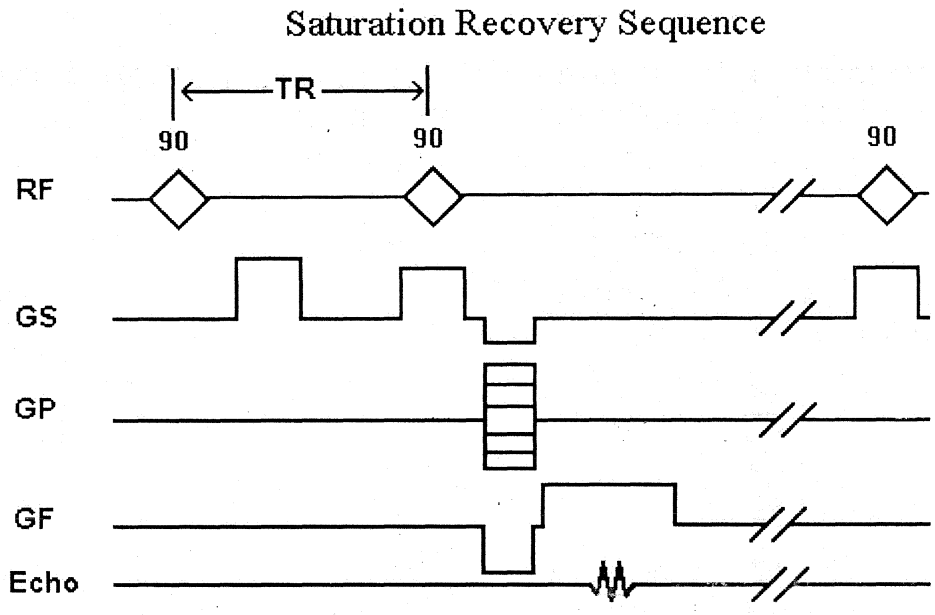

SMASH (Simultaneous Acquisition Of Special Harmony)

SMASH is such a technique. It uses combinations of component coil signals in a radio-frequency (RF) coil array to substitute for omitted gradient steps, reducing the burden on the gradients and allowing multiple components of the spatial encoding required to generate an MR image to be performed in parallel.[12] This technique has been shown to achieve a four- to eightfold reduction in image acquisition time, with no compromise in spatial resolution.

TRICKS

This technique uses an increased sampling rate for lower frequencies, temporal interpolation of k-space views, and zero filling in the slice-encoding direction. When appropriately combined, these elements permit reconstruction of a series of 3-D image sets, having an effective temporal frame rate of one volume every two to six seconds, with no serious compromise in the spatial resolution.

RARE. (Rapid acquisition with relaxation enhancement)

The RARE is a fast spin echo sequence using a series of RF pulses, after an initial P/2 RF excitation pulse, to evoke a train of

multiple individually phase encoded echoes. The RARE method is initiated by a slice-selective P/2 RF excitation pulse applied simultaneously with a gradient in the slice-selective direction, which is inverted after the RF pulse ends for spin rephasing. A short dephasing gradient pulse is then applied in the frequency encoded direction. Next, a P RF pulse is transmitted accompanied by a gradient in the slice-selective direction. A phase encoding gradient pulse follows, after which is applied the readout frequency encoding gradient and the sampling of an echo occurs. Echo acquisition is immediately followed by a rephasing gradient in the phase encoded direction (ie. phase 'unwound'). A subset of sequence events is repeated 4-16 times, including the P RF pulse, slice-selective gradient pulse, phase encoding gradient, readout gradient and rephasing gradient in the phase encoding direction. Optional 'crusher' gradients can be used before and after the slice-selective gradients (simultaneous with the P RF pulse) to improve slice definition. FAISE (Fast acquisition interleaved spin echo) is a hybrid RARE technique with an special phase encode gradient order (ie. special imaging algorithm) that traverses k-space in an interleaved manner giving straightforward T2 contrast manipulation.

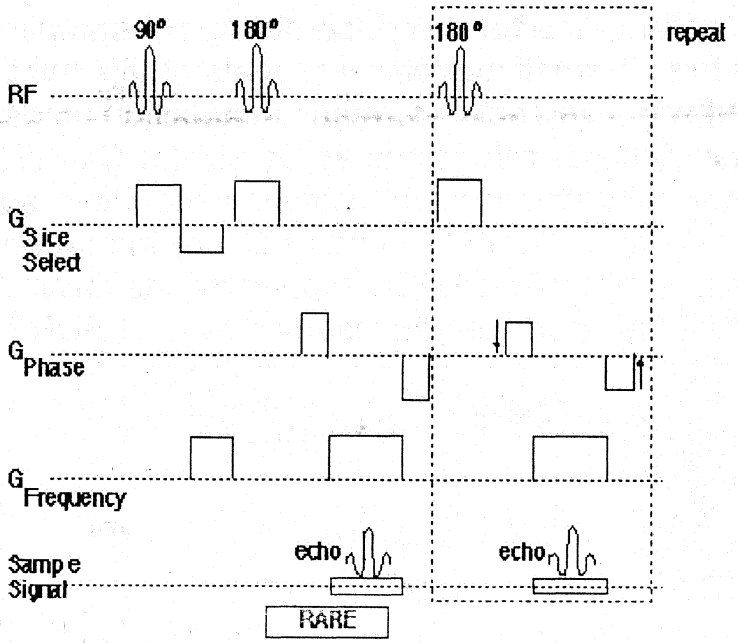

The advantage of fast spin echo methods is that a number of echoes can be acquired in a single TR period yielding a highly efficient method for obtaining proton density-weighted or strongly T2-weighted

es, 3D images [], or for dynamic imaging. The SNR of fast spin
methods is near that of standard spin echo imaging, and
rally surpasses that of images acquired using gradient-recalled
methods]. Several 256x256 images can be obtained in a multi-
acquisition in 30-60 sec. Disadvantages of RARE images are
resence of T2-dependent effects along the image phase
ding axis, insensitivity to susceptibility effects and increased RF
er deposition (due to the multiple P RF pulses) which can be
come by using an a degree RF excitation pulse (a < P) in place
e repeated P RF pulse

ST.

BURST is a ultra-fast imaging method utilizes a rapid sequence
ort very low flip angle RF excitations of varying amplitudes to
rate multiple echoes accompanied by either constant is an
nple of a BURST sequence) or switched gradients to improve
. BURST sequences can be designed in several ways with either
e and frequency encoding gradients occuring during the BURST
ulses and/or after the pulse during RF sampling. An image is
ed from a small number of repeats of this multi-echo sequence
nent with even sub-100 msec acquisition times possible. Related
-fast methods referred to as DUFIS (or OUFIS) imaging] have
been described that can similarly acquire images in about 10
c - similar to BURST in that relatively infrequent gradient
hing is required. BURST-type methods have shown promise for
l 3D imaging. A current disadvantage of BURST-type images is
ow SNR.

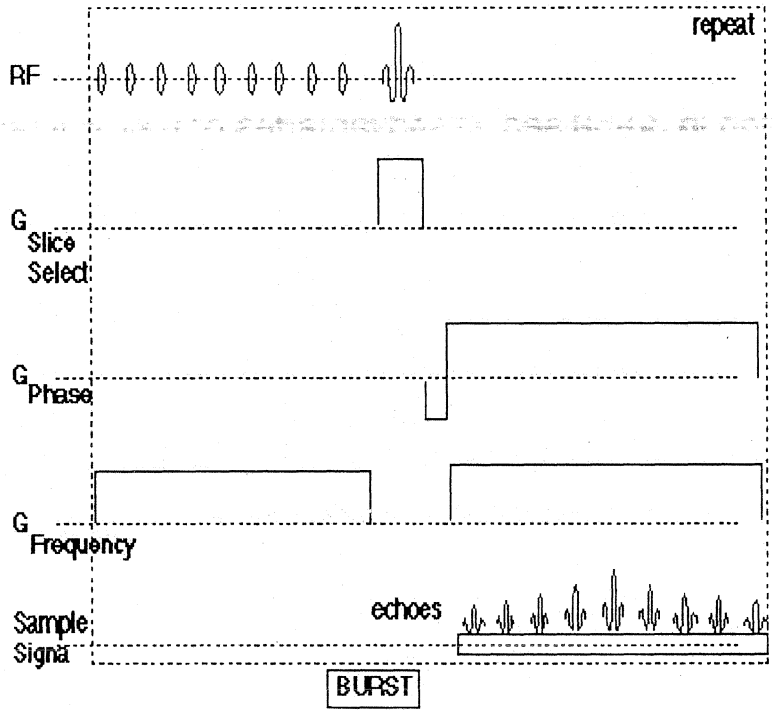

GRASE.

The gradient- and spin-echo (GRASE) method combines magnetization refocusing using □ RF pulses interleaved with refocusing gradient pulses to form a train of echoes. Using the CPMG method, □ RF refocusing pulses are used to create an echo train, similar to fast spin echo techniques. Three or more gradient-recalled echoes are also then created during the period between each RF echo using a combination of stepped phase encoding gradients and switched frequency encoding gradients. An image is formed from a small number of repeats of this multi-echo sequence segment. (Multi-shot spin echo planar imaging is equivalent to GRASE.) Used in multi-slice 3D imaging GRASE imaging can yield more than 20 T2-weighted 256x256 images in about 30 sec. A disadvantage of GRASE, shared by fast spin echo sequences, is that magnetization remains saturated after a single shot, requiring a delay before the next acquisition. GRASE images are less affected by chemical shift and field inhomogeneities, advantageously more sensitive to magnetic susceptibility differences, and are acquired with reduced RF deposition compared to fast spin echo techniques and is more rapid.

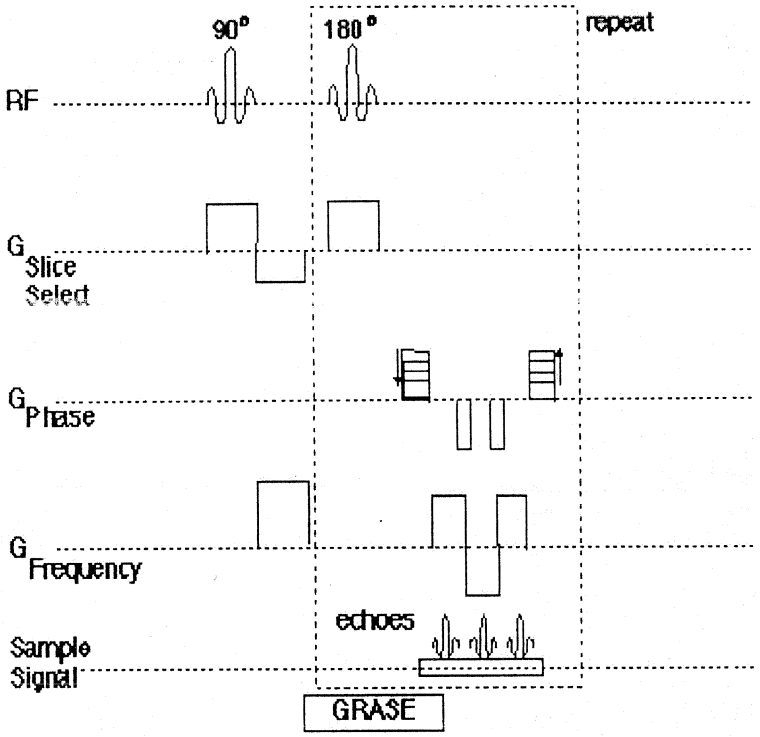

RALLEL Imaging

oduction:

ce the development of the NMR phased array in the late 1980s, icoil arrays have been designed to image almost every part of the an anatomy. These multicoil arrays are primarily used for their eased signal-to-noise ratio (SNR) compared to volume coils or e surface coils. Sensitivity encoding for MRI (SENSE), ultaneous acquisition of spatial harmonics (SMASH), and sitivity profiles from an array of coils for encoding and nstruction in parallel (SPACE-RIP) are MRI techniques designed educe the scan time. The reduction is achieved by under sampling ace and recording images simultaneously from multiple imaging s. Under sampling reduces the acquisition time and the use of iple RF coils eliminates the wraparound caused by the under pling.

is technique the component coils of an array to partially replace ial encoding which would normally be performed using gradients, eby reducing imaging time.

In general, higher acceleration factors can be achieved, approaching the number of coil elements.

- Huchinson & Raff (1988) and Kwiat & Einav (1991) suggested using arrays of coils in place of all phase encoding steps.
- Requires one coil for each line of k-space.
- Signals seen by adjacent coils must be sufficiently distinct.

- Kelton et al: "An algorithm for rapid image acquisition using multiple receiver coils," 8th SMRM proc., 1172 (1989).
- Ra & Rim: "Fast imaging using subencoding data sets from multiple detectors," 10th SMRM proc., 1240 (1991); Mag. Res. Med. 30, 143 (1993).
- A set of aliased images are produced by an array of receiver coils using subencoded data.
- These images are resolved to an aliasing-free image by using the distance-dependant sensitivity information for each coil.

Phased Array

- Phased array is the use of several surface coils.

–Advantages:
- Good SNR
- Large FOV

–Disadvantages:
- Coil coupling - "magic separation" geometry
- Multiple receiver channels ($)

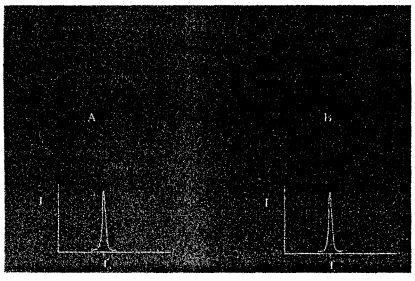

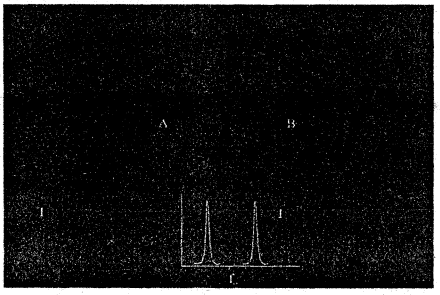

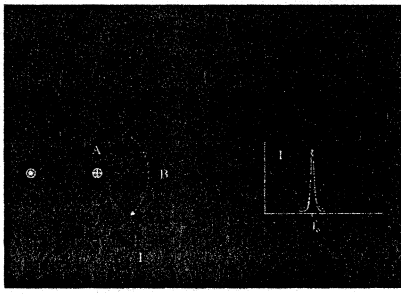

xtending the phased array to more channels:
3 channel "Bucky" array for 1.5T

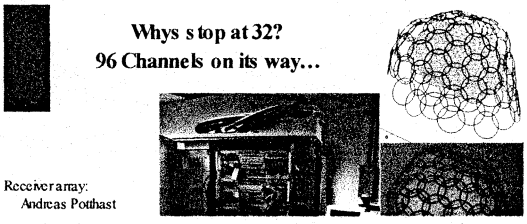

Parallel imaging key points

sing occurs as a result of sub sampling, Parallel imaging
rithms aim at removing aliasing or regenerating the missed *k*-
ce lines using the coil sensitivities. Subsampling factor is limited
retically by the number of coils

allel reconstruction techniques

- SENSE (SENSitivity Encoding)
- PILS (Partially Parallel Imaging with Localized Sensitivites)
- SMASH (SiMultaneous Acquisition of Spatial Harmonics)
- GRAPPA (GeneRalized Auto-calibrating Partially Parallel Acquisitions)

SPACE RIP (Sensitivity Profiles from an Array of Coils for Encoding and Reconstruction In Parallel)

SENSE (SENSitivity Encoding)

sitivityencoding (SENSE) is based on the fact that receiver
sitivitygenerally has an encoding effect complementary to Fourier
aration by linear field gradients. Thus, by using multiple
iver coils in parallel scan time in Fourier imaging can be
siderably reduced. The problem of image reconstruction
sensitivity encoded data is formulated in a general fashion
solved for arbitrary coil configurations and k-space sampling
erns. Special attention is given to the currently most
tical case, namely, sampling a common Cartesian grid with
ced density. For this case the feasibility of the proposed
nods was verified both in vitro and in vivo. Scan time was
ced to one-half using a two-coil array in brain imaging.With
rray of five coils double-oblique heart images were obtained
ne-third of conventional scan time.

THEORY AND METHODS

In this section SENSE theory is presented and methods for image reconstruction from sensitivity encoded data are derived. The theory addresses the most general case of combining gradient and sensitivity encoding. That is, no restrictions are made as to the coil configuration and the sampling pattern in *k*-space. Two reconstruction strategies are discussed. The first approach strictly aims at optimal voxel shape and is called *strong* reconstruction for convenience. In *weak* reconstruction, the voxel shape criterion is weaker in favor of the SNR. With both strategies the reconstruction algorithm is numerically demanding in the general case. This is mainly because with hybrid encoding the bulk of the work of reconstruction can usually not be done by fast Fourier transform (FFT). However, it is shown that in weak reconstruction FFT can still be applied if *k*-space is sampled in a regular Cartesian fashion. For this reason sensitivity encoding with Cartesian sampling is particularly feasible.

Sensitivity Encoding With Cartesian Sampling of k-Space

In two-dimensional (2D) Fourier imaging with common Cartesian sampling of *k*-space, sensitivity encoding by means of a receiver array permits reduction of the number of Fourier encoding steps. This is achieved by increasing the distance of sampling positions in *k*-space while maintaining the maximum *k*-values. Thus scan time is reduced at preserved spatial resolution. The factor by which the number of *k*-space samples is reduced is referred to as the *reduction factor R*. In standard Fourier imaging, reducing the sampling density results in the reduction of the FOV,causing aliasing. In fact, SENSE reconstruction in the Cartesian case is efficiently performed by first creating one such aliased image for each array element using discrete Fourier transform (DFT). The second step then is to create a full-FOV image from the set of intermediate images. To achieve this one must undo the signal superposition underlying the fold-over effect. That is, for each pixel in the reduced FOV the signal contributions from a number of positions in the full FOV need to be separated. As depicted in Fig. 1, these positions form a Cartesian grid corresponding to the size of key to signal separation lies in the fact that in each single-coil image signal superposition occurs with different weights according to local coil sensitivities. Consider one pixel in the reduced FOV and the

rresponding set of pixels in the full FOV (Fig. 1). Let *n*P denote the mber of pixels superimposed and *n*C the number of coils used. ssemble in the vector ***a*** the complex image values the osen pixel has in the intermediate images. The complex il sensitivities at the *n*P superimposed positions form an C 3 *n*P *sensitivity matrix S*:

= *U**a***,

here the resulting vector ***v*** has length *n*P and lists separated pixel lues for the originally superimposed positions. By repeating this ocedure for each pixel in the reduced FOV a non-aliased full-FOV age is obtained.

$$SNR_{\rho}^{red} = \frac{SNR_{\rho}^{full}}{g_{\rho}\sqrt{R}} .$$

his relation confirms an upper bound for SNR haracterized by the square root of the number of samples cquired. The geometry factor describes the ability with the sed coil configuration to separate pixels superimposed by iasing. In practice it allows a priori SNR estimates and ovides an important criterion for the design of dedicated il arrays

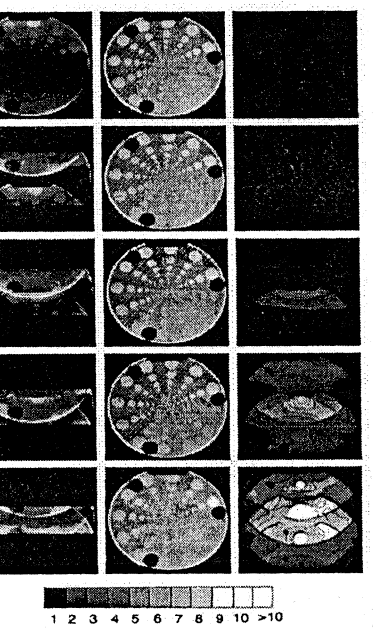

SENSE imaging of a quality phantom with creasingreduction factor Rindicated on the left. Phase encoding in rtical direction. Left: conventional sum-of-squares images. Middle: ENSE reconstruction from the same data. Right: maps of the lative noise level as predicted by SENSE theory, colored according the gray-scale on the far right (arbitrary units).

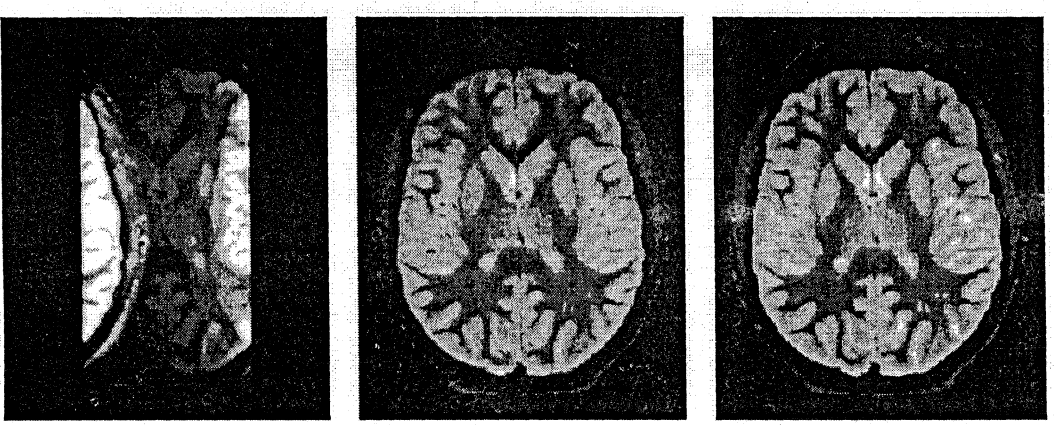

a **b** **c**

G. 7. Transverse brain images obtained with TSE using two coils. **b:** Reduction factor R=2.0, conventional single-coil image and ENSE reconstruction. **c:** SENSE image from fully Fourier encoded ata.

H (SiMultaneous Acquisition of Spatial Harmonics)

MASH is introduced. The SMASH technique exploits
ty variations in a surface coil array to substitute for spatial
ions normally produced by phase-encoding gradients.11 This
oil encoding in place of gradient encoding allows the whole of
to be traversed using a reduced number of phase encoding
steps, thereby reducing image acquisition times. The
of phase-encoding gradients is to impose sinusoidal
ions of magnetization across the image plane. The MR signal
ed against these sinusoids then corresponds to spatial Fourier
ents of the image, or the familiar k-space lines.
MASH technique, some of these sinusoidal modulations, or
harmonics', are generated by manipulations of component
sitivities, rather than by gradient-induced modulations of
ization.

y of rf coils contains spatial information in the form
mponent coil sensitivities (Figure 2). In a linear surface
y with adjacent components, each coil j has a distinct
rlapping sensitivity Cj(x, y). By forming appropriate linear
ations of component coil signals (Figure 3), we may
e composite sensitivity profiles C^{tot} which oscillate in

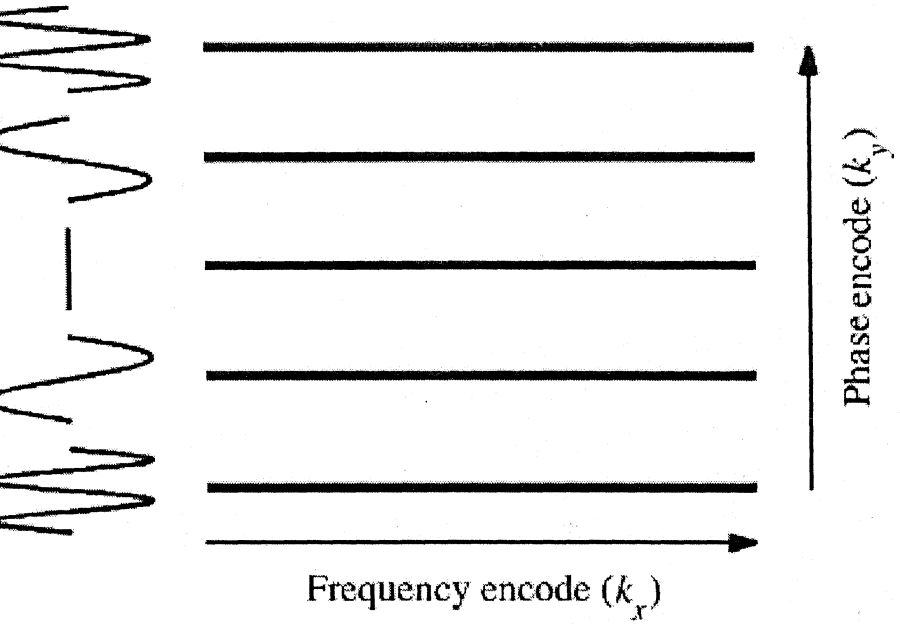

gure 1 A k-space schematic, indicating the spatial modulations sulting from phase-encoding gradients. Gradient steps on either side the central $k=0$ line correspond to various harmonics of spin odulation across the image plane

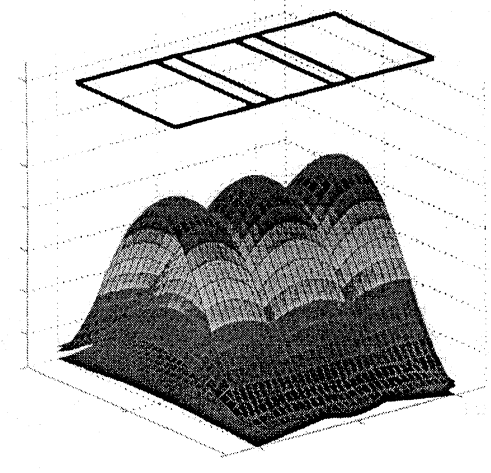

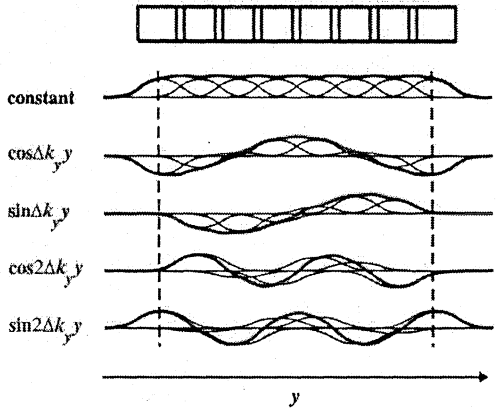

Figure 3 Multiple spatial harmonic profiles derived by linear combination of component coil sensitivities in an eight-element array

Figure 2 The sensitivities of a linear coil array. Each of the three

e 2 The rf sensitivities of a linear coil array. Each of the three
pping sensitivity distributions corresponds to one of the three
nent coils in the array pictured at the top. (The conductor paths
acent component coils are also typically overlapped, as shown in
xample, to minimize inductive coupling between coils.) Only
vity magnitudes are shown here. In practice, coil sensitivities
lso have spatially varying phase distributions

entation

portant first step in a practical SMASH implementation
easure the rf sensitivities of the various array
ts. These sensitivities may be extracted in a straightforward
from images of homogeneous phantoms, since
ensity variations in such images may be traced to variations
sensitivity. Typically, intensity profiles across an
plane of interest are extracted from a stored phantom
t and are used as sensitivity references.

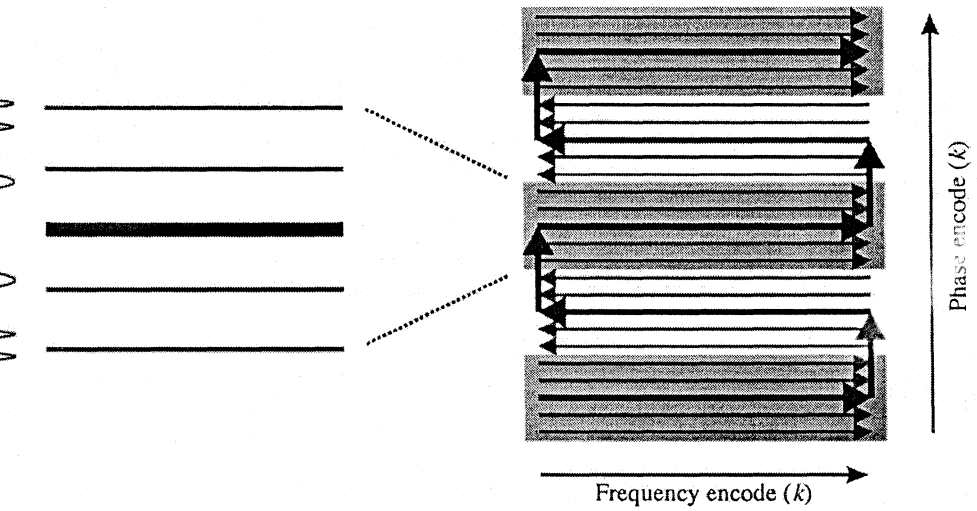

Schematic *k*-space trajectory for a partially parallel acquisition using five spatial harmonics. Thick lines represent *k*-space lines
ing to applied phase-encoding gradient steps, while thin lines represent additional *k*-space lines reconstructed using the linear
ns shown in Figure 3. The additional reconstructed lines substitute for omitted phase-encoding gradient steps

-SMASH,

number of reference k-space lines are added to the
tion, and the relation between these reference lines and the
MR signal data lines are used to `train' SMASH reconstructions

AUTO-SMASH,a small number of reference k-space lines are
ded to the acquisition, and the relation between these reference
es and the usual MR signal data lines are used to `train' SMASH
constructions directly in k-space.

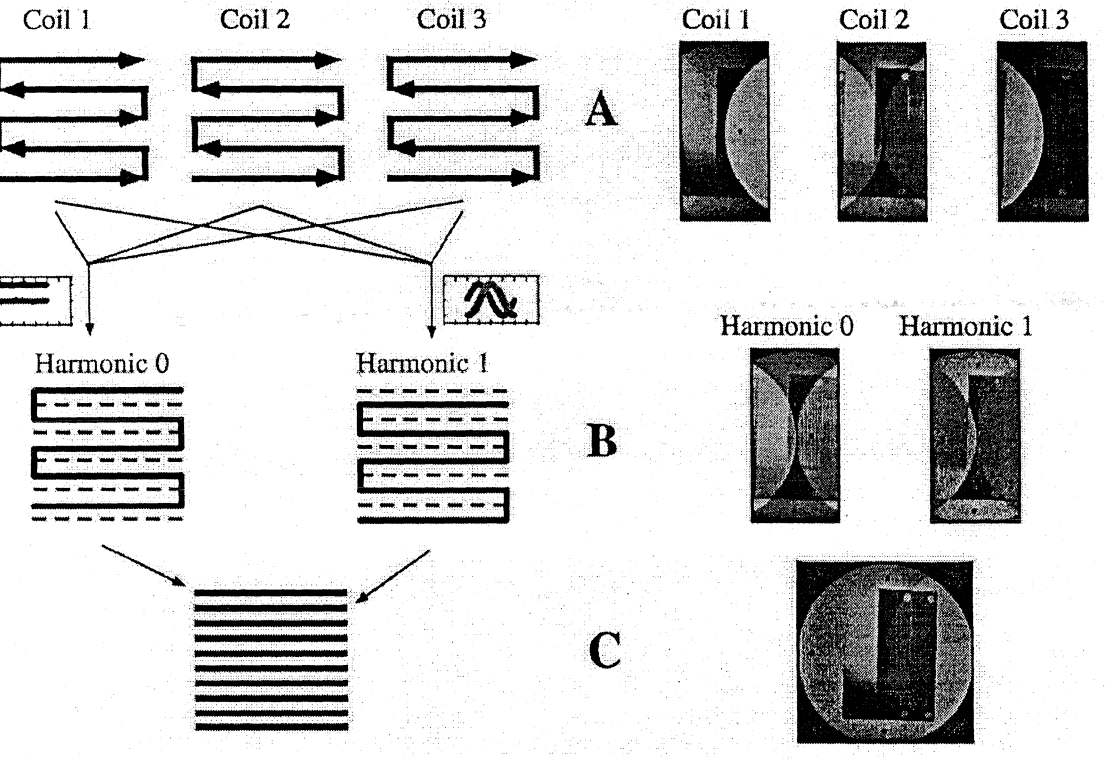

gure 5 Schematic representation of the SMASH reconstruction
ocedure (left: k-space cartoon, right: corresponding phantom
ages). (A) Acquisition of data with reduced phase encoding. (B)
rmation of shifted data sets using spatial harmonic
mbinations.(C) Interleaving of shifteddata sets to generate a full
gnal matrix, corresponding to an image with full FOV

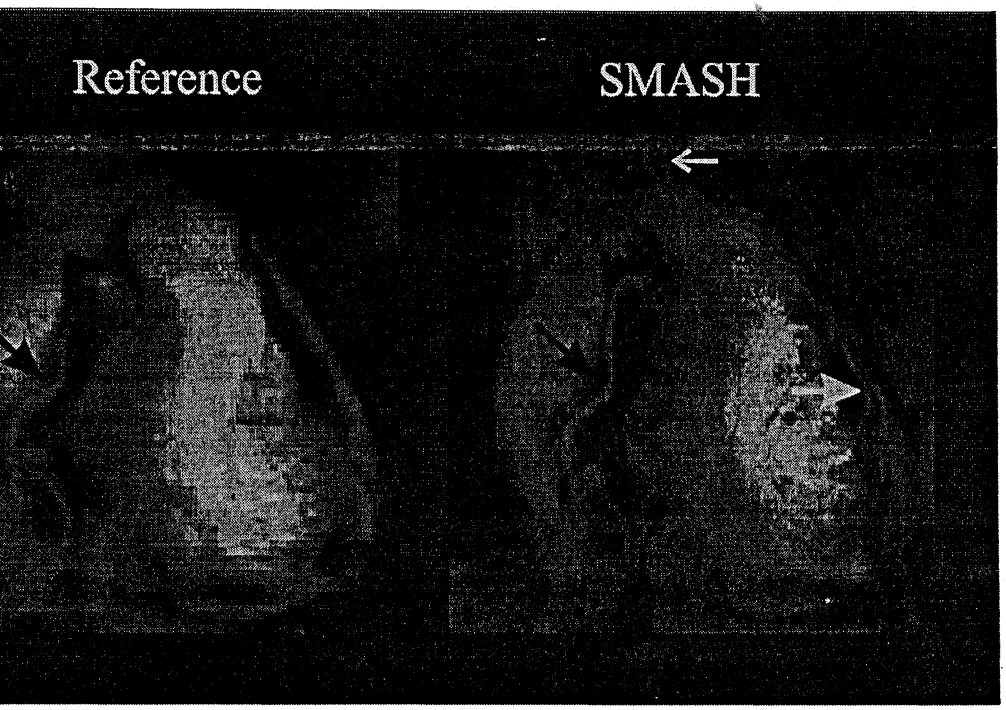

cardiac images showing the use of SMASH for increased
esolution

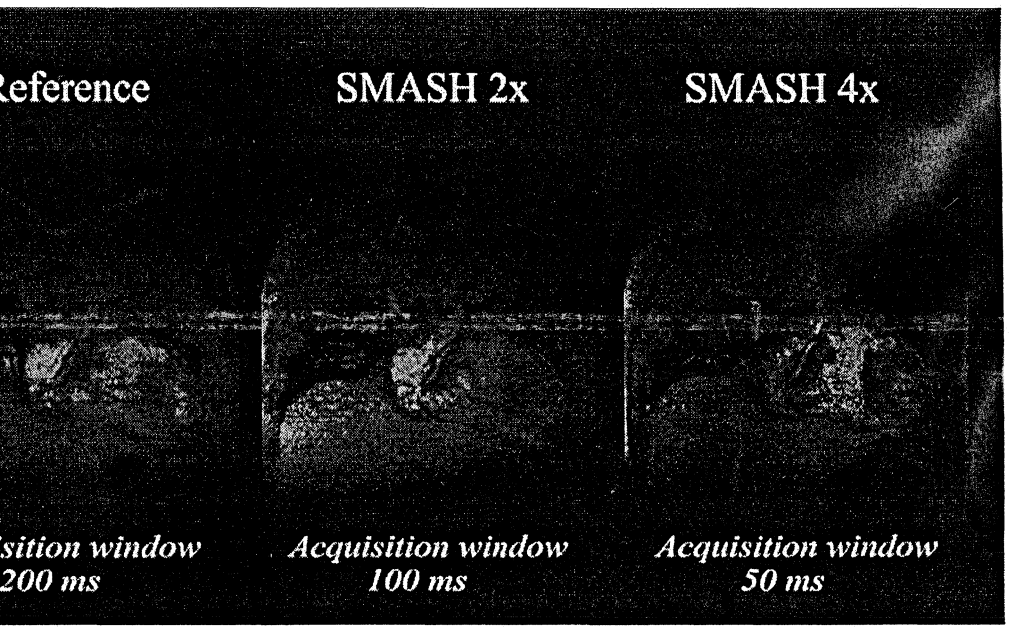

cardiac images from a 3D data set demonstrating the use of
to increase temporal resolution at fixed spatial resolution

UTO-SMASH Imaging

hod uses a VD *k*-space sampling approach and shows
y to improve the image quality without significantly

reasing the total scan time. This new *k*-space adapted calibration
proach is based on a *k*-space–dependent density
nction. In this scheme, fully sampled low-spatial frequency
ta are acquired up to a given cutoff-spatial frequency. Above
s frequency, only sparse SMASH-type sampling is performed.
top of the VD approach, advanced fitting routines,
ich allow an improved extraction of coil-weighting factors
the presence of noise, are proposed. It is shown in simulations and
vivo cardiac images that the VD approach significantly increases
potential and flexibility of rapid imaging with AUTO-SMASH.

RAPPA

rrent parallel imaging techniques for accelerated imaging
quire a fully encoded reference data set to estimate the spatial
il sensitivity information needed for reconstruction. In dynamic
rallel imaging a time-interleaved acquisition scheme can be used,
ich eliminates the need for separately acquiring additional
ference data, since the signal from directly adjacent time frames
n be merged to build a set of fully encoded full-resolution reference
ta for coil calibration. In this work, we demonstrate that a time-
erleaved sampling scheme, in combination with autocalibrated
RAPPA

e GRAPPA parallel imaging reconstruction is performed in *k*-space
calculating the missing *k*-space lines in each coil in the array using
weighted sum of adjacent lines from all coils.

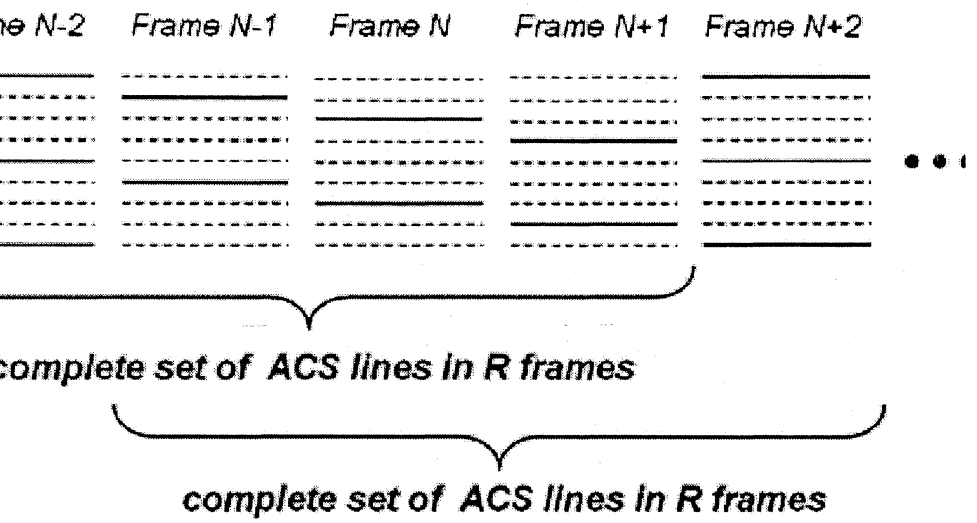

complete set of ACS lines in R frames

ral,more neighboring frames can be averaged to increase the the ACS(autocalibration signal) data, resulting in a potentially d GRAPPA reconstruction.

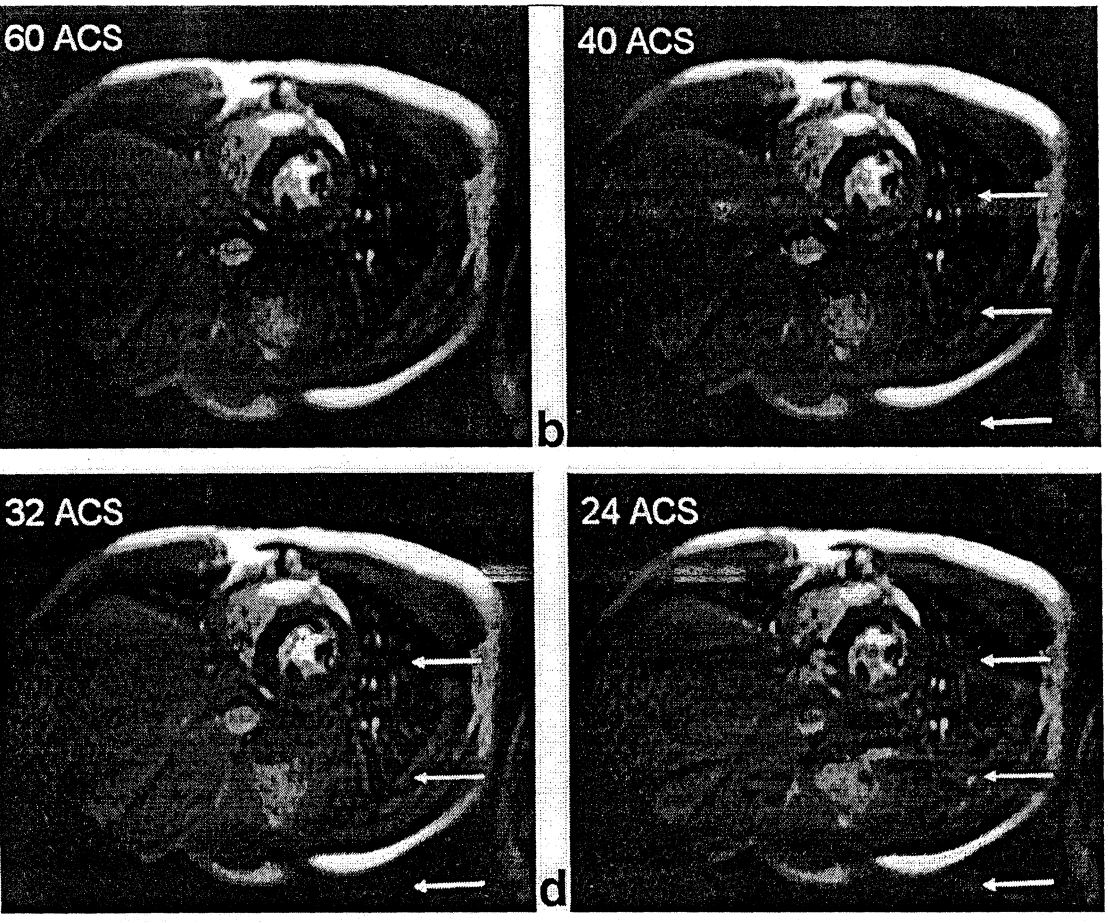
60 ACS
40 ACS
b
32 ACS
24 ACS
d

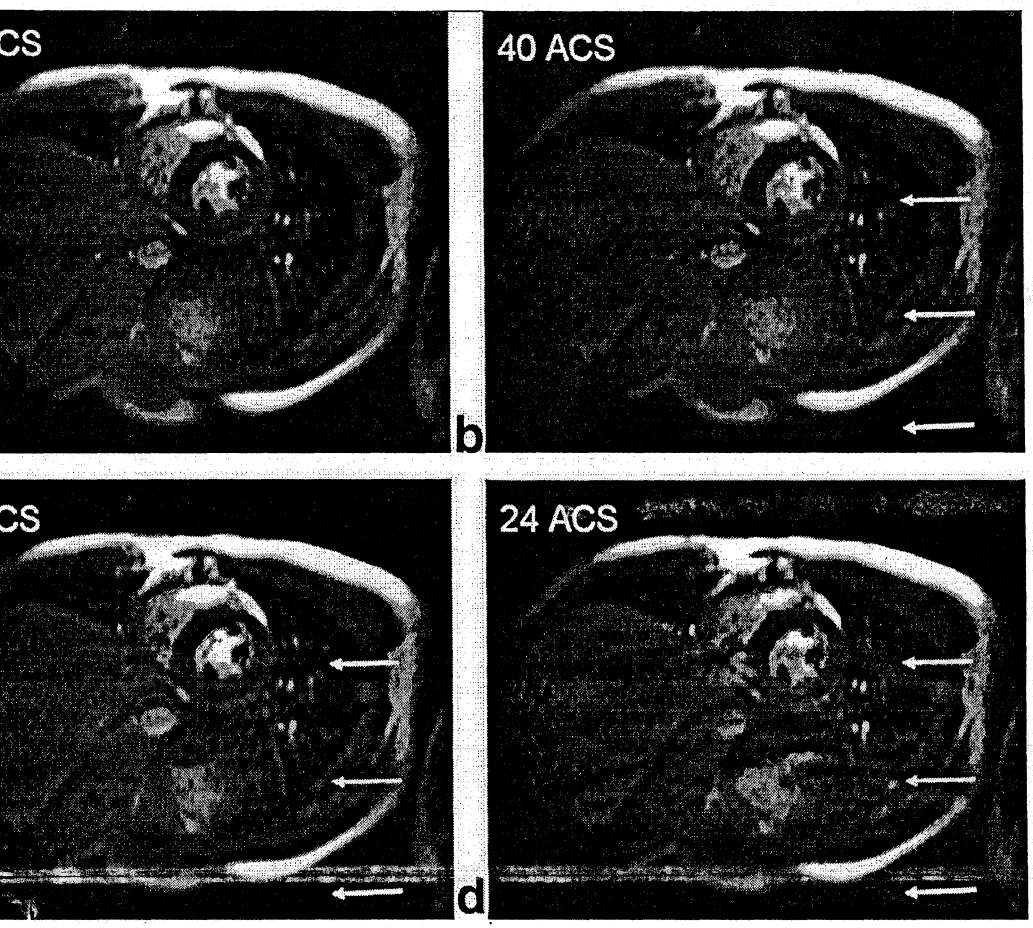

Rate 4 undersampled example images after GRAPPA
truction using (**a**) 60 ACS lines (full spatial resolution),
ACS lines, (**c**) 32 ACS lines,and (**d**) 24 ACS lines as reference
he image quality improves significantly with increased number
lines. Residual aliasing artifacts are visible even
ACS lines as reference data.

NITATIONTRANSFER CONTRAST IMAGING

tization transfer (MT) is a unique contrast mechanism in
tic resonance (MR) imaging that has been known for the past
e. Magnetization transfer contrast (MTC) is most useful in two
reas, improving image contrast and tissue characterization.
as also proven to be extremely useful in the reduction of

ckground signal in MR angiography and improves the appreciation issue enhancement by intravenous contrast agents.

sis of Magnetization Transfer

e signal obtained in clinical MR imaging comes from mobile otons. These are largely present in free water with a smaller ntribution from lipid. There are, in addition, a large number of otons in tissues contained in macromolecules or in water bound to ese macromolecules. No signal is normally detected from these otons by standard clinical imaging techniques because they have a y short T2 value (of the order of 1 ms or less) and any transverse gnetization is rapidly dephased before data collection is possible. ere is, however, a constant exchange of magnetization between protons in these two pools, the free pool and the bound pool, ich occurs by through-space dipole-dipole interactions or probably s importantly direct chemical exchange. By means of this erchange, the bound pool influences the signal obtained from the e pool even though the bound pool cannot be directly visualized. In imaging, the normal equilibrium between free and bound pools is rturbed and the resulting contrast is referred to as magnetization nsfer contrast and indicates the exchange processes with the und pool in that particular tissue. Wolff and Balaban, first produced vivo images with MTC and described two-pool concept of agnetization transfer. They coined the terms free (Hf) and restricted r) proton pools to describe the exchange compartments. These thors perturbed the normal equilibrium between free and bound ols by selectively saturating the bound pool (Fig. 1).

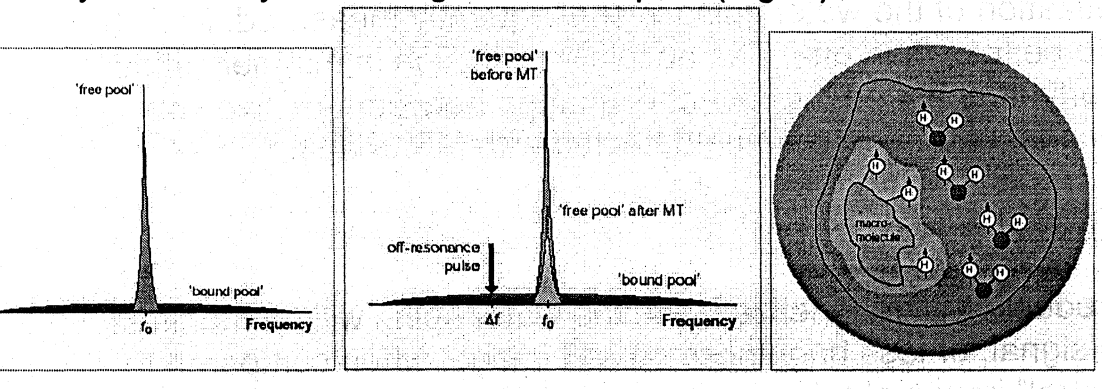

ure: Schematic diagram of water and macromolecule proton widths (top), and the use of an off-resonance pulse to detect gnetization transfer in tissue where both lines overlap (bottom)

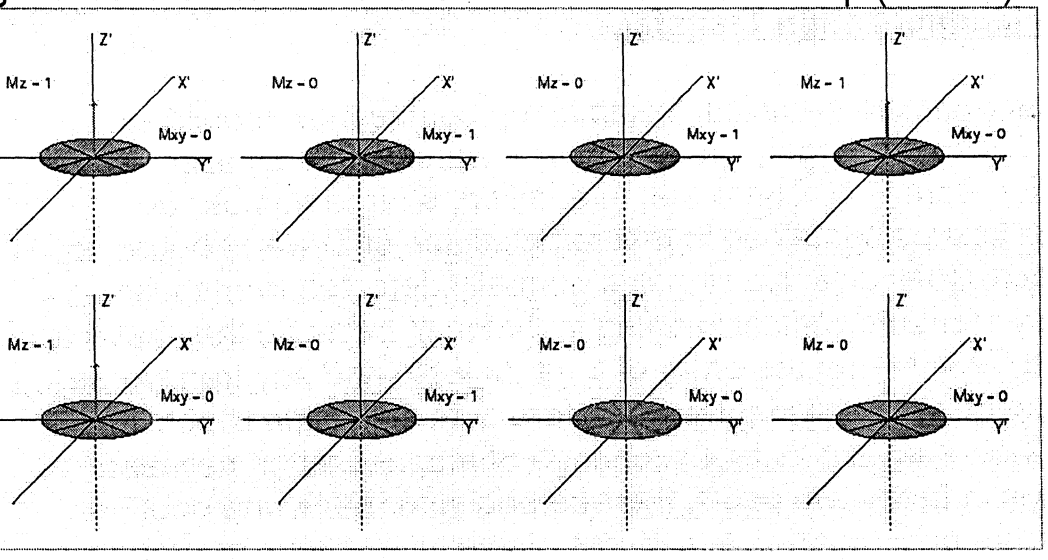

ective saturation:

possible to saturate the macromolecular spins (i.e. to reduce their gnetization to zero) preferentially using radio frequency pulse. The tricted motion of protons results in a very short spin-spin relaxation e (T2). This results in a very broad absorption line shape (20-40 z) than the mobile spins (narrow water resonance peak of 15Hz), king them as much as 106 times more sensitive to an propriately placed radio frequency pulse. The saturated cromolecular spins, with zero magnetization will exchange for ter spins having magnetization of one. Thus, when the gnetization of the water spins is subsequently measured, it will be nd to be less than one. The absolute reduction in magnetization clearly depend, on the rate of exchange between the two spin oulations, and hence can be detected with MR imaging.

Contrast:

he reduction of magnetization in the water spins will be manifest less signal, or less brightness on MR image, when compared to "control" image obtained without the MT preparation. The crease will be larger in regions where exhange of magnetization is re efficient, determined by the relative proportion of the hydrogen

oms of the two pools, their intrinsic relaxation times and the change rate. Although saturation is never perfectly selective in o, contrast between areas exhibiting varying degrees of MT effect developed and superimposed upon the intrinsic contrast of the seline image, be it proton-densitweighted(W) image, T1-W image, some combination.

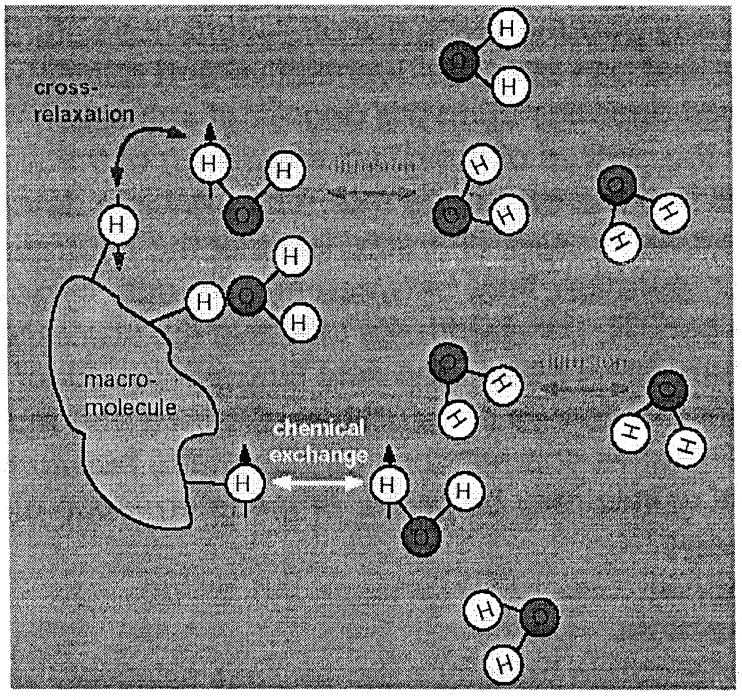

aturation transfer techniques:

hree techniques for saturating the bound water have been studied:) off-resonance (radio frequency pulses applied at a frequency that offset from the "free" water resonance) continuous wave excitation), (b) off-resonance shaped pulses, and (c) on-resonance binomial ulses[4,5]. The off-resonance shaped pulses are now the ommonest saturation transfer techniques for clinical imaging.

agnetization transfer ratio:

is a quantitative measure of the MT effect on tissues. It is the egree of signal suppression of a given tissue compared with the onventional PD or T1-W image. The MT ratio (MTR) may be simply btained by collecting a pair of identical images (PD or T1-W), one ith and one without MT saturation.. For each region of interest ROI), MTR is calculated from the two images using the formula:

$R = \{1 - \frac{Ms}{Mo}\} x\ 100\%$

ere Mo, Ms represent the signal intensity with the saturation pulse nd on, respectively.

trolling parameters in saturation transfer:

re are several key parameters in the off-resonance saturation sfer technique that can alter the quantitative and qualitative MTC. MTR measured depends upon the degree of saturation of the nd water, and the degree of the direct saturation of the signal of mobile protons and the exchange rate. The principle determinants g the base sequence used, characteristics of the saturating pulse se type, power, duration, time between pulses, duty cycle i.e. ber of pulses per TR, bandwidth, its effective flip angle), offset uency of the saturating pulse, and field strength [6]. All of these racteristics alter the degree of saturation obtained and must be wn before quantitative comparisons can be made between clinical lies. Numerical values may be given, or the information displayed a difference image.

ss relaxation:

le-dipole interactions

ough the magnetization transfer mechanismis relatively well erstood at the tissuelevel, much less detailed knowledge is ilableon a cellular and molecular level. Continued advances in deling of magnetization transfer effects will improve the detailed ure of the mechanism underlying this phenomenon.

FMR IMAGING

nctional Magnetic Resonance Imaging (fMRI)

RODUCTION

recent discovery that magnetic resonance imaging can be used nap changes in brain hemodynamics that correspond to mental rations extends traditional anatomical imaging to include maps of nan brain function. The ability to observe both the structures and o which structures participate in specific functions is due to a new

chnique called functional magnetic resonance imaging, fMRI, and ovides high resolution, noninvasive reports of neural activity tected by a blood oxygen level dependent signal (Ogawa, et al, 90 a and b, 1992, 1993; Belliveau, et al, 1990, 1991). This new ility to directly observe brain function opens an array of new portunities to advance our understanding of brain organization, as ell as a potential new standard for assessing neurological status d neurosurgical risk.

HAT IS fMRI

unctional MRI is based on the increase in blood flow to the local sculature that accompanies neural activity in the brain. This results a corresponding local reduction in deoxyhemoglobin because the crease in blood flow occurs without an increase of similar agnitude in oxygen extraction (Roy and Sherrington, 1890; Plum, osner & Troy, 1968; Posner, Plum & Poznak, 1969; Fox and aichle, 1985). Since deoxyhemoglobin is paramagnetic, it alters the 2* weighted magnetic resonance image signal (Ogawa, et al, 1990a nd b, 1992, 1993; Belliveau, et al, 1990, 1991; Turner, et al, 1991; ank, et al, 1992). Thus, deoxyhemoglobin is sometimes referred to s an endogenous contrast enhancing agent, and serves as the ource of the signal for fMRI. Using an appropriate imaging equence, human cortical functions can be observed without the use exogenous contrast enhancing agents on a clinical strength (1.5 T) canner (Bandettini, et al, 1992, 1993; Kwong, et al, 1992; and urner, et al, 1993; Schneider, et al, 1993). Functional activity of the rain determined from the magnetic resonance signal has confirmed nown anatomically distinct processing areas in the visual cortex Belliveau, et al, 1991; Ogawa, et al, 1992; Blamire, et al, 1992; chneider, et al, 1993; Hirsch, et al, 1995), the motor cortex (Kim, et , 1993a; Kim, et al, 1993b), and Broca's area of speech and nguage-related activities (Hinke, et al, 1993, Kim, et al, 1995). urther, a rapidly emerging body of literature documents orresponding findings between fMRI and conventional ectrophysiological techniques to localize specific functions of the uman brain (Atlas, et al, 1996; Puce, et al, 1995; Burgess, 1995; etre, et al, 1995; George, et al, 1995; Ives, et al, 1993). onsequently, the number of medical and research centers with fMRI apabilities and investigational programs continues to escalate.

main advantages to fMRI as a technique to image brain activity
ed to a specific task or sensory process include 1) the signal
not require injections of radioactive isotopes, 2) the total scan
required can be very short, i.e., on the order of 1.5 to 2.0 min per
depending on the paradigm), and 3) the in-plane resolution of the
ional image is generally about 1.5 x 1.5 mm although resolutions
than 1 mm are possible. To put these advantages in perspective,
ional images obtained by the earlier method of positron emission
graphy, PET, require injections of radioactive isotopes, multiple
isitions, and, therefore, extended imaging times. Further, the
cted resolution of PET images is much larger than the usual
pixel size. Additionally, PET usually requires that multiple
idual brain images are combined in order to obtain a reliable
l. Consequently, information on a single patient is compromised
limited to a finite number of imaging sessions. Although these
ations may serve many neuroscience applications, they are not
nally suitable to assist in a neurosurgical or treatment plan for a
ific individual.

at are some common uses of fMRI?

I is becoming the diagnostic method of choice for learning how a
nal, diseased or injured brain is working, as well as for assessing
otential risks of surgery or other invasive treatment of the brain.
term "Functional MRI" (with a capital F) can also include other
techniques that are sensitive to physiologic changes (such as
nges in water motion), whereas fMRI with a lower case f usually
s to the mapping of brain activity using MRI. As a group, these
nctional MRI" techniques appear to provide the most sensitive
nod currently available for identifying, investigating and
itoring brain tumors, strokes and certain chronic disorders of the
ous system such as multiple sclerosis. In addition, these
nods appear to provide a useful means of documenting some
n abnormalities related to dementia or seizures.
utine practice, fMRI studies are often used in planning brain
ery, since they can help physicians monitor normal brain function
well as any disturbed brain function. While research is still
oing, it appears that fMRI can also help assess the effects of
ke, trauma or degenerative disease (such as Alzheimer's) on
n function.

ow should I prepare for the procedure?

ince fMRI uses an MRI device, the standard preparations for an MRI rocedure are necessary. For example, because the strong magnetic eld used for MRI will pull on any ferromagnetic metal object nplanted in the body, MRI staff will ask whether you have a heart acemaker (or artificial heart valve), implanted port, infusion catheter rand names Port-o-cath, Infusaport, Lifeport), intrauterine device UD) or any metal plates, pins, screws or surgical staples in your ody. In most cases, surgical staples, plates, pins and screws pose o risk during MRI. Red dyes used in tattoos and permanent eyeliner ay contain metallic iron oxide and could heat up during MRI, owever this is rare. You will be asked if you have ever had a bullet r shrapnel in your body, or ever worked with metal. If there is any uestion of metal fragments, you may be asked to have an x-ray that ill detect any such metal objects. Tooth fillings are not affected by ne magnetic field, but they may distort images of the facial area or rain, so the radiologist should be made aware of them. The same is ue of braces, which may make it hard to "tune" the MRI unit to your ody. You will be asked to remove anything that might degrade MRI mages of the head, including hairpins, jewelry, eyeglasses, hearing ids and any removable dental work.

he radiologist or an assistant may ask about drug allergies and whether head surgery has been done in the past. If you might be regnant, this should be mentioned. Less than one in 20 patients who ndergo MRI in an enclosed unit may feel confined or claustrophobic

ask Procedure: Patients and subjectsare positioned in the canner as for a conventional scan, and plane lines are set based on onventional imaging methods. During a typical functional imaging eries, 30 images are acquired in a 90 sec run where the initial and ast 10 images are baseline conditions and the middle 10 images (30 ecs) are acquired during a task. For example, in the case of a typical ask designed to identify eloquent brain tissue involved in hand and inger movement, the patient taps fingers and thumb during the ctivity epoch. The beginning and end of this activity period is cued y a visual or auditory signal and occurs at images 10 and 20, espectively. Language, sensory, visual, auditory and other targeted unctions are imaged in a similar manner. A task-induced signal hange is illustrated in Fig. 1 for a sensory task involving tactile timulation (touching) the left hand. The abscissa represents a 30

cquisition run during a 90 sec period. The initial 10 pre-
ion (baseline) images are followed by 10 activation images
nd stimulation) and 10 post-stimulation images. Each 90 sec
series (illustrated by the intensity levels for one voxel) is
repeated twice although only one series is illustrated. In this
e the left hand stimulation results in right hemisphere activity
sumably represents the post central sulcus sensory strip.

fMRI (Blood-Oxygen-Level-Dependent fMRI)

D-fMRI is currently the most common fMRI technique (Table

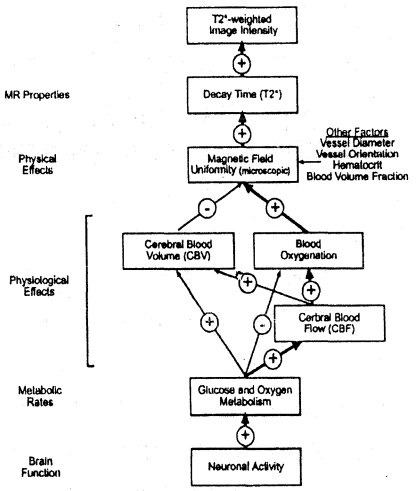

he MRI scanner is tuned to
e and image hydrogen atoms as
entional MRI; however, T2*-
ed images are performed which
vantage of the fact that
enated hemoglobin is magnetic
s oxygenated hemoglobin is not [6-
use of the magnetic properties of
ipped magnetic deoxyhemoglobin
le which causes rapid dephasing, T2* signal is retained longer
gion when it has more oxygenated blood compared to when
less oxygenated blood. Thus, an area with more oxygenated
will show up more intense on T2*-weighted images compared
n there is less oxygenated blood around.

this technique, it is assumed that an area is relatively more
when it has more oxygenated blood compared to another point
[1,6]. This is based on the principle that when a brain region is
used, arterial oxygenated blood will redistribute and increase to
ea. This principle has one caveat: there is a time lag of 3-6
s between when a brain region is activated and blood flow
ses to it [1,9,10]. During this time lag of 3-6 seconds, in fact, the
ed areas experience a relative decrease in oxygenated blood
gen is extracted by the active regional neurons. Afterward, the
t of blood flowing to the area far outweighs the amount of
that is extracted so that oxygenated blood is now higher.
gh images can be acquired every 100 msecs with echoplanar
of rapid acquisition) BOLD fMRI, this predictable but time
delayed onset of the BOLD response limits the immediate

poral resolution to several seconds instead of the 100 msec ential [9]. In the future, researchers may be able to improve the poral resolution of fMRI by measuring the initial decrease in genated blood with activation[11].

OLD fMRI is a relative technique in that it must compare images en during one mental state to another to create a meaningful ure. As images are acquired very rapidly (ie. a set of 15 coronal n slices every 3 seconds is commonly done in our lab), one can uire enough images to measure the relative differences between states to perform a statistical analysis within a single individual. ally, these states would differ in only one aspect so that everything ontrolled for except the behavior in question [10]. Breiter et 1996), for example, scanned Obsessive-Compulsive Disorder ents and healthy controls during activated (ie. holding dirty shcloth) versus rest states (ie. holding clean washcloth) 12 (see re 2).

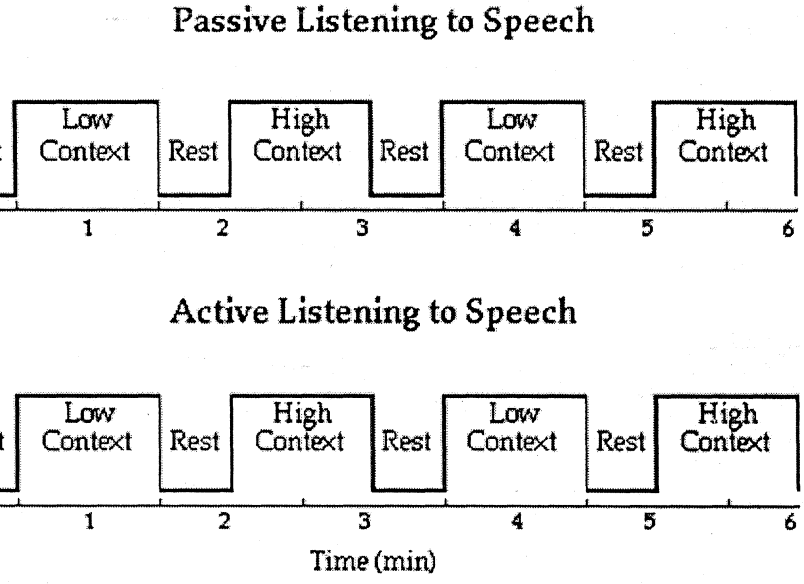

OLD-fMRI paradigms generally have several periods of rest ernating with several periods of activation . Images are then mpared over the entire activation to the rest periods (see figure 3). ages obtained over the first 3 to 6 seconds of each period are nerally discarded due to the delay in hemodynamic response. ernating paradigms are used because the signal intensity nerated by the MRI scanner drifts with time.

current technology, fMRI-BOLD is best used for studying
es that can be rapidly turned on and off like language, vision,
ent, hearing, and memory [9]. The study of emotion is
ed by its slow and variable onset and its inability to be quickly
d [13,14]. Some have, however, succeeded in using this
ue to study emotional processes [12,15]. For example, Whalen et
8) [16] used a backwards masking procedure to present 3
ing conditions to 10 subjects: (1) a baseline condition where
s would see a "+" sign, (2) a "happy" (H) condition where
s would see repeated presentations of 33 msecs of a happy
lowed by 167 msecs of a neutral face, and (3) a "fear" (F)
n where subjects would see repeated presentations of 33
of a fearful face followed by 167 msecs of a neutral face.
earful and happy faces were presented in such a way that 8 of
articipants could not identify them. Despite this unconscious
sing, subjects had relatively increased amygdala activation
rful faces and relatively decreased amygdala activation with
py faces (see Figure 4).

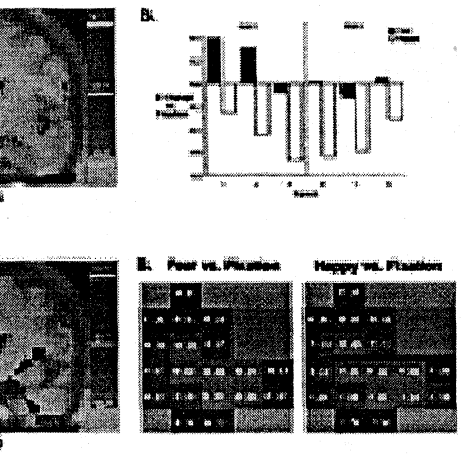

D-fMRI is very sensitive to movement so that tasks are limited
e without head movement, including speaking. BOLD-fMRI is
ited in that artifacts are often present in brain regions that are
air (i.e. sinuses). Thus, there are some problems in
ing important emotional regions at the base of the brain like
itofrontal and medial temporal cortices. Another problem is
metimes observed areas of activation may be located more in
raining veins rather than directly at a capillary bed near the site
onal activation [6].

Currently, there are no indications for BOLD-fMRI in clinical
ychiatry, although this technique holds considerable promise for
raveling the neuroanatomic basis of psychiatric disease. It may be
potential help in sorting out diagnostic heterogeneity and treatment
anning in the future. Neurologists and neurosurgeons are beginning
use this technique clinically to noninvasively map language, motor,
d memory function in patients undergoing neurosurgery [2-6].

old is using gredient echoplanar sequences.In EPI, a gradient echo
formed in the broadening direction by applying an initial dephasing
gradient, and then a series of 'blips' of the opposite polarity which
orm the echo. The time from the r.f. excitation pulse to the centre of
he echo is defined as the echo time in EPI (see Figure 4.1). This is
distinct from the repeated set of echoes formed by the switching of
the read gradient.

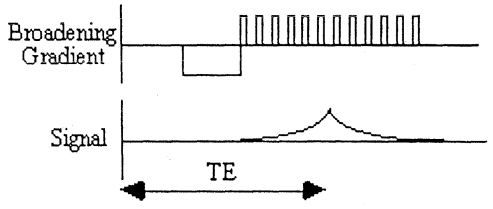

gure 4.1. Formation of a Gradient Echo in EPI using the Broadening
radient.

aving formed one gradient echo, it is possible to form other echoes
mply by reversing the polarity of the blipped gradient. These echoes
l form under the T_2^* decay envelope, and have different echo times
igure 4.2). This is distinct from the multiple spin echo experiment
escribed in section 2.4.3, in which the echoes form under the T_2
ecay envelope.

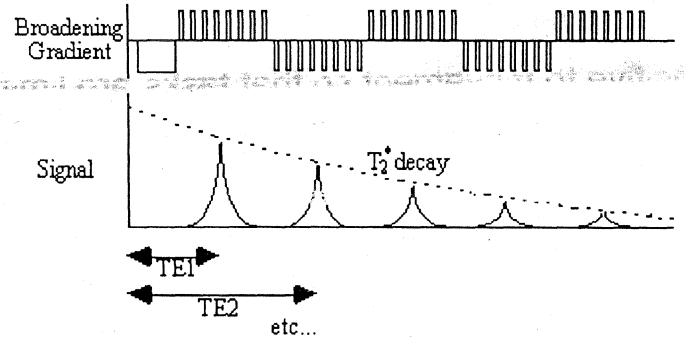

ıradigm

series of images are acquired rapidly while the subject performs at
activation Several such volumes may be collected while the subject
ıs different tasks
relating the signal time course in each voxel it is possible to
y voxels that shows signal change

rom acquired images to
a clinically useful picture"

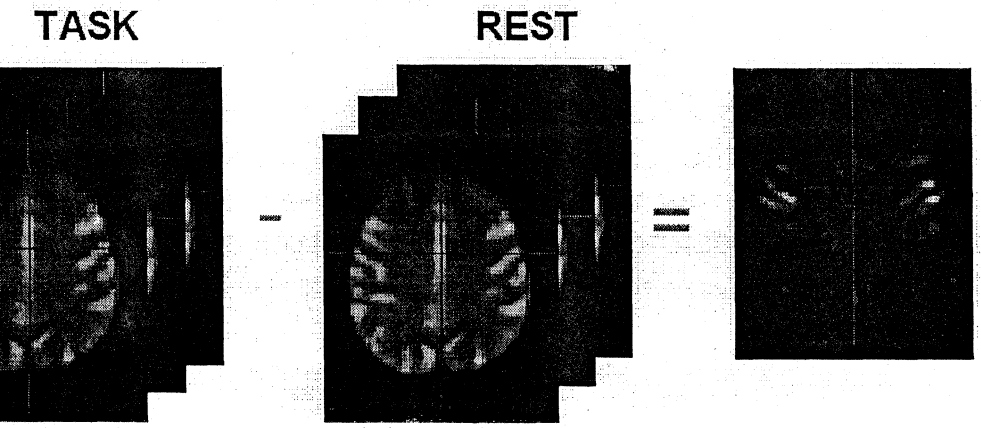

-test

est calculates the difference in signal intensity between the two
,rest and activation Analyzing BOLD data - the calculation of t-

tistic for each voxel .One can take a threshold value of eg:- p < .01, this
ı pick out all voxels whose t value passes the threshold . These voxels are
en displayed in colour over the anatomy images

Visualisation

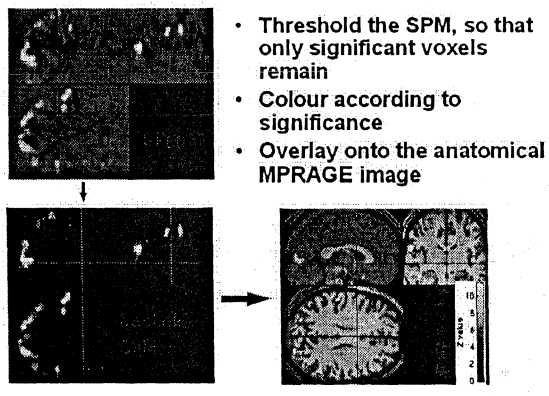

ne kolmogorov –smirnov test

ame like t-test For each population (rest and activation) measured
alues are sorted in an ascending order .From the two
stributions (P act and P rest) KS statistic is calculated as the
aximum difference between the two cumulative distributions

ime Series and Activation Maps

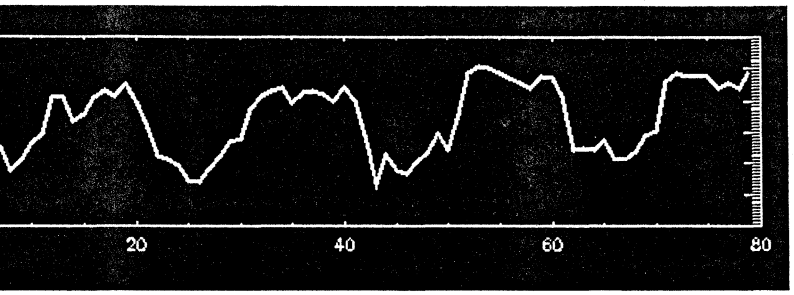

ages in Functional FMRI

ity (Contrast-to-noise ratio)
gnal change is ~1-2% at 1.5 T; signal-to-noise ratio in
hot EPI images is ~100.
gical pulsations (cardiac and respiratory); Head motion;
ntal instability
ity
of activation – neurons or veins
tibility artifacts

ssion of Temporal Fluctuations

Head motion reduction
lder modified from a football helmet
lignment in data processing
ogical pulsations
on using simultaneously recorded cardiac and respiratory

Ultra-fast imaging techniques
hot echo-planner imaging (EPI)
hot Spiral imaging
ocessing
ng
aradigms

age

Motor Paradigm- 'BOX- CAR' Design

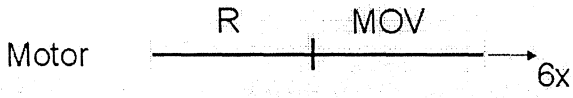

conditions are alternated:

- –Rest (R)
- –Movement (MOV)

Motor function

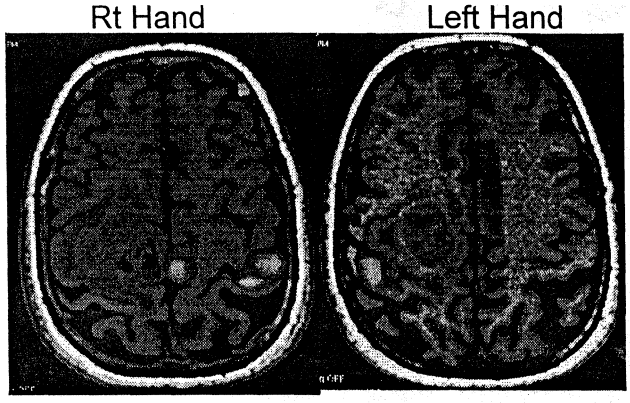

Bilateral finger tapping Vs Rest

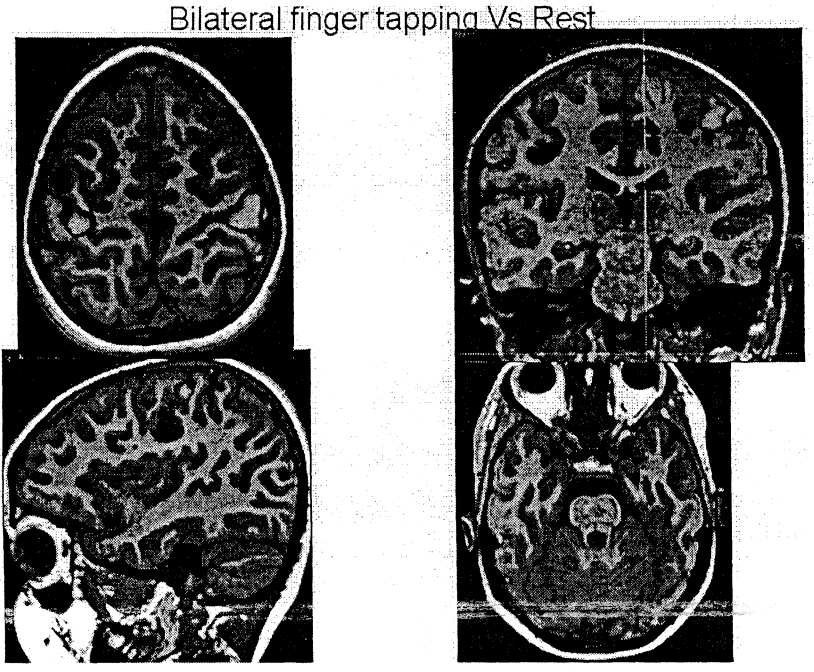

Left finger tapping Vs Rest

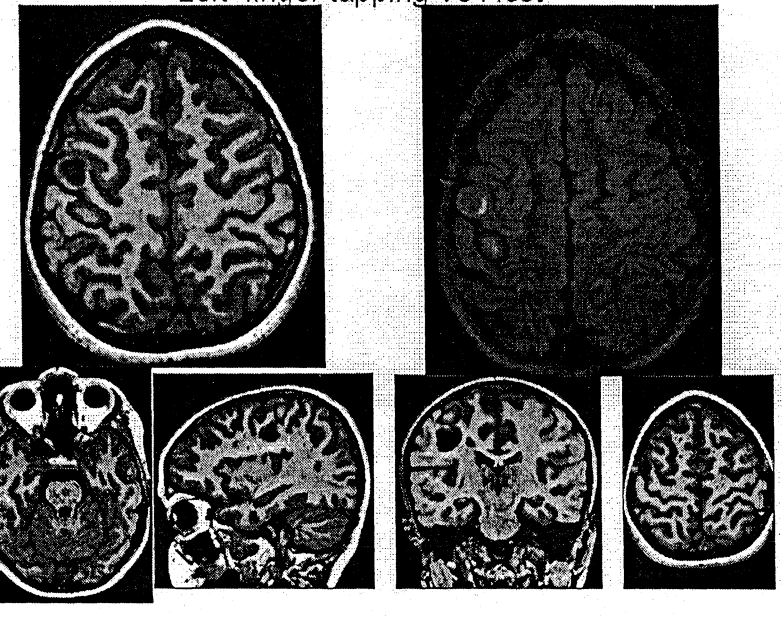

Lip Pouting vs rest

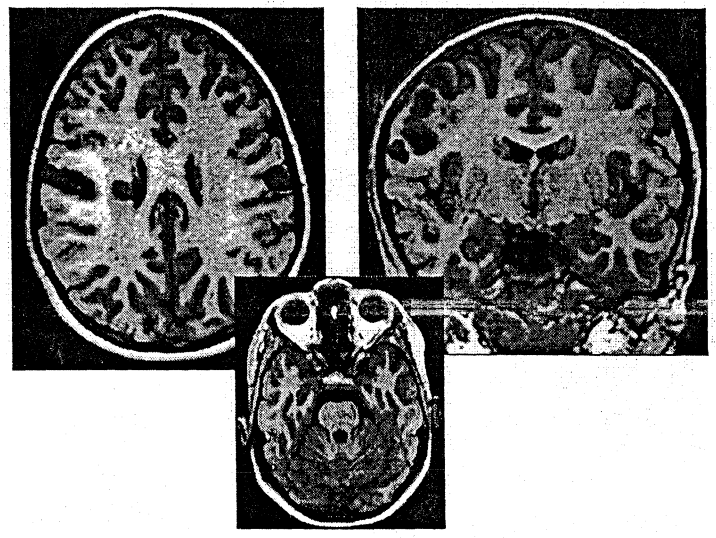

Bilateral leg motor vs Rest

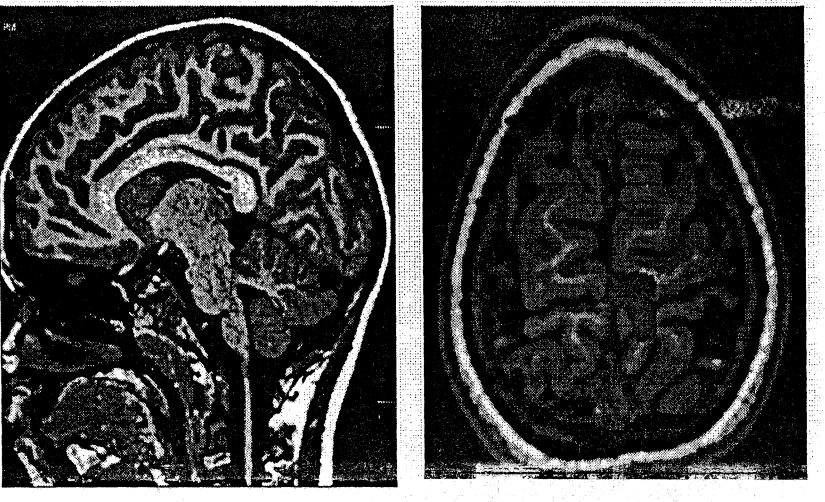

guage Paradigms

Fluency

ntic Decision
age

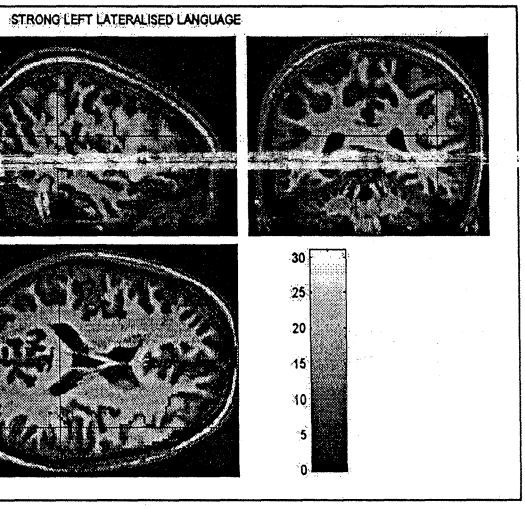

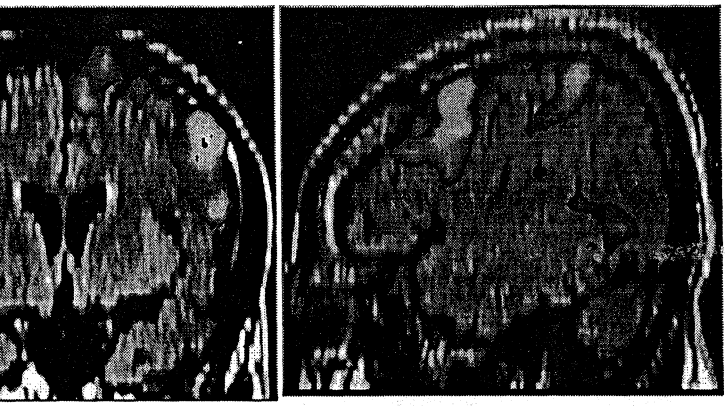

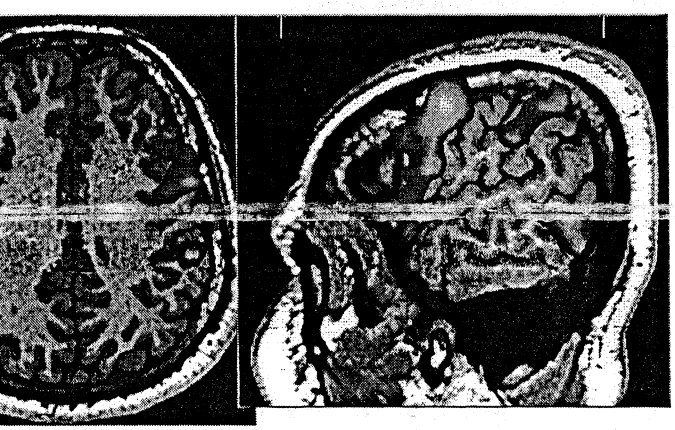

Verbal Fluency_ Inline BOLD
Left lateralized language

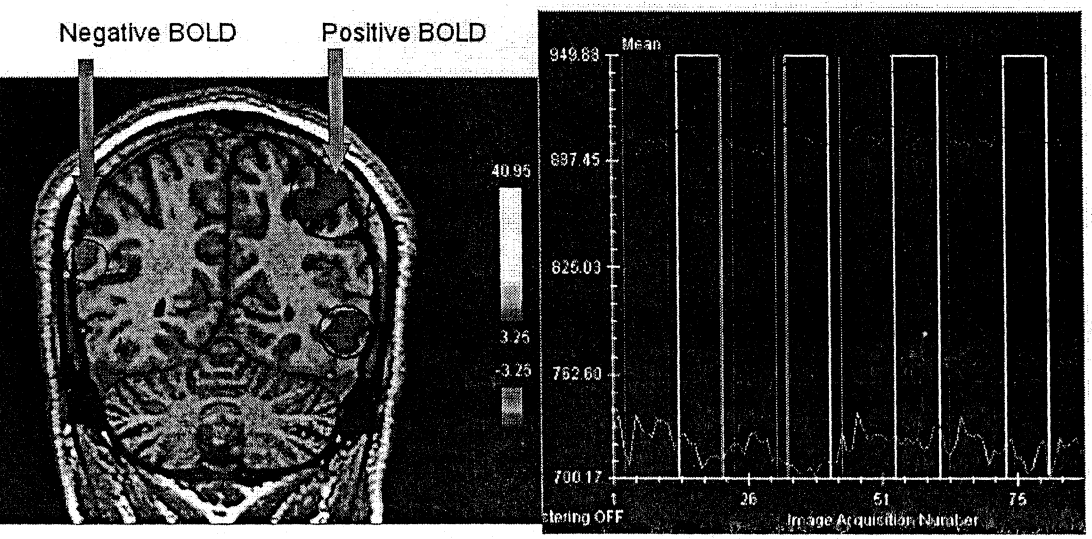

Visual

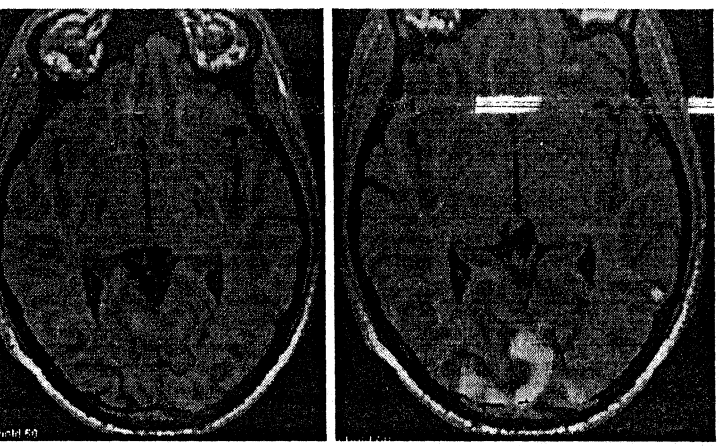

Auditory

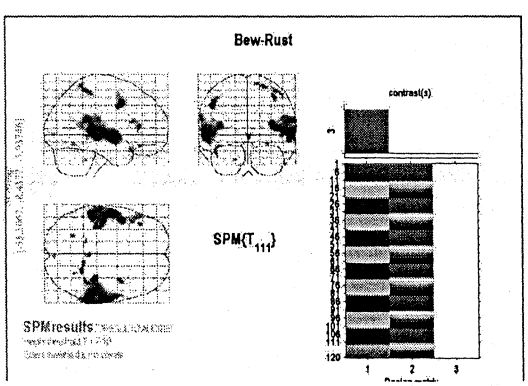

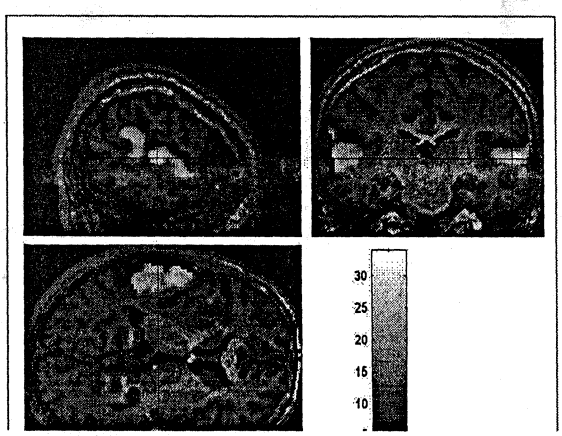

ACT IN BOLD :

pe of artifact which is specific to EPI is the Nyquist. This arises use odd and even echoes are acquired under opposite read gradients, and the data requires reversal prior to image nstruction. Inaccurate timing of the sampling relative to the hed gradient, temporal asymmetries in the analogue filter or nogeneities in the static field cause a modulation of alternate k-space. This leads to a ghost image shifted by N/2 pixels in nase encode direction. In fMRI, ghosting artifact can cause a r of problems. In the first place, the ghosting can spoil the look the image, and ghosting of activated regions could lead to nt 'activation' appearing outside the head. More serious effects r if the artifact changes with time. Movement of the subjects d causes the interference fringes, of overlapping ghost and to change dramatically, with even small displacements having rge effect. Since subject motion is often stimulus correlated, cularly if the experimental paradigm involves movement, the ges of the interference pattern can show up in the statistical analysis as 'activation',

Diffusion-Weighted Imaging:

on Weighted imaging provides a technique for mapping proton st that reflects the microvascular water environmen.Diffusion g makes use of the variability of "Brownian motion" of water les in brain tissue.

ian motion refers to the random movement of molecules. molecules are in constant motion, and the rate of movement or n depends on the kinetic energy of the molecules and is ature dependent. In biological tissues, diffusion is not truly n because tissue has structure. Cell membranes, vascular res, and axon cylinders,for example, limit or restrict the amount

- Turbo STEAM
  - Conventional 1.5T system
  - Gradients - 9 mT/m
  - Single slice - 27 sec
- DWI with EPI
  - Echoplanar system
  - Gradients - 25 mT/m
  - Whole brain - 4 sec

diffusion.
eractions

fusion
ighted
nsitive to
1H in

Also, chemical
of water and
macromolecules affect
properties. Diffusion-
imaging is very
the random movement
water molecules
rownian movement). The amount of water diffusion for a given pixel
n be calculated and is called the apparent diffusion coefficient
DC).

reas with low ADC values (ie.low diffusion) appear more intense.
DC values are direction sensitive. For instance, if images are taken
rpendicular to myelin fiber tracts like the optic chiasm, arcuate
sciculus, or corpus callosum, ADC values will be lower than if the
ages are taken along the length of these fibers. This is thought to
because there is little diffusion across myelin sheaths.

us, ADC direction sensitivity permits detection of myelination and
ay allow researchers to understand in greater detail myelin
velopment in infants. On the other hand, this direction sensitivity
mpers the study of diffusion in other processes as ADC values
ffer, depending on the imaging plane (axial, coronal, or sagittal).
radients are applied in to three orthogonal plain of gradient
,y and Z) and creating a average diffusion weighted image . There
e now ways to calculate average ADC values incorporating all
anes for each pixel, removing "artifacts" due to the direction of
cquisition. Removing the directional diffusion sensitivity has been
lpful in studying stroke.

pair of strong gradient pulses are added to the pulse sequence.
ne first pulse dephases the spins, and the second pulse rephases
e spins if no net movement occurs. The amount of diffusion
eighting is determined by the strength of the diffusion gradients, the
uration of the gradients, and the time between the gradient pulses

FFUSION TENSOR IMAGING:

e basic idea of diffusion tensor imaging is the same as for Phase ontrast Angiographic MRI.It is an anisotropic process with different olecular mobility in x, y and z directions, the diffusion constant"D" s to be replaced by a diffusion tensor

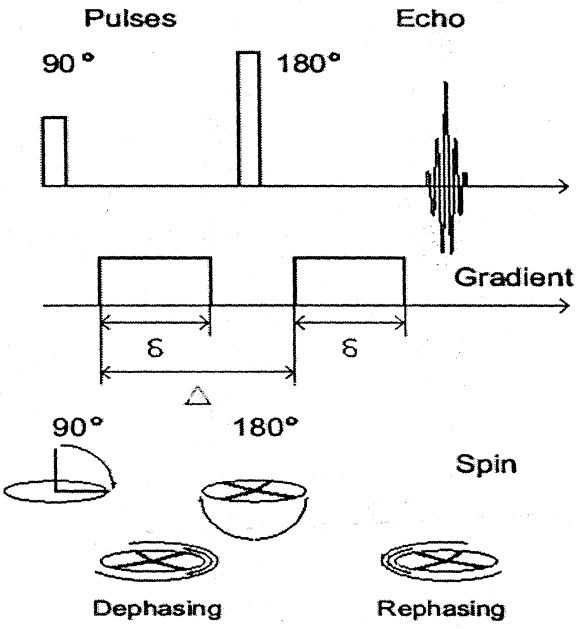

ffusion in white matter is extremely variable. The value of the ffusion co-efficient directly depends on the relative orientation of the bers and the magnetic field gradients, which is known as nisotropic diffusion." Water diffusion in gray matter does not exhibit

nough the individual axons and the surrounding myelin sheaths nnot be revealed with the limited spatial resolution of *in vivo* aging, distinct bands of white matter fibers with parallel orientation y be distinguished from others running in different directions .

lculation of the ADC

el-by-pixel calculation of the ADC was performed by fitting the aracteristic curve, $\log(S_0/S_b) = ADC b$, onto the DW image data, ere S_0 is the signal intensity obtained without diffusion weighting; the signal intensity obtained with diffusion weighting; and b, the V factor. Only those pixels that could be clearly differentiated from ckground noise were considered for calculation.
e trace of the diffusion tensor, Trace (**D**), was calculated by using e equation,

$$ADC_{av} = \frac{1}{3}\text{Trace}(\mathbf{D}) = \frac{1}{3}\sum_{i=x,y,z} ADC_i \quad (2)$$

ere x, y, and z indicate the directions of diffusion weighting, and DC_{av}, the average ADC. The calculation of b values was performed numerical integration of the diffusion-sensitizing gradients

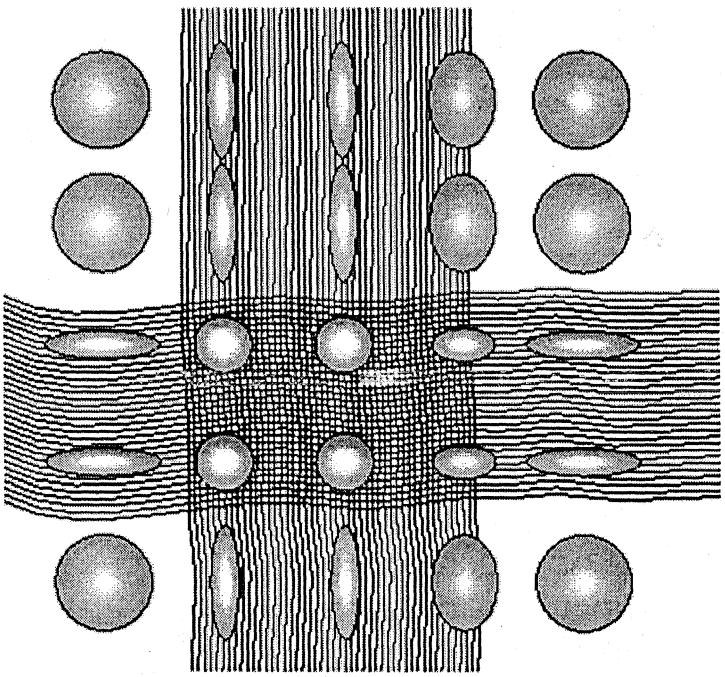

and the magnetic field gradients, which is known as
tropic diffusion." Water diffusion in gray matter does not exhibit
opy or restriction by impermeable walls. White matter on the
hand is extremely anisotropic, the results of the measurements
ding on the respective orientation of the myelin fiber tracts and
adient direction at each different image location. It appears that
on coefficients are significantly decreased when the myelin fiber
are perpendicular to the direction of the magnetic field gradient
o measure molecular displacements

ffusion coefficient measured parallel to the myelin fiber
on is about three times larger than the diffusion coefficient
ndicular to fibers

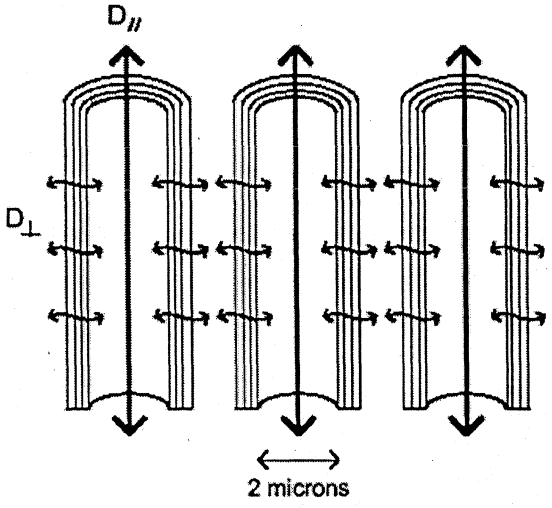

on in mylene fibers

ways obtain a macroscopic measure of a microscopic quantity,
necessarily entails intravoxel averaging, the voxel dimensions
nce the measured diffusion tensor at any particular location in
ain. Factors which would affect the shape of the apparent
on tensor (i.e., the shape of the diffusion ellipsoid) in the white
include the density of fibers, the degree of myelination, the
ge fiber diameter, and the directional similarity of the fibers in
xel. The geometric nature of the measured diffusion tensor
a voxel is thus a meaningful measure of fiber tract
ization.

o crossing fibertracts would ideally be represented by a diffusion nsor image.

BER TRACKING

diffusion tensor can be thought of as an ellipsoid with its three axes iented along the tensor's three perpendicular eigenvectors, with the ree semi-axis lengths proportional to the square root of eigenvalues the tensor - mean diffusion distances

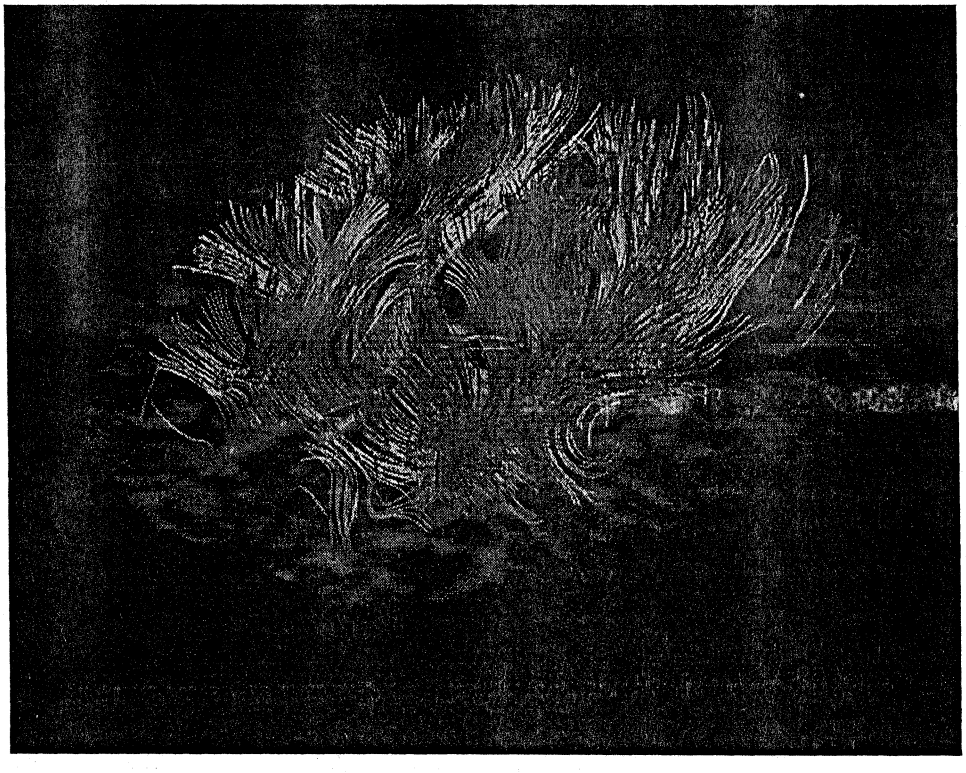

PERFUSION IMAGING

o methods have been developed for measuring cerebral blood Mainly two methods are using to perform perfusion imaging.

avenous bolus tracking,

s on the intravenous (iv) injection of a magnetic compound such adolinium-containing contrast agent and measuring its T2*- ted signal as it perfuses through the brain over a short time of time. Areas perfused with the magnetic compound show gnal intensity as the compound creates a magnetic ogeneity that decreases the T2* signal. The magnetic ound may be injected once during the control and once during tivation task and relative differences in blood flow between the ates may be determined to develop a perfusion image atively, one can measure changes in blood flow over time after le injection to generate a perfusion map.

ugh gadolinium-based contrasts are not radioactive, the number uses that can be given to an individual is limited by the potential lney toxicity with repeated tracer administration. This technique nly generates a map of relative cerebral blood flow, not ute flow as in the next technique. Arterial spin labelling is a T1- ted noninvasive technique where intrinsic hydrogen atoms in al water outside of the slice of interest are magnetically tagged ed") as they course through the blood and are then imaged as nter the slice of interest

sion Weighted Imaging

al techniques have been developed for determination of sion. Both PET and SPECT are relevant for clinical assessment ften use diffusible tracers, which are ideal for measuring sion. Both techniques have drawbacks being invasive, using actively labeled tracers and having relative low spatial and oral resolution. For measuring perfusion, MRI has the

vantages of high temporal and spatial resolution using no
ioactivity, being almost noninvasive and offering combination
dies using other MR techniques (diffusion, spectroscopy,
giography, structural imaging). MR perfusion imaging is divided
o categories: (1) susceptibility based techniques either (a)
ng intravenous bolus injection of a paramagnetic contrast agent or
detecting changes in the endogenous paramagnetic substance
oxyhemoglobin (blood oxygen level dependent, BOLD),
d (2) arterial spin labeling of protons in blood.

e most commonly used of these techniques is (1a): contrast agent
us tracking also known as dynamic susceptibility contrast
gnetic resonance imaging (DSC-MRI). DSC-MRI was applied
our studies and will be further described.

.1. Contrast agents

posite to radioactive tracers, MR contrast agents are considered
fe. Their effect is due to paramagnetic properties causing
ortening in T1 and T2 relaxation (further described below).
R contrast agents containing gadolinium-chelates are approved for
e in humans. Gadolinium is a lanthanide metal being paramagnetic
perty due to seven unpaired electrons. Due to toxicity gadolinium
chelated to different compounds: Gadolinium-DTPA (Dithylen-
amin- Penta-Acetiacid) is known as gadopentate and sold as
agnevist® (Schering), DTPA-BMA
TPA-bismethylamide) known as gadodiamide and sold as
mniscan®.

scular effects

e effect of MR contrast agents on T1 relaxation is caused by so-
lled dipole-dipole interactions i.e. on direct interaction of protons in
e water molecules with the dipole moment
the unpaired electrons of the paramagnetic contrast agent.
adolinium-compounds in the brain are intravascular when the blood
ain barrier is intact. T1 shortening produces signal
hancement in the blood volume, that contributes about 5% of the
tal brain volume. Susceptibility is a measure of the ability of a
mpound to become magnetized when subject to a
agnetic field thus increasing or decreasing the applied external
agnetic field. The intravascular paramagnetic contrast agents cause
sceptibility changes and increase the local

l magnetic field. A magnetic field gradient between the lumen
essel and the surrounding tissue is induced (figure15),
increasing the T2* relaxation rate and dephasing.
fect on T2* relaxation extends beyond the blood vessel, thus
ting relative large and distant signal changes. The method is
re more suitable for MRI perfusion measurements,
e dipole-dipole effect changing T1 relaxation in the vessel only
gnal change caused by a paramagnetic compound also
ds on the distance that the water molecules diffuse compared
ield inhomogenity created by the paramagnetic agent, i.e.,
any different magnetic fields the spins experience during the
n of the pulse sequence (figure 15). Around a larger vessel,
molecules will only experience the same "static" magnetic field
se the distance travel led by diffusion is small in relation to the
teristic distance of field inhomogenity. Dephasing due to static
ogenity leading to signal loss will occur in a gradient-echo
ment but not in a spin-echo experiment. Around smaller
s, the water molecules will experience varying magnetic field
nts due to diffusion (around the vessel and around the
oring vessels), this will lead to dephasing and signal loss in a
nt-echo as well as in a spin-echo experiment. Using gradient-
equences, the T2* effects from both large and small vessels
refore be detected. Using spin-echo sequence the T2* effects
ne large vessels will be suppressed. However, gradientecho
n used in studies due to the better SNR, (greater signal loss
ith spin-echo sequences), when using the same amount of MR
st agent. The susceptibility effect will decrease when the BBB
aged because local field inhomogenity decreases. The
dipole effects shortening T1 will cause a greater signal increase
issue. The MRI sequence can be optimized so T1 effects are
ased and post-processing of the signal time curve has
een proposed (108), (109). Use of paramagnetic contrast
unds causing small T1effects, e.g. dysprosium, can minimize
from leakage of the BBB, although not available for
n studies (110). Perfusion is confined to the capillary bed and
a spin echo sequence will select the relevant compartment for a
ion measurement, (111). Spin echo images have better
st-to-noise (CNR) than gradient echo images and are without
susceptibility artifacts in the inferior frontal and temporal
On the other hand, information on hemodynamics in the large

ssels is abolished. Also, more contrast agent is needed in bolus
cking using a spin echo sequence because)*R2** is smaller than
2.

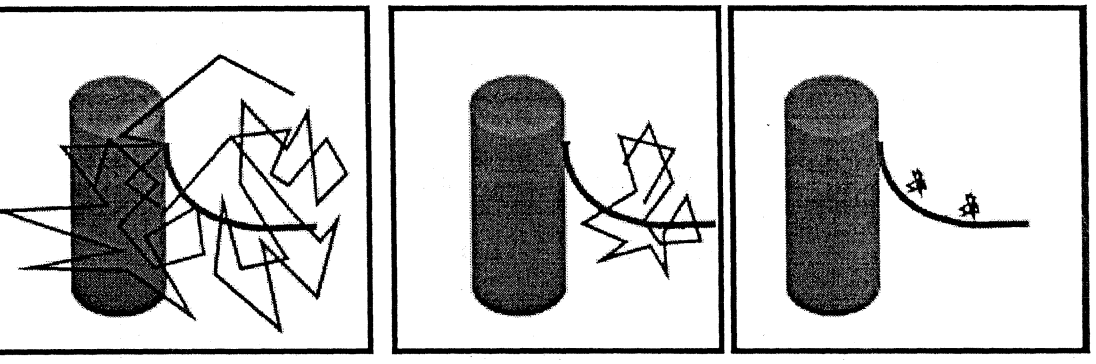

ure 15. Vessel size and susceptibility effects
m left to right: small vessel, intermediate vessel, large vessel

.3. Contrast agent bolus tracking

nen tracking a bolus injection of paramagnetic contrast agent by
st imaging, the MRI signal will drop transiently, due to the
sceptibility effect when the gadolinium-compound passes
rough the detecting plane (figure16). The bolus of 0.1-0.2mmol/kg
injected via the antecubital vein (3-5ml/sec), using a power injector.
ith the availability of EPI, it has become possible in the last five
ars to obtain the passage with high temporal (1-2 seconds) and
gh spatial resolution (~1mm) by multislice imaging (6-11slices). 10-
frames of baseline images should be acquired before the bolus is
ected increasing SNR ratio when calculating)*R2** (see
rmula [2.20]) (111). The TE should be long (60-75 ms) increasing
e susceptibility sensitivity
11).

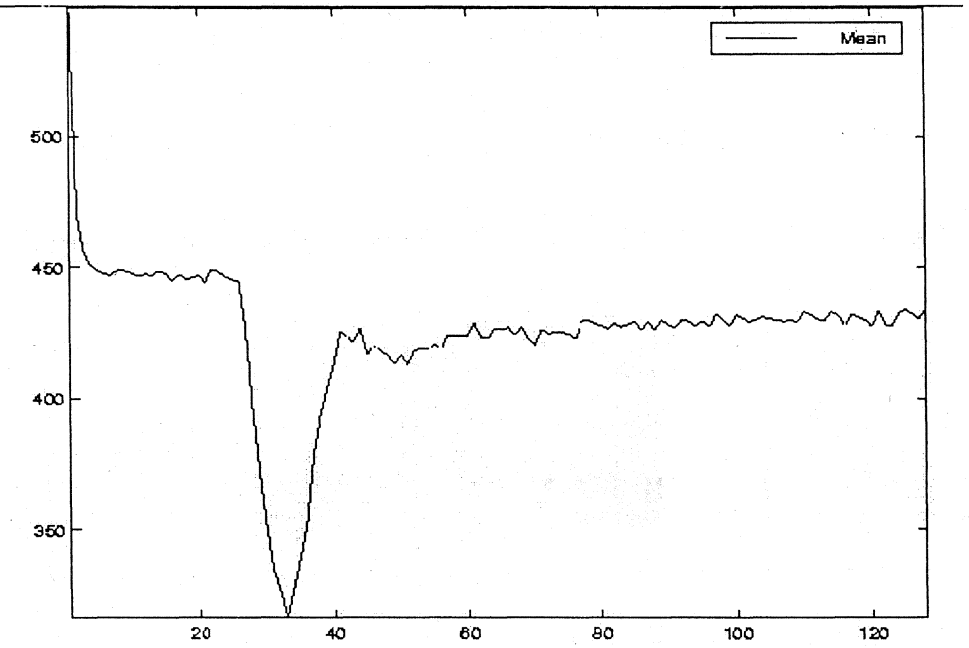

e 16. Contrast agent bolus tracking *signal-time curve*
r kinetics

ification of perfusion is done using the central volume theorem based on certain assumptions describing a systems response njection of a tracer: Flow is constant during observation and the is inert with no metabolism or retention.

entral volume theorem states that: CBF is the perfusion, CBV is ood volume and MTT is the mean transit time. The central e theorem is a general equation for all kind of tracers (diffusible, ascular or intermediate). The model used when calculating ion in DSC-MRI is based on tracer kinetics for nondiffusible ascular tracers (113). When a bolus of contrast agent is ed, the concentration *Cvoi(t)* of the tracer in a volume can be described in terms of

= CBV/MTT [2.14]

s the perfusion, CBV is the blood volume and MTT is the mean time.

e central volume theorem is a general equation for all kind of
cers (diffusible, Intravascular or intermediate). The model used
en calculating perfusion in DSC-MRI is based on tracer kinetics for
ndiffusible intravascular tracers (113). When a bolus of contrast
ent is injected, the concentration *Cvoi(t)* of the tracer in a volume
OI) can be described in terms of *h(t), the frequency distribution*
nction, describing the distribution of transit times through the
OI following an ideal instantaneous bolus.
R(t), the residue impulse response function i.e., the fraction of the
lus still present in the VOI at
ne *t* following a ideal instantaneous bolus. *R(t)* and *h(t) are related*

$$R(t) = \left[1 - \int_0^t h(\tau)d\tau\right] = 1 - H(t) \qquad [2.15]$$

$$H(t) = \int_0^t h(\tau)d\tau \qquad [2.16]$$

.16], represents the accumulated fraction of the bolus that has left
e VOI. Formula [2.15]
ate that after a instantaneous bolus, *R(t)* is the fraction of the bolus
the VOI at time - *t*.
AIF, the arterial input function, Ca(t), the concentration of contrast
gent in the supplying vessel
the VOI.
rom these definitions *Cvoi(t)* is calculated as:

$$Cvoi\ (t) = \rho\ /k_h \cdot CBFvoi\ \cdot (Ca(t) \otimes R(t)) \qquad [2.17]$$

$$= \rho\ /k_h \cdot CBFvoi\ \cdot \int_0^t Ca(\tau) \cdot R(t-\tau)d\tau \qquad [2.18]$$

oi is the perfusion in VOI,
ne density of the tissue,
h is correcting for differences in hemotocrit in capillaries and
arge vessels.

a [2.17] states that *Cvoi* can be expressed as a convolution of
idue impulse response function, *R(t)*, and the arterial input
n, *Ca(t)*. To calculate *CBFvoi*, the arterial input function *Ca(t)*
e *Cvoi(t)* therefore must be deconvolved determining the
e response function *R(t)* and *CBF voi*. Deconvolution is
ically demanding with inherent uncertainties in the estimated
ecause the signal time curve in the artery and the tissue is
identical when using intravascular tracers. However, attempts
ulating the rCBF have shown good agreement with values from
easurements (114), (115). An accurate estimate of the arterial
unction is necessary but can be difficult to obtain due to partial
e effects and bad SNR in EPI. Also it is assumed in the model
e bolus curve in the VOI is not dispersed or delayed compared
AIF, which is certainly not valid in ischaemic regions (116).
BV is expressed as:

$$CBV = \frac{k_h}{\rho} \cdot \frac{\int Cvoi(t)dt}{\int Ca(t)dt} \qquad [2.19]$$

ve CBV can be estimated without knowledge of the *AIF*,
ing the same *AIF* to all parts of the tissue. This approach has
ore often been applied in human studies. For intravascular
s used in DSC-MRI, the time concentration curve obtained in
OI, also depend on the vascular architecture. The first moment
tissue concentration curve differs from the true MTT (117).
ating CBF by the central volume theorem [2.14], with
alculated as the first moment of the tissue curve, is therefore

ncentration dependency

e concentration in the VOI *Cvoi* used in the calculation of the modynamics is related to the change in *T2** relaxation:

$$\Delta\left(\frac{1}{T2^*}\right) = \Delta R2^* = k \cdot Cvoi \qquad [2.20]$$

s the relaxivity constant. Assuming the linear relationship [2.20] tween the concentration of the gadolinium-compound, *Cvoi*, and e change in *R2**.)*R2** is determined from the baseline signal *S0*, d *SVOI(t)*, the signal in the VOI at time t (118), (107), (119). *TE* is e chosen echo time:

$$Cvoi(t) = k \cdot \Delta R2^* = -\frac{k}{TE} \cdot ln\left(\frac{S(t)}{S_0}\right) \qquad [2.21]$$

21], is valid for both the tissue and arterial input function, (however may differ).

erfusion parameter maps

ith the technical and practical difficulty of absolute quantification of erfusion using DSCMRI, various parameters derived from the)*R2** ne curve can been calculated. The time to *R2** peak, (TTP), the lus arrival time (BAT), the peak height, the area under the)*R2** rve (AUC) (which is related the CBV) and the first moment of the 2* time curve used as an approximation for the MTT. The terpretation, except for AUC = CBV is not straightforward because ere is no simple relation between these parameters and the rCBF. so the parameters should be normalized, because they vary epending on the vascular architecture, cardiac output, injection

d dose. In ischemia, the normal contralateral side will often be
r normalization of
erent parametric maps.
ects of re-circulation can be eliminated either by considering
first part of the signal-time curve or by fitting the curve to an
ed model function, most often a gammvariate function (120).
mary aim of fitting a gamma variate function to the data is to
e the area under the first pass curve and to improve the SNR
TP estimate.

the technical difficulties of deconvolution we used TTP and
aps in the study of acute stroke .However, TTP maps have
nherent differences compared to MTT and CBF maps in
ic volumes. For instance, when considering an ischemic area
by a stenosis or an occlusion, the CBV and CBF are
sed in the ischemic area itself, and the "true" calculated MTT
unchanged. However, TTP in the case of stenosis will be
ed in the whole area distal to the stenosis. If collateral blood
is involved, the TTP will be prolonged in the collateral vessels,
e blood is by-passed from the occluded vessel through the
als. In both cases TTP will overestimate the ischemic area. on
aps. Generally, it can be shown that TTP does not depend on
fusion but only on the actual input function and configuration of
due impulse response function. However, it is not known from
al data, if these parameters in ischemic tissue actually have
rations giving changes in TTP occurring parallel to changes in

CBV

TTP

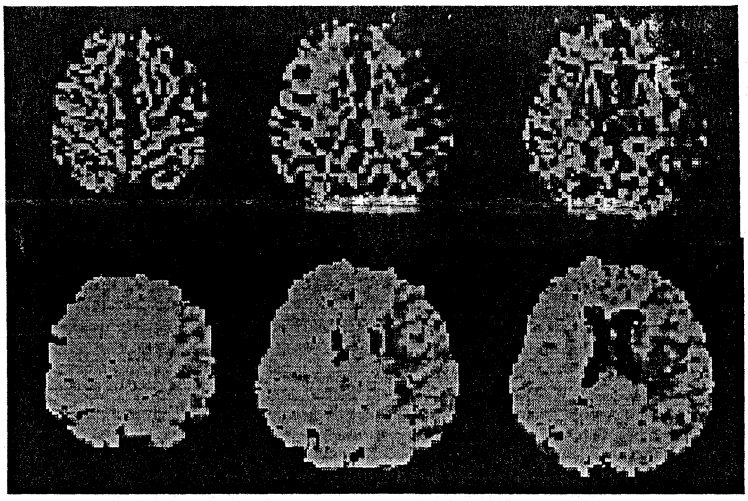

DWI TTP rCBV

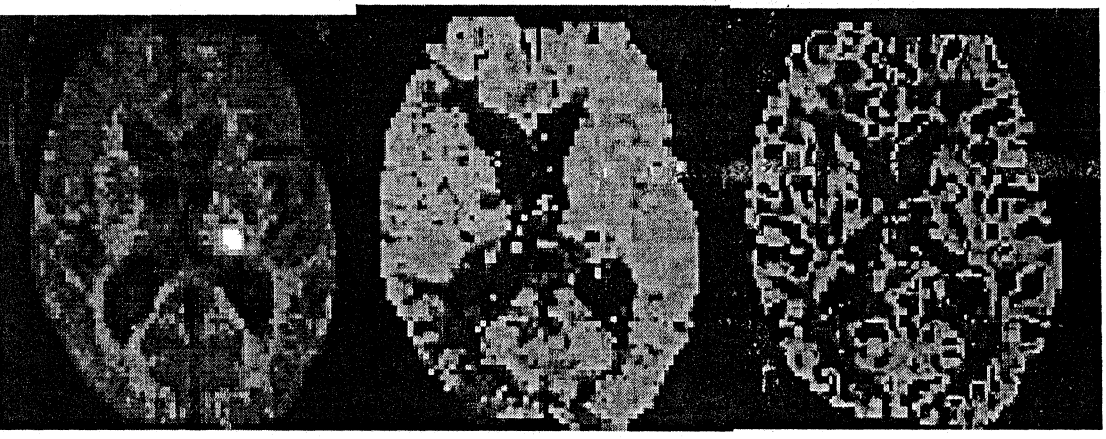

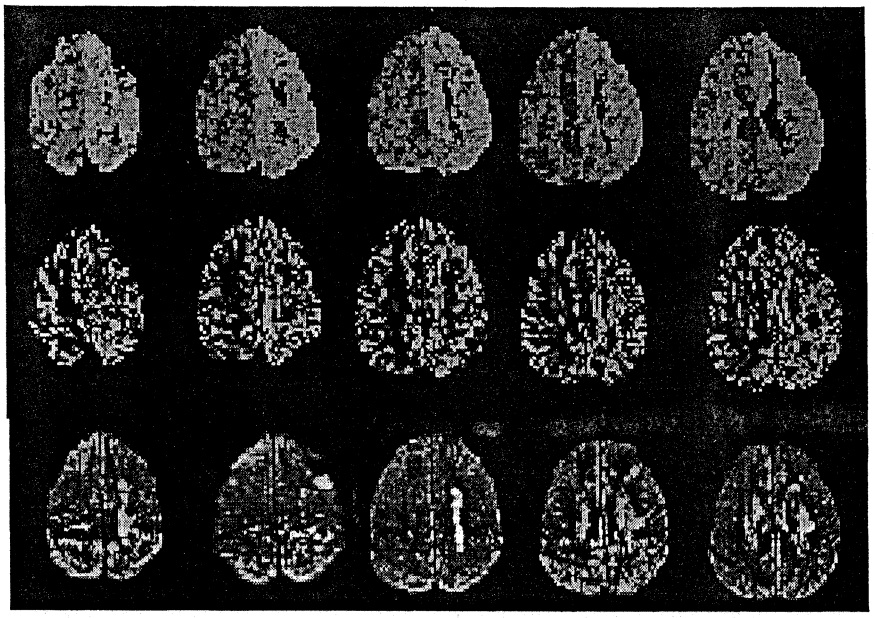

ial spin-labelling,

n-invasive nature **of arterial spin labelling** (ASL) has opened e window into human brain function and **perfusion** ogy. High spatial and temporal resolution makes the technique pealing not only for the diagnosis **of** vascular diseases, but basic neuroscience where the aim is to develop a more ehensive picture **of** the physiological events accompanying al activation. The complete non-invasiveness **of** ASL makes it itable for **perfusion** studies **of** healthy volunteers and in groups requiring repetitive follow-ups . This is especially nt in patients with particular conditions, such as kidney failure, ediatric populations where the use **of** radioactive tracers or ous contrast agents may be restricted.

tative perfusion

r to measure tissue perfusion, one needs to follow the course d flow through the organ, and for this there exist two methods, sed on freely diffusible and the other on intravascular tracers. r names suggest, freely diffusible tracers can leave the

ravascular space without restriction and be distributed throughout e entire tissue volume, whereas intravascular tracers remain in the sculature, which constitutes only a fraction **of** the full volume.

asic arterial spin labeling

e overall goal **of** all existing ASL techniques is to produce a flow-nsitized image or "labelled" image and a "control" image in which e static tissue signals are identical, but where the magnetization **of** e inflowing blood differs. By adding a delay between **labelling** and age acquisition, called inversion delay (TI), the labelled blood **spin**s e allowed to reach the capillaries where they exchange with tissue ater and thereby give rise to the **perfusion** signal. The signal fference, which is only 0.5–1.5% **of** the full signal, depends on any parameters such as the flow, T_1 **of** blood and tissue, as well as e time it takes blood to travel from the **labelling** to the imaging gion. Multiple repetitions are needed for ensuring sufficient signal--noise, and a model **of** the **perfusion** signal is usually used in order quantify the **perfusion**.

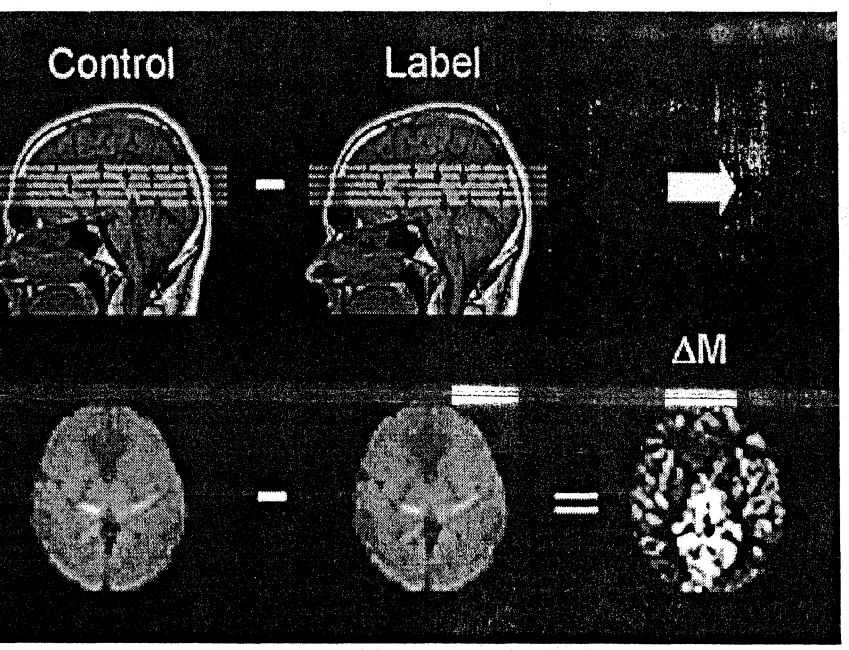

gure 1 Schematic description **of** a **perfusion** weighted image(ΔM) btained by subtraction **of** the labelled images from the control images.

xist two main classes **of** ASL techniques: continuous ASL and pulsed ASL (PASL). In CASL, the supplying blood is ously labelled below the imaging slab, until the tissue ization reaches a steady state (Figure 2a). The PASL ch labels a thick slab **of arterial** blood at a single instance in nd the imaging is performed after a time long enough for that y labelled blood to reach the tissue and exchange at the region est (Figure 2b). Both methods need a control experiment in o visualize and quantify the **perfusion**.

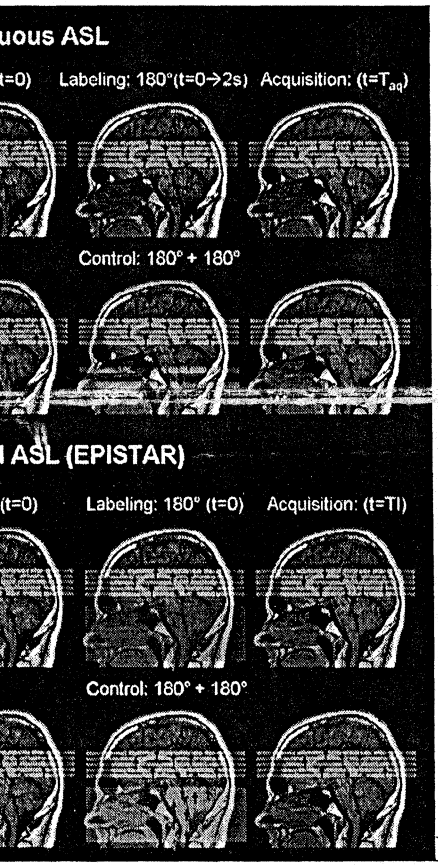

Figure 2. (a) Continuous **arterial spin** g (ASL) multislice experiment, using double adiabatic inversion for trol experiment, where labels get inverted during the passage **of** the ne and returned to equilibrium during the subsequent passage **of** the plane. (b) The EPISTAR pulsed ASL sequence, which labels ing at once and uses two 180° + 180° = 0° pulses for the control

uous arterial spin labelling

iginal ASL method proposed by Williams et al in 1992 used a

ntinuous flow-driven adiabatic inversion scheme, a method that as previously used for angiography . This type of adiabatic inversion the arterial magnetization is realized using a 2–4 s continuous diofrequency (RF) pulse while applying a magnetic field gradient in e flow direction. The moving arterial spins will therefore experience slow variation of the resonance frequency, which will result in their version, while static (tissue) spins will just be saturated. Typically, e inversion "slice" will be selected just proximal to the circle of illis, near the medullospinal junction or at the level of the common arotid, and the spins in blood that flows through this plane will be verted. The inversion efficiency α, which is important for further uantification, depends on factors like the mean velocity of the blood, ngulations of the vessels to the plane and the selected RF mplitude and gradient strength. Typical labelling efficiency is in the nge of 80–95% .

mong the confounding factors of these long lasting inversion pulses e magnetization transfer (MT) effects . When using a single coil for belling and imaging, the off-resonance labelling pulse (with spect to imaging slice) will act as a powerful MT pulse in a way milar to an MT-weighted technique. The resulting saturation effect f the macromolecular pool will result in a reduced signal of the free ater pool from the tissue of interest . This is a very important issue, s the perfusion weighted images are calculated by subtracting a belled from a control acquisition, and if this MT effect is present only uring the labelling scheme, it will lead to overestimated perfusion. the first implementation, these MT-effects were compensated for y applying a distal labelling during the control experiment. This roduces identical saturation effects but, due to the applied gradients uring labelling, this is unfortunately valid only for a single slice. For ultislice acquisition, Alsop et al proposed the use of two closely paced inversion planes, also called double adiabatic inversion (DAI). the control experiment, the magnetization gets inverted while aversing the first plane and returns theoretically to its original state uring the passage through the second plane (the CASL experiment shown in Figure 2a). Double inversion is achieved by applying a inusoidal modulation of the RF waveform. Global control of the MT-ffects is obtained by matching the RF power and the location of the lanes. Another method was also proposed, called simultaneously

al and distal RF irradiation (SPDI) for multislice acquisition [23]. later scheme, the RF power on the control scan is distributed on both sides **of** the acquisition volume. However, a big on **of** these approaches is the doubled RF deposition, resulting er specific absorption rates (SAR).

d arterial spin labelling

4, Edelman et al [31] proposed the first pulsed ASL scheme. ry to CASL, the **labelling** is performed once in a 10–15 cm oximal to the image slices. For the PASL sequences, MT- have to be considered as well, although these are much r compared with CASL. In this first version **of** the "Echo-Planar aging and Signal Targeting with Alternating Radio frequency" TAR) sequence, inversion was performed distal to the image uring the control experiment to induce identical MT effects in ases. Again, this truly compensates for a single slice only and, ore, the sequence was modified for multislice acquisition using e 180° adiabatic pulse for the label experiment and two 180° + ulses **of** half the power for the control experiment at the same al location

erfusion quantification

g acquired the data using either technique, the subtracted l-label images will be **perfusion** weighted (Figure 1). The nship between the ΔM signal and the actual CBF depends on proton density and T_1 relaxation rates **of** tissue and ng blood, the and their respective differences. In addition, the ransit time from the inversion slab to the observed region in the s is also an important factor. Traditionally, quantitative CBF tion is carried out using the tracer clearance theory originally sed by Kety and Schmidt

odified Bloch equation, including the flow dependent exchange term, es:

$$\frac{dM_t(t)}{dt} = \frac{M_{t,0} - M_t(t)}{T_{1t}} + \mathrm{CBF}\left(M_a(t) - \frac{M_t(t)}{\lambda}\right) \quad (3)$$

here M_t, $M_{t,0}$ and M_a are the tissue-, equilibrium- and **arterial**-agnetizations, respectively, λ is the blood–brain partition coefficient, nd T_{1t} is the longitudinal relaxation rate **of** the tissue. In the original uantification model, further assumptions about uniform plug flow and qual T_1 relaxation **of** both tissue and **arterial** blood were made

uxton et al proposed a general kinetic model where all the above entioned parameters can be taken into account. Here, the agnetization difference between labelled and control measurements described using the convolution integral in a way similar to quation (2):

$$\Delta M = 2 \cdot M_{a,0} \cdot \mathrm{CBF} \cdot \int_0^t c(\tau) \cdot r(t-\tau) \cdot m(t-\tau) d\tau \quad (4)$$

here $M_{0,a}$ is the equilibrium magnetization in a blood filled **arterial** oxel, $c(t)$ is the delivery function or fractional **arterial** input function AIF). The residue function $r(t-\tau)$ describes the washout **of** labelled **pins** from a voxel, and $m(t-\tau)$ includes the longitudinal magnetization elaxation effects. The possibility to choose a particular **arterial** input unction and to consider a certain exchange mechanism (single or nulticompartment) allows greater flexibility for data analysis **of** both ASL and PASL experiments.

Comparison with other imaging modalities

t this point, it should be kept in mind that related issues such as the

ghlighted in the previous paragraphs apply to other **perfusion** ies like DSC-**MR**I, CT-**perfusion** and positron emission aphy (PET) as well. Dynamic susceptibility contrast using such as gadolinium-DTPA for instance, suffers from the fact relationship between measured signal and contrast is non- nd depends on parameters such as the field strength, shim **of** gnet and the constitution **of** the vessels In addition, correct **of** the AIF is influenced by partial volume effects in the voxels here it is measured. Altogether, this makes quantification some, and in the general clinical practice only a relative **on** measure is possible. Similar problems exist in CT- **on**, mainly related to the extraction **of** the global AIF . PET said to be a more "pure" method for measuring **perfusion** due se **of** free diffusible tracers and experimental durations that a steady state. However, a relatively low resolution **of** typically m introduces partial volume effects, *i.e.* a mixture **of** grey- white-matter and CSF will be present in almost all voxels, direct comparisons to the abovementioned methods nable.

MR SPECTROSCOPY

ORY

et al[3] and Bloch et al[4] first elucidated the principles of nuclear tic resonance in 1946. The technique of spectroscopy is widely in chemistry for the analysis of compounds in solution, and is rful tool for determining the structure of biological molecules. Similarly, MR spectroscopy can be used to identify ant molecules in living tissue. Protons often are used for MR oscopy because of their high natural abundance and high r magnetic sensitivity.[5] Despite the huge number of ecules in tissue, relatively few are identifiable in vivo because eely mobile compounds that are present in substantial ntrations give enough signals to be detected. The ntrations of metabolites of interest are in the millimolar range; protons are a thousand times as common.[6] For this reason,

ater resonance has to be suppressed so that the other molecules n be detected. The diagnostically resolvable hydrogen MR spectra ay be obtained using clinical instruments (1.5 T or greater) and utinely used surface

RI spectroscopy (MRS) offers the capability of using MRI to non-vasively study tissue biochemistry.The hydrogen atom in water is e main one that is flipped (resonated). In MRS, either 1H atoms in ner molecules or other atoms such as 31P, 23Na, K, 19F, or Li are pped. Within a given brain region called a voxel, information on ese molecules is usually presented as a spectrograph with ecession frequency on the x-axis revealing the identity of a mpound and intensity on the y-axis, which helps quantify the nount of a substance.

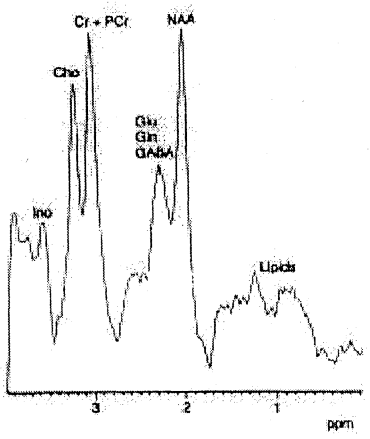

ne quantity of a substance is related to the area under its pectrographic peak; the larger the area, the more of a substance at is present .

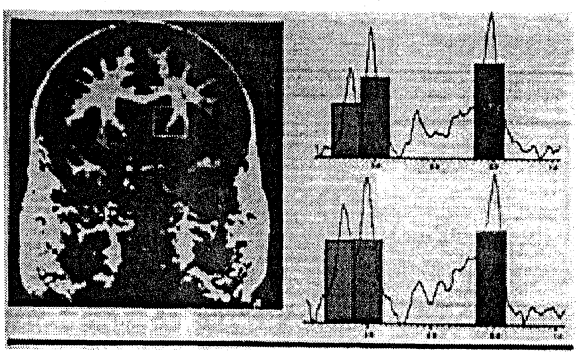

eason why several molecules can be identified and quantified
a singie scan is that the resonant magnetic puise has a
vidth over a narrow precession frequency range so that it can
veral molecules at once. The signal intensity at each of these
ssion frequencies can then be identified using a complicated
matical procedure called a Fourrier transform. For a given
ssion frequency (or spectrographic peak of a given molecule),
ation can also be presented spatially as metabolic maps which
eated with similar principles to the 1H atom in water spatial map
ventional MRI [33]. The spatial resolution of these maps is
ally less than that of conventional MRI as the substance
ntration is much less than that of water. Consequently, the
um area needed to obtain a visible signal is greater.The two
widely used MRS techniques involve either viewing 1H atoms
ecules other than water or 31P-containing molecules [31]. In 1H
the water signal must first be suppressed as it is much greater
ne signal from other 1H-containing compounds and has
pping spectroscopic peaks with these compounds [1].
ounds that can be resolved with 1H-MRS include

on MR Image

nages contain anatomical information based on the distribution
tons and the relative proton relaxation rates in various tissues
nages are based on proton signals from water and fat

Spectrum

R spectroscopy determines the presence of certain chemical mpounds. Stress, functional disorders, or diseases can cause the etabolite concentration to vary. Metabolite concentrations are low, nerating ~10,000 times less signal intensity than the water signal

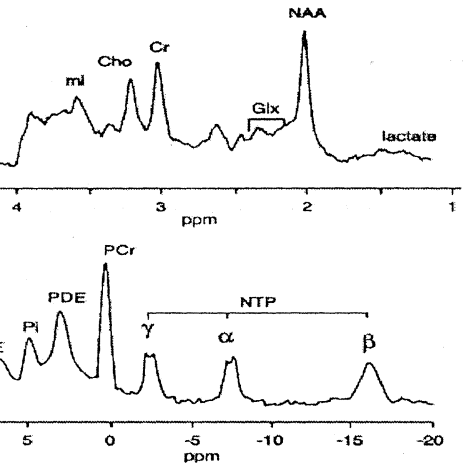

nemical Shift

ne electron cloud around each nuclei shields the external magnetic ld .Because of differences in electron shielding, identical nuclei sonate at different frequencies. The resonance frequency in the esence of shielding s is expressed as:

$$w = (1 - s)gB_o$$

here g is the gyromagnetic ratio and B_o is the external magnetic ld strength

H MR spectra

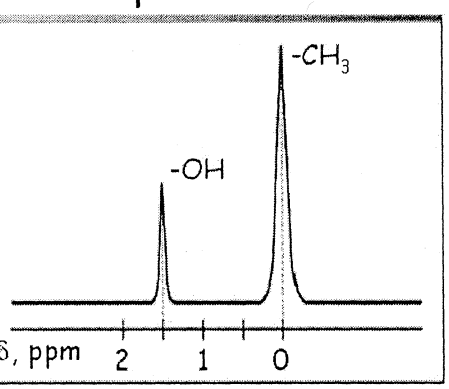

The frequency shift increases with field rength. For example, shift difference between water and fat

(wwater - wfat) at 1.5 T is 255 Hz at 3.0 T is 510 Hzd =
(wwater - wfat) 10^6/gBo, in ppm units
dwater-fat is 3.5 ppm independent of field strength
nvention. Signals of weakly shielded nuclei with higher
ency are on the left Signals of more heavily shielded nuclei with
frequency are on the right Chemical shift of water is set to 4.7
at body temperature

tial Localization

ace Coil Localization

ple surface coil acquisition
h Resolved Surface Coil Spectroscopy, DRESS

le Volume Localization

e Selected *In Vivo* Spectroscopy, ISIS
Resolved Spectroscopy, PRESS
ulated Echo Acquisition Mode, STEAM

ple Volume Acquisition

mical Shift Imaging, CSI

face Coil Acquisition

nple loop of wire and associated circuit tuned to the desired
ency are placed directly over the tissue of interest to obtain
tra

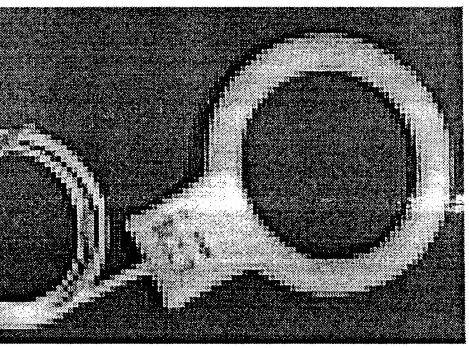

A surface coil

vantages

sy to build and does not require specialized pulse sequence
perb SNR and filling factor

advantages

st be close to region of interest
anging ROI is difficult
omogeneous RF field

Spin Echo Imaging Sequence

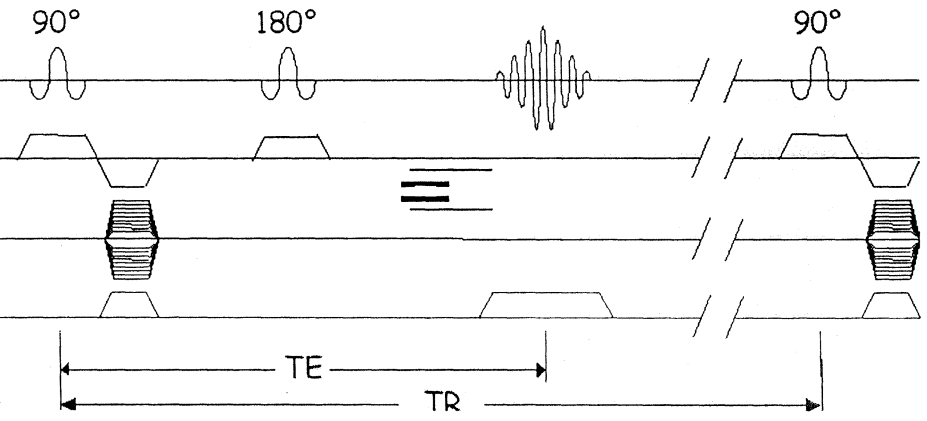

h Resolved Surface Coil Spectroscopy, DRESS

k-shaped slice is excited parallel to the surface coil with a
ency selective RF pulse in the presence of a gradient.

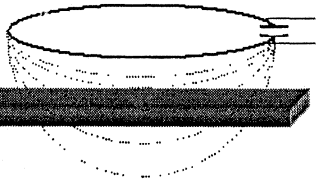

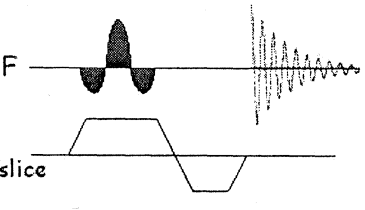

lvantages

elatively simple
ppresses signal from superficial tissue
ulti-slice acquisition, SLIT-DRESS

sadvantages

loss
artial Localization

ingle Volume Localization

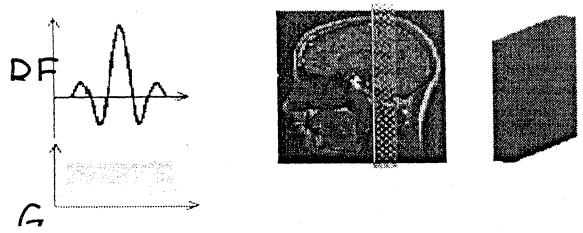

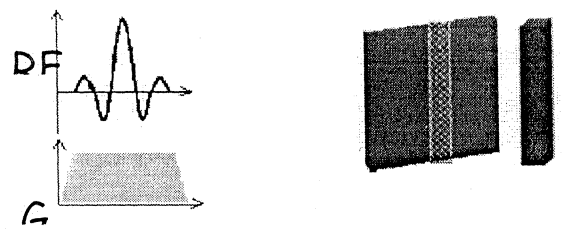

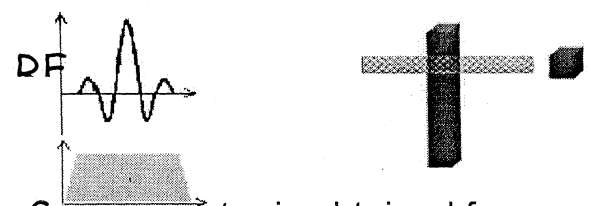

olGalized spectra is obtained from a single volume of interest (VOI)
ocalization is achieved by sequential selection of three orthogonal
ices. The size and location of VOI can be easily controlled
natomic ^{1}H images are used for localizing the VOI

ingle Volume Localization

mage selected *in vivo* spectroscopy, ISIS
oint resolved spectroscopy, PRESS

nical Shift Imaging

e localized spectra are obtained simultaneously from a set of spanning the region of interest No gradient is applied during llection, so spectral information is preserved

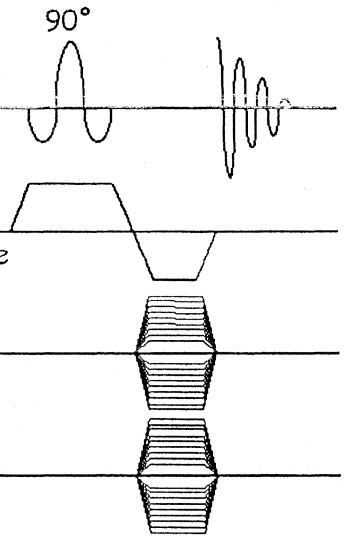

of MR spectroscopy imaging,in which spatially localized a are obtained using this technique. Although the name sts that the data will be in the form of an image, the term CSI is d more generally to any technique in which spectroscopic data quired simultaneously from a large volume of the sample and ecoded into a number of spatially resolved spectra. Spatial ion can be in one, two or three dimensions, but full three- sional CSI demands very long acquisition times. The most mplementation is a slice-selected two-dimensional acquisition. ta can be presented either as a set of spectra representing the cal composition of each spatially-resolved voxel, or as an in which the signal intensity depends on the concentration of vidual chemical species. In the latter case separate images produced for each chemical that is detected in the individual a.

gh most CSI techniques dispense with a read gradient in order etely to preserve the spectroscopic information, an alternative

proach is to employ frequency-selective pulses so that only a gle spectral component is excited. In this way, conventional aging sequences may be employed to produce an image of a rticular chemical compound

ultinuclear MR Spectroscopy

portant Nuclei for Biomedical MR

Nucleus	Spin	γ, MHz/T	Natural Abundance	Relative Sensitivity
^{1}H	1/2	42.576	99.985	100
^{2}H	1	6.536	0.015	0.96
^{3}He	1/2	32.433	.00013	44
^{13}C	1/2	10.705	1.108	1.6
^{17}O	3/2	5.772	0.037	2.9
^{19}F	1/2	40.055	100	83.4
^{23}Na	3/2	11.262	100	9.3
^{31}P	1/2	17.236	100	6.6
^{39}K	3/2	1.987	93.08	.05

– Neurotransmitters, amino acids, membrane constituents

I – Perfusion, drug metabolism, tissue and cartilage structure.

C – Glycogen, metabolic rates, substrate preference, drug metabolism, etc.

F – Drug metabolism, pH, Ca^{2+} and other metal ion Concentration, pO_2, temperature, etc

Na – Transmembrane Na^{+} gradient, tissue and cartilage structure.

P – Cellular energetic, membrane constituents, pH_i, $[Mg^{2+}]$,
etics of creatine kinase and ATP hydrolysis.

MR Spectroscopy

MR Spectra of the Brain Short TE

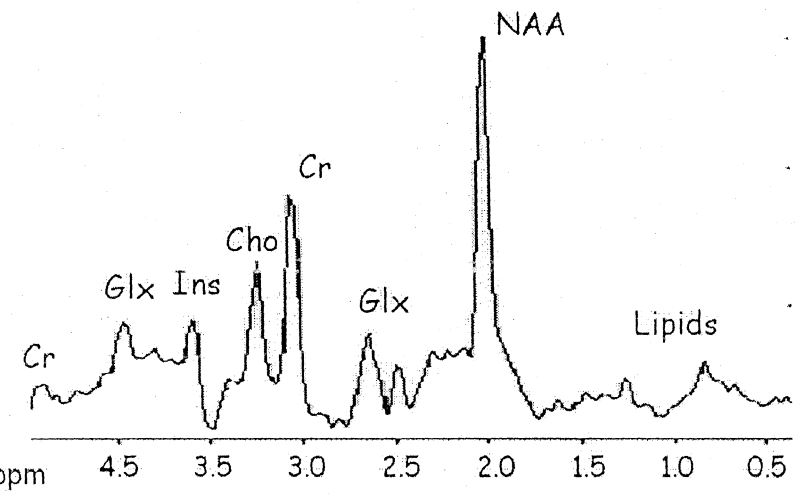

portant ^1H Signals

-Acetyl aspartate (NAA)

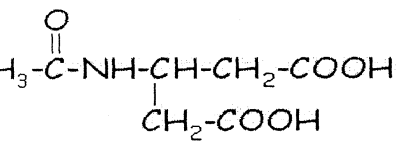

2.02, CH_3
2.52, CH_2
2.70, CH_2
4.40, CH

- NAA is a neuronal marker and indicates density and viability of neurons.
- It is decreased in glioma, ischemia and degenerative diseases.

reatine (Cr), phosphocreatine (PCr)

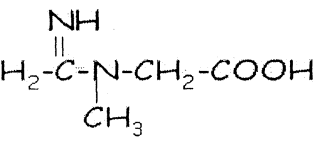

3.04, CH_3
3.93, CH_2

- Cr is a marker of aerobic energy metabolism
- Cr signal is constant even with pathologic changes and may be used as a control value
- However, isolated cases of Cr deficiency may occur in children

holine (Cho), choline compounds

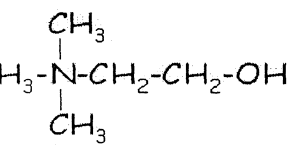

3.24, CH_3
3.56, CH_2
4.07, CH_2

- Cho compounds are involved in phospholipid metabolism of cell membrane.
- Increase Cho mark tumor tissue or multiple sclerosis plaques

lutamate (Glu), glutamine (Gln)

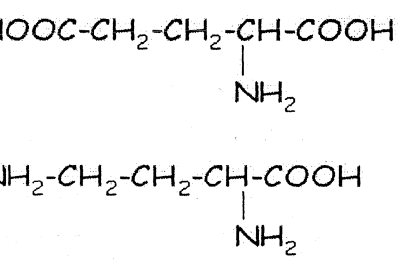

2.1, CH_2
2.4, CH_2
3.7, CH

- Glu is a neurotransmitter, Gln a regulator of Glu metabolism
- It is hardly possible to detect their signals sepratly. The signals are jointly designated "Glx".

e (Lac)

H-COOH
H

1.33, CH_3
4.12, CH

•Lactate is the final product of glycolysis

•It can be detected in ischemic/hypoxic tissue and tumors indicating lack of oxygen

ne (Tau)

H_2-CH_2-S-OH

3.27, NCH_2
3.44, SCH_2

•Cells examination indicates taurine synthesis in astrocytes

nositol (Ins)

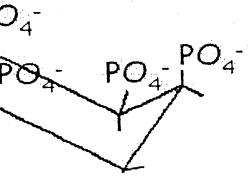

3.56, CH

•Ins marks glia cells in brain

•It is decreased in hepatic encephalopathy and elevated in Alzheimer's disease.

cromolecules from lipids resonate mainly at 0.8-1.5 ppm and thus scure other resonances such as lactate Lipids are commonly due to ination from fat included in the voxel or from extraneous tional contamination In tumors, the presence of lipids mostly es with necrosis Radiation necrosis generally contains a large amount s

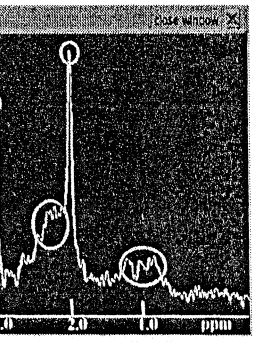

Table 1. METABOLITE PEAKS VISIBLE IN BRAIN AND BRAIN TUMORS

Chemical Structure	Peak Location (ppm)*	Peak Form
Ac methyl	1.92	Singlet
Cholines trimethyl	3.21	Singlet
Creatines CH	3.93	Singlet
Creatines methyl	3.04	Singlet
Gly CH	3.56	Singlet
NAA methyl	2.02	Singlet
NAAG methyl	2.05	Singlet
Suc methylene	2.42	Singlet
Ala	1.48	Doublet
Asp	3.90	Multiplet
Asp	2.81	Multiplet
Asp	2.68	Multiplet
Cholines	3.52	Triplet
GABA	3.01–3.02	Multiplet
GABA	2.30	Multiplet
GABA	1.91	Multiplet
GLN	3.78	Multiplet
GLN	2.46	Multiplet
GLN	2.14	Multiplet
GLU	3.76	Multiplet
GLU	2.35	Multiplet
GLU	2.11	Multiplet
Lac	1.33	Doublet
Myo-inositol	3.63	Triplet
Myo-inositol	3.54	Multiplet
Myo-inositol	3.29	Triplet
NAA	2.70	Multiplet
NAA	2.50	Multiplet
Tau N-CH2	3.27	Triplet
Tau S-CH2	3.43	Triplet
Threonine	3.59	Doublet
Threonine	1.33	Doublet
Valine	3.61	Doublet
Valine	2.27	Multiplet
Valine	1.05	Doublet
Valine	0.99	Doublet

*Resonances at ppm's > 4.0 are not listed.

P MR Spectroscopy

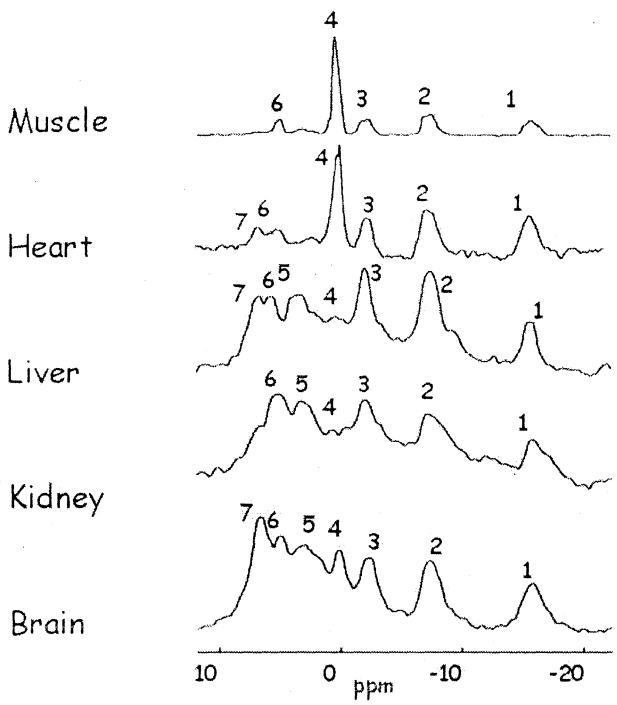

1. β-ATP
2. α-ATP
3. γ-ATP
4. PCr
5. PDE
6. P_i
7. PME

Adenosine triphosphate (ATP)

-16.5	β-ATP
-7.8	γ-ATP
-2.7	α-ATP

ATP is the energy currency in living systems
β- and γ-ATP have contributions from ADP, NAD and NADH
β-ATP is uncontaminated and used for quantification

Phosphocreatine (PCr)

0	PCr

PCr is used for storing energy and converting ADP to ATP
It is absent in liver, kideny and red cells
It is used as an internal reference for chemical shift

organic Phosphate (P_i)

3.7 to 5.7 P_i

- P_i is generated from hydrolysis of ATP and increased in compromised tissue
- its chemical shift is sensitive to pH

hosphomonoester (PME)

5.6 to 8.1 PME

- PME signal contains contribution from membrane constituents and glucose-6-phosphate and glycerol-3 phosphate.
- It is elevated in tumors

hosphodiester (PDE)

0.6 to 3.7 PDE

- PME signal contains contribution from membrane constituents

Measurement of pH by ^{31}P MRS

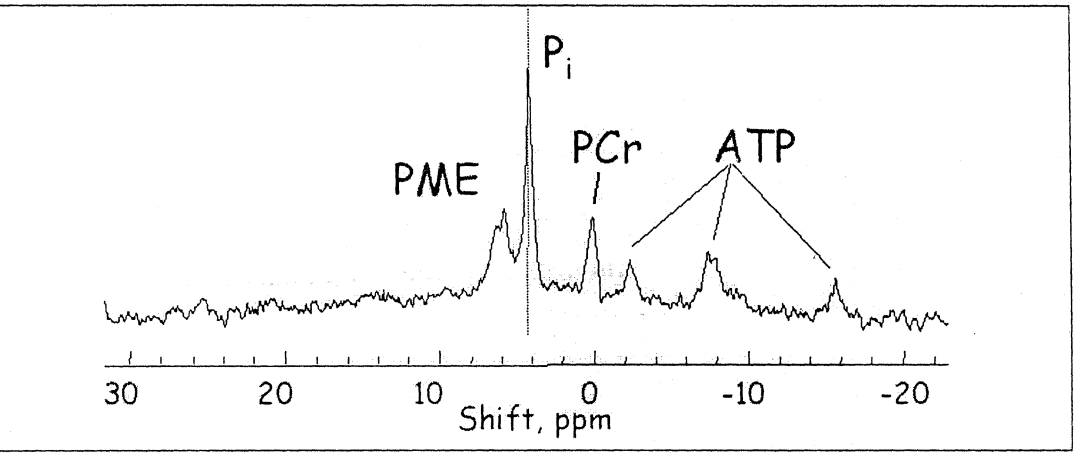

$$pH = pk_a + \log\left[\frac{\delta_{obs} - \delta_{H_2PO_4^-}}{\delta_{HPO_4^{2-}} - \delta_{obs}}\right]$$

Detection of myocardial infarctions by ^{31}P-MR spectroscopy

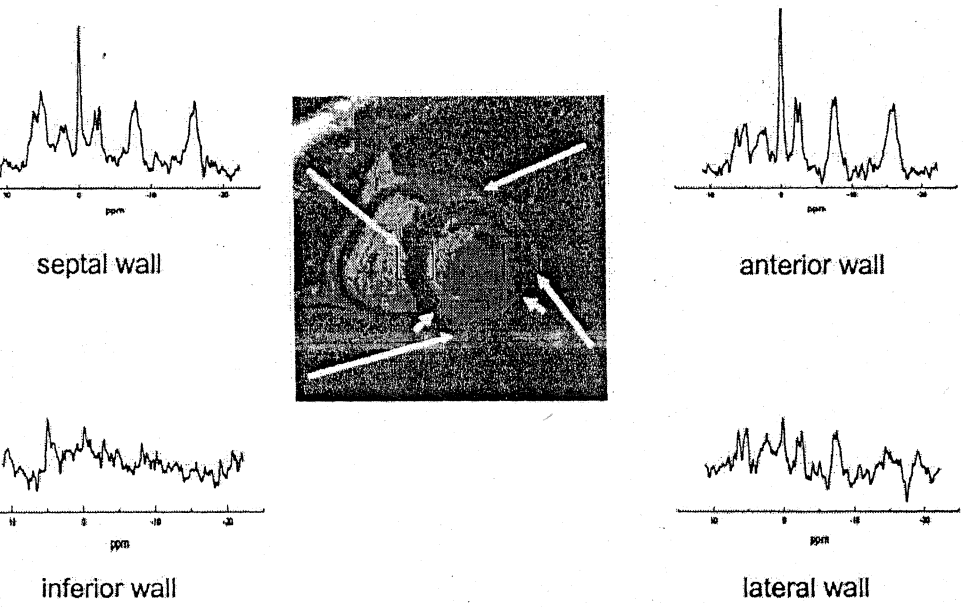

Beer et al., J Magn Reson Imaging. 2004;20:798-802.

MR Spectroscopy and Imaging

gical Importance of Sodium

m and other ions are inhomogeneously distributed across the
nembrane.A transmembrane sodium gradient reflects a dynamic
brium between Na^+-K^+ ATPase versus passive or mediated
The sodium gradient may be altered in certain diseased states.
is the second most sensitive nucleus for biomedical NMR.
and extracellular sodium resonate at the same frequency.
approaches to distinguish between different sodium pools:
Paramagnetic Shift Reagents
Multiple Quantum Filters

Na Shift Reagents

Rs are membrane impermeable negatively charged chelates of anthanide metal ion. They interact with extracellular Na^+, using its signal to be shifted away from intracellular Na^+.

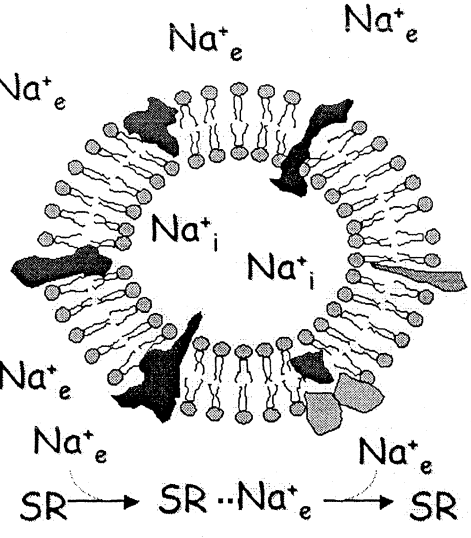

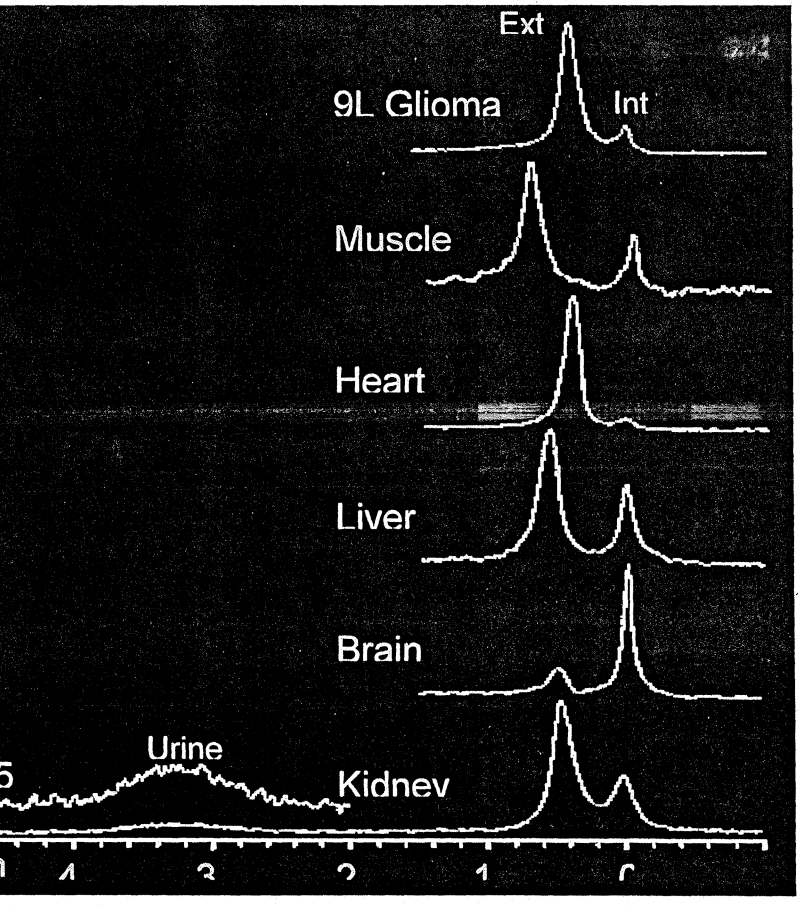

N-acetylaspartate (NAA) which is thought to be a neuronal marker
decreases in processes where neurons die;
actate which is a product of anaerobic metabolism and may
cate hypoxia;
excitatory neurotransmitters glutamate and aspartate;
he inhibitory neurotransmitter gamma-aminobutyric acid (GABA) ;
ytosolic choline which includes primarily mobile molecules
lved in phospholipid membrane metabolism but also small
unts of the neurotransmitter acetylcholine and its precursor
ine;
myoinositol which is important in phospholipid metabolism and
cellular second messenger systems; and
creatine molecules such as creatine and phosphocreatine which
ally have relatively constant concentrations throughout the brain
are often used as relative reference molecules (ie. you may see
A concentration reported as the ratio NAA/creatine in the
ature).
sphorus (31P) MRS allows the quantification of ATP
abolism, intracellular pH, and phospholipid metabolism . ATP
abolism quantification is possible because ATP is involved in the
wing reactions :
ATP ADP + Phosphorus (Pi)
ere the relative concentrations of ATP and Pi can be determined
^{31}P MRS

ADP + phosphocreatine ATP + Creatine
re the relative concentrations of phosphocreatine and ATP can
be determined with ^{31}P MRS .
can be measured because H2PO4 H+ + HPO4-2, and the
onance frequency for H2PO4 is different from HPO4-2. As the
between these two molecules is so rapid, they present as one
ctrographic peak. However, when one of these compounds is
sent at its equilibrium, the peak is shifted closer to that
npound's true precession frequency, allowing changes in pH to be
asured by its position [34]. Mobile phospholipids, including
sphomonoesters (PME - putative cell membrane building blocks)
phosphodiesters (PDE - putative cell membrane breakdown
ducts) can also be measured, supplying information on
spholipid membrane metabolism.
MRS can be used to identify regional biochemical abnormalities.

example, ^{31}P-MRS studies of euthymic bipolar patients have ealed decreased frontal lobe PMEs (cell membrane building cks) compared with healthy controls. However, when bipolar ients become either manic or depressed, their PMEs increase. ese findings appear to be unrelated to medication treatment. The ding of decreased frontal PMEs in euthymic bipolars has also been monstrated in schizophrenia and speculatively accounts for the ding of decreased frontal lobe metabolism in both of these orders. The schizophrenia finding also appears to be medication-ependent [32].

MRS may also be of future help in the differential diagnosis of tain psychiatric diseases such as dementia. In normal aging, there a decrease in PMEs and increase in PDEs [36,37]. In early heimer's Dementia, there appears to be increased PMEs which y be help distinguish it from normal aging[38]. Researchers have o found increased myoinositol and decreased NAA levels in heimer's Dementia compared with healthy controls [39,40]. Some ieve that a decrease in NAA coupled with an increased myoinositol el helps in diferentiating probable Alzheimer's Dementia from althy age-matched controls as well as other dementias (usually creased NAA but normal myoinositol levels) [39].

With MRS, changes in metabolic activity can be measured over e within an individual scanning session. For instance, Dager et al. 995) used ^{1}H MRS to measure changes in lactate concentration h controlled hyperventilation in panic disorder patients and healthy ntrols [41]. MRS can also be used to measure changes in metabolic tivity between sessions, such as before and after medication atment. For example, Satlin et al. (1997) used ^{1}H MRS to measure dparietal lobe cytosol choline levels in 12 Alzheimer's subjects fore and after treatment with Xanomeline, an M1 selective olinergic agonist, or placebo [42]. Additionally, MRS can be used to easure drug levels of certain psychotropic drugs. The magnetic ements ^{7}Li and ^{19}F do not naturally occur in the human body but ey are found in psychotropic drugs; lithium for ^{7}Li and fluoxetine d stelazine for ^{19}F. For example, studies have consistently found at the brain concentrations of lithium are about 0.5 that of serum Li vels and correlate with treatment response.

For psychiatry, MRS is a research tool at this time. In neurology d neurosurgery, however, MRS is starting to be used in the

acterization of tumor, stroke, and epileptogenic tissue and in urgical planning [26,34].

ations

RS is restricted to studying mobile magnetic compounds. As ochemical receptors are not usually mobile, they cannot be sured with MRS. Thus, receptor-ligand studies are still the ain of SPECT and PET. Another problem with MRS is that due to ow concentrations of many of the imaged substances, larger s than with water are needed to obtain detectable signals. Larger me units imaged over longer periods are thus used with this nique, limiting both temporal and spatial resolution compared conventional MRI, and BOLD-fMRI. However, stronger magnetic s which can spread out precession frequencies over a wider e may improve this resolution (ie. a magnetic field twice as g will double the difference between two substances' precession encies, thus increasing resolution). Stronger magnetic fields also allow detection of compounds that are currently considered e in too low a concentration to be seen with current MRS opment.

SEQUENTIAL STEPS OF AN MRs EXAMINATION

IENT POSITIONING
BAL SHIMMING
UISTION OF MR IMAGE FOR LOCALIZATION
ECTION OF MRS MEASUREMENT SEUENCES & AMETERS
ECTION OF AVOLUME OF INTEREST
ALIZED SHIMMING
IMIZATION OF WATER SUPPRESSION
S DATA COLLECTION
S DATA PROCESSING AND DISPLAY

IENT POSITIONING

tient is positioned in the standard head coil Head should be firmly ported to prevents the involuntary.Line broadening ,incorrect lization ,loss of signal.SVS- it causes to collect signal from out the volume. CSI-Phase differences,ghosting on MR images -Motion between the multiple measurements leads to incomplete cellation unwanted signals

OBAL SHIMMING

Optimizing the MF homogeneity It is doing at the Beginning of an aging or MRS. It is Fast and it ensure good quality images & ectra

rovides coil tuning transmitter frequency & power adjustments n alternate approach –store shim sets as data files that may be called and used when needed

SITION OF THE VOLUME

xel is placed over the abnormal tissue.The size of the voxel is justed in order to minimize the normal tissue .Voxel should avoid e scalp,bone sinuses, blood vessels ,csf ,calcification & necrotic ea.Minimize the mixture of gray & white matter

OCAL SHIM

timize the MF homogeneity over the selected volume. Good local im produce a narrower metabolite peak better spectral resolution nproved SNR. Selected MR sequences and it use the water signal. e procedures consist of varying shim currents, one at a time until e narrowest water peak is produced. FWHM– 4-10 HZ, 8 –27 CM^3

ATER SUPPRESSION

rge water signal make it difficult to observe weak signal from etabolites

HESS-Frequency selective 90°pulse ,followed by dephasing adient

0-single CHESS

RYSTEAM

ET– 4 frequency selective RF pulse with different flip angle produce better water suppression than CHESS

EFT

EASUREMENT

6 min –SVS

min-CSI

ATA PROCESSING & DISPLAY OF SPECTRA

tomatically or Manually

me domain signal into frequency domain signal

spectrum is typically displayed with water peak –4.7ppm
mical shift of water with respect to TMS
major metabolites peaks between 0-4.3ppm

CESSING OF THE MR SIGNAL

domain signal –ADC offset correction ,zero filling, apodisation
ection from residual eddy currents ,removal of the water peak
wing the FT—Phase correction ,base line correction ,curve
g

SE CORRECTION

arate pure absorption & pure dispersion mode into the real and
inary part of the complex spectrum
ected with constant or zero order phase factor

SE LINE CORRECTION

e line of the MR spectrum will be flat until the resonance peak is
hed.Delay between the RF-excitation and beginning of the
ction period produces a rolling baseline.Un subtracted water
cause sloping of the base line

K IDENTIFICATION

ermination of the peak position and characteristics
fication of the presence or absence of given metabolites

AK EDITING

arating overlapping peaks for identification

AK AREA CALCULATION

under a peak is directly proportional to the number of spins
ributing to the peak

MR ANGIOGRAPHY

me-of-flight angiography (TOF), phase-contrast angiography (PCA) d contrast enhanced angiography (CEA) are the three common MR giographic techniques. Flow related enhancement is the basis of ne-of-flight angiography.

1. **Time-of-flight MR angiography** (TOF)
2. **Phase contrast MR angiography** (PCA)
3. Contrast enhanced MR Angiography (CEA)

ow-related Enhancement

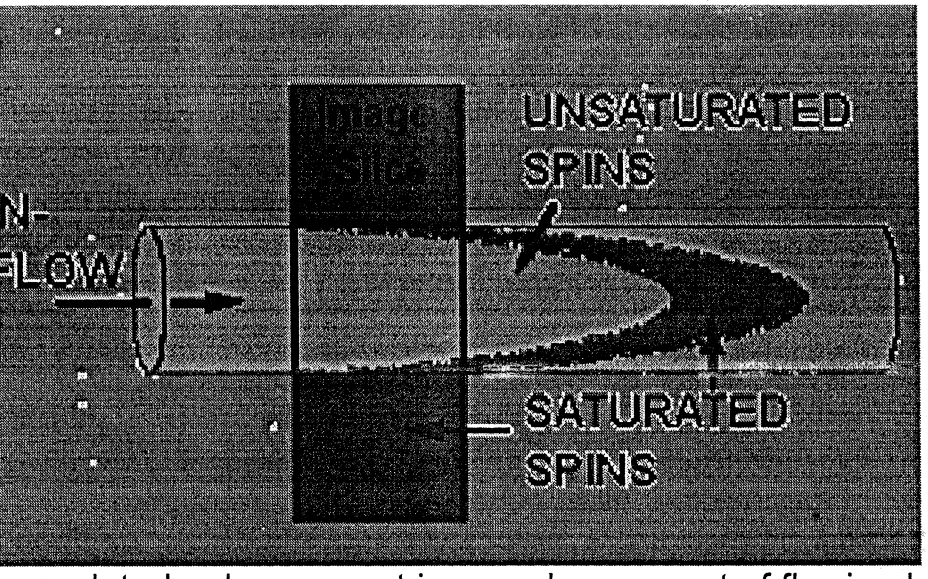

ow-related enhancement is an enhancement of flowing blood seen n gradient echo pulse sequences as well as in entry slices of ultslice spin echo sequences. This enhancement is a result of inflow unsaturated (completely relaxed) spins into a slice plane or naging volume between RF excitations. Stationary spins within the naging volume will undergo incomplete T1 relaxation between RF xcitations resulting in less signal following the next RF pulse when ompared to inflowing, completely relaxed spins in flowing blood. The stance that the unsaturated blood can extend into an imaging

ne and therefore the degree of enhancement is proportional to R and the velocity of the blood. The use of gradient motion g (flow compensation) improves the flow-related enhancement adient echo sequences.

ne-of-Flight MR Angiography

-of-flight (TOF) angiography is based on the phenomenon of related enhancement of spins entering into an imaging slice. As ult of being unsaturated, these spins give more signal that unding stationary spins. With 2-D TOF, multiple thin imaging s are acquired with a flow-compensated gradient-echo ence. These images can be combined by using a technique of nstruction such as maximum intensity projection (MIP), to obtain) image of the vessels analogous to conventional angiography

3-D TOF, a volume of images is obtained simultaneously by e-encoding in the slice-select direction. An angiographic earance can be generated using MIP, as is done with 2-D TOF. eral 3-D TOF volumes can be combined to visualize longer nents of vessels. 3-D TOF angiography will allow greater spatial lution in the slice-select direction than 2-D TOF; however, with volumes and slow flowing blood, loss of signal is seen with the TOF method.
tiple Overlapped Thin Slab Acquisitions (MOTSA).

olume is subjected to multiple RF excitations (as you go from imal to distal) it causes saturation of slow flowing spins. That can voided by using overlapping slabs (MOTSA), this with the ense of increased imaging time. While 3D slabs are stacked ther a dark line crosses the image called Venetian blind artifact. can be avoided by giving 30 – 50 % overlap.

.Phase-contrast MR Angiography .

s that are moving in the same direction as a magnetic field ient develop a phase shift that is proportional to the velocity of spins. This is the basis of phase-contrast angiography. In the olest phase-contrast pulse sequence, bipolar gradients (two

adients with equal magnitude but opposite direction) are used to ncode the velocity of the spins. Stationary spins undergo no net hange in phase after the two gradients are applied. Moving spins will xperience a different magnitude of the second gradient compared to e first, because of its different spatial position. This results in a net hase shift. This information can be used directly to determine the elocity of the spins. Alternatively, the image can be subtracted from he acquired without the velocity encoding gradients to obtain an ngiogram.

Contrast enhanced MR Angiography:

rinciples of 3D Gadolinium-enhanced MR Angiography
adolinium is one of the rare earth elements in the transition group b of the periodic table. Actually, it is not rare at all, but a rather ommon element found throughout the earth's crust. It has eight npaired electrons in its outer shell, which causes its paramagnetic ffects. Gadolinium by itself can cause heavy metal poisoning. owever, when bound to a chelator, it is safe for intravenous jection, yet remains paramagnetic. It shortens the T1 of blood in the egion of the gadolinium molecule according to the following equation):

$$1/T1 = 1/1{,}200 + (R1 \times [Gd]),$$

here R1 is the T1 relaxivity of the gadolinium chelate, [Gd] is the adolinium concentration in the blood, and 1,200 is the blood T1 (in sec) without gadolinium.

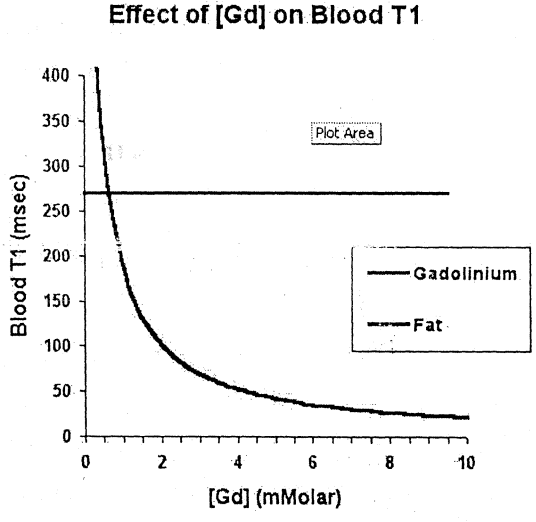

ure 1 Effect of gadolinium concentration on blood T1. (The graph
s calculated with Microsoft Excel 97 [Microsoft, Redmond, Wash]
using the above formula.)
e blood [Gd] must be greater than 1.0 mmol/L for T1 to be less
n 270 msec, which is the T1 of fat at 1.5 T (1, 5). This is the
perty which is important for increasing the MR signal intensity of
od on contrast-enhanced SPGR images. Note that this T1
rtening effect is maximized by using gadolinium chelates with the
hest relaxivity and by having a high gadolinium concentration in
blood.

Space

e most important effect is related to how MR data are mapped in k
ace. K space, or Fourier space, does not map to the image pixel by
el. Rather, the information within k space determines spatial
quency features of the image. The low spatial frequency
ormation, in the center of k space, dominates image contrast, while
higher spatial frequency data, at the periphery of k space,
termines image detail. To obtain an arterial-phase image in which
eries are bright and veins are dark, it is essential that the central k-
ace data (ie, the low spatial frequency data) are acquired while the
dolinium concentration in the arteries is high but relatively lower in
veins. The presence of contrast agent is not as important for
quisition of peripheral k-space data. This trick allows a relatively
ng MR acquisition to achieve the image contrast associated with a
ef window of time. That brief window of time is the instant when
ntral k-space data are acquired. Therefore, it is critical to time the
lus for maximum arterial [Gd] during acquisition of central k-space
ta. With perfect bolus timing, high S/N arterial-phase images are
ssible with smaller doses of gadolinium.

adolinium Extraction

second important effect is the extraction of gadolinium in the
stemic capillary beds. This extraction results in venous blood
nding to have a lower concentration of gadolinium relative to arterial
od, even for relatively long, sustained infusions lasting several
inutes. This effect is not present in the cerebrovascular circulation
ecause of the blood-brain barrier. Consequently, arterial-phase

ging in the central nervous system is more difficult.

sion Rate and Cardiac Output

ird effect is the relationship between arterial gadolinium centration, the infusion rate, and cardiac output as follows:
$_{Arterial}$=Injection Rate/Cardiac Output

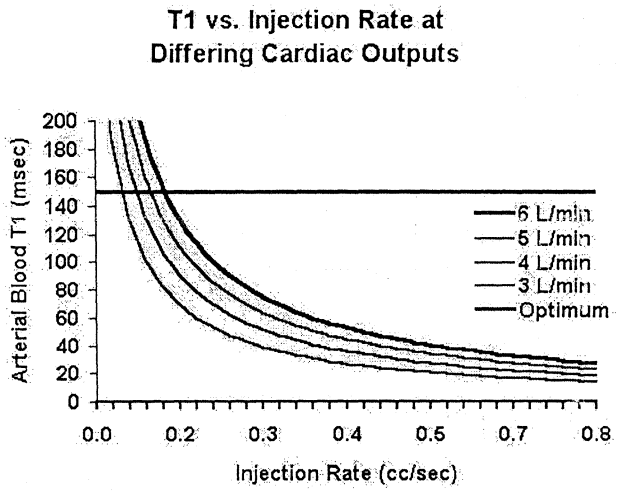

ure 2. T1 versus injection rate at differing cardiac outputs.

s graph is a computer model generated for different cardiac outs. Note that this graph is for static, nonmoving blood. The ual T1 of moving blood is even less than in the above graph. ice that an injection rate of 0.2-0.3 mL/sec is required to decrease blood T1 value to less than 150 msec in a patient with a cardiac out of 5 L/min. This is sufficiently below the T1 of fat (270 msec at T) so that only the gadolinium in blood produces high signal nsity on T1-weighted SPGR images.

erial [Gd] is maximized by relaxing the patient to reduce cardiac out and by using a high infusion rate. However, fast infusion rates ing for at least half of the acquisition time require large doses of olinium. The dose can be kept to a reasonable level by scanning idly. Fast acquisitions (<45 seconds) are possible with high formance gradient systems that allow short repetition and echo es, without having to make the bandwidth too wide. Fast

ition has the additional benefit of making it possible for the rative patient to suspend breathing and to hold perfectly still.

Flush and Intravenous Tubing

portant to use intravenous (IV) line tubing that allows aneous attachment of separate syringes for the contrast agent aline flush.

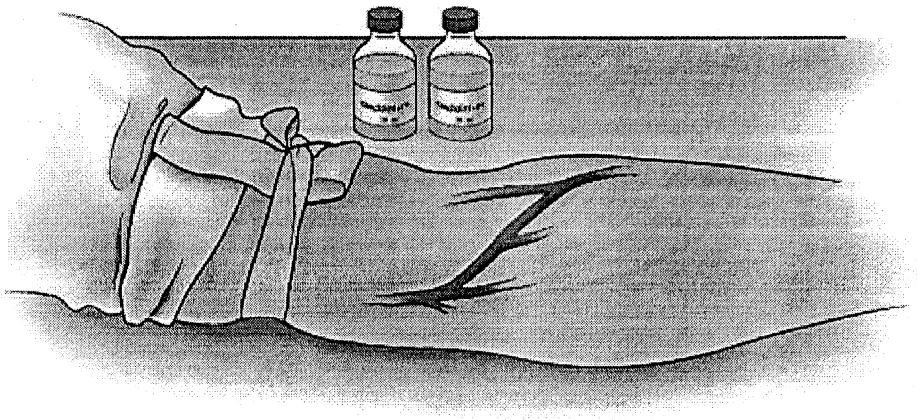

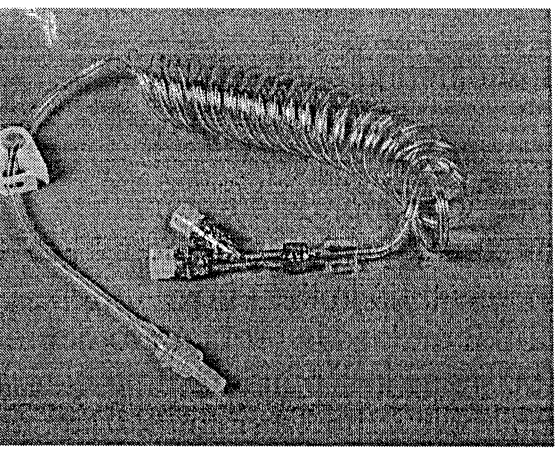

developed at the University of Michigan, has one-way valves llow automatic switching between the contrast agent injection aline flush so that there will be one continuous bolus with no By using the same tubing set for all patients receiving dynamic ast agent injection, the operator becomes familiar with rming the injections and especially with the resistance to ion. It is then easier to concentrate on correctly timing the bolus nstructing the patient to suspend breathing.

ast 20 mL of saline is recommended to adequately flush the

ntrast agent through the IV tubing and arm vein. By starting with a -mL saline-filled syringe, it is possible to initially prime the hartSet with 8 mL of saline, test the IV once or twice with a 1-mL line injection, and still have 20 mL left for the dynamic flush.

adolinium Dose

hen beginning, we recommend use of two bottles (42 mL) for the erage-size patient and three bottles (63 mL) for patients weighing ore than 100 kg. Once you learn how to time the contrast agent ections perfectly, you will find it is possible to reduce the dose and ll obtain diagnostic images.

ontrast Agent Bolus Timing

erfect contrast agent bolus timing is crucial to ensure that the aximum arterial [Gd] occurs during the middle of the acquisition, hen central k-space data are acquired. It is also essential that [Gd] t change too rapidly, as this will create a "ringing" artifact. nimizing the ringing artifact requires that the contrast agent infusion st for at least half the duration of the 3D image acquisition. Bolus ming is difficult because the time required for the contrast agent olus to travel from the injection site (typically an antecubital vein) to e artery being imaged is highly variable. For renal arteries, it may only 10 seconds in a young, healthy person with a central travenous line, or it may be as long as 50 seconds in an older tient with congestive heart failure and an intravenous line in the nd or wrist.

ming for Long Acquisitions

or long acquisitions, lasting more than 100 seconds, timing is easy ecause errors of 10-15 seconds are small relative to the total scan uration. Use sequential ordering of k space, so that the center of k pace is collected during the middle of the acquisition. Sequential dering tends to result in fewer artifacts. Begin injecting the adolinium just after initiating imaging. Finish the injection just after e midpoint of the acquisition, being careful to maintain the

m injection rate for the approximately 10-30 seconds prior to dle of the acquisition. This will ensure a maximum arterial [Gd] he middle of the acquisition, when central k-space data are d. To ensure full use of the entire dose of contrast agent, it is o flush the IV tubing with 20 mL of normal saline. This can be ed by using the SmartSet, which has ports for simultaneous ent of contrast agent and saline syringes and valves for tic switching between syringes. In this way, there is no delay n finishing the contrast agent injection and beginning the ush.

for Fast (Breath-hold) Scans

scans, less than 45 seconds in duration, contrast agent bolus s more critical and challenging. This is because bolus timing f 15 seconds can ruin a fast breath-hold scan. There are approaches to determining the optimal bolus timing for these ns. The simplest, although least successful approach, is to n the basis of patient age, cardiac status, presence of aortic smal disease, and IV location. For a typical breath-hold scan n of 35-45 seconds in a reasonably healthy patient with an IV he antecubital vein, a delay of approximately 10-12 seconds is riate. Therefore, in this scenario, begin the injection, and then nds later start imaging while the patient suspends breathing. is no convenient clock available to time this delay, take age of the natural rhythm of the patient's respiration. One deep n followed by a deep breath out takes approximately 4 s. Two breaths are eight seconds, followed by a deep breath econds, which represents the optimum delay between start of n and beginning of scanning. If a patient is older and has a of cardiac or aortic aneurysmal disease, add one or two extra to the delay. Also, if the IV site is in the wrist, add an extra to the delay. Alternatively, if the patient is a marathon runner are injecting via a central line, it may be suitable to use only aths of delay, or 6 seconds. A firm injection is necessary to e contrast agent bolus together. However, if the injection is rous, it may cause rupture of the vein, with resulting sation of the contrast agent.

eliable and precise techniques for determining the contrast

vel time are also available. These include using a test bolus to
cisely measure the contrast travel time, using an automatic pulse
quence that monitors signal in the aorta and then initiates imaging
er contrast is detected arriving in the aorta (Fluoroscopic triggering
MR SmartPrep), or imaging so rapidly that bolus timing is
mportant. A typical monitor signal graph is shown below.

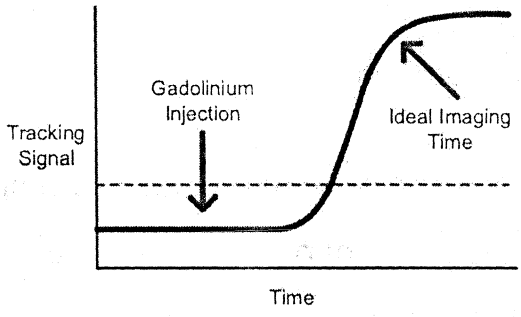

gure 3. Tracking signal versus time.
ue line - MR signal intensity in volume of interest.
een line - Level at which signal is 100% above baseline.
d arrows - Time of injection and optimal time for imaging.

te that the centric ordering of k space for the triggered acquisitions
ay create artifacts if the contrast agent bolus is still arriving when
e scan is started. Sometimes this artifact may be reduced with
quential ordering. This artifact may also be reduced by delaying 5-8
conds after detecting the leading edge of the bolus to give the
ntrast agent time to flow in completely and reach the plateau phase
the bolus.

stprocessing of MR Data

bstantial improvement in image quality, and especially image
ntrast, can be attained through postprocessing techniques.
ro Padding
age resolution can be increased with interpolation. One particularly
eful interpolation scheme is known as zero padding. This involves
ing out peripheral lines of k-space data with zeroes prior to
rforming the Fourier transform. Although no additional time is

d for data collection, the Fourier transform will reconstruct
nages with a smaller spacing. For example, with two-fold zero
g, if the partition thickness is 3 mm, the Fourier transform will
truct additional images that also have a 3-mm slice thickness
.5-mm spacing with 50% overlap. This helps eliminate volume
ng and creates smooth visualization of small vessels on the
atted maximum intensity projection (MIP) images. If available,
d zero padding in the slice direction is recommended.

gital Subtraction Angiography (DSA)

contrast can be improved by digital subtraction of precontrast
data from dynamic, arterial, or venous phase image data. This
ction can be performed either slice-by-slice or prior to the
transform by using a complex subtraction method. The
ement in contrast achieved with DSA may reduce the
nium dose required. However, there must be no change in the
position between the precontrast and dynamic contrast-
ced imaging. This requirement for no motion is easily met in the
and legs, which can be sandbagged and strapped down. It is
difficult to achieve in the chest and abdomen, where respiratory,
c, and peristaltic motions are more difficult to avoid. Note that
ex subtraction is generally performed automatically by the
er before creating any of the images.

planar Reconstructions

nations and MIPs are essential for optimal assessment of
ar anatomy. Single-voxel-thick reformations and narrow
ume MIPs show bifurcations and branch vessels in profile. This
ortant because atherosclerotic disease tends to be most severe
nch points. By creating subvolume MIPs of the 3D image data,
techniques help unfold tortuous vessels and eliminate the
ing overlap of vascular anatomy.

ng an MIP Image

pproach to performing a subvolume MIP is to first load the
3D volume of arterial phase image data into the computer
ation 3D analysis program. Display a coronal MIP of the entire

ıme, an axial reformation, and an oblique view. On the coronal
v, move the dot (which tracks the location) cranially and caudally
e watching the axial reconstruction window to find the renal
ries. Display this subvolume of sagittal data as an MIP. Make this
que MIP thick enough to encompass most of the aorta. Be certain
lign the axis of the subvolume MIP so that it is parallel to the
in of the vessel. Although the entire length of the vessel may not
seen on this image, it will be an accurate representation of the
sel's origin, with no overlap from the aorta. This may then be
eated by moving the tracker dot on the axial image and watching
oblique view to create a sagittal view of the celiac and superior
senteric arteries. This will show the celiac and superior and inferior
senteric arteries, as well as the anterior and posterior margins of
aorta to best advantage.

ıe-Resolved Peripheral MRA

ıe-resolved Gd-MRA techniques are useful when they are
ınbined with 3D Gd-MRA. These are 3D TRICKS and 2D projection
A of the calves and the feet. Time-resolved images shows the
ıtrast arrival time to the calf and gives an idea about how fast the
od flow is. The bolus timing of subsequent 3D bolus chase Gd-
A can be determined based on this information. If the contrast
val time to the calf is less than 25 s, acquisition of 3D Gd-MRA
ıout venous enhancement is almost impossible. In these fast flow
ients, tourniquets (Smart Tourniquet) applied on the thighs are
ecially important for decreasing venous contamination**Time-
olved 2D-projection MRA (calves and feet)**

GR pulse sequence which acquires 30 sequential images of a
k slab (60-120 mm). Display rate of the images is 2 frames/s.
sition the coil over the area from above the knee to mid-tibia,
ndmark on mid-coil
st acquire the pre-contrast sagittal localizer images
sagittal images prescribe a coronal thick slab for imaging the
urcations of both legs
contrast enhanced image acquisition, fill the tubing with Gd, and
n attach to the angiocatheter. Begin administering 6 ml of Gd
us by hand as fast as possible and simultaneously press the
an' button. As soon as the Gd administration finishes, switch to 20

line flush at the same rate. If you are using an injector; 3.5 ml/s
llowed with 25 ml saline flush as 3.5 ml/s.
the coil down to image ankle and the feet. Position with cushion
r knees to that foot will point more horizontally. The toes should
cking out slightly beyond the end of the coil. Tape feet together
mind the patient to hold still.
acquire coronal localizer images. Coronal T1 of ankle-foot is
y to run. No adjustment necessary.
cription of sagittal 2D projection MRA: On the coronal localizer
se a slice 10-30 mm posterior to isocenter) set slab thickness to
of foot-ankle. Use "shift" to place one sagittal thick slab on each
-foot.
sufficient phases so that total scan time is > 1 minute. If patient
ler or expected to have really slow flow, make sure there are
ient slices to image for at least 90 seconds.
g similar parameters and another bolus injection of 6 mL of
linium, acquire sagittal time-resolved ankle and foot images.
nage obtained before the contrast arrival (visually identified on
btracted images) was used as the mask for complex subtraction
the subsequent image data. This is done both calves and feet)
onstruction from remote terminal:

Cardiac MRI

gnetic resonance imaging (MRI) of the heart and great vessels
improved substantially over the past decade, and it is entering
mainstream of diagnostic imaging. As commercial cardiac MRI
ems become more available, demand will grow exponentially.
demand for cost-effective, noninvasive, and safer technology
ensures that cardiac MRI will become a mainstay in cardiac
ging. Diagnosticians must embrace and master the techniques
f cardiovascular imaging and image interpretation if the full
potential of cardiac MRI is to be realized.
rdiac MRI already is considered the procedure of choice in the
luation of pericardial disease and intracardiac and pericardiac
ses, for imaging the right ventricle and pulmonary vessels, and
r assessing many forms of congenital heart disease, especially

after corrective surgery. and the assessment of ischemic heart disease

omplexity of cardiac anatomy

e cardiac anatomy is complex, and cardiac structures have ferent appearances depending on the imaging plane and other tions selected. The most useful imaging planes are those parallel d perpendicular to the cardiac axes. The imager needs to be aware at these planes are not based on external landmarks. Obtaining ages in these double-oblique planes requires the use of multiple calizing sequences and knowledge of the target anatomy.

omplexity of cardiac anatomy

e cardiac anatomy is complex, and cardiac structures have ferent appearances depending on the imaging plane and other tions selected. The most useful imaging planes are those parallel d perpendicular to the cardiac axes. The imager needs to be aware at these planes are not based on external landmarks. Obtaining ages in these double-oblique planes requires the use of multiple calizing sequences and knowledge of the target anatomy. The mplexity of cardiac structures and function must be understood to vise a well-planned imaging scheme. The use of rigid protocols is advised. Each patient's imaging session must be customized to commodate individual variations and distortions caused by cardiac sease.

hoice of pulse sequences

ne choice of pulse sequences and parameters that affect the ppearance of the images obtained with a given sequence greatly epends on the clinical question. The limitations and advantages herent in particular imaging methods such as spin-echo (SE) or adient-echo (GE) techniques must be considered in the selection of lse sequences. GE uses a single excitation pulse to produce aging signals, whereas SE uses both 90° and 180° pulses. Cardiac orphology and anatomy are appreciated better with SE images, hich show higher contrast. Contrast is related to signal intensity fferences, which are chiefly determined by the proton density, T1

relaxation time differences, flow and motion effects, and
tic susceptibility, as they are related to the pulse sequence
. In general, tissue characteristics and pathologic changes
enerally more pronounced on SE images. Signal
ity on GE images largely reflects differences in proton density;
mages inherently show lower tissue contrast. As a result, SE is
eferred method for imaging cardiac masses and diseases of the
rdium.

d pool appearance

ppearance of the blood pool is a factor in selecting the
ition protocol. In general, blood flows too quickly through an
g section for it to be exposed to both the 90° and 180° pulses.
se of this, SE images can fail to depict structures that move out
imaging plane. Because signal generation at SE imaging
ds on refocused spins (protons stimulated by a 90° excitation
and refocused by a 180° inversion pulse), the blood pool, by
of not being exposed to both pulses, appears as a region of
void; the result is termed black-blood imaging. Darkness of the
pool can be further promoted by applying a saturation signal
a double inversion recovery (DIR) technique.

blood imaging improves conspicuity of the endocardial borders
elps demarcate intracardiac masses from normal structures.
nproved delineation of vessel walls with SE also enables
or anatomic evaluation. GE, on the other hand, involves the
ation of only 1 section-selective excitation. After that excitation,
contributes to the image even after it moves out of the imaging
Such contrast is termed bright-blood imaging. Complex
ning vessels, such as the pulmonary veins or arteries, are better
ed with this technique. Another parameter that affects the
rance of the blood flow is the echo time (TE). With GE, the
depends on gradient reversal, without the additional spin
sing of SE. Spins that enter the section during acquisition
ce heightened signal. The bright blood pool can be used to
guish structures such as bronchi from vessels.

al and temporal resolution

tial and temporal resolution

tial resolution is a concern with any imaging modality.Fortunately, size of the major cardiac structures is well within the limit for MRI. tial resolution generally is determined by the field of view (FOV) the number of phase-encoding steps. For comparable FOVs and rix sizes, spatial resolution is equal with SE and GE techniques. ir major difference is with temporal resolution. Adequate depiction ne atrial septum or valve leaflets depends on the temporal olution, as well as the spatial resolution. Regarding time olution, GE imaging has advantages compared with SE imaging. assessment of dynamic heart structures is performed with cine acquisitions because its temporal resolution is better. A trade-off ts between temporal resolution and spatial resolution. For typical ic SE imaging, one may use a matrix of 256 x 256 and a FOV of cm. To make a movie of the beating heart, one may select a GE nique and reduce the number of phase-encoding steps, for mple, to 128. The spatial resolution decreases from 1.33 x 1.33 to 1.33 x 2.66 mm accordingly. That resolution is sufficient to ict cardiac wall motion and to calculate the ejection fraction, but ner resolution may be required if detailed evaluation of the cardiac ves is desired.

G gating

most important factor in the acquisition of diagnostic images is quality of the MRI system's ECG gating. If the gating system lacks sistency or cannot tolerate irregularities of the cardiac rhythm, diac images are severely impaired. Without dependable gating, ny pulse sequences become useless, and if those sequences are uired, the examination is unlikely to yield interpretable data. The a first step, a good ECG tracing must be obtained. Standard MRI-npatible electrodes are placed on the anterior or posterior chest l of the patient. Depending on the gating system, typically 3 or 4 ctrodes are used. The quality of the electrodes is of minor ortance. Experience at the author's institution shows no difference ne performance among electrode pads on the basis of their cost. ctrode contact is important. Thorough cleansing of the contact a with alcohol and/or acetone is sufficient. Body hair should be noved in the area where the electrode is placed because it can

loss of contact. With older systems, adequate tracings required ectrodes be placed within 15 cm of each other, and the leads be straight and could not have loops. The advent of fiberoptic ystems has simplified lead placement and have decreased the rn about looping or degradation of the ECG tracing. However, pping electrodes can significantly degrade the ECG tracing; this ncern in small pediatric patients.

isition protocols

primarily is performed by using SE and GE techniques. As earlier, flowing blood creates a signal void on SE images. ver, the complex pathway of blood flow through the heart s in disordered flow patterns. Focal areas of slow flow create , and the blood pool does not appear homogeneous. nding on the imaging subject, the degree of inhomogeneity can de image quality and limit interpretation of the findings. To eract this affect, two 180° presaturation pulses are used before E acquisition is initiated. This results in images on which the is truly black termed double inversion recovery (DIR) images. echnique provides superior delineation of the endocardial n and vessel walls. Significantly disordered flow on DIR images ests an abnormality, such as a septal defect or valvular disease. s instance, a direct examination of the area is indicated. use DIR is less sensitive to disturbed flow than other techniques, sequence may be required for that evaluation. Any suspected bnormality on DIR images should be confirmed with GE images

cquisition is ECG triggered with a recovery time (TR) equal to -R interval. Common imaging settings include the following:

- TE of 30.5 milliseconds
- Matrix size of 256 x 256
- FOV of 34 x 25 cm in adults, 24 x 18 cm in children, and 16 x 12 cm in neonates
- Number of excitations (NEX) of 1 in adults and children who can hold their breath, 2 in those who cannot, and 4 in neonates
- Section thickness of 8 mm with a gap of 0 mm in adults, usually 5 mm in children, and 3-5 mm in neonates

GE sequence is ECG triggered with a TR/TE of 9.4/5.1 and a matrix size of 256 x 128-256. The flip angle (FA) varies, but it usually is 15-30°. The section thickness, FOV, and NEX are adjusted for the patient's age, with the same considerations as those described for DIR. Vascular structures and connections sometimes are imaged with the white-blood technique to improve their conspicuity.

e GE sequences are used for functional assessment. Cine ging involves multiple acquisitions or cardiac phases throughout a diac cycle in each imaging section. The result is a collection of ges in each section that depict differing degrees of ventricular traction. The images in each section can be stacked and played in a loop to permit visualization of the cardiac chamber and ular motion. Cine GE settings are as follows:

TR/TE of 9.4/5.1
Matrix of 256 x 128
FOV of 34 x 25 cm
Section thickness of 8 mm
NEX of 0.75
FA of 15-30°

Twenty cardiac phases: At least 16 image phases per cardiac cycle are needed to reliably depict end diastole (ED) and end systole (ES) for quantitative analysis.

en wall thickening and wall motion are assessed, significantly ater accuracy can be achieved by using a serial motion essment with reference tracking (SMART) technique to account long-axis and rotational movements.

gmented k-space data acquisition is used widely. A specified mber of phase-encoding steps are applied in each imaging phase cardiac cycle to enable the efficient use of data collection time in tiple phases and sections. The temporal resolution depends on ny factors and is discussed in the following section.

important point to remember is that the FA affects contrast. Small iations in the FA can significantly change the brightness of the od pool, the distinction of the myocardial wall, the appearance of

ent flow, and the imaging time. With the author's system, the sition time for an 8-mm-thick section increases from 5 seconds a FA of 10 to approximately 16 seconds with a FA of 40°.

itivity to blood-flow disturbances increases as the acquisition ncreases. The loss of spin-phase coherence creates a blood- signal void. In addition, the brightness of flowing blood is linearly ed to the FA. These 2 phenomena result in increased blood-pool ast with increased FAs. With an FA greater than 30°, these rs can hamper image interpretation. The appearance of dered flow can obscure the endocardial margin Significant flow rbances may lead to inaccurate qualitative and quantitative ssment, rendering the study useless.

GE imaging, the contrast resolution of the soft tissue improves e FA increases. With a FA smaller than 15°, the dominance of roton density, along with the previously mentioned phenomena, e discrimination of the endocardial and epicardial margins ult. Myocardial distinction is improved with FAs as large as 30° re increased scatter from effects of the blood pool cause ference

mporal resolution and imaging time

ctional evaluation of the cardiac chambers and internal structures ires good time resolution. Temporal resolution is a function of the he heart rate, and the number of phase-encoding steps and ac-imaging phases. The number of phase-encoding steps per ment depends on the matrix and number of segments. In the dard protocol at the author's institution, a matrix with 128 phase-

oding steps and 20 phases per cardiac cycle results in a k-space ment that contains 6 phase-encoding steps.

temporal resolution is equal to the TR multiplied by the number hase-encoding steps, or 9.4 milliseconds x 128, which equals 3 milliseconds per

ging phase. However, the effective temporal resolution is equal to TR multiplied by the number of phase-encoding steps per k-space ment, or 9.4 milliseconds x 6, which equals 56.4 milliseconds.

s time is within the accepted temporal resolution needed to stop diac motion of 70-80 milliseconds, as reported in the literature.

e difficulty in cardiac imaging is related to the heart rate. The TR is ed to the R-R interval for cardiac-triggered imaging. For standard techniques, 1 phase-encoding step is acquired for each section cardiac cycle. A series with a 256 x 256 matrix requires 256 artbeats to complete. In a patient with a heart rate of 60 bpm and R-R interval of 1000 milliseconds, image acquisition requires 4 nutes 16 seconds. With the use of cardiac magnets, SE sequences faster. With the magnet at the author's institution, the DIR has an no train length of 32, and an image in acquired in 8 heartbeats, or 8 conds at a heart rate of 60 bpm. With this imaging time, 2 sections n be imaged per breath hold. Problems arise if the number of quisitions must be increased, because the imaging time is gthened, or if respiratory status is compromised, because the eath-holding time is decreased. In comparison, a heart rate of 100 m with an R-R interval of 600 milliseconds enables quicker aging. In such conditions, an image can be acquired in less than 5 conds, and more sections can be imaged per breath hold; thus, the amination is shortened. Conversely, breath-holding time is shorter, sulting in greater compliance.

naging protocols

e imaging protocol may include the following steps:

- Position the patient supine, with his or her feet first on the table.
- Place the ECG electrodes and leads.
- Position the cardiac radiofrequency coil over the anterior and posterior aspects of the chest. In children weighing less than 50 lb, the head coil is usually used.
- Begin imaging with a sagittal single-shot fast spin-echo (SS-FSE) sequence (TR/TE, 18,738/28.4; matrix, 256 x 128; FOV, 40 x 40; NEX 0.5; section thickness, 8 mm; spacing, 2 mm) with breath holding, if possible.
- Check the adequacy of cardiac coil placement to ensure coverage of the heart, and perform adjustments as necessary.

sagittal series is used to configure a breath-hold coronal SS-FSE
isition through the heart and great vessels

ricular analysis requires a true short-axis plane. This author's
oach begins with the selection of an image from the coronal
s that depicts both the cardiac apex and proximal ascending
a. A few breath-hold GE or DIR sections are prescribed along an
ue axial plane parallel to a line from the cardiac apex through the
lle of the aortic root . The result is a quasi 4-chamber view on
h the interventricular septum can be localized. Cine imaging is
ormed from the apex to the base of the heart in a left parasagittal
e perpendicular to the interventricular septum . This provides
t-axis images with excellent depiction of the aortic and pulmonary
ow tracts for ventricular analysis. The aortic and pulmonary
es can be evaluated in this fashion; image interpretation is limited
8-mm sections but better with contiguous 5-mm sections.

uation of the atrioventricular (AV) valves requires modification of
maging plane. Breath-hold cine sections are prescribed along a
ly oblique plane that is parallel to a line connecting the cardiac
x and middle of the mitral valve and perpendicular to the septum .
result is a standard 4-chamber view . Cine GE imaging in this
e enables dynamic assessment of the tricuspid and mitral valves.
asagittal images parallel to the AV junction can be used to
sure the valve orifice area. Images obtained in a plane
endicular to the long axis of the 4-chamber view are true short-
views.

NTRICULAR ANALYSIS

any methods of ventricular volume calculation are used. Rehr et
s well as Pearlman et al, found excellent correlation between
ngs at volumetric analysis with MRI and findings with ventricular
s (0.99 correlation, 4.9 mL standard error). Accuracy increases
the inclusion of long-axis measurements. Three-dimensional
metric calculations are well correlated with ventriculographic
ings and have low interstudy variability (<5%) compared with
triculographic and echocardiographic results. The first step in

e calculation of ventricular volume is the selection of representative D and ES cardiac-phase images. According to Semelka et al, either ıase images that depict the largest and smallest ventricular volumes the phase images obtained immediately before mitral valve closure e, ED) and opening (ie, ES) are chosen. Next, the right ventricle RV) and left ventricle (LV) are traced along the endocardial margin ı each section obtained in the selected ED and ES phases from the ardiac apex to the section just prior to one that depicts the mitral and cuspid valves. The tracings should exclude trabeculations but may clude papillary muscles inside the endocardial margin, as long as e procedure is performed in systole and diastole

alculations can be made as follows:

- ED and ES volumes for each section are totaled to yield the RV and LV end-diastolic volume (EDV) and end-systolic volume (ESV).
- The stroke volume (SV) equals the EDV minus the ESV, or SV = EDV - ESV.
- The ejection fraction (EF) equals the SV divided by the EDV times 100, or EF = (SV / EDV) X 100 to give a value reported as a percent.
- Cardiac output equals SV multiplied by the heart rate.

or myocardial mass assessment, the RV and LV epicardial borders re traced in ED. The interventricular septum is assigned to the LV nd excluded from the RV tracing of the myocardial mass (see The olumes of all sections are added, and the corresponding EDV is ubtracted to determine the myocardial volume. This result is then ıultiplied by the specific gravity of the myocardium (ie, 1.05 g/mL) to alculate the mass. This measurement is useful in the assessment of ypertrophy and to follow up the ventricular response to therapy.

he AV and ventriculoarterial valves also can be assessed with cine E sequences. Valvular stenosis or regurgitation produces turbulent ts of signal void in the appropriate directions. Regarding the AV alves, regurgitation is graded according to echocardiographic criteria nd is related to the distance to which the jet extends into the atrium. Grades of valvular stenosis are calculated more reproducibly. The

lve orifice areas can be measured and graded according to current andards

ble 1: Ventricular and Valvular Parameters*

Parameter	Men	Women
LV EDV (mL)	77-195	52-141
RV EDV (mL)	88-227	58-154
LV ESV (mL)	19-72	13-51
RV ESV (mL)	23-103	12-68
LV EF (%)	56-78	56-78
RV EF (%)	47-74	47-80
LV SV (mL)	51-133	33-97
RV SV (mL)	52-138	35-98
Cardiac output (L/min)	2.82-8.82	2.65-5.98
LV mass (g)	118-238	75-175
RV mass (g)	30-70	24-55
Septal mass (g)	40-82	26-58

From Lorenz, 1999.

ypical areas for the aortic and mitral valves are 2.5-3.5 and 4-6 cm^2, spectively; areas of less than 0.8 and less than 1 cm^2, respectively, dicate severe stenosis. The values for aortic and mitral valve area pply to both males and females.

ith cardiac MRI imaging, key points include the following:

- Cardiac MRI is an accurate method for the evaluation of structure and function. Although it already is the procedure of choice in many clinical settings, its application continues to expand. The driving force, most likely, is the continuing shift toward diagnosis with noninvasive procedures.
- A complete understanding of the clinical question is needed for proper examination planning.
- Cardiac MRI findings have an excellent correlation with results with other means of functional assessment, with improved

interstudy variability. Calculations are easier to obtain and have fewer limitations compared with calculations with other modalities. In addition, MRI is changing the evaluation of coronary artery disease.

- Cine GE and contrast-enhanced imaging can be used to evaluate MI and predict functional recovery.
- Results of dynamic perfusion imaging at rest and with stress are promising in the evaluation of coronary artery disease.
- Space-time maps summarize the signal intensity changes in the myocardium over time, during transit of the bolus of contrast agent. These show impaired blood delivery as a delayed equitime, or the time to accumulate the LV signal, without a need to induce ischemia.
- Ongoing research and technologic advancements are sure to make MRI the leading cardiac imaging technique.

Planning Cardiac MRI

Anatomy

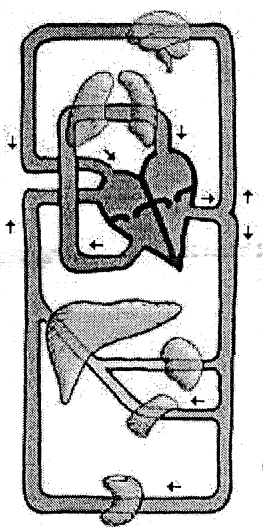

Circulation

Blood flows through the entire body. There are two cles. One circle brings the blood from the heart via the lungs back the heart, the other circle brings the blood to all the other organs d back to the heart again. The main function of the heart is to pump e blood around. Under normal conditions the amount of blood mped out each heartbeat is roughly 100 ml, for each circle. That uals 6 l every minute.

Position

The heart is located in the chest, in between both lungs. ghtly rotated, the apex points towards the left side. On the op two large arteries are connected. The pulmonary artery brings the blood to both lungs, the aorta to the rest of the body.

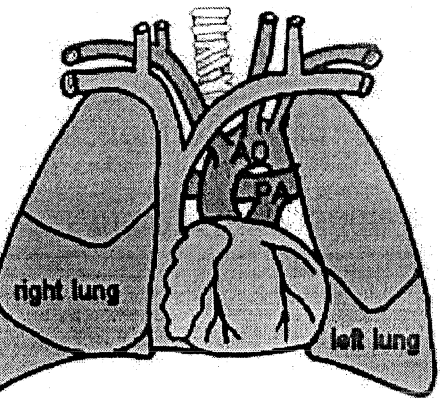

Two sides

The heart is divided into two sides. The left heart receives fresh oxygenated blood from the left and right pulmonary veins (LPV and RPV) in the left atrium (LA). Via the Mitral valve the blood flows into the left ventricle (LV). When the heart contracts the Mitral valve closes and the blood is pushed via the aortic valve into the aorta (AO). When the ood returns from the body it flows via the superior and inferior vena va (SVC and IVC) into the right atrium (RA). Via the tricuspid valve the blood enters the right ventricle (RV). As soon as the heart ntracts the tricuspid valve closes and blood flows via the pulmonary valve into the pulmonary artery (PA). At the bifurcation the blood flows via the left and right pulmonary artery (LPA and RPA) to the lungs.

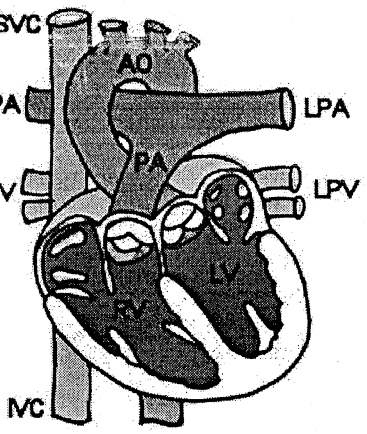

Four chambers

Long axis view

tarting with a transverse plane through the centre of the heart, a ng axis view (LA or LAX) can be defined. Position the slice through pex and centre of the Mitral valve as indicated in Fig 1A. This LA ew shows the left ventricle over its full length from apex to base, cluding the Mitral valve and the left atrium. Note the pulmonary eins that come in from superior into the left atrium.

his view is sometimes also referred to as vertical long axis (VLA).

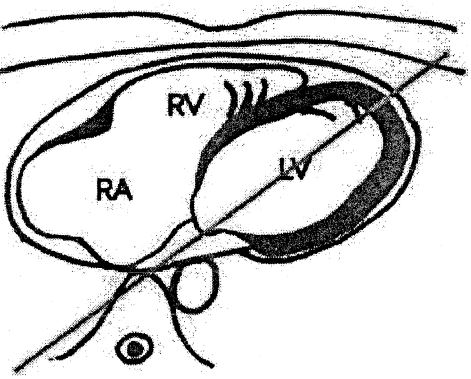

ig 1A: Transverse view.

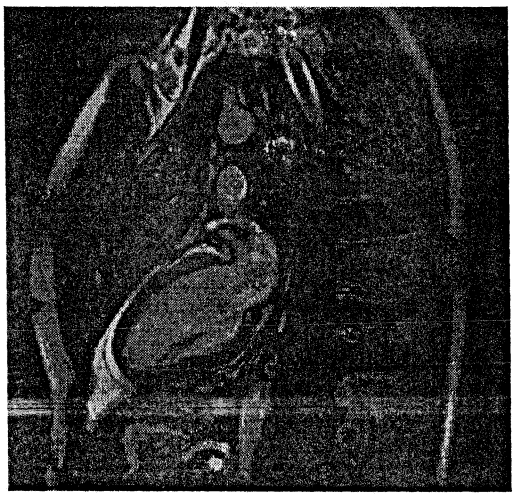

Fig 1B: Resulting LA view.

Semi four-chamber view

ome people like to define all cardiac views using two orthogonal nages. This ensures that the resulting plane is nice orthogonal ligned in both directions. If however the initial transverse plane lready clearly shows the apex and the Mitral valve I usually skip this tep and continue straight with the short axis view. refer to this view s "semi" four-chamber because usually the AP angulation is not recisely right. In this example it's more a semi left ventricular outflow act. I definitely require a short axis view first to ensure a true four-hamber view.

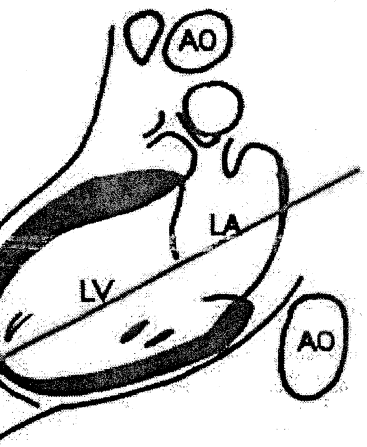

A: LA view.

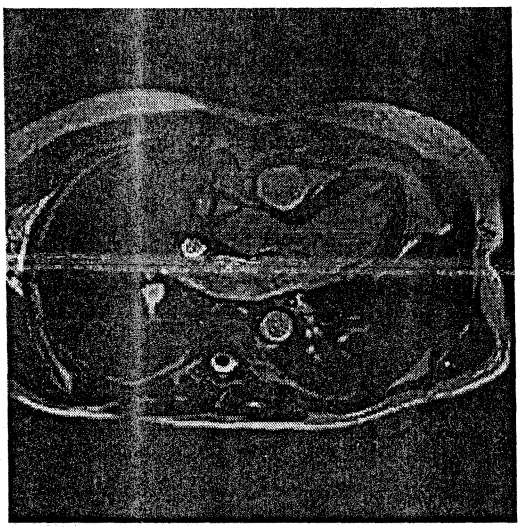

Fig 2B: Resulting (semi) 4CH view

Short axis view

hat we have two orthogonal views of the left ventricle we're to define another cross-section of the heart: the short axis view r SAX). There are several guidelines that can be followed to e a short axis view:

- Orthogonal to the line that connects the centre of the Mitral valve with the apex.
- Orthogonal to the septum. (Not seen on a LA view, but visible on semi 4CH)
- Parallel with the Mitral valve.

sn't matter much which rule to follow here. The accuracy of the netric analysis depends mostly on the decision which slice to ie as the most basel one. For that reason I always choose to go el with the Mitral valve. Sometimes the previously described) four-chamber view (Fig 4A) is used to verify the angulation in er orthogonal direction

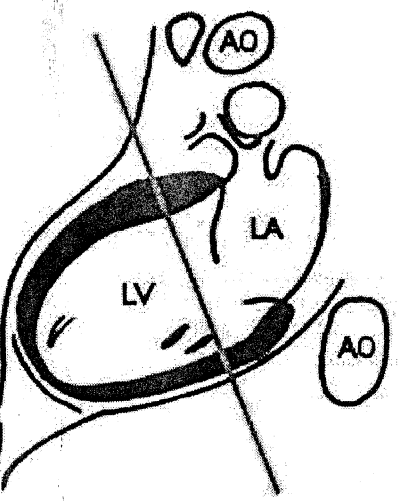

3A: LA view.

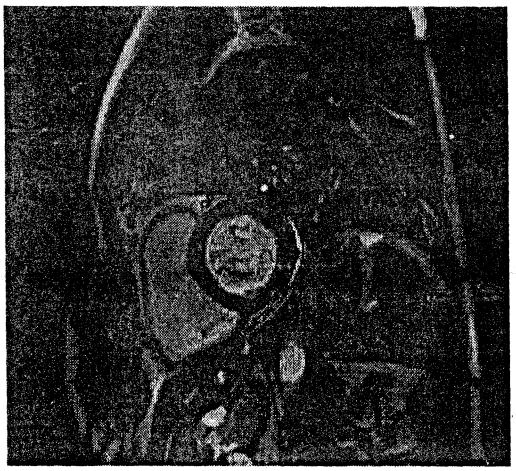

Fig 3B: Resulting SA view.

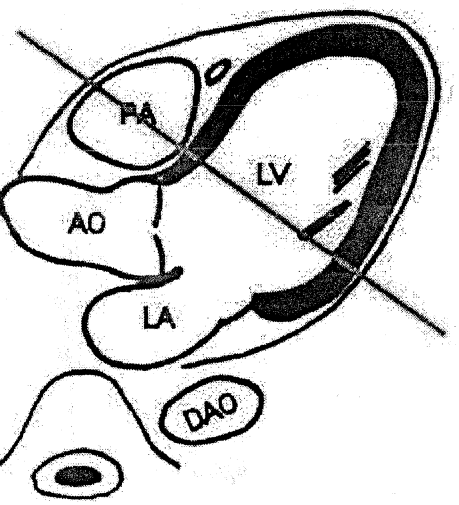

3C: Semi 4CH view.

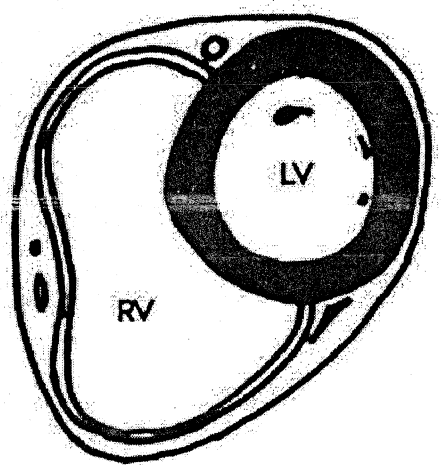

Fig 3D: Resulting SA view.

Four-chamber view

e SA view is used to define the four-chamber view (4CH) that ows us both ventricles and atria in a single plane. This view is metimes also referred to as horizontal long axis view (HLA). Define ne through the centre of the left ventricle and the lower corner pex") of the right ventricle. Many times it's very difficult to tinguish the right ventricle from the right atrium. That is because right ventricular wall is so thin, and the tricuspid valve is not easily cognized.

ood idea to verify the planning of the four-chamber view using axis view. Just to ensure that I am cutting nice through the nd the center of the Mitral valve. Keep in mind that the heart is g with the respiration in feed-head direction. Therefore you nake sure that both views were acquired in the same tion phases. I strongly encourage you to acquire all views in ion phases only because the position of the heart tends to vary ompared to positions acquired in inspiration.

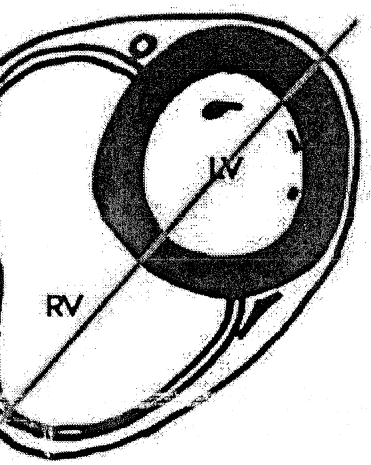

: SA view.

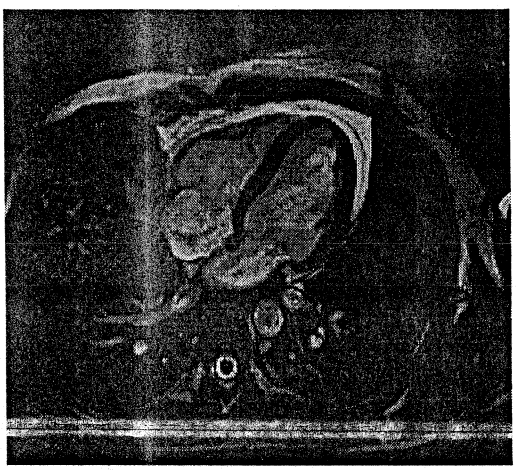

Fig 4B: Resulting 4CH view.

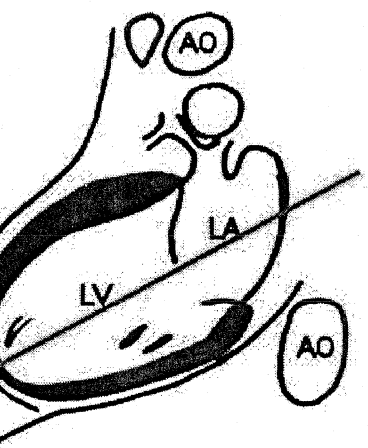

C: LA view.

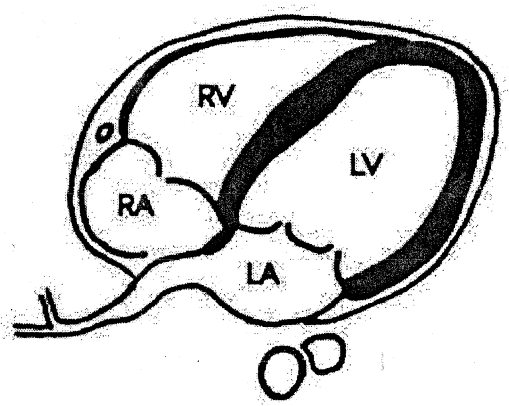

Fig 4D: Resulting 4CH view.

Inflow and outflow tracts

Fresh oxygenated blood comes from the pulmonary veins and flows into the left atrium. The P-wave initiates contraction of the atria. Both the tricuspid valve and mitral valve open and the blood is pushed further into the ventricles. When the R-peak is there the ventricles start to contract and the pressure inside the ventricle increase. Soon the tricuspid valve and mitral valve will close.

Left two chamber view

Very similar to the definition of our first view, the long axis view. The only difference is that this two chamber view is orthogonal to the four-chamber view. (The previously described LA view is perpendicular to the transverse view.) Just describe the line through the apex of the left ventricle and the centre of the mitral valve.

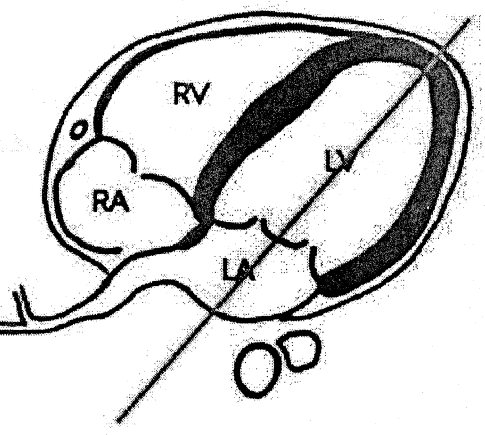

Fig 1A: 4CH view.

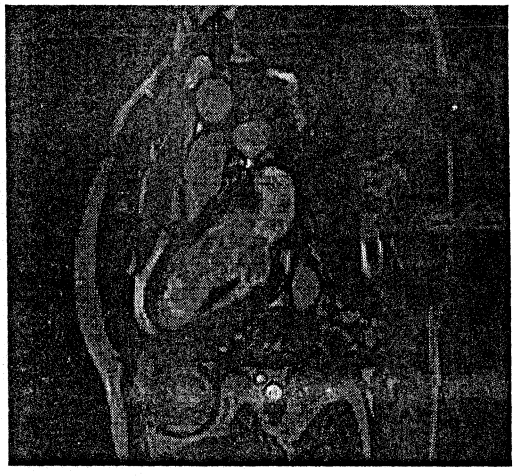

Fig 1B: Resulting L2CH view.

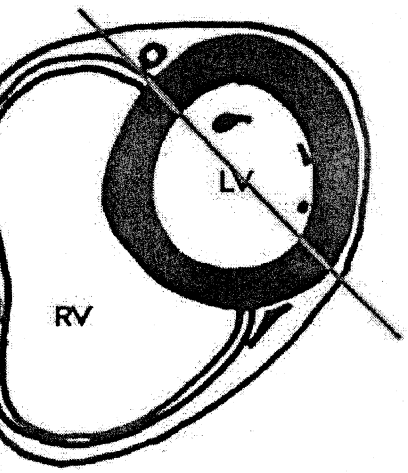

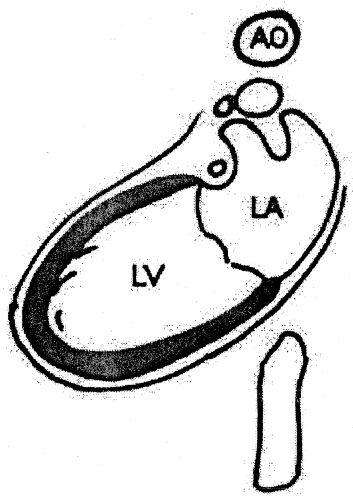

C: SA view.

Fig 1D: Resulting L2CH view.

two chamber view

nove the plane to the right side of the heart. Perhaps rotate it a little bit the plane parallel with the septum. Make sure to cut precisely through ntre of the tricuspid valve.

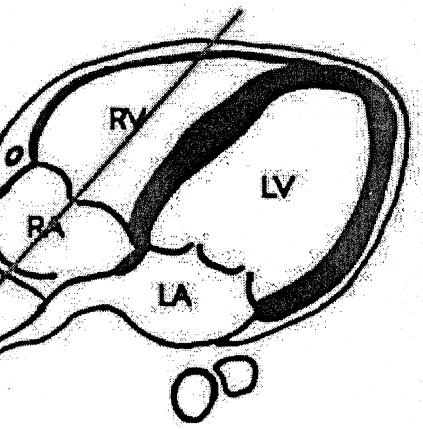

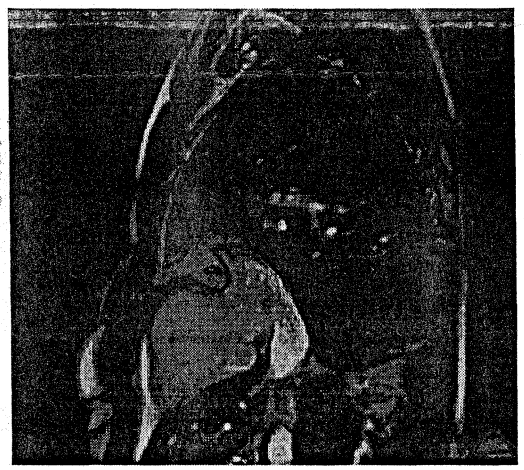

A: 4CH view.

Fig 2B: Resulting R2CH view.

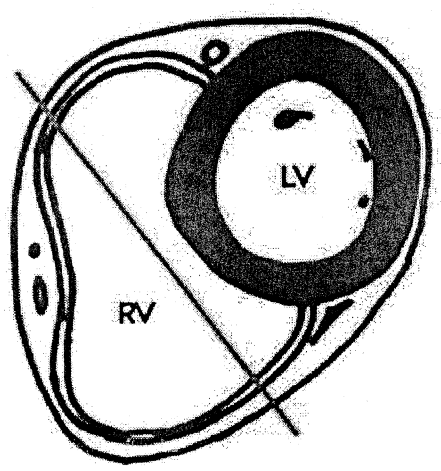

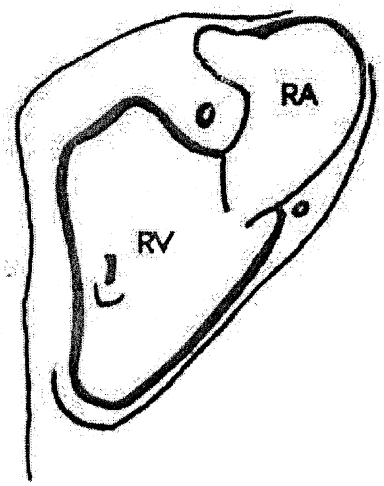

g 2S: SA view. Fig 2D: Resulting R2CH view

Left ventricular outflow tract

here is some disagreement on the precise definition of the Left entricular Outflow Tract. Some sites refer to this view - that sualizes the left atrium, mitral valve, left ventricle, aortic valve and orta - as the "three chamber view". This is a little bit strange ecause this view only shows two chambers: the left atrium and entricle. Perhaps some do count the root of the aorta as third hamber. Nevertheless the idea of this view is to visualize nicely both he mitral valve and the aortic valve. The first landmark we use is the entre of the left ventricle. If more SA slices are available a basel ice could be selected that shows the root of the aorta. The LA view an be used to verify again that the slice cuts through the far end of he apex. Sometimes the plane is angled such that it follows the agittal definition. The result is that those very steep angled views are resented as sagittal views which may lead to some confusion. nterior is presented towards the left side of the image instead of owards the top as for transverse planes. Just "rotate & mirror" the mages and you'll recognize them again as true LVOT views.

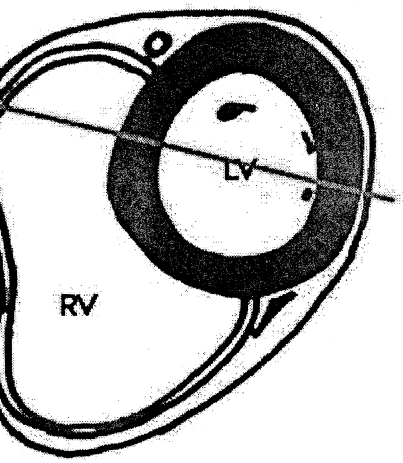

A: SA view.

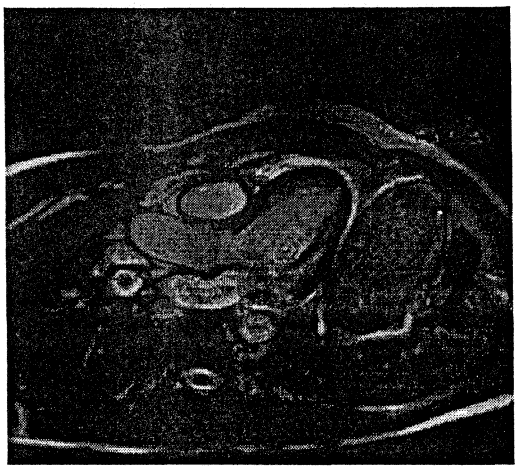

Fig 3B: Resulting LVOT view.

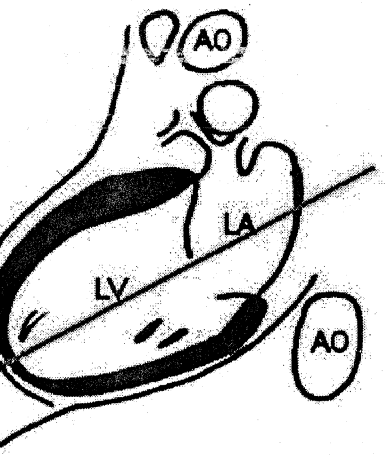

C: LA view.

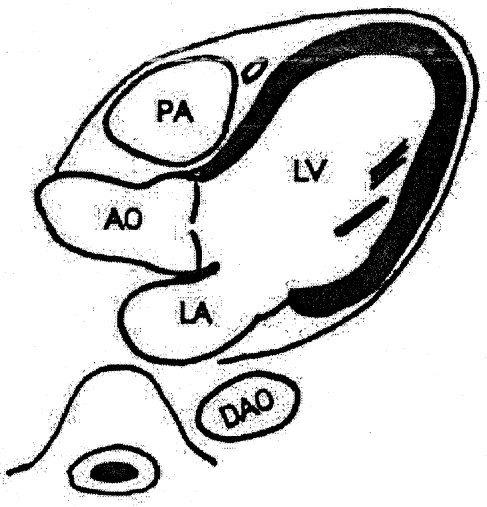

Fig 3D: Resulting LVOT view.

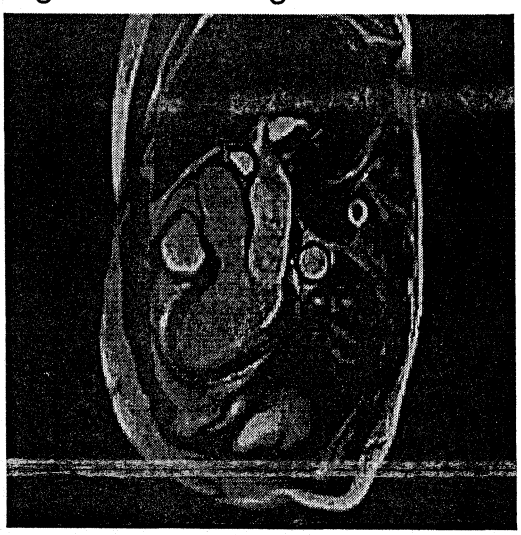

Fig 3F: Steep angled LVOT views might be presented as sagittal images...

Vertical left outflow tract

As said before there is some disagreement on what is meant with "left ventricular outflow tract". Therefore I prefer to the following view as **vertical** left outflow tract. Take the LVOT view as described before and define a line orthogonal to the aortic valve plane. Rotate it a little bit just to capture as much from the aorta as reasonable without loosing too much from the left ventricle ;-). And watch how nice you can see the aortic valve opening and closing...

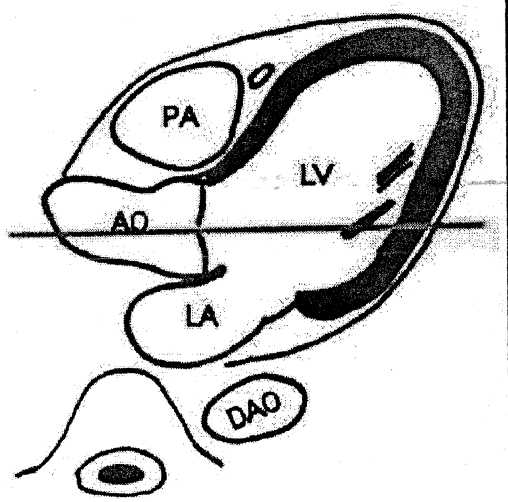

Fig 4A: LVOT view.

Fig 4B: Resulting VLOT view

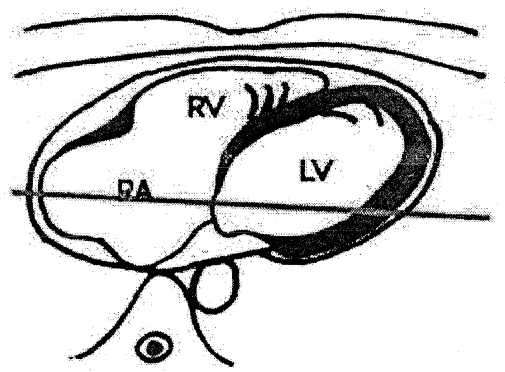

Fig 4A: Transverse view.

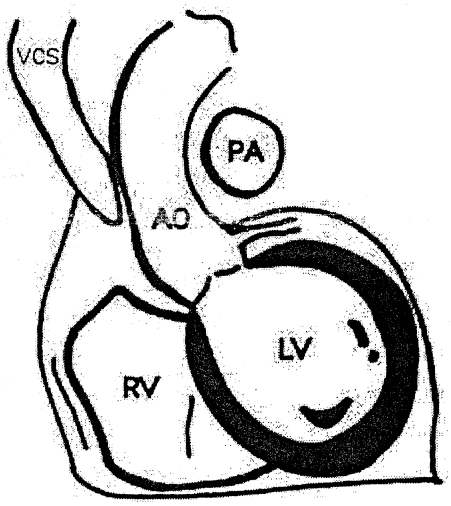

Fig 4B: Resulting VLOT view

Right ventricular outflow tract

m is to visualize the pulmonary valve, such that we can ntiate the left ventricle from pulmonary artery. The easiest way ne this plane is to start with just a sagittal plane. Browse h your transverse slices from a survey scan and look for the the pulmonary artery, it's not difficult to find. Place your slice h the center of the pulmonary artery.

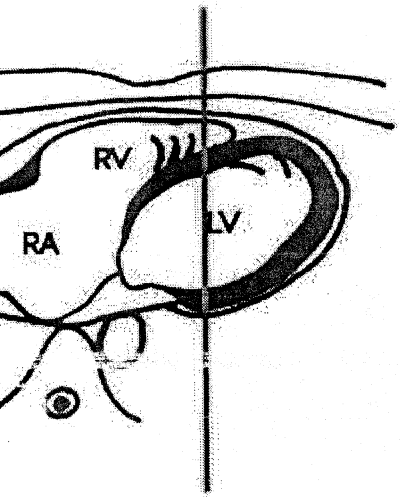

A: Transverse view.

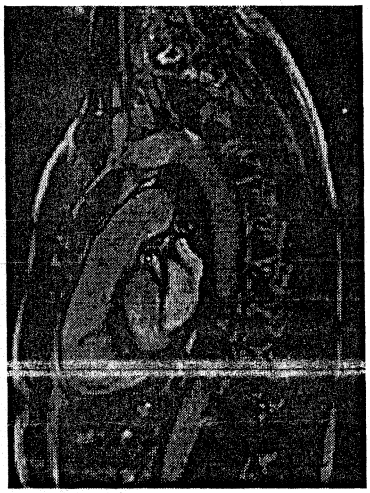

Fig 5B: Resulting RVOT view.

Aortic arch

hree-points-planscan" tool is available than that's the way to go! simply click three points: one in the **ascending aorta**, another ght in the **aortic arch**, and the last one in the **descending** . If no such tools are available then select a straight transverse acquired above the heart. One that shows both the ascending escending aorta. Position the slice through both parts of the Select a vertical outflow tract and align the image plane along ne ascending aorta.

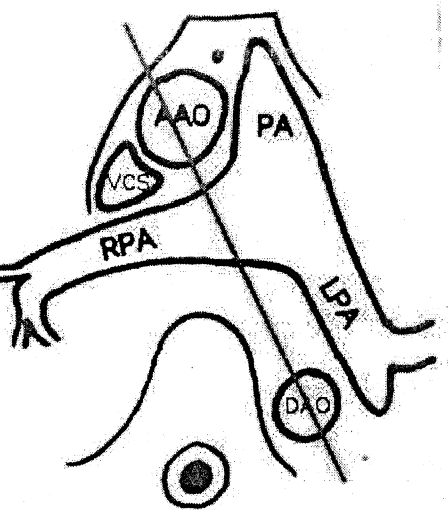

g 1A: 4CH view.

Fig 1B: Resulting aortic arch.

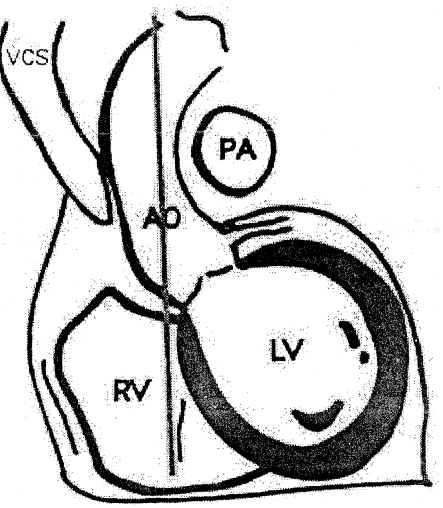

g 1C: VLOT view.

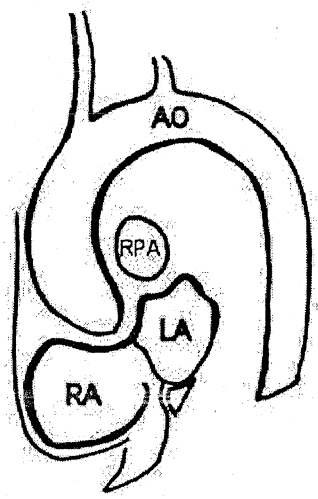

Fig 1D: Resulting aortic arch.

ulmonary artery

s exactly the same view as the RVOT: The aim is to visualize the ılmonary valve, such that we can differentiate the left ventricle from ılmonary artery. The easiest way to define this plane is to start with st a sagittal plane. Browse through your transverse slices from a ırvey scan and look for the root of the pulmonary artery, it's not fficult to find. Place your slice through the centre of the pulmonary tery.

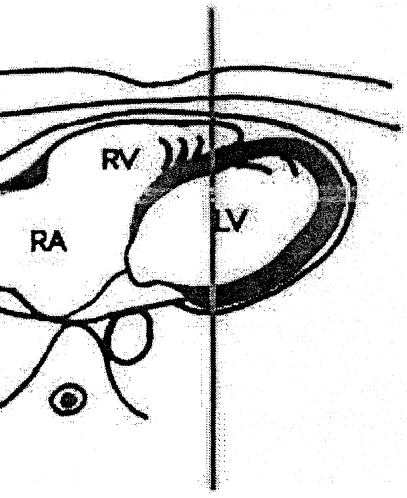

A: Transverse view.

Fig 5B: Resulting pulmonary artery.

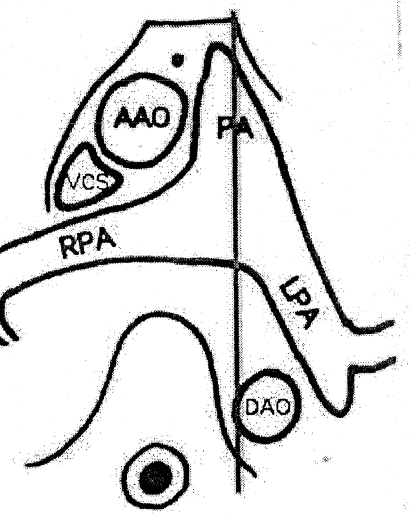

C: Transverse view.

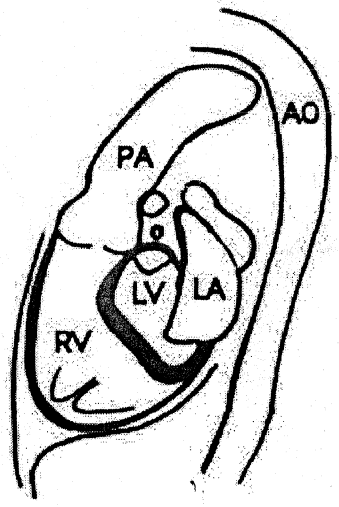

Fig 5D: Resulting pulmonary view.

<u>onary bifurcation</u>

e a straight transverse plane right through the pulmonary artery een on a PA view (or RVOT ;-). I usually take a ride with Active scanning to tilt the plane such that I see both the right and eft pulmonary artery to their full extend.

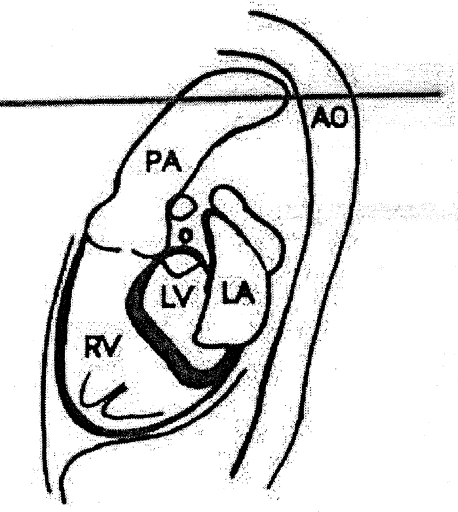

3A: PA view.

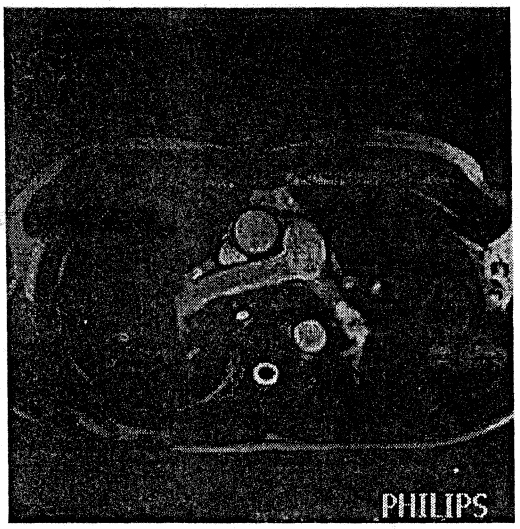

Fig 3B: Resulting pulmonary bifurcation.

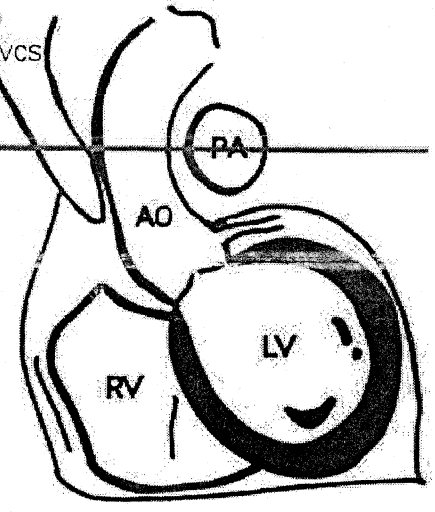

g 3C: LA view.

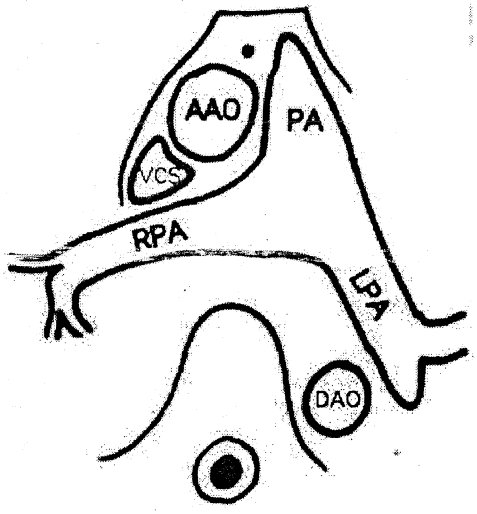

Fig 3D: Resulting pulmonary bifurcation.

ft pulmonary artery

is pulmonary bifurcation view can be used to very easily define the t pulmonary artery. Simply position your slice perpendicular to the urcation view, nicely aligned with the left pulmonary artery.

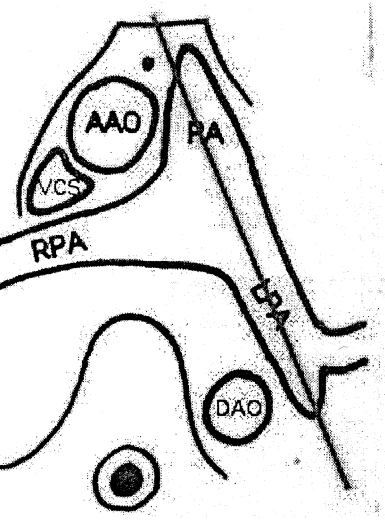

: PT view.

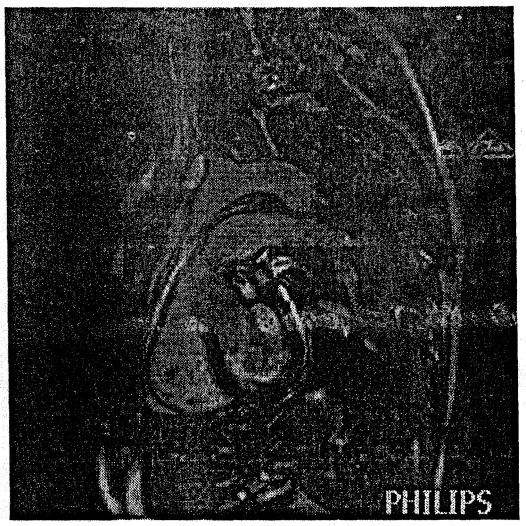

Fig 4B: Resulting left pulmonary artery.

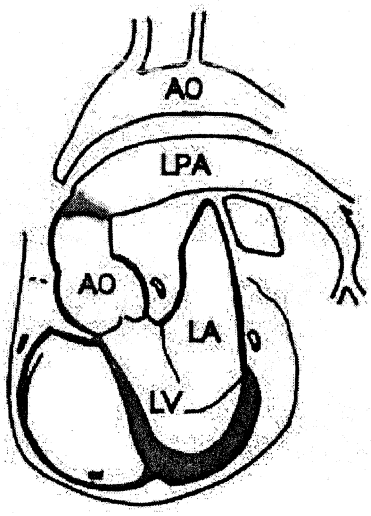

Fig 4D: Resulting left pulmonary artery.

pulmonary artery

ulmonary bifurcation view can also be used to very easily define ht pulmonary artery. Just position your slice perpendicular to urcation view, nicely aligned with the right pulmonary artery. hat the right pulmonary artery tends to slightly descend. That's use InterActive scanning to figure out the amount of tilting that's d to visualize the pulmonary truncus to it's full extent.

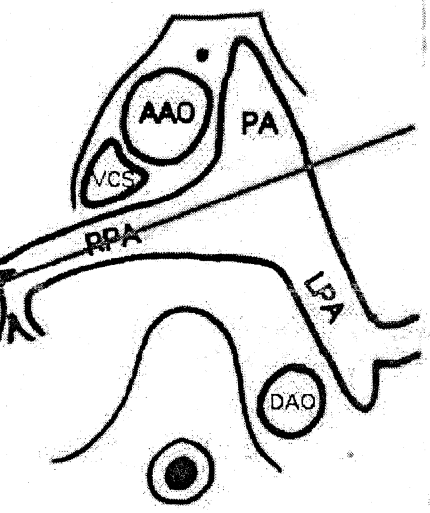

5A: PT view.

Fig 5B: Resulting right pulmonary artery.

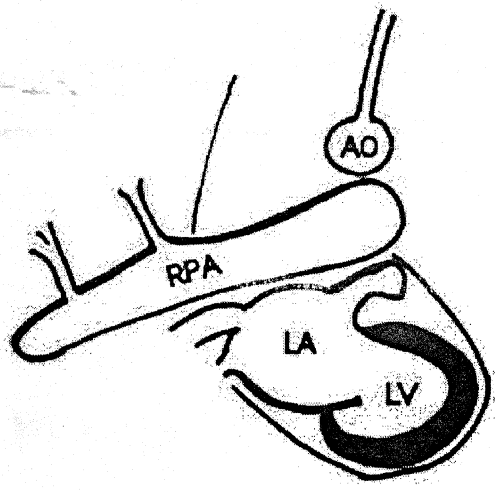

Fig 5D: Resulting right pulmonary

ow through arteries

antification of blood flow is an interesting application. A nice periment includes the comparison between the amount of blood shed into the aorta each heart-beat and the amount of blood mped into the pulmonary artery. This should be - more or less - the me. Another experiment is to add the stroke volumes for LPA and A together and compare this to the PA and AO. And another one ust to take a single slice cutting through ascending aorta, scending aorta and vena cava superior. The difference between cending and descending aorta represents the blood supply to the ad and arms, which should be equal to the amount of blood that urns via the vena cava superior...

ch flow measurement we have to understand the basic rules for flow fication:

Define your scans perpendicular to the vessel as much as possible.
Stay away from areas with fast turbulent flow (stenoses, valves).
Adjust the VENC to the highest expected flow velocity.

tic flow

wo orthogonal views that show the aorta (Aortic Arch and VLOT) osition the slice perpendicular to the aorta. Stay away from the valve to avoid too much interference from turbulent flow. A or less straight transverse orientation at the level of the right onary artery is a good starting point as shown in Fig 1A. If flow is evaluated both for ascending and descending aorta, make sure erage your angulation such that both parts of the aorta are cut gonal.

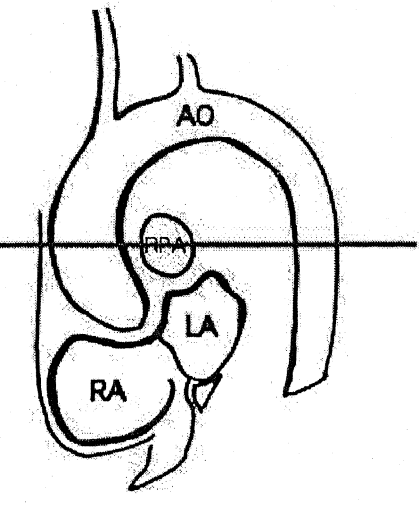

A: Aortic arch.

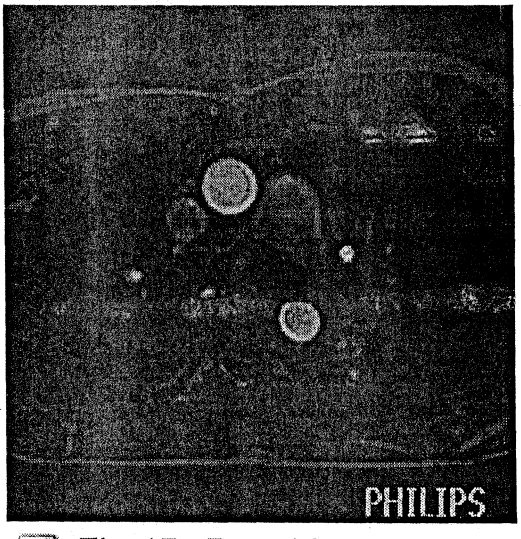

Fig 1B: Resulting aortic cross-section. (FFE-modulus)

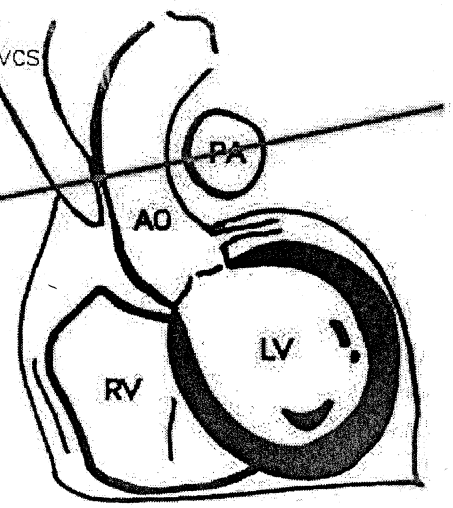

1C: VLOT view.

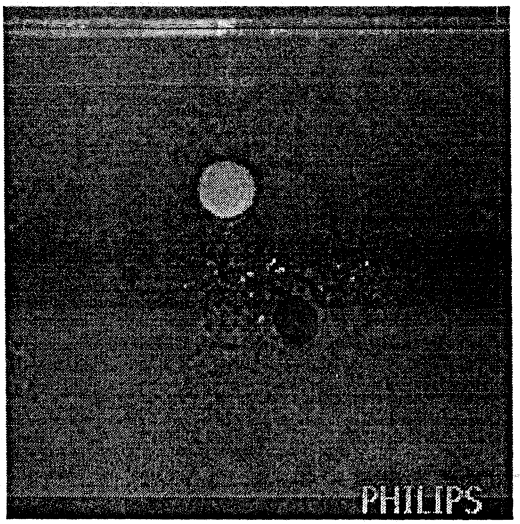

Fig 1D: Resulting aortic cross-section. (PCA-phase)

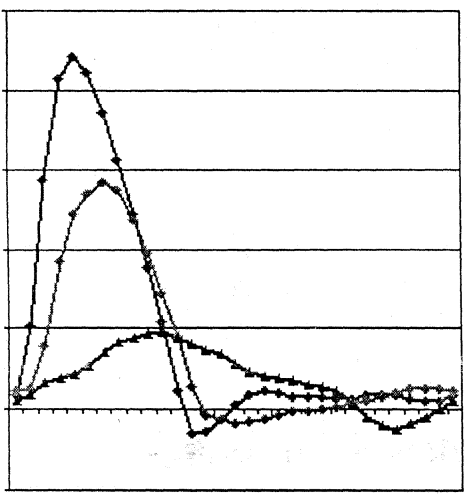

1E: Flow rate (ml/s) Red: AAO, een: DAO, Blue: SVC

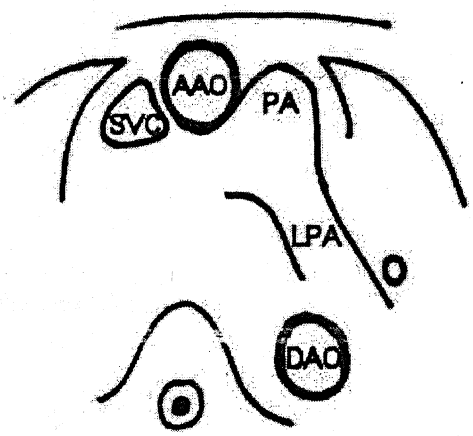

Fig 1F: Resulting aortic cross-section.

ulmonary flow

elect the pulmonary artery view (or RVOT) to position your slice on. sometimes is difficult to recognize the pulmonary valve, but try to ay a few cm away from it. Check on the pulmonary bifurcation view ou're not too close to the bifurcation.

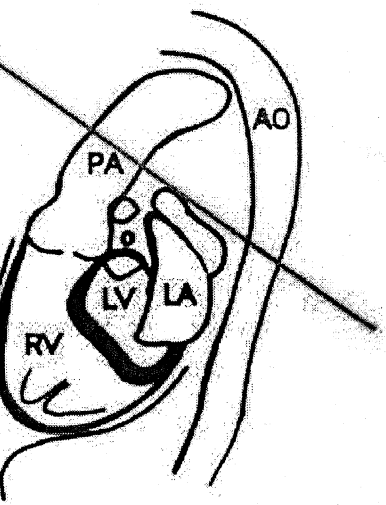

: Pulmonary view (RVOT).

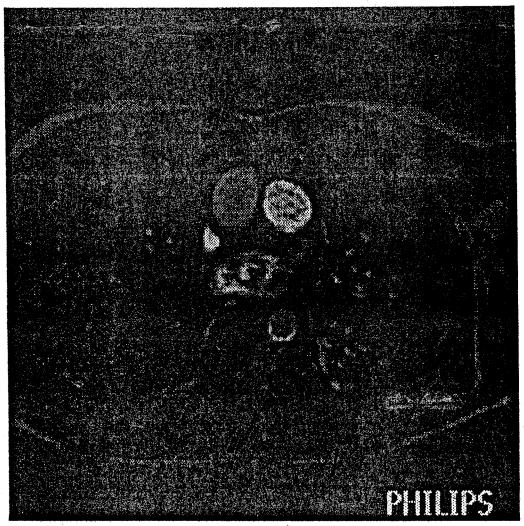

Fig 2B: Resulting pulmonary cross-section. (FFE-modulus)

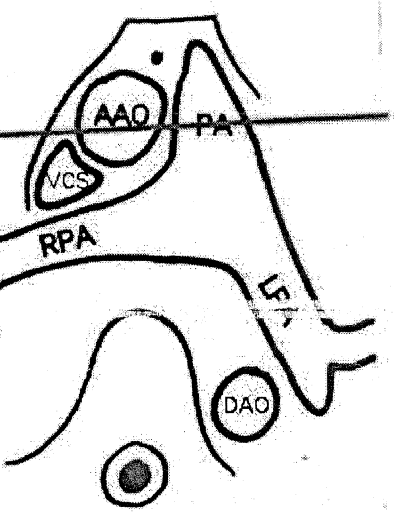

: Pulmonary bifurcation.

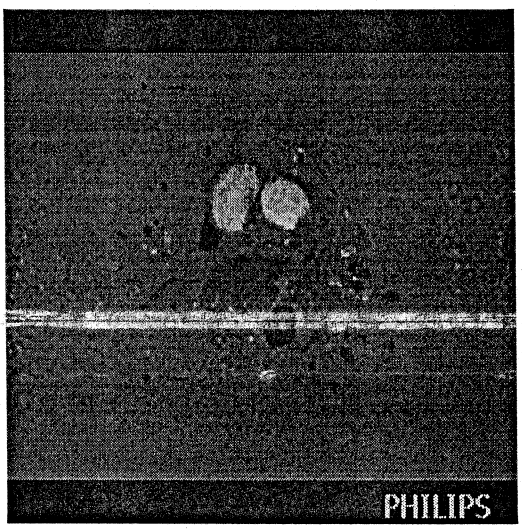

Fig 2D: Resulting pulmonary cross-section. (PCA-phase)

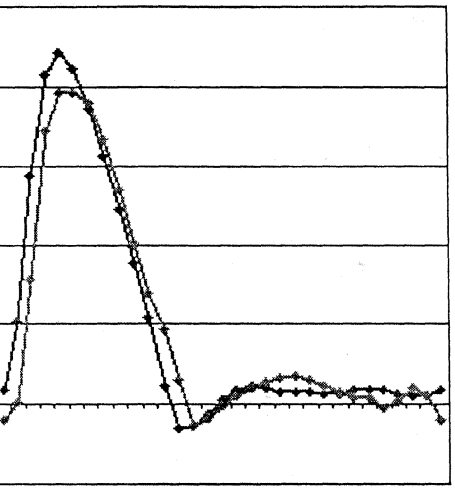

2E: Flow rate (ml/s) Red: AO, een: PA

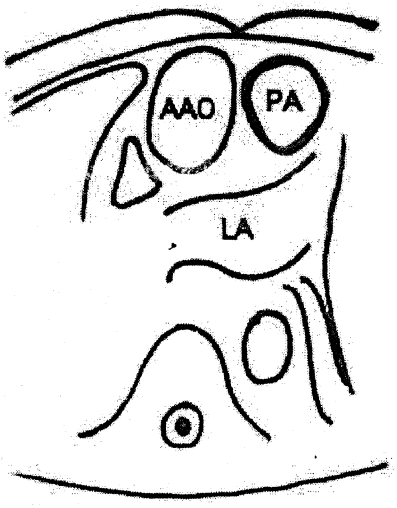

Fig 2F: Resulting pulmonary cross-section.

ft pulmonary flow

ect both the bifurcation view and LPA, and position your slice nogonal to the left pulmonary artery. Position your slice at a place too close to the bifurcation to avoid any chance of turbulent flow.

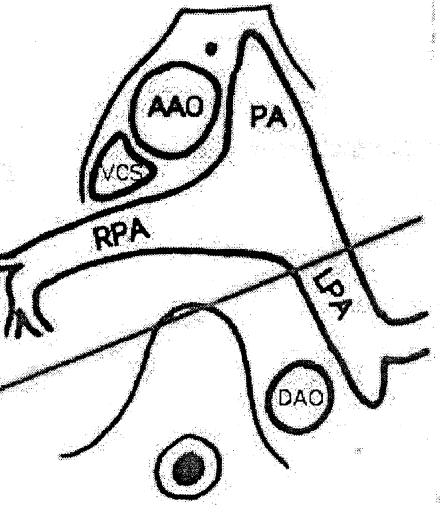

3A: Pulmonary bifurcation.

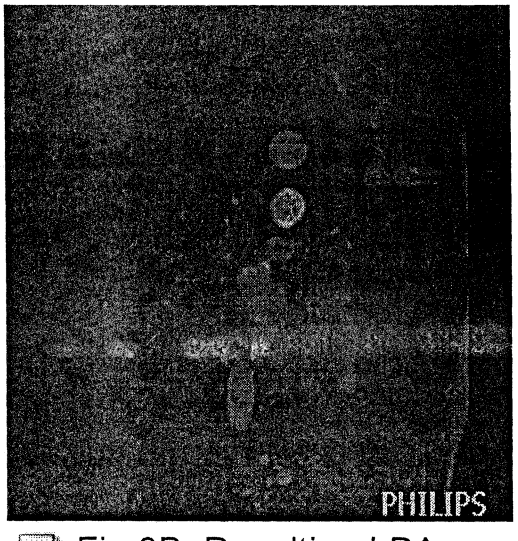

Fig 3B: Resulting LPA cross-section. (FFE-modulus)

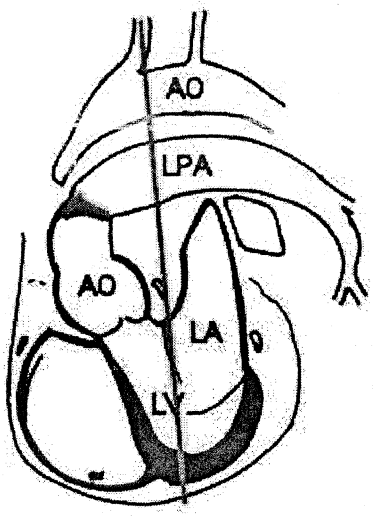

3C: LPA view.

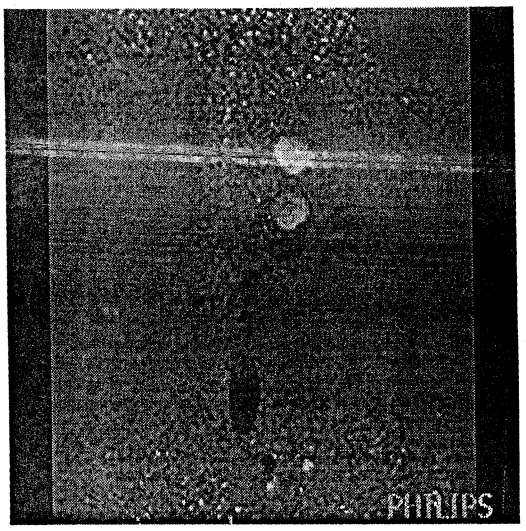

Fig 3D: Resulting LPA cross-section. (PCA-modulus)

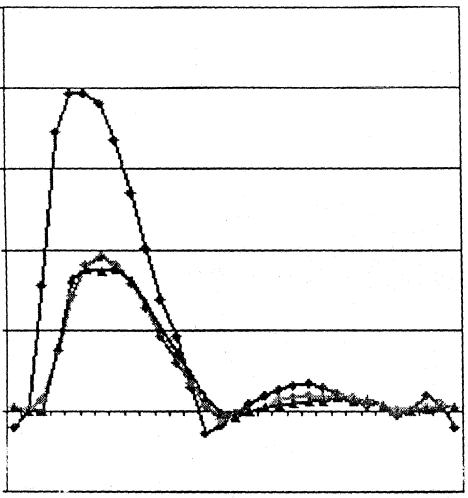

g 3E: Flow rate (ml/s) Red: PA, een: LPA, Blue: RPA

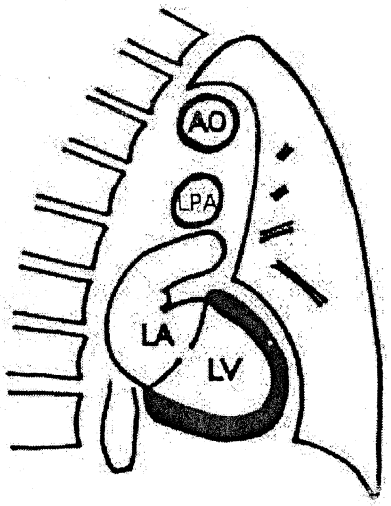

Fig 3F: Resulting LPA cross-section.

ght pulmonary flow

ry similar to the LPA. Now select both the bifurcation view and PA, and position your slice orthogonal to the right pulmonary artery.

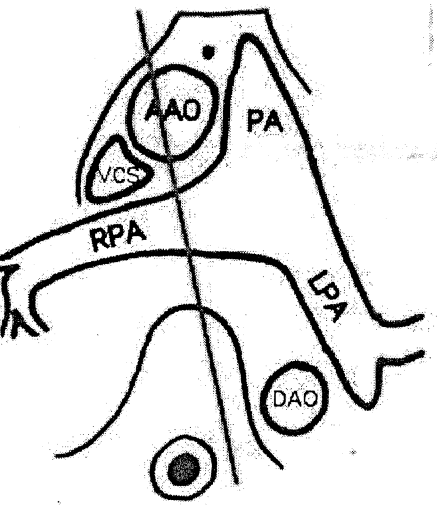

4A: Pulmonary bifurcation.

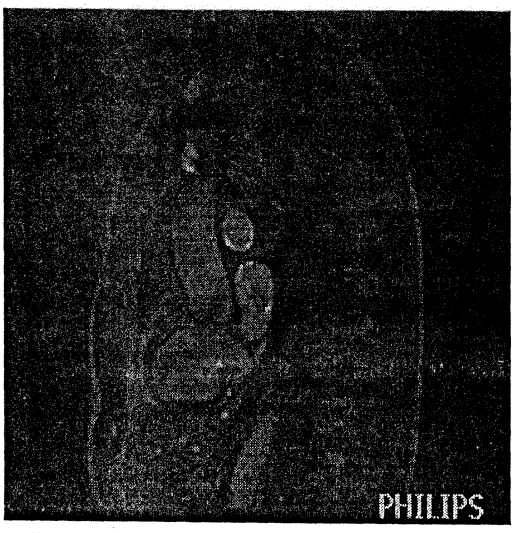

Fig 4B: Resulting RPA cross-section. (FFE-modulus)

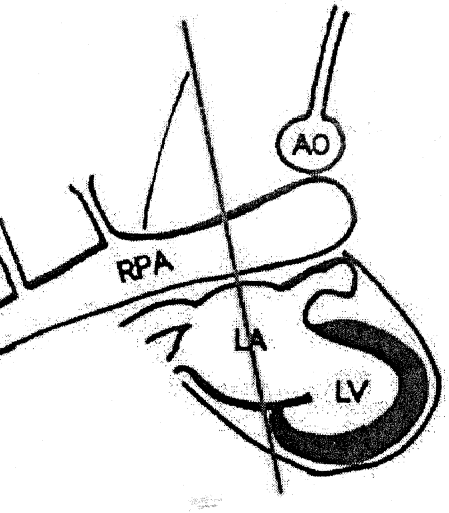

4C: RPA view.

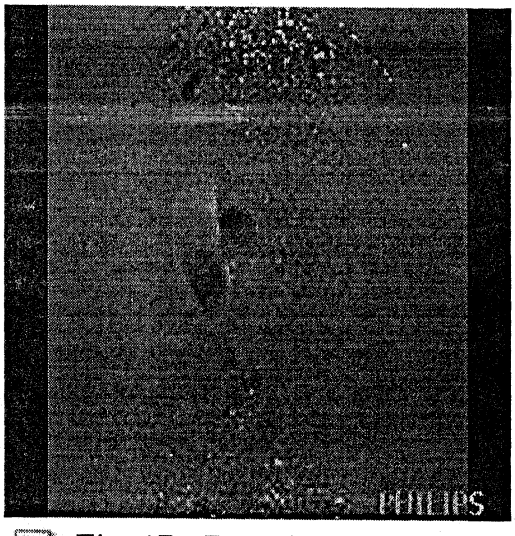

Fig 4D: Resulting RPA cross-section. (PCA-modulus)

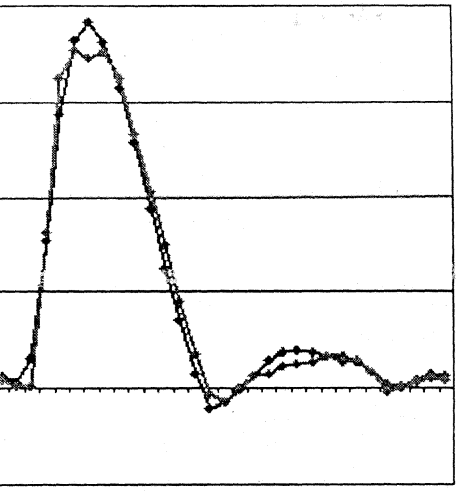

4E: Flow rate (ml/s) Red:
A, Green: RPA

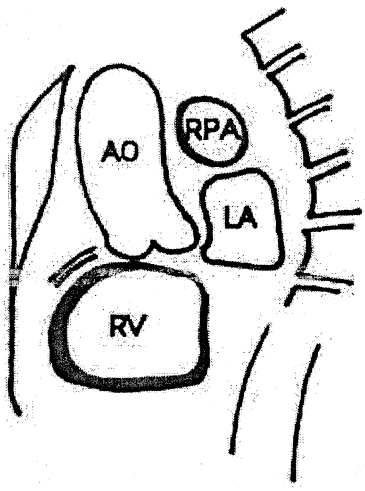

Fig 4F: Resulting RPA cross-section.

Flow through valves

Mitral valve

rhaps the most difficult view of all. Take the four-chamber view and the long axis view (L2CH) that both show the mitral valve. The difficulty lies in the fact that both the mitral valve and the tricuspid alve experience some through-plane movement during the cardiac cycle. For that reason I try to select images that were acquired in early diastole, the moment that the mitral valve opens. On these images I position the slice parallel with the mitral valve plane.

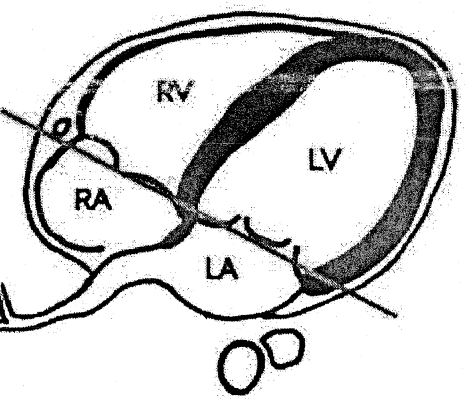

g 1A: Four-chamber view.

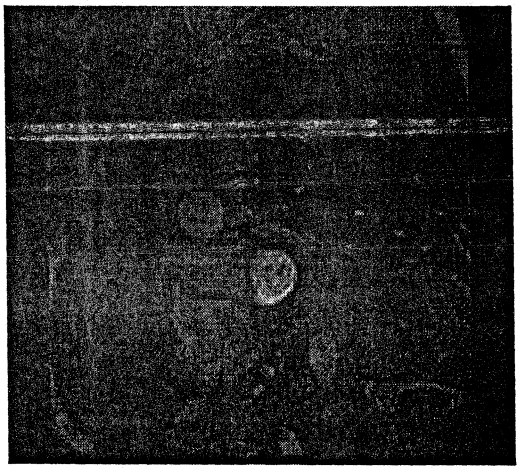

Fig 1B: Resulting mitral valve

view. (FFE-modulus)

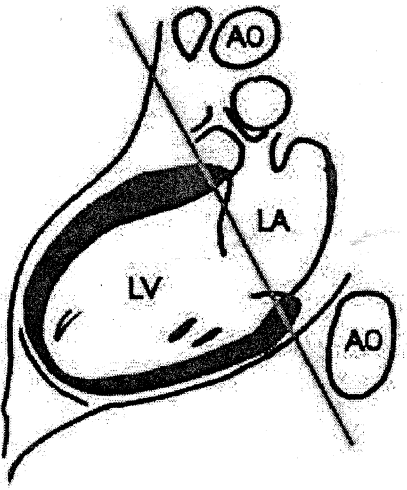

1C: Left 2 chamber view.

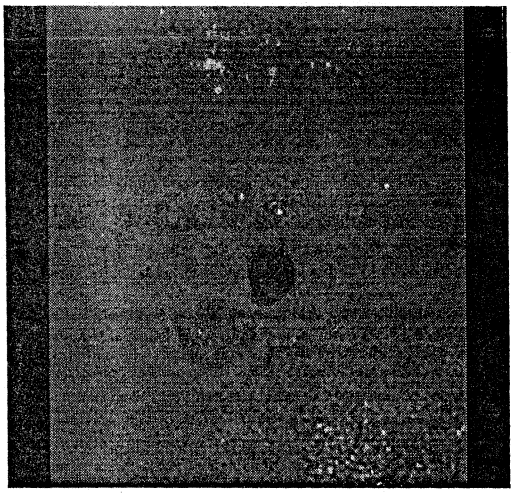

Fig 1D: Resulting mitral valve view. (PCA-modulus)

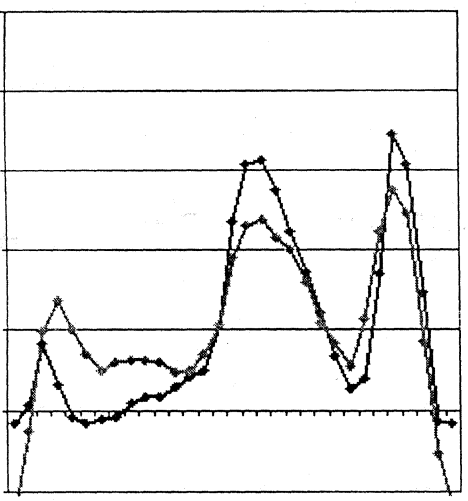

1E: Flow rate (ml/s) Red: Mitral, een: Tricuspid

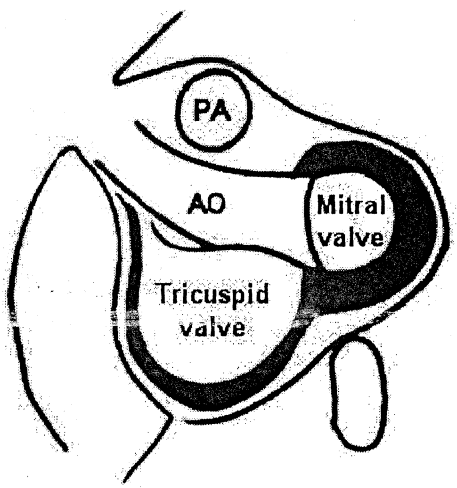

Fig 1F: Resulting mitral valve.

ricuspid valve

sically it's the same position as for the mitral valve. The only ference is that I adjust the angulation such that the plane is now rallel with the tricuspid valve. So select the four-chamber view and e right two chamber view with images acquired in early diastole. On ese images I position the slice parallel with the tricuspid valve ane. valve plane.

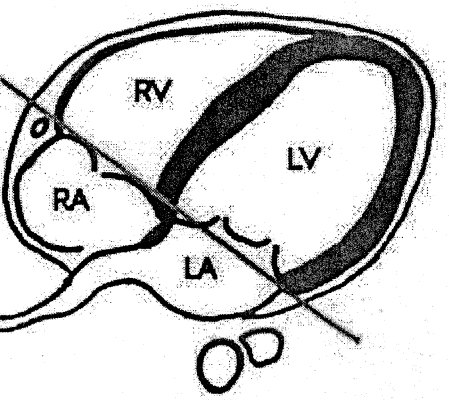

2A: Four-chamber view.

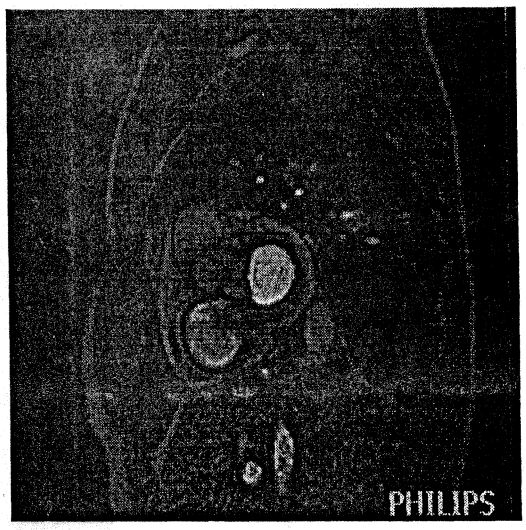

Fig 2B: Resulting tricuspid valve view. (FFE-modulus)

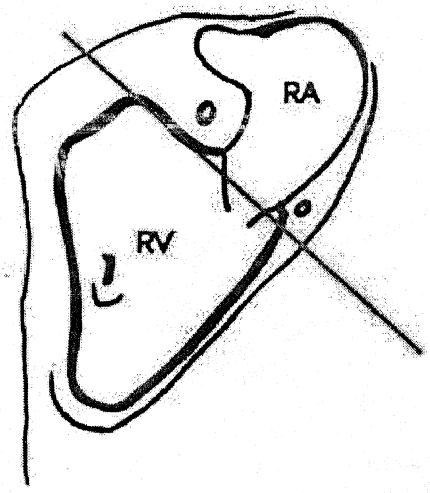

2C: Right 2 chamber view.

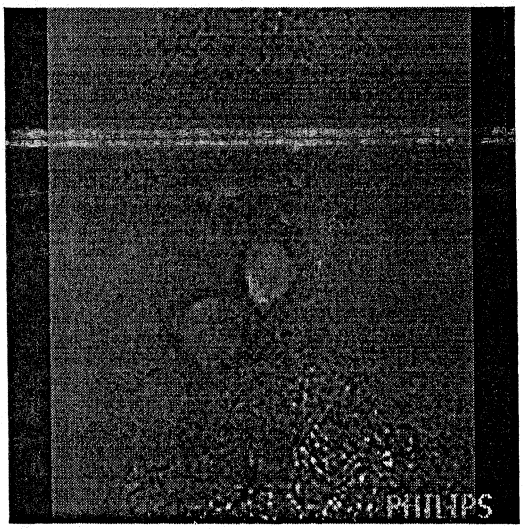

Fig 2D: Resulting tricuspid valve view. (PCA-modulus)

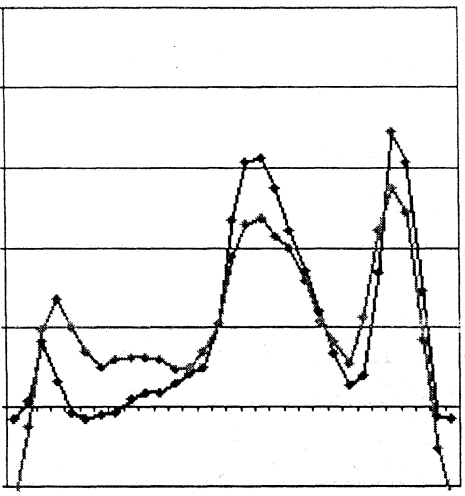

g 2E: Flow rate (ml/s) Red: Mitral, een: Tricuspid

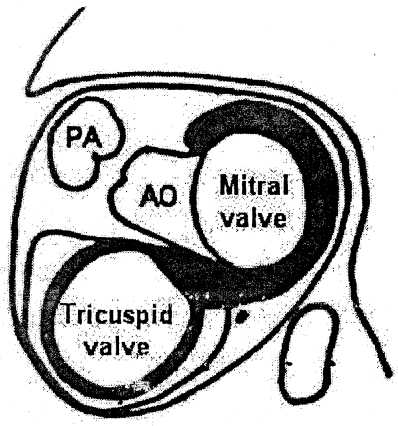

Fig 2F: Resulting tricuspid valve.

yocardial tagging

roduced by Elias Zerhouni
PAMM(spatial modulation of magnetization),line tagging,radial gging,ring tagging are the most commonly using techniques

ysics

tra small saturation pulses are applied immediately after the ECG gger. The RF excitation pulse tags specific parts of the myocardium nulling the magnetization. The tagged tissue will produce arkedly reduced signal intensity during certain phase of the turation pulse. Tagging in short axis is then performed with a ries of radial tagging through the center of myocardium. is possible to track the contraction of left ventricle &estimate the ated wall stress in particular

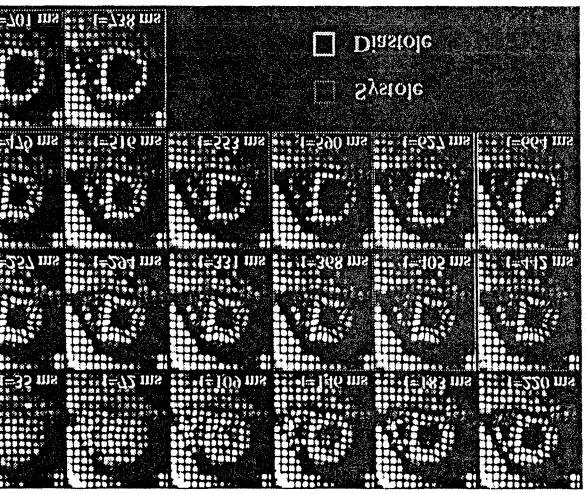

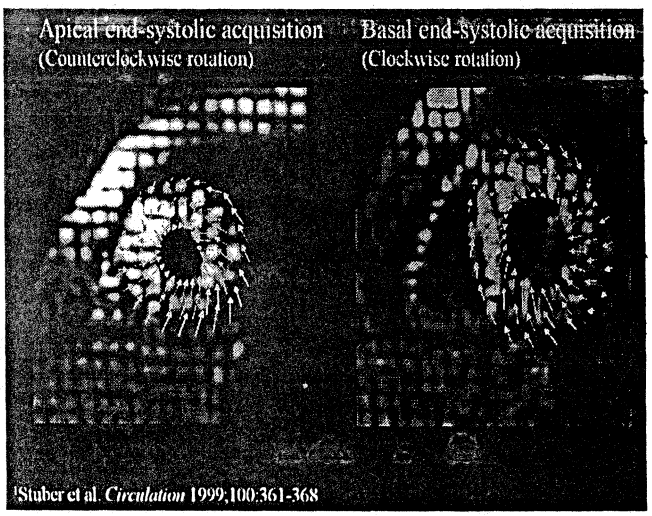

DIAC PERFUSION

ISP-SR-FIRSTPASS-3 SLICE
ardial perfusion of ischemic heart disease can be studied.
linium based contrast agents are injected intravenously and first
metabolism is studied. Fast t1 weighted MR techniques used

gradient echo pulse sequences to be used. Magnetization
red turbo field echo or echo planar or flash. Repetitive
ration in minimum of 3 planes at every heartbeat to be
red. Quantitative image analysis is done with first pass bolus
neters. Level of enhancement, time to peak, mean transit time
easured.

ayed Enhancement

contrast injection ,plasma conc. reaches a maximum value
hen rapidly declines thru diffusion into interstitial space&renal
out. In infarcted tissues ,contrast resorption rate is reduced.
rmal myocardium ,at15-30 min of contrast injection complete
out is noted

al intensity time curve

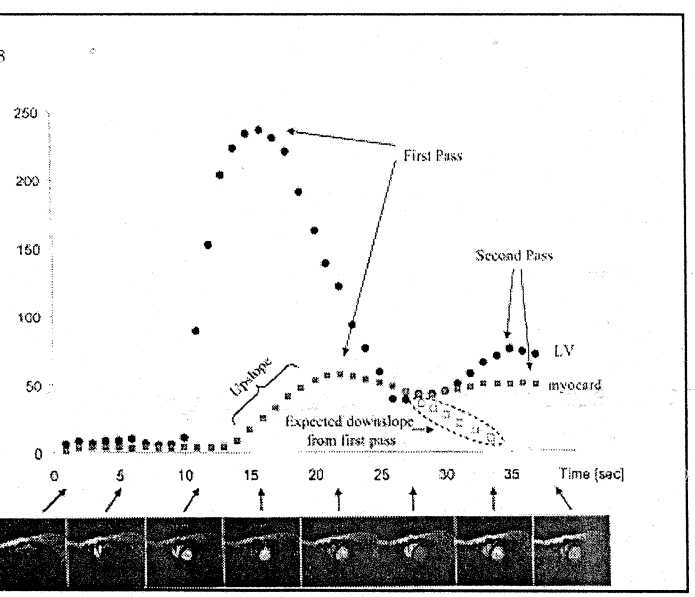

e advent of rapid MRI techniques has made it possible to study in
l-time physiological events such as myocardial perfusion
e ideal MR perfusion sequence is an ultra fast sequence that
irely covers the heart. The ideal contrast agent for perfusion is not
available ,Extra cellular contrast agents are hampered by their
id diffusion in to interstitial space .intra vascular contrast agents
vide lower SNR

ABILITY

65-PSIR-T1-1SLICE

propriate inversion time (approximately 200 msec) is used to null
signal intensity of normal myocardium - critical for accurate
ineation of the infarcted region. The healthy myocardium appears
k, whereas the infarcted myocardium appears bright
arcted or edematous tissue-initially no contrast uptake or little
nal change. After 15min of contrast injection-no complete washout-
ayed enhancement .Bright tissue on delayed images-DEAD tissue.

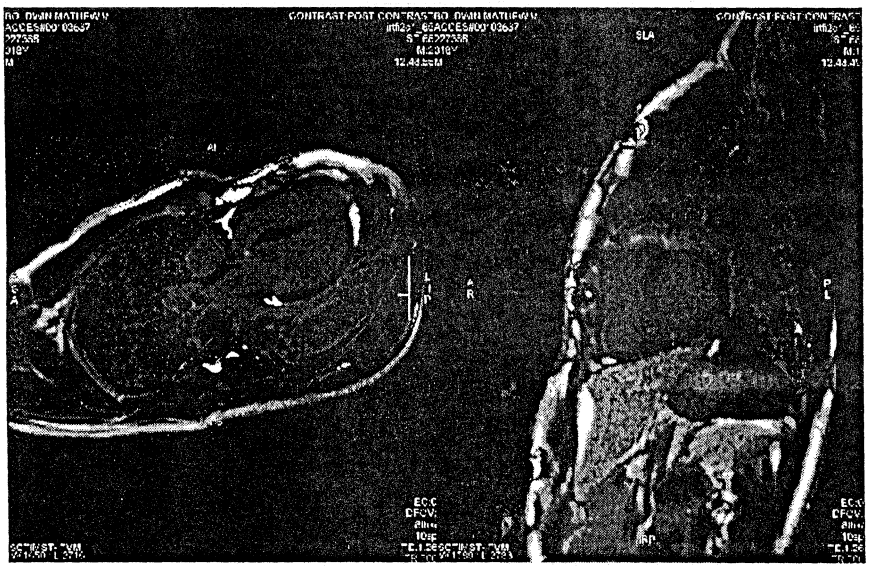

orders, such as tumor, myocarditis, and hypertrophy
diomyopathy. Thus, the location of myocardial enhancement (ie,
endocardial vs midmyocardial) and clinical circumstances are
to proper interpretation of pathologic contrast enhancement.

GNETIC RESONANCE CHOLANGIOPANCREATOGRAPHY

RCP is introduced in 1991;it represents a relatively new
velopment in MR technology that allows for rapid evaluation of the
ary tract, pancreatic duct and gallbladder without contrast material
ministration, instrumentation or radiation.
ecial imaging sequences that are heavily-T2-weighted are utilized
depict the biliary tract, pancreatic duct and gallbladder as high
nal intensity or bright structures owing to the fluid within them. The
curacy of MRCP is comparable to that known as ERCP
doscopic retrograde cholangiopancreatography, the traditional but
asive means of imaging the pancreaticobiliary system) in the
aluation of choledocholithiasis, malignant obstruction, anatomic
iants and chronic pancreatitis.MRCP can be completed in 10
nutes and is easily performed as an outpatient examination.In
RCP and its clinical applications. Technical refinements such as
t MR sequences that allow for imaging of the entire biliary tract
d pancreatic duct in a single breathhold have resulted in marked
provement in the quality and diagnostic yield of MRCPs. As the
ality of MRCPs has improved, the clinical applications of this
chnique have expanded such that MRCP is now replacing
gnostic ERCP in many instances.

me basic principles apply to the acquisition of MRCP images. First
biliary tract and pancreatic duct must be localized; this is often
complished with a scout MRCP performed with a thickness of 40-
mm so that all portions of the pancreaticobiliary tract are included.
is technique is referred to as multislice, thin-slab MRCP

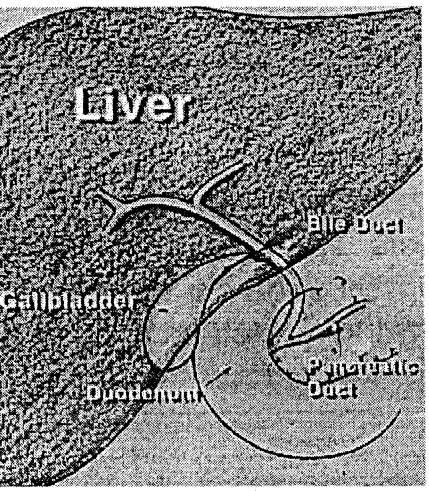

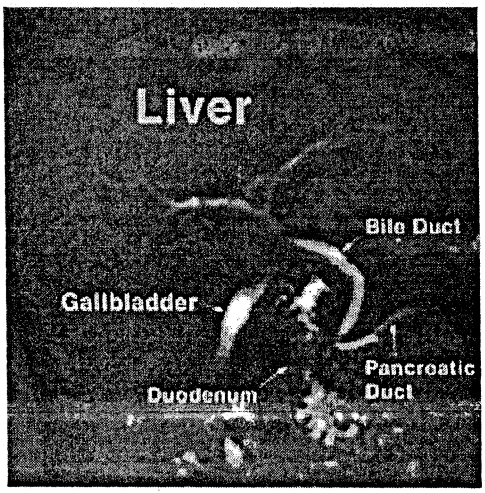

e performance of MRCP does not require intravenous or oral
ntrast material administration because the biliary tract, pancreatic
ct and gallbladder are depicted as high signal intensity or bright
uctures due to the fluid within them. Although patients are not
quired to fast prior to MRCP, patients are asked to avoid heavy
estion of food or liquid immediately prior to the MRCP since a
d-filled stomach may obscure the bile or pancreatic ducts.
or to scheduling a patient for MRCP, the patient is carefully
reened for contraindications to being placed in the MR scanner.
ch contraindications include cerebral aneurysm clips and cardiac
cemakers. If patients give a history of possibly having metallic
gments in their eyes related to grinding metal, a radiograph (x-ray
age) of the eyes is obtained prior to the MRCP.

R TECHNIQUES

cause MRCP is a relatively new imagingtechnique and because of
going advances in software and coils, thetechnique is evolving and
us varies from institution to institution. MRCP is usually performed
h heavily T2-weighted sequences by using fast spin-echo or
gleshot fast spin-echo software and both a thick-collimation
ngle-section) and thincollimation (multisection) technique with a
so phased-array coil. The coronal plane is used to provide a
olangiographic display, and the axial plane is used to evaluate the
ncreatic duct and distalcommon bile duct. In addition, some

tions perform three-dimensional reconstruction
ng a maximum-intensity projection (MIP) algorithm on the
llimation source images. Although the thick-collimation and
dimensional MIP images more closely resemble conventional
ngiograms and are familiar to many clinicians, spatial resolution
raded because of volume-averaging effects. The source
s, which provide greater spatial resolution, must be carefully
nized so as not to overlook small luminal filling defects and
res, which may be obscured on the thicker-collimation
es. Fast spin-echo MRCP is performed by using respiratory
; a long echo train (ie, 32); a long repetition time (three to five
atory cycles, 8,000-10,000 msec); an echo time greater than
nsec; fat saturation; thin collimation (3 mm with no
and three excitations. Imaging time is usually 4-6 minutes.
ugh the use of a long-echo-train sequence considerably
es imaging time compared with that of conventional T2-
ted spin-echo sequences, artifacts from respiration and
alsis are still problematic because the signal is averaged over
le respiratory cycles. Single-shot fast spin-echo is a newer
nore rapid MRCP sequence that can be performed in a single
h hold, thereby significantly reducing motion artifacts and
asing image quality . As a result of less motion artifact (noise)
ingle-shot fast spin-echo MRCP, the signalto- noise ratio
ases compared with that of fast spin-echo MRCP. However,
is also a decrease in signal, albeit not as great as the decrease
se. The result is less spatial resolution. The speed of the
sition is due to a very long echo train (ie, 128); an infinite
tion time; and the ability to reconstruct images after acquiring
nalf of the phase-encoding steps. We use an echo time of
er than 800 msec to suppress signal from most extraductal
ures including fat, eliminating the use of fat saturation. All
formation is acquired in less than 2 seconds from approximately
choes generated from a single 90° pulse. Imaging time for both
e-section and multisection sequences is less than 30 seconds.
use all the image information from one section is
red before proceeding to the next section, breath-hold and non-
h-hold techniques can be used. However, we prefer
reath-hold technique to avoid artifacts from respiratory motion
o avoid section misregistration. The combination of rapid

uences and the torso phased-array coil, which increases signal-oise ratio, makes

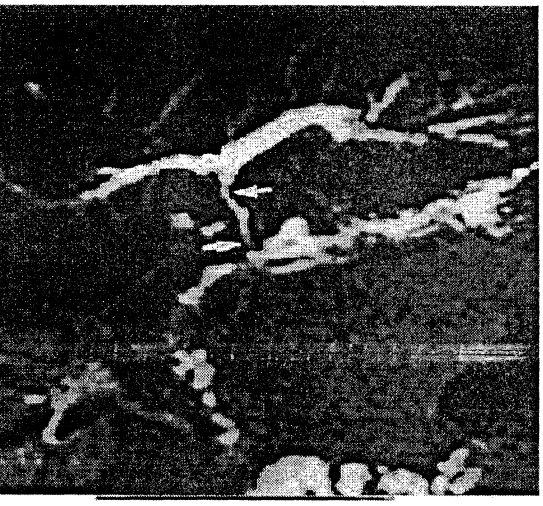

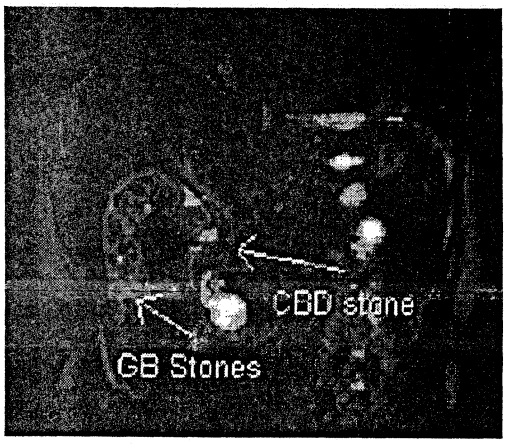

CONTRAST AGENTS FOR MRI

amagnetic Contrast Agents :

neral considerations:

in-lattice relaxation time T1 and spin-spin relaxation time T2 y be shortened considerably in presence of paramagnetic species. e resulting effects can be seen best in NMR spectroscopy. While rtening of T1 leads to increase in signal intensity, shortening of producesbroader lines with decreased intensity . The net result is nlinear relationship between signal intensity and the centration of the contrast agent . At low concentrations, increase in contrast agent provides an increase in signal nsity due to effect on T1 until the optimal concentration is ched. Further increase in concentration reduces the signal ause of effect on T2. Therefore, in clinical practice it is possible achieve less than optimal contrast effect and even produce a gative contrast effect. This dictates the use of agents that have a tively greater effect on T1 than on T2, as well as the use of se sequences that emphasize the changes in T1.

gnetic species are species which have unpaired electrons. be simple substance (i.e. molecular oxygen), stable i.e. nitroxide radical) or metal ion (i.e. many transition metal

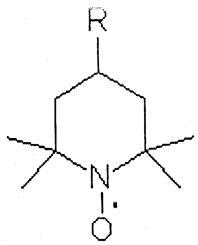

Stable nitroxide radical

Figure 1

dicals generally cause damage to the living tissues. Therefore, e not suitable candidates for medical MRI purposes. The agnetic effect of oxygen, although demonstrable, seems ak for practical applications Paramagnetic metal ions do suitable effect which depends on number of unpaired ns in the ion. The following table shows some of the agnetic metal ions.

N	Ion	3d	4f	Magnetic moment (Bohr magneton)
	Cr 3+	↑ ↑ ↑		3.8
	Mn 2+	↑ ↑ ↑ ↑ ↑		5.9 (weak field)
	Fe 3+	↑ ↑ ↑ ↑ ↑		5.9 (weak field)
	Cu 2+	↑↓ ↑↓ ↑↓ ↑↓ ↑		1.7-2.2
	Eu 3+		↑↓ ↑ ↑ ↑ ↑ ↑ ↑	(6.9)
	Gd 3+		↑ ↑ ↑ ↑ ↑ ↑ ↑	7.9
	Dy 3+		↑↓ ↑↓ ↑ ↑ ↑ ↑ ↑	(5.9)

ere are more transition metals and lanthanide metals with ed spins, but for the metal to be effective as a relaxation the electron spin-relaxation time must match the Larmor

quency of the protons. This condition is met better for the Fe3+, 2+ and Gd3+ ions (about 10-8 - 10-

s, others have 10-11 - 10-12 s).

The main problem with paramagnetic heavy metal ions in their ive form is their toxicity. Investigation has focused on the velopment of stable paramagnetic ion complexes. Both the tal ion and the ligand usually exhibit substantial toxicity in the bound state. Together, however, they may create a rmodynamically and kinetically stable compound which is much s toxic. Complexation of the metal ion with organic ligand, ile considerably decreasing toxicity, may alter paramagnetic perties of the metal.

Chromium-EDTA complex was the first such agent tried, but blems with synthesis and long-term stability prevented its ical application.

Gadolinium-DTPA complex, a renally excreted chelate with a y high formation constant (Table 2), had sufficiently favorable perties to be approved by Food and Drug Administration of USA use in cranial disease diagnostics in mid-1988.

Table 2

Gd-DTPA formation constant = 10^{23}
Half-life in urine = 21.0 min after intravenous injection
in blood = 19.6 min

Compound	LD_{50} with intravenous dose in rats (mmol/kg body weight)
Gd-DTPA	10
Gd-EDTA	0.3
Gd-Cl3	0.4
Meglucamine diatrizoate (common X-ray contrast agent)	18

Another, relatively new type of paramagnetic contrast agents is -called superparamagnetic iron oxide (SPIO) based colloids .

y consist of nonstoichiometric microcrystalline magnetite
es which are coated with dextranes or siloxanes. Use of these
oids as tissue- specific contrast agents is now a well-established
a of pharmaceutical development .

dolinium(III) complexes

e prominent feature of Gadolinium(III) is the high number of
paired electrons - seven. The Gd3+ ion retains a number of
paired spins when bound to the organic ligand. The free Gd3+
is extremely toxic. Number of its complexes are very stable
l thus exhibit much less toxicity. As mentioned before, Gd-
PA complex has been approved to clinical use and is now
rketed in USA under the name "Magnevist".

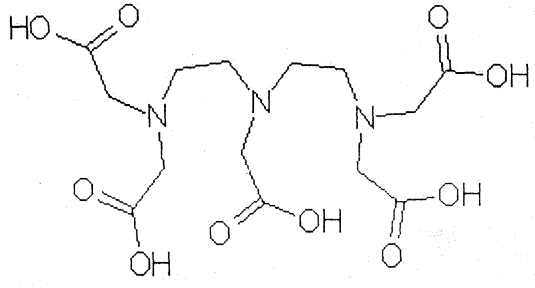

DTPA (diethylenetriaminepentaacetic acid)

1

The relationship between the thermodynamic stability of the
mplex and the acute toxicity in vivo seems to be more complex, as
monstrated by study on that matter. Authors investigated stability
the series of complexes of several ligands with Gd3+ versus acute
icity on mice. They also attempted to measure the rate of
nsmetallation of Gd3+ by Cu2+ and selectivities of different ligands
vards Gd3+ as compared to Zn3+, Cu3+, Ca3+. Iron(III) was not
nsidered because it is tightly bound in vivo by the storage proteins
ritin and hemosiderin and is essentially unavailable for interaction
h Gd3+ complexes. The main competitor to Gd3+ was found to
Zn2+, and the most important thermodynamic criterion of toxicity
the selectivity of the ligand for Gd3+ over other endogenous
etal ions. Zinc transmetallation was found to be the most likely
ode of both acute and subchronic toxicity in experiments on rats.
mplexes whose structure make in vivo transmetallation

actions much slower than renal excretion rates have gnificantly improved toxicities than would be predicted by ermodynamics. Slower clearance from the body is likely to gnificantly increase the toxicity of any Gd3+ complex. The following gure shows other ligands often used in gadolinium studies.

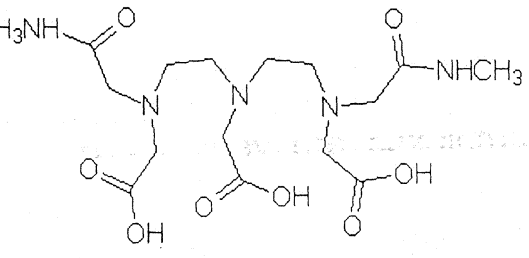

DTPA-BMA
(diethylenetriaminepentaacetic acid bis(methylamide))

2

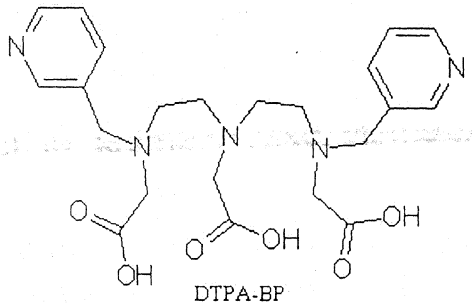

DTPA-BP
(N,N'-bis(2-pyridylmethyl) diethylenetriamine-N,N',N''-triacetic acid)

3

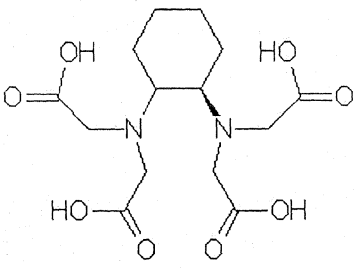

CDTA
(trans- 1,2-diaminocyclohaxane-N,N',N'',N'''-tetraacetic acid)

4

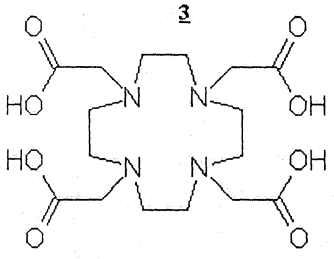

DOTA
(1,4,7,10-tetraazacyclododecane-N,N',N'',N'''-tetraacetic acid)

5

Gd3+ has been shown to inhibit Ca2+ binding to mammalian ardiac sarcoplasmic reticulum. The mechanism of toxicity could nvolve hemodynamic disruption.

An example of two another perspective ligands is shown on igure 3.

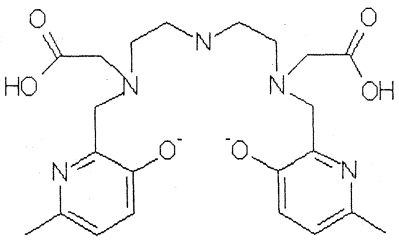

DTTA-HP
(N,N'-bis(3-hydroxy-6-methyl-2-pyridilmethyl)di-ethylenetriamine-N,N',N"-triacetic acid)

6

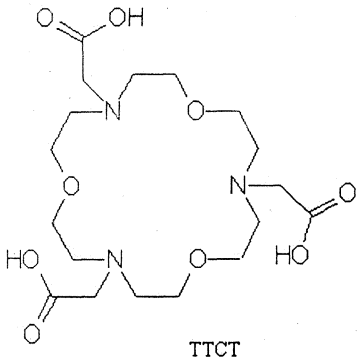

TTCT
(1,7,13-triaza-4,10,16-trioxacyclooctadecane-N,N',N"-triacetic acid)

7

Potential improvement also lies in the idea of covalently
ıpling the ligand to protein to generate tissue- specific contrast
ents .
derstandably, search for new potential ligands for Gd3+
mplexation is still hot area of investigation. The complexes are
aluated against Gd-DTPA, the only approved compound for
man use so far. Criteria include thermodynamic stability,
es of excretion, toxicity, lipophilicity, biodistribution, percent
ange in MR signal intensity. Some of the complexes are slightly
tter than Gd- DTPA in particular tests, others are a little
rse. However, neither of them got as much attention as Gd-
PA itself . This complex is far not be the best choice as of today,
it is relatively well-known choice, widely used in many MRI
ilities on a daily basis. Accumulated experience allows in many
ses offset the shortcomings of Gd-DTPA, so the agent continues
play indispensable role in modern MR imaging.
nocrystalline Iron Oxide Nanocompounds Compounds called
ON constitute relatively new but rapidly evolving area in MRI
ntrast agents. As compared to the single approved gadolinium-
ntaining complex, there are variety of MION (also called SPIO -
perParamagnetic Iron Oxide) reagents available on the market.
ashy names

ridex I.V™., Endorem™, Gastromark™, Lumirem™, Sinerem™
d more patents pending tell us that the last word in the area is yet
be said.

These compounds consist of nonstoichiometric
rocrystalline magnetite cores which are coated with dextrane
ferumoxides) or siloxanes (in ferumoxils). SPIO agents are mu
e effective in MR relaxation than their paramagnetic
nterparts. Since they are nonstoichiometric, there was and
is much interest in studying these compounds with all the vast
y of modern physical-chemical methods: single crystal X-ray
raction, powder X-ray diffraction, Mossbauer spectroscopy,
smission electron microscopy, dynamic light scattering, atomic
orption spectroscopy, spectrophotometry, electron microscopy,
erconducting quantum interference devices etc.
e compositions and physiochemical properties of
stoichiometric magnetites are continuously variablebetween
se of Fe_3O_4 and Fe_2O_3. Conceptually, these cation-deficient,
erse-spinel phases are formed by partial oxidation of
II) in stoichiometric magnetite24.The Fe2+ content is typically
5 mol%. The lattice parameters of these colloids also fall
ween those of Fe_3O_4 and Fe_2O_3.
e particles are usually of varying sizes from several to several
ndred nanometers. They are irregular in shape and highly light-
sorbing. They have no magnetic hysteresis at ambient
mperatures, which is characteristic of superparamagnetic
terials. Mossbauer spectra are characteristic of small
0nm) magnetic domains which undergo superparamagnetic
axation or collective magnetic excitation on the Mossbauer time
le . There is no evidence of covalent bonding between the iron
face and the surrounding dextran .
IO compounds are promising contrast agents since their
perties may be fine-tuned for the specific application. They
non-toxic and rapidly cleared from the organism. Experiments
ve been successful in receptor- specific SPIO delivery.
talloporphyrines of Iron(III) and Manganese(III)

rphyrins have been known for decades as indicators of
ious metabolic disorders and disease states. They are used in
otodynamic therapy of tumors .Low toxicity of metalloporphyrins
d their selective retention in tumors have led recently to their
dy as a MRI contrast media . Article contains theoretical treatment
relaxivity of some of the metalloporphyrins. This is a fairly
w area of development, but metalloporphyrins of Mn(III) and

show favorable properties as MRI contrast agents for tumor
on. No doubt, it will lead to new discoveries soon.
Proteins Acting as Contrast Agents
ne-containing proteins may act as "natural" contrast agents,
e previously discussed iron(III) porphyrins. Hematomas are
identified by MRI. Paramagnetic deoxyhemoglobin within
blood cells causes a local region of high magnetic field
esults in rapid dephasing of water protons diffusing in the
of acute hematoma with shortening of T2, which results in low
A similar phenomenon is observed when magnetically
otible ferritin is deposited in macrophages in
hromatosis.

gh these not a specifically designed contrast agents, their
ties may be successfully used for diagnostics in specific

ointestinal Contrast Agents

he gastrointestinal tract cannot be reliably studied by MRI
t the use of contrast agents. Oral contrast agents may
tically improve utility of MRI for gastro- diagnostics. The only
lly approved agents for that purpose are soluble iron
ounds. (ferrous gluconate, ferric ammonium citrate) and Gd-
There is a problem with dosage of iron salts, which may not
d the levels above those when iron supplementation is used.
are no particulate agents approved for oral use yet.

Contrast Agents

Examples of contrast agents other than paramagnetic involve
mechanical action than changing the characteristics of
rrounding tissue. They are thus similar to agents used in X-
ethods. One recent example successfully utilized vegetable
r rectal MRI applications. Other possibilities include
ation of air to achieve better contrast of intestinal walls .

ARTIFACT

image artifact is a structure not normally present but visible as a ult of a limitation or malfunction in the hardware or software of the l device, or in other cases a consequence of natural processes or perties of the human body. The knowledge of MRI artifacts and se producing factors is important for continuing maintenance of n image quality. Artifacts may be very noticeable or just a few els out of balance but can give confusing artifactual appearances n pathology that may be misdiagnosed.

age distorsions related to changes in patient position, pulse quence, metallic artifacts, or other imaging variables can be ected by the operator; artifacts due specifically to the MR system y require a service engineer.

ny types of artifacts may occur in magnetic resonance imaging. facts in magnetic resonance imaging are typically classified as to ir basic principles,

- Physiologic (motion),
- flow.
- Hard ware (electromagnetic spikes, ringing)
- Inherent physics (chemical shift, susceptibility, metal)

1. Chemical Shift Artifacts
2. Aliasing
3. Black Boundary Artifacts
4. Gibbs or Truncation Artifacts
5. Zipper Artifacts
6. Phase-encoded Motion Artifacts
7. Entry Slice Phenomenon
8. Slice-overlap Artifacts
9. Magic Angle Effects
10. Moire Fringes
11. RF Overflow Artifacts
12. Central Point Artifact

Susceptibility Artifacts

Zero-fill Artifact (Zebra Artifact)

eral techniques are developed to reduce these artifacts (e.g. piratory compensation, cardiac gating, eddy current pensation) but sometimes these effects can also be exploited, for flow measurements

sing Artifact

sing is an artifact that occurs when the field of view (FOV) is ller than the body part being imaged. The part of the body that beyond the edge of the FOV is projected on to the other side of image.

sing in the frequency direction can be eliminated by sampling the al twice as fast or by applying frequency specific filters to the ived signal.

milar problem occurs in the phase encoding direction, where the ses of signal-bearing tissues outside of the FOV in the y-direction a replication of the phases that are encoded within the FOV.

se encoding gradients are scaled for the field of view only, efore tissues outside the FOV do not get properly phase encoded tive to their actual position and 'wraps' into the opposite side of image

a larger FOV, RFOV or 3D Volume, apply presaturation pulses to undesired tissue, adjust the position of the image center, or select maging coil which will not excite or detect spins from tissues side of the desired FOV. In the phase direction, the number of se encoding steps must be increased with a longer study as a ult.

en this is not possible it can be corrected by oversampling the a. Oversampling is used in the frequency direction to eliminate the sing. No Phase Wrap (Foldover Suppression) options typically rect the phase encoding by doubling the field of view, doubling the mber of phase encodes (to keep resolution constant) and halving number of averages (to keep scan time constant) then discarding additional data and processing the image within the desired field iew (but this is more time consuming).

sue outside this doubled area can be folded nevertheless into the ge as phase wrap. In this case combine more than 2 number of citations / number of signal averages with foldover suppression.

ifact by Patient Movement

ient movement during the scans are often an imaging problem.
facts from patient movement are widely varied due to a
pendence when during k-space filling the motion occurs. When the
ient moving causes only in the last few seconds of the scan at that
e the outside edges of K-space were being filled, and as a result
artifact does not overly affect the image (there are only fine lines.

ack Boundary Artifact

e black boundary artifact is an artificially created black line located
water-fat interfaces such as muscle-fat interfaces. If the MR imager
uned or centered to the frequency of water, fat will be shifted or
atially mismapped relative to its true spatial location. When
emical shift is greater than or equal to the size of an individual pixel
ark or bright band of signal intensity will occur at the lipid –water
erface in the frequency encoding direction of the image. This pixel-
pixel misregistration along the frequency encoding direction visibly
nifests itself as a bright or dark band running perpendicular to the
quency encoding direction.
is artifact can occur for a couple of reasons. The most common
ason (for gradient echo sequences) is a result of selecting an echo
e in which the fat and water spins are out of phase, canceling each
er. At 1.5 T, the 3.5 ppm difference in frequency between water
d saturated fat results in cancellation of spins at 4.5 ms multiples;
example at 6.8ms, 11.3ms, and 15.9 ms.

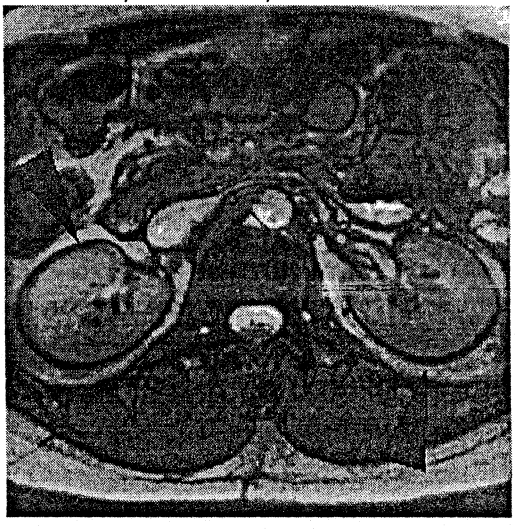

iac Motion Artifact

ement of the heart causes blurring and ghosting in the images. artifacts appear in the phase encoding direction, independent of irection of the motion.
e artifacts can be reduced by using cardiac synchronization: ering, gating or retrospective triggering. Maximum reduction can chieved by using triggering in combination with flow pensation, respiratory triggering or breath hold and regional ration techniques

tral Point Artifact

central point artifact is a focal dot of increased signal in the er of an image. Temperature fluctuations often cause dc-coupled ifiers to have non-zero outputs with zero input. It is caused by a tant offset of the DC voltage in the receiver and therefore an t in signal intensity of all raw data points. Normally software pensation prevent it, by applying a 'dc correction' or 'baseline ection' before the FT.

mical Shift Artifact

e B0 and chemical shift differences between tissues cause acts. The MRI scanner uses the frequency of the signal to cate spatial position. During frequency encoding, fat protons ess slower than water protons in the same slice because of their netic shielding. The signal from the fat protons is incorrectly oded. The net effect is that the fat and water, located in the same el are encoded as located in different voxels and are shifted in the uency direction from their true positions. This chemical shift egistration cause accentuation of any fat-water interfaces along frequency axis of MRI's and may be mistaken for pathology. ere fat and water are in the same location, this artifact can be n as a bright or dark band at the edge of the anatomy.
ons in fat and water molecules are separated by a chemical shift bout 3.5 ppm. The actual shift in hertz (Hz) depends on the gnetic field strength of the magnet being used. The artifact is ater at higher field strengths and lesser at higher gradient ngths. For a 0.3 T system operating at 12.8 MHz the shift will be

3 Hz compared with a 223.6 Hz shift for a 1.5 T system operating
3.9 MHz
artifact reduction helps a smaller water fat shift (higher
dwidth), a higher matrix, an in phase TE or a spin echo technique.
ce the misregistration offset is present in the read out axis the
ent may be rescanned with this axis parallel to the fat-water
rface. Steeper gradient may be employed to reduce the chemical
t offset in mm. Another strategy is to employ specialized pulse
uences such as fat saturation or inversion recovery imaging.
ctically about the best way to eliminate this artifact is to use a fat
pression technique

sscross / Herringbone Artifact

s artifact appears as a herringbone pattern scattered over the
ole image in any direction only on one slice or on multiple slices.
e causes of this are many and various, like e.g. electromagnetic
kes created by the gradients, electronic equipment inside the MR
cedure room, or fluctuating AC current.

osstalk (Artifact)

osstalk is an artifact introduced into images by interference
tween adjacent slices of a scan, caused by a slice profile that is not
al due to the constraints of the measurement technology. If the
ce distances are too small, there is cross talk between the slices,
ich can affect T1 contrast

artifact can be eliminated by limiting the minimum spacing (for
nost sequences a minimum gap 10% and for IR sequences 20%)
een the slices. Crosstalk can also be reduced by selection of
eaved slices (so a slice gap will not be necessary), but
eaved data acquisition can produce large mean intensity
rences between adjacent slices

y Slice Phenomenon (Artifact)

y slice phenomenon occurs when unsaturated spins in blood first
s into a slice or slices. This artifact is characterized by bright
al in a blood vessel (artery or vein) at the first slice that the vessel
rs. Often the signal is seen on more than one slice, fading with
nce.
fusion with thrombosis can be the result of this artifact. The
acteristic location and the use of gradient echo flow techniques
be used to differentiate entry slice artifacts from occlusions

osting Artifact

mage artifact caused through moving (respiratory, bowel motion,
rtbeat) primarily associated with the phase direction
facts can be reduced by respiratory and cardiac triggering, the use
reath holding pulse sequences and flow compensation. Another
hod of reducing ghosting artifacts is to use a pharmaceutical,

n as glucagon or scopolamine, to reduce bowel motion. This will rease artifacts from both peristalsis and breathing.

bs Artifact

s artifact is a series of bright or dark lines that are seen parallel adjacent to borders of abrupt intensity change (sharp intensity e) in an image, as when going from bright CSF to dark spinal cord a T2 weighted image.
ne spinal cord, the gibbs phenomenon can simulate a small syrinx ne unaware. It is also seen in other locations as at the in/calvarium interface.
e lines visible in an image may be due to undersampling of the n spatial frequencies, respectively incomplete digitization of the o. It is related to the finite number of encoding steps used by the urier transformation to reconstruct an image. This means the signal s not decayed to zero by the end of the acquisition window, and echo is not fully digitized.

s related to the finite number of encoding steps used by the Fourier nsformation to reconstruct an image. The more encoding steps, less intense and narrower the artifacts. Therefore, e.g. the artifact nore pronounced in the 256 point dimension of a 512x256 quisition matrix
s problem can be easily resolved by taking more samples - a her acquisition matrix and/or a smaller FOV.

adient Related Artifact

ifacts arising from problems with the gradient system are metimes very similar to those described as B0 inhomogeneities. A adient that is not constant with respect to the gradient direction will tort an image. This is typically only possible if a gradient coil has en damaged. Other gradient related artifacts are due to abnormal rrents passing through the gradient coils.

Artifact

ffects in MRI can produce a range of artifacts. Flow artifacts
ually include intravascular signal void by 'time of flight' effects,
nt dephasing and first echo dephasing, caused by flowing
A liquid flowing through a slice can experience a RF pulse and
ow out of the slice by the time the signal is recorded (because
petition time (TR) is asynchronous with the pulsatile flow). The
flow occasionally produces an intravascular high signal
ty due to flow related enhancement, even echo rephasing and
ic pseudogating. The pulsatile laminar flow within vessels often
ces a complex multilayered band that usually propagates
e the head in the phase encoded direction. Blood flow artifacts
l be considered as a special subgroup of motion artifacts.
ts can be reduced by reduction of phase shifts with flow
ensation (gradient moment nulling), suppression of the blood
with saturation pulses parallel to the slices, synchronization of
aging sequence with the heart cycle (cardiac triggering) or can
ped 90° by swapping the phase/frequency encoding directions.

Angle Effects

angle effects are seen most frequently in tendons and
ents that are oriented at about a 55 degree angle to the main
etic field. Signal from water molecules associates with the
n collagen fibers is not normally seen because of dipolar
ctions that result in very short T2 Times. At an angle of about 55
es to the main magnetic field, the dipolar interactions become
resulting in an increase of the T2 Times about 100 fold. This
s in signal being visible in tendons with ordinary pulse
ences. A bright signal from this artifact is commonly seen in the
r cuff and occasionally in the patellar tendon and elsewhere.
llowing image shows increase signal in the distal patellar
n from this magic angle effect.

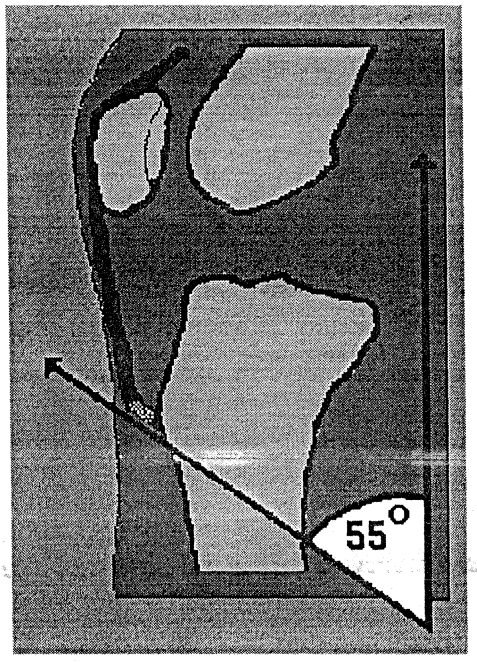

oire Fringes

oire fringes are an interference pattern most commonly seen when ing gradient echo images with the bodycoil . Because of lack of rfect homogeneity of the main magnetic field from one side of the dy to the other, aliasing of one side of the body to the other results superimposition of signals of different phases that alternatively add d cancel. This causes the banding appearance and is similar to the fect of looking though two screen windows.

otion under Control

th Prospective Acquisition Correction (PACE)

D-PACE and 2D-PACE

ethod

ne fastest method of detecting motion is 1DPACE (also known as a avigator" technique). It typically requires only 30 ms and is used imarily for minimizing the effects of breathing motion in cardiac kams. For this purpose, a single line of data from a pencil-shaped olume that crosses the diaphragm is acquired. The volume is teractively placed (Fig. 1) in such a way that the position of the aphragm can be calculated and used for motion rrection – in real time.

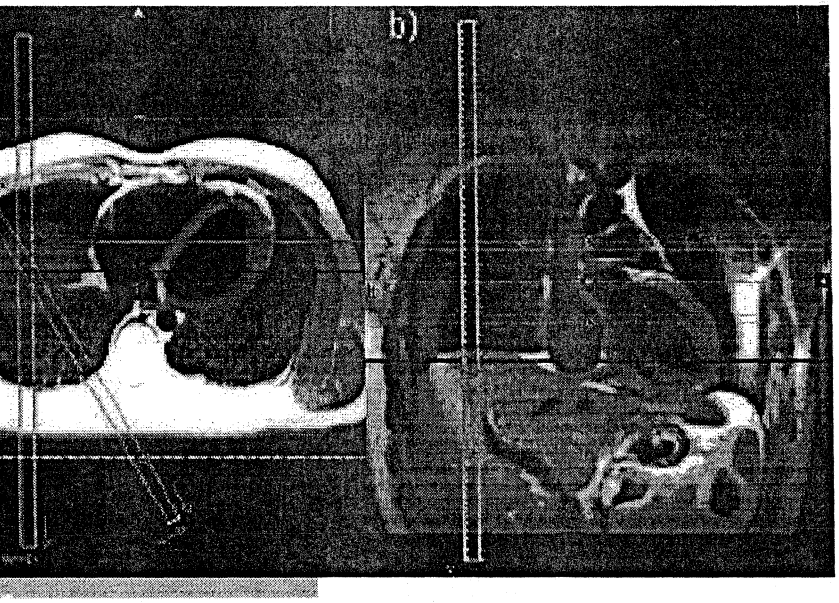

CE,
ge is acquired by means of a low-resolution gradient echo
nce featuring a low flip angle; this ensures that magnetization is
urated, so that dark lines in the image are avoided. The user
a small box across the diaphragm on the 2Dimage
ange in signal intensity along the axis of the box is used to
ine the position of the diaphragm. Since a 2D image provides
nformation than a single line, this method is very robust. The
eeded to acquire an image for 2D-PACE is around 100 ms. The
reliable 2D-PACE technique is unique to Siemens.

olication:

tiple Breath-hold Examinations

patients who can hold their breath for only a short time, the uisition can be split up into multiple breath-holds. The information ut the diaphragm position allows the operator to monitor the athing pattern of the patient online. Furthermore, acquisition of es during different breath-holds can be aligned in order to pensate for imperfect reproducibility of the breathhold position. is way, gaps between slices or overlaps are avoided.

PACE

ctional MR imaging (fMRI) is another application where motion ection, and instantaneous adjustment of the acquisition ording to this information, are crucial. Here, complete multi-slice datasets of the head are acquired in rapid succession during sentation of various stimuli. In order for the statistical analysis to successful, the datasets need to be aligned perfectly. For this pose, each 3D dataset is compared with the previous one and the slation as well as the rotation of the head are calculated (and layed) in real-time. The software is able to compensate for tions and translations in all 6 degrees of freedom (a feat that is natched in the MR industry). The technique can therefore account, eal time, for any so-called "rigid-body motion". For acquisition ne next dataset, slice position and orientation are adjusted ording to the altered position of the head.

MRI- SAFETY

ety can be divided up into three areas:

- Main Magnetic Field
- Varying Magnetic (Gradient) Fields
- Radio Frequency
-

n Magnetic Field and Safety

ıain magnetic field of a 1.5 T magnet is about 30,000 times the gth of the earth's magnetic field. It is strong enough to pull fork-es off of machinery, pull heavy-duty floor buffers and mop ets into the bore of the magnet, pull stretchers across the room urn oxygen bottles into flying projectiles. Deaths have occurred trauma as a result of these effects. Smaller objects such as rs, bobby pins and pens have been known to be pulled off the on carrying them.
strong field also effects common devices such as pacemakers watches. The magnetic reed switch in modern pacemakers is rbed by strong magnetic fields resulting in possible deleterious ts to the patient with one implanted. Mechanic watches will ze up" in a strong field, sometimes permanentely. Many cranial aneurysm clips are ferromagnetic and as a result rience a torque or twisting in a magnetic field. Not everyone with neurysm clip experiences a fatal hemorrhage when placed in a net, but several cases have been reported.
e types of heart valves (e.g., Star-Edwards) are torqued in a netic field: however, this torque is less than the stresses that r normally as a result of blood flow. Therefore heart valves are considered not to be an absolute contraindication for MRI. More annoyance than a safety problem is the ability of the magnetic of a MRI machine to erase the information contained on the netic strip on ATM and credit cards. This may occur a short nce inside of the scanner room of a MRI machine.
e metallic objects that are usually safe near an MRI machine are jewelry and eyeglass frames

rying Magnetic (Gradient) Fields

ing magnetic fields are necessary in order to obtain images from scanners. Changing magnetic field induce electrical currents in luctors .(.this is how an electrical generator works). In patients

metal in their body, the potential exists for electrical currents
ng induced in the metal with subsequent heating. This may occur
metal foreign bodies or some surgical implants. It does not
versally occur and some patients with hip prostheses, for example,
y, be scanned without harm. Very rapidly changing magnetic fields
may be achieved with echo planar imaging can cause nerve
nulation. This stimulation can effect motor nerves with resulting
scle contraction as well as the retina with resulting flickering lights
ed "magnetophosphenes".

adio Frequency and safety.

e radio frequency power that is capable of being produced
tches that of many small radio stations (15-20 kW). As a result
re is the presence of heating effects from the RF. In most pulse
quences, the heating is insignificant and does not exceed the FDA
delines. New pulse sequences such as for echo planar imaging
d some spectroscopy localization techniques are capable of
ceeding the FDA guidelines. Monitoring of the power deposition in
ients is a requirement for FDA approval of clinical MRI
anners.Potential for electrical shock exists with RF coils so proper
unding and insulation of coils is necessary. Any damage to coils or
ir cables needs prompt attention. Also looping of the cable to a coil
result in burns to patients that come into contact with them. It is
st to avoid all contact with the RF coil cables.
man Exposure Considerations.
tential hazards lies in,

1. Static magnetic fields.
2. Gradient magnetic fields.
3. RF electromagnetic fields.

gnetic field Effects.
cording to FDA (Food and Drug Administration - 1982) guidelines
ere
maximum permissible levels for static mag. Fields. They are,

Static field - 2 Tesla.
Rate of varying field - 3 Tesla/sec.

low these suggested guidelines no documented permanent
verse biologic Effects have been observed. The only biological
ect associated with exposure to a static magnetic Field is

entation of the T- wave amplitude observed on an ECG and
no significant effect on health. Gradient fields can induce
nt in the patient's body. The current can produce mild
eous sensation, involentary muscle contraction and cardiac
hmias. Subjective visual effects, light flashes known as
eto phospheres, may result stimulation of retina.

eld effects.

neasure of dose of RF energy is SAR(Specific AbsorptionRate).
of SAR is Watt per Kilogram (W/Kg.)SAR is the power absorbed
nit mass. The main effect of RF exposure is an increase in the
temperature. Exposure to an SAR up to 0.4 W/Kg should
ce no temperature increase. However, additional evaluation
eeded for
sensitive organs such as testes and eyes.

During Pregnancy.

neral MRI is not believed to be hazardous to the fetus. However
y
echanism have the potential to produce harmful interaction
een electro-magnetic field and fetus. By FDA
mmendations, it is considered inadvisable to undergo MRI
nely during pregnancy until more information regarding potential
rds become available.

netic Field Hazards.

e field exists around the magnet. The 0.5 mT field extends about

a 0.5 T magnet and 36ft. from a 1T magnet.One of the greatest
ntial hazard is the missile effect. Hazards also exists for patients
have medical devices implanted in their bodies such as, Cardiac
maker, Aneurysm clips, Shrapnel or other metallic foreign
es, Implanted electrodes, Neuro-stimulators , Joint replacements

cts that may be damaged by a 0.5 mT field includes watches,
t cards, taperecorders, calculators, cameras etc. Careful

eening of any one (worker, patient, visitor) having access to the gnet is required.

MAGNETOM AVANTO - TECHNICAL VIEW

m (total imaging matrix)

- Up to 76 seamlessly integrated coil elements with up to 32 RF channels.
- 205 cm FoV. Whole Body at the highest quality.
- PAT. Unlimited.

dioComfort with strongest gradients

- Hardware + Software measures for acoustic noise reduction up to 30 dB (A) as compared to conventional systems. This is a reduction of 97 % in sound pressure.
- Gradient field strength up to 45 mT/m (72 mT/m effective)
- Slew rate up to 200 T/m/s (346 T/m/s effective)

- Large Field of View up to 50 cm / 20 in., optimized for whole body examinations
- Ultrafast, highly compact, water-cooled gradient amplifier in solid-state technology for best min. TR 1.5 ms and min. TE 0.6 ms (matrix 2562

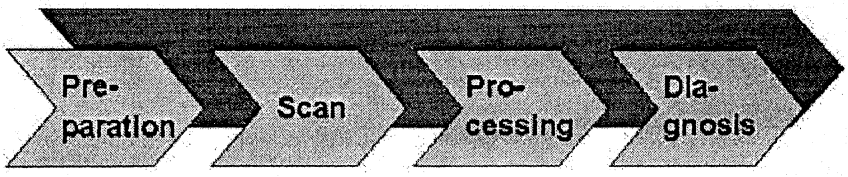

xamples are

- Phoenix
- AutoAlign
- Inline Technology

ompact Magnet

- Ultracompact 1.5T magnet (length: 150 cm/ 5 ft. 3 in.)
- Wide, patient-friendly inner bore diameter (60 cm / 2 ft.)
- Magnet weight only approx. 3,550 kg / 8.900 lbs
- Large DSV (diameter spherical volume) with excellent homogeneity over 50 cm / 20 in.

Computer

syngo speaking user interface.
syngo is the common software platform for all imaging modalities. Enhanced productivity with minimized user interactions per operation step. Based on a powerful Pentium 4 / 3 GHz Panoramic Recon Image Processor reconstructing up to 3226 images per second (256 x 256, 25% recFoV) in combination with a Pentium 4 based Host Computer with two CPU's / 3 GHz and 2 GB RAM capacity.

Cost Effective Siting

- 30 qm / 325 sq.ft. floor space only

No computer room required for a total of just two electronic cabinets (water-cooled

MAGNETOM Avanto – Application

Whole Body Suite

GNETOM Avanto features a unique telescopic patient table which ables a full Field-of-View of 205 cm, without increasing total system gth. No additional table extension is required.
e table top has standard length, additional space is only required at rear part of the magnet. Table movement to its full extent can be trolled from the operator console.
e large FoV helps in imaging metastases with sequences such as RM (Turbo Inversion Recovery). Whole-Body MR Angiography is ssible on the entire volume with iPAT.

- Max. scan range of 205 cm
- Protocols and programs for Whole-Body MR Angiography and metastasis detection

SS & DESS

ique Siemens sequences and protocols

DESS (Double Echo Steady State):

- T2/T1-weighted
- Excellent fluid-cartilage differentiation in orthopedic imaging

CISS (Constructive Interference in Steady State):

- Excellent visualization of fine structures such as cranial nerves
- High resolution imaging of inner ear and spine

nced Cardiac

al sequences and scan protocols for MR studies of the heart.
nology - Heart and Vessel Structure and Valve Function

Dark-blood sequences using breath-hold technique
Ventricular Function and Wall Motion
Dynamic CINE TrueFISP imaging of cardiac function with prospective and retrospective ECG triggering, with or without breath-hold technique
Cine imaging with echo sharing for high temporal resolution
Triggered retrogated cine imaging with arrythmia rejection for automatic adjustment of the number of phases to the heart rate
Real-time cine TrueFISP imaging without need for ECG triggering of breath-hold commands
Real-time radial imaging for high speed and high resolution cine studies
Visualization of myocardial contractility using various tagging techniques
Tissue characterization (differentiation of tissues with different T1 values)
Ultra-fast, high SNR sequences for first pass imaging using TrueFISP iPAT and Half Fourier techniques. These protocols provide multi-slice information for the assessment of coronary heart disease (TrueFISP)
Assessment of myocardial viability in breath-hold with single shot IR TrueFISP for delayed enhancement studies
Robust and reproducible contrast between infarct and normal myocardium with phase-sensitive Inversion recovery.
Adjustment of TI is no longer necessary with this technique
Protocols for pediatrics, plaque imaging and stress imaging

onary Imaging

Dedicated sequences for coronary imaging and angiography providing free breathing navigator (1D PACE) and breath hold techniques (2D and 3D Flash and TrueFISP



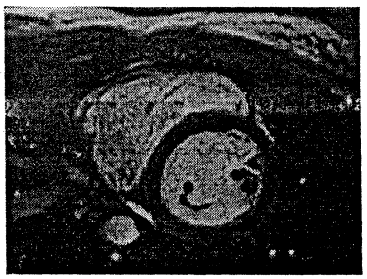

w Quantification

ecial sequences for quantitative flow determination studies

asuring blood/CSF flow non-invasively

quires Physiological Measurement Unit (PMU) option

troGated Flow

- Dynamic representation of temporally changing flow

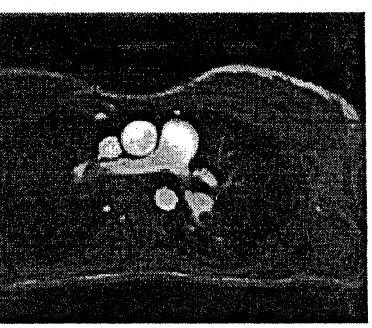
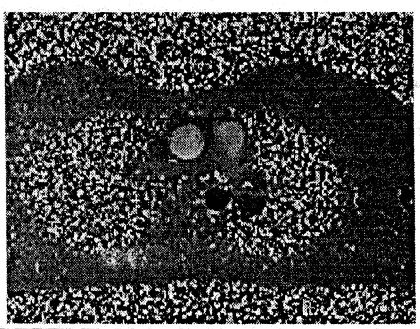

eractive Realtime

equences and hardware for interactive real-time scanning.
ses ultra-fast TrueFISP and other gradient-echo sequences for high
age contrast

eal-time reconstruction of the acquired data

e user can navigate in all planes on-the-fly during data acquisition

- Real-time cardiac examinations
- Real-time interactive slice positioning and slice angulation
- 3D Magellan SpaceMouse included

SE
a-fast sequence providing high-resolution imaging or extremely
rt acquisition times

rid turbo spin echo/gradient echo used primarily for T2-weighted
ging

- Shorter measurement time
- Decreased RF power deposition
- Improved visualization of hemorrhage, due to magnetic susceptibility differences

h resolution imaging of brain and spine

ne DiffusionAutomatic real-time calculation of trace-weighted images
ADC maps with Inline technology. Compatible to single-shot diffusion-
ghted EPI

ne Perfusion
tomatic real-time calculation of
obal Bolus Plot (GBP) and Time-to-
ak map (TTP) with Inline technology

ne Bold Imaging
amination of intrinsic susceptibility changes in different areas of the
in, induced by external stimulation (e.g. motor or visual)

tomatic real-time calculation of z-score (t-test) maps with Inline
hnology, for variable paradigms

- Compatible to single-shot EPI with high susceptibility contrast for fast multi-slice imaging
- ART (Advanced Retrospective Technique) for fully automatic 3D retrospective motion correction, for 6 degrees of freedom (3 translations and 3 rotations)
- Mosaic images for efficient storage and transfer of large data sets
  3D spatial filtering
- Overlay of Inline calculated t-test results on the EPI images

anced Functional Neuro
PACE (Prospective Acquisition CorrEction)

spective motion detection and correction in the volume to
inate motion artifacts during BOLD measurements

- Fully automatic 3D prospective motion correction during data acquisition, for 6 degrees of freedom (3 translations and 3 rotations)
- Motion correction covering the complete 3D volume
- Provides high accuracy
- Substantially reduced motion-related artifacts in t-test calculations
- Significantly increased signal changes in the activated neuronal volume
- Increased functional MRI (fMRI) sensitivity and specificity

Inline fMRI

- Overlay of functional information on 3D dataset during image acquisition

lti-Directional Diffusion-Weighted Imaging (DWI)

- Measurements of multiple diffusion directions and b-values
- Suitable for investigation of anisotropic diffusion in tissue such as calculation of diffusion tensors.
-

Single Voxel Spectroscopy

eamlined for easy push-button operation

S techniques SE and STEAM

ort TEs available
lly automated adjustments including localized shimmering
d adjustment of water suppression pulses
so available: Interactive adjustments and control of
justments
timized protocols for brain applications

l Shift Imaging

ed software package with sequences and protocols for
al Shift Imaging (CSI)

on of the SVS package, offering the same level of user-
ess and automation

D and 3D Chemical Shift Imaging
ybrid CSI with combined Volume selection and Field of View
oV) encoding
hort TEs available (30 ms for SE, 20 ms for STEAM)
utomized shimming of the higher order shimming channels for
timal homogeneity of the larger CSI volumes
eighted acquisition, leading to a reduced examination time
ompared to full k-space coverage while keeping SNR and
patial resolution
uter Volume Suppression
pectral Suppression
rotocols for prostate spectroscopy

Biopsy Software
use *syngo*-based post-processing software helps finding the
ates for needle insertion for biopsy of localization of breast
detected by MR

calculation of the coordinates after clicking the center of the
nd the 0 marker of the breast biopsy device

rintout of working sheet
ulti-lesion calculations

erequisites:

- Breast Biopsy Device
- Loop Flex coil, large

age Filter Software
r noise reduction in MR images and better edge definition

ses high-pass and low-pass filtering and adjusts automatically to the local
age content (adaptive filtering)

ain Benefits:
oise reduction
daptive filtering

pplications:
educes noise in acquired MR images
nproves the visual appearance of the image
nage filtering

his image filtering software uses an adaptive filter from Context
ision that searches for conspicuous structures in the image and then
hecks whether these structures are random or part of other
ructures. It considers local distribution of signal intensity and the
ontinuity of local tissue structures.

ilter strength values from 1-20 can be selected individually. Three
fferent image filter values (smooth, medium, sharp) are individually
orable for frequent use. Single and multiple images or entire series
an be selected together for evaluation. An additional, selectable
indow shows the actual calculation status and provides a preview of
lready filtered images.
rgus Function
utomated tool for cardiac function evaluation

lain Benefits:

Fully automated segmentation of high-contrast TrueFISP cine images
A full set of analyses
- End-diastolic and end-systolic volume
- Ejection fraction, stroke volume and cardiac output
- Cardiac mass
- Ejection and filling rates
- Regional wall thickening calculation

Efficient review of dynamic studies
- Up to 8 series simultaneously in a synchronized movie displayed
- Rapid multi-level sorting

Fast AVI creation
For conferences, presentations and consultation over the internet

us Flow
omated tool for analysis of cerebral spine fluid flow

n Benefits:

Semi-automatic segmentation of through-plane velocity-encoded images
Color-encoded display of velocity in static and movie studies
Quantification of velocity, flow of blood and CSF

us DynamicSignal
ion- of- Interest based analysis of dynamic image intensity
ations

n Benefits:

Semi- automatic detection or manual selection of Regions- of- Interest
Analysis of temporal tissue signal variations (e.g. Peak signal, time- to- peak)

Color output curves and parametric displays
More information about Argus? Go to *syngo* >>

ssel View

eractive analysis of vessel disease using MR or CT angiography
a

in Benefits:

- Clinical protocols for reliable results
- Automatic visualization of vessel trees within the volume of interest
- Automatic visualization and measurement of vessel cross-section in MPR views
- Integrated vessel navigator

VRT - Volume Rendering Technique
in Benefits:

- Fully integrated into the 3D workflow and user interface
- More productive surgical planning and discussion with referring physicians
- Complete visualization modes
  Volume Rendering Technique, Maximum Intensity Projection, Multiplanar Reconstruction or Surface Shaded Display
- Many predefined settings, easily selectable from gallery
- Optimal display quality
  Independent control of color, opacity and shading
- Easy elimination of obstructing anatomy
  3D Object Editor

uro Perfusion Evaluation
edicated task card for quantitative processing of neuro perfusion
ta

ain Benefits:

- Color display of relative Mean Transit Time (relMTT)
- Flexible selection of Arterial Input Function (AIF) for reliable quantification

Planar Imaging, Diffusion imaging, Perfusion and Diffusion or imaging

Single shot and segmented EPI sequences for fast acquisition
Diffusion weighted imaging with b max of 10,000 s/mm2
Single shot EPI for perfusion imaging
Multidirectional Diffusion Weighted (MDDW) imaging for diffusion tensor imaging

) Evaluation
Oxygenation Level Dependent

nvasive MR-technique to detect functionally activated regions of uman brain

ination of intrinsic susceptibility changes in different areas of the induced by external stimulation (e. g. motor or visual)

Benefits:
ed overlay of functional and anatomic data
D

D= Blood Oxygen Level Dependent
roscopy Evaluation

prehensive and user-friendly evaluation of spectroscopy data

Benefits:

Display of spectroscopic data as colored metabolite images or spectral overview maps and overlaid over anatomical images
Protocol driven quantitation for routine use
Flexible algorithms and interactive UI for research use

transferring, exporting and printing of data

COILS

ead Matrix Coil

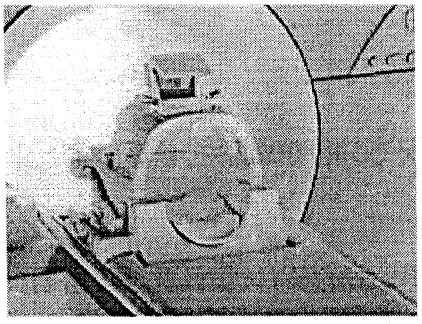

ne multi-element Matrix coil technology is an essential rt supplementing the most innovative Total imaging atrix.

escription:

- 12-element design with 12 integrated preamplifiers, two rings of 6 elements each (i.e. 4 clusters of 3 elements each)
- Upper coil part removable
- Lower coil part may stay on the patient table for most of the examinations
- Smoothly integrated into the patient table for most of the examinations
- Smoothly integrated into the patient table with Neck Matrix coil and Spine Matrix coil
- Open patient-friendly design
- Cushioned head stabilizers (removable)
- No coil tuning
- iPAT-compatible
- Detachable double mirror.
-
-

Applications:

- Head examination
- MR Angiography
- Combined head/neck examination
- TMJ (temporo mandibular joints)
-

e combined with:

leck Matrix coil
pine Matrix coil
ody Matrix coil (up to 4; optional)
A Matrix coil (optional)
ll flexible coils (e.g. CP Flex coil, small, CP Flex coil, large)

Veight: 5 kg
Dimensions: 300 mm x 300 mm x 280 mm (LxWxH)

Matrix Coil

new multi-element Matrix coil technology is an ntial part supplementing the most innovative imaging matrix.

ption:

4-element design with 4 integrated preamplifiers, 2 clusters of 2 elements each
Upper coil part removable
Lower coil part may stay on the patient table for most of the examinations
Operates in an integrated fashion with the Head Matrix coil and Spine Matrix coil, for coverage of the posterior and anterior neck region
No coil tuning
iPAT-compatible

cations:

Cervical Spine
Neck
Larynx/Esophagus
MR Angiography
Mediastinum
Combined head/neck examination

Can be combined with:

- Head Matrix Coil
- Spine Matrix Coil
- Body Matrix Coil (up to 4; optional)
- PA Matrix coil (optional)
- All flexible coils (e.g. CP Flex coils, small, CP Flex coil, large

- Weight: 2.6 kg
- Dimensions: 190 mm x 330 mm x 332 mm (L x W x H)

Spine Matrix Coil

The multi-element Matrix coil technology is an essential part supplementing the most innovative Total imaging matrix.

Description:

- 24-element design with 24 integrated preamplifiers, 8 clusters of 3 elements each
- Smoothly integrated into the patient table and streamlined with Head Matrix coil and Neck Matrix coil
- May remain on the patient table for almost all exams
- No coil tuning
- iPAT-compatible

Applications:

- High resolution imaging of the whole spine
- Various applications in combination with additional coils

Can be combined with:

- Head Matrix Coil
- Neck Matrix Coil

Body Matrix Coil (up to 4; optional)
PA Matrix Coil (optional)
All flexible coils (e.g. CP Flex coils, small, CP Flex coil, large)
Weight: 11 kg; may remain on the patient table for almost all exams
Dimensions: 1185 mm x 485 mm x 33 mm (L x W x H)

Matrix Coil

ew multi-element Matrix coil technology is an essential part ementing the most innovative Total imaging matrix.

ption:

6-element design with 6 integrated preamplifiers, with 2 clusters of 3 elements each
Operates in an integrated fashion with the Spine Matrix coils (2 rings of 6 elements each = 12-element design)
Can be combined with further Body Matrix coils for larger coverage
No coil tuning
iPAT-compatible

cations:

Thorax (incl. Heart)
Abdomen
Pelvis
Hip

be combined with:

Head Matrix coil
Neck Matrix coil
Spine Matrix coil
Additional Body Matrix coils (typically 2 – 3 in total)

ne new multi-element Matrix coil technology is an
sential part supplementing the most innovative
otal imaging matrix.

escription:

- 16-element design with 16 integrated preamplifiers, in 8 CP pairs, i.e. 4 levels with 2 CP elements each
- Operates in an integrated fashion with the Body Matrix coils and Spine Matrix coil and for Whole-Body examinations also with the Head and Neck Matrix coil
- Automatic table feed and active coil switch
- Can be utilized Head and Feet First
- Both legs are independently covered with coil elements, maximizing the coil filling factor and the signal-to-noise ratio
- No coil tuning
- Includes special non-ferro-magnetic coil cart for sage, user-friendly storage
- iPAT-compatible

pplications:

- High-resolution angiography of both legs incl. Pelvis with highest signal-to-noise ratio
- Visualization of the iliac arteries and aorta

an be combined with:

- Head Matrix coil
- Neck Matrix coil
- Spine Matrix coil
- Body Matrix coils (up to 3)
- All flexible coils (e.g. CP Flex coils, small, CP Flex coil, large)
- Weight: 5,75 kg
- Dimension: 970 mm x 300 – 600 mm x 270 mm (L x W x H)

houlder Array Coil

escription:

- 4-coil design with 4 integrated preamplifiers

Two coils are included, one for small and one for large shoulders
For narrow or wide shoulders the coil can be attached at different positions on the base plate
Includes one base plate pad and one head rest for high patient comfort
No coil tuning
iPAT-compatible

ications:

Best visualization of small anatomical structures (e.g. labrum)
Higher SNR and better field homogeneity
Reduced slice thickness and measurement times.

ll Shoulder Array Coil:

Opening: 165 mm
Weight: 1.3 kg

e Shoulder Array Coil:

Opening: 200 mm
Weight: 1.6 kg

Dimension: 445 mm x 490 mm (L x W)
Weight: approx. 5 kg

Extremity Coil

ılarly Polarized no-tune transmit/receive coil for joint
ninations in the region of the lower extremities
cription:

Transmit/receive coil
CP coil with 2 integrated preamplifiers
Upper coil part removable
Holder allows off-center positioning to keep knee or foot which is not under examination in a comfortable position
No coil tuning

lications:

Knee
Ankle
Peripheral MR Angiography

Weight: 6.5 kg
Dimensions: 405 mm x 270 mm x 290 mm (L x W x H)

ıble Loop Array Coil

nsisting of two flexible, anatomically adaptable 7 cm
g coils for simultaneous examination of both TMJs, the
es or the wrist.Including Double Loop Array Holder

scription:

- Circular coil pair with Double- Loop Array Holder
- No coil tuning
- Extra arm rest for wrist imaging
- IPAT-compatible

plications:

- Simultaneous visualization of the left and right TMJs (temporo mandibular joints) with high resolution
- High-resolution imaging of the eye
- High-resolution imaging of the wrist

n be combined with:

- Body Matrix coils
- All flexible coils (e.g. CP Flex coil, small, CP Flex coil, large)
- CP Head Array Coil

- Weight: 1.1 kg

Dimensions: 82 mm x 135 mm x 82 mm (L x W x H)

ad Array Coil

ted coil for head examinations especially for utilization with a tactic frame for therapy planning and for pediatric imaging, e.g. spine.

CP coil design with 2 integrated preamplifiers
Upper coil part removable
Lower coil part usable without upper part
Open patient-friendly design
Highly homogenous illumination
No coil tuning
Cushioned head stabilizers (removable)
Detachable double mirror
Also compatible with MAGNETOM Symphony and Sonata systems
PAT-compatible

cations:

Head examinations
Head examinations with utilization of a stereotactic frame
Pediatric imaging

e combined with:

Body Matrix Coil
All additional flexible coils (e.g. CP Flex coil, small, CP Flex coil, large)
Double Loop Array Coil
Weight: 5.7 kg
Dimensions: 480 mm x 330 mm (L x W)

rature Tx/Rx Head Coil

mit/receive coil for MR proton spectroscopic head nations. It is especially suited for Chemical Shift Imaging (CSI) ingle Voxel Spectroscopy (SVS

CP Send/Receive head coil with integrated preamplifier

- Upper coil part removable
- Open patient-friendly design
- No coil tuning
- Cushioned head stabilizers (removable)
- Detachable double mirror (optional)

plications:

- Head examinations
- High-resolution brain spectroscopy

- Weight: 7 kg
- Dimensions: 400 mm x 360 mm x 360 mm (L x W x H

Flex Coil, large

Flex coils cover all extremities and joints; beneficial for pelvic, spinal pediatric imaging; provide excellent soft tissue contrast, small field of ws and thin slices, cost-effectively.

plications:

- Imaging of large regions such as medium to large shoulder , hip and knee
- MR Angiography
- Abdominal imaging
- Brachial plexus

plications:

- Imaging of large regions such as medium to large shoulder , hip and knee
- MR Angiography
- Abdominal imaging
- Brachial plexus

scription:

- Wrap- around coil made from soft and flexible material provides high patient comfort
- Excellent soft-tissue contrast and delineation of small details

oils are wrapped around the joint and are easily stabilized with elcro straps

ted Panoramic Array™ (IPA)

ptimizes coil positioning and virtually eliminates coil changing mes
p to 4 different coils can be positioned and connected multaneously
p to 16 CP coil elements can be selected simultaneously

cal Data

ircularly polarized Wrap around coil
lo coil tuning
equires Flex Coil Interface
ize: 210mm x 520mm
ircular polarized coil design offers up to 40% higher signal-to-oise than the linear design

ntegrated Panoramic Array

Benefit:

Up to 4 different coils can be positioned and connected simultaneously
Up to 16 CP coils from up to 4 coils can be selected simultaneously via software
No coil changing with multi-exam studies
CP Spine and CP Head Array Coil are integrated into the patient table top
Remain on the table for approx. 95% of all examinations
All IPA coils are time saving 'no tune' coils
Low-noise preamplifiers

IPA Coil Combination

Up to 4 different coils can be positioned and connected simultaneously

Up to 16 coil elements from up to 4 IPA coils can be selected

simultaneously by soft buttons via ergonomic syngo MR user interface at the MR console

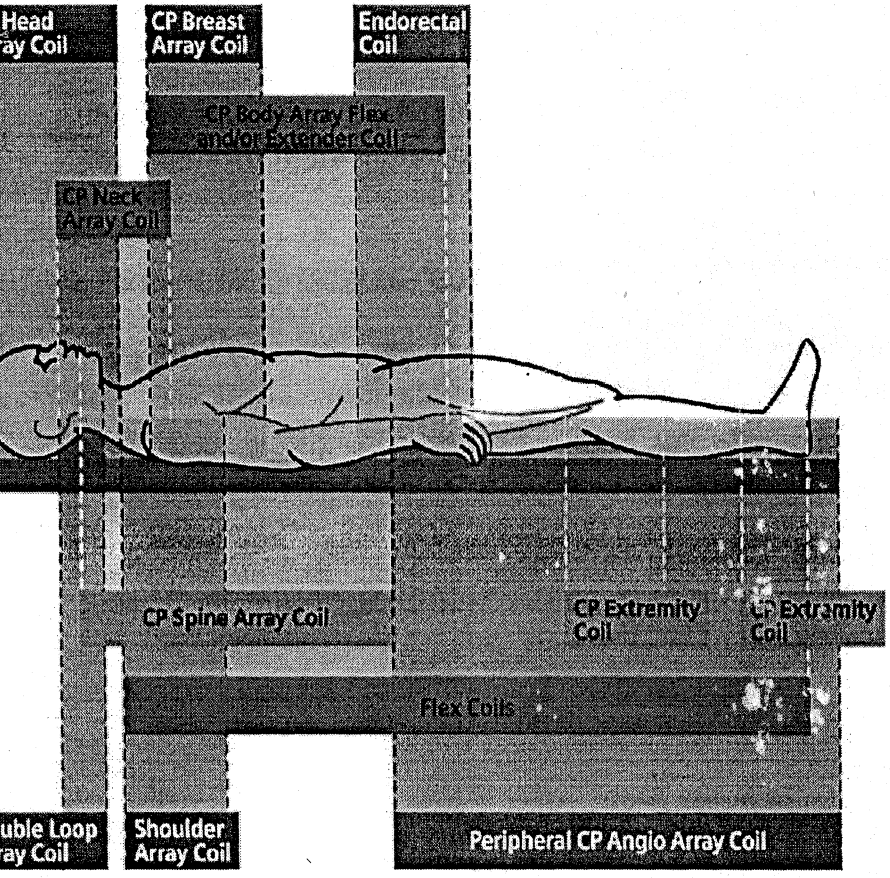

A Coil Combination Matrix MAGNETOM Sonata

ossible combinations
ot necessarily simultaneously)

1. 2nd Flex Coil Interface connectable
2. If CP Spine Array is not used

ombination of up to 4 IPA coils possible

xamples:

- Head+ Neck+ Spine
- Spine+ Body+ Flex
- Peripheral CP Angio + Body Array Flex + Body Array Extender + CP Spine incl. large FOV- Adapter
- Spine+ Body+ Endorectal

c.

ex Coil, large

linear polarized loop coil for shoulder and extremity examinations.
provides excellent soft tissue contrast with small field of views

ations:

xamination of upper or lower extremities (e.g. shoulder, axilla, nee and ankle)
igh soft tissue contrast

ption:

lexible circular coil
he design allows easy access to joints for patients with limited nobility

cal Data

arge, flexible circular coil
lo coil tuning
Requires Flex Coil Interface
Diameter: 190mm, 7.5in

Flex Coil, small

e linear polarized loop coil for examinations of very small res near the surface. The coil provides excellent soft tissue st with small field of views.

ations:

Examination of small structures near the surface (e.g. joints of ngers and toes, wrist, skin, Temporo Mandibular Joints TMJ High soft tissue contrast

ption:

Small circular coil

- The Flex Loop Coil is placed directly on the joint and easily stabilized with Velcro straps

chnical Data

- Small, flexible circular coil
- Easy positioning
- No coil tuning
- Requires Flex Coil Interface
- Diameter: 40mm, 1.6in

ndorectal Coil and Interface

ansrectal surface coils for non-invasive evaluation of pelvic disease.
gh soft tissue contrast to show infiltration and extension of lesion.
nproved treatment planning, evaluation of abnormalities, and staging
malignancies possible

pplications:

- Excellent visualization of the prostate, colon, rectum and cervix without the risk of invasive procedures
- Non- invasive preoperative diagnostic evaluation and treatment planning
- Accurate and reproducible image quality as the coil is positioned inside the patient next to the structure or lesion to be imaged

escription:

- Interface device for connecting either the prostate, colon or cervix receive coil
- The endo coil is plugged into the endo interface which is then plugged into the Flex Coil Interface
- Can be used simultaneously with the CP Spine Array and/ or CP Body Array Flex Coil

ted Panoramic Array™ (IPA)

ptimizes coil positioning and virtually eliminates coil changing
mes
p to 4 different coils can be positioned and connected
multaneously
p to 16 CP coil elements can be selected simultaneously

nation of Endorectal Coil, CP Body Array Flex and CP Spine
Coil

Non-invasive, high resolution imaging of prostate, rectum, colon
nd cervix

cal Data

nterface device to connect; prostate, colorectal, cervix coil
robe
The endo coil is plugged into the endo interface which is then
lugged into the Flex Coil Interface.
Requires Flex Coil Interface
No coil tuning
Field of view 8 to 20 cm
Easily expandable with CP Body Array Flex and CP Spine
Array Coil
Additional probes have to be ordered from MEDRAD Inc. with
he ordering name MR Innervu Disposable Prostate Endorectal
Coil, Colon Endorectal Coil, Cervix Endorectal Coil

le and Plasma Screen.

tor console :
t is multifunctional with its own dedicated computer archive
e system and data base. It supports scan, display, archiving,
, utilities and networking functions. Intercom control provides
unication with the patient.

a Screen:

hen we touch the soft key on the screen, breaking up of an infrared am which sends the commands to the system. The console is 8.5 x inches in size, touch sensitive screen by which the operator can eract with the system. The screen is divided into two as scan reen and image processor(IP).

LSMA SCREEN

inches diagonal monochrome monitor with 512 x 512 pixel display. lse Sequences available.

Optiopns:
SE, GRE, IR, TSE, FMPIR, FLASH, PISIF

Options :
FLASH, PISIF, GRE.CISS,MP-RAGE

ascular Options :
2D & 3D PC,
2D & 3D TOF,
3D Vascular TOF SPGR (MOTSA).

nage enhancement Optons.

ow compensation (FC), respiratory compensation (RC), ECG & ulse gating, graphic Rx (GRx), Phase over sampling (POS), fat water suppression (stF/W), phase offset multi planar (POMP), ariable band width (VBW), image intensity correction (IIC)< xtended dynamic range (EDR), contigous section (CS), classic (CL), quare pixel (SqP), sequential (Sq), magnetisation transfer (MT), ulti phase ramped pulse direction (SPF).

ontiguous slices :

educes chemical shift artifacts, reduces cross talk and provides flow ompensation option with slice thickness below 3mm.

xtended dynamic range:

2-bit data processing, instead of the conventional 16 bits, to SNR, in some applications. It is compatible with virtually all quences and imaging options.

E to minimize the motion artifact in body imaging and fast ating to acquire multiple phases cardiac cycle at single slice This option provides high-resolution images with short scan pending upon the echo train length.

r suppression :

s signal from fat or water. Uses a frequency – selective n pulse to suppress signal with in the imaging volume. This ce the chemical shift artifact .

npensation :

motion artifacts created by the flow of slow moving blood This will cause strain on the gradient hardware.

al Echo (Short Echo)

nore slices in single echo scan and increase T1WI, decreases c susceptibility and decreases flow artifact.

(Number of excitations)

es the indication of how many times signals is averaged oing the fourier transformation. Fractional nex allow to maging time but with decrease in SNR.

CL)

s the variance between muscle and fat signals. Classic are annotated CL.

Equilibrium Preparation (DE prepped)

A fast grad option that uses 90/180/90- degree pulse series where the longer the time between the 180 –degree pulse and the last 90-degree pulse, the more T2 weighted is the image.
Graphic Rx (GRx)

Prescribe the imaging locations by graphically.

Image intensity correction

Activates a filtering process to minimize excessive brightness of anatomy close to surface coil. IIC minimize the fat signal when using extremity coil. This is equivalent to the TGC of ultra sound imaging. IIC increase the image reconstruction time by adding 1.7 seconds to the first echo display and 1 second to subsequent echoes.

Magnetization Transfer (MT).

Improves contrast by saturating the short T2 component of tissue, such as grey white matter and skeletal muscle. Magnetization enhances inferior to superior flow.

Phase Over Sampling

Prevent wrap around(aliasing) artifacts and in small FOVs. Phase wrap takes "close-up", high resolution images of FOVs smaller than available anatomy. NPW doubles the FOV and image acquisition matrix in phase direction and during data reconstruction , discards data from outside the FOV.

Phase Offset Multi-Planar (POMP).

Acquires twice the number of allowable slices in a given TR without increasing scan time. Designed for rapid coverage of anatomy including the head, c-spine, and L-spine, particularly T2 axis. POMP excites two adjacent slices at once, with a pulse combining two frequency bands and reconstructs as two separate images.

ratory Compensation (RC).

ces the ghosting artifacts from respiratory motion in chest or
nen and reduces motion caused by respiration in flow analysis .
es chest wall motion to identify the best time for motion
ed imaging. The bellow is positioned exactly over the imaging
get better triggering.

ation parameters (SAT).

s addition RF pulse that chemically or spatially saturate
ied structures. Sat pulses helps to minimize flow artifacts,
e residual signal, suppress phase encoding ghosts caused by
elated enhancement.

oncatenated.

ventional studies, moves slice select pulses along with the
sitions and saturating tissues before acquiring each slice.

ping of phase and frequency.

allow to change the phase and frequency direction of an
sition.

ble Bandwidth (VB).

s the operator to select the receiving frequency range of the
l. Decrease band increases SNR , decrease the number of
ng slice.

ential (SQ).

ires all the images at the first slice before moving to the next
on. With sequential, total number of acquisition equals to the
er of slices.

re Pixel(SqP).

nits scans with an FOV scaled by the ratio of phase to frequency
ts in the phase direction, resulting in a square pixel resolution at
ver scan time.
e thickness, Spacing, FOV and Excitation.

es :
2D : 3 –20 mm in 0.7 increments.
3D : 0.7 – 5 mm with volume of 28, 60 and 124,
iguous slices.

cing : Can be varied with an increment of 0.0mm.

/ :
Head coil : 8 – 28 cm in 1cm increments.
Body coil : 8 – 48 cm in 1cm increments.
(Variable FOV and off centre FOV are available.)
Extremity coil : 8 – 18 cm.
QuardT/L coil : 30cm. S/I direction.
Post neck coil : 24cm. S/I direction.

X :
ctional NEXs : 0.5, 0.75, and 1.5 (1.5 NEX is only available with
W and POMP & 0.5 NEX is not available with GRE, SPGR,
FP and Fast sequences.)

Multiple NEXs : 1 – 150.

quisition matrix.

Frequency Matrix : 256 and 512.
Phase Matrix : 128 – 512 in steps of 32.

ed of pre Scanning :

timizes the image quality by providing shim accuracy (Ensure
cise flip angle, optimize receiver dynamic range).
ne the frequency you are interested in, by adjusting the centre of
frequency. It ensure the optimal excitation of proton.
s the volume / slice at just right level by fine tuning the transmit
d receive gain or amplification.
ygen Monitoring :

Oxygen monitor gives alarm when oxygen level falls below
%.
rking : Oxygen gas in the space surrounding the cell (oxygen
ection transducer cell) diffuses through a Teflon membrane and
ches on the surface of the cathode, corresponding oxidation
urs at the anode. Electrical current generated is proportional to
oxygen. Cell output is limited by the rate at which the oxygen
ers the cell and by the amount of anode material stored within the
. The resulting cell output drives the meter circuit of the oxygen
nitor.
erating temperature : 32 – 131 °F.
l Electrolyte used : Potassium Hydroxide in a barrier bag.
ench.
expected loss of superconductivity in a superconducting magnet
t causes heating and very rapid vaporization of the cryogen such
iquid Helium. This can cause damage to the magnet and can
ce oxygen out of the scanner room potentially causing anoxic
ndition.

d Head and Compressor (Chiller).

d head use simple compression-expansion process. Helium is
ed for compression and compressed heat is removed by air cooled
at exchanger and He gas is allow to expand. The flow of low and
h pressure He is controlled by control valve located at the base of
d head. The control valve is rotated clockwise by 72 rpm by an
ctronic synchronized stepping motor. As the control valve rotates
the top of the control disc, Helium in the valve align with different
es in the disc. When one set of holes are aligned, high pressure
flows in to the expansion chamber. As the valve rotates this valve
sealed and another set of holes align, this second set aligned holes
ms a channel which allows the He in the chamber to expand, cool
d escape. The volume of expansion chamber is also controlled by
other control valve. A relief valve pressure from cold head if it is
posed to hot ambient temperature when shut off. This relief valve
o protect the cold head from internal damage if the flux lines are
moved while the helium inside the cold head is expanding. The
ium connection have self sealing coupling which keep the cold
ad under pressure and gas line is removed.

d head is a two stage cryo-refrigerator. Its first stage produces a p. 40 – 60K and its second stage produces a temp. between 10 – K. The available cold head capacity is 40 Watt for first stage and 2 t for second stage. The cold head require compressor (chiller) to rate. The compressor provides power and high pressure helium d to produce low temp. in the cold head. Helium gas circulated ween cold head and compressor through flux lines. Cold head is rted and stopped by start and stop button situated in front of mpressor. Compressor have a guage to monitor the helium ssure. The pressure should be between 305 – 334 psi (21 – bar) during operation and 218 – 232psi (15 – 16bar) when mpressor is not operated. Cooling water temperature is between – 80°F and circulating with a rate of 3.5 litter per minute. The pH of oling water is between 6 – 8.

* * * * * * * * * * *

ain Routine **Rf Coil-Quad Head**
il

naging arameters	Views				
	SAGITTAL. Loc	Axial T1	Axail T2	Coronal T1	Coronal T2
ulse Seqs	SE	SE	SE/V	SE	SE/V
-	SAGITAL	OBLIQUE	OBLIQUE	OBLIQUE	OBLIQUE
D	2D	2D	2D	2D	2D
SD	-	-	-	-	-

	NONE	GRx	VB, EDR, FC,GRx	GRx	VB,EDR, FC, GRx
	380	450	2000	450	2000
	16	16	30/90	16	30/90
	-	-	-	-	-
)	-	-	-	-	-
	24	22	22	22	22
NES	5	5	5	5	5
E	3	3	3	3	3
TION	13	16	16/16	16	16/16
X	256X192	256X192	256X192	256X192	256X192
	2	2	1	2	1
UENC	S/I	NOT SWAPP ED	NOT SWAPP ED	NOT SWAPP ED	NOT SWAPP ED
	16	16	16/3.20	16	16/3.20
	2.29	2.10	5.12	2.10	5.12

ituitary **Rf Coil-Quad Head Coil**

NG MET	VIEWS				
	Sag. Loc	Axial T1	Axail T2	Coronal T1 Thin	Axial T1 Thin
Seqs	SE	SE	SE/V	SE	SE
	SAGITA L	OBLIQU E	OBLIQU E	OBLIQU E	OBLIQU E
	2D	2D	2D	2D	2D
	-	-	-	-	-

ptions	NONE	GRx	VB, EDR, FC,GRx	CS,GRx	CS, GRx
R	360	480	2000	300	300
E	Min.Full	Min.Full	30/90	Min.Full	Min.Full
	-	-	-	-	-
LIP (^{0})	-	-	-	-	-
OV	24X24	22X16	22X16	22X16	22X16
HICKNES	5	5	5	3	3
ITER PACE	3	3	3	0	0
OCATION	13	16	16/16	10	10
ATRIX	256X192	256X192	256X192	256X192	256X192
EX	2	2	1	2	2
REQUEN Y	S/I	NOT SWAPPED	NOT SWAPPED	NOT SWAPPED	NOT SWAPPED
BW / BW2	16	16	16/3.20	16	16

rain Epilepsy **Rf Coil-Quad Head Coil**

MAGIN ARAM TERS	Views						
	Axial Loc	Coronal Loc	Sag.T1	Axial T1	Axail T2	Coronal T2	Coronal T1
Pulse Seqs	SE	SE	SE	SE	SE/V	SE	FLASH 3D

	AXIAL	CORONAL	OBLIQUE	OBLIQUE	OBLIQUE	OBLIQUE	CORONAL
	2D	2D	2D	2D	2D	2D	3D
	-	-	-	-	-	-	-
s	NONE	GRx	GRx	GRx	VB, EDR, FC,GRx	VB,EDRFC,GRx	FC, GRx, NPW
	300	300	400	480	2000	2000	36
	Min.Full	Min.Full	Min.Full	Min.Full	30/90	30/90	Min.Full
		-	-	-	-	-	45
N	22X16	22X16	24X24	22X16	22X16	22X16	16X16
E	5	5	5	5	5	4	1.5
TI	3	5	3	3	3	2	0
IX	10	10	13	16	16/16	16/16	60
	256X192	256X192	256X192	256X192	256X192	256X192	256X128
UE	0.75	0.75	2	2	1	1	2
	A/P	S/I	NOT SWAPPED	NOT SWAPPED	NOT SWAPPED	NOT SWAPPED	S/I
	16	16	16	16	16/3.20	16/3.20	16
	0.38	0.38	2.37	2.22	5.12	5.12	9.53

Spine

Rf Coil-Post Neck Coil

MAGING ARAME ERS	Views					
	Coron al Loc	Sag.T1	Sag.T2 *	Axial T1	Axail T2*	Axial 3D Gradien t
ulse eqs	SE	SE	GRE	SE	GRE	GRE
L	CORO NAL	SAGGI TAL/O BLIQU E	SAGGI TAL/O BLIQU E	AXIAL/ OBLIQ UE	AXIAL/ OBLIQ UE	AXIAL
ID	2D	2D	2D	2D	2D	3D
SD	-	-	-	-	-	-
ptions	NPW	CS,GR x	FC,GR x	CS,GR x	FC,GR x	FC,GRx
R	450	320	300	380	340	33
E	Min.Ful l	16	Min.Ful l	19	Min.Ful l	Min.Full
LIP (^{0})		-	12	-	16	9
OV	32X32	24X18	24X18	18X13	18X13	18X13
HICKNES S	5	4	4	5	5	1.5
NTER SPACE	3	1	1	0	0	0
OCATIO NS	11	9	9	11	11	28

IX	256X128	256X192	256X192	256X192	256X192	256X192
	1	4	4	4	4	2
UE	S/I	S/I	S/I	NOT SWAPPED	NOT SWAPPED	R/L
	32	16	16	16	16	16
	1.10	3.08	2.56	3.42	3.19	5.08

ACIC SPINE

Coil-Quad T/L Coil

atient lies supine on the examination couch with the coil
ng from the top of the shoulders to the lower costal margin to
the total coverage of the total thoracic spine and conus (Q/D,
). The patient is positioned so that the longitudinal alignmrnt
s in the midline and the horizontal alignment light passes
n the level of the thoracic vertebra

i T2 localizer
Slices are prescribed from on either side of the longitudinal
ent light and left borders of the vertebrae. The area from the
f the skull to the conus is included (Body coil). As the first
l vertebrae is visualized, the offset allows easy assessment of
ral levels and easy placement of pre saturation pulses
al T2 Localizer
Slices are prescribed relative to the vertical alignment light,
osterior aspect of spinous process to anterior border of the
ral bodies. The area from C7- conus is included
l T1
Slices are prescribed from right to left borders of the vertebrae
ravertebral areas if needed. The area from C7-conua is
ed

nal sequences

Post contrast sag. T1& Axial T1 fat sat (If needed –bone and
rd tumors, infectious diseases M S plaques , metastatic diseases)
IR – For metastatic diseases of vertebral bodies

NG ME	Views						
	Sag.Loca Body Coil	Cor.Loc	Sag.T1	**Sag.T2FSE**	**Axial T1**	**Axail T2 FSE**	**Axial 3D Gradient**
	SE	SE	SE	SE	SE	SE	FLASH 3D
E	SAGITTAL	CORONAL	SAGGITAL/OBLIQUE	SAGGITAL/OBLIQUE	AXIAL/OBLIQUE	AXIAL/OBLIQUE	AXIAL
	2D	2D	2D	2D	2D	2D	3D
tion	-	-	Ant.Sat		Ant.Sat	-	-
s	RC.CS	CS,GRx	FC/VB/ED/FAST	RC, GRx FC,NPW	RC,NPW GRx	FAST/FC/VB/ED/NW	FC,NPW, GRx
	200	260	340	2000	400	3000	38
	Min.Full	Min.Full	Minimum	108	Min.Full	108	Min.Full
	48x48	32	32	28	18	18	18X18
NE	5	4	4	4	7	7	2
E	0	2	0	0	2	2	-
TIO	7	11	9	9	11	11	28
IX	512x128	256X128	256X192	256X192	256X192	256X192	256X192
	2	0.75	4	4	4	4	1.5
UE	S/I	S/I	A/P	S/I	SWAP-PED	SWAP-PED	A/P
2	16	16	16	16	16	16	16
	1.16	0.30	4.11	2.3	5.28	3	5.54

MBO SACRAL SPINE

f Coil-Quad T/L Coil

tient lies supine on the examination couch with their knees flexed
er a foam pad, for comfort and to flatten the lumbar curve so that
ne lies nearer to the coil. The coil (Q/D /T/L) Should extend from
e xiphisternum to the bottom of the sacrum for adequate coverage
the lumbar spine. The patient lies so that the longitudinal alignment
nt lies in the midline and the horizontal alignment light passes
ough the lower costal margin

OUTINE SEQUENCES INCLUDE

Coronal T1 Localizer
ces are prescribed from the posterior aspect of the vertebtral
lumn to the anterior aspect of the vertebral bodies. The area from
e conus to the sacrum is included

&3 Sagital Spin Echo T1 &T2
e slices are prescribed from right to left borders of the vertebral
dies (If needed paravertebral area is included)

&5 Axial Spin Echo T1 & Axial T2 TSE
ces are prescribed parallel to the conus, vertebral bodies, and disc
aces Continous multiple slices are obtained at L4-L5 & L5-S1

dditional sequences

ost contrast Sagittal.Axial & Coronal T1 fat sat . (if indicated
rtebral body or cord tumours, fragment discs, post operative IVDP,
etastatic disease etc.
D Gredient Sagittal & Axial across the level of L3-S1
ronal SE/FSE T1 for some cord syndrome

UMBOSACRAL SPINE

G ET	Views					
	Coronal Loc	**Sag.T1**	**Sag.T2 TSE**	Axial T1	**Axail T2TSE**	**Axial 3D Gradient**
	SE	SE	SE	SE	SE	FLASH
	CORONAL	SAGGITAL/OBLIQUE	SAGGITAL/OBLIQUE	AXIAL/ OBLIQUE	AXIAL/ OBLIQUE	AXIAL
	2D	2D	2D	2D	2D	3D
	-	-	-	-	-	-
s	None	RC,CS, GRx	RC, FC,/VB GRx/ED	RC,NP W GRx	RC/FC /FAST/ VB/ED	FC,NP W, GRx
	400	300	3000	400	3000	38
	Min.Full	16	108	18	108	Min.Full
		-	-	-	-	-
		-		-		
	32X32	28X28	28X18	18X18	18X18	18X18
NES	5	5	5	5	5	2
	3	0	0	5	5	-
ION	11	9	9	11	11	28
X	256X192	256X192	256X192	256X192	256X192	256X192
	0.75	4	4	4	4	1.5
EN	S/I	A/P	S/I	SWAPPED	SWAPPED	A/P
	16	16	16	16	16	16

Joint
Coil- Body Coil

GING RAMET S	Views					
	Coron al Loc	Axial T1	Axail T2	Coronal T1	Coronal T2	Sag.T1
se Seqs	SE	SE	GRE	SE	GRE	SE
NE	CORO NAL	AXIA L/OB LIQU E	AXIAL/ OBLIQ UE	CORON AL /OBLIQ UE	CORON AL /OBLIQ UE	SAGITAL / OBLIQU E
DE	2D	2D	2D	2D	2D	2D
D	-	-	-	-	-	-
ions	None	CS, GRx, NPW	FC, GRx, NPW	CS,GRx	FC,GRx	CS, GRx
	400	420	350	360	250	350
	16	16	16	18	Min.Full	Min.Full
	-	-	-	-	-	-
P (^{0})	-	-	15	-	15	-
V	42	42	42	40	40	38
ICKNES	5	5	5	5	5	5
TER ACE	3	1	1	1	1	1.5
CATION	14	14	14	11	10	11
TRIX	256X1 92	256X 192	256X1 92	256X19 2	256X19 2	256X192
X	0.75	1	2	1	2	1

QUEN	S/I	R/L	R/L	NOT SWAPPED	NOT SWAPPED	NOT SWAPPED
/2	16	16	16	16	16	16
	1.04	1.34	1.30	1.16	1.36	1.11

E JOINT
oil - Extremity Coil

The patient lies supine with the knee relaxed, slightly flexed
on with in the coil (Extr. Knee coil). The knee is immobilized with
The patient is positioned so that the longitudinal alignment light
long the midline of the leg under examination. The horizontal
passes through the center of the coil which correspond to the
border of the patella
ial T2*GRE-Localizer

as a localizer. If the knee is not at iso center the FOV is offset so
he knee is in the middle of the image. Coronal and Sagittal
zers may also be used
With the axial localizer the slice in which the patella is clearly
onstrated is chosen to prescribe the following sequences

Coronal SE T1&TSE T2/PD

s are prescribed from the femoral condyles posteriorly to the
ior patella and oriented parallel to the posterior surface of the
ral condyles

Sagittal SE T1&TSE T2/ PD (fat sat)

s are prescribed from the lateral side of the knee

	18	19	18	Min.Full/ 18	10	18	30/90
	-	-	-	170-STIR	-	-	-
P (^{0})	-	22	-	-	20	-	-
V	16	16	16	16	16	16	16
CKNS	5	5	5	5	5	3	5
ER ACE	0	0	0	0	0	0	0
CATIS	15	14	14	14	20	10	16
TRI	256X224	256X192	256X256	256X224	256X192	256X192	256X256
X	1	1.5	1	1	1	1	1
EQUCY	R/L	NOT SWAPPED	NOT SWAPPED	NOT SWAPPED	NOT SWAPPED	NOT SWAPPED	R/L
W / W2 lz)	16	16	16	16	16	16	16
IE	2.17	2.53	2.24	5.12/2.44	2.10	2.22	5.2

r Cruciate ligament : Obl/Gre – 20o – 300/19 – 16x16 – 3/0-:
Nex =>

Oblique sag T1

display of the anterior Cruciate ligament is essential for trauma
pected joint damage . The ligament is best seen in oblique
l scans oriented to the ligament .Slices are prescribed from the
to the medial collateral ligament and aligned parallel to the
r Cruciate ligament which runs at an angle 5-10°
onal sequences

al GRE T2*

JOINT **KNEE COIL**

N M S	Views						
	Axial Loc	**Coronal T2***	**Cor.T1**	**Cor. T2-FSE/STIR**	Sag.GRE	**Sag.T1**	**Sag.T2**
	SE	GRE	SE	SE/FSE	GRE	SE	SE
E	AXIAL	CORONAL /OBLIQUE	CORONAL /OBLIQUE	OBLIQUE	SAG/ OBLIQUE	OBLIQUE	SAGITTAL /OBLIQUE
E	2D	2D	2D	2D	2D	2D	2D
	-	-	-	FAT-FSE	-	-	-
ns	NPW, CS	NPW,FCGRx,	NPW, CS, GRx,	VB,EDR, NPQ,GRx	NPW, GRx	NPW, CS, GRx	FC, EDR, VB,NPW,GRx ,CS
	540	440	500	2000/4500	440	640	2000

EART

Coil - Body Coil

tient positioning

The patient lies supine on the couch with respiratory mpensation bellows and ECG gating leads attached . The patient is sitioned so that the longitudinal alignment light lies in the midline d the horizontal alignment light passes through the 4th Thoracic rtebra

ARDIAC GATING

Cardiac gating uses the electrical signal detected by the leads ced on to the patient's chest to trigger each RF excitation pulse .In s way each image is always acquired at the same phase of the rdiac cycle so phase mismapping from cardiac motion is reduced . e correct placement of leads is very important to optimize the age quality

ad placement

There are usually four leads that are color coded for easy use. ads can be placed either anteriorly or posteriorly. Usually anterior acement is done it is simpler and easy to assess the landmark

The white and red leads are placed across the heart as the ltage difference between the two produces the ECG trace

The green lead is positioned as close, but not touching the red acing as the ground

The black lead is placed right upper chest below the clavicle

ROUTINE SEQUENCES

oronal Spin Echo T1 localizer

Slices are prescribed relative to the vertical alignment light from e posterior chest muscle to the sternum

3,4 Axial spin echo T1, T2/PD&Obloque

ices prescribed from inferior border of the heart to the arch of the rta

Sagittal oblique SE T1

elect an image that demonstrate ascending and descending aorta. ices are angled through the ascending aorta and prescribed from e lateral edge of the vessel to the other

dditional sequences include

Oblique cine GRE T2*

Used to assess cardiac function. Two chambers are best strated on sagittal/ oblique view, four chambers in the coronal/ plane.

T

ING AMET	Views			
	Coronal T1	**Oblique Axial**	**Axial T1**	**Sagittal T1**
	SE	SE	SE	SE
E	CORONAL	OBLIQUE	AXIAL / OBLIQUE	SAGITTAL
E	2D	2D	2D	2D
	-	S/I & A/P	S/I & A/P	R/L & A/P
ns	RC, Gating	CS,NPW, EDR,VB GRx, RC, Gating	RC,Gating ,NPW CS, GRx,	RC,Gating. CS,GRx NPW
	1 RR	1 RR	1 RR	1RR
	Min.Full	20	Minimum	Minimum
	-	-	-	-
(°)	-	-	-	-
	36	36	36	36
KNES	10	7	10	10
R CE	3	3	2.5	3
ATION	23	11	12	12

IATRIX	256X128	256X128	256X128	256X128
IEX	4	4	4	4
REQUEN CY	S/I	NOT SWAPPED	R/L	S/I
RBW / RBW2 KHz)	16	16	16	16
TIME	8.54	8.54	8.54	8.54

bdomen
f Coil - Body Coil

MAGING PARAME TERS	Views					
	Corona l Loc	**Axial T1**	**Axial T2**	**Sagitta l T1**	**Coron al T1**	**Axial Breat h Hold**
Pulse Seqs	SE	SE	SE	SE	SE	FLAS H 3D
PLANE	CORO NAL	AXIAL /OBLI QUE	AXIAL /OBLIQ UE	SAGIT TAL /OBLIQ UE	CORO NAL /OBLI QUE	AXIAL
MODE	2D	2D	2D	2D	2D	2D
PSD	MEMP	MEM P	MEMP	MEMP	MEMP	MEMP

ons	NoneSQ	NPW, RC, GRx,	FC, GRx, EDR,RC,NPW VB	RC,GRx	RC,GRx	SEQ, RC, FC, GRx
	400	400	2000	400	400	30
	18	16	30/90	18	18	Min.Full
	-	-	-	-	-	-
(°)	-	-	-	-	-	45
	40	42	42	38	40	42
CKNE	5	10	10	10	10	5
ER CE	3	5	5	5	5	5
ATIO	14	13	16	12	12	1
TRIX	256X192	256X192	256X192	256X192	256X192	256X256
	0.75	4	1	4	4	1
QUE	S/I	R/L	R/L	S/I	S/I	R/L

GING AMETE	Views	
	2D PC	**3D PC**
e Seqs	Vascular PC	Vascular PC
NE	SAGITTAL , AXIAL , CORONAL	SAGITTAL , AXIAL , CORONAL

DE	2D	3D
	Vascular Options	
rojection ges	**Collapse -2**	Collapse -19
quisition ction	**All**	All
dditional ges	**Magnitude**	Magnitude
ow on- ction Time	**Complex Difference**	Phase Difference
city	**10-70cm/sec**	10-70cm/sec
ons	FC,GRx, SEQ	FC,GRx,
	24	33
	8.6	6.9
	-	-
P (^{0})	30	30
V	22X22	22X16
CKNESS	80	1.5
ER ACE	0	0
CATIONS	1	60
TRIX	256X192	256X128
X	8	1
EQUENCY	S/I	A/P
W / RBW2 z)	16	16

	1.51	13.32

: MRA **RF Coil - Head Coil**

MAGING ARAMET RS	Views		
	2D TOF	**3D TOF**	**3D MOTSA**
ulse eqs	Vascular TOF SPGR	Vascular TOF	Vascular TOF SPGR
LANE	SAGITTAL , AXIAL , CORONAL	SAGITTAL , AXIAL , CORONAL	AXIAL
ODE	2D	3D	3D Multiple Slab
Vascular Options			
rojection mages	**Collapse -19**	Collapse -19	Collapse -19
.Ramp ulse	-	S→I or I→S	S→I or I→S
ptions	FC,GRx, SEQ	FC,GRx,	FC, SQP, EDR, VB, GRx,MT
R	46	33	56
E	Min.Full	6.9	6.4
I	-	-	-

FLIP (^{0})	40	30	30
FOV	22X22	22X16	22X16
THICKNESS	1.5	1.5	1.5
LOCATIONS/SLAB Overlap	-	-	32 33%
LOCATIONS	120	60	SLAB : 3
MATRIX	256X128	256X128	256X192
NEX	2	2	1
FREQUENCY	R/L	A/P	A/P
RBW / RBW2 (KHz)	16	16	16
TIME	9.02	9.04	15 43

terial & Venous flow can be obtained by giving appropriate
t. Pulse (S or I)
rta : Gd enhanced MRA **RF Coil - Body Coil**

IMAGING PARAMETERS	Views		
	Coronal T1 Localiser	**Sagittal 40ml Gd**	**Coronal 40ml Gd**
Pulse Seqs	SE	Vascular TOF SPGR	Vascular TOF SPGR
PLANE	CORONAL	SAGITTAL	CORONAL
MODE	2D	3D	3D

cular ions	-	Ramp Pulse: R/L	Ramp Pulse: R/L
ions	RC,Gating,GRx	GRx,	GRx
	-	27	27
	Min.Full	Min.Full	Min.Full
ing	ECG/PULSE	-	-
P (^{0})	-	30	30
V	40	36	36
CKNE	10	2.5	2.5
er ace	3	0	0
CATIO	23	60 +19 Collapsed	60 +19 Collapsed
TRIX	256X128	256X192	256X192
X	4	1	1
EQUEN	S/I	S/I	S/I
W / W2 Hz)	16	16	16
ME	8.54	5.35	5.35

Angiogram

il - Body Coil

PC MRA is the technique of choicein spine is done
ferent flow velocities

IMAGING PARAMETERS	Views	
	2D PC	**2D PC**
Pulse Seqs	Vascular PC	Vascular PC
PLANE	CORONAL	SAGITTAL
MODE	2D	2D
Vascular Options		
1. Projection Images	**Collapse**	Collapse
2.Acquisition Flow Direction	**All**	All
3. Additional Images	**Magnitude**	Magnitude
4.Flow Recon-struction Time	**Complex Difference**	Complex Difference
5.Velocity	**6-20 cm/sec**	6-20/sec
Options	FC,GRx,NPW	FC,GRx,NPW
TR	70	70
TE	11.20	11.20
TI	-	-
FLIP (^{0})	30	30
FOV	30	30
THICKNESS	15	30
INTER SPACE	0	0
LOCATIONS	1	1
MATRIX	256X192	256X192

NEX	10	10
FREQUENC Y	S/I	S/I
RBW / RBW2 (KHz)	16	16
TIME	8.58	8.58

Vol. Of IV. Gadolinium contrast 2-4ml is given prior to o.

Myelogram
oil – Quad T/L Coil
Heavily weighted FSE T2

IMAGING PARAMETERS	Views	
	SAGITTAL	**CORONAL**
Pulse Seqs	FSE	FSE
PLANE	SAGITTAL /OBLIQUE	CORONAL / OBLIQUE
MODE	2D	2D
1. Projection Images	**Collapse**	Collapse
2.Acquisition Flow Direction	**All**	All
3. Additional Images	**Magnitude**	Magnitude
4.Flow Recon-struction Time	**Complex Difference**	Complex Difference

Options	FAST,FC,GRx,NPW, EDR,VD	FAST,FC,GRx,NPW,ED R,VD
User's CV : FSE Optimisation	0	0
TR	10000	10000
Eff.TE	300	300
ETL	16	16
FOV	26 : Sat - A,P,F	26 : Sat - A,P,F
THICKNESS	3	3
INTER SPACE	1	1
LOCATIONS	18	18
MATRIX	256X192	256X192
NEX	2	2
FREQUENCY	NOT SWAPPED	NOT SWAPPED
RBW / RBW2 (KHz)	16	16
TIME	4	4

R Cholangiogram

F Coil - Body Coil

IMAGING PARAMETERS	Views

	Axial Localiser	Coronal Localiser	Coronal	Coronal/ Oblique
ulse eqs	SPGR/BH	SPGR/BH	FSE/BH	FSE/BH
LANE	Axial	Coronal	CORONAL	Coronal / Oblique
ODE	2D	2D	2D	2D
ptions	RC, FC,EDR, SEQ,Gat, GRx	RC, FC,EDR, SEQ,Gat,G Rx	FAST,FC, NPWEDR, VB,GRx	FAST,FC,N PWEDR,V B,GRx
R	35	35	4000	9000
ffect.TE	Minimum	Minimum	750	340
OV	40	40	24	24
HICKNE S	10	10	20	3
ter pace	2.5	2.5	1	0
OCATIO S	1	1	1	13
IATRIX	256X192	256X192	256X128	256X192
EX	1	1	1	1
REQUEN Y	R/L	S/I	NOT SWAPPED	NOT SWAPPED
BW / BW2 KHz)	16	16	16	32
IME	0.38	0.38	0.16	1.30

Compensation direction selected according to the plane of sition,

: Axial – Slice & Coronal / Sagittal – Frequency.

riotactic – For Globus Pallidus Internanal capsule

ad RF Coil Coil

IMAGING PARAMETERS	Views				
	Sag Localiser	Axial Localiser	Coronal Localiser	Axial FMPIR	Coronal FMPIR
Pulse Seqs	SE	SE	SE	IR	IR
PLANE	SAGITTAL	AXIAL	CORONAL	AXIAL	CORONAL
MODE	2D	2D	2D	2D	2D
Options	None	None	None	FAST,FC, SEQ,SQP EDR,VB, GRx	FAST,FC, SEQ,SQP EDR,VB, GRx
TR	420	420	420	4000	4000
TE/Effect. TE	Minimum	Minimum	Minimum	38	38
FOV	30	30	30	30	30

HICKNE S	5	5	5	3	3
ter pace	3	3	3	0	0
OCATIO S	11	11	11	12	12
ATRIX	256X25 6	256X256	256X192	256x25 6	256x256
EX	2	2	2	4	4
REQUEN Y	S/I	A/P	S/I	A/P	S/I
BW / BW2 (Hz)	16	16	16	16	16
ME	2.45	2.45	2.45	14.08	14.08

ELLANEOUS

GIN AME S	Views					
	Internal Ear	Urogra phy	FLAIR	STIR	HEAD	SPINE
e	FSE	FSE	FMPIR	FMPIR	FSE	FSE

LANE	CORL. OBL/ AXIAL. OBL	CORL. OBL	OBLIQUE	OBLIQUE	OBLIQUE	OBLIQUE
ODE	2D	2D	2D	2D	2D	2D
	-	-	2500	155	-	-
ptions	FC, GRx, EDR,,NPW, SQ, VB	VB,EDR ,NPW,GRx,StF	VB,EDR,GRx, FC	VB,EDR ,GRx,FC	VB,EDR , FC,GRx	VB,EDR , FC,GRx ,StF,a:Sat
R	6000	10,000	10,000	5,000	3,000	3,000
ff.TE	360	340	34	Min.Full	17/34	68
TL	12	32	12	8	8	8
LIP (^{0})	-	-	-	-	-	-
OV	16X16	36	22X16	22X16	22x16	-
HICKNSS	5/20	3	5	5	5	5
NTER PACE	0	0	3	3	3	1
OCATINS	6/1	11	9	16	16	13
IATRIX	256X256	256X192	256X192	256X192	256X192	256X192
EX	2	2	1	1	1	2
REQUECY	NOT SWAPPED	NOT SWAPPED	NOT SWAPPED	NOT SWAPPED	NOT SWAPPED	NOT SWAPPED
RBW / RBW2 KHz)	16	16	16	16	16/3.2	16

	4.48	2	6	3	2	2

S ROUTINE

positioning

tient lies supine and positioned so that the longitudinal
ent light lies in the midline and the horizontal light passes
the point midway between the pubic symphysis and iliac
When local rectal coil is used it is carefully inserted and
ned prior to the investigation

onal T1-Localizer

lices/spacing are prescribed from coccyx to the anterior aspect
ubic symphysis

gittal SE T1&T2 FSE

lices are prescribed from left to right pelvic side walls. Unless
node involvement is suspected, small structures such as the
e requireshigh resolution imaging using thin slices/ gapis
d

kial SE T1 & T2 FSE

are prescribed from the pelvic floor to the iliac crests

Options	TR	TE	ETL	FOV	Thick	SP	Loc	Matrix	Nex	RBW	Time
RC/NP	440	18		32	5	1	14	256X 192	1	16	1.5
RC/NPW	580	18		28	4	1	20	"	2	16	3.4
Fast/FC VB/ED NPW	3000	120	6	28	4	1	20	"	2	16	2.5
CS/NP W	580	18		28	5	1	20	"	2	16	3.4
Fast/FC VB/ED NPW	3000	120		28	5	1	20	"	2	16	2.5
CS/NP W	440	18		28	4	1	15	"	2	16	2.2

SE	Fast/FC VB/ED/ NPW	2400	110	6	28	4	1	15	"	2	16	1.5

dditional sequences

Sagittal TSE fat sat T2

Coronal GR for bony lesions

Post contrast sag. Axial, Coronal T1(If indicated)

HOULDER- ROUTINE

The patient lies supine with the arms resting omfortably by the side. Slide the patient across the table to bring the houlder under examination as close as possible to the center of the ore The arm to be examined is strapped to the patient thump up and added so that the humerus is horizontal. Place the coil (12"GP) to over the humeral head and superior and medial to the natomy.Centre the FOV to the Glenohumeral joint

. Axial Localizer SE T1

Slices are prescribed relative to the horizontal lignment light so that

supraspinatus muscle is included in the image

Coronal oblique SE T1

hin slices are prescribed from the infraspinatus posteriorly to the upraspinatus anteriorly and angled parallel to the supraspinatus nuscle. The superior edge of the acromion to the inferior aspect of he subscapularis & deltoid muscle laterally and distal third of the upraspinatus muscle medially are included in the image

. Coronal oblique TSE T2 Fat sat

at suppressed T2 images clearly display muscle tear, trabecular njury,joint fluid and tendon tears

. Sagittal oblique TSE-T2

lices are prescribed from medial to the glenoid cavity to the bicipital roove laterally

itional sequences
xial GRE T2*
slices are prescribed from top of the accromio clavicular joint to
w the inferior edge of the glenoid

ptions	TR	TE	FLIP°	ETL	FOV	Thk	SP	Loc	Matx	Nex	Rb	Time
S/NP	380	17			24	5	1	11	256X 192	1	16	1.4
S/NP	440	18			24	4	1	14	"	2	16	2.5
st/FC 3/ED PW	240 0	120		7	24	4	1	14	"	2	16	1.5
st/FC/ 3/ED PW	240 0	120		7	24	4	1	14	"	2	16	1.5
C/NP	540	18	16°		24	4	1	14	"	2	16	2.1

COMPUTED TOMOGRAPHY

CT is in the fourth decade of clinical use and has been proved to be an in valuable diagnostic tool in many clinical purposes, from cancer diagnosis, trauma to osteoporosis screening. CT was the first imaging modality that made it possible to probe the inner depths of the body, slice by slice. Since 1972, when the first head ct scanner was introduced, ct has matured greatly and gained technological sophistication. Concomitant changes have occurred in the quality of ct images. The first ct scanner, an EMI MARK I, produced images with 80 x 80 pixel resolution (3 mm pixel resolution, and each pair of slices required approx. 4.5 min of scan time and 1.45 min of reconstruction time. Because of the long acquisition times required for the early stage scanners and the constraints of cardiac and respiratory motion, it was originally thought that CT would be practical only for the head scanning.

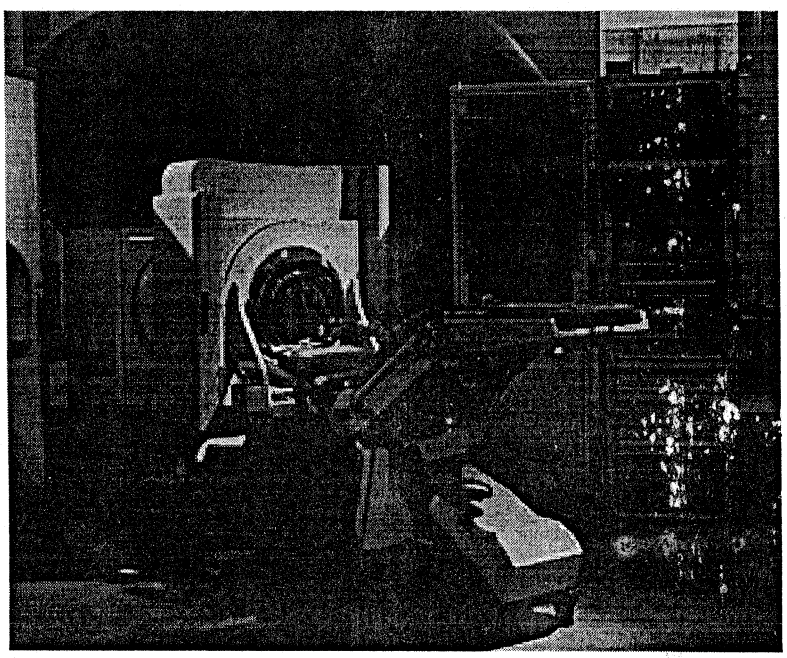

EMI Scanner

CT is one of the technologies that was made possible by the invention of the computer. The clinical potential of the CT became obvious during its early clinical use, and the excitement

ver solidified the role of computers in medical imaging.
ent advancement in the acquisition geometry., detector
nology, multiple detector arrays, and the x-ray tube design
e led to scan times that have now measured in fraction of
onds. Modern equipments deliver computational power that
ws reconstruction of the image data essentially in real time.

Godfrey Hounsfield Allan Cormack

invention of the ct scanner earned Godfrey Hounsfield of
ain and Allan Cormack of united states the Nobel prize for
dicine in 1979. CT scanner technology today is used not only
nedicine but in other industrial application, such as
destructive testing and soil core analysis.

sic principle.

e mathematical principles of CT were first developed by
adon in 1917. Radon's treatise proved that an image of
known object could be produced if one had an infinite number
projections through the object.

nographic acquisitions

ingle transmission measurement through the patient made by
ngle detector at a given moment is called a ray. A series of
s that pass through the patient at the same orientation is

called a view or a projection. There are two types of projection geometries, these are the parallel beam geometry and the fan beam geometry, the rays at a given projection angles diverge and have an appearance of a fan beam. All modern ct scanners incorporate fan beam geometry in the acquisition system and reconstruction process. The purpose of the CT scanner hardware is to acquire a large number of transmission measurements through the patient at different positions. The acquisition of a single ct image may be involving approx.800 rays taken at 1,000 different projection angles, for a total of approx 800,000 transmission measurements. Before the axial acquisition of the next slice , the table that the patient is lying down is moved slightly in the cranio-caudal direction, which positions a different slice of tissue in the path of the x-ray beam for the acquisition of the next image.

Tomographic reconstruction

Each ray is acquired in ct is transmission measurement through the patient along a line, where these detectors measures an x-ray intensity. I_t. the unattenuated intensity of the x- ray beam is also measured during the scan by the reference detector. And this detects an x-ray intensity I_o. The relationship between I_t and I_0 is given by the following equation.

$I_t = I_0 e^{-\mu t}$

Where t is the thickness of the patient along the ray and μ is the average linear attenuation coefficient along the ray. Notice that I_t and I_o are machine dependent values, but the product μt is an important parameter related to the patient anatomy along a ray. When the equation is rearranged, the measured values I_t and I_o can be used to calculate the parameter interest:

$/n\ (Io/It) = \mu t$

where /n is the natural logarithm (to base e, e = 2.79....),t ultimately cancels out, and the value μ for each ray is used in the CT reconstruction algorithm. This computation, which is preprocessing step performed before the image reconstruction,

uces the dependency of the CT image on the machine
endent parameters, resulting in an image that depends
narily on the patients anatomic characteristics. This is very
ch a desirable aspect of imaging in the general, and the high
ical utility of CT result, in part, from this feature. By
nparison, if a screen film radiograph is underexposed itr
ears white, and if it is overexposed it appears dark. The
sity of Ct images is independent of I_o although the noise in
image is affected.

er preprocessing of the raw data, a CT reconstruction
orithm is used to produce the ct images. There are numerous
onstruction strategies; however, filtered back projection
onstruction is most widely used in the clinical scanners.
e back projection method builds up in the CT image in the
mputer by essentially reversing the acquisition steps. During
quisition, attenuation information along the known path of the
row X-ray beam is integrated by a detector. During the back
jection reconstruction, the μ value from each ray is smeared
ng this same path in the image of the patient. As the data
m a large number of rays are back projected onto the image
trix, areas of high attenuation tend to reinforce on each other,
the areas of low attenuation also reinforce, build up the image
to the computer.

EOMETRY AND HIS TORICAL DEVELOPMENT

GENERATIONS OF CT SCANNERS.

rst Generation: Rotate/Transilate, Pencil Beam

T scanners represent a marriage of diverse technologies,
cluding computer hardware, motor control systems, X-ray

detectors, sophisticated reconstruction algorithms, and X-ray tube/ generator systems. The first generation of CT scanners employed a rotate/ translate, pencil beam systems. Only two X-ray detectors where used, and they measured the transmission of X-rays through the patient for two different slices. The acquisition of numerous projections and the multiple rays per projection required that the single detector for each CT slice be physically moved through out all the necessary positions. The system used the parallel ray geometry. Starting at a particular angle, the X-ray tube and the detectors translated linearly across the FOV, acquiring 160 parallel rays across the 24 cm FOV. When the X-ray tube/ detector system completed its translation, the whol;e system was rotated slightly, and then another translation was used to acquire 160 rays in the next projection. This process was repeated until 180 projections where acquired at 1^0 interval. A total of 180 X 160 = 28,800 rays where measured.

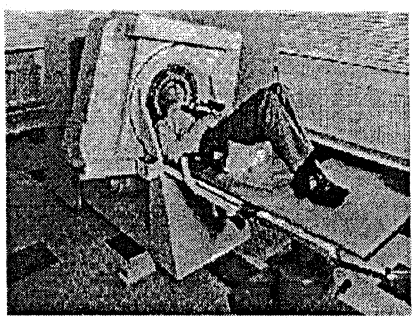

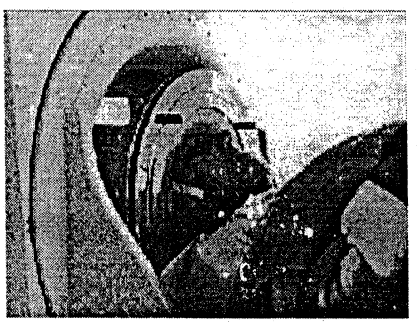

As the system translated and measured rays from the thickest part of the head to the areas adjusent to the head, a huge change in the X-ray flux occurred. The early detector system couldnot accomadate such a large change in the signal, and consequently the patients head was pressed into a flexible membrane filled with water bath. The water bath acted as to bolus the X-rays, so that the intensity of the X-rays outside the patients head was similar in intensity to that inside the haed. The NaI detectors also had significant amount of "after glow"meaning that the signal from the measurement taken at one period of time decayed slowly and carried over into the next measurement if the measurements were made temporarily too close together.

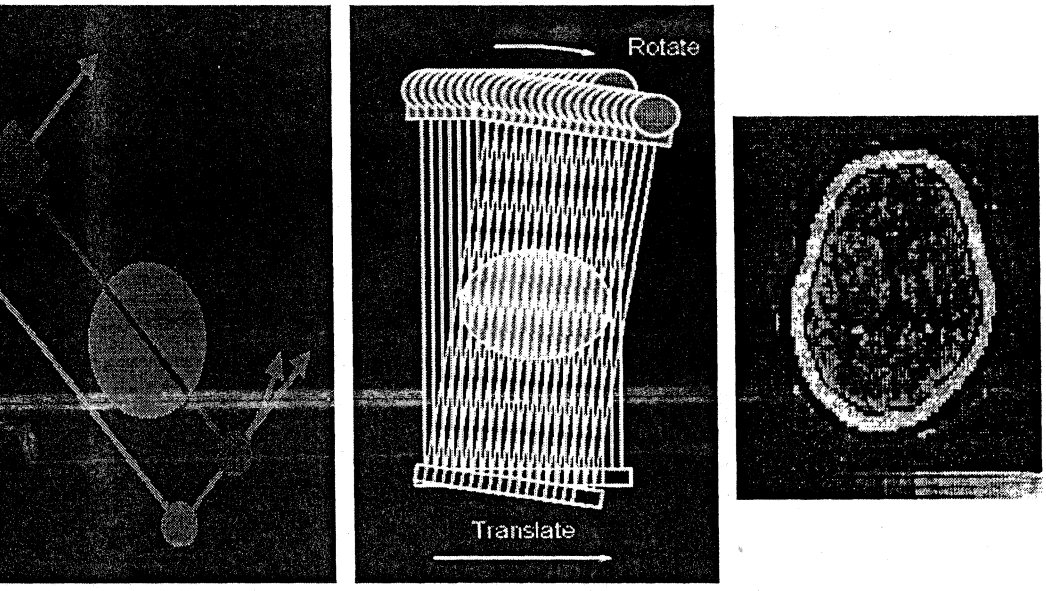

ne advantage of the first generation CT scanners was that it ployed a pencil beam geometry- only two detectors measured transmission of X-rays through the patient. The pencil beam wed very efficient scatter reduction, because scatter that was ected away from the pencil ray was not measured by the ector. With regards to the scatter rejection, the pencil beam metry used in the first –generation CT scanners were the t.

cond generation ct scanners: rotate/transilate, narrow fan am.

next increment improvement to the CT scanners was the orporation of a linear array of 30 detectors. This increased the zation of the X-ray beam by 30 times, compared with the gle detector used per slice in the first- generation system. A tively narrow afn angle of 10^0 as used. In principle a uction of scan time by 30 fold could be expected. However, reduction time was not realized, because more data 0rays X 540 views = 324,000 data points) were acquired to

improve image quality. The shortest scan time wit a second generation scanner was 18 s/ slice, 15 times faster than the first generation.

In corporation of an array of detectors instead of just two, required the use of a narrow fan beam of radiation. Although a narrow fan beam provides excellent scatter rejection compared with the plain film imaging, it does allow more scattered radiation to be detected than that with the pencil beam used in the first generation CT.

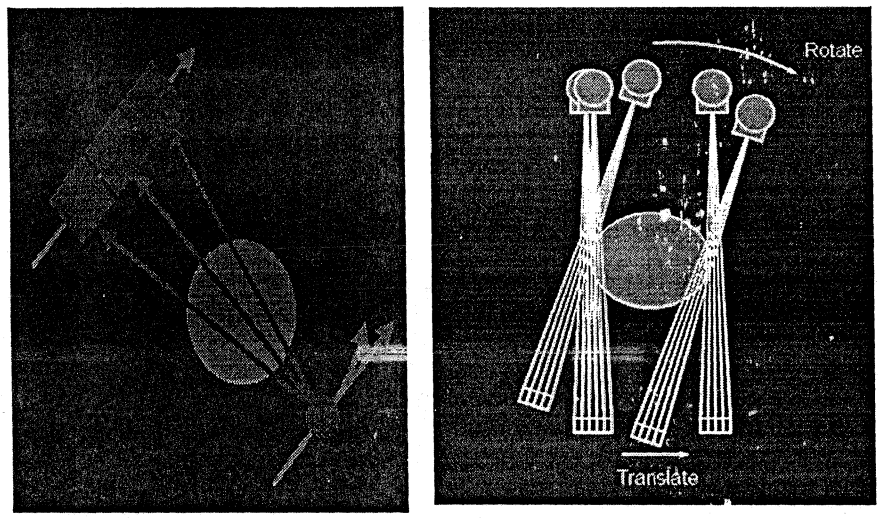

Third Generation :Rotate/ Rotate, Wide Fan Beam

The translational motion of first and second generation CT scanners was a fundamental impendiment to fast scanning. At the end of each translation, the motion of the X-ray tube/detector system had to be stopped, the whole system rotated, and the traslation motion restarted. The success of CT as a clinical modality in its infancy gave manufacturers reason to explore more efficient, but more costly, approaches to the scanning geometry.

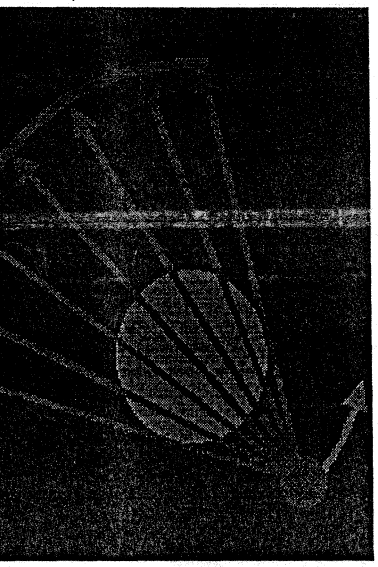

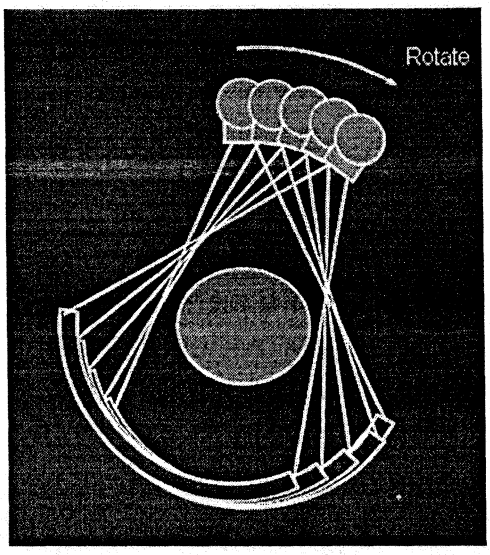

e no: of detectors used in the third generation scanners was
reased substantially (more than 800 detectors), and the angle
the fan beam was increased so that the detector array formed
arc wide enough to allow the X-ray beam to interrogate the
tire patient. Because detectors and the associated electronics
e expensive, this led to more expensive CT scanners.
owever, spanning the dimensions of the patient with an entire
w of detectors eliminated the need for the translational motion.
e multipkle detector in the detector array capture the same
mber of ray measurements in one instance as was required by
complete translation earlier. The mechanically joined X-ray
be and the detector array rotate together around the patient
thout translation. The motion of the third generation CT
anners is called as "rotate/ rotate" referring to the rotation of
e X-ray tube and the rotation of the detectors. By eliminating
e translational motion, the scan time has reduced substantially.
ne early third generation scanners could deliver scan times
orter than 5 seconds. Newer systems have scan times of one-
lf the second.

The evolution from first to third generation involved radical
provement with each step. Developments of the fourth and the
h generation scanners led not only to some improvements but
so some compromises in clinical CT images.

Fourth Generation: Rotate/Stationary

Third generation scanners suffered from the significant problem of the ring artifacts and in the late 1970's forth generation scanners where designed specifically to address these artifacts. It is never possible to have a large number of detectors in perfect balance with each other, and this was especially true 25 years ago. Each detector and its associated electronics in the system has a certain amount of drift , causing the signal levels of each detector to shift over time. The rotate/ rotate geometry of the third generation scanners leads to a situation in which each detector is responsible for the data corresponding to a ring in the image. Detectors towards the center in the detectora array provide the data in the reconstructed image in a ring that is small in diameter, and more peripheral detectors contribute to large diameter rings.

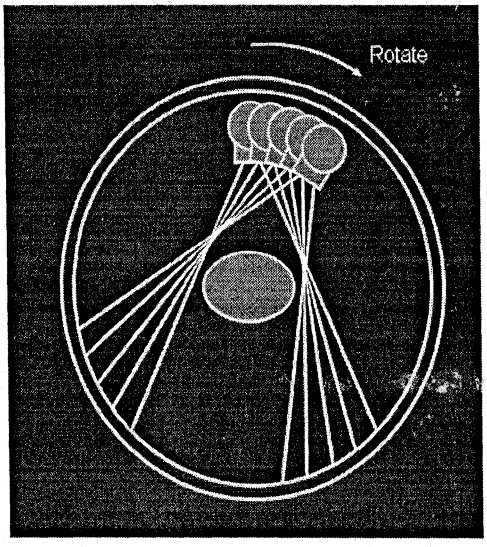

Third generation CT uses a fan beam geometry in which the vortex of the fan is in the X-ray focal spot and the rays fan out from the X-ray source to each detector on the detector array. The detectors towards the center of the array make the transmission measurement I_t, while the reference detector that measures I_0 is positioned near the edge of the detector array. If g1 is the gain of the reference detector, and g2 is the gain of the other detector, then the transmission measurement is given by the following equation:

$$/n(g1i_0/g2i_t) = \mu t$$

ourth generation CT scanners were designed to overcome problems of the ring artifacts. With fourth –generation nners, the detector removed from the rotating gantry and are ced in a stationary 360- degree ring around the patient uiring many more detectors. Modern fourth –generation CT tems are stationar, fourth generation CT is said to use a te/stationary geometry. During acquisition with a fourth- eration scanner, the divergent X-ray beamemerging from the ay tube forms a fan- shaped beam. However, the data are cessed for a fan beam reconstruction with each detector as vertex of a fan beam. The rays acquired by each detector ng fanned out to a different positions of the X-ray source. In vernacular of CT, third- generation design uses a source fan. ereas fourth generation uses a detector fan. The third eration fandata are acquired by the detector array ultaneously, in one instant of time. The fourth generation fan am data are acquired by a sigle detector over the period of e that is required for the x-ray tube to rotate through the arc gle of the fan. With fourth generation geometry, each detector s as its own reference detector. For each detector with its own n, g, the transmission measurement is calculated as follows.

$$\ln (g\, I_0 / g\, I_t) = \mu t$$

ere the single term g cancels out, therefore the ring artifact eliminated in the fourth generation scanners. It should be ntioned, however,that with the modern detectors and more phisticated calibration software. Third- generation CT nners are essentially free of the ring artifacts as well.

th Generation: Stationary/Stationary

ovel CT scanner has been developed specifically for cardiac nographic imaging. This " cine-CT" scanner does not use a nventional X-ray tube; instead, a large arc of tungsten circles the patient and lies directly opposite to the detector g. X-rays are produced from the focal track as a high-energy ctron beam strikes the tungsten. There are no moving parts to s scanner gantry. The electron beam is produced in a cone- e structure (a vacuum enclosure) behind the gantry and is ctronically steered around the patient so that it strikes the

annular tungsten target. Cine CT system is called electron beam scanner, are marketed primarily to cardiologists. They are

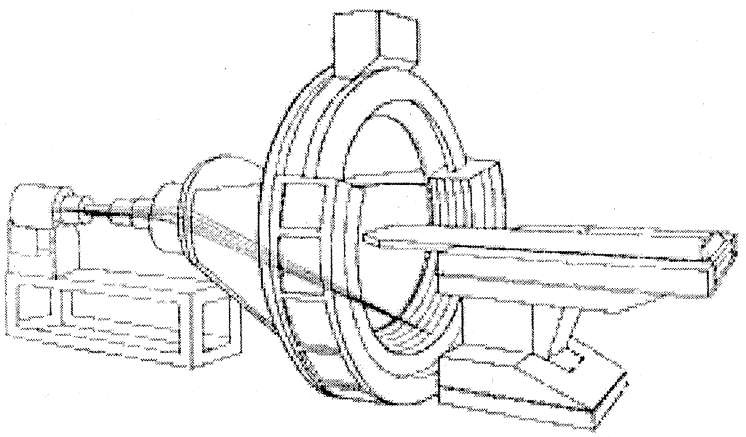

EBCT

capable of 50 msec scan times and can produce fast-frame- rate CT movies of the beating heart.

Sixth Generation: Helical

Third- generation and the fourth generation scanning geometries solved the mechanical inertia limitation in acqusition of the individual projection data by eliminating the translation motion used in the first- and second- generation scanners. However, the gantry had to be stopped after each slice where acquired, because the detectors and the X-ray tube had to be connected by wires to the stationary scanner electronics. The ribbon cable used to connect the third generation detectors with the electronics had to carefully rolled out from a cable spool as the gantry rotated , and then as the gantry stopped and began to rotate in the opposite direction and the ribbon cable had to retracted . in the early 1990's, the design of the third-and the fourth generation scanners evolved to incorporate slip ring technology. A slip ring is a circular contact with sliding brushes that allow the gantry to rotate continuously, un winded by wires. The use of slip- ring technology eliminated the inertial limitation

ne end of each slice acquisition, and the rotating gantry was
to rotate continuously throughout the entire patient
mination. The design made it possible to achieve greater
tional velocities than with systems not using a slip ring,
wing shorter scan times.
lelical CT scanners acquire data while the table is moving; as
sult, the X-ray source moves in a helical pattern around the
ent being scanned. Helical CT scanners use either third-or
th- generation slip ring design. By avoiding the time required
anslate the patient table. The total scan time required to
ge the patient can be shorter. Consequently, helical scanning
ws the use of less contrast agent and increases patient
oughput. In some instances within a single breath hold of
ent, avoiding inconsistent level of inspiration.

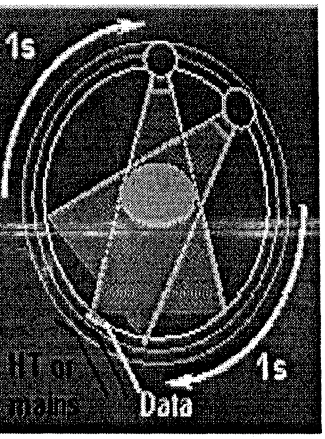

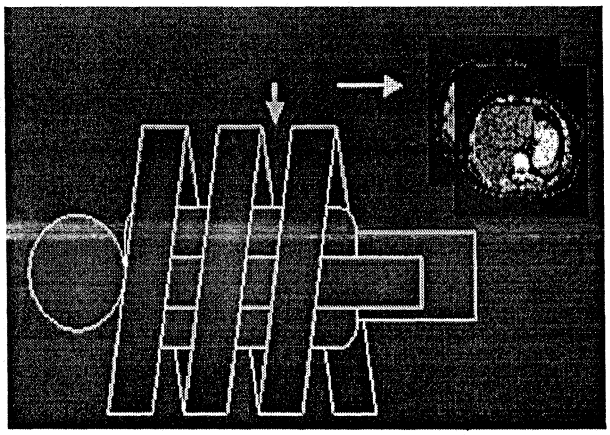

e introduction of helical CT has introduced many different
nsiderations for data acquisition. In order to produce
onstructions of planar sections of the patient, the raw data
m the helical data set is interpolated to approximate the
quisition of planar reconstruction data. The speed of the table
tion relative to the rotation of the CT gantry is very important
nsideration, and the pitch is the parameter that describes this
ationship.
The table movement during one gantry rotation to the aperture
limation is expressed as the pitch ratio.

$$\text{Pitch} = \frac{\text{Table feed(s) x Gantry rotation / sec.}}{\text{Collimation width.(D)}}$$

In spiral CT the data acquired is a volume data instead of a single 2D data that is acquired in conventional CT. This 3D volume of data can be reconstructed retrospectively for any inter scan spacing (overlapped images), which is useful in detecting very small lesions. Also the area of missed scan is eliminated due to volume data acquisition.

The hardware part of the system uses a built in High-Frequency high-tension generator, and a high heat capacity x-ray tube.

MSHCT refers to the helical CT system equipped with multiple row of detector array for simultaneous collection of data at different slice locations along z direction. It offers substantial improvement of the volume coverage speed and high z axis resolution. It enables sub second scanning (.25sec for 1 slice) and facilitates reduced motion artifact and better temporal resolution.

The multiple detector rows enable to further divide the total x-ray beam into multiple sub beams (by the post collimators, which are equal in number as the detector rows). Let D' be the X-ray beam collimation and d' be the detector row collimation respectively and N' be the number of detector rows; $d = D/N$

The thickness of the individual X-ray beam is determined by the detector row collimation(d) as opposed to X-ray beam collimation in conventional CT. So the helical pitch (P) of multislice CT is given by

$$P = S/d$$

Thus the extended pitch allows high volume coverage without loss of z-axis resolution.

antages of spiral CT.

metric Data Acquisition.
uced motion and misregistration artifacts.
uced overall study time - increased patient comfort and
ity of the images in seriously ill or un co-operative patients.
uced radiation and IV contrast dose.
er multiplanar and 3D image reconstruction.

enth Generation: Multiple Detector Array CT (MDCT)

introduction in 1998 of multi–detector row computed
ography (CT) by the major CT vendors was a milestone with
ard to increased scan speed, improved z-axis spatial
olution, and better utilization of the available x-ray power. In
review, the general technical principles of multi–detector row
are reviewed as they apply to the established four- and eight-
ion systems, the most recent 64-section scanners, and
re generations of multi–detector row CT systems.

Evolution Of Spiral Ct: From One Section To 64

introduction of spiral CT in the early 1990s constituted a
damental evolutionary step in the development and ongoing
nement of CT imaging techniques .For the first time, volume
a could be acquired without misregistration of anatomic detail.
ume data became the basis for applications such as CT
iography ,which has revolutionized the noninvasive
essment of vascular disease. The ability to acquire volume
a also paved the way for the development of three-
ensional (3D) image-processing techniques such as
tiplanar reformation (MPR), maximum intensity projection,

surface-shaded display, and volume-rendering techniques ,which have become a vital component of medical imaging today. Ideally, volume data are of high spatial resolution and are isotropic in nature: Each image data element (voxel) is of equal dimensions in all three spatial axes, and this forms the basis for image display in arbitrarily oriented imaging planes. For most clinical scenarios, however, single-section spiral CT with a 1-second gantry rotation is unable to fulfill these requirements. To prevent motion artifacts and optimally utilize the contrast agent bolus, body spiral CT examinations need to be completed within a certain time frame of, ordinarily, one breath hold (25–30 seconds). If a large scan range such as the entire thorax or abdomen (30 cm) has to be covered within a single breath hold, a thick collimation of 5–8 mm must be used. While the in-plane resolution of a CT image depends on the system geometry and on the reconstruction kernel selected by the user, the longitudinal (z-axis) resolution along the patient axis is determined by the collimated section width and the spiral interpolation algorithm. Use of a thick collimation of 5–8 mm results in a considerable mismatch between the longitudinal resolution and the in-plane resolution, which is 0.5–0.7 mm, depending on the reconstruction kernel. Thus, with single-section spiral CT, the ideal of isotropic resolution can only be achieved for very limited scan ranges .Strategies to achieve more substantial volume coverage with improved longitudinal resolution include the simultaneous acquisition of more than one section at a time and a reduction in the gantry rotation time. A first multi slice CT scanner was introduced in 1993 (Elscint TWIN; Elscint, Haifa, Israel) In 1998, several CT manufacturers introduced multi–detector row CT systems, which provided considerable improvement in scanning speed and longitudinal resolution and better utilization of the available x-ray power .These systems typically offered simultaneous acquisition of four sections at a gantry rotation time of 0.5 second.

Simultaneous acquisition of *m* sections results in an *m*-fold increase in speed if all other parameters (eg, section thickness) are unchanged. This increased performance of multi–detector row CT relative to single-section CT allowed the optimization of a variety of clinical protocols. The examination time for standard protocols could be substantially reduced, which proved to be of

ediate clinical benefit for the quick and comprehensive
ssment of trauma patients and uncooperative patients
rnatively, the scan range that could be covered within a
ain time was extended by a factor of *m,* which is relevant for
logic staging or for CT angiography with extended coverage
the lower extremities).
most important clinical benefit, however, proved to be the
y to scan a given anatomic volume within a given scan time
substantially reduced section width at *m* times increased
itudinal resolution. Because of this, the goal of isotropic
lution was within reach for many clinical applications.
minations of the entire thorax or abdomen could now be
nely performed with a 1.0- or 1.25-mm collimated section
h. Despite these promising advances, clinical challenges and
ations remained for four-section CT systems. True isotropic
lution for routine applications had not yet been achieved,
ause the longitudinal resolution of about 1 mm does not fully
ch the in-plane resolution of about 0.5–0.7 mm in a routine
mination of the chest or abdomen. For large volumes, such
or CT angiography of lower extremity vessels ,thicker (eg,
mm) collimated sections had to be chosen to complete the
n within a reasonable time frame. Scan times were often too
to allow image acquisition during a purely arterial phase. For
angiography of the circle of Willis, for instance, a scan range
bout 100 mm must be covered .With four-section CT at a
mated section width of 1 mm, pitch of 1.5, and gantry rotation
e of 0.5 second, this volume can be covered in about 9
onds, not fast enough to avoid venous overlay, assuming a
ebral circulation time of less than 5 seconds.
a next step, the introduction of an eight–detector row CT
tem in 2000 enabled shorter scan times but did not yet
vide improved longitudinal resolution (thinnest collimation,
nt sections at 1.25 mm). The latter was achieved with the
oduction of 16–detector row CT .which made possible the
ine acquisition of substantial anatomic volumes with isotropic
millimeter spatial resolution and scan times of less than 10
onds for 300 mm of coverage. While in-plane spatial
lution is not substantially improved, the two major
antages of fast multi–detector row CT are a true isotropic
ugh-plane resolution and a short acquisition time that enable

high-quality examinations in severely debilitated and severely dyspneic patients .

Traditional CT applications have been enhanced and strengthened by the remarkable, although incremental, improvement in scanner performance by the addition of more detector rows. Multi–detector row CT also dramatically expanded into areas previously considered beyond the scope of third-generation CT scanners that were based on the mechanical rotation of an x-ray tube and detectors, such as cardiac imaging with the addition of electrocardiographic (ECG)-gating capability. With a gantry rotation time of 0.5 second and dedicated image-reconstruction approaches, the temporal resolution for acquisition of an image was improved to 250 msec and less,which proved to be sufficient for motion-free imaging of the heart in the mid- to end-diastolic phase when the patient had a slow to moderate heart rate (ie, up to 65 beats per minute .With four simultaneously acquired sections, coverage of the entire heart volume with thin sections (ie, four sections at 1.0- or 1.25-mm collimation) within a single breath hold became feasible. This 1.0–1.25-mm longitudinal resolution combined with the improved contrast resolution of modern CT systems enabled noninvasive depiction of the coronary arteries .Initial clinical studies demonstrated the potential of multi–detector row CT to not only demonstrate but to some degree also characterize noncalcified and calcified plaques in the coronary arteries on the basis of plaque CT attenuation .
The limitations of four– and eight–detector row CT systems, however, have so far prevented the successful integration of CT coronary angiography into routine clinical algorithms: Stents or severely calcified arteries constitute a diagnostic dilemma, mainly because of partial volume artifacts as a consequence of insufficient longitudinal resolution . For patients with a higher heart rate, careful selection of separate reconstruction intervals for different coronary arteries has been mandatory .It is almost impossible for patients with manifest heart disease to comply with the breath-hold time of about 40 seconds required to cover the entire heart volume (approximately 12 cm) with four-section CT. The ongoing technical refinement of multi–detector row CT, however, holds the promise of gradually overcoming some of

e limitations. The most important steps toward this goal are
ry rotation times faster than 0.5 second for improved
poral resolution and robustness of use, 16-section
millimeter acquisition for increased longitudinal resolution
shorter breath-hold times, and novel sophisticated
oaches for image acquisition and reconstruction.

RRENT TECHNIQUES

tem Design

ector Design.—For clinical purposes, different section
ns must be available to adjust the optimum scan speed,
itudinal resolution, and image noise for each application.
a single–detector row CT scanner, different collimated
ion widths are obtained by means of prepatient collimation of
x-ray beam . For a very elementary model of a two-section
scanner (m = 2, or two detector rows), figure demonstrates
different section widths can be obtained by means of
patient collimation if the detector is separated midway along
z-axis extent of the x-ray beam. For m > 2, this simple design
ciple must be replaced by more flexible concepts requiring
e than m detector rows to simultaneously acquire m sections.

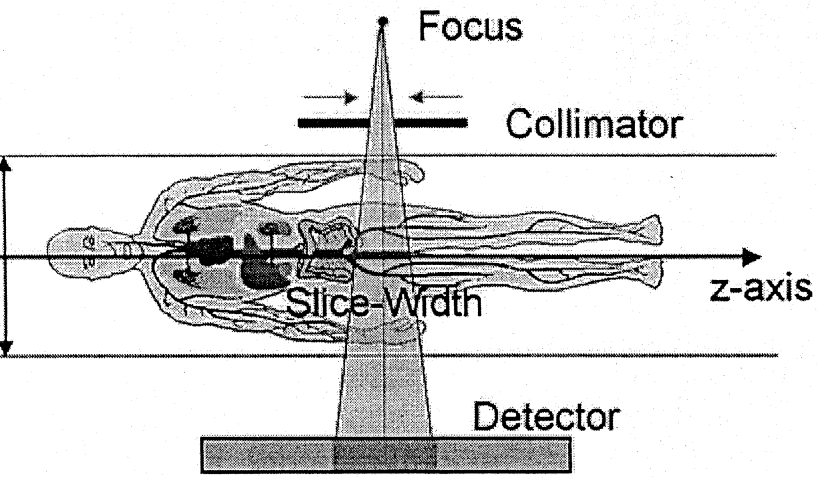

erent manufacturers of multi–detector row CT scanners have
oduced different detector designs. In order to be able to
ect different section widths, all scanners combine several

detector rows electronically to a smaller number of sections according to the selected beam collimation and the desired section width.
For established four-section CT systems, two detector types are commonly used.

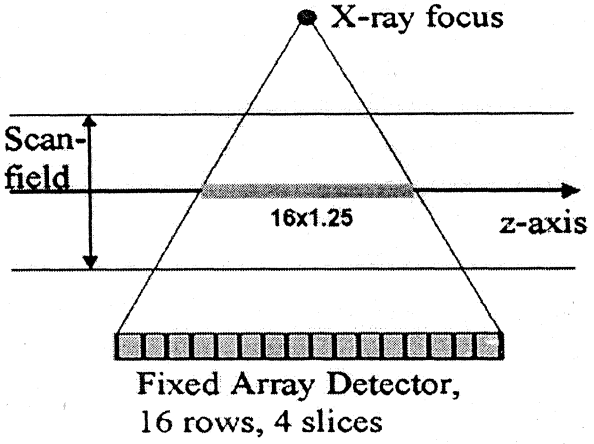

The fixed-array detector consists of detector elements with equal sizes in the longitudinal direction. A representative example of this scanner type, the Lightspeed scanner (GE Medical Systems, Milwaukee, Wis), has 16 detector rows, each of them defining a 1.25-mm collimated section width in the center of rotation .The total coverage in the longitudinal direction is 20 mm at the isocenter; owing to geometric magnification, the actual detector is about twice as wide. By means of prepatient collimation and combination of the signals of the individual detector rows, the following section widths (measured at the isocenter) can be realized: four sections at 1.25 mm, 2.5 mm, 3.75 mm, and 5.0 mm .The same detector design is used for the eight-section version of this system and provides eight sections at 1.25- and 2.5-mm collimated section widths.

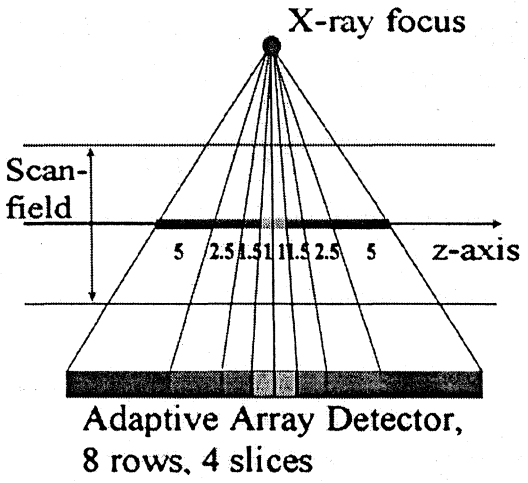

ifferent approach uses an adaptive-array detector design, ch comprises detector rows with different sizes in the gitudinal direction. Scanners of this type, the Mx8000 four- ction scanner (Philips Medical Systems, Best, the therlands) and the Somatom Sensation 4 scanner (Siemens), ve eight detector rows .Their widths in the longitudinal ection range from 1 to 5 mm at the isocenter and allow the owing collimated section widths: two sections at 0.5 mm, four 1.0 mm, four at 2.5 mm, four at 5.0 mm, two at 8.0 mm, and o at 10.0 mm

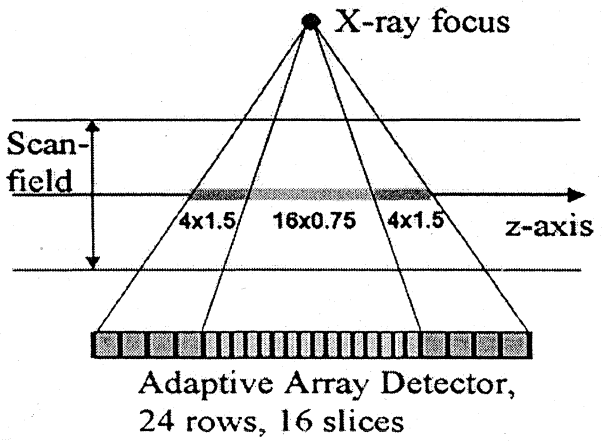

e selection of the collimated section width determines the rinsic longitudinal resolution of a scan. In a "step-and-shoot" quential mode, any multiple of the collimated width of one tector section can be obtained by adding the detector signals

during image reconstruction. In a spiral mode, the effective section width, which is usually defined as the full width at half maximum (FWHM) of the spiral section-sensitivity profile (SSP), is adjusted independently in the spiral interpolation process during image reconstruction. Hence, from the same data set, both narrow sections for high-spatial-resolution detail or for 3D postprocessing and wide sections for better contrast resolution or quick review and filming may be derived.
Sixteen-section CT systems usually have adaptive-array detectors. A representative example for this scanner type, the Somatom Sensation 16 scanner (Siemens), uses 24 detector rows The 16 central rows define 0.75-mm collimated section widths at the isocenter, and the four outer rows on both sides define 1.5-mm collimated section widths .The total coverage in the longitudinal direction is 24 mm at the isocenter. By means of appropriate combination of the signals of the individual detector rows, either 12 or 16 sections with 0.75- or 1.5-mm collimated section width can be acquired simultaneously. The Lightspeed 16 scanner (GE Medical Systems) uses a similar design: It provides 16 sections with either 0.625- or 1.25-mm collimated section width. The total coverage in the longitudinal direction is 20 mm at the isocenter. Yet another design, which is implemented in the Aquilion scanner (Toshiba, Tokyo, Japan), can provide 16 sections with either 0.5-, 1.0-, or 2.0-mm collimated section width, with a total coverage of 32 mm at the isocenter.

Radiation Dose

Radiation dose and dose efficiency.—Radiation exposure to the patient at CT and the resulting potential radiation hazard have recently gained considerable attention in both the public and the scientific literature .Typical values for the effective patient dose for selected CT protocols are 1–2 mSv for a head CT, 5–7 mSv for a chest CT, and 8–11 mSv for abdominal and pelvic CT.This radiation exposure must be appreciated in the context of the average annual background radiation, which is 2–5 mSv (3.6 mSv in the United States). Despite the undisputed clinical benefits, multisection CT scanning is often considered to require increased patient dose compared with the dose from

ngle-section CT. Indeed, a certain increase in radiation dose is navoidable owing to the underlying physical principles.
the x-ray tube of a CT scanner, a small area on the anode ate, the focal-spot, emits x-rays that penetrate the patient and e registered by the detector. A collimator between the x-ray be and the patient, the prepatient collimator, is used to shape e beam and to establish the dose profile. In general, the llimated dose profile is a trapezoid in the longitudinal direction. the umbral region (ie, plateau region of the trapezoid), x-rays mitted from the entire area of the focal spot illuminate the etector. In the penumbral regions, only a part of the focal spot uminates the detector, while the prepatient collimator blocks off her parts.
/ith single-section CT, the entire trapezoidal dose profile can ontribute to the detector signal, and the collimated section width determined as the FWHM of this trapezoid. The relative dose tilization of a single-section CT system can therefore be close to 00%. In most cases with multi–detector row CT, only the ateau region of the dose profile is used to ensure an equal gnal level for all detector elements. The penumbral region is en discarded, either by a postpatient collimator or by the trinsic self-collimation of the multisection detector, and epresents "wasted" dose. The relative contribution of the enumbral region increases with decreasing section width, and it ecreases with increasing number of simultaneously acquired nages. This is demonstrated in Figure 4, which compares the minimum width" dose profiles for a four-section CT system and corresponding 16-section CT system with equal collimated idth of one detector section. Correspondingly, the relative dose tilization with four-section 1-mm-collimation CT is 70% or ess,depending on the scanner type. With 16-section CT systems nd submillimeter collimation, dose utilization can be improved to 4%, again depending on scanner type .Some multi–detector ow CT systems offer special implementations of even more ose-efficient modes that use a portion of the penumbral region.

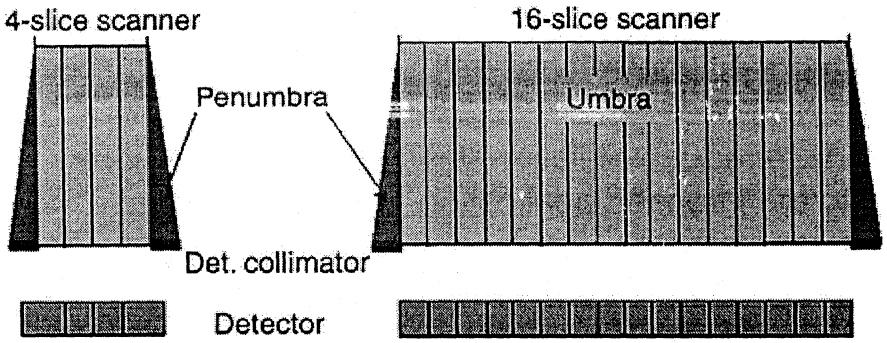

Dose profiles for four- and 16-section CT systems with identical collimated width of one detector *(Det.)* section. The relative contribution of the penumbral region, which represents wasted dose, decreases with increasing number of simultaneously acquired sections.

A clinically appropriate measure for dose is the weighted CT dose index, or $CTDI_w$,which uses the absorbed dose in a polymerized methyl methacrylate (acrylic plastic) phantom as an approximation of the dose delivered to a cross section of the patient's anatomy Figure shows $CTDI_w$ at 120 kV for the 32 cm body phantom as a function of the total collimated width of the detector for a four-section CT system and a 16-section CT system with a similar system geometry. The $CTDI_w$ for 16-section CT at 0.75-mm collimation is 7.8 mGy/100 mAs, whereas the $CTDI_w$ for four-section CT at 1.0-mm collimation is 9 mGy/100 mAs. Thus, different from the transition from single-section CT to 4-section CT systems, a further increase in radiation exposure with the more widespread availability of 16-section CT systems is not to be expected.

Concepts for radiation dose reduction.—The most important factor for reducing radiation exposure is an adaptation of the dose to the patient's size and weight .As a general rule, the dose necessary to maintain constant image noise has to be doubled if the patient diameter is increased by 4 cm. Correspondingly, for a patient diameter that is 4 cm smaller than average, half the standard dose is sufficient to maintain adequate image quality. This is of particular importance in pediatric imaging. Dose reduction can be achieved by reductions in the milliampere-seconds and voltage settings. Most CT manufacturers provide

icated pediatric protocols with, for example, milliampere-
onds and voltage settings adjusted according to the weight of
child.
other means to reduce radiation dose is to adapt the x-ray
e voltage to the intended application. In contrast agent–
anced studies such as CT angiography, the contrast-to-noise
o for fixed patient dose increases with decreasing x-ray tube
age. As a consequence, to obtain the desired contrast-to-
se ratio, the patient dose can be reduced by choosing a lower
age setting. The potential for dose saving is more substantial
patients with a smaller diameter. This can be demonstrated,
example, by means of phantom measurements of small tubes
d with diluted contrast agent embedded in acrylic plastic
antoms with different diameter. Compared with a standard
n at 120 kV in a 32-cm-diameter phantom (corresponding to
t for an average adult), the same contrast-to-noise ratio is
ained with 0.49 times the dose (1.3 times the milliampere-
conds setting) for 80 kV and 0.69 times the dose (1.1 times the
liampere-seconds) for 100 kV. Thus, ideally, 80 kV should be
ed for CT angiography in order to reduce patient dose.
nical studies have confirmed these findings and
monstrated a potential for dose reduction of about 50% when
kV is used for CT angiography instead of 120 kV. In reality,
wever, the maximum x-ray tube current available at 80 kV is
nerally not sufficient to scan bigger patients, which limits the
utine application of this approach. Therefore, use of 100 kV
pears to be a suitable compromise and the method of choice
CT angiography. Figure 5 shows pulmonary CT angiographic
ages of a patient with pulmonary embolism; the scan was
rformed on a 16-section scanner at 100 kV and 120 mAs, and
e effective patient dose for this scan was 2.3 mSv, 25% less
n that for the standard 120-kV protocol.

approach that is finding increased implementation in clinical
actice is anatomic tube current modulation. With this
chnique, tube output is adapted to the patient geometry during
ch rotation of the scanner to compensate for strongly varying
ay attenuation in asymmetric body regions such as the
oulders and pelvis. The variation of the tube output is either
edefined by means of an analysis of a localizer scan

(topogram, scout view) or is determined online by evaluating the signal from a detector row. With this technique, dose can be reduced by 15%–35% without degrading image quality, depending on the body region .
In more sophisticated approaches, tube output is modified according to the patient geometry not only during each rotation but also in the longitudinal direction (automatic exposure control), to maintain adequate dose when moving to different body regions (eg, from thorax to abdomen). In one implementation, the attenuation for each body region of a "standard-sized" patient is stored in the control computer. This attenuation corresponds to the milliampere-seconds setting of the standard protocol. If the actual attenuation of the patient deviates from the "standard" attenuation, the tube output is adapted correspondingly. Figure shows the variation of the milliampere-seconds output for a CT scan of the chest and abdomen in a 6-year-old child. Although the standard protocol with 165 mAs was used—which would have resulted in substantially higher radiation dose than necessary in a standard mode of operation—the average milliampere-seconds value throughout the scan was adjusted to 38 mAs by means of automatic exposure control. Automatic adaptation of tube current to patient size prevents both over- and underirradiation, considerably simplifies the clinical workflow for the technician, and eliminates the need for look-up tables of patient weight and size for adjusting the milliampere-seconds settings.

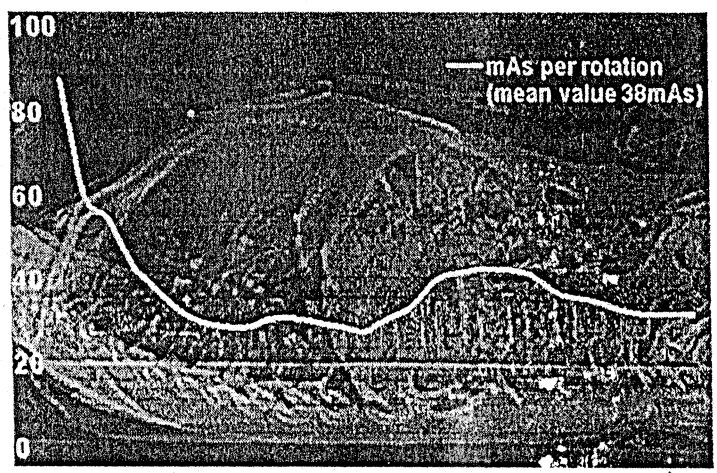

diation dose for ECG-synchronized CT for cardiac
plications has been a topic of considerable controversy.
cent studies based on four-section CT systems find an
ective patient dose of roughly 1 mSv for ECG-triggered
cium scoring with 3-mm section width and roughly 10 mSv for
G-gated CT angiography of the coronary arteries with 1.0- or
5-mm section width. Radiation dose in ECG-gated spiral CT
n be reduced by 30%–50% with use of ECG-controlled dose
dulation (42,43). During the spiral scan, the output of the x-ray
e is modulated according to the patient's ECG trace. It is kept
ts nominal value during a user-defined phase of the cardiac
cle—in general, the mid- to end-diastolic phase. During the
t of the cardiac cycle, the tube output is typically reduced to
% of the nominal values, although it is not switched off
tirely, to allow image reconstruction throughout the entire
rdiac cycle. Thus, although the signal-to-noise ratio is
creased at certain phases of the cardiac cycle, the low-dose
ages are still sufficient for evaluation of functional parameters
ch as ejection fraction, should this kind of information be
sired.

EQUENTIAL SCANS AND IMAGE-RECONSTRUCTION CHNIQUES

th the advent of multi–detector row CT, sequential "step-and-
oot" scanning has remained in use for only a few clinical
plications, such as head CT, high-spatial-resolution lung CT,
rfusion CT, and interventional applications. The number of
ages acquired during a sequential scan corresponds to the
mber of active detector sections. By adding the detector
gnals of the individual sections during image reconstruction,
e number of images per scan can be reduced, and the image
ction width can be increased. As an example, a scan with four
ctions at 1.0-mm collimation provides either four images with
0-mm section width, two images with 2.0-mm section width, or
e image with 4.0-mm section width.
he option to realize a wider section by summing several thin
ctions is beneficial for examinations that require narrow
llimation to prevent partial volume artifacts and low image

noise to allow detection of low-contrast details (eg, neurologic examinations of posterior fossa or cervical spine). In the head, partial volume artifacts typically manifest as dark streaks or areas of hypoattenuation and are due to a nonlinear effect .Figure shows an example of a patient who underwent follow-up CT after surgical removal of a pituitary tumor. From the same scan data—four sections at 1.0-mm collimation—both 4.0-mm-thick images with a standard head kernel for soft-tissue evaluation and 1.0-mm-thick images with a bone kernel were reconstructed. For best image quality, the posterior fossa should be scanned with a collimated section width not larger than 1.25 mm, whereas wider collimation can be used in the supratentorial region

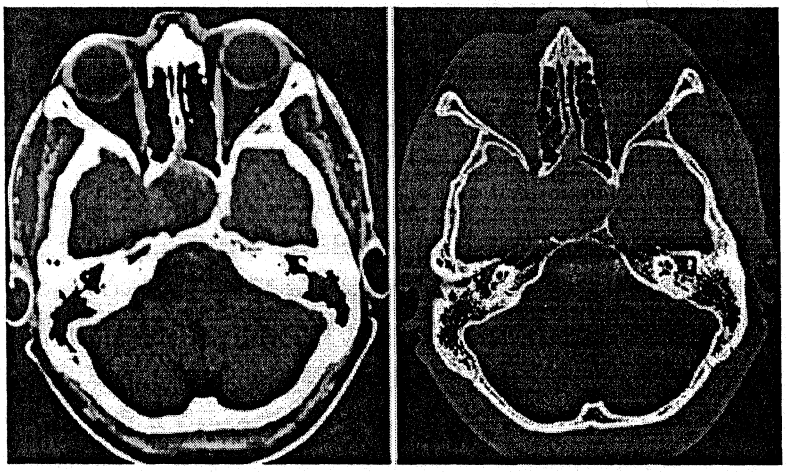

SPIRAL SCANS AND IMAGE-RECONSTRUCTION TECHNIQUES

Spiral scanning is the method of choice for the majority of all multi–detector row CT examinations and requires more attention than does sequential multi–detector row CT because it is conceptually more demanding.

Definition of Spiral Pitch

An important parameter for characterizing a spiral CT scan is the pitch. According to International Electrotechnical Commission specifications, the pitch *(p)* is given by

$$p = TF/W$$

e expense of section broadening—if the collimation is kept nstant—and increased spiral artifacts. For CT angiographic plications in particular, it is more favorable to scan a given lume in a given time by using narrow collimation at a high pitch ther than wider collimation at a low pitch. The motivation for creasing pitch and reducing collimation is to improve ngitudinal resolution by narrowing the SSP .

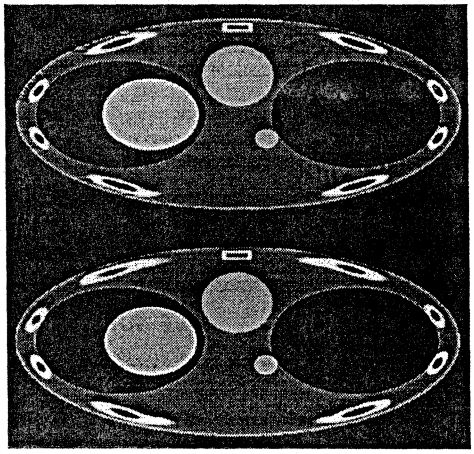

ransverse sections of anthropomorphic thorax phantom from 6-section CT at 0.75-mm collimation and pitch of 1. Images ere reconstructed with adaptive multiplanar reconstruction AMPR; Siemens), with 1.0-mm (top) and 3.0-mm (bottom) ection width. Spiral interpolation artifacts are reduced with ections widths that are thick relative to collimation. In clinical ractice, best image quality for a desired section width is btained by acquiring narrow-collimation data.

he Cone-Angle Problem in Multi–Detector Row CT

wo-dimensional image-reconstruction approaches used in ommercially available single-section CT scanners require all neasurement rays that contribute to an image to run in a plane erpendicular to the patient's longitudinal axis. In multi–detector ow CT systems, this requirement is violated. Figure shows the eometry of a four-section scanner: The measurement rays are lted by the so-called cone angle with respect to the center lane. The cone angle is largest for the sections at the outer dges of the detector, and it increases as the number of detector

rows increases, if their width is kept constant. As a first approximation, the cone angle is neglected in multi–detector row CT reconstruction approaches: The measurement rays are treated as if they traveled perpendicular to the z-axis, and modified two-dimensional image-reconstruction algorithms are used. The data are then inconsistent, however, and produce cone-beam artifacts at high-contrast objects such as bones. It has been demonstrated that cone-beam artifacts can be tolerated if the maximum number of simultaneously acquired sections does not markedly exceed four. As a consequence, the image-reconstruction approaches of all commercially available four-section CT systems and of some systems with even more sections neglect the cone angle of the measurement rays.

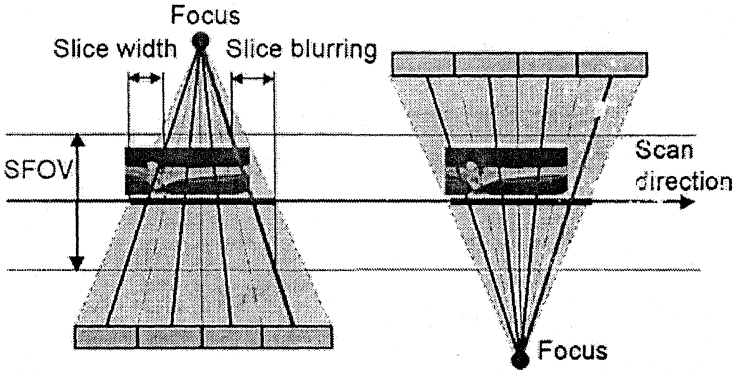

Diagram shows geometry of four-section CT scanner demonstrating the cone-angle problem: Measurement rays are tilted by the so-called cone angle with respect to the center plane. Left and right: Two view angles from sequential scan that are shifted by 180° so that positions of x-ray tube and detector are interchanged. With single-section CT, identical measurement values would be acquired. With multi-detector row CT, different measurement values are acquired. *SFOV* = scan field of view.

MULTI–DETECTOR ROW SPIRAL CT RECONSTRUCTION APPROACHES THAT NEGLECT CONE-BEAM GEOMETRY

Multi–Detector Row 180° and 360° Linear Interpolation

The 360° and 180° linear interpolation single-section spiral reconstruction approaches can be extended to multi–detector

v spiral scanning in a straightforward way. Both 360° and 180°
ltidetector linear interpolation methods are characterized by a
jection-wise linear interpolation between two rays on either
e of the image plane. The cone angle of the measurement
s is not taken into account. In the 360° linear interpolation
ral reconstruction approach, rays measured either at the same
jection angle by different detector rows or in consecutive
ations of the scanner (ie, 360° apart) are used for spiral
erpolation. In the 180° spiral reconstruction approach, both
ect and complementary rays are considered. At the isocenter,
ect and complementary rays interleave in the z-axis direction
selected pitch values. This way, the distance between
easured samples is substantially reduced and equals half the
limated section width, which results in the desired narrow
Ps. Appropriate pitch values are 0.75 for four-section
anning and 0.5625 or 0.9375 for 16-section scanning. The
0° and 360° multidetector linear interpolation approaches are
nematically illustrated in Figure E4 for the example of a four-
ction CT scanner.

general, scanners that rely on 180° or 360° multidetector linear
erpolation techniques and extensions thereof provide selected
screte pitch values to the user, such as 0.75 and 1.5 for four-
ction scanning or 0.5625, 0.9375, 1.375, and 1.75 for 16-
ction scanning. These pitch values are intended to provide
timized sampling schemes in the longitudinal direction and,
nce, optimized image quality.

e user has to be aware of pitch-dependent effective section
dths. For low-pitch scanning (pitch of 0.75 for four sections and
5625 or 0.9375 for 16 sections), the effective section width
proximates the collimated section width; for a 1.25-mm
llimated section width, the resulting effective section width
mains 1.25 mm. The narrow SSP, however, is achieved by
ing 180° multidetector linear interpolation reconstruction with
njugate interpolation at the price of increased image noise. For
gh-pitch scanning (pitch of 1.5 for four sections and 1.375 or
75 for 16 sections), the effective section width is approximately
27 times the collimated section width, and a 1.25-mm
llimated section width results in a 1.5–1.6-mm effective section
dth.

When comparing dose and image noise for different pitch values, the widening of the SSP has to be taken into account. To obtain the same image noise as in a sequential scan with the same collimated section width, 0.73–1.68 times the dose (depending on spiral pitch) is required, with the lowest dose at the highest pitch (see reference 50). Some manufacturers provide a semiautomatic adaptation of the milliampere value to keep the image noise constant if the pitch is changed. In clinical practice, therefore, it is permissible to assume that scanners offering discrete optimized pitch values based on 180° and 360° multidetector linear interpolation techniques are comparable to single-section CT systems in some core aspects: At high pitch, the section widens and the longitudinal resolution degrades; at low pitch, the narrowest possible SSP (comparable to that of 180° single-section linear interpolation at pitch of 1) can be obtained, but a higher dose is necessary to maintain the signal-to-noise ratio. Thus, as a take-home point, when one selects the scan protocol for a particular application, scanning at low pitch optimizes image quality and longitudinal resolution at a given collimation but at the expense of increased patient dose. To reduce patient dose, either milliampere settings should be reduced at low pitch values or high pitch values should be chosen.

Z-Filter Approaches

In a z-filter multi–detector row spiral reconstruction, the spiral interpolation for each projection angle is no longer restricted to the two rays closest to the image plane. Instead, all direct and complementary rays within a selectable distance from the image plane contribute to the image. The weighting function for the rays is selectable, which allows one to adjust both the functional form and the FWHM of the spiral SSP. Still, the cone angle is neglected. A representative example of a z-filter approach is the adaptive axial interpolation algorithm implemented in Siemens CT scanners (Another example is the "multislice cone-beam tomography," or MUSCOT, algorithm used by Toshiba. Z filtering allows the system to trade off z-axis resolution (the SSP) with image noise (which directly correlates with required dose).

adaptive axial interpolation, the spiral pitch is freely
ctable in the range 0.5–2.0, and the same effective section
h, which is defined as the FWHM of the spiral SSP, is
erated at all pitch values. Therefore, longitudinal resolution is
pendent of pitch, unlike single-section spiral CT and multi–
ctor row CT that relies on 180° and 360° linear interpolation.
a consequence of the pitch-independent spiral section width,
image noise for a fixed tube current (in milliamperes) would
rease as pitch is decreased, owing to the increasingly
rlapping spiral acquisition. Instead, the user selects an
ective" milliampere-seconds value, and the tube current is
automatically adapted to the pitch of the spiral scan to
pensate for dose accumulation. The dose for fixed effective
ampere-seconds is independent of the spiral pitch and
als the dose of a transverse scan with the same milliampere-
onds setting
s, as a take-home point, unlike in single-section spiral CT a
nge in pitch does not result in a change in dose to the
ent. Accordingly, the use of a higher pitch does not result in a
e saving, which is an important practical consideration with
systems that rely on adaptive axial interpolation.
intrinsic resolution of a multi–detector row spiral scan is
ermined by the choice of collimation (eg, four sections at 1.0
.5 mm). Z filtering makes it possible to reconstruct images
ospectively with different section widths from the same raw
data set. Only section widths equal to or larger than the
tion width of one active detector row can be obtained. In
ny cases, both thick sections for initial viewing and recording
thin sections for detailed diagnosis or as an input for
anced 3D postprocessing are routinely reconstructed.
thinnest available section width is the collimated section
th (1.0 mm for four sections at 1.0-mm collimation), which is
ated by using nonlinear spiral weighting functions at the
ense of increased image noise and increased susceptibility to
facts. Thus, as a take-home point, the thinnest available
tion should only be used for high-contrast applications such
high-spatial-resolution lung imaging. For general purpose
nning, a 1.25-mm section width for four-section CT at 1.0-mm
imation (and 3.0-mm section width for four sections at 2.5-
collimation) is recommended as the most suitable trade-off

noise to allow detection of low-contrast details (eg, neurologic examinations of posterior fossa or cervical spine). In the head, partial volume artifacts typically manifest as dark streaks or areas of hypoattenuation and are due to a nonlinear effect .Figure shows an example of a patient who underwent follow-up CT after surgical removal of a pituitary tumor. From the same scan data—four sections at 1.0-mm collimation—both 4.0-mm-thick images with a standard head kernel for soft-tissue evaluation and 1.0-mm-thick images with a bone kernel were reconstructed. For best image quality, the posterior fossa should be scanned with a collimated section width not larger than 1.25 mm, whereas wider collimation can be used in the supratentorial region

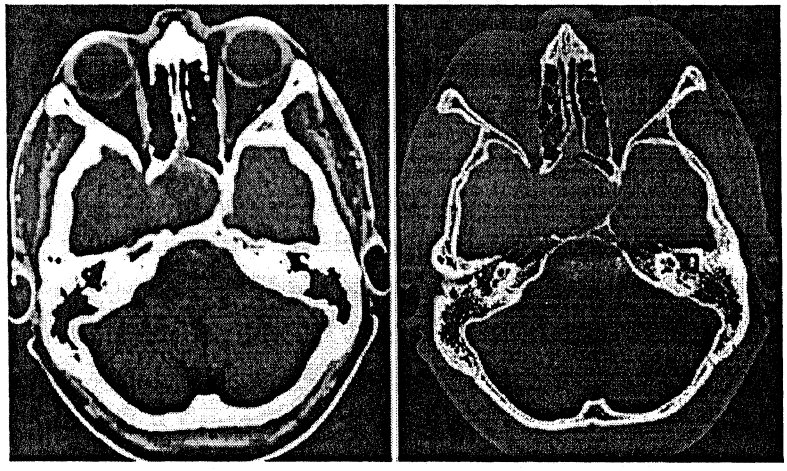

SPIRAL SCANS AND IMAGE-RECONSTRUCTION TECHNIQUES

Spiral scanning is the method of choice for the majority of all multi–detector row CT examinations and requires more attention than does sequential multi–detector row CT because it is conceptually more demanding.

Definition of Spiral Pitch

An important parameter for characterizing a spiral CT scan is the pitch. According to International Electrotechnical Commission specifications, the pitch *(p)* is given by

$$p = TF/W$$

/here TF is the table feed per rotation, and *W* is the total width f the collimated beam. This definition holds for both single-ection and multi–detector row CT. It shows whether data cquisition occurs with gaps ($p > 1$) or with overlap ($p < 1$) in the ngitudinal direction. With 16 sections at 0.75-mm collimation nd a table-feed of 18 mm per rotation, the pitch is $p = 18/(16 \times .75) = 18/12 = 1.5$. With four sections at 1.0-mm collimation and table-feed of 6 mm per rotation, the pitch again is $p = 6/(4 \times 1) = 6/4 = 1.5$. In the early days of four-section CT, the term *etector pitch* had been additionally introduced, which accounts or the width of a single section in the denominator. For the sake f clarity and uniformity, the detector pitch should no longer be sed.

hort Review of Single-Section Spiral CT Reconstruction

piral CT requires an interpolation of the acquired measurement ata in the longitudinal (through-plane) direction to estimate a omplete CT data set at the desired plane of reconstruction. The ost commonly used single-section spiral interpolation schemes re the 360° and 180° linear interpolation methods.

he 360° linear interpolation method exploits the 360° periodicity f the projection data. For each projection angle, a linear nterpolation is performed between those two projections on ither side of the image plane that are positioned closest to the mage plane and are 360° apart (ie, are measured in subsequent otations). The 180° linear interpolation technique makes use of he fact that for each measurement ray, an interpolation partner s already available after approximately half a rotation, when the -ray tube and detector have exchanged positions. This is the o-called complementary ray. In spiral CT, z-axis resolution is etermined not only by the collimated beam width (as in sequential scanning) but also by the effective section width, vhich is established in the spiral interpolation process. Usually, he effective section width is defined as the FWHM of the SSP. Effective section width increases with increasing pitch for both 360° and 180° linear interpolation, and longitudinal resolution degrades

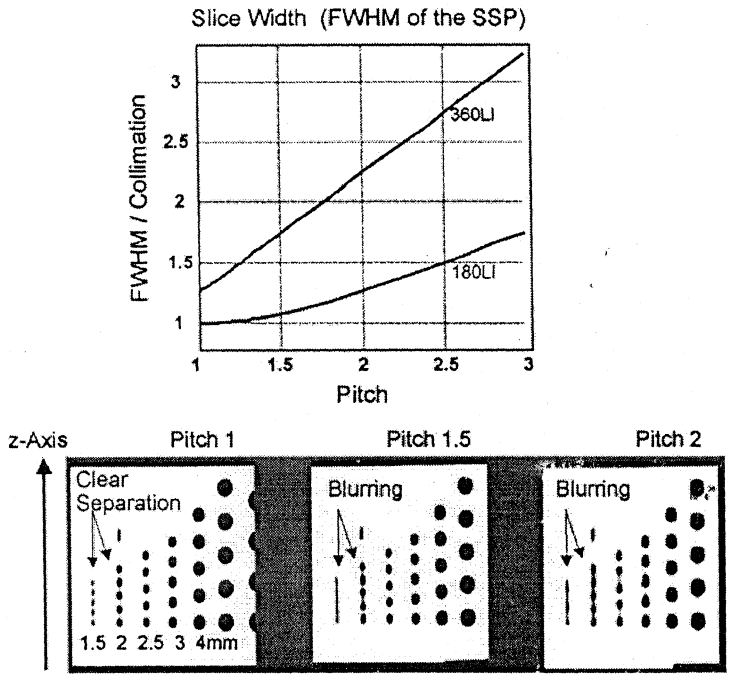

This is a consequence of the increasing longitudinal distance of the projections used for spiral interpolation. With 180° linear interpolation, the effective sections width equals the collimated section width at a pitch of 1, but effective section width equals 1.27 times the collimated width at a pitch of 2, so that a collimated 5-mm-thick section is an actual 6.4-mm-thick section at a pitch of 2. The image noise in single-section spiral CT is independent of the pitch if the tube current (in milliamperes) is left unchanged, and patient dose decreases with increasing .Single-section spiral CT is based almost exclusively on 180° linear interpolation, owing to the narrower SSP of this algorithm, despite its increased susceptibility to artifacts and increased image noise. For the same milliampere-seconds setting, image noise is about 15% higher than that in sequential CT mode. Spiral artifacts gradually increase as pitch is increased. Spiral artifacts typically manifest as hyper- or hypoattenuating "windmill" structures surrounding z-axis inhomogeneous high-contrast objects (eg, bones), which rotate when scrolling through a stack of images. Spiral artifacts are caused by the spiral interpolation process and can also be observed on multi–detector row CT images (see Fig 8). With single-section CT, scanning at a higher pitch is often used to reduce patient dose at

e expense of section broadening—if the collimation is kept nstant—and increased spiral artifacts. For CT angiographic plications in particular, it is more favorable to scan a given ume in a given time by using narrow collimation at a high pitch her than wider collimation at a low pitch. The motivation for creasing pitch and reducing collimation is to improve ngitudinal resolution by narrowing the SSP .

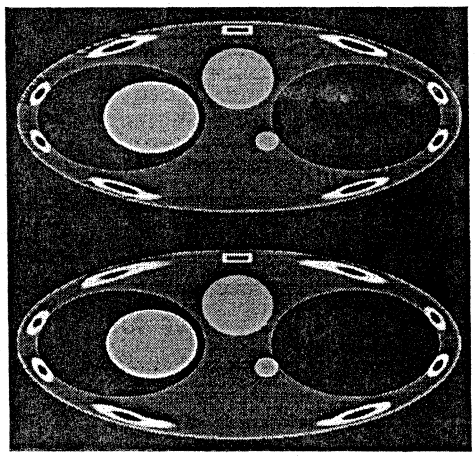

ansverse sections of anthropomorphic thorax phantom from -section CT at 0.75-mm collimation and pitch of 1. Images ere reconstructed with adaptive multiplanar reconstruction MPR; Siemens), with 1.0-mm (top) and 3.0-mm (bottom) ction width. Spiral interpolation artifacts are reduced with ctions widths that are thick relative to collimation. In clinical actice, best image quality for a desired section width is btained by acquiring narrow-collimation data.

ne Cone-Angle Problem in Multi–Detector Row CT

wo-dimensional image-reconstruction approaches used in ommercially available single-section CT scanners require all easurement rays that contribute to an image to run in a plane erpendicular to the patient's longitudinal axis. In multi–detector w CT systems, this requirement is violated. Figure shows the eometry of a four-section scanner: The measurement rays are ted by the so-called cone angle with respect to the center ane. The cone angle is largest for the sections at the outer dges of the detector, and it increases as the number of detector

between longitudinal resolution, image noise, and artifacts, in particular when thin sections are reconstructed as an input for 3D postprocessing such as for MPR, maximum intensity projection, or volume-rendering techniques. For a 1.25-mm spiral section width reconstructed from four-section CT at 1.0-mm collimation, 0.61–0.69 times the dose (depending only slightly on spiral pitch) is required to maintain the image noise of a sequential scan at the same collimation. Unlike 180° and 360° multidetector linear interpolation, image noise is therefore practically independent of pitch at constant dose.

For a given collimation, such as four sections at 2.5 mm, image quality can be optimized with regard to spiral artifacts by lowering the pitch. Another means to reduce spiral artifacts is to use narrow collimation: A given section width (eg, 3.0 mm) can be obtained with different collimations, in this case four sections at 1.0 mm and at 2.5 mm. For optimum image quality, collimation that is narrow relative to the desired section width is preferable. Furthermore, a more rectangular SSP can be established. Figure shows the SSPs of a 3.0-mm section for four-section CT at both 1.0- and 2.5-mm collimation.

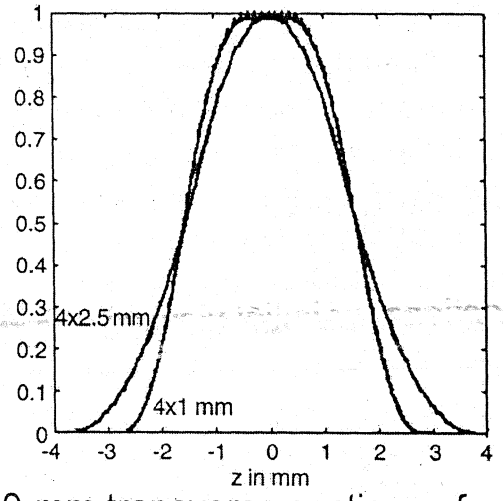

Figure shows 3.0-mm transverse sections of a thorax phantom scanned with four-section CT at 2.5- and 1.0-mm collimation. Despite the higher pitch, the 3.0-mm image obtained at 1.0-mm collimation shows fewer artifacts. Similar to single-section spiral CT, narrow collimation at high pitch is preferable to wide collimation at low pitch for artifact reduction.

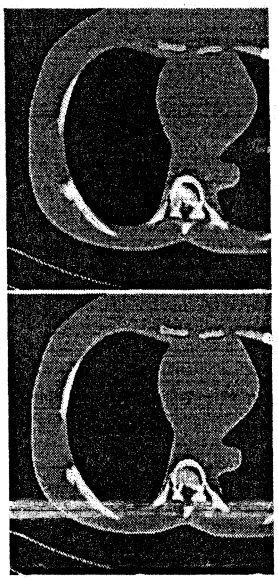

cept for a minor dose increase due to the different relative
ntributions of the penumbral zones of the dose profile,
anning at narrow collimation does not result in higher radiation
se to the patient as long as the effective milliampere-seconds
el is kept constant. Narrow-collimation scanning should,
refore, be the protocol of choice for all applications that
uire 3D postprocessing as part of the clinical evaluation. In
clinical treatment of uncooperative or trauma patients or for
otocols such as routine oncologic staging, the use of wider
limation can be considered. The best suppression of spiral
facts is achieved by using both narrow collimation (relative to
desired section width) and reduced spiral pitch.
general, more challenging clinical protocols, such as CT of the
ne and of the skull base, are reliant on a combination of
rrow collimation and low pitch. When multi–detector row spiral
of the head is performed with narrow collimation, low pitch,
d z-filter reconstruction of wider sections, the results are
uivalent to those of traditional sequential CT. Figure shows an
ample of a head scan performed with a four-section CT
stem in which a sequential image (two-section CT at 8 mm)
d a spiral image (8-mm section width from four-section CT at
mm collimation) are compared in the same patient.

Some manufacturers who use a z-filter approach do not provide completely free selection of the spiral pitch but recommend a selection of fixed pitch values (eg, pitch of 0.625, 0.75, 0.875, 1.125, 1.25, 1.375 and 1.5 for four-section CT with the MUSCOT algorithm that are aimed at optimizing the z-axis sampling scheme and reducing spiral artifacts.

MULTI–DETECTOR ROW SPIRAL RECONSTRUCTION APPROACHES THAT ACCOUNT FOR CONE-BEAM GEOMETRY

Overview of Cone-Beam Reconstruction Algorithms

For CT scanners with 16 or more detector rows, modified reconstruction approaches that account for the cone-beam geometry of the measurement rays have to be considered. Some manufacturers (Toshiba, Philips) have extended the Feldkamp algorithm, an approximate 3D convolution back-projection reconstruction that was originally introduced for sequential scanning, to multisection spiral scanning. With this approach, the measurement rays are back projected into a 3D volume along the lines of measurement, accounting in this way for their cone-beam geometry. Three-dimensional back projection is computationally demanding and requires dedicated hardware to achieve acceptable image-reconstruction times. Other manufacturers use variations and extensions of nutating-section algorithms for image reconstruction. These algorithms split the 3D reconstruction task into a series of conventional two-

nensional reconstructions on tilted intermediate image planes, his way benefiting from established and very fast two-nensional reconstruction techniques. Representative examples e AMPR (Siemens) and the weighted hyperplane construction (proposed by GE Medical Systems) techniques.

MPR Method

e AMPR approach is an extension and generalization of the dvanced single-slice rebinning" method. AMPR allows free ection of the spiral pitch with optimized dose utilization, which beneficial for medical applications. With advanced single-slice binning, a partial scan interval (about 240° of scan data) is ed for image reconstruction. The image planes are no longer rpendicular to the patient axis; instead, they are tilted to match e spiral path of the focal spot; see Figure for a 16-section anner at a pitch of 1.5. For every view angle in this partial scan erval, the focal spot is positioned in or near the image plane—at is, measurement rays running in or very close to the image ane are available. These conditions need to be fulfilled for a andard two-dimensional reconstruction. In a final z-axis formation step, the traditional transverse images are calculated interpolating between the tilted original image planes.

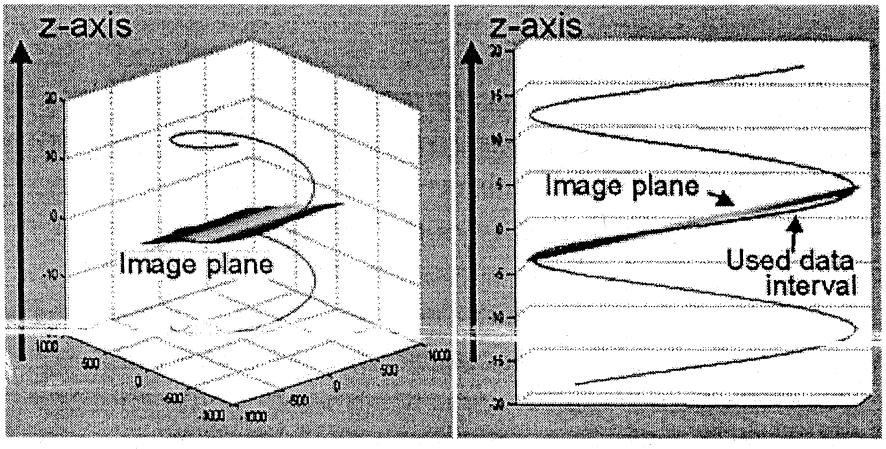

dvanced single-slice rebinning encounters its limitations when e spiral pitch is reduced to make use of the overlapping spiral cquisition and the resulting dose accumulation. The AMPR

algorithm addresses this problem: Instead of all available data being used for a single image, the data are distributed to several partial images on double-oblique image planes, which are individually adapted to the spiral path and fan out like the pages of a book (Fig left). To ensure full dose utilization the number of partial images ("pages" in the book), as well as the length of the data interval per image, depend on the spiral pitch. The final transverse (or arbitrarily oriented) images are calculated by means of z-axis interpolation between the tilted partial image planes (Fig right). The shape and the width of the z-axis interpolation functions are selectable. Different SSPs and different section widths can therefore be adjusted, so that z-axis resolution (SSP) can be traded off with image noise. The spiral pitch is freely selectable and the section width—and consequently the z-axis resolution—are independent of the pitch. The concept of effective milliampere-seconds and automatic adaptation of the tube current to the pitch also apply to AMPR

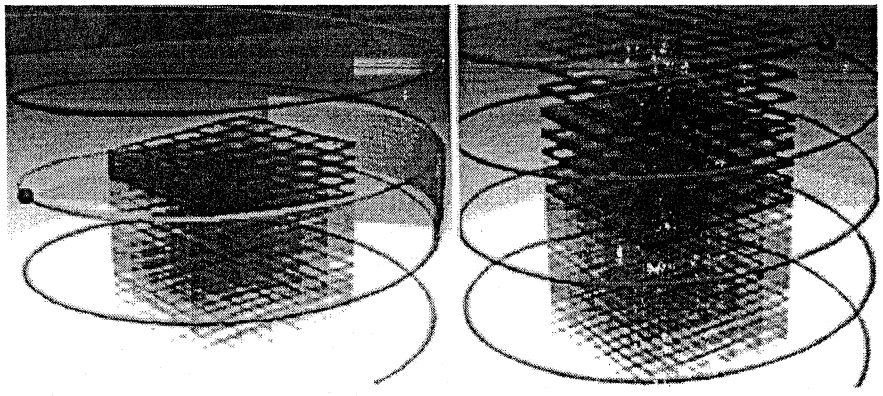

With the AMPR approach, sufficient image quality is obtained for all pitch values between 0.5 and 1.5. Figure shows transverse sections and MPRs of an anthropomorphic thorax phantom. Scan data for 16 sections at 0.75-mm collimation and pitch of 1 were reconstructed with 1-mm section width with z filtering, the AMPR algorithm, and 3D back projection. Neglecting the cone angle leads to artifacts at high-contrast objects and geometric distortions, particularly in MPRs (Fig top). Both AMPR and 3D back projection restore the spatial integrity of the high-contrast objects, reduce cone-beam artifacts, and are fully equivalent for 16-section scanning. Recent studies have demonstrated the

quacy of extended versions of AMPR for medical CT systems
up to 64 detector rows.

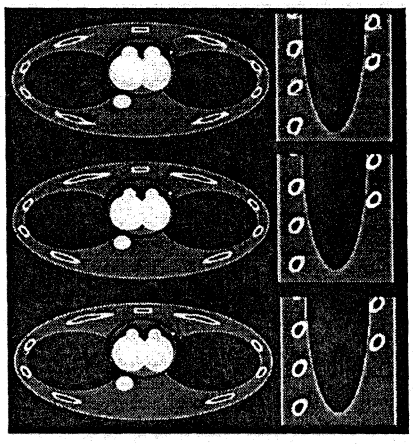

remaining artifacts in Figure are spiral interpolation artifacts
dmill artifacts), not cone-beam artifacts. Windmill artifacts are
related to the cone-beam geometry and result from the finite
h of the detector rows, which require interpolation between
ows for image reconstruction. Hence, windmill artifacts occur
pendent of the reconstruction approach. They are
ggerated in the mathematic phantom shown (Fig) and can
educed by decreasing the pitch and/or

easing the reconstruction section width relative to the
mation. Figure shows MPRs of a z-axis resolution phantom
nned with 16-section CT at 0.75-mm collimation and pitches
.75, 1.0, 1.25, and 1.5. Independent of the pitch, all cylinders
n to 0.6 mm in diameter can be resolved, the MPRs are
tively free of geometric distortions, and the spatial integrity of
3D image is maintained.

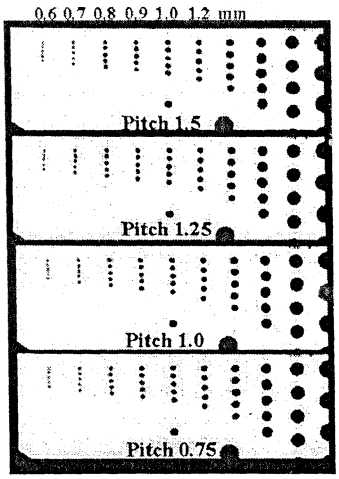

Multi–detector row spiral CT with AMPR is characterized by the same key properties as adaptive axial interpolation, which can be directly derived from information in the section on z-filter reconstruction presented earlier in this review. Thus, all recommendations regarding selection of collimation and pitch that were discussed there also apply for AMPR. In particular, a change in pitch does not result in a change in radiation exposure to the patient, and the use of higher pitch does not result in dose saving. Narrow collimation should be used whenever possible. With 16-section 0.75-mm-collimation CT, the thinnest available reconstruction section width of 0.75 mm is created by using nonlinear weighting functions at the z-axis image-reformation step, at the expense of increased image noise and increased susceptibility to artifacts. As a take-home point, this approach again should only be used for high-contrast applications such as high-spatial-resolution lung imaging. When thin sections are reconstructed as input for 3D postprocessing such as MPR, maximum intensity projection, or volume-rendering techniques, a 1.0-mm section width is recommended as the most suitable trade-off between longitudinal resolution, image noise, and artifacts.

Weighted Hyperplane Reconstruction

The weighted hyperplane reconstruction method, which has been described elsewhere, uses concepts related to AMPR but is derived differently. Similar to AMPR, 3D reconstruction is split

nto a series of two-dimensional reconstructions. Instead of econstruction of traditional transverse sections, convex yperplanes are proposed as the region of reconstruction. The ncreasing spiral overlap with decreasing pitch is handled by ntroducing subsets of detector rows, which are sufficient to econstruct an image at a given pitch value. At pitch of 0.5625 vith a 16-section scanner, the data collected by detector rows ne to nine form a complete projection data set. Similarly, rojections from detector rows two to 10 can be used to econstruct another image at the same z-axis position. Projections from detector rows three to 11 yield a third image nd so on. In a way, these "subimages" are related to the "book ages" of AMPR. The final image is based on a weighted verage of the subimages. By performing parameter ptimizations, an optimal balance among various system erformance parameters, such as noise, artifacts, and SSPs, can e achieved.

ECG-SYNCHRONIZED SCAN AND IMAGE-RECONSTRUCTION TECHNIQUES

One of the most exciting new applications of multi–detector row CT is the ability to image the heart and the cardiothoracic anatomy without motion artifacts. For ECG-synchronized scanning of the cardiothoracic anatomy, either ECG-triggered sequential scanning or ECG-gated spiral scanning can be used. In ECG-triggered sequential scanning, the heart volume is covered by subsequent transverse scans with a step-and-shoot technique. For each transverse scan, the number of images corresponds to the number of active detector sections. A partial scan data interval is acquired with a predefined temporal offset relative to the R waves of the patient's ECG trace, which can be either relative (as a certain percentage of the R-R interval) or absolute (in milliseconds) and either forward or reverse. Some 16-section CT systems offer gantry rotation times shorter than 0.5 second (eg, 0.42, 0.40, or 0.37 second). In this case, temporal resolution can be as good as 0.21, 0.20, or 0.185 second.

With retrospective ECG gating, the heart volume is covered continuously by a spiral scan. The basic concepts for ECG-gated spiral imaging, such as single-segment and multisegment reconstruction, had already been developed in 1998. The patient's ECG signal is recorded at the same time the CT data are acquired to allow retrospective selection of the data segments used for image reconstruction. Only scan data acquired in a predefined cardiac phase, usually the diastolic phase, are used for image reconstruction. The data segments contributing to an image begin with a user-defined offset relative to the onset of the R waves, similar to ECG-triggered sequential scanning. Image reconstruction generally consists of two steps: multi–detector row spiral interpolation to compensate for the continuous table movement and to obtain scan data at the desired image z-axis position, followed by a partial scan reconstruction of the transverse data segments. The temporal resolution of an image can be improved up to $t_{rot}/(2N)$ by using scan data of N subsequent heart cycles for image formation in a so-called multisegment reconstruction mode, where t_{rot} is the gantry rotation time of the CT scanner. With increased N, better temporal resolution is achieved but at the expense of slower volume coverage: Increased N and slower patient heart rate require a reduction in spiral pitch.

Multisegment approaches rely on a complete periodicity of the heart motion, and these approaches encounter their limitations in patients with arrhythmia or a heart rate that changes during scan acquisition. Multisegment reconstruction may improve image quality in selected cases, but the reliability of good-quality image acquisitions with N-segment reconstruction is compromised with increases in N.

In general, clinical practice suggests the use of one segment at lower heart rates and two or more ($N \geq 2$) segments at higher heart rates. Use of single-segment versus multisegment reconstruction is integrated in the data acquisition process in a variety of ways, depending on the scanner type. One approach consists of automatic division of the partial-scan data segment into one or two subsegments, depending on the patient's heart rate during acquisition ("adaptive cardio volume" algorithm. With a different approach, single-segment partial-scan images are prospectively reconstructed as baseline images, followed by

etrospective two-segment reconstruction for improved temporal esolution in patients with a higher heart rate. Yet another pproach is prospective adjustment of the gantry rotation time to e heart rate of the patient to obtain an optimized temporal esolution for a multisegment reconstruction. Again, this pproach requires a stable and predictable heart rate during can acquisition.

rospective ECG triggering combined with sequential step-and-hoot acquisition of transverse sections has the benefit of maller patient dose than that of ECG-gated spiral scanning, ecause scan data are acquired only during the desired heart hases. However, this technique does not provide continuous olume coverage with overlapping sections, and misregistration f anatomic details cannot be avoided. Furthermore, econstruction of images in different phases of the cardiac cycle or functional evaluation is not possible. Since ECG-triggered equential scanning depends on a reliable prediction of the atient's next R-R interval by using the mean of the preceding R- intervals, the method encounters its limitations in patients with rrhythmia. To maintain the benefits of ECG-gated spiral CT but educe patient dose, ECG-controlled dose modulation has been eveloped .The major improvements of 16-section CT, ompared with established four-section scanners, include mproved temporal resolution due to shorter gantry rotation time, etter spatial resolution owing to submillimeter collimation, and onsiderably reduced scan acquisition times. The time to cover he entire heart volume (about 12 cm) with four-section CT at .0-mm collimation is about 40 seconds, which is at the limit for a can requiring patient breath holding. ECG-gated CT of the ntire thorax or the aorta is not possible within reasonable scan urations. For a 16-section CT system, the time to cover the ntire heart volume with submillimeter collimation is about 15 econds. With 16-section CT, coverage of the entire thorax (30 m) can be completed in about 38 seconds at 0.75-mm ollimation and in about 19 seconds at 1.5-mm collimation. ECG-ated examinations of extended cardiothoracic anatomy became easible with 16-section CT, which lends itself to a spectrum of pplications where suppression of cardiac pulsation is desired. ypical diagnostic pitfalls caused by transmitted cardiac ulsation can be avoided, such as an artifactual intimal flap

resembling dissection in the ascending aorta. Suppression of cardiac pulsation improves the assessment of paracardiac lung segments and allows confident exclusion of small peripheral pulmonary emboli in segmental and subsegmental arteries. In routine thoracic studies, which are not synchronized to the patient's ECG signal, cardiac motion usually precludes the assessment of coronary bypass grafts.

FUTURE DIRECTION OF MULTI–DETECTOR ROW CT

Sixty four section CT, which has become widely available, enables truly isotropic submillimeter imaging for virtually any application. In the case of cardiac imaging, 64-section CT sets today's benchmark in spatial resolution for noninvasive coronary artery imaging. Motion artifacts in patients with a higher heart rate remain the most important challenge for multi–detector row coronary CT angiography, although diagnostic image quality can be achieved in most cases by administering ß-blockers to such patients. Improved temporal resolution is desirable in the future to prevent the need for heart rate control. Increased gantry rotation speed, rather than multisegment reconstruction, appears to be preferable for robust clinical performance. Obviously, substantial development efforts are needed to account for the notable increase in mechanical forces (about 17*g* for 0.42-second rotation, >33*g* for 0.3-second rotation) and increased data transmission rates. A rotation time of less than 0.2 second (mechanical force > 75*g*), which is required to provide a temporal resolution of less than 100 msec independent of heart rate, appears to be beyond today's mechanical limits. An alternative to further increases in rotation speed is to reconsider the scanner concept with multiple tubes and multiple detectors that had already been described in the early years of CT.

Owing to its ease of use and its widespread availability, general-purpose CT continues to evolve into the most widely used diagnostic modality for routine examinations, especially in emergency situations or for oncologic staging. CT primarily provides morphologic information; in combination with other modalities, however, functional and metabolic information can also be obtained. Therefore, combined systems for obtaining

omprehensive structural and functional diagnoses will gain ncreasing importance in the near future.
he combination of state-of-the-art multi–detector row CT with ositron emission tomographic (PET) scanners, for instance, pens a wide spectrum of applications ranging from oncologic taging to comprehensive cardiac examinations. The clinical otential of these scanners is currently being evaluated.
econstruction of the CT images in a sufficient field of view ithout truncation of anatomic structures (eg, arms) is a rerequisite for adequate attenuation correction of the PET mages. An enlarged field of view of up to 70 cm can be realized y extrapolating from the measured CT data. Pertinent lgorithms can be found in, for example, Figure shows MPRs om CT images in a 46-year-old man with renal cancer who had ndergone nephrectomy and chemotherapy, with PET images uperimposed. Areas with increased metabolism are enhanced, nd a metastatic mediastinal lymph node can be identified, which upports the notion of PET as adding a "new contrast agent" to T.

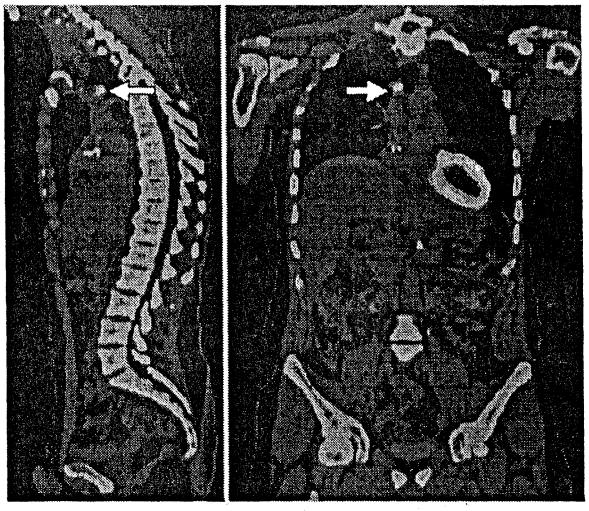

ystems that combine CT and single-photon emission computed omography are another promising modality. Potential applications are currently being investigated and range from the ocalization of parathyroid lesions and heterotopic splenic tissue o detection of recurrent nasopharyngeal carcinomas to imaging f aortic prosthesis infection.

CT virtual simulation is gaining increasing importance with a more widespread adoption in 3D conformal and intensity-modulated radiation therapy. With general-purpose CT systems that have a gantry opening with a typical diameter of 70 cm, some patients (eg, women with breast cancer) cannot always be scanned in the treatment position. Such applications, along with interventional procedures and trauma protocols, will be facilitated by CT systems with a larger bore. Recently, concepts have been introduced for four- and 16-section CT scanners with a bore diameter of up to 85 cm and a reconstruction field of up to 82 cm, owing to image reconstruction based on data extrapolation. These systems will probably gain considerable importance in the near future, in particular with regard to the dramatically increasing number of severely obese patients in the Western countries.

For general purpose CT, we will witness a moderate increase in the number of simultaneously acquired sections in the near future. A new generation of CT systems with 32, 40 and—in combination with refined z-axis sampling techniques—64 simultaneously acquired sections are currently being introduced. However in contrast to the transition from single-section to four- and 16-section CT, clinical performance will improve only incrementally with further increases in the number of detector rows. The achievable clinical benefit will have to be carefully considered in the light of the necessary technical efforts and the cost. Clinical progress can more likely be expected from further improvements in spatial resolution rather than from an increase in the volume-coverage speed. In clinical reality, the latter has only rarely been a limiting factor since the introduction of 16-section CT. As soon as all relevant examinations can be performed in a comfortable breath hold of not more than 10 seconds, a further increase in the number of sections will not provide a substantial clinical benefit.

At this point, a qualitative enhancement of CT that allows new clinical applications may again bring substantial clinical progress with, for example, the introduction of area detectors large enough to cover entire organs such as the heart, kidneys, or brain in one sequential scan (approximate scan range, 120 mm). With these systems, dynamic volume scanning would become feasible,

ich would open up a whole spectrum of new applications such
functional or volume perfusion studies.
ea-detector technology is currently under development, but no
mmercially available system so far fulfills the requirements of
edical CT with regard to contrast resolution and fast data
adout. A scanner with 256 0.5-mm detector elements has been
oposed by one manufacturer and appears to be conceptually
omising, but this system is still in the prototype stage.
ototype systems by other vendors use cesium iodide–
norphous silicon flat-panel detector technology that was
ginally used for conventional angiography, which is limited in
ms of low contrast resolution and imaging speed. Owing to the
rinsic slow signal decay of flat-panel detectors, rotation times
at least 20 seconds are needed to acquire a sufficient number
projections (≥600 projections). The spatial resolution of such
stems is excellent, though, because of the small detector pixel
ze. Excessive dose requirements to date, however, preclude
e examination of larger objects. Initial experimental results are
us limited to small high-contrast objects such as joints, the
ner ear, or contrast material–filled vessel specimens.
gure shows a prototype set-up, where a flat-panel detector was
corporated into a standard CT gantry (Somatom Sensation 16;
emens). The detector covers a 25 x 25 x 18 cm scan field of
ew, and the pixel size is 0.25 x 0.25 mm, both measured at the
nter of rotation.

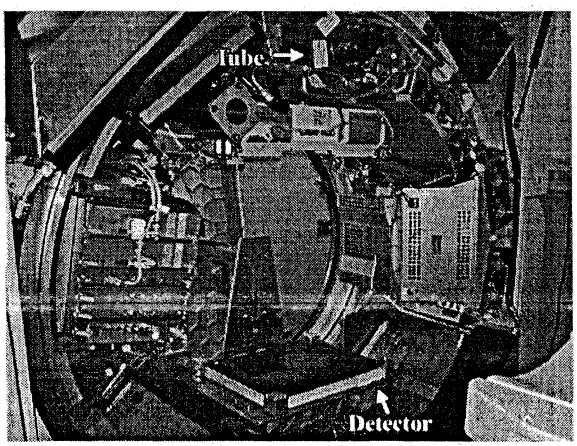

igure shows volume renderings of a heart specimen (80 kV, 20
A, 20-second gantry rotation) that demonstrate excellent

spatial resolution, which enables visualization of even very small side branches of the coronary artery tree.

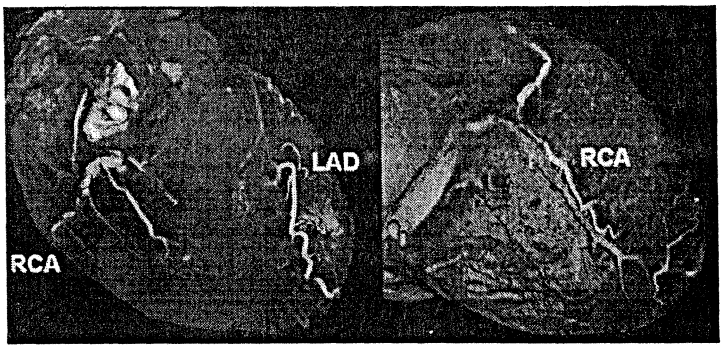

The combination of area detectors that provide sufficient image quality with fast gantry rotation speed will be a promising technical concept for medical CT systems. The vast spectrum of potential applications may bring about another quantum leap in the evolution of medical CT imaging; however such systems will probably not be available in the near future.

POST PROCESSING THE DATA

The raw data acquired by the CT scanner is preprocessed before reconstruction. Numerous pre-processing steps are performed. Electronic detector systems produce a digital data set that is easily processed by a computer. Calibration data determined by the air scans provide correction data that are used to adjust the electronic gain of each detector in array. Variation in geometric efficiencies caused by imperfect detector alignments is also corrected. For example: in fourth generation scanners, the X-ray source rotates in an arch around each of the detectors in the array. As the angle and the distance between the detectors and the X-ray tube changes. These geometric efficiencies are measured during the calibration scans and stored in the computer. They are corrected in preprocessing steps.

After the digital data are cal liberated. The logarithm of the signal is computed by the following equation

$$\ln(I_0/I_t)=\mu t$$

here I_0 is the reference data, I_t is the data corresponding to
ch ray in each view, t is the patients overall thickness (in cm)
each ray. And μ is the linear attenuation coefficient (in cm^{-1}).

TERPOLATION HELICAL:

elical CT scanning produces a data set in which the X-ray
urce has traveled in a helical trajectory around the patient.
esent- day CT reconstruction algorithms assume that the X-ray
urce has negotiated a circular, not helical, path around the
tient. To compensate for these differences in the acquisition
eometry, before the actual CT reconstruction the helical data
t is interpolated into a series of planar image data set.
though interpolation represents an additional step in
mputation, it also enables an important feature. With
nventional axial scanning, the standard is to acquire
ntiguous images, which abut one another along the cranio-
udal axis of the patient. With helical scanning, however, CT
ages can be reconstructed at any edge of the scanned
lume. Helical scanning allows the production od additional
erlapping images with no additional dose to the patient. The
nsitivity of the CT images to objects not centered in the voxel
reduced, and therefore subtile lesions, which lay between two
ntiguous images, may be missed. With helical scanning, in
terleaved reconstruction allows the placement of additional
ages along the patient, so that the clinical examination is
most uniformly sensitive to subtle abnormalities. Interleaved
construction adds no additional radiation dose to the patient,
t additional time is required to reconstruct the images.
though an increase in the image count would increase the
terpretation time for tradiational side-by- side image
esentation, this concern will ameliorate as more CT studies
e read by the radiologist at computer workstation.
is important not to confuse the ability to reconstruct CT images
short intervals along the helical data set with the axial
solution itself. The slice thickness dictates the actual spatial
solution along the long axis of the patient.
or example: images with 5 mm thickness can be reconstructed
very 1mm, but this does not mean that the image is sampled at
mm intervals. To put the example ion technical terms, the

sampling pitch is 1mm but the sampling aperture is 5mm. In practice, the use of interleaved reconstruction much beyond a 2:1 interleave yields diminishing in returns, except for multiplanar reconstruction or 3D volume rendering.

SIMPLE BACK PROJECTION

Once the image raw data have been pre- processed, the final step is to use the planar projection data sets to reconstruct the individual tomographic images. As a basic introduction to the reconstruction process, assume that a very simple 2X2 "image" is known only by the projection values. Using algebra, one can solve for the image values in the simple case of 4-pixel image. A modern CT image contains approx. 205,000 pixels or "unknowns", and each of the 800,000 projections represent an individual equation. Solving this kind of a problem is beyond simple algebra, and back projection is the method of choice. Simple back projection is a mathematical process, based on trigonometry, which is designed to emulate the acquisition process in reverse. Each ray in each view represents an individual measurement of μ. In addition to the value of μ for each ray, the reconstruction algorithm also "knows" the acquisition angle and position in the detector array corresponding to each ray. Simple back projection starts with an empty image matrix, and the μ value from each ray in all views are smeared or back projected onto the image matrix. In other words, the value of is added to each pixel in a line through the image corresponding on the rays path.

Simple backprojection comes from vary close to reconstructing the CT image as desired. However a characteristic l/r blurring is a byproduct of simple back projection. Imagine that a thin wire is imaged by a CT scanner perpendicular to the image plane; this should ideally result in a small point on the image. Rays not running through the wire will contribute little to the image (μ =0). The back projected rays, which do run through the wire, will converge at the position of the wire in the imaging plane, but these projections run from one edge of the reconstruction circle to the other. These projections will therefore "radiate" geometrically in all directions away from a point input. If the image gray scale is measured as a function of

stance away from the center of the wire, it will gradually minish with a I/r dependency. Where r is the distance away m the point. This phenomenon results in a blurred image of e actual object. When simple back projection is used. A filtering ep is therefore added to correct this blurring, in a process own as filtered back projection.

LTERED BACKPROJECTION RECONSTRUCTION

filtered back projection, the raw view data are mathematically ered before back projection onto the image matrix. The filtering ep mathematically reverses the image blurring, restoring the age to an accurate representation of the object that was anned. The mathematical filtering step involves convoluting e projection data with a convolution kernel. Many convolution rnels exist, and the different kernels are used for varying nical application such as soft tissue imaging and bone aging.
ne kernel refers to the shape of the filter function in the spatial omain, whereas it is common to perform the filtering step in the equency domain. Much of the nomenclature concerning filtered ck projection involves an understanding of the frequency omain. The fourier transform is used to convert a function in the patial domain into the spatial frequency domain, the inverse ourier transform is used to convert it back. Convolution is an tegral calculus operation.

The difference between filtered back projection and mple back projection is the mathematical filtering operation. arious convolution filters can be used to emphasize different haracteristics in the CT images. The Lak filter, named for Dr. akshminarayanan, increases the amplitude linearly as a nction of frequency and is also called a ramp filter. The I/r urring function is the spatial domain becomes a I/f blurring nction in the frequency domain. Therefore, multiplying with lak ter, where L(f) = f, exactly compensates the unwanted I/f urring, because I/f x f = 1, at all f. this filter works well when ere is no noise in the data, but in X-ray images there is always -ray quantum noise, which tends to be more noticeable in the gher frequencies.

The Shepp- logan filter is similar to the Lak filter but incorporates some roll –off at higher frequencies, and this reduction in amplification at higher frequencies has a profound influence in terms of reducing high-frequency noise in the final CT image. The Hamming filter has even more pronounced high frequency roll-off, with better high frequency noise suppression.

BONE KERNELS AND SOFT TISSUE KERNELS

The reconstruction filters derived by Lekshminarayanan, Shepp and Logan, and hamming provide the mathematical basis for CT reconstruction filters. In clinical CT scanners, the filters have more straightforward names, and terms such as "bone filter" and "soft tissue filter" are common among the CT manufacturers. The term kernel is also used. Bone kernel have less high- frequency roll- off and hence accentuate higher frequencies in the image at the expense of increased noise. CT images of the bone typically have very high contrast(high signal), so the SNR is inherently quite good. Therefore, these images can afford a slight decrease in SNR ratio in return for sharper detail in the bone region of the image.

For clinical application in which high spatial resolution is less important than high contrast resolution. For Example: in scanning for metastatic disease in the liver- soft tissue reconstruction filters are used. These kernels have more role off in higher frequencies and therefore produces images with reduced noise but lower spatial resolution. The resolution of an image is characterised by the modulation transfer function (MTF); The high spatial resolution MTF corresponds to use of the bone filter at small FOV, and the standard resolution corresponds to images produced with the soft tissue filter at large FOV.

CT NUMBERS AND HOUNSFIELD UNITS

After CT reconstruction, each pixel in the image is represented by a high precision floating point number that is useful for

mputation but less useful for display. Most computer display ardware makes use of integer images. Consequently, after CT construction, but before storing and displaying. CT images are rmalized and truncated to integer values. The number of T*(x,y),* in each pixel, *(x,y),* of the image is converted using the llowing expressions:

$$CT(x,y) = 1000 \frac{M(x,y) - \mu_{water}}{\mu_{water}}$$

here μ(x,y) is the floating point number of the (x,y) pixel before nversion, μ_{water} is the attenuation coefficient of water, and CT ,y) is the CT that ends up in the final clinical image. The value f μ_{water} is about 0.195 for the X-ray beam energies typically sed in the Ct scanning. This normalization results in the CT umbern ranges from about –1000 to +3000, where –1000 rresponds to air, soft tissue ranges from –300 to –100, water is and dense bone and areas filled with contrast agent range up +3000.

T images are produced with a highly filtered, high KV X-ray eam, with an average energy of about 75keV. At this energy in ne muscle tissue, about 91% of X-ray interactions are Compton catter. For fat and bone, Compton scattering interactions are 4% and 74% respectively. Therefore, CT numbers and hence T images derive their contrast mainly from the physical roperties of tissue that influence Compton scatter. Density g/cm^3) is a very important discriminating property of tissue, and ne linear attenuation coefficient, μ, tracks linearly with density. ther than physical density.

ETECTORS AND DETECTOR ARRAYS.

enon Detectors:

Xenon detectors use high-pressure (about 25 atm) non-radioactive Xenon gas , in long thin cells between two metal plates. Although a gaseous detector does not have the same efficiency as a solid one, the detector can be made very thick (e.g.: 6 cm) to compensate in part for its relatively low density. The metal septa that separates the individual xenon detectors can also be made quite thin, and this improves the geometric efficiency by reducing the dead space between the detectors. The geometric efficiency is the fraction of the primary X-rays exiting the patient that strike the active detector elements

The long thin ionization plates of the xenon gas detector are highly directional. For this reason, xenon detectors must be positioned in a fixed orientation with respect to the X-ray source. Therefore, xenon detectors cannot be used for the fourth generation scanners, because those detectors have to record the X-ray source as moves over a very wide angle. Xenon detectors can be used only for third generation systems.

Xenon detectors for CT are ionization detectors- a gaseous volume is surrounded by two metal electrodes, with a voltage applied across the two electrodes. As X rays interact with the Xenon gas atoms and cause ionization., the electrical field between the plates cause the ions to move the electrodes, where the electronic chrge is collected. The electronic signal is amplified and then digitized, and its numerical value is directly proportional to the X-ray intensity striking the detector. Xenon detector technology has been surpassed by solid-state detectors, and its ues is now relegated to inexpensive scanners.

Solid state detectors

A solid state detector is composed of a scintillator coupled tightly to a photodetector. The scintillator emits visible light when it is struck by X-rays, just as in an X-ray intensifying screen. The light emitted by the scintillator reaches the photodetector, typically a photocathode, which is an electronic device that converts light intensity into electrical pulse proportional to the intensity. This scintillator-photocathode design of solid state CT detector is very similar in the concept to many digital radiographic X-ray

letector systems. However, the performance requirements of the CT are slightly different. The detector size in CT is measured in millimeters., whereas detector elements in igital radiography systems are typically 0.01 to 0.20mm on each side. CT requires a very high fideluity, low noise signal, typically digitized to 20 or more bits.

The scintillator used in solid state CT detectors varies among manufacturers, with $CdWO_4$, yttrium and gadolinium ceramics, and other materials being used, because the density and effective atomic number of the scintillators are subsequently higher than those of pressurized xenon gas, solid-state detectors typically have better x-ray absorbtion efficiency. However to reduce rosstalk between adjuscent detector elements, a small gap between detector elements is necessary, and this reduces geometric efficiency somewhat.

The top surface of solid state CT detectors is essentially flat and therefore is capable of x-ray detection over a wide range of angles, unlike the xenon detector. Solid-state detectors are required for fourth-generation CT scanners, and they are used in most high-tier third generation scanners as well.

ARTIFACTS IN CT.

In CT the final image is formed by some mathematical econstruction process, which make use of X-Ray neasurements in reconstructing the density of tissue at every oint in the slice. Any error of measurement will reflect as an rror in the reconstructed image, which may be a qualitative one r may be less obvious. Such a distortion of the image is called n artifact. Artifacts can be classified according to where their ause stem from - geometric errors, algorithm effects, ttenuation measurement error or photon spectrum effects.

Geometric Error.

hese are due to the situation in which not all rays measurement ccurred along line with the proper orientation in space - a

detector that is not located in its proper position, motion of the patient etc.

Algorithmic effects.

Those caused by the form of recon. algorithm used. Some of the algorithms helps to enhance the image for certain purposes, but this manipulation may often create image that can be misleading. Two effects both of which are due to geometric spreading of the imaged object will be considered

Point spread effect: It is noted that the size of an object with high +ve or

–ve contrast measured from the scan shows some apparent change in the measurement, and this increases with narrow window.

Edge enhancement effect: Arises from a deliberate effort to distort the true density relationship at sharp edges, and is known as edge enhancement. Example : False subarachnoid space in head scan with edge enhancement algorithm.

Attenuation Measurement Errors

These are caused by any malfunction of the detectors that causes an inaccurate attenuation measurement. Even this kind of errors in not completely independent of the patient. Eg: Streak artifacts produced from surgical clips.

There are three main causes of measurement errors.

Scattered radiation.

Faulty Detector.

Faulty x-ray source.

Faulty Detector:

Consider a condition in which one detector in the array is faulty, the resulting ray also became bad. As the source and detector rotate to form subsequent image the same ray will be inaccurate in every view. All these rays are targeted to a circle to form ring artifact. An error of only 0.1 % will cause easily observable circle in the image.

aulty x-ray source:

f the x-ray output varies during the scan process, an nconsistency in the collected data will immediately occur, since ne detectors can't distinguish this change in output. Fixed etector geometry are more sensitive to this output variations. Due to this effects some noise pattern will develop and can be orrected with a separate reference detector which rotate with ne x-ray tube in constant geometric relationship. Other possible -ray source error is momentarily high voltage arching and uctuations.

Photon spectrum Effect.

This is caused due to the attenuation produced in the x-ray energy spectrum as the beam passes through the patient. It is patient related in the sense that bone and barium produces serious artifacts.
There are two reasons why most CT artifacts appears as streaks.
Regardless of the algorithm used any single ray represent a measurement of x-ray transition along a specific straight path through the slice. Thus any error that affects only one ray would appear primarily on those pixels which lies along that ray – as a streak.
Rays that shows abrupt change from one view to another. Eg: streak due to patient movement.

Partial Volume Effect.

A voxel represent some finite volume of tissue in the body. If such a voxel contains more than one tissue type then the total content of the voxel are in effect linearly arranged. This effect is significant for relatively small anatomic structure size or for tissue volumes which are rapidly changing in size. These artifacts can be minimized by diminishing the slice thickness although it cannot be eliminated entirely unless beam hardening is also corrected for.

Motion artifacts

When the patient motion occurs the computer has no means to keeping track of where the pixels are in space and which ray path belongs to which row and column. This inconsistency leads to severe streaking and is specially aggravated by the presence of high density structures. The motion not only produces artifactual streaks but as in clinical radiography may cause both a loss of spatial resoln. and a loss of tissue resoln.

Poly chromatic effects.

The best known effect is beam hardening artifact. The basis of this artifact is the fact that in the reconstruction process one attempts to assign an attenuation coefficient value to each voxel within the patient. However attenuation value depends highly on energy of the x-ray beam. As the beam passes through the patient the lower energy photons are preferentially absorbed and we say that beam become harder. Any given voxel within the patient is viewed along different ray path for each different angular projections. The overall effect will be general decrease in the CT number. The visual result of these effect is dark streaks. Eg: inter petrous hypodensity streaks.

Couping artifact.

Seen in the interface of bony structure with adjoining soft tissue due to beam hardening effect. This is evident at the edge of the skull. The ray passing through the periphery of the structure suffers more hardening than those of the centre. So the central region appears darker.

Artifacts related to Spiral CT.

Stair Step artifacts.

Seen in high contrast longitudinal reformations and is manifested as a disruption of inclined surfaces in regular stair step fashion. It results from the use of interpolation algorithm associated with high contrast interfaces aligned obliquely to the direction of table motion. This artifact is more pronounced when high contrast

structures are more oblique to the direction of patient motion. To eliminate the artifact, both the collimation and the table feed should be less than the longitudinal dimension of the important features on inclined surface and the recon. interval should be less than the table feed.

Break up artifact.

Here the smooth transverse surface of a structure may be seen as irregular with break up at the edges. It is associated with cubic spline interpolation algorithm.

Flow / Contrast Enhancement Artifact

One of the practical problem of spiral CT is that images may be acquired too early after contrast injection. In the liver, unopacified hepatic vein in such instance should not be mistaken as pathological lesion. Filling defects in IVC are extremely common due to unopacified blood and should not be mistaken as thrombus. When thorough IVC delineation is required a second series of delayed images has to be obtained.

Aortic (Ghosting) Artifacts

A more noticeable artifact seen in the ascending aorta and that can simulate aortic dissection. This results from a combination of z - axis blurring and aortic pulsation. Careful inspection images will reveal that the curved thin lucency has extended just beyond the aortic wall in one of the images. This artifacts can be minimized by segmentation of image acquired under 2 sec. Instead of using data throughout 360^0 cycle, using only data in 60 - 120^0 rotation will yield images which are not affected by heart movement

HiSpeed CT/*i*-System specifications

HiSpeed CT/i (GE) is a top of the line helical CT scan system. Using 6.3 MHU x-ray tube which enables 60 sec. Continuous scan with 1 sec. rotation speed.
Generation: Third generation.

X-Ray tube:

Anode - Tungsten Rhenium focal track on a Molybdenum alloy substrate backed by Graphite.
Max. Potential - 140 kVp.
Filament supply - 7 V / 6.5A / 50Hz.
Heat storage : Anode – 6.3MHU..
Focal Spot : Small focus - 0.4 mm x 0.7 mm & 0.6 mm x 0.9 mm
Large focus - 1.2 mm x 1.2 mm
Target angle : 7^0

The system automatically select the filament as,
Small : When the technique is 24 KW or less.
Prescription includes detailed, bone or edge recon. Algorithm with KW fall in the range of 24-28.
Large : Technique more than 24 KW.
Technique : 24KW - 28 KW and prescription without bone, detail or edge recon. Algorithm.

KV Choices : 80, 100, 120, 140.
mA Choices : 40 - 400 in 10mA increments.

Exposure time :
Axial Scan - 1, 2, 3, and 4 Seconds.
Cine & Helical – 0.8 sec& 1 Sec.

Scout - 0.26 Sec. - 13.3 Sec. (Scan range 20-1000mm at 75 mm/sec.).

Collimation : 1, 3,5,7,& 10 mm.
Detectors : Hi Light Detectors.
Number: Scanning - 852 & Reference - 12.
Material : Solid Scintillator.
Channel spacing 1mm.
Dose Efficiency: 80% (Generative) and 99% Absorption.

AS (Data Acquisition System / Analog to Digital Converter

Channels : 752 Nos.
Sample rate : 984 Hz. Provides 984 views / m Sec.
Tube Control. Regulate : Rotor start and stop time.
Generators : High frequency.
- Comprised of anode and cathode tanks.
- Provides 36 - 48 KW of power.

n Board Computer.

his Computer controls KV, mA and provides mechanism for
formation input and put put across the slip ring.

antry.

Tilt : $+30^0$ to -30^0
Tilt speed : 1^0 / Sec.
Opening Diameter : 700 mm.
Isocentre to tube distance: 630 mm.
Tube focus to Detector : 1999 mm.
Alignment Light: O/P : < 1mW / Laser Beam.

able :

Load Capacity - 180 kg. With +/- 0.25 mm accuracy.
250 kg with +/- 1mm acuracy.
Cradle Travel: 1703 mm max.
Cradle speed : 5mm / Sec. minimum & 75mm/sec. max.

CT.Protocols

lead. – Non traumatic
Routine Head.

atient supine.
hin tucked down to make the anthropological line vertical.

- Scout lateral view of the whole skull.
- Section planes parallel to supra orbito metal line.
- Thin sections (3-5mm) through posterior fossa.
- 10mm sections above.

Technique: Thin sections in 2 seconds with 200mA.& 120 kVp.
10mm sections in 2 seconds with 170mA & 120 kVp.

Facial Bones.

- Patient supine and eyes should be closed to avoid eyeball movements.
- Chin tucked down to make the anthropological line vertical.
- Lateral scout scan.
- Scan sections parallel to IOM line.
- Scan through orbit.
- Slice thickness 3mm.

Technique: 3mm sections in 2 sec. with 200mA & 120kVp.

Coronal.

- Patient supine with neck hyperextended or prone with chin resting in the axial head holder.
- A lateral scanogram is used to select the gantry angulation.
- 3mm images from the orbital apex through the orbit.

Technique: 3mm sections in 2 sec. with 200mA & 120 kVp.

Orbits.

Axial.

- Patient supine & eye should be closed to avoid eye movements.
- Angle of mandible as the zero centering point.
- Lateral localiser scan of the whole skull.
- Scan sections parallel to the IOM line.
- Scan through orbits.
- 3mm slices.

Technique: 3mm sections in 2 seconds with 200 mA & 120 kVp.

Coronal.

Patient supine with neck hyperextended or prone with chin resting in the axial head holder.
A lateral scanogram to select gantry angulation.
3mm Images from the orbital apex through the orbit.

Technique: 3mm sections in 2 seconds with 200 mA & 120 kVp.

Posterior Fossa.

Patient supine & eye should be closed to avoid eye movements and radiation to eye.
Angle of mandible as the zero centering point.
Lateral localiser scan of the whole skull.
Scan sections parallel to the IOM line.
3mm Sections from foramen magnum to above the third ventricle.

Technique: 3mm sections in 2 seconds with 200 mA & 120 kVp.

Internal Auditory Canals.

Axial.
Patient supine with OM line perpendicular to the table.
Lateral scout.
Scan sections parallel to IOM line.

Technique: 5mm Sections in 2sec. with 170 mA & 120 kVp. to localise the IACs.
After localising the IAC use 1mm scan through the entire IACs using 2sec. 200mA & 120 kVp.

Coronal.

Patient supine with neck hyperextended or prone with chin resting in the axial head holder.
A lateral scanogram to select gantry angulation.

1mm scans through IAC with smaller FOV.
5mm Sections in 2sec. with 170 mA & 120 kVp. to localise tne IACs.
After localising the IAC use 1mm scan through the entire IACs using 2sec. 200mA & 120 kVp.

Temporal Bone.

Axial.

- Patient supine.
- Angle of mandible as zero centre point.
- Lateral Scout scan.
- 1mm Scan to include mastoid and temporal bone.
- Scan sections parallel to IOM line.

Technique: 1mm sections in 2 sec. with 100 mA & 140 kVp or
1sec with 200mA & !40 kVp.
Bone algorithm.

Coronal.

- Patient supine.
- Lateral localiser scan.
- 1mm Scan to include mastoid and temporal bone.
- Scan sections perpendicular to the IOM line.

Technique: 1mm sections in 2 sec. with 100 mA & 140 kVp or
1sec with 200mA & !40 kVp.
Bone algorithm

Sella and Optic Chiasma.

- Patient supine with neck hyper extended.
- Lateral localiser scan.
- 1mm scan through the entire sella.

echnique: 1mm Sections in 2 sec. with 200mA & 120 kVp.
nd
3mm sections in 2 sec. with 200mA & 120 kVp. if the
ella is large.

ead –Traumatic or Emergency.

acial Trauma.

gorithm – bone and standard for soft tissues.
mm thick direct coronal scan with pitch 1 from front of the nasal
one to behind the sphenoid sinus.
mm Thick axial scans with pitch 1 from below maxillary to above
ne frontal sinus and include mandible in case of suspected
acture of mandible.
mm helical scans with overlaping for 3D and later reformations,
direct coronal is not possible.

Orbital foreign body.

lgorithm - detailed.
mm thick helical axial & coronal slices with pitch 1 through orbit.

Cervical Spine – Non traumatic.

Routine (for discs).

atient supine, chin extended and the shoulders stretched down.
andmark – Sternal notch.
P & Lateral scout scans.
cans are parallel to and throgh the disc spaces.
mm or 3mm scans with 2sec. 200mA & 120 kVp.

Thoracic Spine and Chest.

atient supine.
P & Lateral Scout.
lice thickness depending upon the pathology (3 – 10 mm).
Tecniques: 2sec. scan with 200mA & 140 kVp.

1sec. scan with 300mA & 140 kVp.

Routine Chest Survey.

- Patient supine.
- Scan from thoracic inlet to adrenals.
- Slice thickness 7 – 10 mm.
- Scan in inspiration (breath hold).

Technique: 1 sec. scan with 240 – 300 mA & 120 – 140 kVp.

HRCT Lung.

- Patient supine.
- Area –whole lung or region of interest.
- 1mm slices with 10mm spacing.

Technique: 2sec. scan with 150 – 200 mA & 140 kVp.
Algorithm. – Lung.

Chest Mediastinum.

- Patient supine.
- Regions.

a. Apices to arch – 10mm slices with 10 interval.
b. Arch to below carina - 5mm slices with 5mm gap.
c. Below carina – 10mm slices with 10mm interval

Technique: 10mm – 1sec scan with 210 – 240 mA & 120 kVp.
5mm - 1sec scan with 250 – 280 mA & 120 kVp.

Lumbar Spine – For disc.

- Patient supine.
- Iliac crest as landmark.
- AP & Lateral localisers.
- Plan sections through the disc and parallel to it.
- 3mm slices.

Technique: 2sec. scan with 240mA and 140 kVp.

Abdomen Routine.

- Patient supine.
- Landmark – Xyphisternum.
- AP & Lateral Scouts.
- 5 – 10 mm slices.
- Scan at breath hold.

Technique: 1 sec. scan with 240 – 300mA & 120 – 140 kVp.

Pancreas.

- Patient Supine.
- Localise pancreas.
- 3 – 5 mm thick slices.
- 1 sec. scan with 250 – 280 mA & 120 kVp.
- Scan during Breath hold.

Kidneys.

- Patient Supine.
- Localise Kidney.
- 3 – 5 mm thick slices.
- 1 sec. scan with 250 – 280 mA & 120 kVp.
- Scan during Breath hold.
-

Pelvis.

- Patient supine.
- Landmark – Iliac crest.
- AP & Lateral Scouts.
- 7 – 10 mm Thick slices.
- 1 sec. Scans with 300 mA & 120 kVp.
- Breath hold technique.

CT Angio. Protocols.

Carotid artery.

- Patient supine, neck extended and shoulders stretched down.
- AP and Lateral scout scans.
- Scan thickness 3mm with 50% overlap.

- Pitch 1 - 1.4 as required the area of coverage.

Technique: 1 sec. scans, 250 - 280mA & 100kVp.
Contrast : 90 - 120 cc non-ionic contrast at a rate of 3 - 4 cc / sec.
Scan delay: 8 - 12 sec.

Circle of Willis.

- Positioning as routine axial head scan.
- AP & Lateral Localiser of the skull.
- 1-3mm Thick slices with 1-1.3 pitch.

Technique: 250 – 280mA & 120 kVp . 1 sec. scans with Scan delay 12 – 18 sec.
Contrast: 75 – 125 cc of non-ionic contrast at a rate of 2 – 3 cc/ sec.

Pulmonary Artery.

- Position as for chest scan.
- AP & Lateral Scouts.
- Breath hold should be strictly followed.
- Scan Thickness 5mm with 50% overlap.
- Pitch 1 -1.3.

Technique : 1 sec scan 250 - 280 mA & 120 kVp helical scan.
Contrast : 90 - 120 cc non-ionic contrast at a rate of 3 - 4 cc / sec.
Scan delay : 8 - 12 sec. or smart prep. can be used.

Thoracic Aorta.

- Position as for chest scan.
- AP & Lateral Scouts.
- Scan Thickness 5 - 7 mm with 50% overlap.
- Pitch 1 -1.3.
- Breath hold should be strictly followed.

Technique : 1 sec scan 250 - 280 mA & 120 kVp helical scan.
Contrast : 100 - 125 cc non-ionic contrast at a rate of 2 - 4 cc / sec.
Scan delay : Smart Prep. or 12 - 20 sec. delay.

Coronary artery.

Position as for chest scan.
AP & Lateral Scouts.
Scan Thickness 1 - 3 mm with 50% overlap.
Pitch 1 -1.3.
Breath hold should be strictly followed.
Technique : 1 sec scan 250 - 300 mA & 120 kVp helical scan.
Contrast : 100 - 125 cc non-ionic contrast at a rate of 2 - 4 cc / sec.
Scan delay: Smart Prep. or 12 - 15 sec. delay.

Abdominal Aorta.

Position as for abdominal scan.
AP & Lateral Scouts.
Scan Thickness 5 - 7 mm with 50% overlap.
Pitch 1 -1.4.
Breath hold should be strictly followed.
Technique : 1 sec scan 250 - 280 mA & 120 kVp helical scan.
Contrast : 100 - 125 cc non-ionic contrast at a rate of 2 - 4 cc / sec.
Scan delay : Smart Prep. or 18 - 25 sec. delay.

Renal Artery

Position as for abdominal scan.
AP & Lateral Scouts to localize kidneys.
Breath hold should be strictly followed.
Scan Thickness 3 mm with 50% overlap.
Pitch 1 - 1.2.
Technique : 1 sec scan 250 - 280 mA & 120 kVp helical scan.
Contrast : 100 - 125 cc non-ionic contrast at a rate of 2 - 4 cc / sec.
Scan delay : Smart Prep. or 12 - 20 sec. delay.

Renal Donors Angio.

CT angiography / pyelography may be used in preferance to intravenous urography and catheter aorto-renal angiography.

Preliminary non contrast helical CT with 5mm collimation and 1.4 pitch to access the renal calcification.
Begin the CTA at the level of SMA so that scanning trhough the renal vascular pedicle occurs prior to significant opacification of the renal vein. Extend the scan sequence inferior to the level of common iliac artery bifurcation.
Obtain AP Scout Image 3 - 4 minute after the injection for pyelogram.

Injection : 5cc / sec. for 30 sec.
Scan Delay: Smart prep. Or by mini bolus testing (4cc / sec. for 4 sec.).
Scanning : SMA to iliac bifurcation.
Scan thickness: 3 - 5mm with 50% overlap and pitch of 1- 1.3.

Clinical Applications of CT.

Spiral CT has wider clinical application than initially anticipated. It can be used in head, thorax, abdomen, spinal region as well as for 3D CT angiography.

Thorax.

Volumetric CT data from a spiral acquisition can be used to obtain contiguous overlapping thin sections, which improve the sensitivity for detection and characterization of pulmonary nodules.
Determination of the site of origin of the masses adjacent to the diaphragm is improved by the use of multiplanar images generated from the spiral CT data. Spiral CT also improves all the evaluation and local staging of lung of lung cancer compared to conventional CT, for example sensitivity ratio of pleural involvement increases to a dramatic 92%.
Spiral CT helps in better assessment of the lung parenchyma for the evaluation of interstitial lung diseases and bronchiectasis. It improves detection of lymph adenopathy in anatomically complex location like aorto-pulmonary window and hilar region. Mediastinal vascular anomalies such as dissection, aneurysms, and coarctation can be rapidly, accurately and reliably accessed.

Abdomen.

For the liver, spiral CT has obvious advantages. Spiral CT due to very fast scanning optimizes the contrast dynamics in the liver and has improved detection of metastatic lesion. Both hypovascular and hypervascular metastasis can be detected with better accuracy. Most gastrointestinal neoplasm's are hypovascular, whereas lesions from islet cell tumours, renal neoplasms, sarcomas, lymphomas and melanoma can be hypervascular.Depending upon the type of the primary tumour, spiral CT could be tailored to image the liver either during the arterial phase,(for hypervascular lesions) or during the portal venous phase(at these time there is peak enhancement of the liver parenchyma, maximizing liver to lesion difference) for hypovascular lesions. For suspected hypervascular metastasis a delay time of 25 - 30 sec can be used, whereas for hypovascular metastasis a delay time of 60 sec. is used.

For pancreatic pathologies spiral CT has became the gold standard. Vascular opacification is optimum which is very important for evaluating pancreatitis and malignant tumours of pancreas. In pancreatitis spiral CT can detect the vascular patency and evaluate for pseudo- aneurysms. In pancreatic tumours it is important to opacify the portal vein well to look for enhancement.

In the kidneys, Spiral CT is extremely useful to evaluate and characterize renal masses which re smaller than 1.5 cm in size. Spiral CT with overlapping sections and 3D reconstruction is particularly useful for planning surgical exploration in small indeterminate lesions and for planning resections of large corners in solitary kidneys.

In this initial series, the cortex enhances whereas medulla may still be hypodense. It is important to note that when the kidneys are being evaluated, small tumours of the medulla may not be missed. Some unique application of spiral CT that has been recently advocated is its use in renal colic and for CT urograms. A 40 - 50 sec. Unenhanced spiral CT study from the top of the kidney to the base of the bladder for renal colic is an accounted way of detecting renal calculi.

It is feasible to use data from a contrast enhanced spiral CT to obtain CT renal angiography and to evaluate the renal parenchyma at the same time. Using 3D reconstruction from the delayed images the dense contrast within the collecting system can be used to obtain intra venous urogram like images.

Cranio- Spinal Applications.

For the brain, conventional scan are still preferred for routine indications, as the resolution obtained is slightly better than with spiral acquisition. However in case of un co-operative and pediatric patients, it is extremely useful to use a spiral acquisition. 3D Spiral CT angiography can be used for the carotid bifurcation and intra cranial vascular abnormalities. 3D recon. For evaluation of congenital diseases like cranio stenosis and complex facial trauma are better performed with spiral CT.

Musculoskeletal Applications.

Spiral CT can be used in the evaluation of complex musculoskeletal disease processes like bone or soft tissue tumours, infective processes or complex traumatic processes. In areas where the anatomy is complex, trauma can be reliably and more completely evaluated with 3D recon.(Cranio- vertebral region, acetabular fractures etc.).

CT Angiography.(CTA).

CT angiography is a relatively non-invasive technique to obtain vascular details. If an intravenous bolus of contrast material is administrated and timed correctly, images can be obtained at the peak of arterial enhancement with helical scanning. New software timing sequences such as 'smart prep' further improves the quality of CT angiography by allowing accurate timing of the contrast bolus. These images can be post processed to display three dimensionally.

3D CTA gives images which are more or less similar to the DSA images.

3D WORK STATION.

dvantage Windows (AW).

perating System: Sun OS 5.4 / Type: SUNW, SPARC station
ocessor type: Spare/ Processor No: I
Processor1. Clock . 150MHz / Memory Size: 128MB
. of Disks: 3

is a multitasking, multifunctional workstation, based on Sun crosystem, designed for the display and analysis of the ages. AW is networked with MRI, CT and DSA. It is equipped h several software like 3D, Reformat, Denta (Dental CT), BMD Navigator (Virtual Endoscopy).

) Analysis Package.

is a software application designed to be used with AW. It nerate reconstructed 3 Dimensional volume and reformatted t plates on CT and MR series. 3D imaging can be performed ing two physical methods: Thresholding & Percentage based. e basic different between the two techniques is that resholding based software assumes a particular voxel to be of iform density, where as percentage based software assumes at a voxel contains more than one type of tissue. Advantage ndows is a thresolding based software. Here thresolding, osion, dilation and select object are the four most often used ols for segmenting anatomy for 3D Surface/volume rendering. e reconstructed images can be displayed as Shaded Surface splay (SSD), Maximum Intensity Projection (MIP), High finition MIP (HD MIP), minimum Intensity Projection, Raysum d Integral.

urface rendering was one of the earliest methods of 3D splay and is now incorporated in most commercially available) medical imaging packages. In this method, each voxel within e data set is determined to be a part of or not a part of the ject of interest. Usually by comparing the voxel intensity to me threshold value, thereby defining the 'Surface' of the ject.

It is feasible to use data from a contrast enhanced spiral CT to obtain CT renal angiography and to evaluate the renal parenchyma at the same time. Using 3D reconstruction from the delayed images the dense contrast within the collecting system can be used to obtain intra venous urogram like images.

Cranio- Spinal Applications.

For the brain, conventional scan are still preferred for routine indications, as the resolution obtained is slightly better than with spiral acquisition. However in case of un co-operative and pediatric patients, it is extremely useful to use a spiral acquisition. 3D Spiral CT angiography can be used for the carotid bifurcation and intra cranial vascular abnormalities. 3D recon. For evaluation of congenital diseases like cranio stenosis and complex facial trauma are better performed with spiral CT.

Musculoskeletal Applications.

Spiral CT can be used in the evaluation of complex musculoskeletal disease processes like bone or soft tissue tumours, infective processes or complex traumatic processes. In areas where the anatomy is complex, trauma can be reliably and more completely evaluated with 3D recon.(Cranio- vertebral region, acetabular fractures etc.).

CT Angiography.(CTA).

CT angiography is a relatively non-invasive technique to obtain vascular details. If an intravenous bolus of contrast material is administrated and timed correctly, images can be obtained at the peak of arterial enhancement with helical scanning. New software timing sequences such as 'smart prep' further improves the quality of CT angiography by allowing accurate timing of the contrast bolus. These images can be post processed to display three dimensionally.

3D CTA gives images which are more or less similar to the DSA images.

3D WORK STATION.

dvantage Windows (AW).

perating System: Sun OS 5.4 / Type: SUNW, SPARC station
rocessor type: Spare/ Processor No: I
Processor1. Clock : 15OMHz / Memory Size: 128MB
o. of Disks: 3

is a multitasking, multifunctional workstation, based on Sun icrosystem, designed for the display and analysis of the nages. AW is networked with MRI, CT and DSA. It is equipped th several software like 3D, Reformat, Denta (Dental CT), BMD Navigator (Virtual Endoscopy).

D Analysis Package.

is a software application designed to be used with AW. It enerate reconstructed 3 Dimensional volume and reformatted ut plates on CT and MR series. 3D imaging can be performed sing two physical methods: Threshholding & Percentage based. he basic different between the two techniques is that resholding based software assumes a particular voxel to be of niform density, where as percentage based software assumes at a voxel contains more than one type of tissue. Advantage indows is a thresolding based software. Here thresolding, rosion, dilation and select object are the four most often used ols for segmenting anatomy for 3D Surface/volume rendering. he reconstructed images can be displayed as Shaded Surface isplay (SSD), Maximum Intensity Projection (MIP), High efinition MIP (HD MIP), minimum Intensity Projection, Raysum nd Integral.

urface rendering was one of the earliest methods of 3D splay and is now incorporated in most commercially available D medical imaging packages. In this method, each voxel within he data set is determined to be a part of or not a part of the bject of interest. Usually by comparing the voxel intensity to ome threshold value, thereby defining the 'Surface' of the bject.

With the surface determined, the rest of the data is discarded, Surface contours are typically modeled as a collection of polygons and displayed with surface shading. The resulting image is a simplified and possibly misleading representation of a structure, particularly if the surface is difficult to determine precisely, as is often the case in medical imaging.

By converting data from a volume to a surface, a large portion of the data available is forfeited in exchange for faster, easier computation. This can be an advantage by allowing real-time rendering and thereby enhancing user interactivity, but the usefulness of surface-rendered medical images is generally limited by their inconsistent image fidelity.

Like surface rendering, Maximum intensity projection (MIP) is also commercially available in 3D software packages and has been extensively clinically evaluated, particularly in reconstruction angiographic images from CT and MR data.. The MTP algorithm evaluates each voxel along a line from the viewer's eye through the data set and select the maximum voxel value as the value of the corresponding display pixel. The resulting images are typically not displayed with surface shading or other devices to help the user appreciate the 'depth' of the rendering, making three-dimensional relationships difficult to assess.

If there is another high-intensity material along the ray through a vessel, such as a calcification, the displayed pixel will represent the calcification and will contain no information from the intravascular contrast material. Selection of the heighest pixel value also increases the background mean of the image, which enhances structures such as the kidney and liver, there by decreasing the visibility of vessels in these structures.

What is worse, volume averaging coupled with the MIP algorithm typically produces artifacts. a normal vessel passing obliquely through a volume may look like a string of beads. In spite of its shortcomings, MIP is generally more accurate than surface rendering for CT angiography.

s its name implies, Volume rendering makes use of the entire olume of data rather than just surfaces and so potentially nveys more information than a surface model.

olume rendering techniques sum the contributions of each xel along a line from the viewer's eye through data set. This is one repeatedly to determine each pixel value in the displayed nage. Because the entire data set is incorporated into the sulting image, computers that are more powerful are ecessary to do volume rendering at a reasonable speed.

We view volume rendering as the most advanced form of 3D image processing available creating accurate, clinically useful images, Volume rendering is just now being incorporated into commercially available software. With general availability and continued increase in computer power, volume rendering will likely become the most important technique for 3D medical imaging.

enta scan (Dental CT)

It is a software programme, which allows us to evaluate the teeth, and teeth bearing portion of the jaws in a manner differ from routine axial sections and sagittal or coronal reconstructions.

he software is constructed such a way that multiple, contiguous axial sections are fed in to it to yield panoramic(OPG like) and para axial reconstructions. Para axial reconstructions are perpendicular to the plane of the tooth and are the only image, which shows all four cortices of the mandible well.

The technique: Axial images of 1 to 2 mm thickness with 1mm gap are obtained with a low kV setting of 90-1 1 0 and a low mA setting of 120-180, Use a matrix of 512 X 512 and a high definition bone algorithm with a display FOV of 15cm . The mandible and maxilla have to be scanned separately. A bite is placed in the mouth to adequately separate the mandible and maxilla. For mandible place the patient so that the mandible **is**

perpendicular to the floor plane. For maxilla place the patient so that the maxilla is perpendicular to the floor plane.

Bone Mineral Densitometry (BMD)

Quantitative computer tomography (QCT) is the technique used to measure the trabecular BMD in the lumbar spine and trabecular and cortical bone in the fore arm. These measurements have been used to provide normal reference values and to assess diseases that affect both bone mineral density and body composition. BMD measurements is currently the most accurate method for predicting patients at a risk of osteoporotic fracture. These measurements are also useful for monitoring the response to therapy for prevention of bone loss and fracture.

The QCT-5000 bone densitometry system allows highly automated vertebral bone mineral density measurements. The hardware consists of a calibration phantom, a QA Torso phantom, phantom cushion and bolus bag.

Technique : Taking a lateral scout image and axial scans through 3 or 4 vertebrae of the patient while they are laying on the calibration phantom. Care should be taken to perform the scans with a standard mA, Scan time, Slice thickness, Scan FOV and Table height.

NAVIGATION (Virtual Endoscopy)

The navigator package generates 3-dimensional volumes of hollow structures on advantage windows system. The multiple screen displays the position and direction of the navigator, in 3 planes. A mouse and keyboard driven navigator provides luminal views in real time.

Virtual endoscopy or fly-through methods that combine the features of endoscopic viewing and cross sectional volumetric imaging may provide and advances in diagnosis. Virtual endoscopy presentations of image data enables the operator **not**

only to explore the inner wall surfaces but also to navigate in side the virtual organs extracted from CT Scan or MR images.

Imaging requirements - All routine CT or MR imaging techniques that provide high-resolution cross-sectional images can be post processed to obtain 3D re-constructions. CT scanning for virtual endoscopy is performed using a continuously rotating helical CT system. Typical helical CT data acquisition parameters are 120 kVp, 70-165 mA , 20-40 sec exposure, 5-3mm collimation, 5-6mm/sec table feed (pitch of 1.2), and 512 X 512 matrix. Reconstruction parameters include 180 linear interpolation, standard reconstruction kernel, and 3mm table incrementation. For virtual colonoscopy studies, after oral colonoscopy preparation, patients are scanned after ingestion of oral contrast agent (1000 ml of 2% Barium Sulfate suspension) or, alternatively, air insufflation can be applied. Glucagon may have a role in improving image quality by reducing bowel peristalsis. The optimal CT technique for virtual colonoscopy has not yet well established. For CT abdominal angiography studies, helical CT scans are obtained after IV injection of contrast agent.

For MR imaging, T1 weighted 3D volumetric gradient-echo sequences provide isotropic voxels that are applicable for 3D rendering- For vessel fly-through method, 3D Time-of-flight MR angiography is preferred over phase contrast angiography because of the better delineation of vessel wall.

Leksell Streotactic System.

Introduction

In 1920 Clarke, who interestingly was not a ,surgeon himself, suggested the use of mechanically directed instruments for surgery in the depth of the brain. However, the first intracerebral sterotactic operation was not performed until 1947 when Spiegel and Wycis introduced " stereoencephalotomv **"** for the treatment of intractable pain,

The Leksell Stereotactic instrument was introduced and used for the first time in 1949. Although continuous technological

improvements and many valuable modifications have been made, the original basic principle of the instrument, with the target in the center of the semicircular arc, has been maintained since that time.

Stereotaxy is often considered the simplest and safest approach to the deep areas. It is a highly suitable technique for making deep functional lesions and often the only desirable method for biopsies, for the treatment of deep-seated tumors such as cranio pharyngiomas and cysts of the foramen Munro and for the evaluation of deep hemorrhages. Implantation of radioactive seeds for interstitial irradiation necessitates the precision offered by stereotaxy inorder to comply with dose-planning requirements.

With the development of the Leksell Stereotactic Gamma Knife in 1968, which is based on the same principles as the open technique, the number of indications for stereotactic treatment, now also by radiosurgery, has increased further. With this technique conditions such as A V M s, acoustic tumors, pituitary adenomas, pineal tumors, as well as other benign and malignant tumors can be treated without opening of the skull. The very high precession of the gamma Knife lends itself particularly well to small and critically located targets. Radiosurgery in functional disorders and in the treatment of vascular malformations in the brain stem are good examples for such targets.

The combination of stereotactic surgery and computerized tomography (CT) has been very fruitful and, with magnetic resonance imaging (M R I) new dimensions have opened up.

The Leksell micro - Stereotactic System.

The principal components of the Leksell Micro Stereotactic system are the coordinate frame and the semicircular arc.

The Co-ordinate Frame

It has the shape of the rectangle, which is 25mm high, 206mm

vide and 236mm low. It is made of light weight aluminium and has four feet which connect it to the x-ray equipment, the CT and MR adapters as well as the May field frame fixation. The rectilinear coordinate system has its origin outside the frame, superior, posterior and lateral to it on the right side. It conforms to the X, Y and Z noman- clature used in CT and MRI scanning. The coordinate scales on the frame indicate positive values only,Thus for instance, confusion between right and left is precluded.

The frame is provided with six posts for fixation to the patient. The frame is provided with two earplugs, which are used as an aid for the orientation of the frame on the patient's head, prior to its fixation.

The Stereotactic Arcs.

The semi circular arc is composed of the arc itself, to axes with side rings and sliding instrument carrier. Its design is such that when using needles, electrodes or other instruments whether the standard Leksell length, or active part will always enter in the center of the arc, i.e. at the selected target point. This gives the surgeon the unique opportunity to place the burr hole anywhere on the skull. The arc is positioned on to the coordinate frame according to the target coordinates obtained from a MR or CT scan or from an X-ray film.

C.T. PERFUSION

C.T Perfusion is used to measure the heamodynamic properties such as CBf,CBv,MTT and time to peak(TTP).The principle of these method involves continous acquisition of data from a particular area performed during the first passage of a pheripherally administrated contrast meadium through the cerebral vasculature.From the images obtained in this way, the shortterm changes in the density of the brain tissue can be

presentd in the form of a time density(TD) curve for every volume element of the slice being examined

Analysis of the resultent TD curve is used to calculate the blood heamodynamic properties.

CT Perfusion, commonly use either a non-diffusible tracer(iodine)or diffusible tracer(xenon).

Xenon CT used as an accurate technique in CT perfusion but involves inhalation of stable xenon by the patient,with possible side effects and necessitates expensive and complex equipment.

Non –diffusible tracer(iodine)is the commonly used tracer in PCT.In this two region of interest(ROI) are placed on a non contrast enhanced image and contrast enhanced CT scan was done.This will produce a TD graph. Later analysis of this TD curve with perfusion software produce heamodynamic parameters. MDCT Technique allows imaging different slices at the sametime.

Knowledge of cerebral blood flow (CBF) alterations in cases of acute stroke could be valuable in the early management of these cases. Among imaging techniques affording evaluation of cerebral perfusion, perfusion CT studies involve sequential acquisition of cerebral CT sections obtained in an axial mode during the IV administration of iodinated contrast material. They are thus very easy to perform in emergency settings.
Viability of the cerebral parenchyma is dependent on cerebral blood flow (CBF) .Complex autoregulation processes ensure the adjustment of regional CBF to local energetic needs, determined by the activity level of local neurons .CBF alterations are encountered in association with a variety of pathologic conditions, the most frequent being strokes. .Cerebral infarcts occur when CBF values are <10 to 15 cc/[100 g x min], whereas penumbra, relating to reversible cerebral ischemia, happens with CBF between 15 and 20 cc/[100 g x min] .Present indications for a thrombolytic therapy rely on the time interval between the beginning of symptoms (inferior or superior to 3 hr) and the native cerebral CT findings .Knowledge of a quantitative map of

CBF, indicating the severity and potential reversibility of neuronal damages, would perhaps allow for the clinical use of the theoretical thresholds mentioned above; thrombolysis achieved when the penumbra prevails over the infarcted area might not only be more profitable but furthermore might decrease the risk of intracranial bleeding .Different imaging techniques are now available to evaluate CBF, notably stable xenon CT and perfusion CT studies. Stable xenon CT relates to dynamic CT scanning during inhalation by the patient of a gas mixture containing stable xenon and oxygen. Alveolar xenon accumulation is measured end-tidally by a thermoconductivity analyzer and assumed to be equal to arterial xenon concentration. Stable xenon is a diffusible gas that progressively pervades cerebral blood and neurons on a well-balanced basis. Its radiopacity relates cerebral increase of CT units on successive cerebral CT sections to an increase of the parenchymal concentration of stable xenon. Stable xenon CT data analysis is realized through applying the equilibrating indicator model ,which relies on the Fick principle:

$$\frac{dQ(t)}{dt} = CBF \cdot (C_a(t) - C_v(t)) \qquad (1)$$

where $C_a(t)$ and $C_v(t)$ designate the instantaneous arterial and venous concentration of the indicator at time t, whereas Q(t) designates the amount of indicator in the local vascular networks in connection with time t. The equilibrating indicator model supposes a balance between the venous, $C_v(t)$, and the parenchymal, $C_b(t)$, concentrations of the indicator:

$$C_b(t) = \lambda * C_v(t)$$

where λrelates to the cerebral parenchyma-blood partition coefficient of the indicator. Combination and development of equations 1 and 2 result in the supporting equation of the equilibrating indicator model:

$$C_b(T) = \lambda \cdot K \cdot \int_{t=0}^{T} C_a(t) \cdot e^{-K \cdot (T-t)} \cdot dt$$

with

$$K = \frac{CBF}{\lambda}$$

Stable xenon CT necessitates excellent collaboration from the patient, as well as specialized and expensive equipment. It may occasionally be responsible for a decrease in the respiratory rate,headaches, nausea, vomiting, and convulsions.

Perfusion CT studies involve sequential acquisition of cerebral CT sections achieved on an axial mode, during the IV administration of iodinated contrast material. Perfusion CT data consist of contrast enhancement profiles obtained at each pixel, the latter relating linearly to the time-concentration curves of the contrast material. Analysis of these curves is realized according to the central volume principle.The regional cerebral blood volume map is inferred from a quantitative estimation of the partial volume averaging effect, completely absent in a reference pixel at the center of the large superior sagittal venous sinus:

$$CBV = \frac{\text{area under the curve in a parenchymal pixel}}{\text{area under the curve in the reference pixel}}$$

where CBV stands for cerebral blood volume with a correction factor to take into consideration that iodinated contrast material is restricted to the plasma phase of the blood .The impulse function and the related mean transit time maps result from a deconvolution of the parenchymal time-concentration curves by a reference arterial curve. Finally, combination of cerebral blood volume and mean transit time at each pixel leads to a CBF value

.

$$CBF = \frac{CBV}{MTT}$$

here MTT stands for mean transit time.

The imaging protocol for stable Xe gas perfusion

six contiguous 10-mm sections located on the cerebral emispheres. This protocol was repeated two times before and our times during an inhalation of a gas mixture containing 28% table xenon, 25% oxygen, and 47% air, to a total of 6 min. The btained data were analyzed on a computer with a post-rocessing software.

he imaging protocol for perfusion CT

two adjacent levels among the six examined ones were elected at the level of the basal nuclei. Twenty-five successive 0-mm CT sections were obtained every 2 s at these two djacent levels, with a total acquisition time of 50 s. Acquisition arameters were 80 kVp and 200 mAs. CT was initiated 2 s efore the IV administration of 1.3 cc/kg of iohexol by means of a ower injector at a rate of 5 cc/s. The delay before injection of he contrast material allowed for the acquisition of baseline mages without contrast enhancement. This perfusion CT rotocol involved an additional radiation dose of 291 mSv. Regarding the stochastic effects of radiations, this dose, once edistributed on the entire cerebral volume, amounted to 29 mSv, hich is inferior to the dose of a standard cerebral CT xamination (40–60 mSv).

Stable xenon CT results and perfusion CT data were transferred o a workstation for computer processing and comparison. Perfusion CT rely on the central volume.There are two different econvolution methods: the singular value decomposition (SVD) nd the conventional least mean square (LMS) methods . In both echnique, the reference artery was automatically selected by the oftware (thus avoiding interobserver variability) as the pixel with he shorter time to peak on the corresponding time-concentration urve in the area drawn by the operator, either around the nterior cerebral artery (ACA) or around the middle cerebral rtery (MCA).

Perfusion CT studies have the same complications as that of CT ngio, whereas stable xenon CT examinations were responsible or a decrease in respiratory rate .

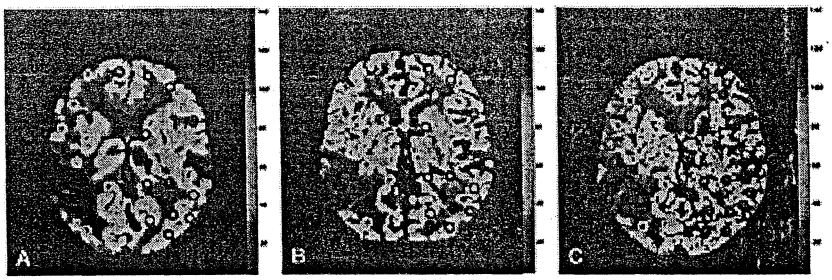

xe gas perfusion svd lms

Stable xenon CT relies on the equilibrating indicator model, which indicates that the balance of concentrations of a diffusible indicator between blood and cerebral parenchyma is more or less rapidly realized in the various cerebral areas, according to the importance of the corresponding local CBF. Knowledge of the blood (or alveolar) and parenchymal concentration curves leads to the balance rates and to the CBF values for each pixel. On the other hand, perfusion CT data analysis is realized through the central volume principle .The latter describes the behavior of an iodinated contrast material bolus crossing the cerebral capillary networks, with subsequent modifications of contrast enhancement profiles. Iodinated contrast material is limited to blood vessels, at least at first pass and in healthy cerebral parenchyma.

Perfusion CT studies of CBF are not time-consuming and are well tolerated. They verify classical contraindications regarding the IV administration of iodinated contrast material. On the other hand, the IV administration of nonionic iodinated contrast material can reasonably be achieved even in patients who have suffered acute stroke .

Perfusion CT studies do not require any special equipment. Even with a multi-detector CT unit, perfusion CT coverage of the brain is inferior to that of stable xenon CT, because only two 10-mm cerebral CT sections can be examined. This is mainly because of the much quicker kinetics of iodinated contrast material compared with that of stable xenon CT. However, the purpose of our study was to compare the corresponding sections in perfusion CT and stable xenon CT and not brain coverage.

rfusion CT studies were performing at low kVp (80) rather
n high kVp (120), allowing for a statistically significant
rease in contrast enhancement. This results from the more
portant perfusion of gray matter compared with that of white
tter. Moreover, after contrast enhancement, radiographic
eraction with soft tissues at 80 kVp relates to the photoelectric
ect, due to the 33 keV K-edge of the iodine included in the
ntrast material. On the other hand, radiographic interaction
fore contrast material administration is mainly due to the
mpton effect.Although the use of 80 kVp involves a lower
oton flux, it does not result in a statistically significant increase
noise, allowing 80 kVp images to be used in perfusion CT
alysis.Finally, performance of perfusion CT examination at 80
p, keeping milliamperes constant, lowers the radiation dose by
actor of 2.8.

th stable xenon CT, there is no concern regarding the choice
a reference artery, because the arterial time-concentration
rve is assumed to be the same as that measured in the end-
al breathed air. However, this leads to other pitfalls, notably for
tients with chronic respiratory disease or with cardiac or
scular shunts.

AL SUBTRACTION ANGIOGRAPHY(DSA)

is the generic term for any digital radiographic method for
menting subtraction. DSA offers the advantage of image
oulation, plus the instantaneous viewing of the images, and
ivity to low contrast images, with smaller amounts of contrast
m injected, are all desirable technical considerations. DSA has
applications for low-contrast examinations. DSA can be very
l in patients who are at risk for a high rate, high volume contrast
nation because less contrast media is needed to obtain
ostic images. Film framing rates on the order of 3 to 4 fps is
able.

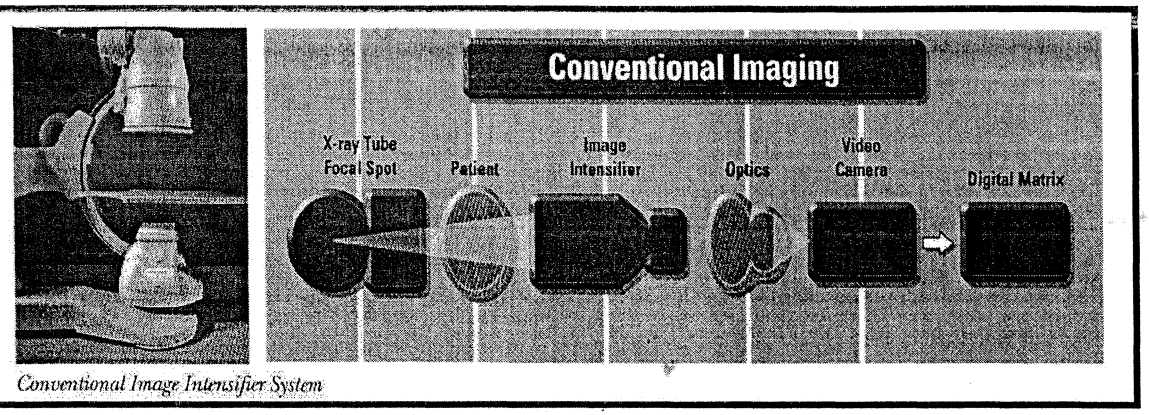

Conventional Image Intensifier System

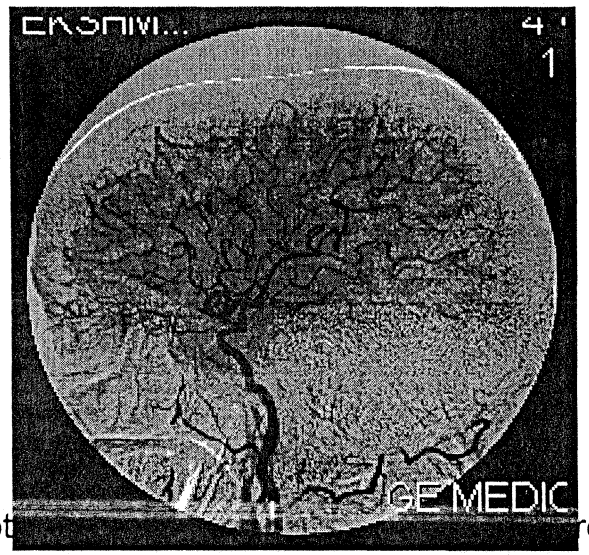

ne various subt re;

1. **MASK SUBTRACTION**
2. **DUAL ENERGY SUBSTRACTION**
3. **TIME INTERVAL DIFFERENCING**
4. **TEMPORAL FILTERING**

MASK SUBSTRACTION

Mask subtraction is the DSA technique, which closely esembles film screen angiography. The patient is prepared and catheter is placed under fluoroscopy control. Contrast media is then njected and exposures made, starting before contrast media is

pected to arrive the vessel of interest and extending pass the time en it is expected to have cleared the vessel. Subtraction of pre ntrast mask image from contrast containing image is the basis of s mask subtraction technique.

AL ENERGY SUBSTRACTION

In dual energy subtraction, two images are taken with in a very rt period, during which time there is no change in the patients. ese two images are obtained by making exposures with different x- energy spectra. E.g.; from a high kvp exposure and a low kvp osure.

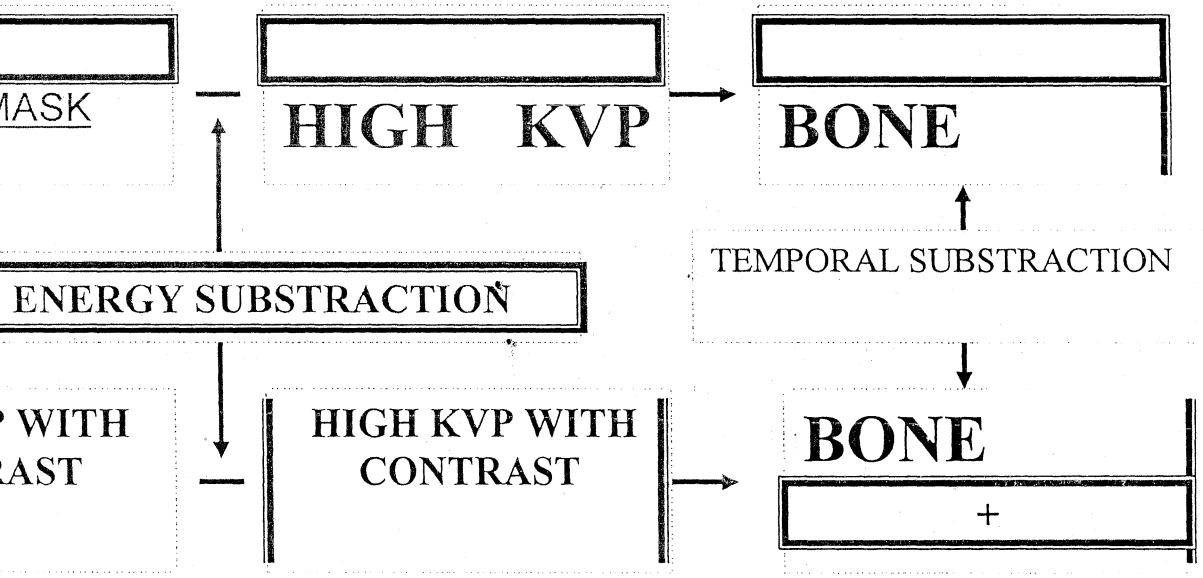

INCIPLES

The differential attenuation between bone and soft tissue at low p is much greater than their differential attenuation at high kvp. The ne contrast in the high kvp film is reduced much more than the soft sue contrast. In the regions that do not contain bone, the soft sues cancel but bone containing regions do not cancel completely. us the final images consists of only bone plus the inevitable noise.

OPLEMS WITH DUAL ENERGY SUBSTRACTION

All the problems associated with radiographic imaging in ral and DSA in particular are still present. Additional problems nay be encountered are;

The high kvp image still has some bone with in it when the soft tissue densities are eliminated by subtraction, some of the bone densities are eliminated by subtraction, and some of the bone density is also removed.

A more complex x-ray machine is required, as an x-ray generator capable of switching kvp and mAs rapidly is needed to overcome problems with anatomic motions.

Due to differential beam hardening of the two beams in the different thickness of bone and S/T in the body there is improper subtraction of bone.

ER DUAL ENERGY SUBSTRACTION

K-SHELL SUBSTRACTION
HYBRID SUBSTRACTION

E INTERVAL DIFFERENCING

has seen some application in cardiology. The technique is ely related to simple mask subtraction. In simple mask raction an early image is chosen as a mask and this mask is acted from each succeeding image of the series of subtracted es. In TID technique, a new mask is chosen for each subtraction each subtracted image is the difference between images rated by some fixed interval of time.

PORAL FILTERING

is technique, several of the early frames are added to obtain a k and several of the later frames added to obtain a contrast aining image and the two are subtracted. This reduces the image e with out an increase in tube mA being required for the same.

obvious advantage of the technique is the reduced tube loading ired as compared to single mask subtraction.

disadvantage is that a large number of individual frames must be lled for temporal filtering.

re are two catheterization laboratories; one equipped with nens Polydoros 100 & DGITRON 3 and other with GE Advantx -LCV

ipment Parameters:

mens Polydoros 100

mens Polydoros 100 is a high frequency X-ray generator with roprocessor control. The equipment is a bi plane C-arm System cine attachment. It has DSA provision to.

ITRON 3

itron 3 is a fully digital DSA unit designed for cardiac work as well routine intraarterial and intravenous subtraction angiography. It is eal time image acquisition and processing system.

Image post processing features are mask selection, electronic tter, Grey-scale inversion, image re-registration, horizontal/ tical (pixel shift), image zoom, land scape road map, edge nancement, image integration up to sixteen images, ROI's, image ring, cardiac analysis etc.

Advantx DLX-LCV

SYSTEM SPECIFICATIONS

MAINCOMPONENTS

1. X-RAY TUBE
2. IMAGE INTENSIFIER
3. GENERATOR
4. TV -CAMERA
5. COMPUTER CONSOLE

X-ray tube

X 135 HEXAGRAPH(SIX FOCAL SPOT)
FILAMENTS →1.1,0.6,0.3
ASED FOCAL SPOTS→ 0.30b, 0.20b, 0.15b

nage intensifier

TYPE	SIZES
UAL FIELD	6"
RIPLE FIELD	9"
UADRIPLE FIELD	12" / 16"

ray generator – LFX generator

0KW, 12 PULSE
TOR CONTROLLER- TIRC 10,800 rpm

V TRANSFORMER

se bias tank – control grid

CK UP TUBES

con
nicon, saticon (Philips)
mbicon, newicon, chimicon

RAMETERS SELECTION

e, Focalspot, FOV, MA, KVP

AL → System estimates the exposure factors
→ 60-120
ME RATES → 12.5-25 F/S-CINE
CULAR MAX → 8.3 F/S

DOSE VASCULAR CARDIAC

A	100	4
B	250	7
C	500	7
D	1000	15

UORO DOSE

X KV –120 KVp, CONTROLLED ABC
SE 10R/M - max dose at tabletop
des → low – med -high

The system offers facilities such as last image hold (LIH), auto ction of contrast, edge enhancement, noise filtering, roadmap etc, age processing include different subtraction modes, pixel shift, y scale inversion, remasking, image filter, image integration, egrated mask, maximum opacification, temporal scale, dscaping, shutter, stenosis analysis, cardiac analysis and notation.

ARM

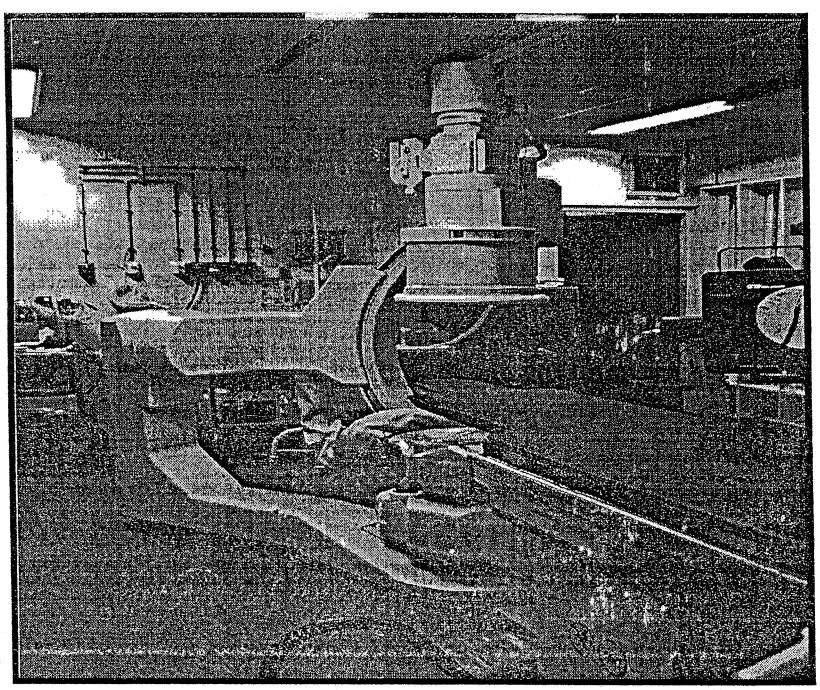

SOLE

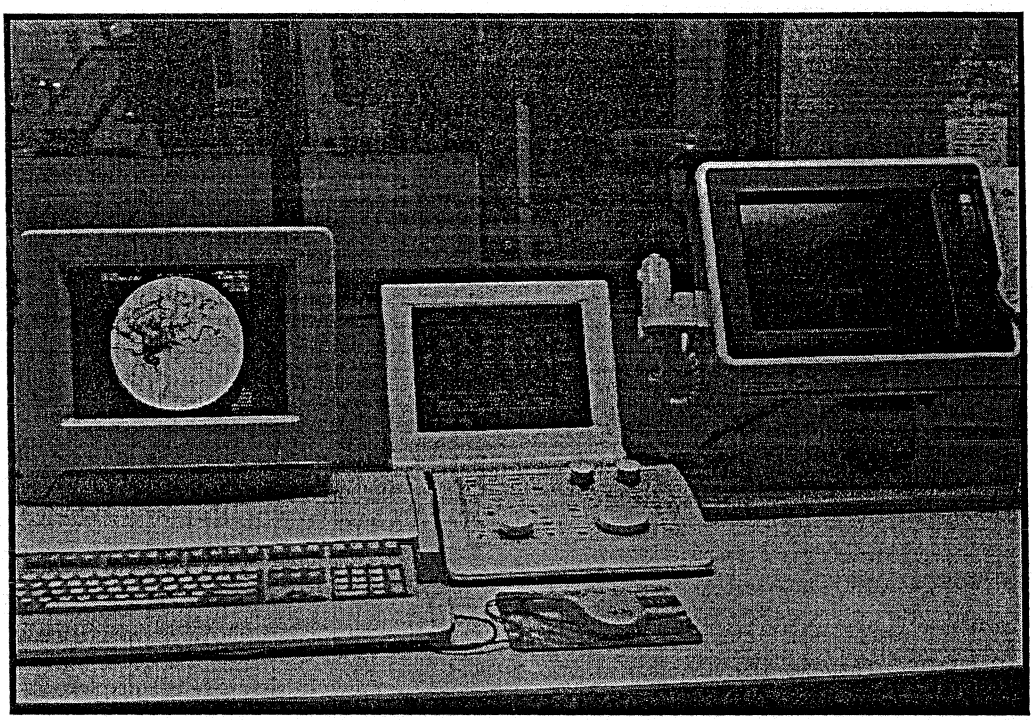

T A : Equipments & Accessories

eration
mponents of the Digital Imaging System
thods of manipulating and archiving the DSA Image

peration

stores images electronically and with the aid of a computer, acts images in real time. Real-time digital imaging permits 30 es per second. The images can be manipulated to change the ow levels and contrast, a function that is invaluable in low ast examinations. The DSA system operates at a fluoroscopic mperage level on the average of 10 to 20 mA, depending on the pment being used. The image is processed as the run is being rmed, so that subtraction image can be viewed and the sure terminated once the area of interest is viewed. What occurs at the image from the image intensifier is converted from analog

ata into digital information and processed by the computer for splay and storage.

Components of the Digital Imaging System

television image chain is one of the most important links in the gital system. The light produced by the image intensifier is roportional to the amount of remnant x-ray photons. The image tensifier (II) input phosphor is coated with an x-ray sensitive nosphor, such as cesium iodide (CsI). The television chain produces electronic video signal at the output phosphor in proportion to the mount of light, but exceedingly intensified. The television camera Plumbicon, CCD, or Saticon) then forms an image by electronically canning a target or semiconductor. The video signal produced is ent to the digital processing unit Digital Subtraction Angiography ystem

haracteristics needed in the TV chain of a DSA system include low g and low noise. Plumbicon TV camera tubes are usually used for SA because of their intrinsic low lag. Excessive lag would produce ghosting" Ghosting occurs when the image viewed actually contains nformation belonging to the previous images. Studies can be greatly ffected by this artifact. The signal to noise ratio (SNR) is the signal oltage ratio to the noise voltage. Conventional fluoroscopy requires 200:1 SNR. Digital requires about 1000:1 SNR. Generally noise an mask or hide the signal. Because subtraction studies are usually erformed on low -contrast studies it is especially important that the mount of electronic noise must be kept to a minimum, much more so nat in standard film screen radiography or fluoroscopy. Digital adiography images can be degraded by noise from the fluctuations n x-ray photon intensity (quantum mottle) and noise from the elevision chain (electronic noise). Techniques have been devised to elp overcome the problem of noise in DSA . Frame integration verages together several frames, thereby diminishing the effects of lectronic and quantum noise.

light diaphragm or filtering device is used to control the amount of ght from the image intensifier that reaches the television camera ube. Without the use of apertures, either not enough or too much ght (saturation) is allowed to reach the television camera.

The analog-to-digital converter (ADC) is the component that converts the video images from the TV chain into digital form. The video signal has a voltage that varies during the scan, representing the number of x-ray photons that are received by the image intensifier. Measurement of the voltage of each individual pixel of every line results in conversion of the video image into a digital image. So it is easy to see that the size of the matrix will greatly influence the image resolution.

Television scan modes are a component of the actual television monitor and are of various types.

Interlaced: the 525-raster or line frame is scanned in 1/30th of a second. This means each 262.5 line field is scanned every 1/60th of a second. The interlaced mode reads the information in two separate fields and then combines, or interlaces, the information. This mode is adequate to avoid the perception of flicker. The human eye can detect flicker on a television monitor below 50 pulses per second. The major drawback of interlaced mode is that certain images are discarded, so the patient receives some unnecessary x-ray exposure.

Progressive: Every line is read in order, rather than in field - interlaced manner. This method involves the TV camera scanning being paused while an exposure is made so that it is not as rapid as interlaced but eliminates motion.

Slow: This method is inadequate for real - time DSA. It has application in the 1024x1024 pixel digital fluoroscopy imaging, with a 1050 line TV frame. The slow scan mode is limited to 7.5 frames per second. Real-time continuous digital fluoroscopy requires 30 frames/second. Pulsed digital fluoroscopy typically allows for only 1 to 6 images per second but could not use the slow scan mode. These images have less noise but require high mA.

3.DIFEERENT METHODS FOR IMAGE MANIPULATION

Window and Level Adjustments:

DSA allows for post-procedural manipulation of images. The simplest way to manipulate an image is to vary the window level, which

ontrols the density or vary the contrast by adjusting the window idth.

ANDSCAPING

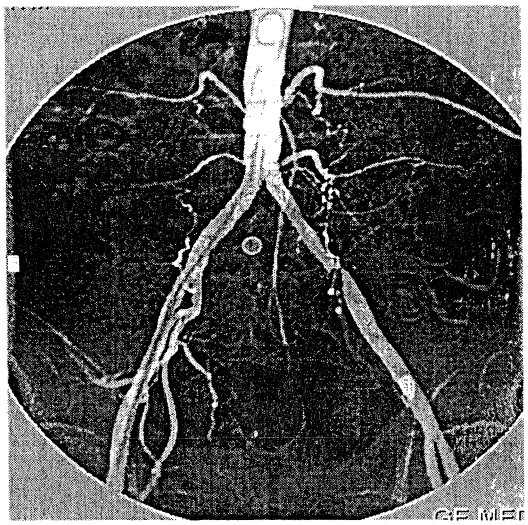

A small amount of the mask image is added back to the subtracted mage, but not so much that the subtracted image is overwhelmed. andscaping is usually done to assist the radiologist in preparation of nvasive procedures.

dge Enhancement:

Edge enhancement is intended to increase the visibility of small tructures with moderate to high contrast. The basic goal is to discard nost of the information about the large structures and keep the nformation relates to small structures. Edge enhancement is ccomplished by subtraction of low pass filtered image from the rginal which yields an image in which edges and small structures emain. Unfortunately noise also prominent in this edge enhanced mage.

NOISE SMOOTHING

BEFORE FILTERING AFTER FILTERING

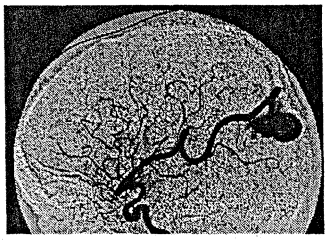

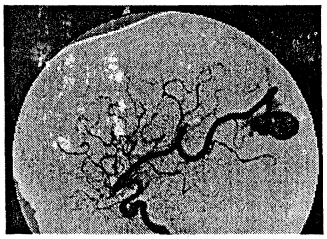

It is an attempt to decrease the visual prominence of noise so low contrast objects of moderate to large size may be better eciated. The technique operates by reducing the statistical uation in each pixel by averaging the pixel with its closest hbours. The visual prominence of noise is suppressed through process. The disadvantage is that resolution is decreased.

SK RE-REGISTRATION

It's sometimes useful when there is yet patient motion between time the mask is taken and the time that contrast material arrives e vessel of interest.

The re-registration of mask may be accomplished either;

1. **MANUALLY (VIEWER-CONTROLLED)**
2. **AUTOMATICALLY (COMPUTER CONTROLLED)**

FORE RE-MASKING **AFTER RE-MASKING**

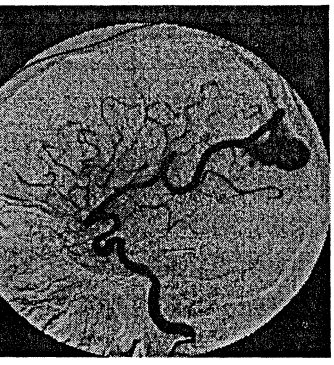

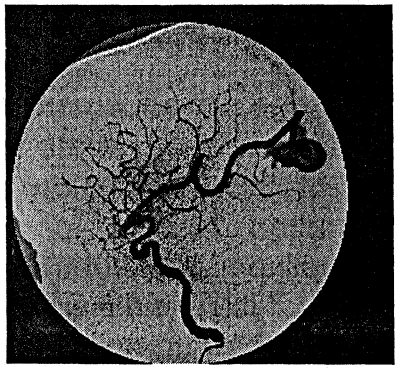

The patient is 3-dimenssional and mask re-registration rations are effective only for motions confined to a plane;

Upper structures project on to different lower structures when the patients roll on to one side as compared to being flat on his

back. Re-registration cannot exactly compensate for this type of motions.

- Motion of structures with in the patient(especially bowel gas and larynx) also changes the relative positions of prominent structures, and again re-registration cannot compensate exactly.

MAGE ZOOM :

ITH OUT ZOOM

WITH ZOOM

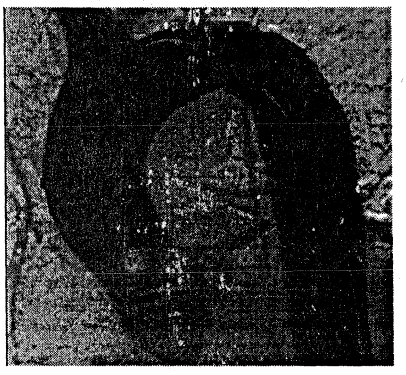

mage zoom allows for magnification of an area of interest but owever it does not increase visibility of detail.

mage Reregistration or Remasking :

hese two tools can be helpful to reregister or remask the image, hich is helpful in eliminating motion artifacts. Misregistration, which ccurs when the mask and the series images are not aligned, can be orrected through this process.

ixel Shifting:

This is a post processing technique. Mainly two types of pixel hifts are there;

1. AUTOMATIC PIXEL SHIFTING
2. MANNUAL PIXEL SHIFTING

UTOMATIC PIXEL SHIFTING

The automatic pixel shift is used to perform the registration on either the left or right side of the image using a ROI positioned by the operator; the calculation in the ROI shall always be limited to the useful part of the image. The box

should be positioned so that it covers a ROI containing vessels and subtraction artifacts, which disturb the visibility of vessels. The calculated shift would be more effective if the edges of the horizontal and vertical bone structures are present in the ROI. If the shift is greater than 7.5 pixels, the system unable to register the image and ROI is needed to reposition.

WITH OUT PIXEL SHIFTING

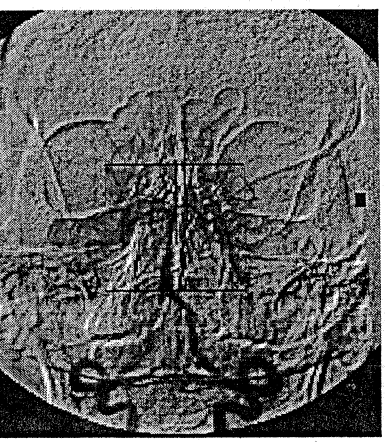

AFTER AUTOMATICPIXEL SHIFTING

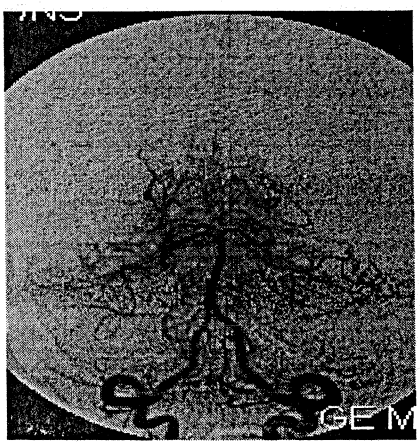

NUAL PIXEL SHIFTING

The joystick can be used to shift the image to reduce the registration error. The manual pixel shift adjustments let you to register subtracted images when movement occurred between mask selection and image acquisition.

The pixel shift is equal to 0.1 pixels in 512 matrix and 0.2 pixel in 1024 matrix.

TH OUT PIXEL SHIFT

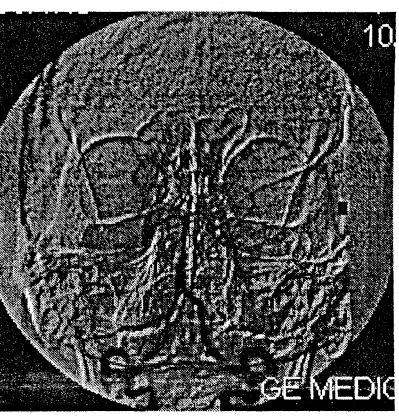

WITH PIXEL SHIFT

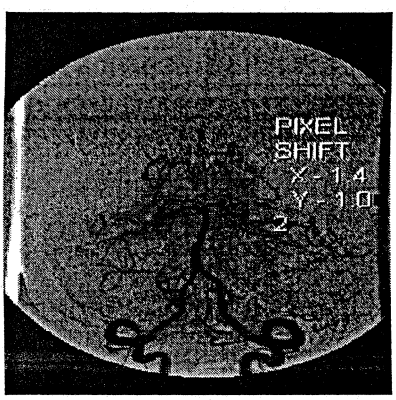

oad Mapping:

oad mapping is a means of tracking or tracing with small amounts of ontrast material injected. The vascular path is remembered by the ystem, and a print can be made or it can be subtracted from a image ith no contrast media. Road mapping that provides a continuous eal-time DSA image is widely used and is extremely helpful for ngioplasty, embolization and difficult or superselective procedures. he catheter, as well as the contrast filled artery, appears on the onitor, and acts as a guide for the catheter.

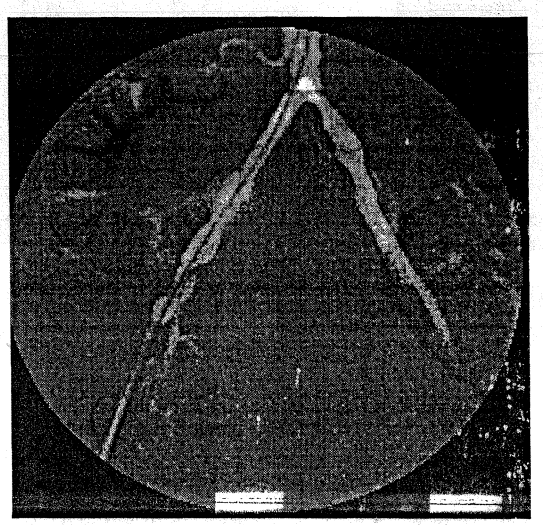

AXIMUM OPACIFICATION

Lets the operator view the maximum density reached by each ixel in a range of images. This function is useful to show on a single mage the vessel opacified at their higher intensity.

NTEGRATED MASK

It creates an average image from a range of images; the ing image is used as a mask.

GRATED IMAGE

It creates an average image from a series of images. The vement in SNR makes it suitable for poorly injected sequence

iving of DSA Images:

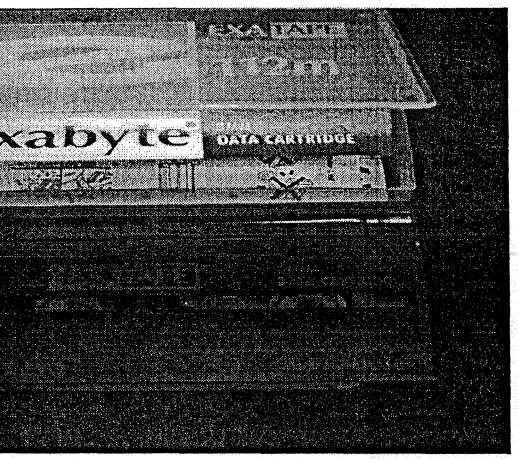

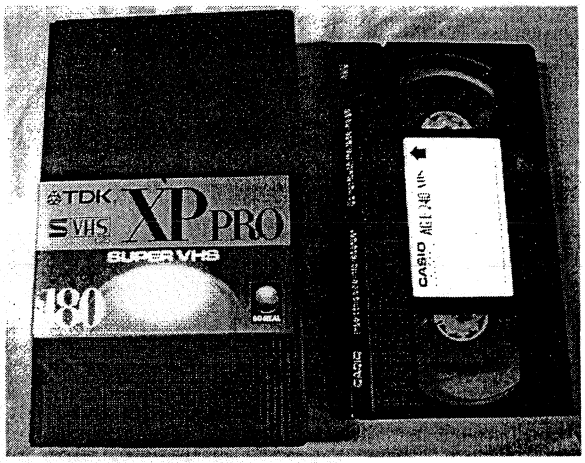

is possible on video tape recorders and digital disk. Final hard es of digital images are printed on either multiformat or laser eras.

AN CIRCULATORY SYSTEM

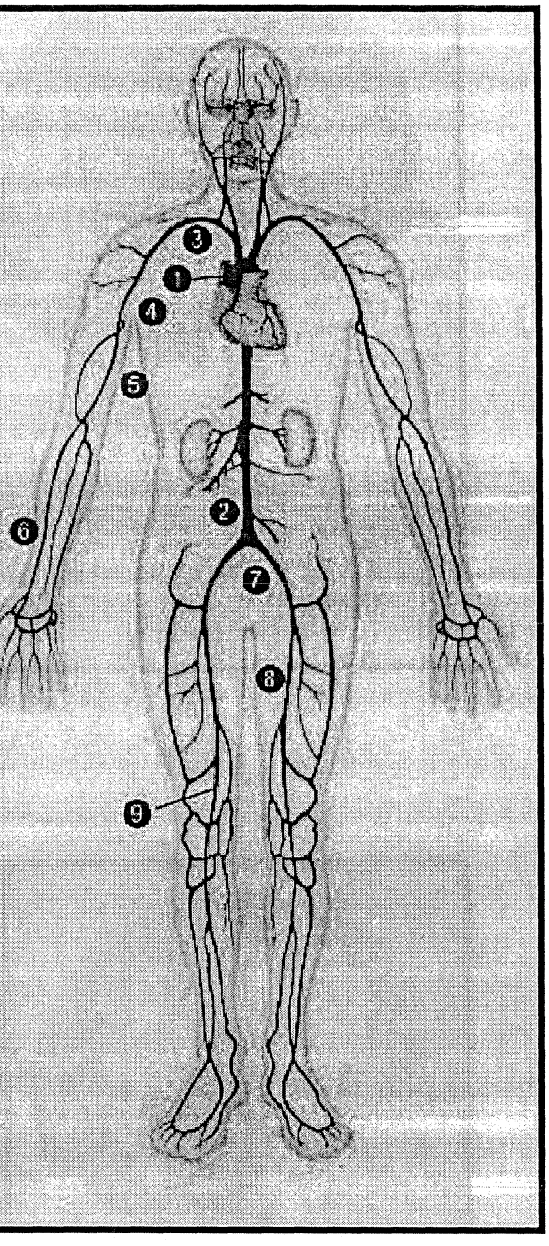

ARTERIES

1. Ascending aorta
2. Abdominal aorta
3. Subclavian artery
4. Axillary artery
5. Brachial artery
6. Radial artery
7. Common iliac artery
8. Femoral artery
9. Popliteal artery

nternal Carotid Artery

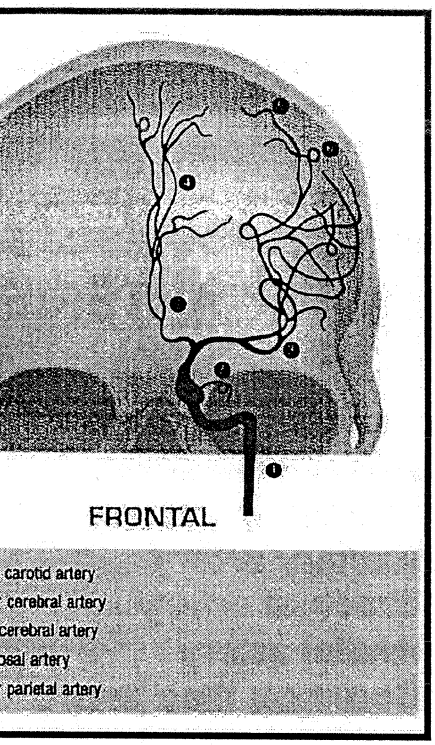

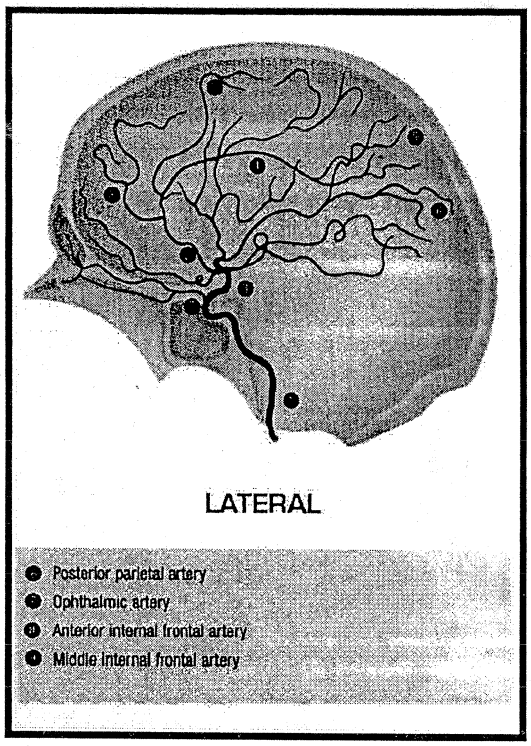

Vertebral Artery

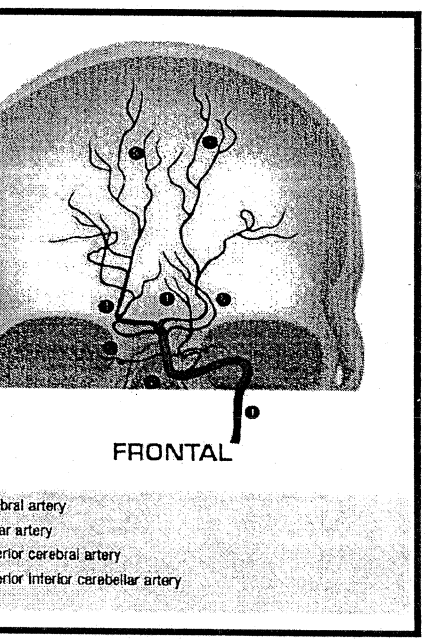

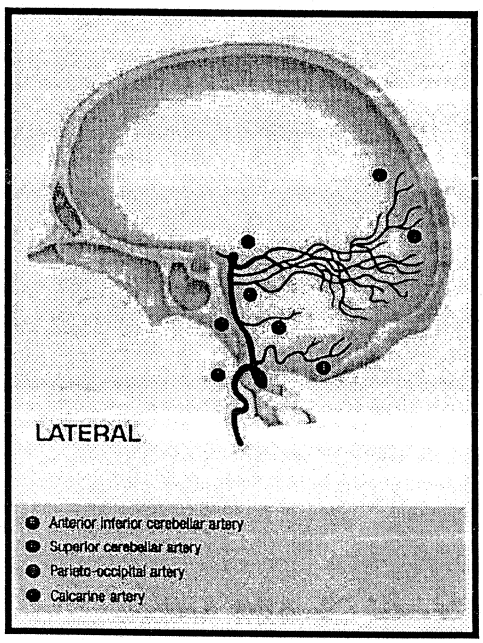

ternal Carotid

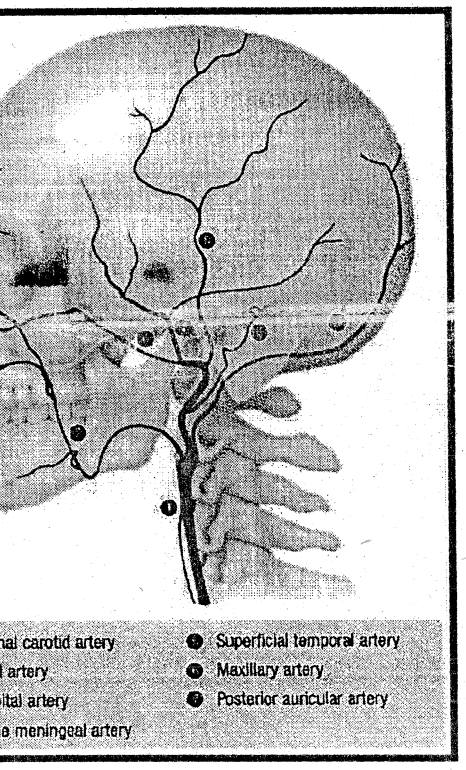

Neck vessels

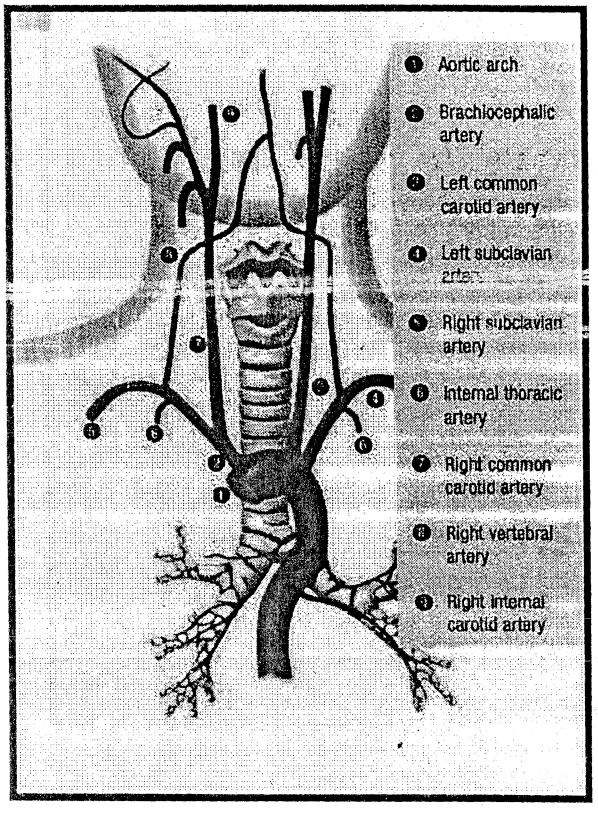

Right Coronary Artery

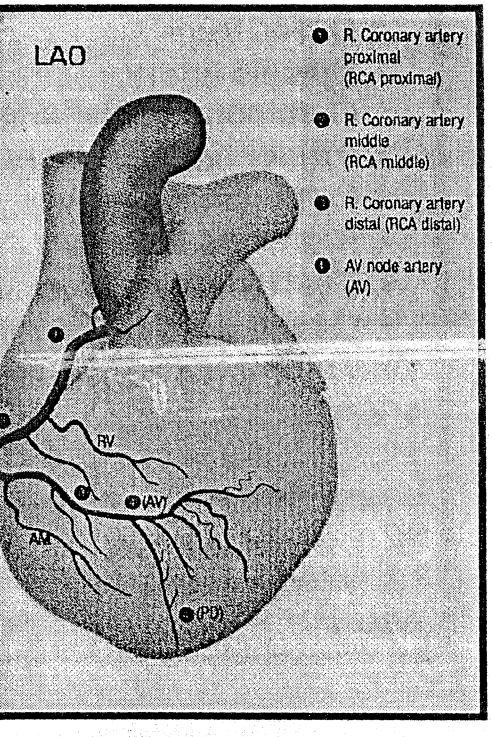

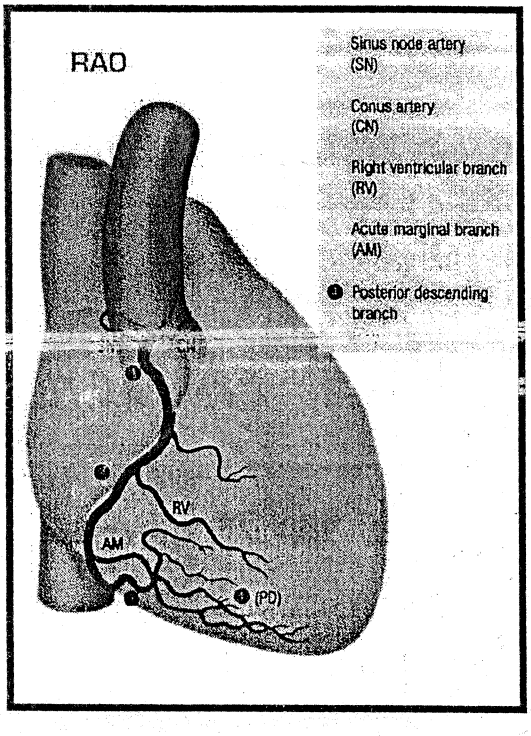

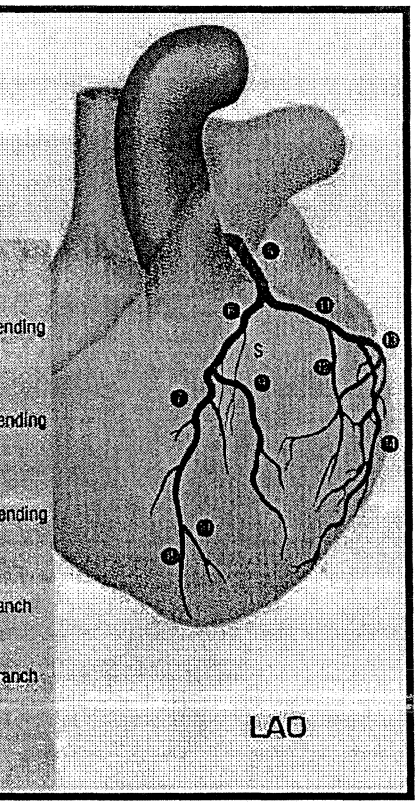

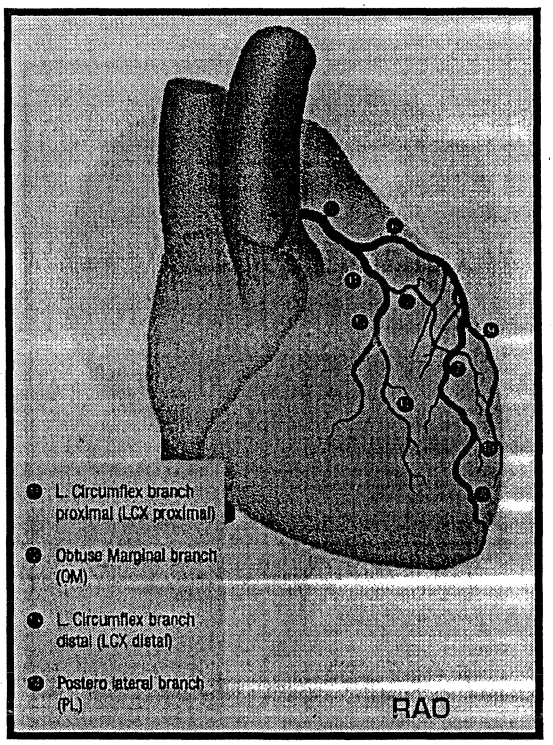

Abdominal

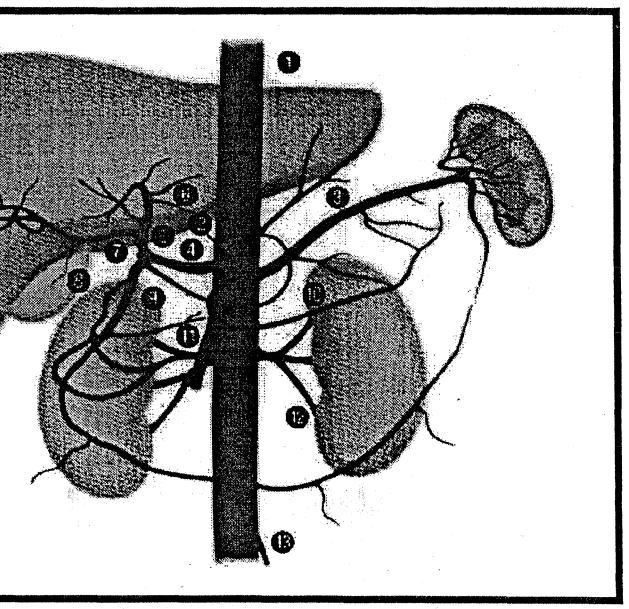

1. Abdominal aorta
2. Celiac trunk
3. Splenic artery
4. Common hepatic artery
5. Proper hepatic artery
6. Left hepatic artery
7. Right hepatic artery
8. Cystic artery
9. Gastro duodenal artery
10. Transverse pancreatic artery
11. Superior mesenteric artery
12. Left renal artery
13. Inferior mesenteric artery

Hepatic Arteries

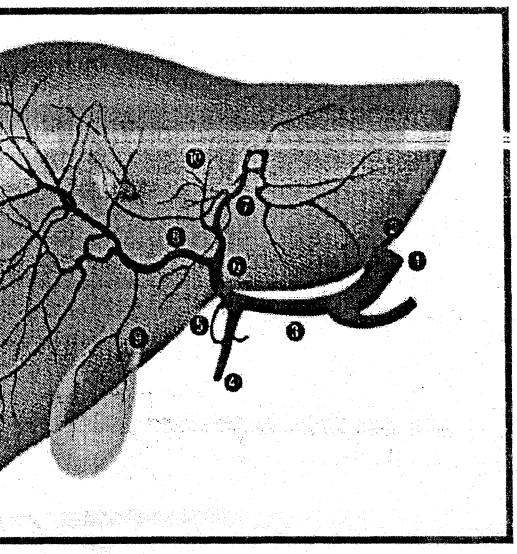

1. Celiac trunk
2. Left gastric artery
3. Common hepatic artery
4. Gastro duodenal artery
5. Right gastric artery
6. Proper hepatic artery
7. Left hepatic artery
8. Right hepatic artery
9. Cystic artery
10. Middle hepatic artery

Portal Vein and Pancreas

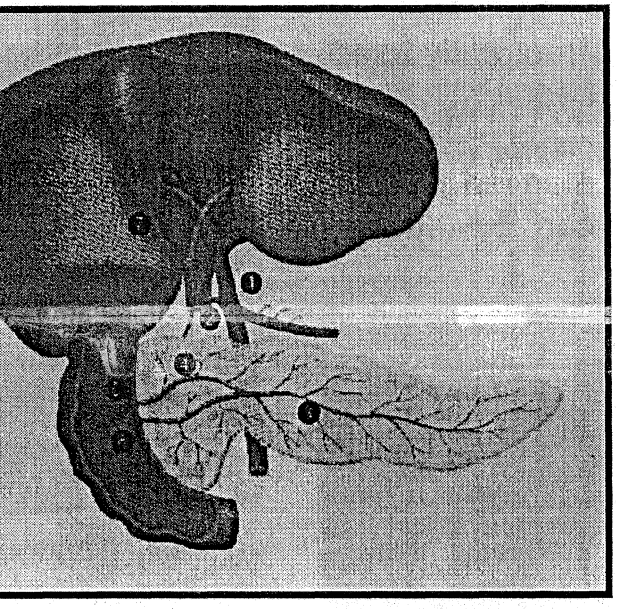

1. **Portal vein**
2. **Common bile duct**
3. **Pancreatic duct**
4. **Accessory pancreatic duct**
5. **Lesser duodenal papilla**
6. **Greater duodenal papilla**
7. **Cystic duct**

RODUCTION TO CATHETER TECHNIQUE

e basic technique of arterial catheterization is applicable to veins

IENT PREPRATION

1. The patient will need to be admitted to hospital, as careful preparation before and observation for 24 hours after the procedure will be required.
2. The arrangements should be made to discontinue anticoagulants.
3. The radiologist may wish to see the patient on the ward prior to the examination. This will be the time when:
    a. The procedure is explained and questions answered
    b. Informed consent is obtained
    c. The patient is examined, with special reference to blood pressure and peripheral pulses as a base line for post angiographic problems.
4. The puncture site is shaved.
5. Pre medication - pethedine
   phenergan

UNCTURE SITES

1. Femoral artery – the most frequently used.
2. Axillary artery.
3. Brachial artery
4. AORTA- by using Teflon sleeved needle for trans lumbar aortography the sleeve can be directly antegradely or retrogradely in the aorta.

FEMORAL ARTERY PUNCTURE

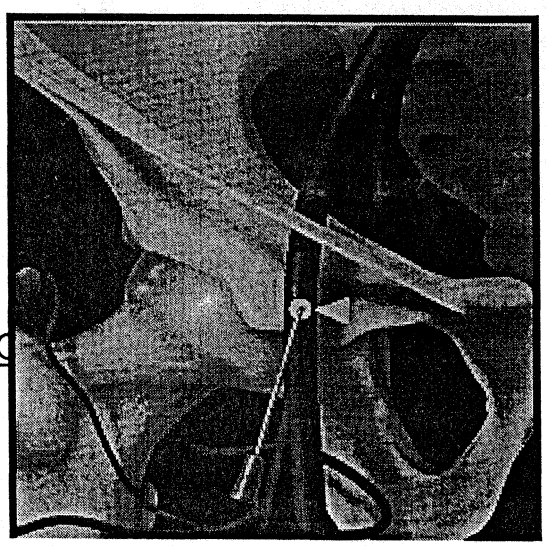

ONTRAINDICATI

1. Severe aortic,iliac or femoral artery artheroscierosis.
2. Blood dyscrasis.
3. Femoral artery aneurysm.
4. Marked tortuosity of the iliac vessels may preclude further advancement of the guide wire or catheter. In such a case axillary artery puncture or direct puncture, e.g. of a carotid artery, will be necessary.

PUNCTURING TECHNIQUE

SELDENGIER METHOD

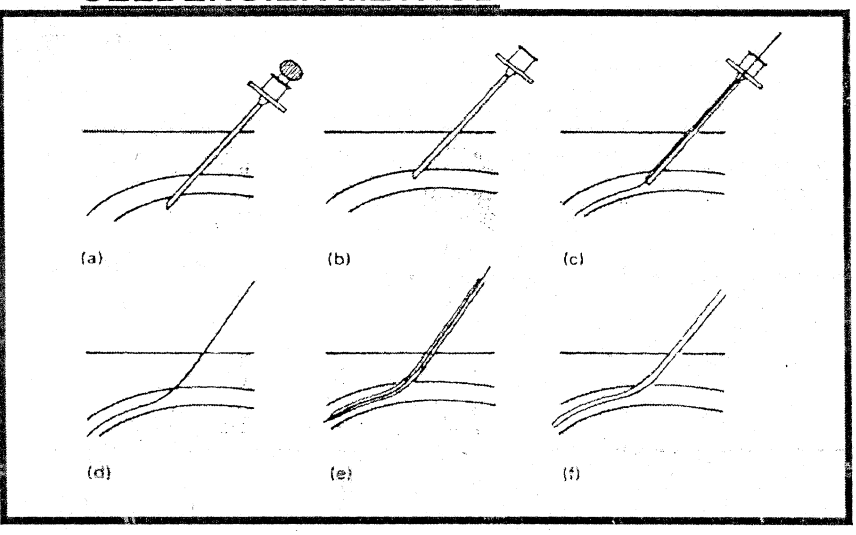

a. Both walls of the vessel punctured.
b. Stillette removed.needle with drawn so that the bevels is with in the lumen of the vessel and blood flows from the hub.
c. Guide wire inserted through needle
d. Needle with drawn, leaving guide wire in situ
e. Catheter threaded over wire.
f. Guide wire withdrawn.

TECHNIQUE

1. The patient lies supine on the x-ray table. Both femoral arteries are palpated and the easiest is selected for puncture. If the pulsation are equal, the right side is used

2. Before beginning, the appropriate catheter and guide wire are selected and their compactability checked by passing the guide wire through the catheter and needle.
3. Using aseptic technique, local anaesthetic is infiltrated either side of the artery down to the periosteum. A 5mm transverse incision is made over the artery to avoid binding of soft tissue on the catheter.
4. The actual point of puncture of the femoral artery must be considered. The femoral artery arches medially and posteriorly as it becomes the external iliac artery. Attempts to puncture the artery cephalad to the apex of the arch will result either in failure to puncture the artery or puncture of the artery deep in the pelvis at a point where haemostasis cannot be secured by pressure. Puncture distal to the arch may result in catheterization of the profunda femoris artery. Correct puncture is made at the apex of the arch with the needle directed to the 45° cephalad to the skin surface and slightly medially. The needle is then in direct line with the lumen of the artery .
5. The artery is immoblised by placing the index and middle fingers of the left hand on the either side of the artery and the needle is held in the right hand . The needle is advanced through the soft tissues until pulsation are felt transmitted through its tip. If the pulsations are localized to one side or other,the needle is either medial or lateral to the artery and should,therefore,be re-positioned. Both walls of the artery are punctured with a stab. The stilette is removed and the needle is slowly withdrawn until pulsatile blood flow from the end of the needle indicates a satisfactory puncture.poor flow may be due to:
    a. Femoral vein puncture
    b. The end of the needle lying sub intimally
    c. Hypo tension → due to vasovagal reactions during the puncture.
    d. Atherosclerosis
    e. Polycythaemia
6. When good flow is obtained the guide wire is inserted ɔugh the

    Needle and advanced up the artery using fluoroscopy to follow its travel. It should not be forced . When it is in the

descending aorta the needle is withdrawn over the guide wire keeping firm pressure on the puncture site to prevent bleeding. The guide wire is then wiped clean with a wet swab and the catheter threaded over it. The catheter is advanced up the descending aorta, under fluoroscopic control and when in a satisfactory position the guide wire is withdrawn.

6. The catheter is connected via two-way tap to a syringe of heparinised saline and after aspiration of air bubbles is flushed.
7. At the end of the procedure and the withdrawal of the catheter compression of the puncture site maintained for 10 min. if continued becomes a concern, consideration should be given to neutralizing the effect of heparin by giving protamine sulphate.

AXILLARY ARTERY PUNCTURE

Indications – as for femoral artery puncture but as this approach is associated with a higher incidence of complications it should only be used if femoral artery catheterization is unsuccessful.

Contraindications

1. Atherosclerosis of the axillary or subclavian arteries.
2. Subclavian artery aneurysm

Technique

1. The patient lies supine on the x-ray table with his/her arm fully abducted. Peripheral arm pulses and blood pressure are compared in each arm. The puncture point is just distal to the axillary fold and using aseptic technique the area is infiltrated with local anesthetic.
2. A small incision is made in the skin, 1-2cm distal to the point of arterial puncture.
3. The needle is directed more horizontally than in the femoral approach and along the line of the humerus.

4. Following satisfactory puncture the remainder if the technique is as for femoral artery catheterization.

ACHIAL ARTERY PUNCTURE

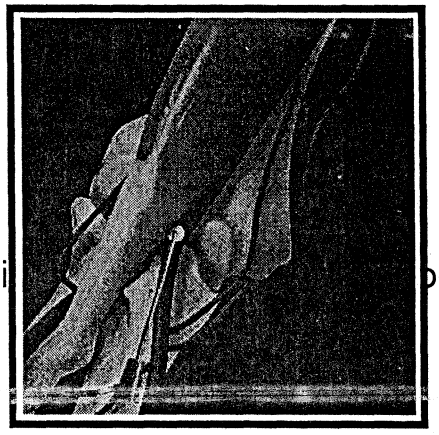

brachial artery i ographic procedures.

CATIONS

- Angiography when both ilio femoral arteries severely diseased or occluded.
- Common femoral artery region infection or recent surgical graft.

ONTRAINDICATIONS

- Uncorrectable bleeding diathesis.
- Known occlusion of brachial artery.
-

ETTING STARTED

INGS TO CHECK

- Check Brachial, Radial, Ulnar Pulses In Arm.
- Left arm is used because only cross-vertebral artery on way to aortic arch.
- On the right side cross right vertebral and carotid ostia as well as left carotid and left subclavian.

General complications of catheter technique

1. Due to anesthetic
2. Due to contrast medium

3. Due to the technique

Due to the anesthetic:- 1. General anesthesia
2. Local anesthesia:

The maximum adult dose of lignocaine is 0.2g. Anesthetic lozenges contribute to the total dose.

Symptoms are of paraesthesia and trembling which may progress in to convulsions, cardiovascular and respiratory depression and death.

Treatment is symptomatic.

Due to the contrast medium

ALLERGIC AND IDIOSYNCRATIC

Non fatal reactions are much less common with intra-arterial injections than with intravenous injections.

TOXIC

1. Hot feeling : This is localized to the region supplied by the injected artery. Injection of conventional contrast media may cause severe pain typically when injected in to the arm, the artherosclerotic lower limb or the external carotid artery . symptoms are due to the high osmolarity and it is for this reason that the new low-osmalar contrast media are preferred.
2. A large dose delivered to a specific organ may have a chemotoxic effect.

    a. Coronary arteries – pure sodium or meglumine salt produce impaired myocardial contractility and ECG changes. Addition of calcium to the contrast medium improves contractility but also increases the subjective feeling of the warmth.
    b. Cerebral arteries - Sodium salts are more neurotoxic than meglumine salts.
    c. Spinal cord – direct injection to a lumbar or intercoastal artery which feeds the artery of the Adamkiewicz, or diversion of contrast medium in

to the spinal vascular bed in low aortic obstruction, can results in spinal cord damage.

d. Kidneys – Acute renal failure is a rare complication and is more likely association with :

- Pre-existing renal disease, diabetes or myelomatosis.
- Decreased renal perfusion(hypotension,dehydration,low-out put cardiac failure)
- Large volumes of contrast medium
- Recent administration of nephrotoxic drugs.

Due to technique:

LOCAL

1. Haemorrhage/haematoma.
2. Arterial thrombus. May be due to:
   a. Stripping of thrombus from the catheter wall as it is withdrawn
   b. Trauma to the vessel wall.

   Factors implicated in increased thrombus formation are:

   a. Large catheters
   b. Excessive time in the artery
   c. Many catheter changes
   d. Inexperience of the radiologist
   e. Polyurethane catheters, because of their rougn surface.

   The incidence is decreased by the use of:
   a. Heparin-bonded catheters
   b. Heparin – bonded guide wires
   c. Flushing with heparanised saline
3. Infection at the puncture site
4. Damage to local structures, especially the brachial plexus during axillary artery puncture.

5. False aneurysm.Rare.Present as a pulsatile mass at the puncture site, usually 1-2 weeks after angiography and is due to the communication between the lumen of the artery and a cavity with in an organized haematoma.Treatment is surgical.
6. Arteriovenous fistula. Rare.

DISTANT

1. Peripheral embolus from the stripped catheter thrombous. Emboli to small digital arteries will resolve spontaneously; emboli to large arteries may need surgical embolectomy.
2. Atheroembolism. More likely in old people. J- shaped guide wires are less likely to dislodge atheromatous plaques.
3. Air embolus. May be fatal in a coronary or cerebral artery. It is prevented by:
    a. Ensuring that all taps and connectors are tight.
    b. Always sucking back when a new syringe is connected.
    c. Ensuring that all bubbles are excluded from the syringe before injecting.
    d. Keeping the syringe vertical,plunger up, when injecting.
4. Cotton fibre embolus. Occurs when syringes are filled with from a bowl containing swabs prevented by,
    a. Separate bowls of saline for flushing and wet swabs, or
    b. A closed system of perfusion.

5. Artery dissection, due to entry of catheter guide wire or contrast medium in to the subintimal space. It is recognized by resistance to the movement of the guide wire or catheter or increased resistance of injection of contrast medium. The risk of serious dissection is reduced by:

    a. Floppy J- shaped guide wires
    b. Pig tail catheter
    c. A test injection prior to a pump injection

d. Careful and gentle manipulation of the catheters.

6. Catheter knotting
7. Catheter impaction
8. Guide wire breakage

TERIALS USED FOR ROUTINE ANGIOGRAPHY AND ERVENTIONS

YRINGES

Syringes used for flushing of the microcatheter, ography,and injection of the embolic agents must have luerlocks ppropriately secure them to the hub of the microcatheter. The el and sturdy enough for repeated use. Most operators use either or 3cc syringes because adequate injection rates are difficult to in with larger volume syringes. The 1cc syringes are made up of r poly carbonate barrels and plungers that are provided in several rs.

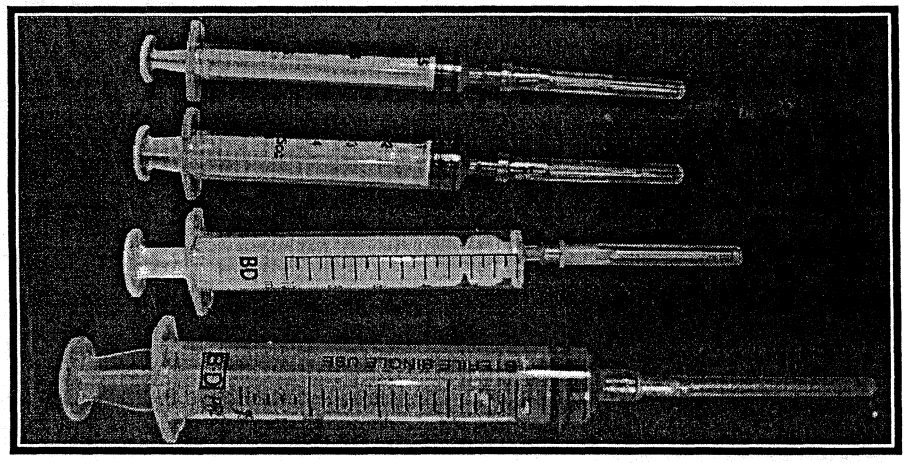

licro puncture Needles

d to reduce complications in patients when they are at a risk for eding, or to prevent accidental puncture of nearby nerves or vital

organs. They are also useful in arteries that are prone to spasm or in patients with grafts or poorly palpable arteries

One- Piece or single-walled needles are multipurpose needles that consist of a beveled needle with a base plate; there is no stylet . Two-Piece or double-walled needles consist of an outer cannula with an inner stylet and obturator . Examples include the two piece Seldinger or modified Potts needle.
Three-piece or sheath needles consist of a cannula, stylet and sheath. The stylet is in the cannula, and this system is inside the sheath. Examples include the three-piece Potts Cournand.

NEEDELS

- Single Wall
- Seldinger Type
- Modified Cournand Type

SELDINGER NEEDLE

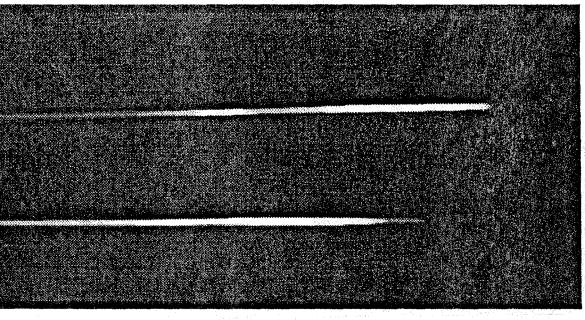

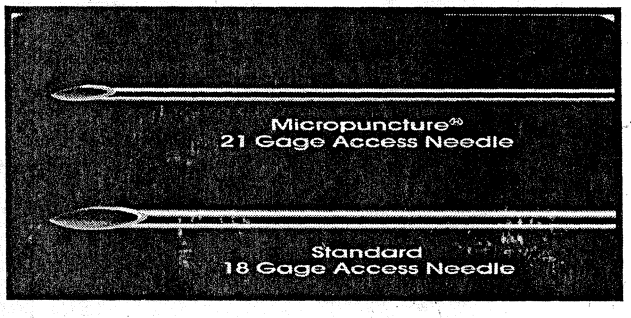

Arterial needles generally are 2 1/8" or 3 1/4" long and come in a variety of gauge sizes. The 16 to 20 gauge needles are generally used, with the 18 gauges being the standard. All needles used in angiography are thin-walled in comparison to hypodermic needles, which are not. This allows the passage of the guide wire through the needle. A variety of needles are also available for special interventional procedures. Percutaneous arterial needles are available in a variety of designs .

ODUCER SHEATH

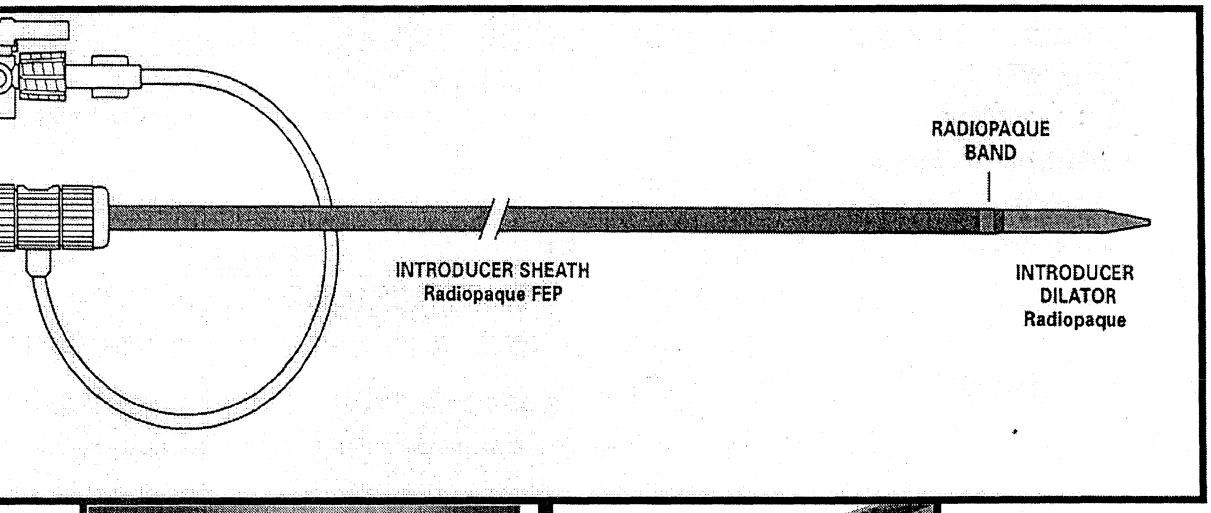

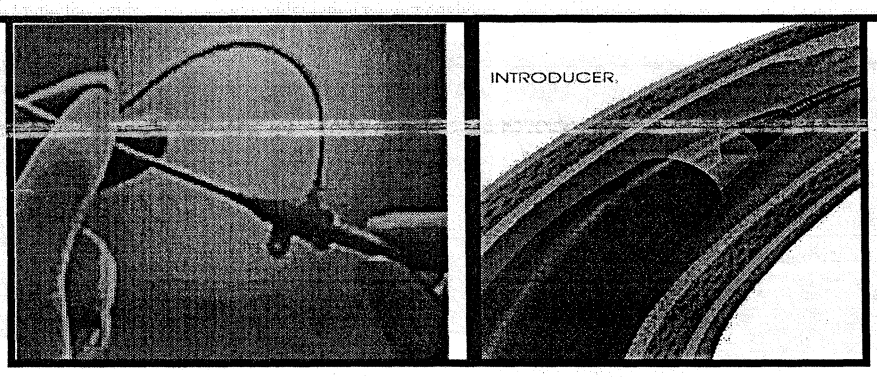

aths provide smoother and safer catheter introduction during edures that require multiple catheter exchanges or arduous ipulation of the catheter. Sheaths usually come with safety ures such as a sideport for heparin and or contrast installation for obtaining pressure measurements. There should also be a ostasis valve to prevent air aspiration and blood backflow. ath also come with a interlocking dilator to aid in the insertion of sheath, once the sheath dilator is in the artery, the interlocking can be detached and the dilator portion can be removed

For most interventional procedure, after arterial access has been obtained, the placement of sheaths offers significant advantages.

1. Repeated access to the artery
2. Ease of catheter maneuverability.
3. Lessened bleeding.

The placement of a sheath of appropriate length may also allow the operator to negotiate tortuous anatomy only once. There are numerous sheaths available in from various manufactures.

INTRODUCER SET

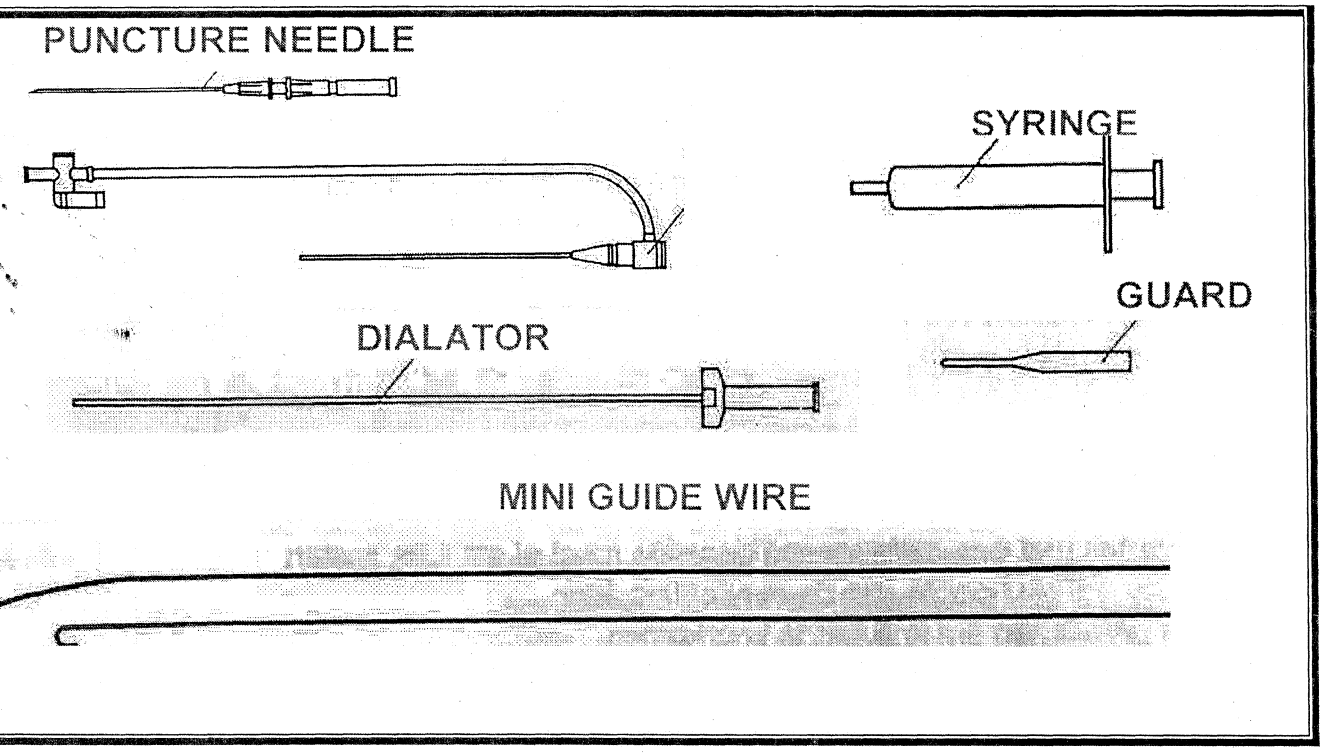

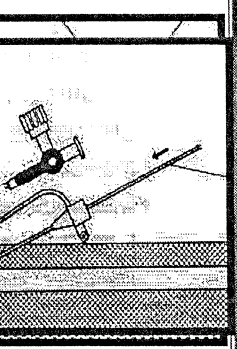

Fig-2

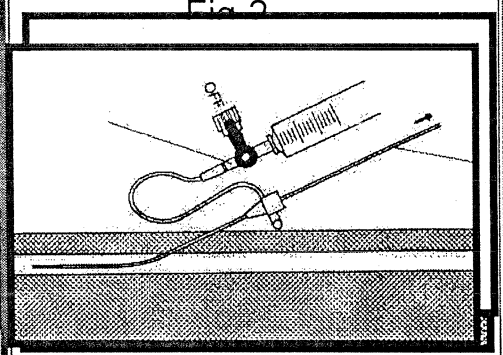

Fig-3

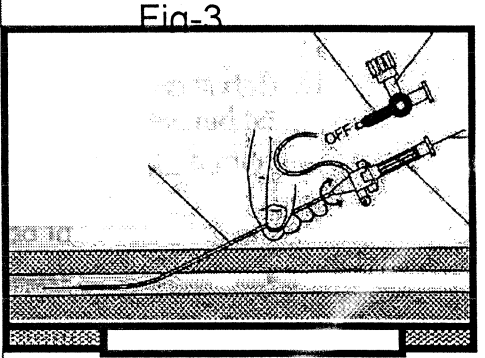

Fig-5

Fig-6

Fig-8

Fig-9

INSTRUCTION FOR USE

1. Make a small incision at the puncture site with surgical knife.
2. Insert an entry needle to puncture the blood vessel. Then remove the inner metallic needle (fig-1) reinsert the inner needle of the entry needle in to the plastic cannula. Dispose the removed inner metallic needle safely being careful to avoid infections.
3. Before inserting angled/spring mini guide wire, set the guide inserter at the plastic cannula hub for easy insertion. Insert the flexible end of the mini guide wire through the plastic cannula in to the vessel. (Fig-2).
4. Remove the plastic cannula over the mini guide wire.
5. Connect flushing line to the 3-way stopcock of the introducer sheath. Fill the sheath assembly completely with heparanized saline, removing all air.
6. Prime the dilator using the syringe with heparanized saline.
7. Insert the vessel dilator fully in to the sheath. The female hub of the sheaths connects with the male hub of the dilator, and locks in place by means of grip. (Fig-3)
8. Insert the dilator and sheath together over the mini guide wire, and in to the blood vessel (fig-4)
9. Unlock the dilator hub from the sheath hub by bending the dilator hub downward. (Fig-5)
10. Slowly remove the dilator and mini guide wire, leaving the outer sheath in the vessel (fig-6). If injection or sampling is necessary at this point, remove the mini guide wire, and use the dilator hub as an injection port before removing it.
10. Insert the catheter in to the valve center of the sheath.
11. Insert a catheter through the sheath and in to the blood vessel, and advanced to the desired location (fig-7). When

exchanging catheters, remove the used catheter and repeat the same step.

12.When inserting, manipulating or withdrawing a catheter from the sheath always hold it in place .to temporarily suture the sheath

11. After the intended procedure is completed, remove the catheter and then the sheath.

12.

ONTRAINDICATION

1. Patient must not exceed a 60° angle position post procedure.
2. An introducer obturator must be inserted in to the sheath before a patient can sit up.

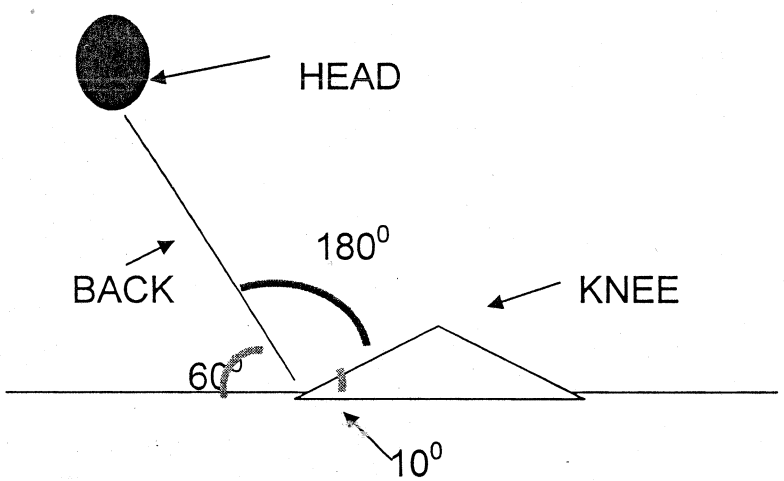

VARIOUS SIZES	COLOUR
4F (1.35mm)	
5F (1.65mm)	
6F (2.0mm)	
7F (2.3mm)	
8F (2.7mm)	
9F (3.0mm)	
10F (3.3mm)	
11F (3.7mm)	

DILATORS

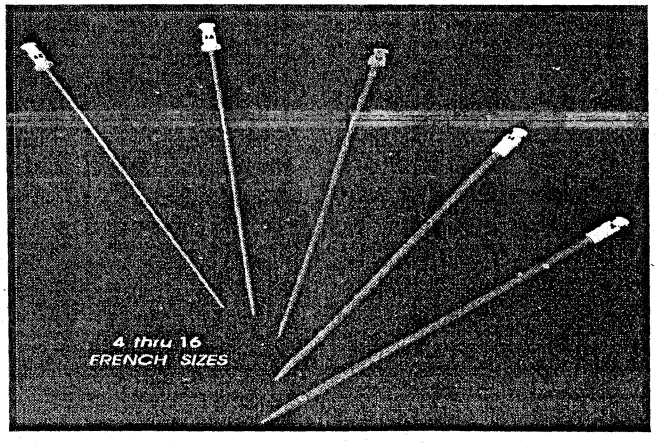

tors are thick-walled plastic tubing with a tapered end that provide act from the skin surface to the vessel, assuring smooth catheter y. The dilator is most commonly used when a guide wire is in a sel but catheter placement is difficult, when a vessel is heavily rred, when plaque is present at the puncture site, or in the sence of a graft. In the case of dilation of a graft, the rventionalist will find it necessary to overdilate , by going up one nch size

APTERS

vides a means of connection between instruments; classified as e and female; the female adapter can only be connected to a e connector and the male adapter to a female connector.

STOPCOCKS

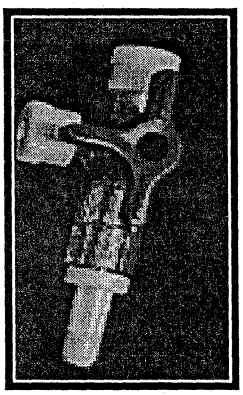

re valve attachments to control the passage of fluid (blood , trast, parenteral fluids) that opens and closes with the turn of a er

MANIFOLD

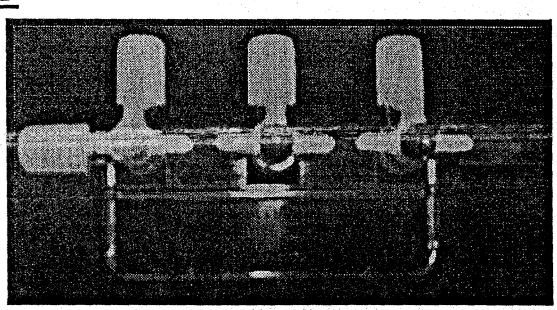

A series of stopcocks placed in either a Y formation or a linear formation. The linear formation allows for the discreet regulation of individual stopcocks.

TUOHY-BORST

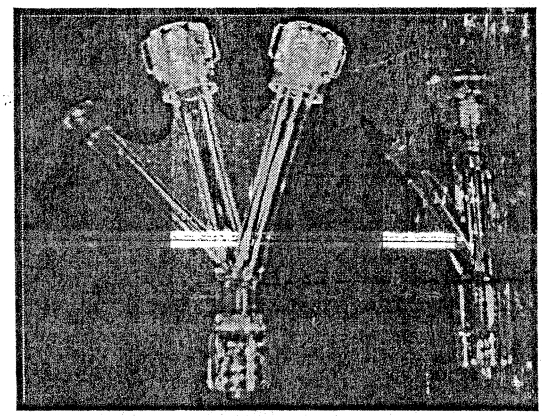

It is an adapter that provides a continuous flush in a coaxial system between the two systems.

PRESSURE SALINE BAG

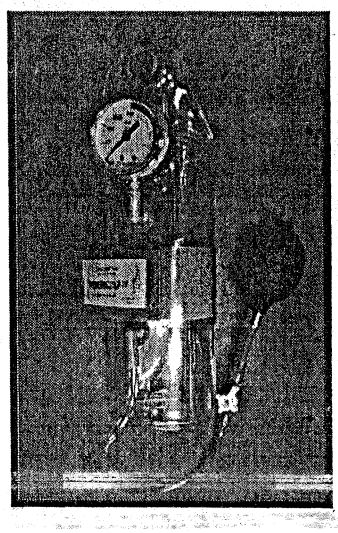

CONTRAST

The contrast material used for interventional procedure should be non-ionic for several reasons.

1. Perforation or extravasation can occur at any time.

. non-ionic contrast media are less toxic to the CNS tissue and less likely to provoke seizures.
. Non-ionic contrast has been shown to cause less renal failure in those patients with underlying renal disease, and it seems reasonable that in other patients there may also be less renal toxicity with non-ionic contrast usage.
. In the awake patient, the non-ionic contrast cause less movement on injection , allowing for superior images.

rawback of non-ionic contrast has been the possible increase in formation , which has been somewhat controversial.

ther suggested drawback has been the greater coast of non-ionic.

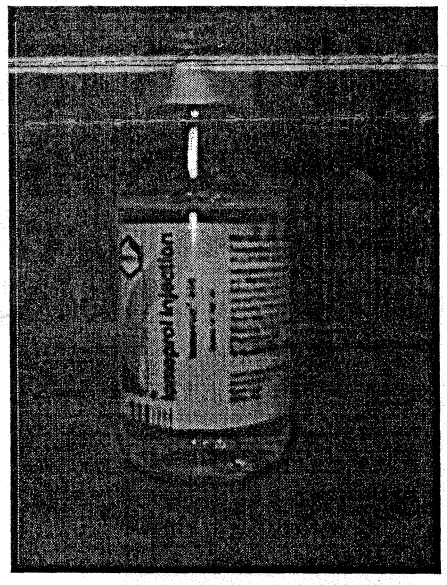

omatic Pressure Injectors

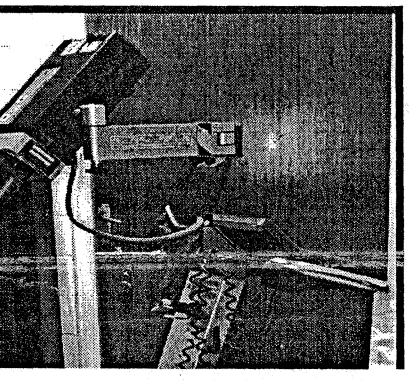

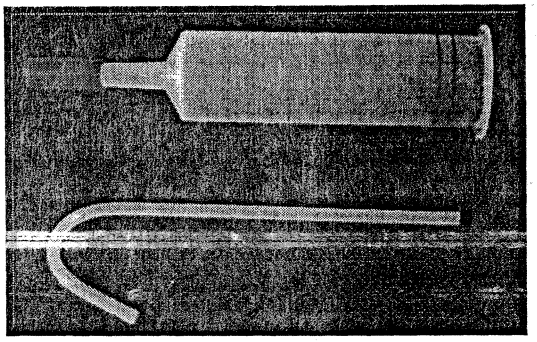

The automatic power injector most commonly used today allows for specific volume of contrast to safely be delivered at a precise flow rate, regardless of the variables. Using the electromechanical injector, the parameters can be set at a control panel, directing the amount (ml) of contrast media to be delivered over a set period of time (per second). For example, 15 ml/sec for 4 seconds would be a total volume of 60 ml. The components of the pressure injector include: Syringe Removable; usually sterile disposable type Heating Device Reduces viscosity of the contrast media High Pressure Mechanism Electromechanical system with a motor drive connected to a screw, that drives the plunger piston plate and transmit motion to the syringe Control Panel Allows for programming and display of the injection parameters, i.e., volume flow rate, PSI, injection delay, film delay, linear rise, reset/abort button, visible and audible warning alarms.

Functions of an automatic injector include:
Flow rate - the rate at which the contrast media is going to flow. Variable introduce into flow rate include catheter length, diameter and the number of side holes, as well as contrast viscosity
Volume - the desired amount of contrast you want to deliver Linear rise- the time it take to reach the desired flow PSI (pounds per square inch)- the pressure at which you inject the contrast media. The pressure should never be higher than the catheter can accept or higher that the vessel can tolerate. The smaller the vessel, the lower the pressure.
Injection delay - the filming will start and the injection, according to the delay set Filming delay- the injection will start first, and then the filming will begin.

Automatic pressure injectors are equipped with multiple safety features to prevent inadvertent damage to the patient or damage to the catheter.

ction monitoring devices : A flashing red light, audible warning or rinted message to notify the operator that a setting has been tted or that there is some mechanical malfunction
ume limiting device: The maximum limit on the amount of contrast inistered is set on the control panel, but a backstop lever is ted on the head of the injector. Pressure limiting device: Sets a ximum pressure (PSI) to be induced, prevents catheter breakage ecoil and vessel damage; ensures safe use with low-pressure neters.
elerator regulators : Allows the drive motor to propel over an ct duration of time, to guard against recoil
e rise control: Allows gradual rise in (PSI) instead of an instant ge or pressure all at once

dditionally, the radiographer must take care to properly load the nge. With the syringe pointing up straight up, clear all air bubbles n the syringe. Automatic injectors have loading and unloading ons to draw up and empty contrast. When hooking up to the neter, point the injector head down. In the event any air bubbles in the syringe, they would rise away from the catheter. A high ssure connector is usually used to connect to the catheter . This ws for better visualization of any air bubbles. The radiologist will ct the radiographer to first advance contrast. Once the connection nade, aspirate back blood and check for any air bubbles in the necting tube. Care should be taken not to aspirate too much od, as this will dilute the contrast and could possibly cause clot nation in the injector syringe. Before the injection begins, the iologist and radiographer should confirm the parameters selected. ce the injection begins, the radiographer must be prepared to minate the injection, in the event of an emergency .

ctors in use:
giomat 6000

. Range : 0.1ml – 9.9 ml in 0.1ml increments .
: 1ml – 150ml in 1ml increment.
w rate range : 0.01ml – 40ml/sec in 0.01ml increments.
ration range : 0 – 10/255sec in 0.01sec increment.
ssure limit : 127 to 1200 psi in 1psi increment.

Medrad Envision CT injector
EOM 700 E

Fluid delivery perfomance:

Vol. Range : 1ml to max. syringe capacity (125ml)
Flow rate range : 0.1 – 9.9ml /sec in 0.1ml/sec increments
Duration range : 1sec – 20:50Min for 125ml syringe.
Pressure limit : 25 – 300 psi in 1psi increments
- 1.7 – 20.7 Bar in 0.1 bar increments

CATHETERS

Catheters are long, hollow tubes that supply an avenue or passageway for contrast media, embolizing materials or therapeutic medications or instruments. Catheters come in a variety of sizes that are measured in the term called French as general rule: 3F to 5F for children and 4F to 9F for adults. This term French refers to the outer diameter of the catheter.

Catheters also have a variety of shapes which include single and multiple curves. Catheters are designed to be either radiolucent to view bubbles or radiopaque for better visualization. Memory refers to a catheters ability to retain its shape. Torque refers to the catheters ability to twist and turn. Another term use to discuss catheters is Tractability this refers to how well a catheter can track over a guide wire Ordinary catheters cannot normally be directed into a CC-fistula or into the most distal external and internal carotid artery branches that may be supplying an AVM. So micro catheters are used they range in the order of 2.5fr. to 3.5fr. These are made of highly flexible silicone. These catheters may be either flow directed or may require the use of a guide wire.
Units Useful for Angiographic Catheters & Guide wires
1" = 25.4mm
1mm = 3F = 0.039"
1F = 0.013"

French FR	Sizes mm
1F	1/3mm
2F	2/3mm
3F	3/3mm

ample 9F catheter = 3mm Diameter

giographic Catheter

n-Braided Catheters

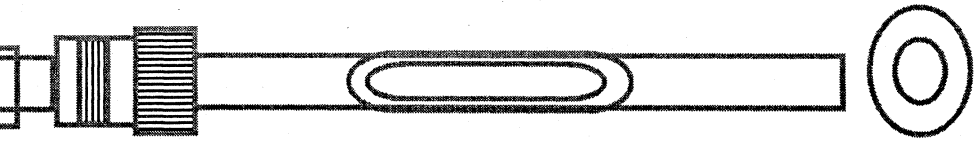

atheter Construction Cross
ction

pes:

dio opaque Polyethylene – has a medium coefficient of friction and s stiffness than TFE. It does absorb some moisture. Polyethylene ing contains Bismuth Salts for radio opacity. Suitable for selective d super selective angiographic studies.

hin wall radio opaque Nylon – has low friction coefficient and is kink esistant. Bismuth salts for radio opacity. Suitable for maximum high flow administration of contrast medium.

adio opaque TFE – has a lower coefficient of friction and higher urst point than polyethylene of similar wall thickness and out side iameter. TFE is stiffer than polyethylene. It doesn't absorb moisture. ismuth salts are used for radio opacity. Suitable for non-selective ngiographic studies. (! Never sterilise TFE by irradiation; complete isruption results.

adio opaque vinyl – is more flexible than standard polyethylene naterial. Suitable for selective and sub selective angiographic studies vhen standard catheter can't be advanced over wire guide to desired osition.

raided Catheters

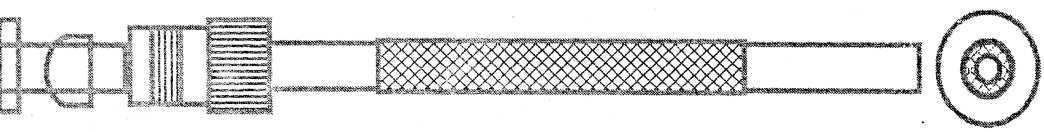

Catheter construction

Cross section

Types:

Thin wall radio opaque polyethylene with torque control – has tainless steel braided construction within catheter shaft which mparts torque control to catheter tip. Bismuth salts are used for radio

ity. Suitable for high flow administration of contrast medium in ctive angiographic studies.

wall Radio opaque Nylon with Torque control – has low icient of friction surface characteristics; incorporates stain steel ed construction with catheter shaft which imparts torque control theter tip for a One to One response. Bismuth salts are used for opacity. Suitable for high flow administration of contrast um in selective angiographic studies.

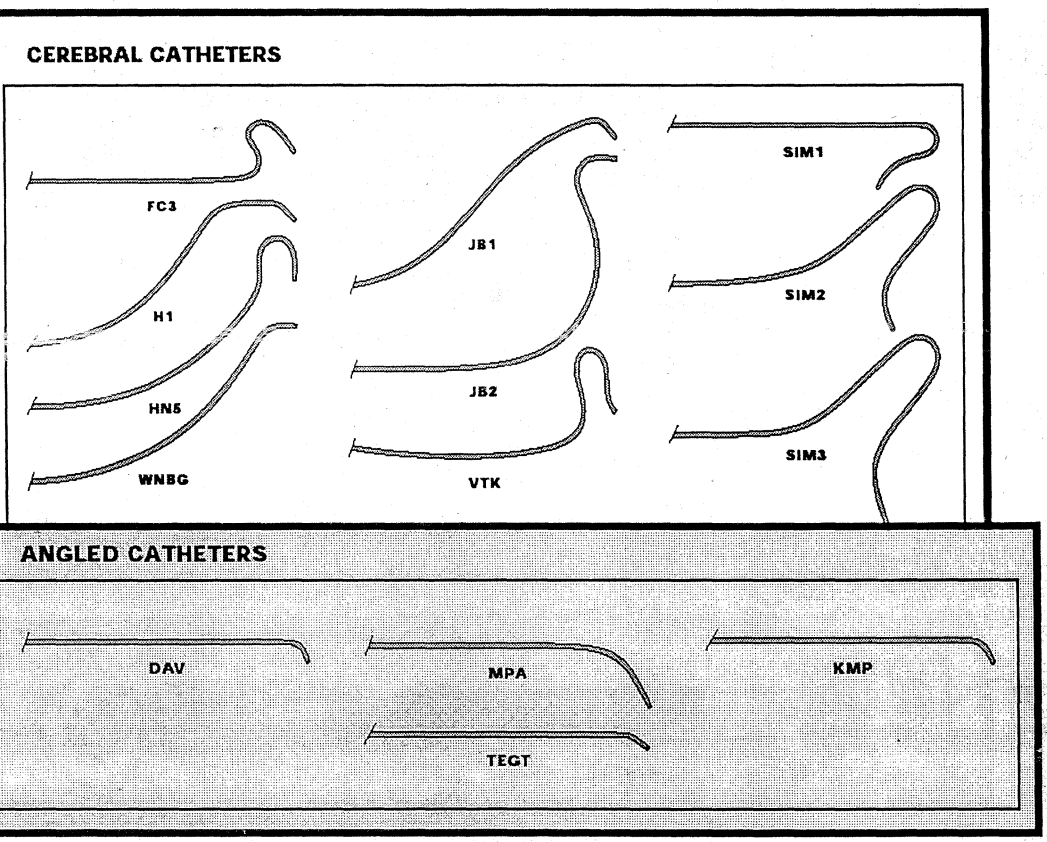

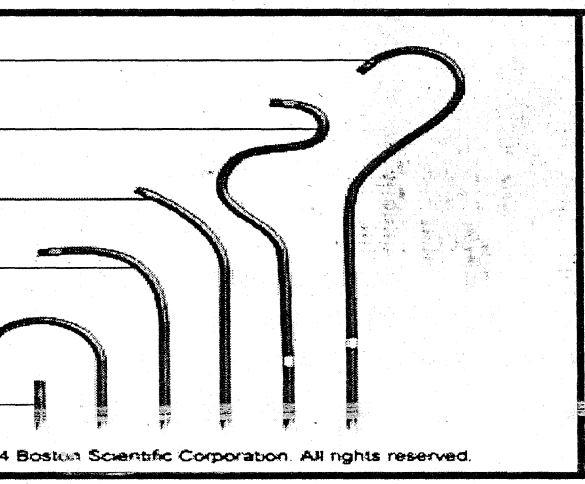

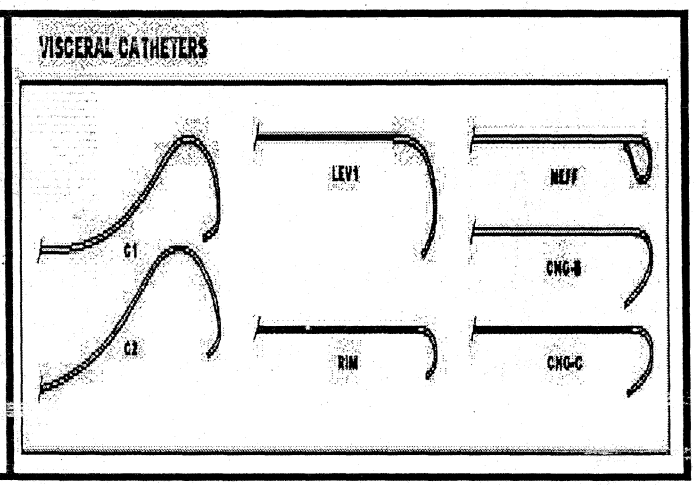

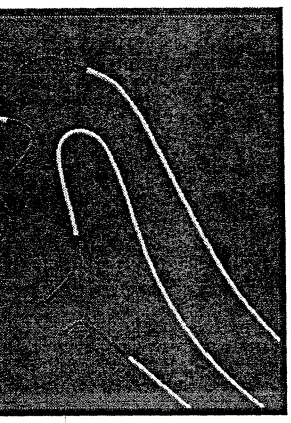
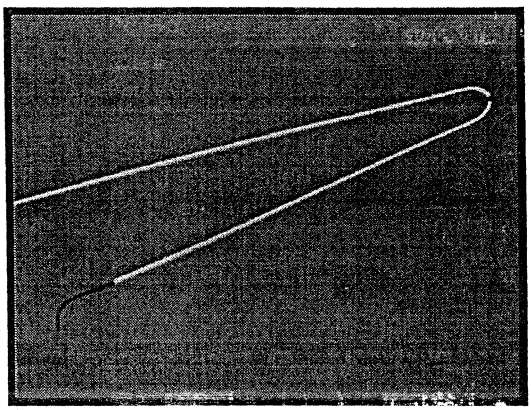
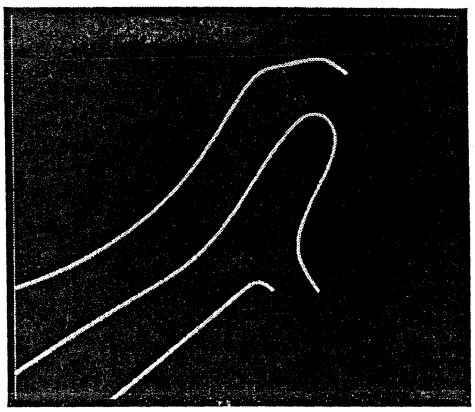

UIDE CATHETERS

sed in interventional procedures for introducing microcatheters. In electing the size of the micro catheter, the operator must always emember the goals of the procedure. This requires matching of the uide catheter inner lumen with the outer diameter of the micro atheter. In addition one must also keep in mind the inner lumen of ne micro catheter, so that appropriate embolics can be delivered .In electing the guiding catheter, the stiffness and shape of the tip are nportant. The guide catheter frequently will move with respiration nd with placement of the micro catheter. This can cause the tip of ne guide catheter to dig in to the intima, which seems to be occurring nore frequently with the pre shaped models. The stiffness of the uide catheter shaft also is important, because the micro catheters an exerts force against the guide catheter and push it from the esired vessel. However, too stiff a catheter may make initial lacement difficult and may also lead to undesired straightening of essels and sometimes-intimal damage. The length of the guide atheter is important in very tall individuals, in whom a 90-cm length nay be inadequate for appropriate positioning of the guide catheter.

lach 1™ Guide Catheter

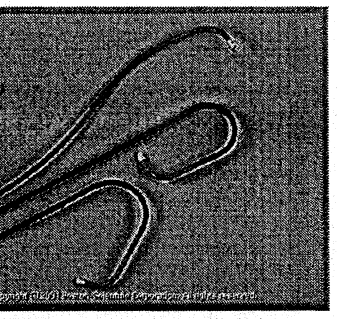

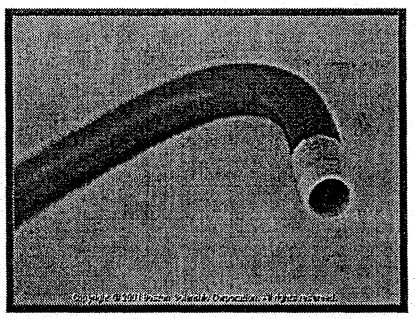

OAXIAL DESIGN LUMAX® FLEX GUIDING CATHETERS

sed as a support catheter for angioplasty catheters and other vices for intervention. The inner coaxial catheter is tapered to a 38-inch end hole to facilitate percutaneous placement of the guiding theter, without use of an introducer sheath, into the vessel. Device ovement through the catheter into the vessel is enhanced by a rge ID and low friction lumen surface. Catheter construction ovides excellent support without softening during procedural use. Max® Flex tip allows atraumatic engagement of target vessel while viding high radiopacity for precise positioning. Supplied sterile in eel-open packages. Intended for one-time use

VISTA BRITEV TIP

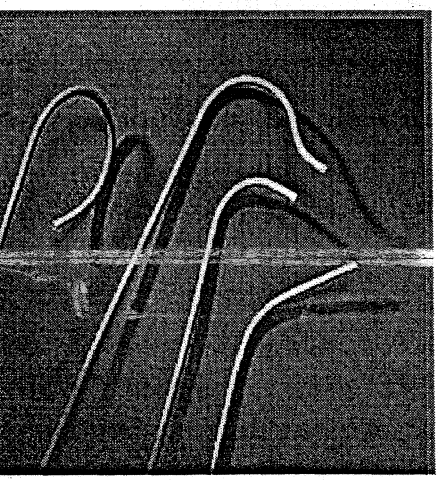

CROCATHETERS: - All of the commercially available micro theters are constructed of polyethylene and are hydrophilically ated. Many micro catheters wall contain braided materials, which proves flexibility, pushability, and trarckability of the microcatheter. ne braided construction lessens the incidence of micro catheter nking or ovalizing as it traverses bends. This braid feature can also

ANUFACTURES	OUTER DIAMMETER			INNER DIAMMETER		
	F	mm	Inch	F	mm	Inch
BALT	3F	0.95	0.040	1.6	0.60	0.023
	4.5	1.50	0.059	3.00	1.00	0.039
	5F	1.67	0.066	3.60	1.20	0.047
	6F	2.00	0.079	4.5	1.50	0.059
	7F	2.33	0.093	4.8	1.60	0.063
	8F	2.67	0.104	6.00	2.00	0.079
	9F	3.00	0.118	7.2	2.40	0.094
	10F	3.33	0.133	7.8	2.60	0.102
NYCOMED	5F	1.67	0.066	3.68	1.23	0.04797
	6F	2.00	0.079	4.44	1.48	0.05772
	7F	2.35	0.092	5.28	1.76	0.06864
	8F	2.68	0.105	6.00	2.00	0.079
	9F	3.00	0.118	6.99	2.33	0.093
	10F	3.35	0.131	7.80	2.60	0.102
	6F	2.00	0.079	4.92	1.64	0.064
CORDIS	6F	2.00	0.079	4.92	1.64	0.064
	7F	2.35	0.092	6.00	2.00	0.078
VISTA BRITE TIP	8F	2.68	0.105	6.768	2.256	0.088
	9F	3.00	0.118	7.53	2.51	0.098
	10F	3.35	0.131	8.46	2.82	0.110

use the microcatheter to move forward and suddenly to retract as e guide wire is removed. Most
urrently available micro catheters have similar performance aracteristics. All the catheters have a marker at the tip, and most e available in a two-marker variation for the deployment of coils.

ON BRAIDED

sTRACKER-10

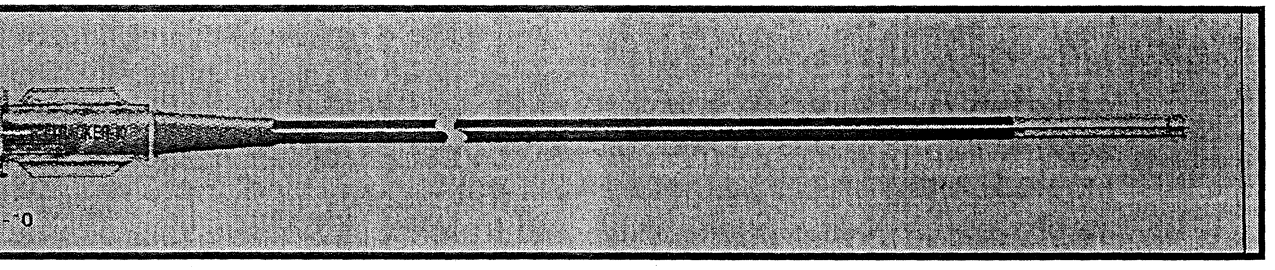

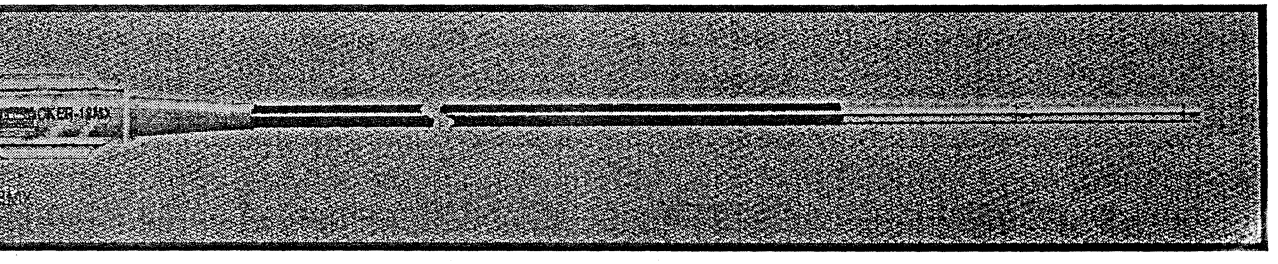

xcel-14

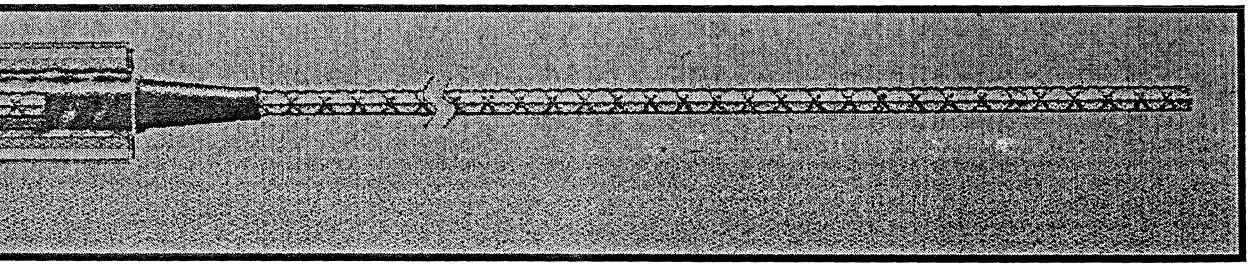

ENEGADE

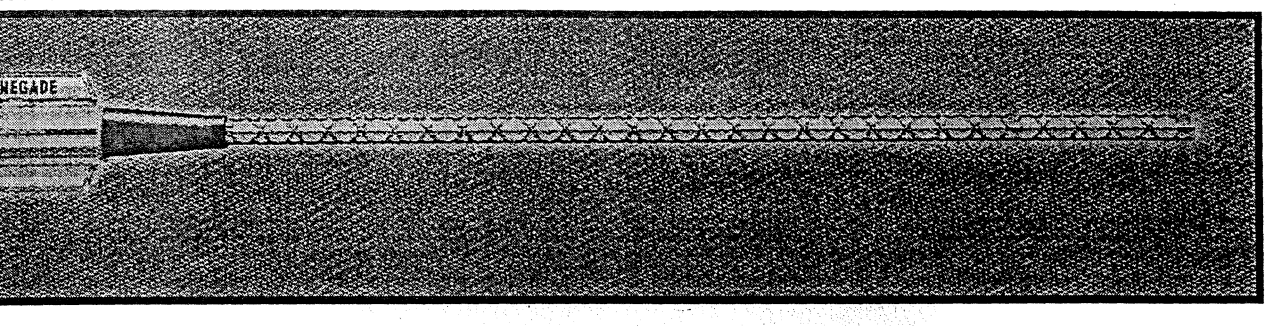

URBOTRACKER

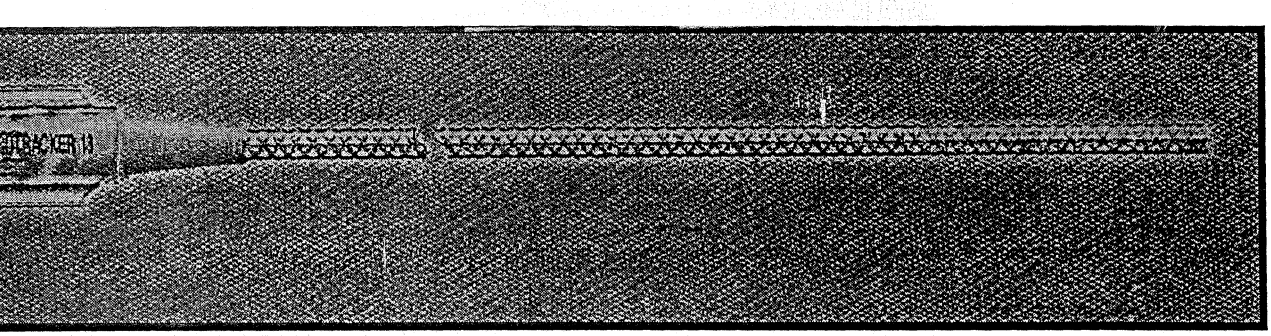

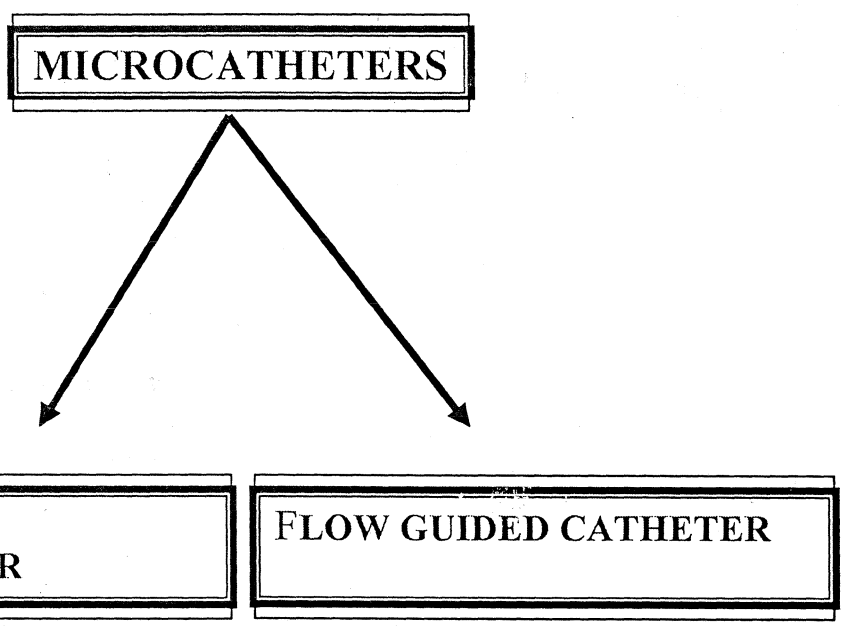

R THE WIRE MICROCATHETERS

Used for the infusion of thrombolytic agent.

OSOFT STREAM(BOSTON),

h requires a 0.042-inch lumen guide catheter. This is a 150 cm phillic-coated 0.021-inch inner diameter microcatheter that has side holes in the distal 2cm. These side holes are smaller mally and larger distally to promote equal distribution of flow.

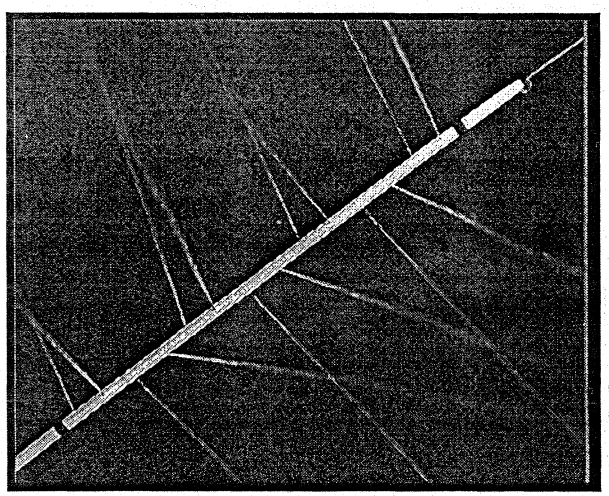

me Infusion catheter (Boston)

A 160 cm hydrophilic coated microcatheter to which 17mm of istal portion of a transend micro guide wire have been added. wire tip is shapeable and eliminates the need for a micro guide The distal 1cm of the microcatheter, which is just proximal to the paque micro guide wire tip, has six side holes for the infusion. In-Time microcatheter may be delivered through a 0.035-inch n catheter.

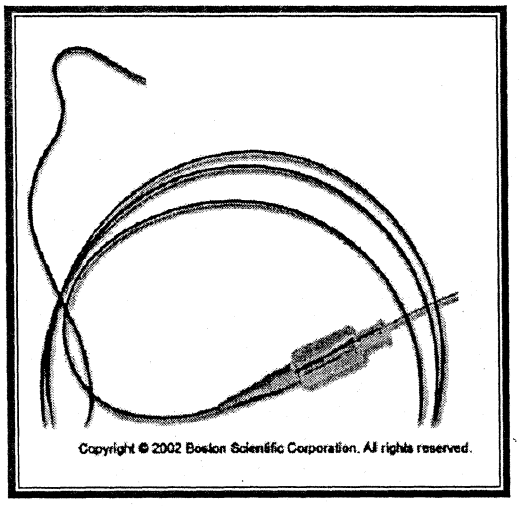

CROFERRET -18

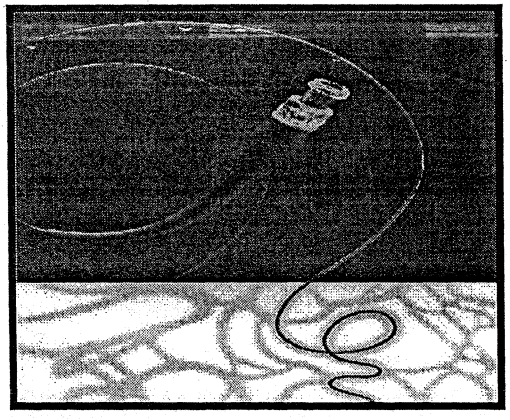

ed for diagnostic or interventional procedures in small vessels or per selective anatomy including neuro, peripheral or coronary plications. The microferret-18 catheters tapers from a proximal 3.0 ench to a distal 2.4 French diameter. The catheter features are ee-step multiple stiffness polyethylene catheter shaft to facilitate acement in tortuous or super selective vascular anatomy. The distal ft, flexible portion resists kinking and is available in 12 or 20cm gth. The rigid proximal and intermediate portions facilitate shability. Slip-coat hydrophilic coating on the distal two segments the catheter provides an extremely lubricious surface for enhanced aneuverability. The catheters accept0a wide variety of embolisation vices including .018 inch microcoils and appropriately sized PVA

sation foam. The catheter is available with one or two platinum aque band.

COOK→ MICROFERRET-18

ng length	150
nal OD French	3.0
nal ID(IN.)	0.018
material	NONE
OD French	2.4
ID (IN.)	0.018
arker OD French	2.4
rs	1or2
al guide (in.)	0.038
nal wire OD (IN.)	0.016
umen construction	Polyethylene

er microcatheter(braided)

The prowler micro catheters are also available in a preshaped gree, 90-degree angle, J-tip. The preshaped curves keep the tor's fingers from the steam, and the microcatheter seems to ain their shape longer .At times, as mentioned earlier, the ed catheter will retract as the guide wire is removed. Similarly ed catheters have a tendency to suddenly move forward .

CORDIS

	PROWLER	PROWLER	PROWLER
D			
	10	14	PLUS
ISIT			

g length	150/50	150/20	150/20	150/50
flexible nt	170/50	170/50	150/45	170/50
al OD French	2.3	2.3	3.0	3.0
al ID INCH	0.015	0.0165	0.021	0.021
MATERIAL	Platinum coil distally Stainless steel proximally	Platinum coil distally Stainless steel proximally	Platinum coil distally Stainless steel proximally	Platinum coil distally Stainless steel proximally
L OD CH	1.7	1.9	2.3	2.3
L ID INCH	0.015	0.0165	0.021	0.021
MARKER OD CH	1.7	1.9	2.3	2.3
ERS	1or2	1or2	1or2	1or2
AL GUIDE	0.035	0.035	0.042	0.042
WIRE OD	0.012	0.014	0.018	0.018
R LUMEN TRUCTION	PTFE	PTFE	PTFE	PTFE
SPACE	0.32	0.35	0.50	0.50

OW GUIDED MICROCATHETERS

These are very flexible hydrophilic-coated catheters that are marly designed to deliver liquid embolics such as glue, onyx, and hydrated alcohol, PVA (less than 500µm) can be administrated ough these microcatheters as well.

INNAKER ELITE

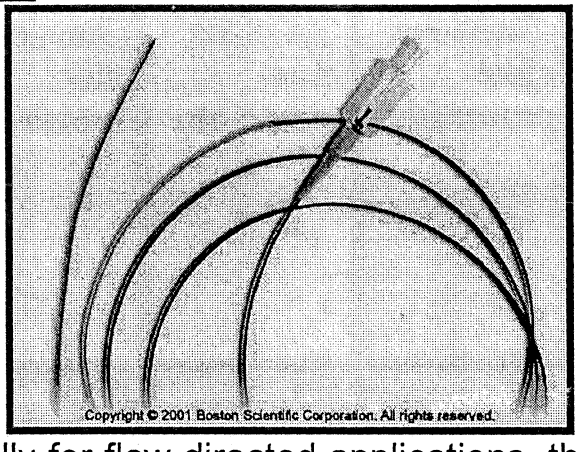

veloped specially for flow directed applications, the spinnaker elite w directed microcatheter might be used for regional infusion of gnostic agents and vascular occlusion with berenstein liquid coil- The flow-directed spinnaker elite (Boston) is not approved for use h glue or other liquid agents, which would seem to be its purpose.

ATURES

DVANCED COMPOSITE SHAFT CONSTRUCTION

egment- specific, composite shaft construction is designed to liver the most desirable performance attributes in each shaft gment.

tra flexible distal segment

1. Atraumatic, unbraided distal segment promotes flow directed navigation and vessel selectively.
2. Steam shapeable tip.
3. Offered n 1.5F and 1.8F OD and a choice of distal segment lengths.

sponsive proximal shaft

1. High durometer
2. unbraided shaft,body for support, control, and pushability.
3. smooth mid shaft transitions facilitate advancement through tortuous vasculature.

ydrolene- hydrophilic polymer surface

Ultra-lubricious outer surface facilitates advancement and anipulation of the spinnaker elite with in the guide catheter and ough challenging anatomy.

adiopaque distal tip marker

Platinum distal tip marker provides superb fluoroscopic sualization.

ptional stylet

An optional stylet may be used to facilitate introduction of the innaker elite in to the guiding catheter.

pinnaker Elite

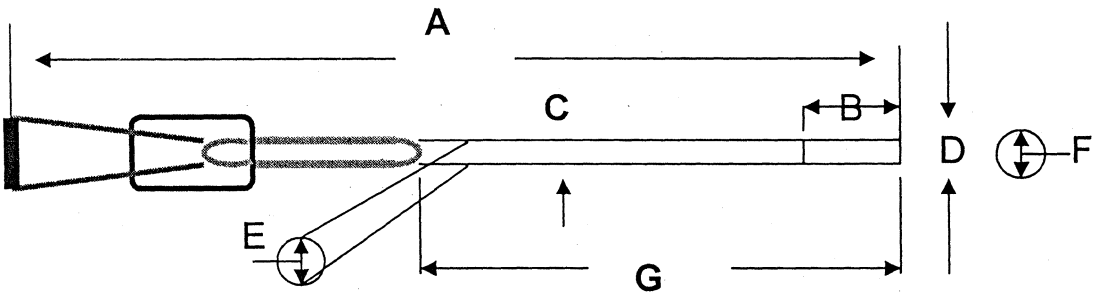

A	B	C	D	E	F	G
6cm	15cm	1mm/3F	0.5mm/1.5F	0.46mm/.018in.	0.28mm/.011in.	160cm
6cm	20cm	1mm/3F	0.5mm/. 011in.	0.46mm/. 018in.	0.28mm/. 011in.	160cm
6cm	30cm	1mm/3F	0.5mm/1.5F	0.46mm/.	0.28mm. 011in.	160cm

				018in.		

	B	C	D	E	F	G
m	10cm	1mm/3F	0.6mm/1.8F	0.46mm/. 018in.	0.28mm/. 011in.	160cm
m	20cm	1mm/3F	0.6mm/1.8F	0.46mm/. 018in.	0.28mm/. 011in.	160cm
m	30cm	1mm/3F	0.6mm/1.8F	0.46mm/. 018in.	0.28mm. 011in.	160cm

T MAGIC

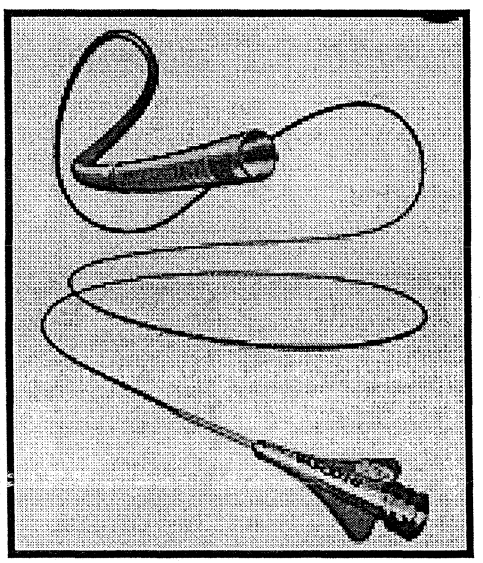

GIC catheters are designed for general intravascular use. They y be used for the controlled, selective regional infusion of rapeutic agents or embolic materials in to vessels. The MAGIC neter is intended to facilitate access through distant, tortuous sculature. Progressive suppleness ranging from a super supple tal shaft to a rigid proximal shaft allows the catheter to be vanced by the physician. The rigid proximal shaft allows torque ntrol to facilitate the advancement of the catheter. The MAGIC heter tip (ring) and shaft are radiopaque.

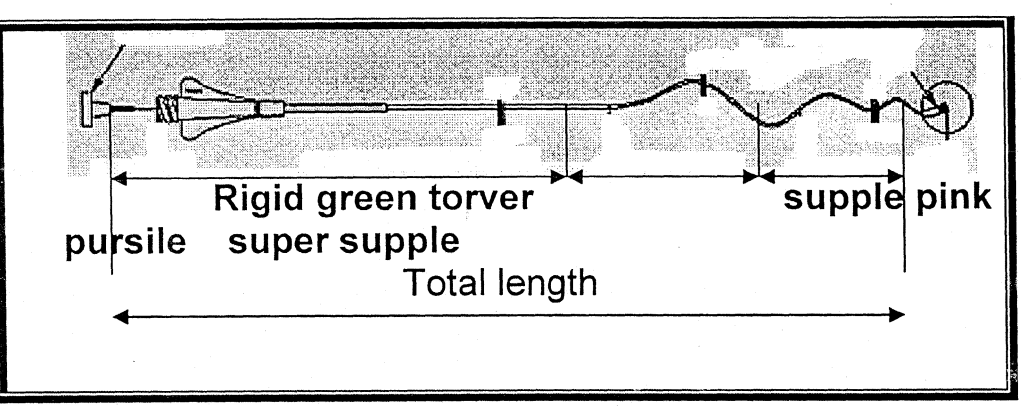

LENGTH (CM)

eference	Total	Green TORVER	Pink PURSIL	White PURSIL	REMARK
AGICSTD AGICMP	155 165	120 120	25 25	10 20	TIP 1.8F
AGICOLIVE AOLIVEMP	155 165	120 120	25 25	10 20	Olive TIP 1.8F
AGIC 1.5F A 1.5F MP	155 165	115 120	25 25	15 20	TIP 1.5F
A 1.5F LIVEMP	165	120	25	20	OLIVE TIP 1.5F

LENGTHS (CM)

ence	Total	Green TORVER	Pink PURSIL	White PURSIL	Turquoise PURSIL	REMARKS
IC	165	120	30	3	12	TIP 1.2F
IC M	165	120	30	12	3	TIP 1.2F
2F E	165	120	30	3	12	OLIVE TIP 1.2F

PARTICLE INJECTION MAGIC CATHETERS

Lengths (cm)

rences	Total	Green TORVER	Pink pursil	White pursil	REMARKS
IC3F	155	120	-	35	Particules up to**1000µ**

ATTA (CORDIS)

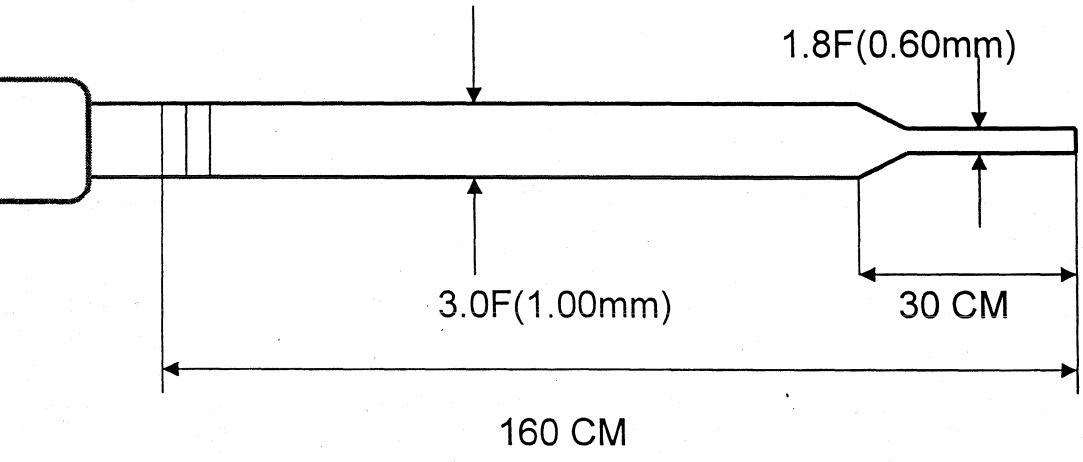

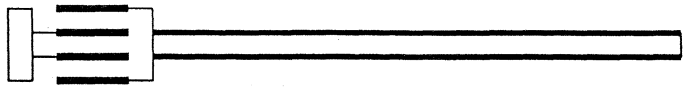

WORKING LENGTH	160/10
DISTAL FLEXIBLE SEGMENT	160/20
PROXIMAL OD FRENCH	3.0
PROXIMAL ID (INCH)	0.021
DISTAL OD FRENCH	1.8
DISTAL ID (INCH)	0.014
TIP MARKER OD FRENCH	1.8
MINIMAL GUIDE (INCH)	0.042
MAXIMUM WIRE OD (INCH)	0.010
INNER LUMEN CONSTRUCTION	N/a
DEAD SPACE	0.27
BURST PRESSURE	150

MICRO THERAPEUTICS

	Rebar-10	Rebar-14	Rebar-18
ing n	153	153	153
l le ent	170	170	170
mal French	2.3	2.4	2.8
mal CH)	0.015	0.017	0.021
rial	Stainless steel	Stainless steel	Stainless steel
l OD ch	1.7	1.9	2.3
l CH)	0.015	0.017	0.021
marker rench	1.7	1.9	2.3
ers	2	2	2
nal e(inch)	0.035	0.035	0.035

ximum e (in..)	0.012	0.014	0.018
er lumen struction	PTFE	PTFE	PTFE
ad space	?	0.27	0.27

TARGET

rking length	150/6	150/15	150/10	150/3
tal flexible gment(cm)		150/7.5	150/20	155/15
ximal OD nch	2.6	2.4	3.0	2.6
ximal ID(IN.)	0.019	0.017	0.021	0.016
id material	Stainless steel	Stainless steel	Fiber Weave	None
tal OD nch	2.0	1.9	2.5	2.0
tal ID(IN.)	0.019	0.017	0.021	0.015
marker OD nch	2.0	1.95	2.5	2.6
rkers	1or2	1or2	1or2	1or2
nimal de(in.)	0.042	0.035	0.038	0.038
ximal wire D(IN.)	0.016	0.014	0.018	0.010
er lumen nstruction	PTFE	PTFE	PTFE	PP/EVA proximai PE/EVAdistal
ad space(cc)	0.35	0.30	0.47	0.30

th in centimeters and the diameters both in inches and in
meters.

erial.

Guide wires are all constructed of fine stainless steel. Some guide
s are coated with Teflon (PTFE-Poly Tetra Flouro Ethylene) to
ce the friction coefficient of the guide wire within the catheter.
e must taken when a Teflon coated guide wire is passed through
etal needle or catheter hub,as the Teflon coating can become
ded and flake off.

es.

Guide wires basically are of two shapes, straight and J curve and
have either a movable core or a fixed core.

ight guide wires.

ne straight guide wire has a straight flexible tip generally 3cm and
opropriate for passage through linear vessels. Since both the
imal (stiff) and the distal (flexible) ends of the straight guide wires
ear the same, it is imperative to check the ends before insertion
nsure that the flexible end is inserted. Some straight wires are
structed such that both the ends are flexible to avoid this
plication.

rve guide wires.

The J-curved guide wire generally has a 1.5,3,or 6 mm-curved
us at its tip. It is particularly used for passage through tortuous
sels. Many percutaneous catheter introducer sets now supply a
n curve J curve wire with the kit. The larger 6mm curve wire is
n appropriate for negotiating a tortuous femoral vein. An even
er 15mm radius J-curve is for cases of extreme vessel tortuosity.
A multipurpose, double end guide wires offer a long 10cm flexible
ight tip at one end with a small 1.5 mm J curve on the other end.
rve guide wires are packaged with a small plastic sleeve that
n advanced over the tip of the guide wire straightens the guide

imum in..)	0.012	0.014	0.018
r lumen struction	PTFE	PTFE	PTFE
d space	?	0.27	0.27

TARGET

rking length	150/6	150/15	150/10	150/3
al flexible ment(cm)		150/7.5	150/20	155/15
ximal OD nch	2.6	2.4	3.0	2.6
ximal ID(IN.)	0.019	0.017	0.021	0.016
d material	Stainless steel	Stainless steel	Fiber Weave	None
tal OD nch	2.0	1.9	2.5	2.0
tal ID(IN.)	0.019	0.017	0.021	0.015
marker OD nch	2.0	1.95	2.5	2.6
rkers	1or2	1or2	1or2	1or2
imal de(in.)	0.042	0.035	0.038	0.038
ximal wire (IN.)	0.016	0.014	0.018	0.010
er lumen struction	PTFE	PTFE	PTFE	PP/EVA proximai PE/EVAdistal
ad space(cc)	0.35	0.30	0.47	0.30

Excelsior Excel Renegade

Tracker-10

de Wires:

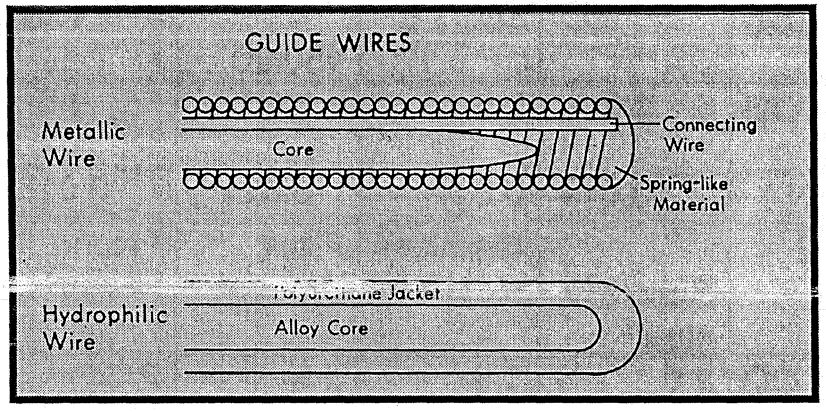

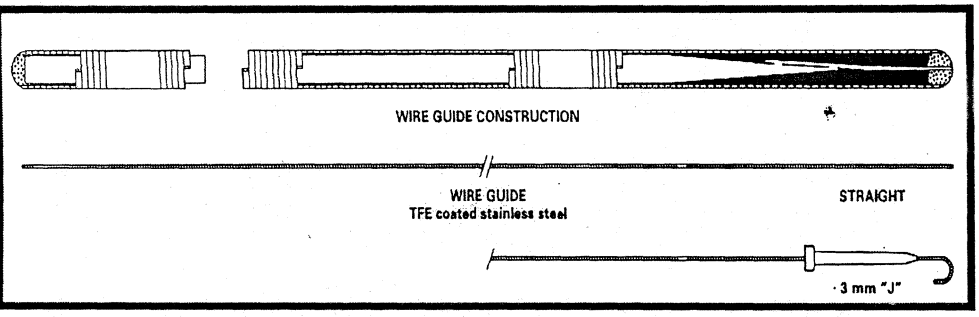

- Guide wires are thin and are constructed of stainless steel wire.
- Guide wires are very flexible and vary in size and length.

IDEWIRE USED FOR DIAGNOSTIC ANGIOGRAPHY

e length of guide wires vary from 100 to 300 cm and sizes range n 0.025 " to 0.045 " in diameter. Guide wires may be coated with on, polyurethane, polyethylene or a hydrophilic coating (Glide es) to lower the friction coefficient and prevent damage to the sel walls. Guide wires may also treated with heparin to reduce the nce of blood clotting and emboli formation.

NSTRUCTION.

The usual guide wire has mainly two parts one is the coil and other is the core or mandrel. Spinning a thin strand of round wire und a metal tube or rod usually makes the coil. The coil is vanced over a core or mandrel and fixed at the ends by a soldered nd. At the flexible end or tip a safety ribbon is soldered and runs length of guide wire adjacent to the core.

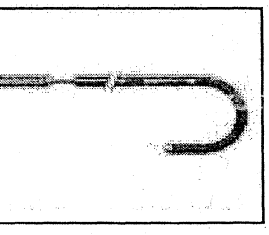

All guide wires have an inner safety wire, which is bonded or lded at both ends to prevent separation in the event of guide wire eakage and to contain the coils of the spring wire during nipulation. The wire tips are welded and polished for strength and oothness to minimize vessel trauma. We usually refer guide wire

h in centimeters and the diameters both in inches and in
neters.

rial.

uide wires are all constructed of fine stainless steel. Some guide
s are coated with Teflon (PTFE-Poly Tetra Flouro Ethylene) to
ce the friction coefficient of the guide wire within the catheter.
must taken when a Teflon coated guide wire is passed through
tal needle or catheter hub,as the Teflon coating can become
ded and flake off.

s.

Guide wires basically are of two shapes, straight and J curve and
have either a movable core or a fixed core.

ght guide wires.

ne straight guide wire has a straight flexible tip generally 3cm and
propriate for passage through linear vessels. Since both the
imal (stiff) and the distal (flexible) ends of the straight guide wires
ear the same, it is imperative to check the ends before insertion
nsure that the flexible end is inserted. Some straight wires are
tructed such that both the ends are flexible to avoid this
plication.

rve guide wires.

The J-curved guide wire generally has a 1.5,3,or 6 mm-curved
us at its tip. It is particularly used for passage through tortuous
sels. Many percutaneous catheter introducer sets now supply a
n curve J curve wire with the kit. The larger 6mm curve wire is
n appropriate for negotiating a tortuous femoral vein. An even
er 15mm radius J-curve is for cases of extreme vessel tortuosity.
multipurpose, double end guide wires offer a long 10cm flexible
ght tip at one end with a small 1.5 mm J curve on the other end.
rve guide wires are packaged with a small plastic sleeve that
n advanced over the tip of the guide wire straightens the guide

re and permits it to be introduced into the hub of a needle or
theter.

xed core guide wires.

Fixed core guide wires have a straight inner core (mandrel) that is
ed at one end and terminates usually 3cm from the tip .The core
ovides necessary stiffness to the body of the coiled wire, while
lowing flexibility at the tip. Variations in the tapered length 10 or 15
n of the mandrel alter the degree of tip flexibility and improve the
ansition from the flexible distal coil to supported mandrel. This is an
nportant feature in PTCA guide wires. Both straight and J-curved
uide wires are available with a fixed core.

ovable core guide wires.

Guide wires that have the straight core attached only at the
stal end are designed to allow movement of the tip of the core for
e purpose of increasing or decreasing the length of the flexible tip.
his is accomplished by not welding the proximal end of the mandrel
ore to the end of the guide wire, but instead securing the inner
andrel to a 5cm handle that is attached to the distal end of the wire.
variation in the tapered length of the core (5cm, 10cm, 15cm) alters
e degree of tip flexibility or in case of J-curve wires the radius of the
ppy wire. The ability to increase or decrease the length of the
ire's flexible tip of ten desirable for traversing local areas of
rtuosity. On occasion, re advancement of inner mandrel may be
fficult. This may be due to bending or kinking of the UN supported
exible tip. In general the inner mandrel should never be forced
gainst a resistance, if this occurs the entire guide wire should be
emoved.
ore-flex guide wires.

Core-flex guide wires have a solid stainless steel mandrel with a
afety wire constructed of spring coil soldered to the end. Although
e out side diameter of this guide wire is 0.018inch, the guide wire
ffers the same support and rigidity as an 0.035 inch guide wire
ecause of its solid steel mandrel. All usual PTCA wires are Core-flex
ires. The rigidity of the guide wire permits percutaneous cannulation

n a smaller 22-gauge cannula rather than a standard 18-gauge nnula.

e Exchange guide wires.

The exchange guide wire is a straight wire unique only in its gth of 260 or 300 cm. It is used exclusively for heter exchange purposes as it is long enough to allow the removal d insertion of a catheter while the wire tip remains in the selected amber. This is often used for exchanging catheters in LV if difficulty s encountered in crossing the aortic valve. Exchange guide wires also used in coronary angioplasty.

en-end guide wire/catheter.

This new type of Teflon wire has an open end and a removable er mandrel. In this way it can function both as a guide wire and h the mandrel removed as a catheter. This guide is of greatest use raversing tortuous or stenotic arteries during peripheral gioplasty. Pressures can be monitored during this procedure ough the lumen of the guide wire.

mensions of the guide wires.

The guide wires for CAG are available in sizes ranging from 018 to 0.038 inches in diameter. The guide wire most commonly ed for coronary angiogram is 0.035inch guide wire as it will support d passes through 6,7 and 8 Fr. catheters. Ideally the catheter tip ould fit closely over the guide wire, with no excess space between e catheter and the guide wire. This promotes the smooth insertion the catheter into the vessel.

Guide wires are available in lengths varying from 50 to 300 cm. e length of the specific catheter to be used dictates the guide wires gth. The guide wire should be at least 20cm longer than the theter to allow insertion of the catheter over the wire with some es always exposed at the hub for manipulation and retension. ually for coronary angiogram a 145cm wire is used.

esired features of a guide wire.

Important considerations in guide wire selections include *tiffness, flexibility, and smoothness*. These features are important for oth patient safety and improved operation.

tiffness.

The stiffness of the guide wire is a function of both the core and ne diameter of the wire. The wire must be sufficiently stiff to be ushed forward without collapsing back on itself or coiling within the asculature. Increased stiffness can be obtained by use of a larger uide wire, if possible or use a guide wire with heavy-duty larger nandrel.

lexibility.

The degree of flexibility of the guide wire is related to the core as vell as to the single helix of stainless steel wire around it.

Smoothness.

The smoothness of the wire is a result of its surface. Certainly the Teflon coated wires are smoother and produce less friction when passed through catheters. Some guide wires are treated with benzalkonium heparin to reduce thrombogenicity

MICROGUIDE WIRE

The selection of a micro guide wire can be difficult because there is he trade-off between increased flexibility and decreased ability of the microcatheter to pass over the microguidewire. Increased stiffness of he microguidewire may make traversing numerous curves very difficult. Most micro guide wires have a stain less steel core; a few nave a nitinol core. This core provides most of the torquing. A few nave polymer outer coatings and nearly all have hydrophilic coatings. The core diameter is so small that microguidewires are not adiopaque unless the manufactures have added platinum coils to the distal segments, distal radiopaque polymer coatings, or gold-tipped,

kers. Some microguidewires tip are shapeable, and others are shaped by manufactures. The softness of the tip, although ortant when the microguidewire has been deployed several timeters, is moot when the micro guide wire is first emerging from microcatheter because the microcatheter buttresses even the bies tip to make it almost needle like on its initial emergence from catheter. Almost all microguidewires have a hydrophilic coating improves performance. The smallest micro guide wires for neuro rventional use are 0.08 inch in diameter; other ranges up to 0.018 in diameter.

RANSEND STEERABLE GUIDE WIRE

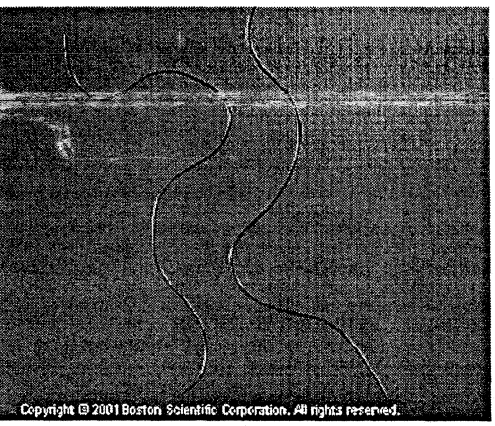

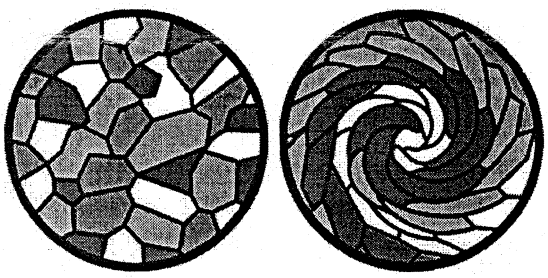

Conventional stainless steel alloy core construction

Proprietary SCITANIUM alloy core construction

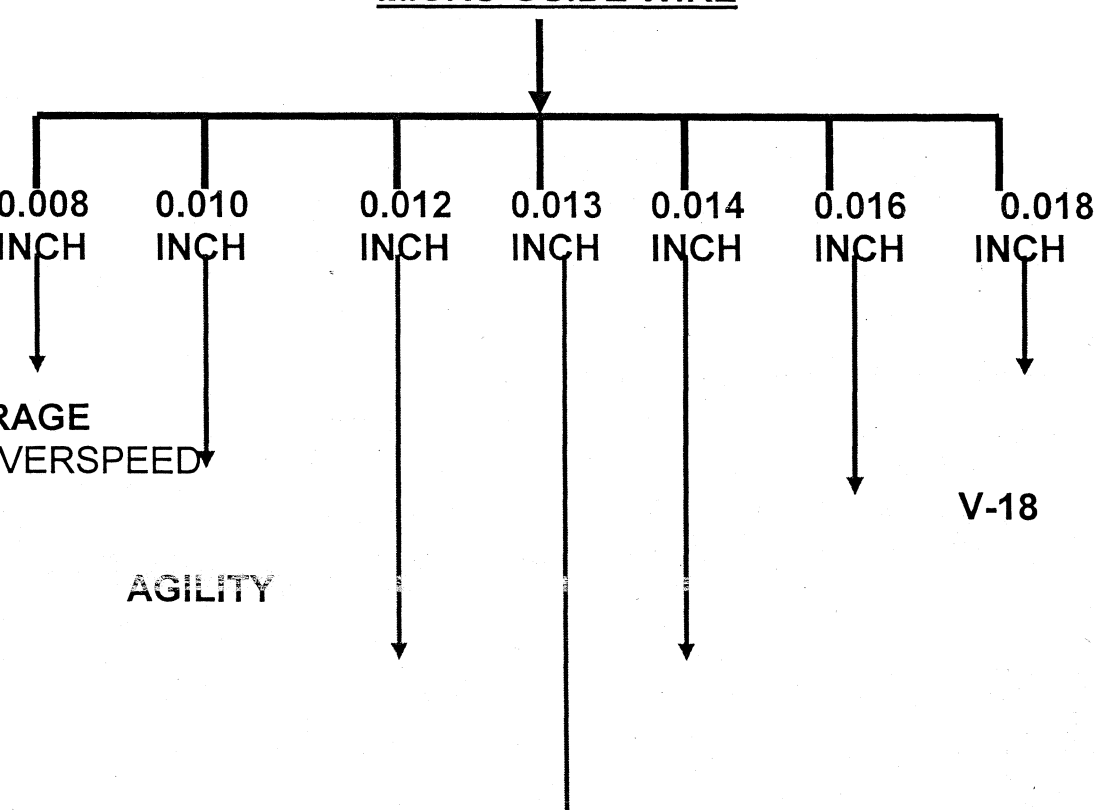

TRANSEND SILVER
EED
SILVER SPEED HEDLINER

HEDLINER AGILITY
SILVER SPEED
STRATEGY
TRANSEND
FasDasher
CHOICE
MIZEEN

CORDIS

	AGILITY-10	AGILITY-14
e diameter ximal (inch)	0.009	0.014
e diameter al (inch)	0.010	0.014
gth (cm)	195	205,350
e material	Stainless steel	Stainless steel
er jacket al	Hydrophilic on metal	Hydrophilic on metal
diopaque gth (cm)	10 PT COIL	10 PT COIL
drophilic ting gth (cm)	158	170
apeable tip	Yes	Yes
shapeable	No	No
xible length	35	42
designs	Straight	Straight

	MIRAGE	SILVER SPEED 10	SILVER SPEED 14,16,18
e diameter ximal (inch)	0.012	0.0095	0.0095
e diameter al (inch)	0.008	0.010	0.014 0.016 0.018
gth (cm)	200	205	175,200
e material	STAINLESS STEEL	STAINLESS STEEL	STAINLESS STEEL
er jacket al	Hydrophilic	Hydrophilic	Hydrophilic
iopaque gth (cm)	10 PT COIL	10 PT COIL	20 PT COIL
rophilic ing gth (cm)	170	170	145,200
peable tip	Yes	Yes	Yes

Reshapeable ip	No	No	No
Flexible length	30	35	35,40
Tip designs	Straight	Straight	Straight

TARGET

Transend 10 TRANSEND FasDasher-14 MIZZEN HEDLINER

EX-.014

ter nal	0.01	0.014	0.014	0.013	0.012 0.016
ter	0.010	0.014	0.014	0.013	0.012 0.016
n	205	182,205	195	195	200
al	STAINLESS STEEL	STAINLESS STEEL	STAINLESS STEEL	NITINOL	NITINOL
	TUNGSTEN LOADED POLYMER HYDROPHILIC	TUNGSTEN LOADED POLYMER HYDROPHILIC	NONE	HYDROPHILIC	HYDROPHILIC
paqu n	205	182/205	4 PT COIL	5 GOLD COIL	2 GOLD COIL

c	205	182/205	42	95	200
e	YES 2.0CM	YES 2.0CM	YES 4.0CM	YES 2.5CM	PRESHAPED
	YES	YES	NO	NO	NO
	39	39	50	35/60	N/a
	straight	Straight	straight	straight	45°-70° 90/150

BOLISATION MATERIALS

The ideal embolic agent procedures should have several racteristics

1. Readily available
2. Easily prepared and injected
3. The agent should have little or no toxicity and cause minimal or no inflammation.
4. Embolic should produce reliable occlusion that will persist for the desired duration at times, permenantly.
5. The agent should be radiopaque to illustrate delivery and should not hinder surgical removal of the embolised lesion.

EMBOLISATION MATERIALS

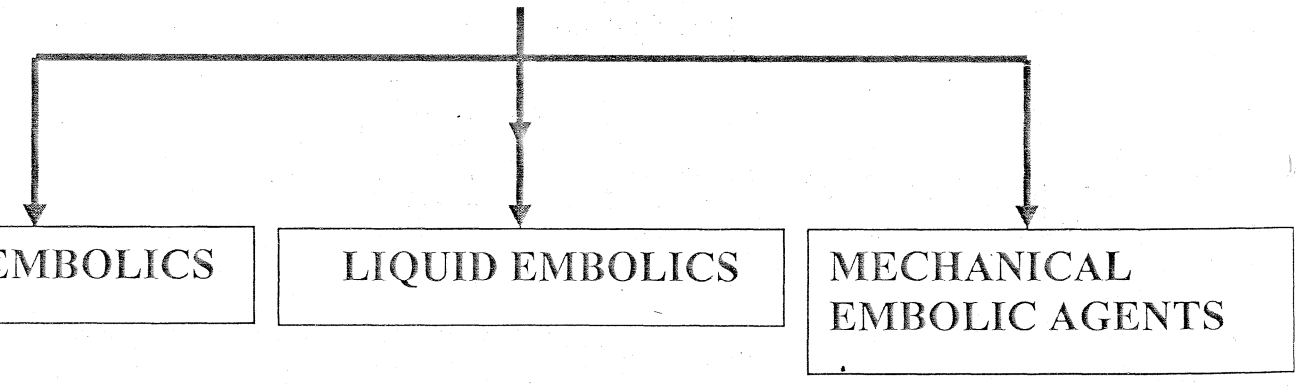

olid embolic agents

Solids that have been used as a embolic agents include

1. **POLYVINYL ALCOHOL (PVA) PARTICLES**
2. **SILK SUTURES**
3. **EMBOSPHERES**
4. **AVITENE**
5. **GEL FOAM**

All of these agents mechanically obstruct the vessels, which lead to slowing of the flow and eventually clot formation with in ne embolised vessel.

Polyvinyl alcohol

These are artificial embolisation devices. These devices are ntended to provide vascular occlusion up on selective placement via n angiographic catheter. It is nearly water insoluble polymer made y the reaction of foamed PVA with formaldehyde. The polymer is not near but composed of cross-linked chains that determines the hysical properties such as swelling, suspension in contrast material, nd viscosity. They are available in different sizes and different brand ames.

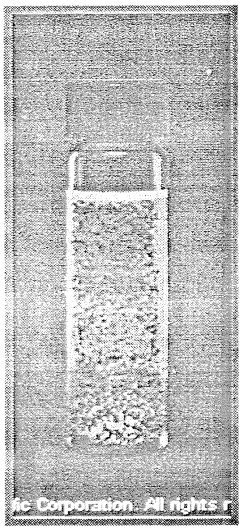

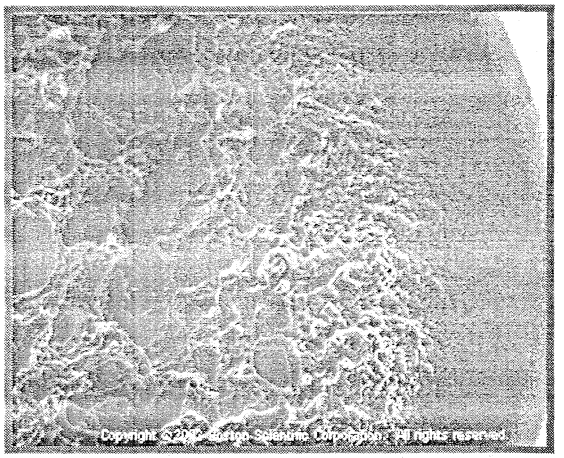

BRAND NAME	MANUFACTURES
BIODYNE	COOK
CONTOUR	BOSTON

COOK

SIZE RANGE
50-100μ
100-200μ
200-300μ
300-500μ
500-700μ
700-1000μ
1000-1500μ
1500-2000μ
2000-2800μ

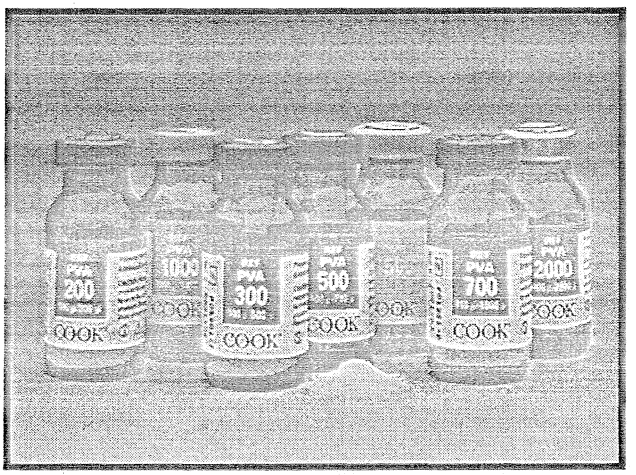

BOSTON

SIZERANGE
45-150µ
150-250µ
250-355µ
355-500µ
500-710µ
710-1000µ
1000-1180µ

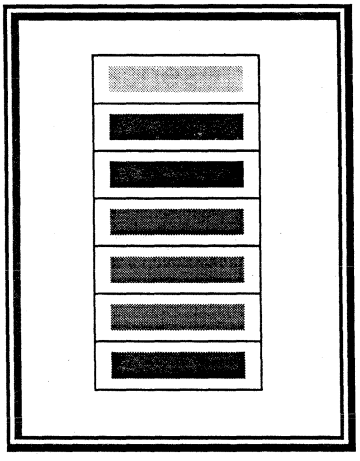

Contour SE™ Microspheres

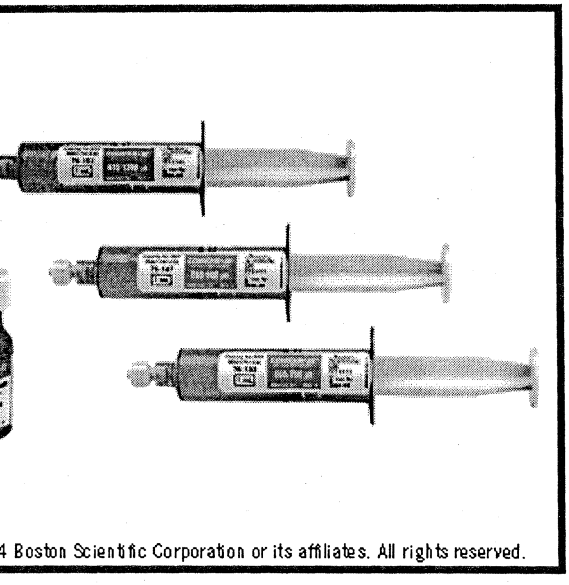

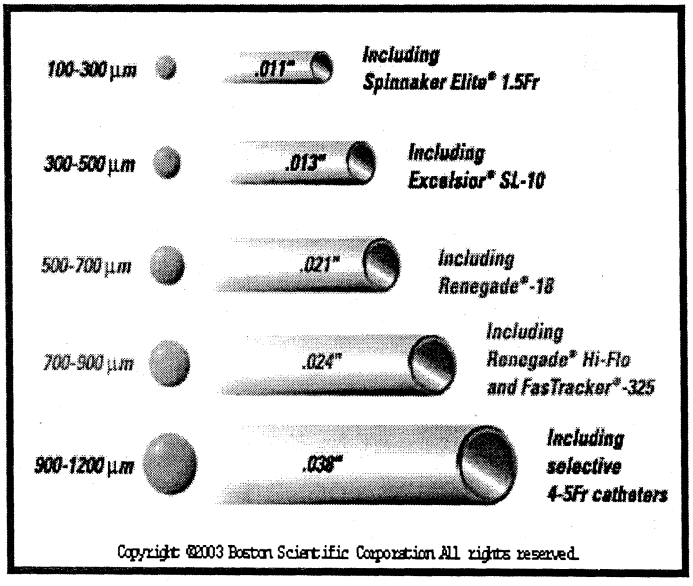

NDICATION FOR USE

Emboli are used for the embolisation of hyper vascular tumours and arteriovenous malformation.

ONTRA INDICATIONS

1. Patient intolerance to temporary occlusion procedures
2. Vascular anatomy or blood flow precludes stable, selective emboli or catheter placement.
3. Presence of likely onset of vasospasm.
4. Presence of likely onset of hemorrhage
5. Presence of artheromatous disease.
6. Presence of feeding arteries smaller than distal branches from which they emerge
7. Presence of patient extra-to-intracranial anastomoses or stimuli
8. Presence of collateral vessel pathways potentially endangering normal territories during embolisation
9. Presence of end arteries leading directly to cranial nerves
10. Presence of arteries supplying the lesion not large enough to accept emboli
11. Vascular resistance peripheral to the feeding arteries precluding passage of emboli in to the lesion.

OTENTIAL COMPLICATIONS

1. Clot formation of the tip of catheter and subsequent dislodgement
2. Ischemia at an undesirable location
3. Capillary bed saturation and tissue damage
4. Ischemic stroke or ischemic infarction
5. Vessel or lesion rupture and hemorrhage
6. Recurrent hemorrhage.
7. Vasospasm
8. Death
9. Undesirable reflux or passage of emboli into the arteries adjacent to the target lesion or through the lesion into the other arteries or arterial beds such as internal carotid artery, pulmonary or coronary circulation.

When the PVA particles used for mbolisation of the AVMs, the choice of particle size is based on the w through the lesion. For PVA embolisation of tumors, the particles e as small as possible to occlude as distally as possible. Epistaxis mbolisation usually is performed with 200μm- sized PVA particles,

vhich lessens the risks of mucosal slough that can occur when maller particles are used.

ILK SUTURES

Some operators have used silk suture in the embolisation f AVMs, The 5-0or 6-0 silk suture is cut in to appropriate lengths 5mm to 30mm), suspended in contrast material because the silk is ot radiopaque, and injected through a micro catheter in to a feeding edicle of the AVMs, until the flow slows. Further injection may cause eflux of the silk in to more proximal vessels. The silk is easily ectioned during the surgical removal of the AVM.

The two major advantage of the silk are

1. Ready availability
2. Low coast

The disadvantages include,

1. Pressure necessary for injection
2. The difficulty in determining the site of deposition.(feeding arteries or draining veins)
3. The acute intravascular and extravascular inflammation that ensues.

EMBOSPHERES

Embospheres is a new particle product that has been specially designed for particle embolisation. It is composed of an acrylic polymer core covered with collagen in gelatin form. The surface is hydrophilic and smooth, which prevents aggregation. These particles are somewhat compressible for delivery through the micro catheter. They obstruct when the vessel lumen size matches their size. Sizes, which are more uniform than with PVA particles, range from 40-1200µm. The tissue reaction to embo spheres and PVA is similar, both embolics elict chronic transmural and per vascular inflammation.

EMBOSPHERES

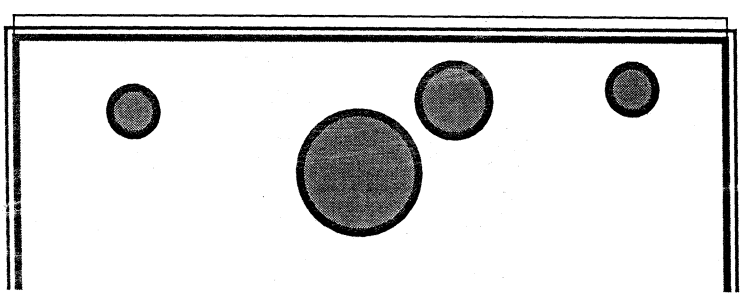

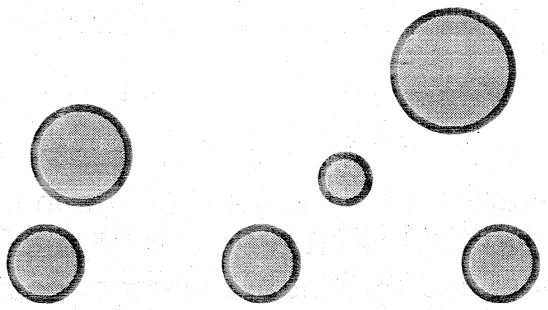

VITENE

It is a powder composed of purified bovine collagen. The micro rils, which are 75-150μm in size, function by obstructing the ssels. Avietene is designed to attract platelets to the fibrils and to tivate the platelet to release the aggregation factors that result in a ombus in the interstices of the fibrous mass. It is less effective in ombocytopenic patients. The powder is absorbable and therefore a temporary agent if fibrous tissue has not replaced the thrombus. stimulates a mild chronic cellular inflammatory response. It has en used as a preoperative embolic agent for hyper vascular head d neck lesion.

ELFOAM

It is a water insoluble, porous, pliable product that is absorbed the body in 7-21 days with little tissue reaction. It is prepared from rified pork skin and should not be used in patients with known ergies to procine collagen. The haemostatic properties are not fully derstood but seem to be due to the formation of an artificial clot as trix forms for platelets that are damaged by contact with the foam. This cause release of thromboplastin, which reacts with ombin and calcium to produce thrombin, which acts on the rinogen in the blood. Gelfoam has the ability to absorb and hold up 45 times its weight of blood and other fluids. This capacity makes it very effective vascular occlusive agent.It is available in a sponge

orm that can be cut into the desired pledged size, suspended in contrast, and injected though the micro catheter for non permanent occlusion of larger arteries supplying the lesion. Gel foam is not adiopaque, and the contrast in which it is suspended serves as an ndirect indication of its course and destinatio. Although compressible, he gel foam pledges can lodge in the catheter, causing it to become obstructed. The delivery catheter must not be over pressurized or the catheter will rupture and result in a proximal embolisation.

LIQUID EMBOLICS

Liquid agents for neuro interventional use consist of

CYANOACRYLATES (GLUE)

- Histoacryl-(n-butyl 2-cyano acrylates) is commonly used
- Need skill full& care full handling.
- Capable of reaching distal small vessel.
- Exposure of glue to the ionic solution causes polymerization.
- Polymerization can be slowed by addition of iophendylate or glacial acetic acid.
- Tantalum, bismuth or lipidol gives better radiopacity to the glue.
- Speed of the polymerization can control by addition of lipidol.

Complications

1. Stroke due to occlusion of undesired branches.
2. Obstruction of venous out flow.
3. Obstruction of catheter.
4. Polymerization leads to a degree of angionecrosis.

HISTOACRYL CONCENTRATION CHART

NO	CONCENTRATION	HISTOACRYL	LIPIDOL
1	15%	0.5ml	2.8ml
2	17%	0.5ml	2.4ml
3	20%	0.5ml	2ml
4	22%	0.5ml	1.7ml
5	25%	0.5ml	1.5ml
6	33%	0.5ml	1ml
7	40%	1ml	1.5ml
8	50%	0.5ml	0.5ml
9	60%	1.5ml	1ml
10	66%	1ml	0.5ml
11	75%	1.5ml	0.5ml
12	80%	2ml	0.5ml

EHYDRATED ALCOHOL

is a liquid agent used in the same way as cyanoacrylates for the eatment of AVM's and some tumors. In the past the alcohol was acified by dissolving metrizamide powder in it, and the solution was ected under fluoroscopic control. Because metrizamide powder is longer available, operators opacify the alcohol with a small amount concentrated nonionic contrast material.

Alcohol injures tissue by denaturing proteins of the cell all, particularly the endothelial cells, and causing precipitation of the otoplasm. This leads to the thrombus formation and a coagulative crosis. Alcohol injection is very painful, general anesthesia is ually required. The maximum volume of alcohol used in a treatment ssion is 1cc/kg body weight and this is usually well tolerated .The cohol may cause a significant rise in pulmonary vascular resistance d pulmonary arterial pressures.

Besides brain AVM's and head, neck, and spine tumors, cial venous malformations can be treated with successfully with ese agent Care must be taken to confine the alcohol to the venous al formation, because tissue necrosis and superficial skin necrosis n be significant complications.

THIBOLIC

This is a 60% alcohol solution of zein (corn protein), sodium atriazoate (ionic contrast), oleum papaveris, and propylene glycol

for sterility). This biodegradable solution produces thrombosis, ecrosis, and a fibrotic reaction with a short –lived inflammatory esponse that may produce pain and fever, possibly requiring medical nanagement. Ethibolic is safer and produce less ischemia and ecrosis of the skin than alcohol does. Injection is less painful than lcohol injection is; it does require sedation and analgesia but not eneral anesthesia.

ONYX

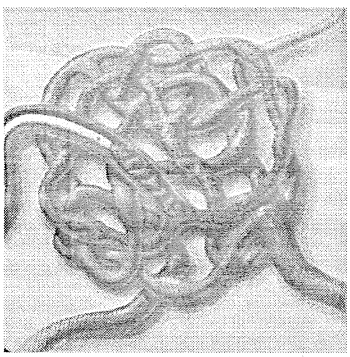

This liquid is a proprietary ethylene alcohol copolymer suspended in DMSO and opacified with tantalum powder. It stays in liquid form until contacts blood or other aqueous solutions. The onyx then begins to precipitate, quickly changing from a liquid to a solid from the out side o the inside. Its major advantage is that it adheres to itself but not to he delivery catheter, so that slow injections with slight reflux along he micro catheter tip can be used without fear of adherence of the ast to the micro catheter. However, if significant reflux occurs, atheter retrieval may be impossible.

HYDROGEL

- Available in either liquid or particle form.
- It forms soft shapeless mass when exposed to water and not produce inflammatory response.
- Similar to EVAL (ethylene vinyl alcohol co-polymer)
- Delivered through micro catheter.

DC COILS
ATRIX 3D-COILS
OOK DETACHABLE COILS
TI COILS

ECHANICAL EMBOLIC AGENTS

ETRIEVABLE COILS

NON-RETREIVABLE COILS.

DC COILS (electrically etachable)

- They are platinum micro coils.
- It is soldered to one end of an insulated stainless steel

TRUFILL PUSHABLE COILS
FIBERED PLATINUM COILS
LIQUID COILS

guide wire, a short segment of the soldered end is exposed

- After coil positioning, low voltage current employs electrolysis to detach coils.
- Advantage is withdrawal of the coil before final placement.
- Available in two systems
    1. GDC-18 SYSTEM
    2. GDC-10 SYSTEM

They are available in various size and shape.

- STANDARD COILS
- 2D-COILS
- 3D-COILS
- SOFT COILS
- ULTRA SOFT COILS
- STRECH RESISTANT COILS
- THROMBOGENIC GDC COILS

GDC-10, 18 & DELIVERY WIRE

The GDC coils are manufactured from a platinum alloy, which permits them to confirm to the often-irregular shape of sacular aneurysm. The delivery wire has been designed to provide two important benefits of the GDC technology:

1. **CONTROLLED DEPLOYMENT.**
2. **ELECTROLYTIC DETACHMENT.**

The GDC system is a fast, accurate and effective endovascular approach to treating high surgical risk intracranial aneurysm. At the heart of the GDC system is a soft, platinum coil that is attached to a stainless steel delivery wire. The softness of platinum allows the coil to conform to the often-irregular shape of intracranial aneurysm. And because the coils are available in a variety of helical diameters and lengths, the interventionalist can deploy and release the optimal combination of coils necessary to occlude the aneurysm sac.

GDC-18&10 SYSTEM STANDARD COILS
18&10 SOFT COILS

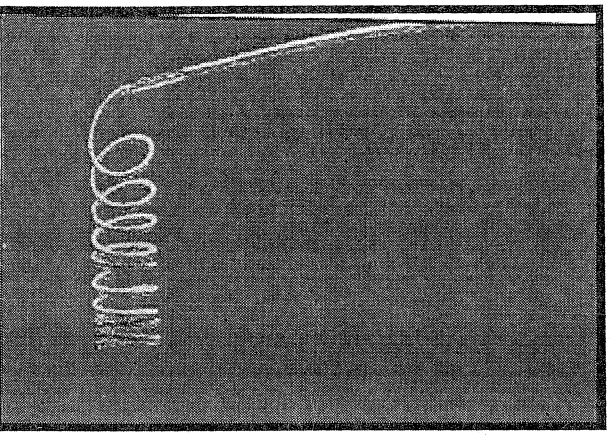

GDC

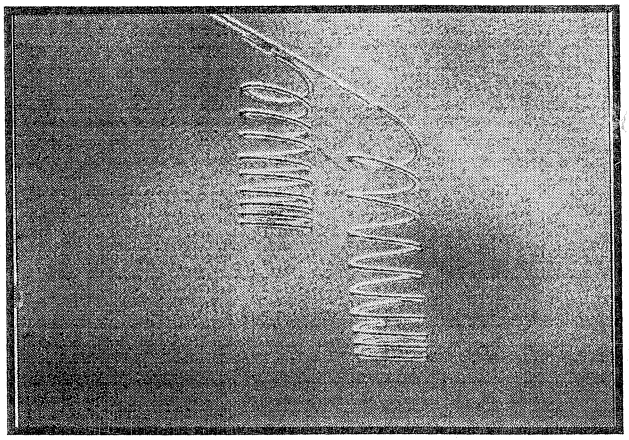

GDC 18&10 2-DIAMMETER

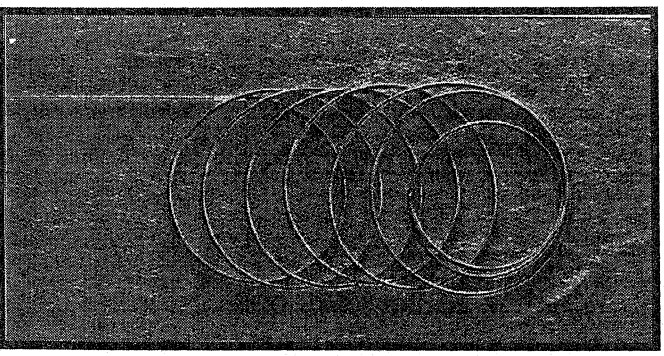

GDC SOFT SR

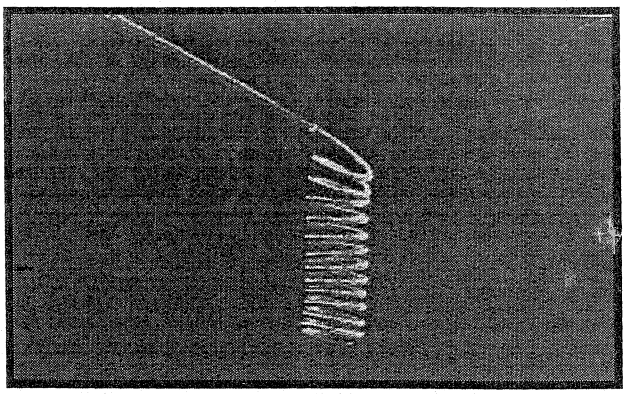

GDC 18 3D SHAPE

GDC-DELIVERY SYSTEM

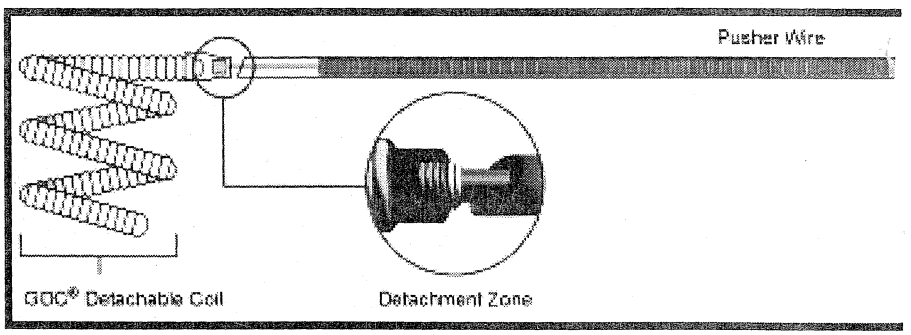

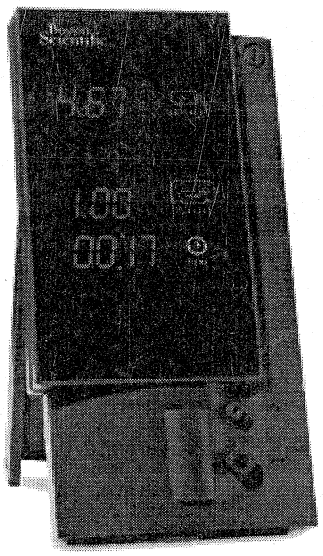

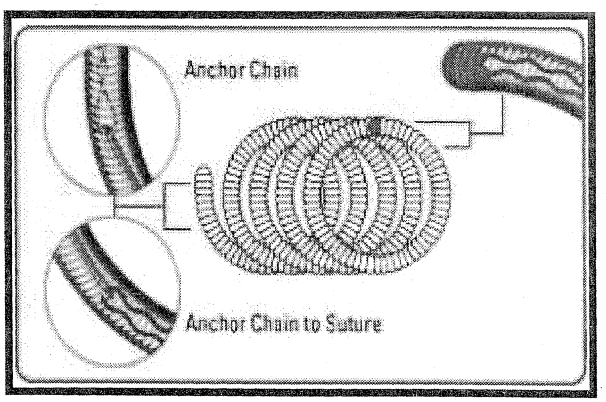

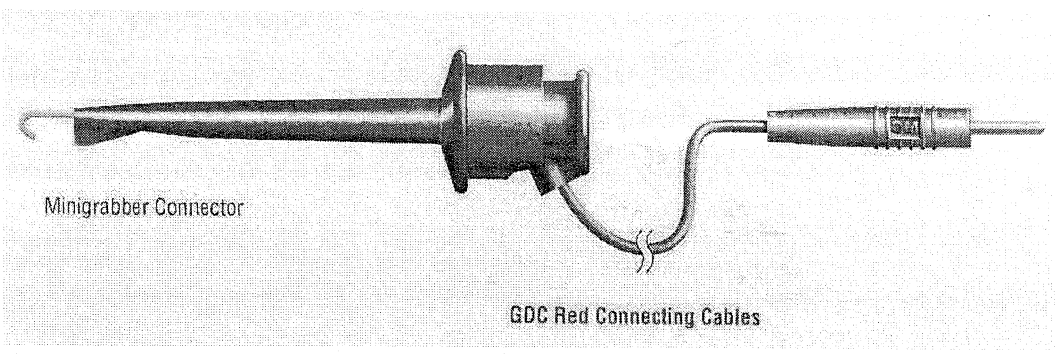

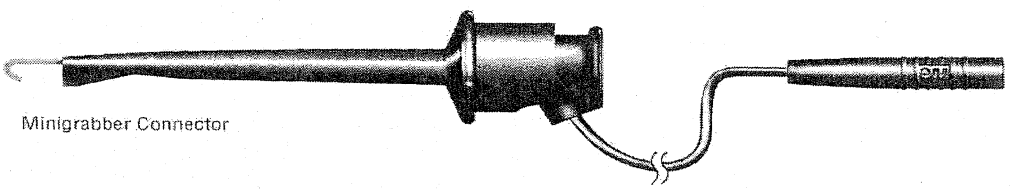

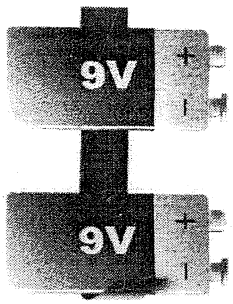

MATRIX COILL

Matrix detachable coils are platinum coils covered with an absorbable polymer and attached to a stainless steel delivery wire. Matrix detachable coils are designed for use with Boston scientific target 2 tip infusion catheters and a GDC power supply.

Matrix detachable coils:-

- Increased the amount of mature connective tissue present with aneurysm at 14 days.
- Increased neck tissue thickness of aneurysm at 14 and 90 days.
- Reduced cross sectional area of the aneurysm at 90 and 180 days as measured from angiograms and histological sections.
- Did not impact average parent artery diameter.

MATRIX 2D-COILS

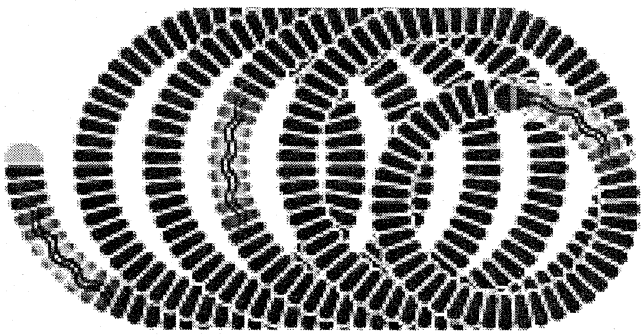

MATRIX 3D-COILS

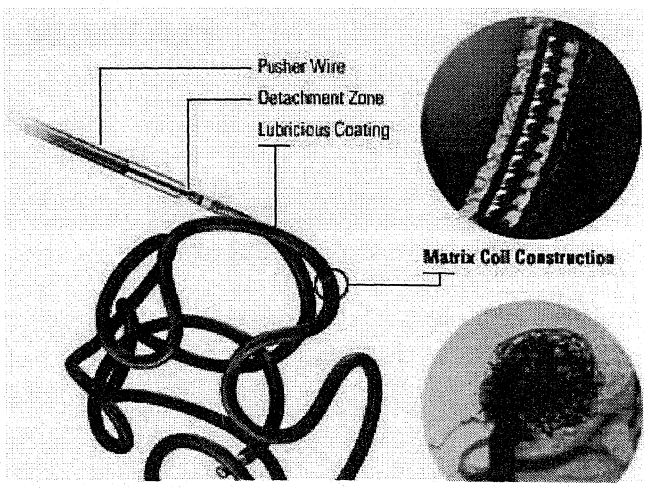

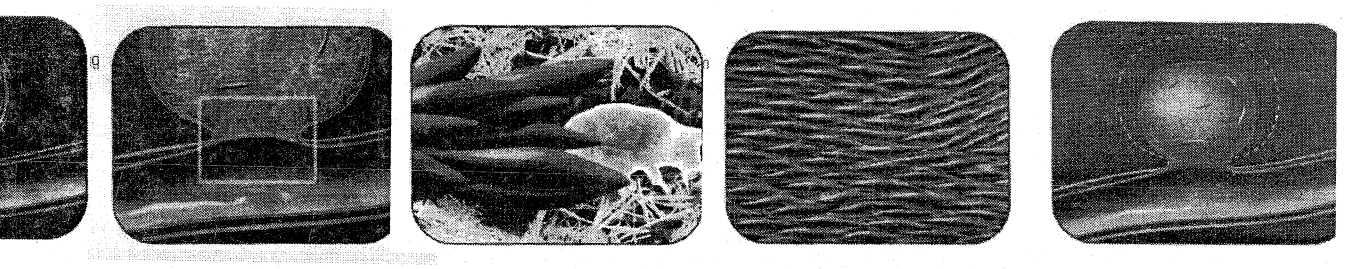

TORNADO®

EMBOLISATION COILS
PLATINUM .018 INCH

EMBOLISATION COILS
PLATINUM .035 INCH

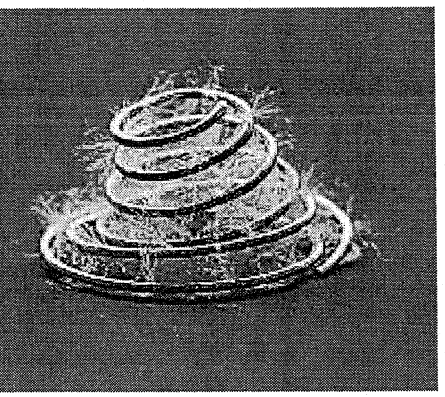

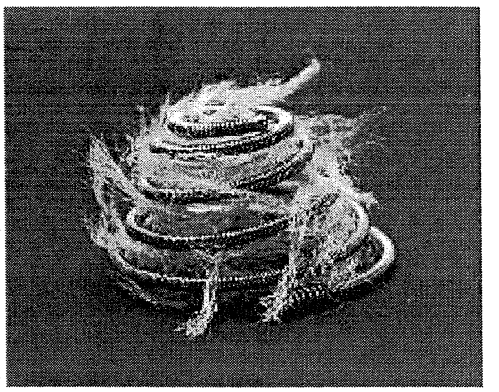

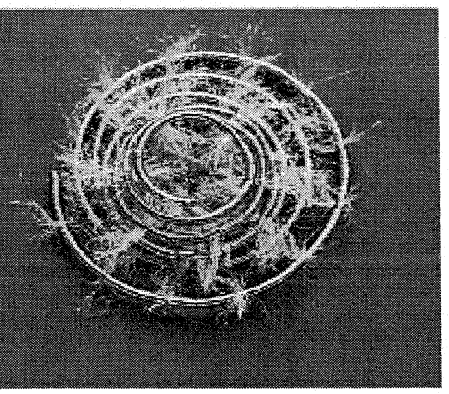

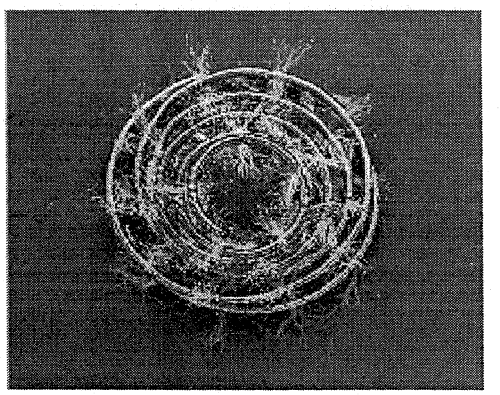

MICRONESTER® PLATINUM EMBOLIZATION COILS

HILAL EMBOLISATION COILS-PLATINUM

PLATINUM

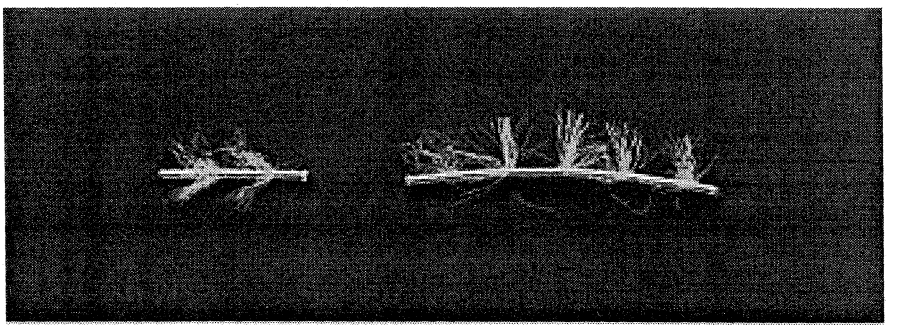

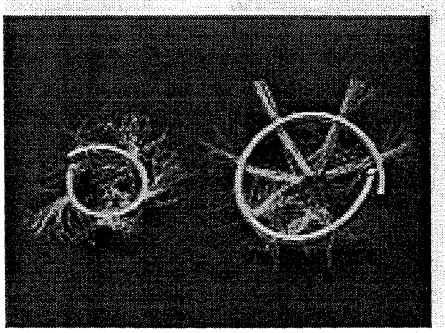

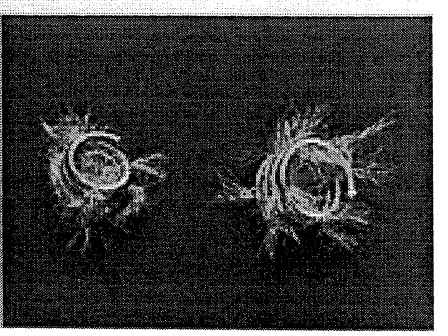

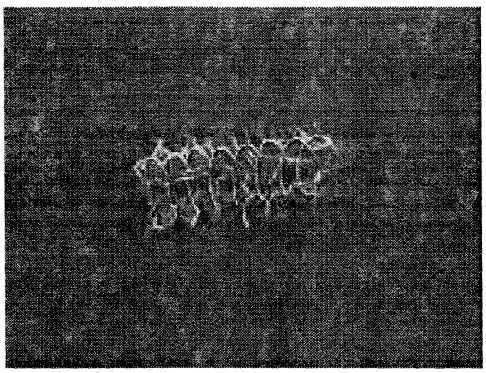

NESTER® EMBOLIZATION COILS
PLATINUM

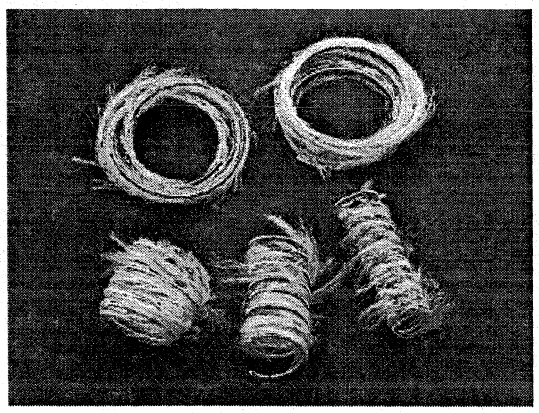

DETACHABLE TORNADO®
EMBOLIZATION COILS – PLATINUM
EMBOLIZATION COILS - STAINLESS STEEL

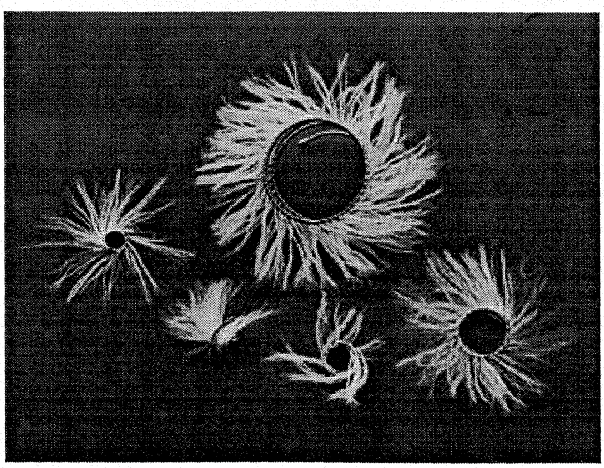

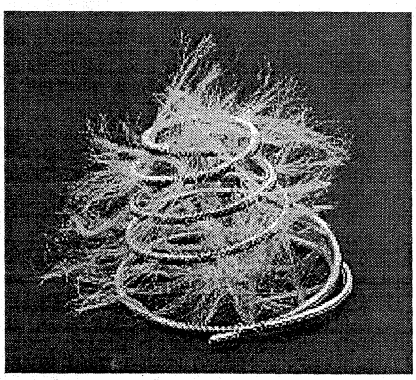

DETACHABLE EMBOLIZATION COILS

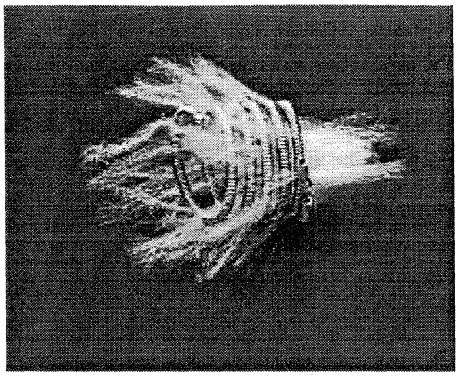

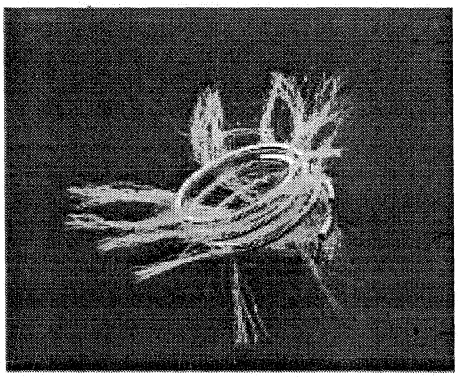

GIANTURCO-GRIFKA VASCULAR OCCLUSION DEVICE

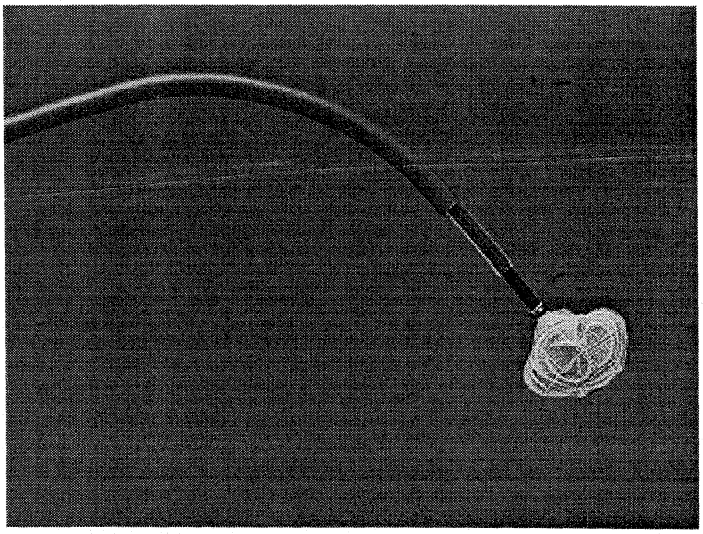

DIAMOND SHAPE COILS **VORTX 35 COILS**

FLIPPER™ DETACHABLE EMBOLIZATION COIL DELIVERY SYSTEM

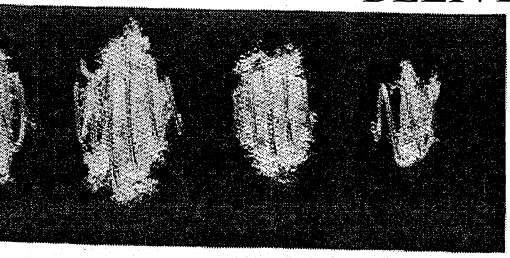

TEIN LIQUID COILS

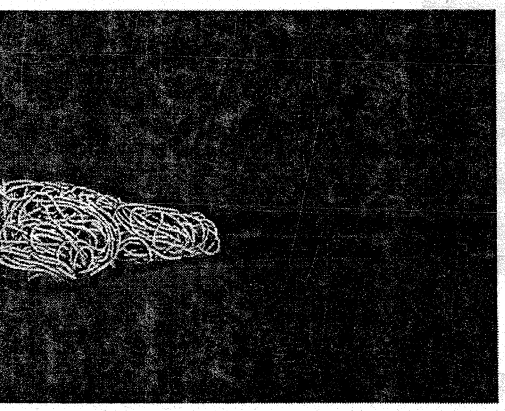

.035 FIBERED PLATINUM MICRO COILS

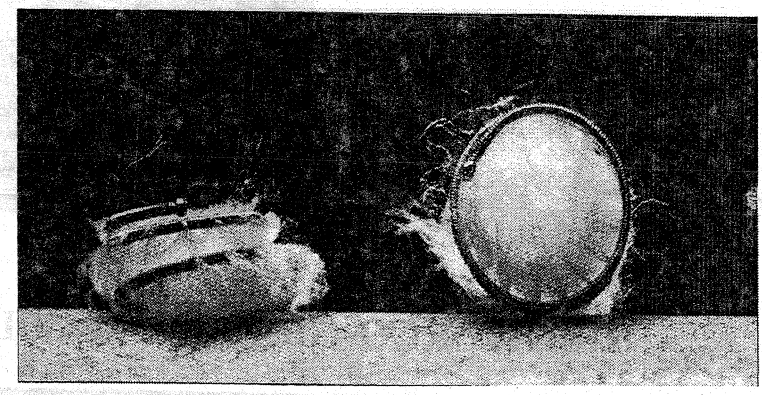

IVC FILTER

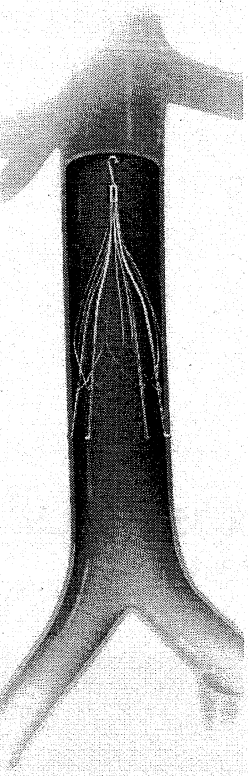

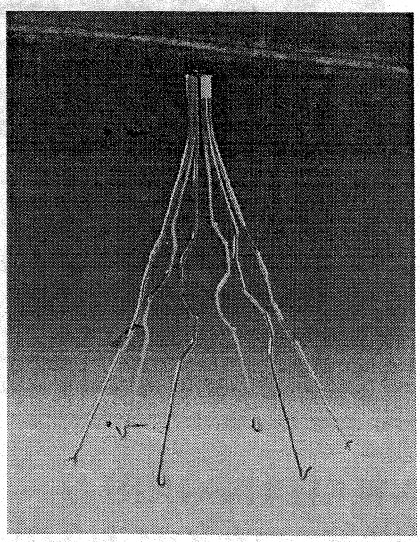

The design of a Gunther tulip venacava filter is a complex construction consisting of 4 main struts 0.45 mm in diameter. Each struts carries an elongated wire loop extending along threeforths of its length. A cross sectional view of Gunther tulip filter demonstrates twice the number of filter wire found as compared to the leading conical filter design

FEMORAL AND JUGULAR SYSTEM:

Used for the prevention of recurrent pulmonary embolism via placement in the venacava in the following situations.

1. Pulmonary thrombo embolism when anticoagulation therapy is contraindicated.
2. Failure of anticoagulation therapy in thrombo embolic disease.
3. Emergency treatment following massive pulmonary embolism where anticipated benefits of conventional therapy are reduced etc...

UROKINASE

Is a plasminogen activator and is used as a thrombolytic agent. Urokinase is an enzyme obtained from the human urine or from the tissue cultures of human kidney cells. It converts tissue plasminogen to enzyme plasmin. Plasmin degrades fibrin clots, fibrinogen and other plasma proteins.

INDICATIONS

- Coronary artery thrombosis associated with an evolving transmural myocardial infarct
- Acute pulmonary embolism

- Deep vein thrombosis
- Peripheral vascular thrombo-embolism

Urokinase therapy should be started 6 hours after the onset of symptoms.
Loading dose: 4,400 i.u/ kg of urokinase re-constituted in 15 ml of sterile physiological saline or 5% dextrose and give i.v. over 10 minutes.
Maintenance dose:
On the first day, the loading dose is followed by 4,400 i.u/kg of urokinase dissolved in 200 ml of sterile physiological saline is given over a period of 8-12 hours. On the second day, the therapy is continued with a daily dose of 4,400 i.u/kg. The total duration of the treatment usually lasts for 6-13 days. For a longer duration, higher doses can be given depending on the clinical urgency, hematological status and the findings of the angiography of the patient.

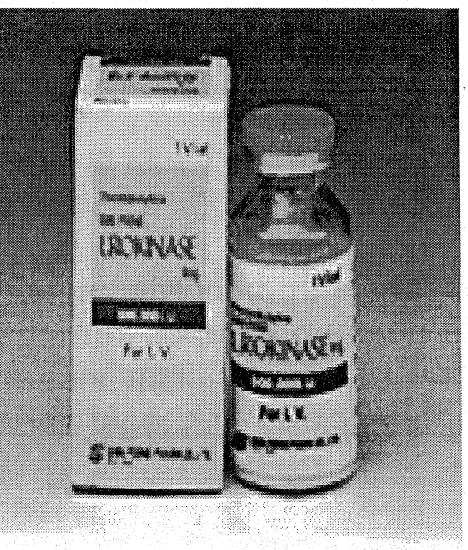

DETACHABLE BALLOONS

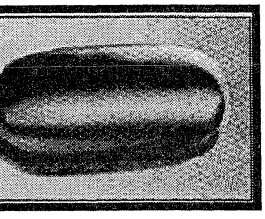
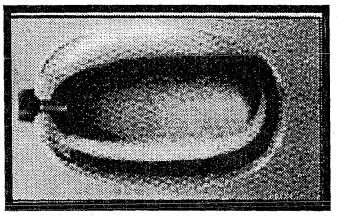
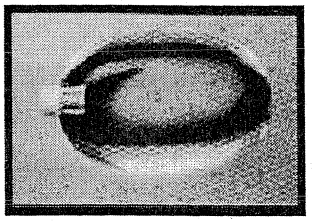

Detachable balloons are designed to occlude the entire vessel with one application. Balloons can sometimes deflate and migrate causing a stroke; they can cause embolus formation and release, vessel rupture and hemorrhage, or infarction. They may also cause Neurological or functioning deficit, vasospasm, ischemia at an undesirable location and death.

Contraindications to balloon occlusion are the patience intolerance to temporary occlusion procedures. Vascular anatomy or blood flow that precludes stable catheter placement. The presence or likely onset of vasospasm. Friable vascular constriction that may cause rupture of a blood vessel and clips, bone fragments, calcifications or any irregularities which may cause damage to the balloon.

ART B. Procedures

adiological Interventions can be broadly classified into

Vascular Techniques
. Non-vascular Techniques

Vascular Techniques

hese procedures are done to correct diseases originating in the lood vessel system of the human body by obtaining arterial or enous vascular access.

asically these procedures are divided into:

. RECANULISATION OF OCCLUDED VESSELS
. OCLLUSION OF ABNORMAL VESSELS
VASCULAR THERAPY TECHNIQUE

.RECANALIZATION TECHNIQUE
ERCUTANEOUS TRANS LUMINAL ANGIOPLASTY

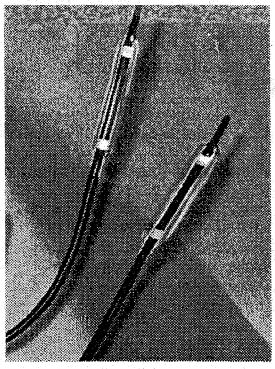

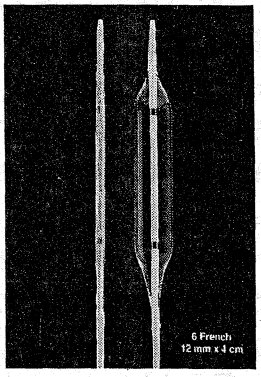

PRE PTA-RENAL ARTERY (LT)

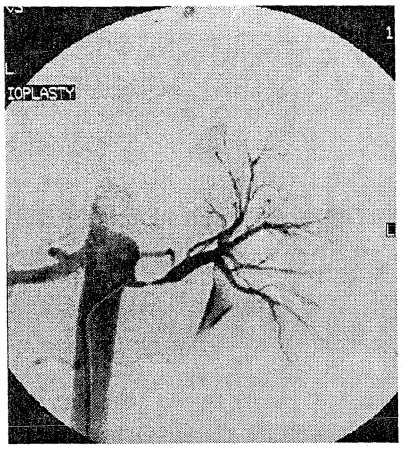

POST PTA

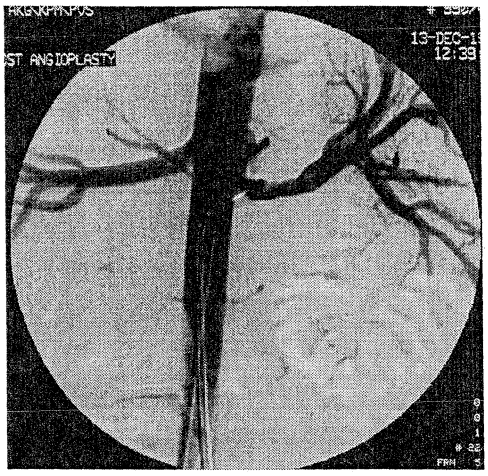

This procedure helps to open up occluded blood vessels using small catheters with distensible balloons attached to it, via intravascular access made through small percutaneous needle punctures. As compared to more extensive and difficult surgical approach this proves definitely beneficial in most instances.

BALLOON CONSTRUCTION

Balloons are constructed with specially treated polymers and processes, which provide maximum strength.

Each balloon inflates to its stated diameter and length over a range of 4ATM/BAR to its rated burst pressure.

The minimal dilating force required to dilate should be applied, minimizing the risk of balloon over inflation or rupture.

CATHETER CONSTRUCTION

The lumen marked distal is the central lumen of the catheter, which terminates at the distal tip. This lumen is used to pass the

catheter over a guide wire. The lumen can also be used for infusion of contrast medium.

The catheter shaft tapers beneath the balloon segment to achieve the lowest possible deflated profile.

Radiopaque markers are placed under the balloon segment of the catheter to provide visual reference points for balloon positioning with in the vessel.

INDICATIONS FOR USE

Balloon dilation catheters are recommended for percutaneous transluminal angioplasty of the iliac, femoral and renal arteries and for the treatment of obstructive lesion of native or synthetic arteriovenous dialysis fistulae.

POTENTIAL COMPLICATIONS

The complications that may result from a balloon dilation procedure include:

- Vessel perforation
- Vessel spasm
- Hemorrhage
- Hematoma
- Hypotension
- Pain and tenderness
- Arrhythmias
- Systemic embolisation
- Endocarditis
- Vascular thrombosis
- Drug reactions
- Allergic reaction to contrast media
- Pyrogenic reactions
- Arteriovenous fistulae
- Thromboembolic episodes
- Vessel dissection
- Infection
- Death

CUTTING BALLOON

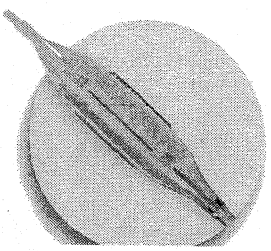

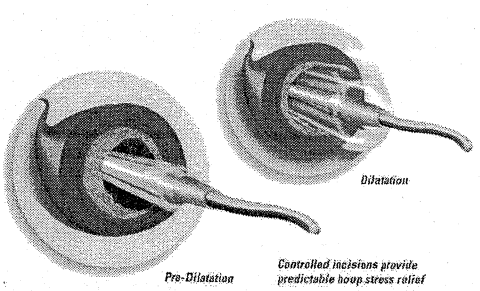

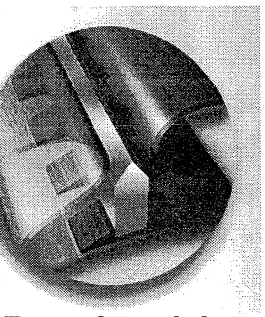

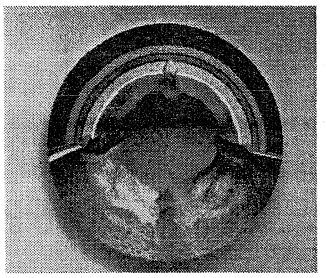

Rotational Angioplasty (Rotablator)

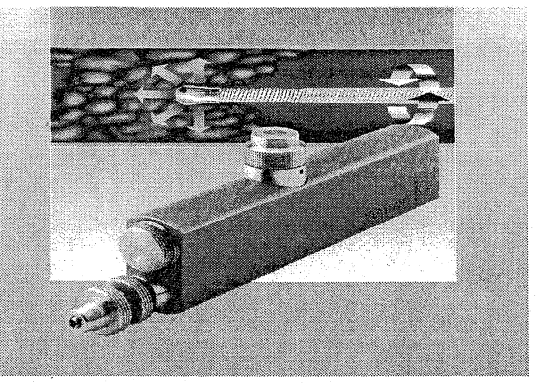

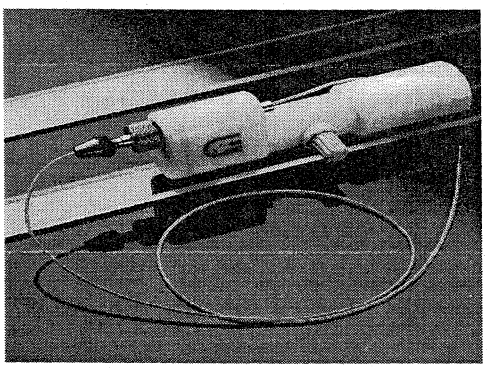

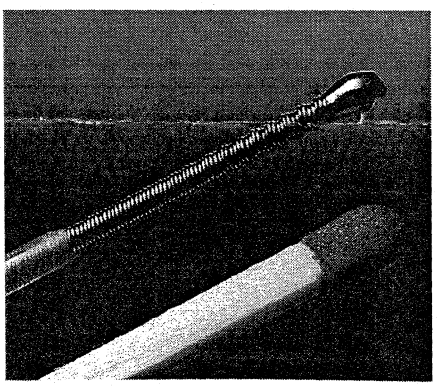

The Rotational angioplasty system is a catheter based angioplasty device utilizing a diamond – coated elliptical burr at the tip of flexible drive shaft. Tracking co-axially over a guide wire and rotating at upto 190,000 RPM, the burr ablates plaque into fine particle that are disposed by the body's reticuloendothelial system.

Indications for use

Percutaneous rotational angioplasty is a sole therapy or adjunctive balloon angioplasty, is indicated in patients with coronary artery disease who acceptable candidates for coronary artery bypass graft surgery and who meets one of the following selection criteria*single vessel atherosclerotic coronary artery disease with a stenosis that can be passed with a guide wire*multiple vessel coronary artery disease that in the physician's judgement does not pose undue risk to the patient. *Certain who have had prior percutaneous transluminal angioplasty (PTCA), and who have a restenosis of the native vessel *native vessel atherosclerotic coronary artery disease that less than 25 mm in length.

Contraindications

1. Occlusions through which a guide wire will not pass.
2. Last remaining vessel with compromised ventricular function
3. Saphenous vein grafts
4. Angiographic evidence of thrombus prior to treatment with rotational angioplasty. Such patients may be treated with thrombolytics (e.g. urokinase when thrombus has been resolved for two or four weeks, lesion may be treated with the rotational angioplasty.
5. Angiographic evidence of significant dissection at the treatment site. The patient may be treated conservatively for approximate for four weeks to permit the dissection to heal before treating the lesion with rotational angioplasty.

STENTS. Desirable stent characteristics 1. Biocompatibility.

2. Metallurgic properties
   * **LOW THROMBOGENICITY**
   *CORROSION RESISTANCE

High radiopacity
Physical properties
*High expansion ratio
*Predictable expanded size.
*Stable after delivery

esistant to external deformation once deployed.
(Palmaz > Wall stent > Strecker.)
*Available in a range of lengths and diameters.
*Delivered on a low profile catheter.
*Precise delivery.
*Retrievable in case of errant placement.
*Amenable to non-invasive imaging follow up,
Including MRI.
Inexpensive.

asic types – Self expanding / Balloon expanded
Covered / Uncovered.

ELF-EXPANDING STENT
Vorks by
Spring action triggered by unloading the
Device from delivery catheter.
Thermal shape memory - Stent assumes
Configuration when warmed to body temperature

ELF-EXPANDING STENTS

Wall stent (Schneider)

dvantages 1.Flexible
2. Available in varying lengths
rawbacks 1. Poor radiopacity.
2. Maximal shortening (30-40%)
ther uses
TIPS, esophageal dilatation,
Tracheobronchial , Enteral end prosthesis
ELF-EXPANDING STENTS

. Nitinol spring coil stent. Made of nickel-titanium alloy; thermally iggered shape.

. Gianturco Z stent (Cook)
Stainless steel; zigzag wire

. Memotherm stent (Bard):
litinol stent with diamond pattern.

ALLOON EXPANDABLE STENTS
. Palmaz stent (Johnson & Johnson).
Made of stainless steel.

dvantages: Ease and accuracy of delivery.
More radiopaque than Wall Stent.
Excellent compression resistance.

)isadvantages:
Lack of flexiblity.
Needs large sheath for introduction

BALLOON EXPANDABLE STENTS

.Strecker stent.
High radiopacity.
lon-ferromagnetic; so MR compatible

.Cordis stent
Made of Tantalum; flexible in undeployed state

.Gianturco-Roubin (Book binder) Flex stent. Stainless steel stent.

.Wiktor stent
Sinusoidal wire; made of Tantalum

COVERED STENTS : Stents with a sleeve (cover) of thin Expandable material.

Uses:
*To exclude aneurysms, both true and false.
*To exclude traumatic vessel disruption
*In esophagus / trachea to cover fistulae

COVERED STENTS

. Cragg endopro system: (Mintec) Cragg nitinol stent covered with 0.1 mm thin Dacron.
2. Wall Graft Covering sleeve made of polyethylene terephthalate.
3. Bifurcated stent system also available for AAA Repair.

COVERED STENTS
Contraindications:
1. Lesion within 0.5 cm of bifurcation or essential branch.
2. Patients in whom ant platelets, anticoagulants or thrombolytic drugs are contraindicated.
3. Connective tissue disorder.
4. Mycotic vascular lesion.
5. Where lesion crosses a joint, Wall Graft cannot

be used.

Vascular Stents:

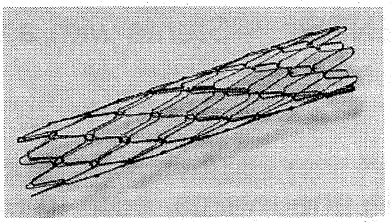

Stents are metallic endo prosthetic materials, which help to maintain the patency obtained through angioplasty. They can also be percutaneously deployed in the precise location, under imaging guidance.
These procedures are extensively used in diseases of blood vessels of neck, limbs, heart etc.

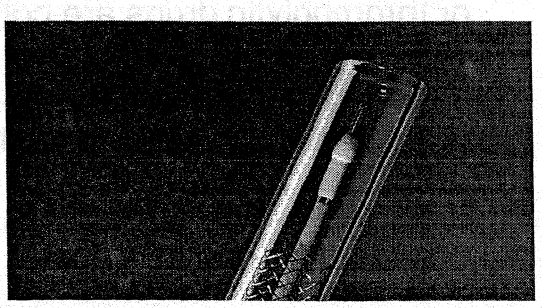

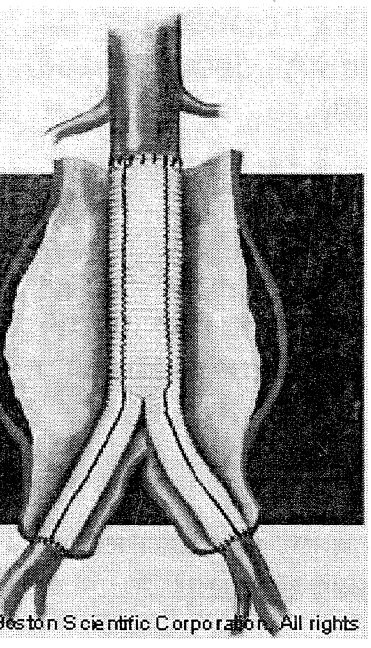

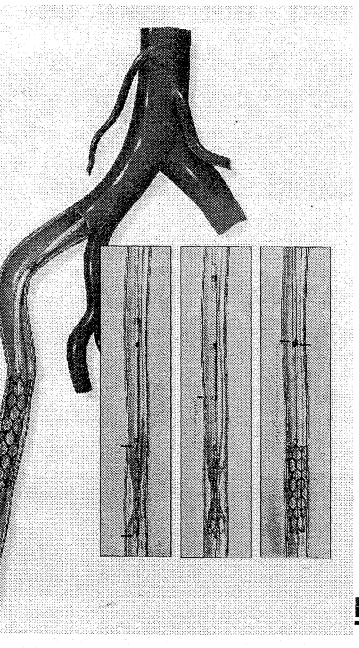

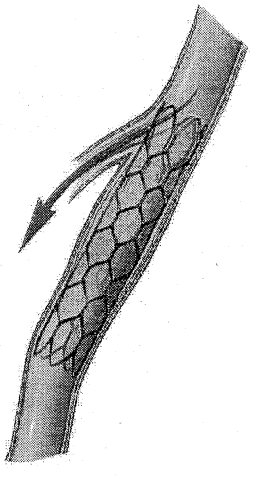

rmal Vessels

Otherwise referred to as 'Therapeutic Embolisation', using particulate materials delivered through micro catheters can be used in settings of acute bleeding from torn vessels, vascular malformations, Aneurysms, Vascular tumors. Embolic materials in use include alcohol, metallic coils, gel foam, etc.

Vascular Therapy

his includes 'thrombolytic therapy' - meaning lysis of clotted blood side important vessels and 'Selective Chemotherapy' - designed to dminister ideal therapeutic concentrations to a tumor.

Non Vascular Interventions

Biopsy Procedures

amples can be taken even from inaccessible sites of human body sing special needle systems, under imaging guidance for diagnostic urposes.

Percutaneous Drainage Procedures

rainage of abscesses and collections can be done by percutaneous eedle placement, which would otherwise need open surgery.

Percutaneous decompression

bstructions of stomach, Intestine, Renal System, etc. can be elieved through guided procedures

Removal of Foreign Bodies

letallic and non-metallic foreign bodies can be located and removed nder X-Ray screening

1. Hepato Biliary interventions

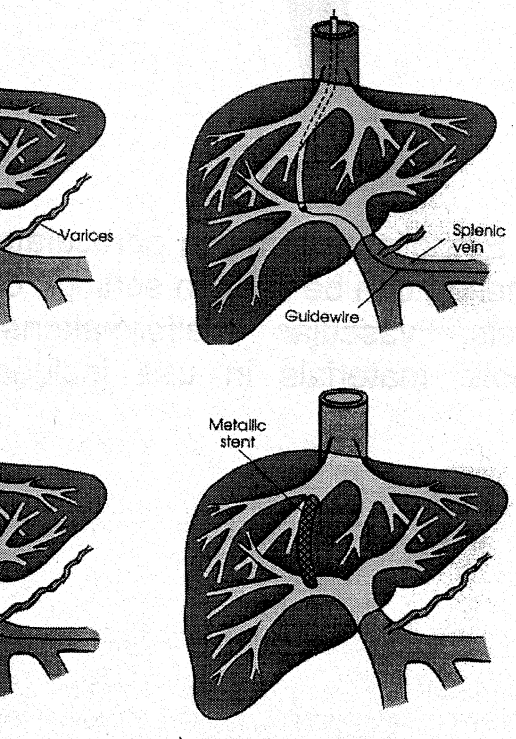

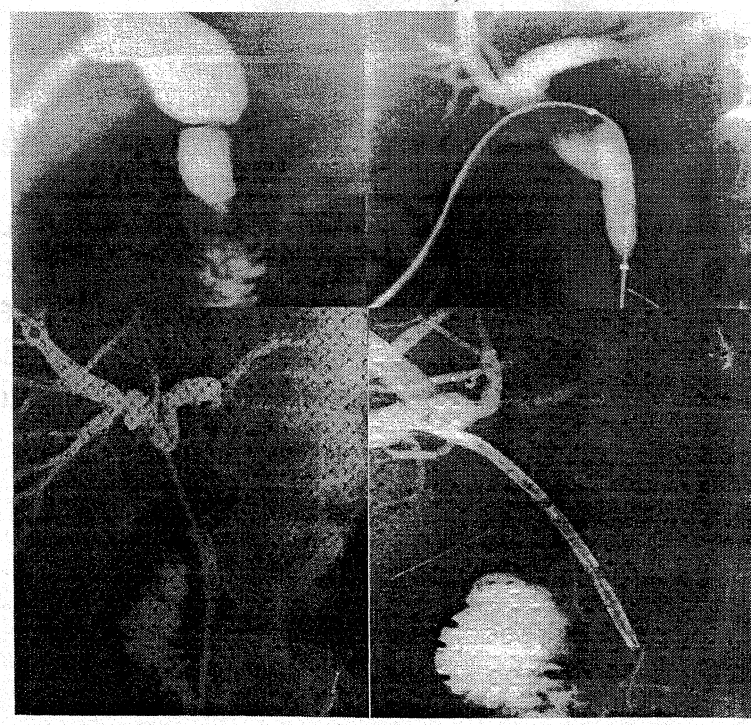

The Interventional procedures done in the liver and biliary system is coming up as a subspecialty in itself.
In addition to routine biopsy techniques and abscess drainage the main emphasis is given to percutaneous removal of gallstones, biliary decompression, drainage and even endobiliary stenting in cases of obstruction to the biliary tree. Patients with obstructive jaundice are treated like this, who otherwise stands a high risk for surgery. Hepatic tumours can also be treated by 'Chemoembolisation'.

6.Genito Urinary System

Obstruction to urinary tract can also be tackled successfully by imaging guided procedures. Stones in the Kidneys, ureters and bladder also can be removed.
Now Interventional Radiology offers treatment for impotence, Pelvic pain syndromes, etc.

7.The Nervous System
In addition to the vascular interventions described earlier, imaging guided procedures like Steriotactic brain biopsy, radiotherapy and surgery are extensively being practiced.

8.The Heart
The angioplasty and stenting procedures are particularly useful in coronary artery diseases. This has come up as a routine procedure and even replaced some of the indications of coronary bypass grafting.

9.Skeletal System
The spinal disc prolapse can be treated by percutaneous laser decompression. Other musculoskelital applications include biopsies, bone reinforcement etc.

The list of Interventional procedures describe are innumerable are every day newer ones are added to it.

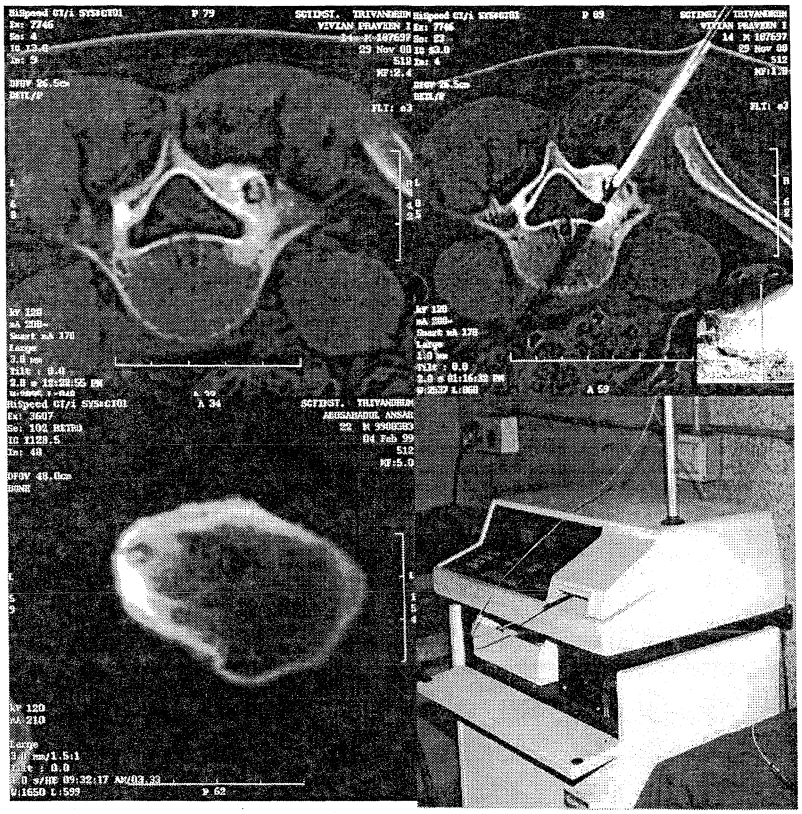

Complications:

Like any other field of invasive medicine interventional radiology is also not devoid of potential risk and side effects. The procedures are to be undertaken with extreme care and even the slightest error can lead on to devastating consequences. But with increasing experience and ever improving technology this relatively newer branch of medicine is assuming a pivotal role in patient management.

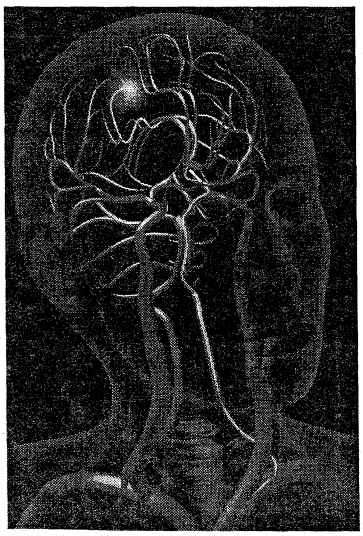

Introduction To Neuro Interventional Procedures

troduction To Neuro Interventional Procedures

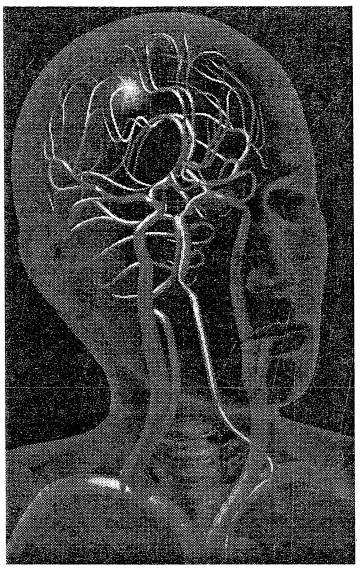

ne of the newest and most promising areas of medical imaging is in ıe field of Neuro interventional radiology. It offers the patient an ternative to surgery and the long healing process that surgery ntails. Viewing the human circulatory system as interconnected oadways, the radiologist has devised methods of entering and aveling within the system to reach the most inner recesses of the ody. The utilization of these arterial passageways is at the heart of ıterventional radiology. Radiologist's that specialize in the brain and oinal cord can guide tiny flexible micro-catheters, metal coils, and ther mini devices into minuscule blood vessels of the brain and eck.

heir goal is to correct the life threatening abnormality of the patient, hich is either beyond the surgeons reach or would bleed too much if urgery were to be performed. Patient's with bizarre symptoms that rise because some parts of their brain are either starved for or verwhelmed by blood are mildly sedated or given a general nesthetic while the radiologist delicately intervene to correct the bnormality, whether it be removing various obstructions to normal lood flow or to close off abnormal openings (fistulas) or utpouchings of blood vessel walls (aneurysm) which may cause emorrhage if it was to rupture. Because the work takes place inside

eoples brains and uses devices guided from outside the body, the sk of failure or causing a second problem while trying to correct the st one is high. But if all goes well, people get their lives handed ack to them.

EWER TRENDS
I DSA
LAT PANNEL DSA
YNA CT
D-ROTATIONAL ANGIOGRAPHY

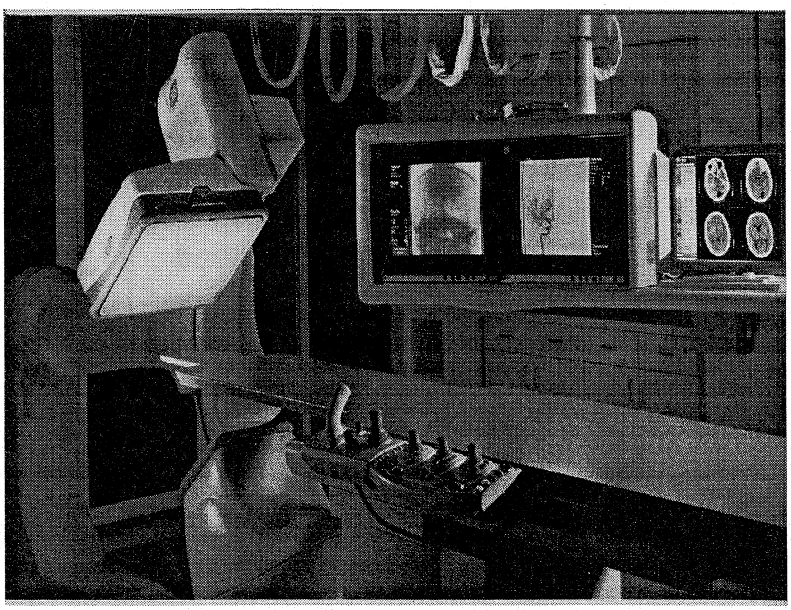

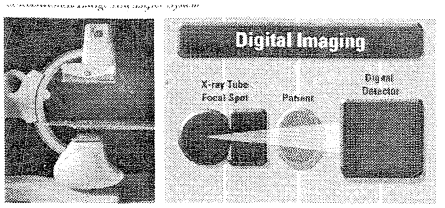

All-Digital Flat Panel Detector System

NUCLEAR MEDICINE

Nuclear medicine is a branch of medicine and medical imaging that uses unsealed radioactive substances in diagnosis and therapy. These substances consist of radionuclides, or pharmaceuticals that have been labeled with radionuclides (radiopharmaceuticals). In diagnosis, radioactive substances are administered to patients and the radiation emitted is measured. The majority of these diagnostic tests involve the formation of an image using a gamma camera. Imaging may also be referred to as radionuclide imaging or nuclear scintigraphy. Other diagnostic tests use probes to acquire measurements from parts of the body, or counters for the measurement of samples taken from the patient. In therapy, radionuclides are administered to treat disease or provide palliative pain relief. For example, administration of Iodine-131 is often used for the treatment of thyrotoxicosis and thyroid cancer.

Nuclear medicine imaging tests differ from most other imaging modalities in that the tests primarily show the physiological function of the system being investigated as opposed to the anatomy. In some centres, the nuclear medicine images can be superimposed on images from modalities such as CT or MRI to highlight which part of the body the radiopharmaceutical is concentrated in. This practice is often referred to as image fusion

ONTENTS

DIAGNOSTIC TESTING

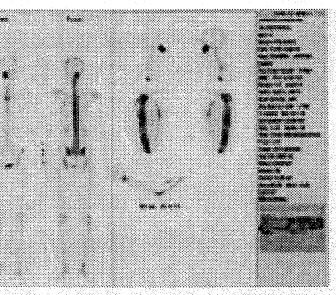

one scintigraphy of a young woman.

iagnostic tests in nuclear medicine exploit the way that the body andles substances differently when there is disease or pathology resent. The radionuclide introduced into the body is often chemically ound to a complex that acts characteristically within the body; this is ommonly known as a tracer. In the presence of disease, a tracer will ften be distributed around the body and/or processed differently. For xample, the ligand methylene-diphosphonate (MDP) can be referentially taken up by bone. By chemically attaching technetium-9m to MDP, radioactivity can be transported and attached to bone

or imaging. Any increased physiological function, such as due to a racture in the bone, will usually mean increased concentration of the racer. This often results in the appearance of a 'hot-spot' which is a ocal increase in radio-accumulation, or a general increase in radio-accumulation throughout the physiological system. Some disease processes result in the exclusion of a tracer, resulting in the appearance of a 'cold-spot'. Many tracer complexes have been developed in order to image or treat many different organs, glands, and physiological processes. The types of tests can be split into two broad groups: *in-vivo* and *in-vitro*:

- *In-vivo* tests are measurements directly involving the patient. By far the most common are gamma camera imaging investigations, though non-imaging probes are also used to measure the levels of radioactivity within a patient.

- *In-vitro* tests are measurements of samples taken from the patient (e.g. blood, urine, breath).

TYPES OF STUDIES

A typical nuclear medicine study involves administration of a radionuclide into the body by injection in liquid or aggregate form, inhalation in gaseous form or, rarely, injection of a radionuclide that has undergone micro-encapsulation. Some specialist studies require the labeling of a patient's own cells with a radionuclide (leukocyte scintigraphy and red cell scintigraphy). Most diagnostic radionuclides emit gamma rays, while the cell-damaging properties of beta particles are used in therapeutic applications. Refined radionuclides for use in nuclear medicine are derived from fission or fusion processes in nuclear reactors or cyclotrons, or take advantage of natural decay processes in dedicated generators, i.e. Molybdenum/Technetium or Strontium/Rubidium.

The most commonly used liquid radionuclides are:

- Technetium-99m
- Iodine-123 and 131
- Thallium-201
- Gallium-67
- Fluorine-18

- Indium-111

ıe most commonly used gaseous/aerosol radionuclides are:

- Xenon-133

IAGING EQUIPMENT

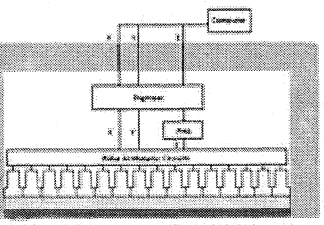

iagrammatic cross section of gamma camera detector
ne radiation emitted from the radionuclide inside the body is usually etected using a gamma camera. Traditionally, gamma-cameras ave consisted of a gamma-ray detector, such as a single large odium iodide *NaI(Tl)* scintillation crystal, coupled with an imaging ub-system such as an array of photomultiplier tubes and associated ectronics. Solid-state gamma-ray detectors are available[1], but are ot yet commonplace. Gamma-cameras employ lead collimators to crease the image resolution by limiting the detection of unwanted amma-rays.
amma-camera performance is usually a balance of spatial esolution against sensitivity. A typical gamma-camera will have a esolution of 4 to 6 mm and will be able to capture several hundred housand gamma-ray 'events' per second. The gamma-camera etects the X and Y position of each gamma-ray event, using these oordinates to place a pixel in an image matrix to build a recognisable

nage. The units of a raw nuclear medicine image is 'counts' or ilocounts', referring to the number of gamma-ray events detected. In uclear medicine, the value of an image pixel is the integral of amma-ray events in that pixel position over time. That is, the pixel ppears brighter as more counts are detected in that position. In non-omographic images, the pixel can also be thought of as the line ntegral of radionuclide distribution of a perpendicular line extending rom the pixel position through the body of the patient.
Since each nuclear medicine radionuclide has a unique gamma-ray mission energy spectrum, and since the energy of a gamma-ray is etected in a gamma-camera by the brightness of the scintillation ssociated with an event, gamma-cameras employ energy 'windows' o gate or limit the imaging process to gamma-ray events of particular nergies. An energy window is usually tailored to the peak of the nergy spectrum of a particular radionuclide, and to ignore other amma-rays that would otherwise contribute noise to the image. This llows noise caused by Compton scattering to be gated out.

ANALYSIS

The end result of the nuclear medicine imaging process is a "dataset" omprising one or more images. In multi-image datasets the array of mages may represent a time sequence (ie. cine or movie) often alled a "dynamic" dataset, a cardiac gated time sequence, or a patial sequence where the gamma-camera is moved relative to the atient. SPECT (single photon emission computed tomography) is ne process by which images acquired from a rotating gamma-amera are reconstructed to produce an image of a "slice" through ne patient at a particular position. A collection of parallel slices form slice-stack, a three-dimensional representation of the distribution of adionuclide in the patient.
The nuclear medicine computer may require millions of lines of ource code to provide quantitative analysis packages for each of the pecific imaging techniques available in nuclear medicine.

RADIATION DOSE

A patient undergoing a nuclear medicine procedure will receive a radiation dose. Under present international guidelines it is assumed that any radiation dose, however small, presents a risk. The radiation doses delivered to a patient in a nuclear medicine investigation represent a very small risk of inducing cancer. In this respect it is similar to the risk from X-ray investigations except that the dose is delivered internally rather than externally.

The radiation dose from a nuclear medicine investigation is expressed as an effective dose with units of sieverts (usually given in millisieverts, mSv).

The effective dose resulting from an investigation is influenced by the amount of radioactivity administered in megabecquerels (MBq), the physical properties of the radiopharmaceutical used, its distribution in the body and its rate of clearance from the body.

Effective doses can range from 6 μSv (0.006 mSv) for a 3 MBq chromium-51 EDTA measurement of glomerular filtration rate to 37 mSv for a 150 MBq thallium-201 non-specific tumour imaging procedure. The common bone scan with 600 MBq of technetium-99m-MDP has an effective dose of 3 mSv

BASIC PRICIPLES OF ULTRASOUND

PHYSICAL PROPERTIES

Definition of Ultrasound (US):

Sound with frequency greater than 20,000 cycles per second or 20kHz. Audible sound sensed by the human ear are in the range of 20Hz to 20kHz.

Advantages:

Ultrasound can be directed as a beam.
Ultrasound obeys the laws of reflection and refraction.
Ultrasound is reflected by objects of small size.

Disadvantages:

Ultrasound propagates poorly through a gaseous medium.
The amount of ultrasound reflected depends on the acoustic mismatch.
The Four Acoustic Variables:

Pressure - the amount of force over a given area.
Distance - particle displacement with the wave
Temperature -
Density

Reflection and Propagation:

Effect of propagation through gaseous zones - poor propagation, inadequate imaging.

Effect of propagation through dense zones - nearly all of the US is reflected. Structures below dense zones are poorly imaged.

Examples of dense materials - bone, calcium, metal.

Material	Speed of Propagation
bone	4080 m/s
blood	1570 m/s
tissue	1540 m/s
fat	1450 m/s
air	330 m/s

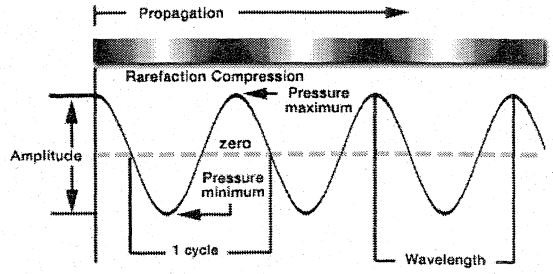

efinitions:

ycle - the combination of one rarefaction and one compression
uals one cycle.
mplitude - the maximum displacement of a particle or pressure
ave.
tensity - the amount of force or energy of sound.
ecibel (dB) - a numerical expression of the relative loudness of
und.
avelength - the distance between the onset of peak compression or
cle to the next.
elocity - the velocity is the speed at which sound waves travel
rough a particular medium. Velocity is equal to the frequency x
avelength.
= f x λ
ae velocity of US through human soft tissue is 1540 meters per
econd.

equency - the number of cycles per unit of time. Frequency and
avelength are inversely related. The higher the frequency the
naller the wavelength.

coustic Impedance - simply put, acoustic impedance is dependent
the density of the material in which sound is propagated through.
ne greater the impedance the more dense the material.

eflection - the portion of a sound that is returned from the boundary
a medium. (echo) The angle of incidence influences the reflected
ad refracted waves.

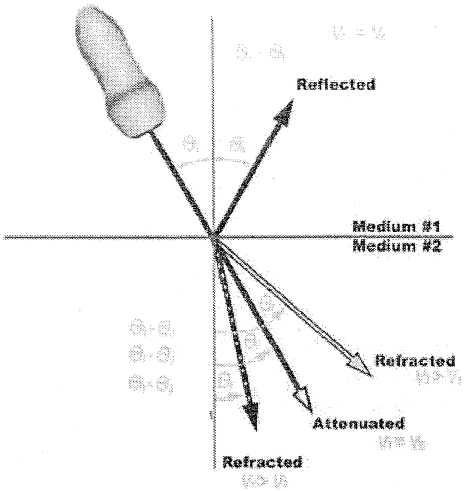

efraction - the change of sound direction on passing from one
ıedium to another.

coustic Mismatch - the boundary between two different media where
eflection and refraction occurs.

ttenuation - the decrease in amplitude and intensity as a sound
ave travels through a medium.

Types of Echoes:

pecular - echoes originating from relatively large, regularly shaped
bjects with smooth surfaces. These echoes are relatively intense
nd angle dependent. (i.e. IVS, valves)

cattered - echoes originating from relatively small, weakly reflective,
regularly shaped objects are less angle dependant and less intense.
e. blood cells)

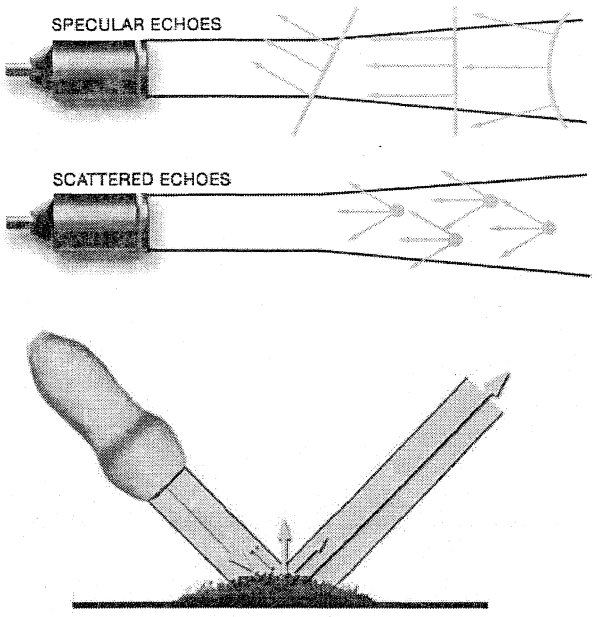

cattering: Reflection and Refraction are affected by the material
eing imaged.
requencies:
requencies for adult imaging - 2.0mHz to 3.0mHz.

requencies for pediatric imaging - 5.0mHz to 7.5mHz to 12mHz.

ffect of higher frequencies on penetration - the higher the frequency
e less penetration, the lower the frequency the greater the
enetration.
rtifacts:

coustic Shadowing - the loss of information below an object
ecause the greater portion of the sound energy was reflected back
y the object. This occurs in objects like prosthetic valves.

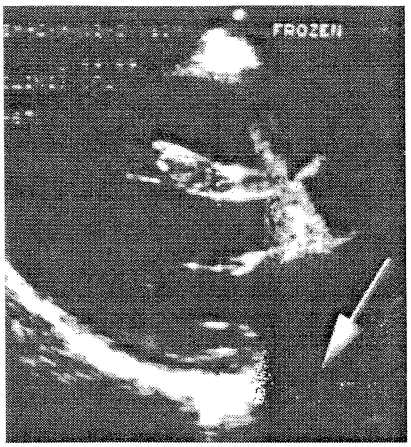

nhancement - the increase in relection amplitude from objects that e behind a weakly attenuating structure. Enhancement may occur in tructures below a cyst.

everberation - the unsuitable reflections generated when the sound ave strikes a highly reflective object creating artifacts that degrade ne image. The peak of the sector scan window is usually filled with everberations due to the initial transmission of sound energy eflecting off of the chest wall and being reflected off the transducer ace in a repetitious fashion. Reverberations may occur in more nternal structures like the diaphragm or from dense objects such as a nechanical valve prothesis. Mirroring may occur as sound energy is eflected off dense structures and displayed on the screen as a ouble image.

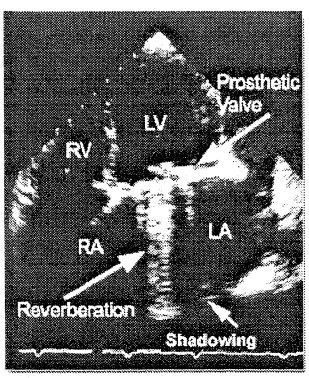

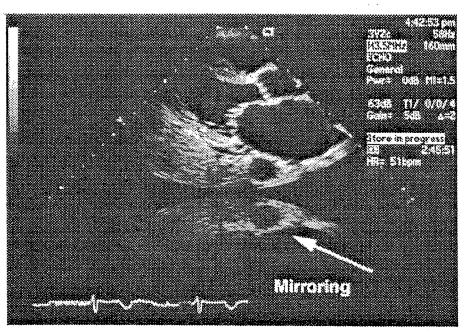

ide-Lobe - produced from the side lobes of the ultrasound beam. his artifact appears as false structures in the scan plane.

DOPPLER PRINCIPLES

Christian Johann Doppler described the effect of motion of sound sources and its effect on the frequency of the sound to the observer. In medical applications we find that the frequency of the reflected signal is modified by the velocity and direction of blood flow. If blood cells are moving towards the transducer, they increase the frequency of the returning signal. As cells move away from the transducer, the frequency of the returning signal decreases.
The mathematical formula is:

$\Delta F/F = 2V/C \cos \Phi$ or rearranged: $Fd = Fr - Fo$

The frequency difference is equal to the reflected frequency minus the originating frequency. If the resulting frequency is higher then there is a positive Doppler shift and the object is moving toward the transducer and if the resulting frequency is lower, there is a negative Doppler shift and it is moving away from the transducer.The angle theta, cos D component is the angle of incidence of the beam upon the object. For the most accurate determination of flow, the beam should be parallel to the flow of blood where the angle theta is zero. If the angle of incidence is greater, the results are less reliable. It is generally accepted that results from the Doppler shift where the angle theta is greater than 20 degrees is not used for calculation.

Doppler Instrumentation:

Doppler techniques are dependent on the transducers used. The transducer operating in continuous wave mode utilizes one half of the element(s) and are continuously sending sound energy while the other half is continuously receiving the reflected signals.
If the transducer is being used in a pulsed wave mode, the whole transducer is used to send and then receive the returning signals.
Comparing the two modes of Doppler techniques describes the advantages and disadvantages.

	Advantages	Disadvantages
Continuous	Accurately measures	Lacks range resolution

Vave	high velocity flows	
ulsed wave	Ability to measure velocities at a specific location (range resolution)	Aliasing of velocities above the Nyquist limit (inability to measure high velocities accurately)

ulsed wave techniques have proven to be very valuable in blood ow studies. The technique allows the accurate measurement of lood flow at a specific area in the heart and detection of both velocity nd direction. Measurement is performed by timing the reception of ne returning signals giving a view of flows at specific depths. The egion where flow velocities are measured is called the sample olume. Errors in the accuracy of the information arise if the velocities xceed a certain speed. The highest velocity accurately measured is alled the Nyquist limit.

lyquist Limit - defined as ½ the Pulse Repetition Frequency (the umber of pulses per second.) If the velocity of flow exceeds the lyquist limit, the direction and velocity are inaccurately displayed nd, in fact, appear to change direction. Color flow Doppler apitalizes on this effect allowing us to detect flow disturbances from aminar to turbulent flow.

ligh PRF - a Doppler technique that attempts to overcome the ffects of the Nyquist limit. This technique may be seen as a ompromise of pulsed wave and continuous wave properties and nvolves the use of multiple sample volumes thereby increasing the ccuracy of velocity measurements at the cost of range ambiguity.

Doppler Displays:

The display of Doppler velocity data is the Doppler frequency shifts ersus time. Included in the display are the Doppler settings such as requency, calibration, range, and timing markers.

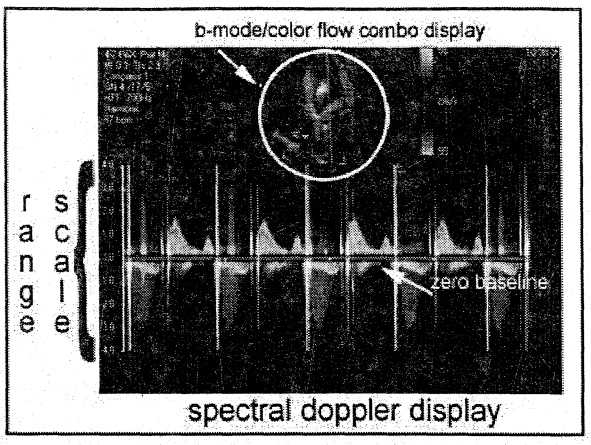

oppler Controls:

ontrols used during the Doppler examination are dependent on anufacturers specifications and the modes available. Controls for e cursor, sample volume length and depth, angle correction, gain, ters, and spectral averaging are typically included.

olor Flow Imaging:

ampling methods - CFI is based on pulsed Doppler technology here multiple sample volumes among multiple planes are detected nd displayed utilizing color mapping for direction and velocity flow ata. Common mapping formats are BART (Blue Away, Red Towards or RABT, and enhanced or variance flow maps where saturations nd intensities indicate higher velocities and turbulence or cceleration, respectively. Some maps utilize a third color, green, to dicate accelerating velocities and turbulence.

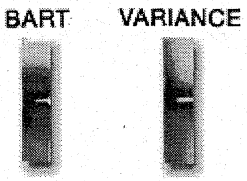

rtifacts - aliasing of the data displayed in pulsed wave technology utilized as a benefit in determining transitions from laminar to rbulent flow. Other artifacts associated with CFI and spectral oppler are artifacts due to gain set too high, "ghosting" from nproperly set wall filters (low frequency), mirroring, crying/talking rtifacts, and signal loss from data sharing.

imitations of CFI - CFI is a "qualitative" examination and has not yet een "quantified", that is, results cannot be measured to give discrete umbers for diagnosis. Qualitative assessment gives comment on the verall view or quality of the results as in flow conditions and jet irection, velocity, and pattern. Quantitative results are those neasured and given discrete numbers used in calculations. There re some current semi-quantitative results given as ratios of jet length y jet width to determine the degree of regurgitation given as mild, noderate or severe.

Piezoelectric Properties:

"crystalline" material such as quartz that changes shape when an lectric current is applied creating sound waves and when struck by ound waves creates electrical currents.

Types:
Nonimaging - transducers that are used in detection of blood flow uch as a continuous wave transducer. The CW transducer, also alled a Pedoff transducer, is two separate elements. One element is lways transmitting while the other element is always receiving.

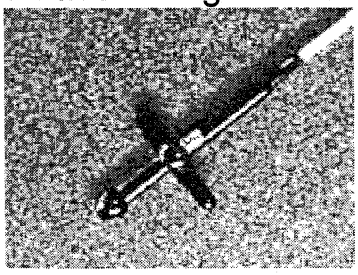

maging - transducers that are used to image cardiac structures but lso have the capability of using various Doppler techniques to detect lood flow. This transducer, sometimes called a duplex transducer, is nade up of multiple elements spending part of the time transmitting nd part of the time receiving sound energy. Continuous wave, pulse vave, high PRF, ColorFlow, m-mode, and 2D are the various modes

at this type of transducer can perform.

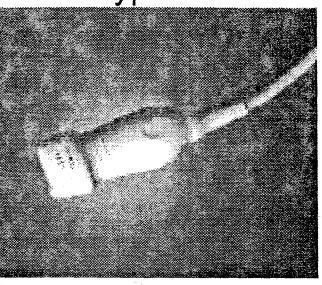

aterials:
ements - commercial echocardiographs use ceramics such as
arium titanate or lead zirconate titanate.

BEAM PROPERTIES:

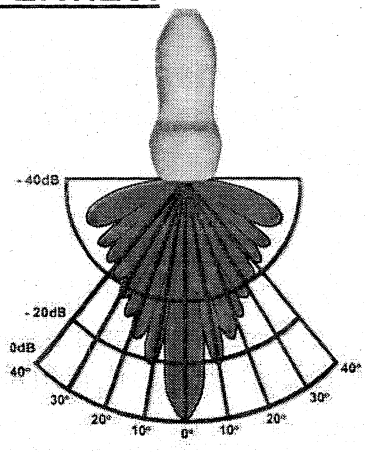

ound wave profile - the wavefront generated by the transducer is a
dimensional beam that contains useful and unuseable components.
ongitudinal Waves - the wave in which the particle motion is parallel
the direction of the wave travel. A series of longitudinal waves
ake up the ultrasound beam.

neer Waves - waves that travel perpendicular to the direction of the
ound beam. These occur mainly in the bone and are not considered
imaging soft tissue.

de-Lobes - artifact that is generated from extraneous side beams.

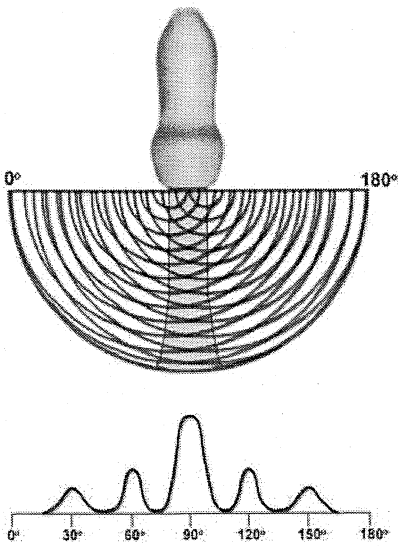

ound wave intensity variations and side lobe generation

ones

lear - the region of a sound beam in which the beam diameter ecreases as the distance from the transducer increases. This zone s called the Fresnel (Fra-nel, the s is silent) zone.

ocal - the region where the beam diameter is most concentrated iving the greatest degree of focus.

ar - the region where the beam diameter increases as the distance om the transducer increases. This zone is called the Fraunhoffer one

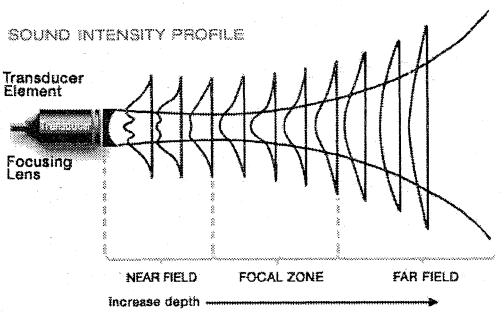

Focusing:

Mechanical - performed by placing an acoustic lens on the surface of he transducer or using a transducer with a concave face.

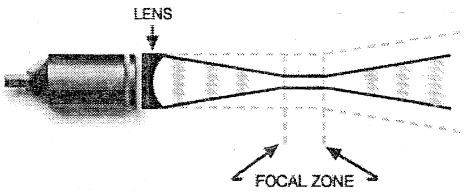

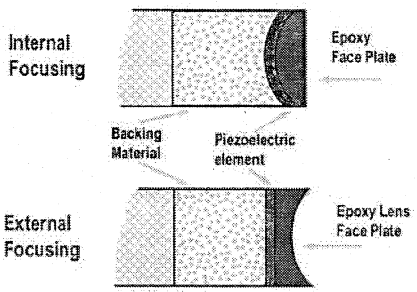

xternal Focusing - a lens is used on the transducer face to bend the oundwaves to a focal point.
ternal Focusing - the piezioelectric element is formed in a curved ement that focus the beam.
lectronic - using a process called phased array, multiple elements re fired sequentially to focus the beam .

eam Focusing

rray transducers have the ability to be dynamically focused by imulating each element as shown in the diagram below. The dividual wave fronts add up to a tight beam of ultrasound energy.

Beam Steering:

rray transducers have the ability to be steered as well as focused. ke focusing, the beam is directed by sequentially stimulating each ement as shown. This feature creates the sector scan by rapidly eering the beam from left to right to give the two dimensional cross ectional image.

esolution:
ateral resolution - the ability to resolve objects side by side. Lateral esolution is proportionally affected by the frequency, the higher the equency the greater the lateral resolution. Higher frequency ansducers are used in fetal and pediatric echocardiography

ecause the lateral resolution displays the smaller structures in those atients and there is less need for depth penetration. Lower equencies are used for adults where structures are larger and the eed for greater depth penetration is important.

xial Resolution - Axial resolution is the ability to resolve objects that e one above the other. Axial resolution is inversely proportional to ne frequency of the transducer depending on the size of the patient. he higher the frequency the lower the axial resolution is in large atients. This state results from the rapid absorption of the ultrasound nergy with lower penetration. Lower frequencies are utilized to ncrease depth of penetration.
epth of Penetration - Higher frequencies are attenuated by tissue nore than lower frequencies. This means that the higher the equency the greater the resolution but the lower the depth of enetration. User lower frequencies for adults and higher frequencies r children. The advent of harmonic imaging allows the use of a wer frequency pulse to be picked up and sampled at a higher equency (the second harmonic) where the low frequency allows reater penetration and high frequency provides better resolution.

	2.0mHz	5.0mHz
Axial	Decrease	Increase
Lateral	Decrease	Increase
Penetration	Increase	Decrease

asic Components of the Imaging System:

ransducer - the probe housing the elements, backing material, lectrodes, matching layer and protective face that both sends and eceives the sound waves.

ransmitter - the component that creates the impulses sent to the ansducer to generate sound energy. Also called the pulser.

eceiver - the component that receives the current generated in the ansducer from the returning sound energy.

mplifier - the component that amplifies the returning signals and repares them to be displayed on the CRT.

PU - the central processing unit that

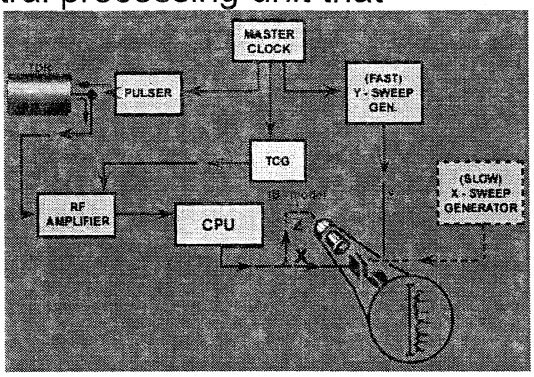

ulsing:
ulse Repetition Frequency (PRF) - the number of pulses per econd.

uty Factor - the amount of time that the transducer is transmitting ound energy. Most transducers are acting as the receiver 99 % of ne time. the duty factor is 1.

ledical Application PRFs -
igh PRF - the range for most commercial echocardiographs is etween 200 and 5000 pulses per second. The varies with the type of ıode in operation.

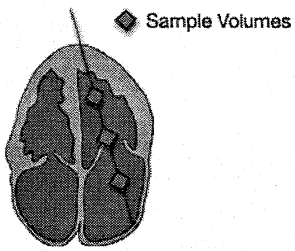

lodes:
A Mode - amplitude mode. Where the signals are displayed as spikes ıat are dependent on the amplitude of the returning sound energy.
B Mode - brightness mode. Where the signals are displayed as arious points whose brightness depends on the amplitude of the eturning sound energy.

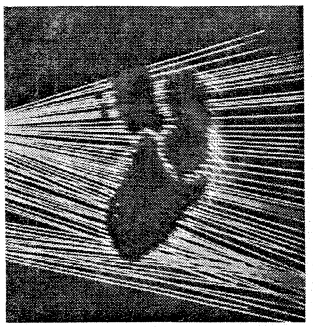

ld format B-mode type scan

l Mode - motion mode. The application of B-mode and a strip chart ecorder allows visualization of the structures as a function of depth nd time.

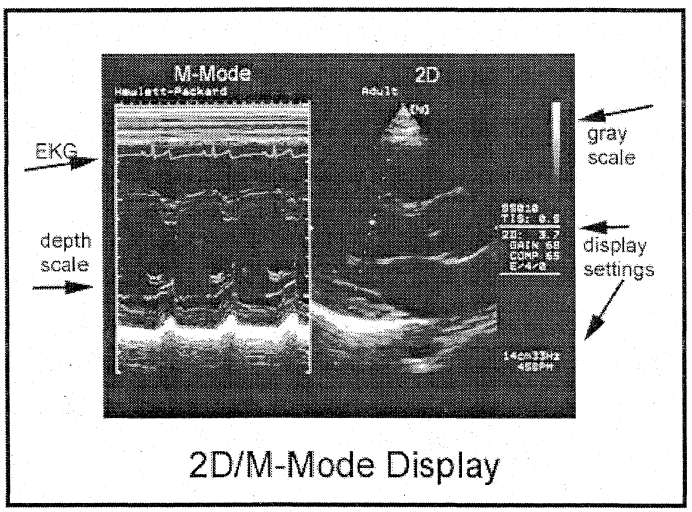

2D/M-Mode Display

D Mode - 2 dimensional mode name is usually reserved to indicate -mode imaging of the heart. The spatially oriented B-mode where tructures are seen as a function of depth and width. The beam is apidly swept back and forth to create a cross section of the imaged tructures.

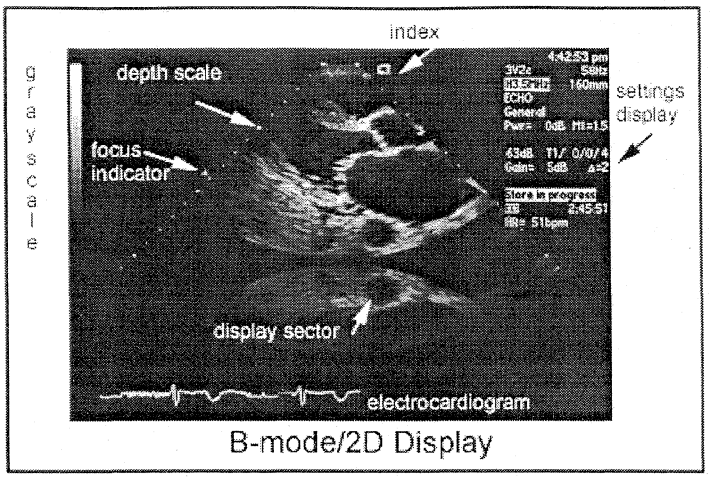

B-mode/2D Display

can Types:

Mechanical - transducers that use a combination of single lement oscillation back and forth, rotating multiple elements, r a single element and set of acoustic mirrors to generate the sweeping beam for 2D imaging. This transducer type is sometimes called the "wobbler" because of the vibration created as the mirrors rotate or oscillate inside the housing.

Electronic or Phased

ector - creates a sector or pie shaped scan plane. This is most seful for cardiac work where the beam is directed between the ribs image the heart. The beam is electronically swept in a fan shape transmit and receive ultrasound signals.

near - creates a linear or rectangular shaped scan plane. This is ost useful in abdominal, OB/GYN, and small parts work where the rgans are not blocked by bones or ribs. A wide footprint allows the perator to image larger organs. This method is simplified because ere are no obstructions to the signal by ribs and other bones.

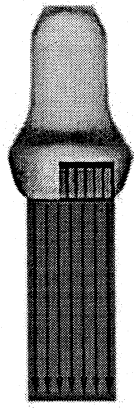

Transesophageal -

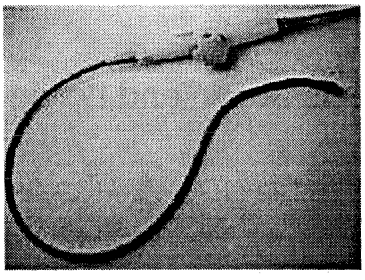

The piezoelectic device has been placed at the end of an endoscope so that the transducer may be passed into the esophagus to image the heart from inside the body.

Advantages of Electronic over Mechanical - dynamic focusing, smaller housing.

Disadvantages of Electronic over Mechanical - more expensive.

SIGNAL PROCESSING

Terms:
Decibel (dB) - a unit describing the ratio of logarithmic power amplification of the signal.

Dynamic range - the range between the minimum low intensity and maximum high intensity signals that a system is capable of displaying.

Reject - The control that allows the operator to ignore the weak

noes that may clutter the display and obscure the higher amplitude nals. It filters out all signals below a fixed amplitude to improve the ording

C - Time Gain Compensation. The control that allows the operator amplify the returning signal from deeper structures in the body. e sector is divided into depths and altering the TGC control can mpen or amplify the returning signals

mping - a method of reducing the pulse duration, or ringing of the nsducer, and thereby increasing lateral resolution.

mpress - a control on some systems that affects the gray scale d overall gain.

ial Resolution - the resolution of objects above and below each ner.

teral Resolution - the resolution of objects that are side by side.

de-Lobe - produced from the side lobes of the ultrasound beam. is artifact appears as false structures in the scan plane.

verberation - produced from the multiple reflections from an object the sound energy bounces back and forth between the object and e transducers face or dense structure.

adowing - the loss of data below a dense object because the ajority of the sound energy has been reflected. This occurs typically prosthetic valves.

ologic Effects and Safety:

vo bioeffects of ultrasound are heat and cavitation. As sound ergy is transmitted through tissue, some energy is reflected and me energy is absorbed as heat. It has not been determined that edical ultrasound causes any deleterious effects. Cavitation is the rmation, growth, and dynamic behavior of gas bubbles neither hich have been determined harmful at the level of the medical age. Mechanical effects of ultrasound include sheer forces and

coustic streaming.

AIUM Statements:

The American Institute of Ultrasound in Medicine states that as of 982, no independently confirmed significant biologic effects had been observed in mammalian tissue below (medical usage) 00mW/cm2.

Measures of Intensity for Ultrasound:

Spatial Peak, Temporal Peak Intensity (SPTP) - the peak intensity at he point in space where the intensity is highest and that occurs when he ultrasonic emitting device is "on". It is highest of the measured ntensities.

Spatial Average, Temporal Average Intensity (SATA) - the average power output of the device over the pulse repetition period divided by a reference, usually that of the transducer face. This measurement of intensity is the most quickly determined and most requently quoted by manufacturers. It also yields the lowest more commonly used measures of intensity.

Spatial Average, Temporal Peak Intensity (SATP) - the peak ntensity over a selected area, such as the transducer face, that occurs when the ultrasonic emitting device is "on."

Spatial Peak, Temporal Average Intensity (SPTA) - the maximal spatial intensity when the sound beam is "on" average over the pulse repetition period.

Spatial Peak Pulse Average Intensity (SPPA) - the pulse-averaged ntensity measured at the point in space where the value is maximal.

Spatial Average Pulse Average (SAPA) - the pulse average ntensity averaged over the beam cross sectional area.

PICTURE ARCHIVING AND COMMUNICATION SYSTEM

In medical imaging, **picture archiving and communication systems** (PACS) are computers or networks dedicated to the storage, retrieval, distribution and presentation of images

PES OF PACS

l PACS handle images from various modalities, such as asonography, magnetic resonance imaging, positron emission nography, computed tomography, endoscopy, mammography and iography (plain X-rays).

all-scale systems that handle images from a single modality ually connected to a single acquisition device) are sometimes ed *mini-PACS*

USES

CS replaces hard-copy based means of managing medical ages, such as film archives. It expands on the possibilities of such nventional systems by providing capabilities of off-site viewing and orting (distance education, tele-diagnosis). Additionally, it enables ctitioners at various physical locations to peruse the same rmation simultaneously, (teleradiology). With the decreasing price digital storage, PACS systems provide a growing cost and space vantage over film archives.
CS is offered by virtually all the major medical imaging equipment nufacturers. There are also several PACS open-source projects. e most difficult area for PACS systems is interpreting the DICOM age format which is slightly variably implemented between different liology equipment vendors. The ability to point the tags in the COM format coming from vendors equipment to useable titles in a CS is a feature common to most vendors and software offerings

ARCHITECTURE

pically a PACS network consists of a central server which stores a tabase containing the images. This server is connected to one or re clients via a LAN or a WAN which provide or utilize the images. eb-based PACS is becoming more and more common: these

ystems utilize the Internet as their means of communication, usually a VPN or SSL. The software (thin or smart client) is loaded via ctiveX, Java, or .NET Framework. Definitions vary, but most claim hat for a system to be truly web based, each individual image should ave its own URL. Client workstations can use local peripherals for canning image films into the system, printing image films from the ystem and interactive display of digital images. PACS workstations ffer means of manipulating the images (crop, rotate, zoom, rightness, contrast and others).
Iodern radiology equipment, modalities, feed patient images directly o the PACS in digital form. For backwards compatibility, most ospital imaging departments and radiology practices employ a film igitizer.
he medical images are stored in an independent format. The most ommon format for image storage is DICOM (Digital Imaging and Communications in Medicine), a NEMA standard

INTEGRATION

A full PACS system should provide a single point of access for mages and their associated data (i.e. it should support multiple nodalities). It should also interface with existing hospital information ystems: hospital information system (HIS) and radiology information ystem (RIS).
nterfacing between multiple systems provides a more consistent and nore reliable dataset:

- Less risk of entering an incorrect patient ID for a study – modalities that support DICOM worklists can retrieve identifying patient information (patient name, patient number, accession number) for upcoming cases and present that to the technologist, preventing data entry errors during acquisition. Once the acquisition is complete, the PACS can compare the embedded image data with a list of scheduled studies from RIS, and can flag a warning if the image data does not match a scheduled study.

Data saved in the PACS can be tagged with unique patient identifiers (such as a social security number or NHS number) obtained from HIS. Providing a robust method of merging datasets from multiple hospitals, even where the different centers use different ID systems internally.

interface can also improve workflow patterns:

When a study has been reported by a radiologist the PACS can mark it as read. This avoids needless double-reading. The report can be attached to the images and be viewable via a single interface.

Improved use of online storage and nearline storage in the image archive. The PACS can obtain lists of appointments and admissions in advance, allowing images to be pre-fetched from nearline storage (for example, tape libraries or DVD jukeboxes) onto online disk storage (RAID array)

cognition of the importance of integration has led a number of pliers to develop fully integrated RIS/PACS systems. These may r a number of advanced features:

- Dictation of reports can be integrated into a single system. The recording is automatically sent to a transcriptionist's workstation for typing, but it can also be made available for access by physicians, avoiding typing delays for urgent results, or retained in case of typing error.
- Provides a single tool for quality control and audit purposes. Rejected images can be tagged, allowing later analysis (as may be required under radiation protection legislation). Workloads and turn-around time can be reported automatically for management purposes.

COMPUTED RADIOGRAPHY

The last few decades have seen numerous technological advancements in the field of radiology with the introduction of newer technologies such as Sonography, Color Doppler, CT, MRI and DSA. In fact this has prompted the change of the nomenclature of this speciality from radiology to medical imaging. Alas the modality that invented this specialty, conventional radiology or more fondly known as plain films has been bereft of any significant technological advancement. The other modalities have significantly benefited because of their reliance on computer technologies. As the hard ware and soft ware revolution has progressed globally in all fields, this has naturally benefited these modalities but not conventional radiology, which has practically no reliance on computer technologies. The key to advancements in conventional radiology is in digitizing the images so they can be manipulated in an electronic format and thus enhanced.

There are two means available to obtain Digital X-Rays

1. Digital Radiography
2. Computed Radiography

Digital Radiography: The X-Ray machines are digital machines with flat panel detectors. There are no available portable digital X-Ray machines. So portable X-rays would still remain conventional.

Computed Radiography: CR uses standard X-Ray machines. There is no need to change existing X-Ray machines as is required in Digital Radiology. There is only a change in the recording device i.e. the cassette. In CR rather than a film, the image is exposed on a digital plate. The Digital image is then transferred to a reader, where the image is displayed on a monitor. This image being digital can be modified to adjust the exposure. Once the quality is approved the image may be printed on film in a laser camera. The images may also be stored in an electronic format on CD or sent to a remote location in the hospital via a local area network or even emailed to any location

in the city, country or world. The images may also be transferred to a workstation similar to a CT or MRI workstation. If the department has existing CT and MRI workstations these can be used without the need to obtain a new workstation. There are numerous advantages of a workstation, the images can be modified, cropped, magnified and labeled

There are numerous advantages of obtaining Digital images for conventional Radiology

1. Marked Improvement in image quality:
Chest, Spine and bone images are of exceptional quality, with better trabecular details.

2. No need for retakes.

Conventional X-Rays are still a manual procedure; the technician sets the exposure depending on the size of the patient. This could occasionally be faulty resulting in an over or under exposure. When this occurs it will need to be corrected by repeating the X-Ray after readjusting the exposure factors. This results in additional radiation to the patient as well as loss to the institution, as the first film will need to be discarded.

With Digital X-Rays the exposure factors do not need to be so accurate, variations in exposure can be adjusted on the monitor after the image has been obtained. Thus a perfect image can then be printed.

Spoil film rates range from 10-15%, similar to most top class institution obtaining X-Rays using conventional means. Conversion to digital will result in a saving of 10-15% on the film bill.

3. No loss of Films

Occasionally in very busy departments films may get misplaced. These films need to be repeated, again resulting in additional radiation exposure and loss of revenue.

4. Multiple images from one exposure
In post bypass patients the physician would like soft exposure X-Rays

so as to see how wet the lungs are and the cardiac surgeon would ike to have a X-Ray with a harder exposure so as to see inserted hard ware, drains etc. In one exposure with a conventional X-ray it is difficult to achieve both. This results in one of the two being unhappy with the quality. This problem does not occur with digital X-rays as the images can be manipulated to provide a softer and harder image with the same exposure thus keeping both the physician and cardiac surgeon satisfied.

5. Multiple images on one film
at present in a Barium X-ray study or IVU, about 8-10 films may be taken. With Digital all these pictures can be placed on one film. Further the abnormal portions can be enlarged, highlighted and labeled. Placing multiple images on one-film results in saving on film.

5. Images can be provided on medium other than film. Images can be documented on CD, high quality paper or viewed on a monitor. The benefit of this is as film is an expensive medium; cheaper options to cut cost can be explored.

With any imaging technique there are disadvantages. There are essentially two disadvantages and these are cost related. The first is capital cost of equipment. DR or Digital Radiology is very expensive, each machine costs at least 1.5 crores, so if a department had 4 X-Ray machines to switch digital would cost at least 6 crores. CR is much cheaper the total cost is between 50 and 60 lacks. The second disadvantage is the cost of film; images are documented on laser films which are approximately double the cost of routine conventional films. The initial reaction is that this makes CR an unviable modality. However there are numerous means as mentioned above of cutting the film bill down and using other recording means. A successful formula will be the key to exploiting the numerous advantages of this new technological advance. The driving force of this technological advance is the far superior image quality.